Development of Novel Anti-viral Strategies for Hepatitis E

Wenshi Wang

王文世 著

The studies presented in this thesis were performed at the Laboratory of Gastroenterology and Hepatology, Erasmus MC-University Medical Center Rotterdam, the Netherlands.

The research was funded by:

- Netherlands Organization for Scientific Research (NWO)
- Dutch Digestive Foundation (MLDS)
- Daniel den Hoed Foundation

Financial support for printing of this thesis was provided by:
Erasmus MC-University Medical Center Rotterdam, ChipSoft and Sanbio B.V..

Cover design: Hongbo Guo.
Cover design acknowledgement: PROTEIN DATA BANK (http://www.rcsb.org/pdb/explore.do?structureId=2ztn) and Tim's Printables (https://www.timvandevall.com/science/animal-cell-diagram/)

Layout design: the author of this thesis.

Printed by: Ridderprint BV, Ridderkerk, the Netherlands

ISBN: 978-94-6299-862-9

Development of Novel Anti-viral Strategies for Hepatitis E

Ontwikkeling van nieuwe anti-virale strategieën tegen hepatitis E

Thesis

to obtain the degree of Doctor from the
Erasmus University Rotterdam
by command of the
rector magnificus

Prof. dr. H.A.P. Pols

and in accordance with the decision of the Doctorate Board

The public defense shall be held on

Tuesday 06th February 2018 at 15:30

by

Wenshi Wang

born in Qingdao, Shandong Province, China

Erasmus University Rotterdam

Doctoral Committee

Promoter:

Prof. dr. M.P. Peppelenbosch

Inner Committee:

Prof. dr. H.J. Metselaar

Prof. dr. R.A.M. Fouchier

Prof. dr. B. Berkhout

Copromoter:

Dr. Q. Pan

CONTENTS

Part II Drug-based strategies

Part III Virus-host interaction-based strategies

Chapter 1

General Introduction

Hepatitis E virus (HEV) infection

HEV is a single-stranded positive-sense RNA virus that was first discovered in 1983. HEV belongs to the *Orthohepevirus* genus within the *Hepeviridae* family and at least four genotypes can provoke human infections. It is the most common causative agent for acute viral hepatitis worldwide with an estimated 20 million infections annually and around 56,000 related deaths (1). HEV genotypes 1 and 2 are indigenous predominantly in countries of the developing world, especially in Asia and Africa. They are transmitted via a fecal-oral route through contaminated water sources in conjunction with poor sanitary conditions, thus these genotypes responsible for many water-borne outbreaks of hepatitis E (2). In contrast, HEV genotypes 3 and 4 infect humans and animals and are transmitted from animal reservoirs (like pigs) to humans. They are reported mainly in developed countries (3). In general, HEV causes a self-limiting infection with low mortality. However, fulminant hepatitis may develop and a high mortality rate (as high as 20%–30%) is reported in the population of pregnant women. Chronic HEV infections are increasingly documented in immunocompromised patients, and provoke liver fibrosis and cirrhosis in some cases (4). As thus, HEV constitutes an important threat to global health.

Molecular virology of HEV

Knowledge as to the molecular mechanism employed by HEV to prey on the human may hold clues to better treatment and prevention of disease. HEV contains a single positive-stranded RNA genome of approximately 7.2-kb in size. The whole genome composes of three open reading frames (ORFs) with 7-methylguanylate (m^7G) capped at the 5' end and a poly-A tail at the 3' end. ORF1 encodes a nonstructural multi-functional protein essential for viral replication. ORF2 encodes the viral capsid protein. And ORF3 is a small functional protein involved in viral secretion step (5) Recently, a novel ORF4 was also defined (6).

ORF1 translates into a polyprotein with a molecular mass of $186\ \mathrm{kDa}$. Its main putative functional domains include a methyltransferase (MeT), a Y domain (Y), a papain-like cysteine protease (PCP), a proline-rich hinge domain, a X domain, an RNA helicase (Hel) domain, an RNA-dependent RNA polymerase (RdRp) domain (7). The enzymatic function of the methyltransferase domain has been experimentally verified. It can catalyze both guanine-7-methyltransferase and guanylyl-transferase activities required for capping of HEV mRNAs (8). The function of the putative

PCP domain during HEV replication is still controversial. Generally, positive-strand RNA virus express proteases for processing viral polyproteins or host proteins in turn facilitating viral infection. In apparent agreement, some studies indicate that HEV PCP also processes the ORF1 polyprotein (9, 10). However, an absence of processing activity by PCP has also been reported (11, 12). Further studies are still needed for a clear understanding of the functionality of this domain. Hel domain is a nucleoside triphosphate (NTPase) with the ability to unwind RNA duplexes into the 5'-to-3' direction. It also possesses the ability to mediate the first step of 5' cap synthesis (13, 14). The RdRp domain can specifically bind to the 3' end of the HEV RNA with poly (A) stretch, which then acts as the template to synthesize RNA (15). Of note, recent reports indicated that HEV mutations emerged in this domain is associated with altered viral fitness and ribavirin sensitivity (16, 17) and thus this part of the virus is subject to evolutionary pressure emanating from human strategies to combat the virus.

ORF2, the second largest ORF, encodes the major viral capsid protein and constitutes of 660 AA and is as thus the major target for HEV-evoked antibody responses. Structural analysis revealed three domains: the shell domain (S), the middle domain (M), and protruding domain (P). These studies postulated that the neutralizing epitope(s) interacting with human immunity locate to the P domain of ORF2. Also functional analyses indicated that the P domain is involved in the binding to cells susceptible to HEV infection and contains epitopes mediating antibody-dependent neutralization of viral activity (18, 19). ORF2 contains 3 putative N-glycosylation sites (Asn 132, Asn 310 and Asn 562), but the biological function of such potential post-translational modifications is still unclear (20). It was also reported that ORF2 can specifically bind to the HEV genome RNA via a 76-nucleotide (nt) region at the 5' end of the HEV genome and plays an essential role in virus assembly process (21). As the capsid protein, ORF2 not only protects the integrity of the viral genome but is also involved in many important regulatory activities. One od these appears to be interfering with host responses to viral infection. The activation of general immune response activating transcription factor NF-κB requires the phosphorylation and degradation of I-kβ, which unmasks a nuclear localization signal and thus allows translocation of NF-κB dimmer to the nucleus. ORF2 can block the degradation of Ikβ, and, as a result, NF-kB activity is inhibited in HEV-infected human hematoma cells (22).

The ORF3 is the smallest among the canonical ORFs of HEV. It partially overlaps with ORF2 in a different reading frame, and encodes a protein product of 13 kD (VP13). VP13 contains two hydrophobic domains in its N-terminal and two proline-rich domains in its C-terminal part. A phosphorylation site (Ser71) was identified in the first proline-rich domain and this site can be phosphorylated by MAP kinase (23). Studies have suggested that VP13 plays multiple roles during HEV infection. VP13 is dispensable for viral replication in cultured cells, however it is indispensable for both virus release and infection (24, 25). The ORF3 protein was also reported to interact with HEV viral proteins such as Hel, PCP, Met and RDRP domains, suggesting its potential roles during HEV replication and viron formation (26). However, elucidating the full function of HEV ORF3 protein still needs further investigations. In conjunction these viral constituents exploit host cell machinery for viral reproduction but also provide opportunities for host defense through both innate and adaptive immunity. In this thesis I focus on cell-autonomous element of former to create enhanced understanding of HEV biology and to uncover potential novel avenues for rational treatment of disease.

Interferon-stimulated genes

Interferon-stimulated genes (ISGs) are a group of gene products that coordinately combat pathogen invasions, in particular viral infections. Classically, upon IFN binding to its cognate cell-surface receptors, a signal is transmitted through the membrane into the cell via the JAK–STAT pathway, leading to rapid transcriptional activation of ISGs. There are hundreds of ISGs that are thought to be the ultimate antiviral effectors (27). Some ISGs control pathogen infection by directly targeting pathways and functions required during pathogen life cycle, whereas others have potent activity against a broad spectrum of pathogens. They are thought to enhance further IFN production, in turn inducing strong and broad induction of ISGs capable of combating infection, also through other positive feedback loops. Some ISGs act as negative regulators in these processes apparently to constrain and maintain the expression of ISGs at a certain stable levels, and appear essential for balancing beneficial antiviral versus detrimental pro-inflammatory effects of this signaling system. Thus, ISGs constitute a complex web of host defense machinery (28). Importantly, how this web interacts with HEV to mount defensive responses against this virus remains only partly understood.

Treatment of HEV infection

In general, the vast majority cases of acute hepatitis E are either asymptomatic or the illness is mild and self-limiting, not necessitating special treatment. However, patients with underlying chronic liver disease or those immunosuppressed patients who develop acute HEV display high mortality, and treatment should be considered (29). Chronic HEV infection was mainly described in immunosuppressed patients. Around one-third of those patients chronically infected with HEV will clear the virus when the level of immunosuppressive therapy is diminished. Hence, a reduction of immunosuppressive therapy is generally considered the first step in the treatment of chronic HEV infection. In those of whom this strategy fails, the use of an antiviral therapy is required (30). Pegylated interferon α (PegIFN-α) or ribavirin monotherapy or a combination of both have been used in this respect. PegIFN-α has achieved success in a small number of liver transplant patients. However, interferon has an immunostimulatory effect that sometimes lead to graft rejection and thus should be used with care in transplantation patients. Therefore, ribavirin as monotherapy is the most widely used therapy, although both antiviral treatments obtain strong antiviral response (31). Ribavirin monotherapy is effective for treating chronic HEV, with sustained virological responses (SVRs) of 85–90%. For patients who relapse, retreatment with ribavirin for a longer period achieves viral clearance in some but not all patients. Indeed, a few cases of ribavirin-treatment failure have been reported (16, 32). Currently, still no alternative treatment to ribavirin exists. In one study, it has been shown that sofosbuvir may inhibit HEV replication and may display enhanced antiviral effects when combined with ribavirin (33). However, the in-vitro efficacy of sofosbuvir against HEV reported in this study is modest (even at high concentrations). Other both in-vitro and in-vivo studies showed that sofosbuvir appears not very effective with respect to HEV, neither in monoinfection nor in HCV–HEV co-infection (34-36). Therefore, sofosbuvir is unlikely to develop into the drug of choice for patients who fail to ribavirin therapy. Further studies are urgently needed to identify novel antiviral agents in treating HEV infected patients.

Virus-host interaction

Virus infection universally elicits dynamic interactions between the virus and host. Host cells are equipped with mechanisms that rapidly detect and respond to virus invasion. These defense mechanisms largely rely on receptors that monitor the cytosol for the presence of atypical nucleic acids from the virus. For example, Toll-like receptor 3 (TLR3) can recognize ds-RNA (double-stranded RNA) in the endosome (37). Retinoic acid-inducible gene 1 (RIG-I) and melanoma differentiation associated protein 5 (MDA5) detect viral RNA through the unique signatures of the RNA involved, in the cytoplasm (38). For DNA viruses, their viral DNA can be recognized by cyclic GMP-AMP synthase (cGAS). Upon the detection of virus by these PRRs, downstream pathways will be activated, ultimately leading to the production of anti-viral cytokines (*e.g.* type I IFNs) (39). Once secreted, IFNs bind to their corresponding cell surface receptor complexes. This leads to the phosphorylation and activation of STAT (signal transducers and activators of transcription) 1 and 2. The phosphorylated STAT1, STAT2 together with IRF9 will form a transcriptional complex, denominated as IFN-stimulated gene factor 3 (ISGF3). This complex will translocate to the nucleus and bind to IFN-stimulated response elements (ISRE) and finally leading to the transcriptional activation of more than 300 IFN-stimulated genes (ISGs). The products of these genes are the ultimate antiviral effectors to constrain virus replication (27). Until now, there are still very limited studies on the cellular innate immune response following HEV infection. For instance, it remains unknown whether the HEV RNA genome can be efficiently recognized by the host and evoke antiviral response. There is thus an urgent need for fundamental studies elucidating the interaction of cell-autonomous innate immunity and HEV.

Nevertheless, it has become clear that such mechanisms are important as the virus has evolved strategies to combat host innate immune response. One study has identified an antagonistic activity to IFN-signaling exerted by the HEV ORF1 polyprotein, suppressing poly (I:C)-initiated IFN-β expression and IFN-related innate immune response (40). Similarly, the ORF3 protein of HEV also inhibits IFN-α-induced phosphorylation of STAT1, provoking downregulation of ISGs (41). In apparent contrast, however, another study indicated that ORF3 could stimulate the poly (I·C)-initiated IFN response through the activation of retinoic acid-inducible gene I (RIG-) (42). Besides IFN-related pathways, other immune response may also be modulated by the HEV infection, for instance, TNF-α induced NF-κB signaling activity (43). However, it is fair to say that the mechanisms that HEV on one hand and the cell-autonomous immune system on the other hand exploit to combat each other remain obscure at best and require further study.

Aim of this thesis

Based on the former, I try in this thesis to address three important issues relating to the molecular mechanisms that the HEV virus and the cell-autonomous innate immune system employ to exert their effects or that relate to the development of novel therapy. The main aims of this thesis are: (1) to investigate the regulatory mechanisms of IFN-stimulated genes and the resulting antiviral effects against HEV (**Part I, Chapter 3-7**), (2) to evaluate the effects of direct-acting antiviral drugs or compounds for HEV (**Part II, Chapter 8-11**), (3) to dissect virus-host interactions between HEV and host cells (**Part III, Chapter 12-15**). As will become evident, these efforts have yielded progress and novel insights in all three of these issues and thus may help develop novel relational therapeutic avenues of dealing with HEV infection.

References

1. Blasco-Perrin, H., F. Abravanel, V. Blasco-Baque, and J. M. Peron. 2016. Hepatitis E, the neglected one. *Liver Int* 36 Suppl 1: 130-134.
2. Hakim, M. S., W. Wang, W. M. Bramer, J. Geng, F. Huang, R. A. de Man, M. P. Peppelenbosch, and Q. Pan. 2017. The global burden of hepatitis E outbreaks: a systematic review. *Liver Int* 37: 19-31.
3. Dalton, H. R., N. Kamar, and J. Izopet. 2014. Hepatitis E in developed countries: current status and future perspectives. *Future Microbiol* 9: 1361-1372.
4. Kamar, N., L. Rostaing, and J. Izopet. 2013. Hepatitis E virus infection in immunosuppressed patients: natural history and therapy. *Semin Liver Dis* 33: 62-70.
5. Debing, Y., D. Moradpour, J. Neyts, and J. Gouttenoire. 2016. Update on hepatitis E virology: Implications for clinical practice. *J Hepatol* 65: 200-212.
6. Nair, V. P., S. Anang, C. Subramani, A. Madhvi, K. Bakshi, A. Srivastava, Shalimar, B. Nayak, C. T. Ranjith Kumar, and M. Surjit. 2016. Endoplasmic Reticulum Stress Induced Synthesis of a Novel Viral Factor Mediates Efficient Replication of Genotype-1 Hepatitis E Virus. *PLoS Pathog* 12: e1005521.
7. Panda, S. K., and S. P. Varma. 2013. Hepatitis e: molecular virology and pathogenesis. *J Clin Exp Hepatol* 3: 114-124.
8. Magden, J., N. Takeda, T. Li, P. Auvinen, T. Ahola, T. Miyamura, A. Merits, and L. Kaariainen. 2001. Virus-specific mRNA capping enzyme encoded by hepatitis E virus. *J Virol* 75: 6249-6255.
9. Paliwal, D., S. K. Panda, N. Kapur, S. P. Varma, and H. Durgapal. 2014. Hepatitis E virus (HEV) protease: a chymotrypsin-like enzyme that processes both non-structural (pORF1) and capsid (pORF2) protein. *J Gen Virol* 95: 1689-1700.
10. Parvez, M. K. 2013. Molecular characterization of hepatitis E virus ORF1 gene supports a papain-like cysteine protease (PCP)-domain activity. *Virus Res* 178: 553-556.
11. Perttila, J., P. Spuul, and T. Ahola. 2013. Early secretory pathway localization and lack of processing for hepatitis E virus replication protein pORF1. *J Gen Virol* 94: 807-816.
12. Suppiah, S., Y. Zhou, and T. K. Frey. 2011. Lack of processing of the expressed ORF1 gene product of hepatitis E virus. *Virol J* 8: 245.
13. Karpe, Y. A., and K. S. Lole. 2010. NTPase and 5' to 3' RNA duplex-unwinding activities of the hepatitis E virus helicase domain. *J Virol* 84: 3595-3602.
14. Karpe, Y. A., and K. S. Lole. 2010. RNA 5'-triphosphatase activity of the hepatitis E virus helicase domain. *J Virol* 84: 9637-9641.
15. Agrawal, S., D. Gupta, and S. K. Panda. 2001. The 3' end of hepatitis E virus (HEV) genome binds specifically to the viral RNA-dependent RNA polymerase (RdRp). *Virology* 282: 87-101.
16. Debing, Y., A. Gisa, K. Dallmeier, S. Pischke, B. Bremer, M. Manns, H. Wedemeyer, P. V. Suneetha, and J. Neyts. 2014. A mutation in the hepatitis E virus RNA polymerase promotes its replication and associates with ribavirin treatment failure in organ transplant recipients. *Gastroenterology* 147: 1008-1011 e1007; quiz e1015-1006.
17. Debing, Y., C. Ramiere, K. Dallmeier, G. Piorkowski, M. A. Trabaud, F. Lebosse, C. Scholtes, M. Roche, C. Legras-Lachuer, X. de Lamballerie, P. Andre, and J. Neyts. 2016. Hepatitis E virus mutations associated with ribavirin treatment failure result in altered viral fitness and ribavirin sensitivity. *J Hepatol* 65: 499-508.
18. Yamashita, T., Y. Mori, N. Miyazaki, R. H. Cheng, M. Yoshimura, H. Unno, R. Shima, K. Moriishi, T. Tsukihara, T. C. Li, N. Takeda, T. Miyamura, and Y. Matsuura. 2009. Biological and immunological characteristics of hepatitis E virus-like particles based on the crystal structure. *Proc Natl Acad Sci U S A* 106: 12986-12991.
19. Guu, T. S., Z. Liu, Q. Ye, D. A. Mata, K. Li, C. Yin, J. Zhang, and Y. J. Tao. 2009. Structure of the hepatitis E virus-like particle suggests mechanisms for virus assembly and receptor binding. *Proc Natl Acad Sci U S A* 106: 12992-12997.
20. Zafrullah, M., M. H. Ozdener, R. Kumar, S. K. Panda, and S. Jameel. 1999. Mutational analysis of glycosylation, membrane translocation, and cell surface expression of the hepatitis E virus ORF2 protein. *J Virol* 73: 4074-4082.
21. Surjit, M., S. Jameel, and S. K. Lal. 2004. The ORF2 protein of hepatitis E virus binds the 5' region of viral RNA. *J Virol* 78: 320-328.
22. Surjit, M., B. Varshney, and S. K. Lal. 2012. The ORF2 glycoprotein of hepatitis E virus inhibits cellular NF-kappaB activity by blocking ubiquitination mediated proteasomal degradation of IkappaBalpha in human hepatoma cells. *BMC Biochem* 13: 7.
23. Zafrullah, M., M. H. Ozdener, S. K. Panda, and S. Jameel. 1997. The ORF3 protein of hepatitis E virus is a phosphoprotein that associates with the cytoskeleton. *J Virol* 71: 9045-9053.
24. Emerson, S. U., H. T. Nguyen, U. Torian, D. Burke, R. Engle, and R. H. Purcell. 2010. Release of genotype 1 hepatitis E virus from cultured hepatoma and polarized intestinal cells depends on open reading frame 3 protein and requires an intact PXXP motif. *J Virol* 84: 9059-9069.
25. Huang, Y. W., T. Opriessnig, P. G. Halbur, and X. J. Meng. 2007. Initiation at the third in-frame AUG codon of open reading frame 3 of the hepatitis E virus is essential for viral infectivity in vivo. *J Virol* 81: 3018-3026.
26. Osterman, A., T. Stellberger, A. Gebhardt, M. Kurz, C. C. Friedel, P. Uetz, H. Nitschko, A. Baiker, and M. G. Vizoso-Pinto. 2015. The Hepatitis E virus intraviral interactome. *Sci Rep* 5: 13872.
27. Wang, W., L. Xu, J. Su, M. P. Peppelenbosch, and Q. Pan. 2017. Transcriptional Regulation of Antiviral Interferon-Stimulated Genes. *Trends Microbiol* 25: 573-584.

28. Schneider, W. M., M. D. Chevillotte, and C. M. Rice. 2014. Interferon-stimulated genes: a complex web of host defenses. *Annu Rev Immunol* 32: 513-545.
29. Dalton, H. R., and N. Kamar. 2016. Treatment of hepatitis E virus. *Curr Opin Infect Dis* 29: 639-644.
30. Kamar, N., S. Lhomme, F. Abravanel, O. Marion, J. M. Peron, L. Alric, and J. Izopet. 2016. Treatment of HEV Infection in Patients with a Solid-Organ Transplant and Chronic Hepatitis. *Viruses* 8.
31. Nelson, K. E., C. D. Heaney, A. B. Labrique, B. L. Kmush, and L. J. Krain. 2016. Hepatitis E: prevention and treatment. *Curr Opin Infect Dis* 29: 478-485.
32. Todt, D., A. Gisa, A. Radonic, A. Nitsche, P. Behrendt, P. V. Suneetha, S. Pischke, B. Bremer, R. J. Brown, M. P. Manns, M. Cornberg, C. T. Bock, E. Steinmann, and H. Wedemeyer. 2016. In vivo evidence for ribavirin-induced mutagenesis of the hepatitis E virus genome. *Gut* 65: 1733-1743.
33. Dao Thi, V. L., Y. Debing, X. Wu, C. M. Rice, J. Neyts, D. Moradpour, and J. Gouttenoire. 2016. Sofosbuvir Inhibits Hepatitis E Virus Replication In Vitro and Results in an Additive Effect When Combined With Ribavirin. *Gastroenterology* 150: 82-85 e84.
34. Donnelly, M. C., S. N. Imlach, F. Abravanel, S. Ramalingam, I. Johannessen, J. Petrik, A. R. Fraser, J. D. Campbell, P. Bramley, H. R. Dalton, P. C. Hayes, N. Kamar, and K. J. Simpson. 2017. Sofosbuvir and Daclatasvir Anti-Viral Therapy Fails to Clear HEV Viremia and Restore Reactive T Cells in a HEV/HCV Co-Infected Liver Transplant Recipient. *Gastroenterology* 152: 300-301.
35. Kamar, N., W. Wang, H. R. Dalton, and Q. Pan. 2017. Direct-acting antiviral therapy for hepatitis E virus? *Lancet Gastroenterol Hepatol* 2: 154-155.
36. Wang, W., M. S. Hakim, V. P. Nair, P. E. de Ruiter, F. Huang, D. Sprengers, L. J. Van Der Laan, M. P. Peppelenbosch, M. Surjit, and Q. Pan. 2016. Distinct Antiviral Potency of Sofosbuvir Against Hepatitis C and E Viruses. *Gastroenterology* 151: 1251-1253.
37. Schlee, M., and G. Hartmann. 2016. Discriminating self from non-self in nucleic acid sensing. *Nat Rev Immunol* 16: 566-580.
38. Wu, J., and Z. J. Chen. 2014. Innate immune sensing and signaling of cytosolic nucleic acids. *Annu Rev Immunol* 32: 461-488.
39. Goubau, D., S. Deddouche, and C. Reis e Sousa. 2013. Cytosolic sensing of viruses. *Immunity* 38: 855-869.
40. Nan, Y., Y. Yu, Z. Ma, S. K. Khattar, B. Fredericksen, and Y. J. Zhang. 2014. Hepatitis E virus inhibits type I interferon induction by ORF1 products. *J Virol* 88: 11924-11932.
41. Dong, C., M. Zafrullah, T. Mixson-Hayden, X. Dai, J. Liang, J. Meng, and S. Kamili. 2012. Suppression of interferon-alpha signaling by hepatitis E virus. *Hepatology* 55: 1324-1332.
42. Nan, Y., Z. Ma, R. Wang, Y. Yu, H. Kannan, B. Fredericksen, and Y. J. Zhang. 2014. Enhancement of interferon induction by ORF3 product of hepatitis E virus. *J Virol* 88: 8696-8705.
43. Xu, J., F. Wu, D. Tian, J. Wang, Z. Zheng, and N. Xia. 2014. Open reading frame 3 of genotype 1 hepatitis E virus inhibits nuclear factor-kappaappa B signaling induced by tumor necrosis factor-alpha in human A549 lung epithelial cells. *PLoS One* 9: e100787.

Chapter 2

The global burden of hepatitis E outbreaks: a systematic review

Mohamad S. Hakim[1,2], **Wenshi Wang[1]**, Wichor M. Bramer[3], Jiawei Geng[4], Fen Huang[5], Robert A.de Man[1], Maikel P. Peppelenbosch[1] and Qiuwei Pan[1]

[1]Department of Gastroenterology and Hepatology, Erasmus MC-University Medical Center and Postgraduate School Molecular Medicine, Rotterdam, the Netherlands

[2]Department of Microbiology, Faculty of Medicine, Gadjah Mada University, Yogyakarta, Indonesia.

[3]Medical Library, Erasmus MC-University Medical Center Rotterdam, Rotterdam, the Netherlands.

[4]Department of Infectious Diseases, The First People's Hospital of Yunnan Province, Kunming, China.

[5]Medical Faculty, Kunming University of Science and Technology, Kunming, China.

Liver International, 2017, 37(1): 19-31

Abstract

Hepatitis E virus (HEV) is responsible for repeated water-borne outbreaks since the past century, representing an emerging issue in public health. However, the global burden of HEV outbreak has not been comprehensively described. We performed a systematic review of confirmed HEV outbreaks based on published literatures. HEV outbreaks have mainly been reported from Asian and African countries, and only a few from European and American countries. India represents a country with the highest number of reported HEV outbreaks. HEV genotypes 1 and 2 were responsible for most of the large outbreaks in developing countries. During the outbreaks in developing countries, a significantly higher case fatality rate was observed in pregnant women. In fact, outbreaks have occurred both in open and closed populations. The control measures mainly depend upon improvement of sanitation and hygiene. This study highlights that HEV outbreak is not new, yet it is a continuous global health problem.

Keyword: global burden, hepatitis E, outbreaks

Key Points

- India represents a country with the highest number of reported HEV outbreaks.
- The number of reported HEV outbreaks is most likely underestimation of the actual burden of HEV outbreaks globally.
- In recent years, the burden of HEV outbreaks come from refugee camps in African countries.
- The availability of HEV vaccine should contribute to better control of HEV disease.

Introduction

Hepatitis E virus (HEV) infection is a major cause of outbreaks and acute sporadic hepatitis worldwide. HEV infecting humans consists of four different genotypes (genotype 1–4), with several sub genotypes exist in each. However, only one single HEV serotype was recognized.[1, 2] HEV genotypes 1 and 2 are found mainly in developing countries. They are transmitted via faecal-oral route through a contaminated water source, exclusively infect humans, and are thus responsible for many water-borne outbreaks. In contrast, HEV genotypes 3 and 4 infect humans and animals. They are found mainly in developed countries and are responsible for sporadic cases seen in the western world.[3, 4] In 2005, it was estimated that HEV genotypes 1 and 2 were responsible for about 20.1 million incidents of HEV infections, 3.4 million symptomatic cases, 70,000 fatalities, and 3000 stillbirths.[5] In general, HEV causes a self-limiting infection and does not need specific treatment. The mortality rate is low. However, fulminant hepatitis may develop and a high mortality rate (as high as 20%–30%) is reported in the population of pregnant women after infection with genotype 1.[1]

HEV is a spherical, non-enveloped, single-stranded positive sense ribonucleic acid (RNA) virus that mainly infects the hepatocyte.[6] HEV genome was first entirely cloned in 1991.[7, 8] Historically, HEV was suggested as a causative agent during jaundice outbreaks with a high attack rate among young adults and resulted in a high mortality rate among pregnant women.[9] Many large, water-borne, jaundice outbreaks in the past were described as non-A, non-B (NANB) hepatitis outbreaks due to failure in identifying hepatitis A (HAV) and hepatitis B virus (HBV) as the responsible agent of the outbreaks.[10, 11] The existence of HEV was already suggested in 1980 during the investigation of the causative agent of a NANB hepatitis outbreak in Kashmir Valley, India.[12]

Since the discovery of HEV, many archived samples obtained during NANB hepatitis outbreaks were tested for the presence of HEV.[13] The first retrospectively identified HEV outbreak was a large jaundice outbreaks in New Delhi, India, in 1955–1956 with more than 29,000 suspected cases.[13, 14] Along with the development of serology- and reverse transcription-polymerase chain reaction (RT-PCR)-based diagnostic methods, many HEV outbreaks were then identified (confirmed), both in the past (NANB hepatitis outbreaks) and in the recent years. Understanding the global distribution of confirmed HEV outbreaks could heighten our awareness of this under-recognized and under-reported human pathogen and improve HEV surveillance.

Therefore, we comprehensively reviewed the confirmed HEV outbreaks in the literature. More specifically, we described the global geographical distribution of (confirmed) HEV outbreaks, the severity (case-fatality rates), outbreak settings and modes of transmission, control measures, and the distribution of HEV genotype responsible for the outbreaks.

Materials and Methods

Literature search

A systematic search of available literature (conducted on 10 March 2015) was performed using the electronic database Embase.com, Medline (Ovid), the Cochrane library, Web of Science, Scopus, and Cinahl (EBSCOhost). Additional references were retrieved from unindexed references from PubMed, Lilacs, Scielo and Google Scholar. Additional references were sought by reviewing the reference list of selected studies. The search terms were designed by an experienced information specialist (WB).

The search was executed without any restrictions of publication date or language. The search terms were consisted of two main elements: hepatitis E virus (HEV) and outbreak. For each element, multiple synonyms were searched in title and/or abstract, and when available thesaurus terms (Mesh for medline, Emtree for embase and CINAHL headings for CINAHL). The search strategies for all databases are available in Table S1.

Study selection, inclusion and exclusion criteria

After removing the duplicates, we screened the articles based on the title and abstract. The full-text copies of included studies based on title and abstract screening were then assessed for eligibility. The inclusion criteria include: (i) Original research articles or reports, informing an outbreak of hepatitis E. An outbreak was identified by: (a) reporting an attack rates; (b) clearly demonstrated the epidemiological curve; (c) reporting large scale, affect several hundred to several thousands of people; (d) specify the time course, either short (few weeks) or long period (few months until year[s]); (ii) This study used PCR-based and/or serology-based diagnostics (IgM and IgG anti-HEV antibody to confirm the presence of HEV as a responsible agent for the outbreak; (iii) Studies showing NANB hepatitis outbreak that was confirmed later by another study showing that the outbreak was due to HEV; (iv) Any studies that confirmed previous NANB hepatitis outbreak as an HEV outbreak; (v) Any studies reported sequencing analysis of HEV strains derived from the outbreak. The following exclusion criteria were used for full-text screening: (i) full-text not available; (ii) language other than English; (iii) not primary study during the outbreak; (iv) not sufficient information. The selection procedure was performed by two independent investigators (M.S.H. and W.W.). Disagreements were resolved by discussion.

Data extraction

M.S.H. extracted the data with help of W.W. Data were extracted from the full-text papers of the included studies. The following items were extracted: author, year of publication, country, specific region (if available), the time of the outbreak (month and year), number of suspected cases, attack rate in general population, diagnosis used (serology, RT-PCR, sequencing), number of sample tested, number of confirmed cases, case fatality rates (CFR) both in general population and pregnant women, outbreak settings, risk factors (modes of transmission), control measures, and HEV genotype. Attack rate was defined as the number of suspected cases divided by the number of exposed population times 100. CFR was defined as the number of deaths divided by the number of suspected cases times 100. Our procedures accorded with the PRISMA guidelines for reporting systematic review and/or meta-analysis (Table S5).

Results

Description of the included studies

Using our search strategy, we identified potentially relevant 3776 articles. After removal of duplicates, 1653 articles were recorded for title and abstract screening. Of these, 191 articles met the eligibility criteria based on full-text and abstract screening and 10 articles identified from manual

search. After assessing 201 full-text articles, we ultimately included 98 articles in this systematic review (Fig.1).

Since we did not restrict the publication date and considering the fact that HEV has caused NANB hepatitis outbreak far before its identification, the publication dates of the included studies ranged from 1978 to 2015. Most of these studies describe the incident of HEV outbreaks in Asian and African countries, and only five studies describe HEV outbreaks in American and European countries. Interestingly, a large number of the included studies describing HEV outbreaks occurred in one country, India.

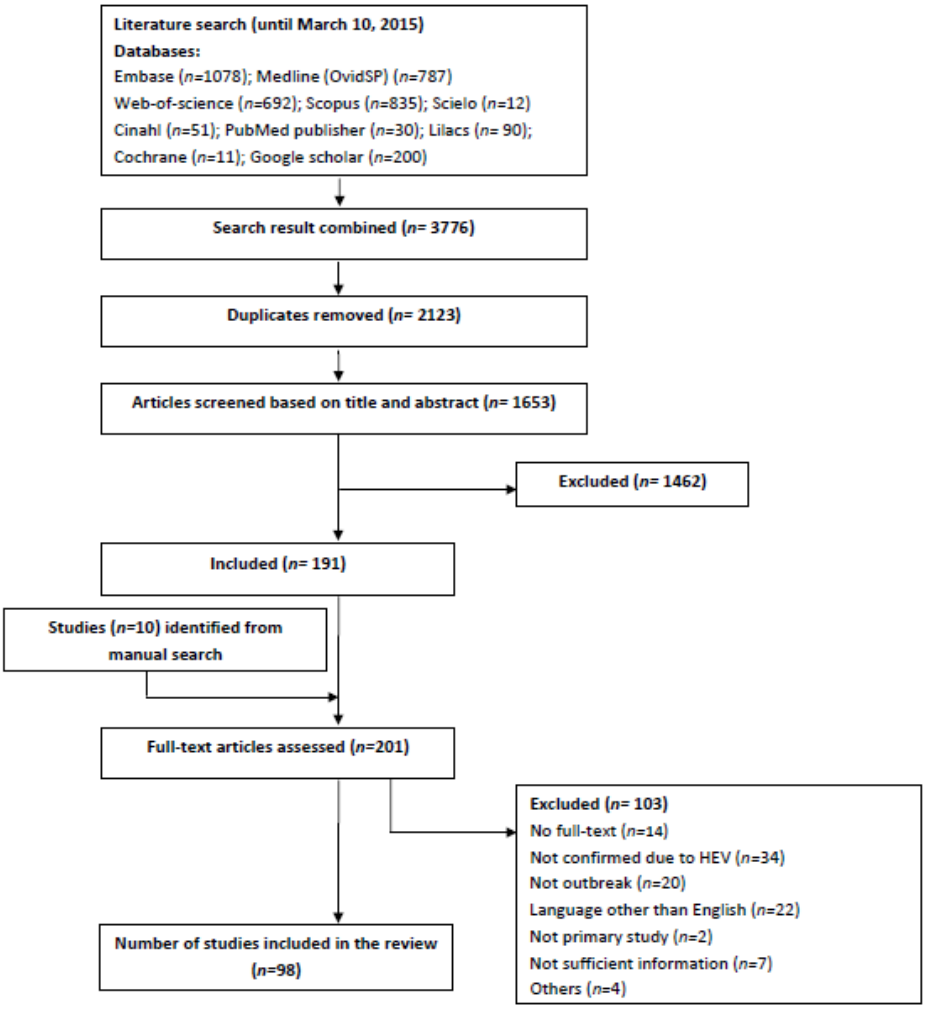

Figure 1. Flow diagram showing literature search and selection results.

Confirmed HEV outbreak and overall attack rate

Asia

HEV outbreaks have been reported from 12 countries: Indonesia,[15-17] Myanmar,[18] Vietnam,[19] Japan,[20] China,[21] Bangladesh,[22, 23] Pakistan,[24-29] Nepal,[30] Iraq,[31] Uzbekistan,[32] Turkmenistan,[33] and India [12-14, 34-65] (Fig.2 and Table S2 and S3). The first confirmed HEV outbreaks occurred in New Delhi, India in 1955.[13] During this outbreak, about 29,000 suspected

cases were reported, with an attack rate 2.05%. Retrospective analysis of archived serum samples from 28 patients successfully detected IgM anti-HEV antibodies in all samples (100%) to confirm that HEV was responsible for this large historical outbreak.[13] After this large outbreak, India has repeatedly reported large HEV epidemics, affecting hundreds to thousands of people (Fig.3). The largest HEV outbreak in India was reported in Kanpur, India during December 1990–April 1991. About 79,000 suspected cases (jaundice patients) were reported, with an attack rate of 3.76%. Analysis of 41 serum samples showed evidence of NANB hepatitis outbreak.[43] Analysis of stool samples from this epidemic demonstrated the evidence of HEV RNA in six of 10 samples analysed (60%), confirming that HEV was the aetiologic agent of this NANB hepatitis outbreak.[42] Another large HEV outbreak was reported from Nellore (south India) with 23,915 suspected cases.[62] From 1975 to 1994, India experienced 21 HEV outbreaks, 13 of them (62%) reported more than 1000 of suspected cases. The most recent epidemic in India was reported from Lalkuan (Nainital District, Uttarakahand) with approximately 240 suspected cases.[65] The attack rate ranged from 0.34%[37] to 8.61%.[65] There were only three outbreaks that reported attack rate of more than 10%, i.e. Saharanpur, 1992–1993 (14%);[45] Nainital district, Uttarakhand, July 2005 (16%);[56] and Baramulla district, Kashmir, 2007–2008 (21.6%).[60] These data suggest that India is highly endemic for hepatitis E.

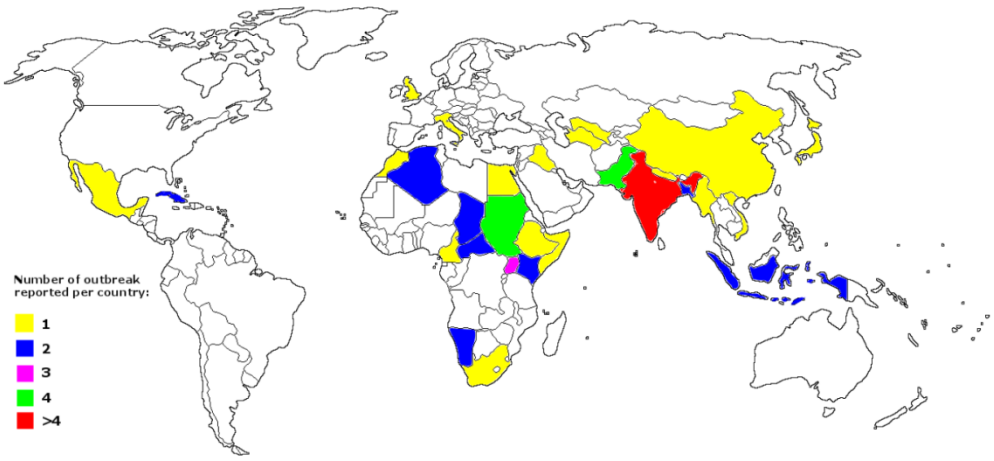

Figure 2. The Global HEV outbreak distribution. (Note: Sudan and South Sudan are regarded as one country).

There were four HEV outbreak reported from Pakistan.[24-28] The first reported HEV outbreak was Sargodha outbreak which occurred during March–April 1987.[24, 25] A large water-borne outbreak was reported from the city of Islamabad, affecting 3827 people, with 10.4% attack rate.[27] A localized HEV outbreak was occurred in the military unit of Abbottabad (August–September 1988), in which more than 100 suspected cases were recorded.[26] In all these outbreaks, the reported attack rates were more than 10%, ranging from 10.4%[27] to 20%.[24]

Bangladesh reported only two HEV outbreaks.[22, 23] An outbreak with more than 4000 cases was reported from Arichpur, an urban area near Dhaka, with 4% attack rate.[22] From south-east Asian countries, Indonesia reported two HEV outbreaks, in East Java [17] and Kalimantan island.[15, 16] Other south-east Asian countries, such as Myanmar and Vietnam only reported one outbreak.[18, 19]

In east Asia, the largest reported outbreak in the world so far was reported from Xinjiang, China. A huge number of 120,000 suspected cases was reported during prolonged outbreak that lasted from September 1986–April 1988, with an overall attack rate of 3.0%.[21] In the middle-east region, HEV outbreak was only reported from Baghdad, Iraq at 2005, after the Iraq war. More than 250 suspected cases were reported during this outbreak.[31] From central Asia, a large HEV outbreak occurred in the Dashoguz province of Turkmenistan, with more than 16,000 cases were reported.[33]

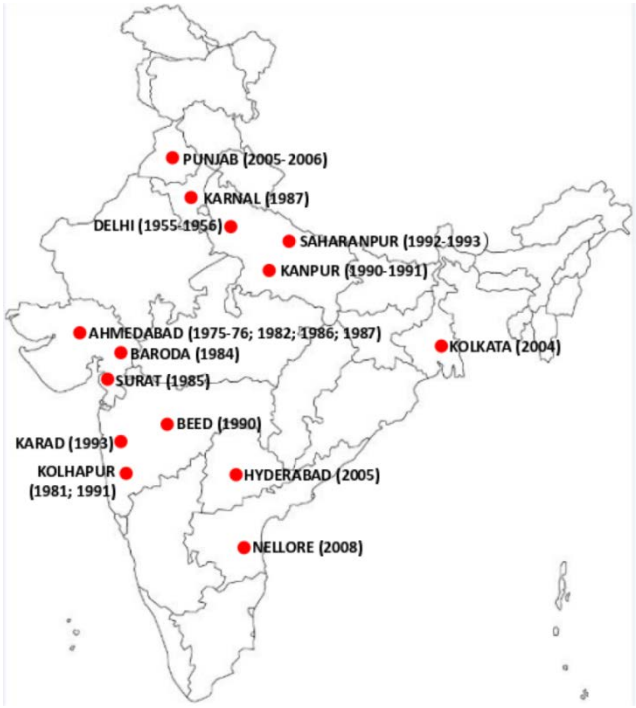

Figure 3. The Epidemic history of large HEV outbreak in India with more than 1,000 suspected cases.

Africa

HEV outbreaks have been reported from 14 countries: Egypt,[66] Kenya,[67, 68] Sudan and South Sudan,[69-76] Central African Republic (CAR),[77-79] Uganda,[80-84] Chad,[73, 76, 85-89] Republic of Djibouti,[90] Algeria,[85, 86, 89, 91] Namibia,[92, 93] Morocco,[94, 95] Somalia,[96, 97] Ethiopia,[98] South Africa,[99] and Cameroon[100] (Fig.2 and Table S2). The first, large, laboratory-confirmed HEV outbreak involved more than 140 villages in Somalia on early 1988 – late 1989. There were more than 11,000 suspected cases reported with an overall attack rate of 4.6%.[96, 97] A large HEV outbreak was also reported from Kitgum district, Uganda. More than 10,000 suspected cases from October 2007–June 2009 were reported with an overall attack rate of 25.1%.[80-82] During the investigation, the outbreak was still ongoing and therefore, the number of suspected cases might be increasing. In the last decade, outbreaks of hepatitis E have been reported from several area with warfare and conflict, causing human displacement. Several large HEV outbreaks, involving hundreds to thousands cases, were reported from refugee camps in Kenya (1702 cases);[67] South Sudan (>5000 cases);[75] Darfur, Sudan (2621 cases);[70, 71] and Chad (>900 cases).[73, 87]

America and Europe

Only few outbreaks were reported from European and American countries. In Europe, a confirmed HEV outbreak probably related to shellfish exposition and involving genotype 3 was reported on cruise ship returning to UK after a world cruise. Thirty-three of 789 passengers (4%) who provided blood samples were IgM anti-HEV positive, confirming a recent acute HEV infection.[101] A small HEV outbreak was reported from Lazio, Italy. Five suspected cases were reported and all of them were HEV positive (genotype 4).[102] In America, HEV outbreak was first reported from two villages, Huitzililla and Telixtac, Mexico in 1986, with more than 200 suspected cases. The overall attack rate was 5%–6%.[103-105] No HEV outbreak was reported from Mexico thereafter. Another country, Cuba, reported two HEV outbreaks.[106]

Case fatality rate (CFR)

The CFRs were reported in 38 studies (Table S4). In overall population, CFRs were relatively low, between 1% and 3%. The highest reported CFR of overall population was 3.6%, in the Kashmir valley outbreak, India, in 1978–1979, involving 275 suspected cases.[12] One study reported an overall CFR of 33% (six fatalities out of 18 cases).[28] This outbreak occurred among patients in neurosurgery ward in the hospital. Therefore, the underlying disease and condition might be important factors influencing this high CFR.

Compared with overall population, fatalities are higher in pregnant woman. The CFR among pregnant woman ranging from 5.1% in Rajasthan, India during February 2006[58] to 31.1% in refugee camp, Darfur, Sudan during July–December 2004.[70, 71] From 15 studies which reported CFR of both overall and pregnant women population, we found a significantly higher CFR in pregnant women compared to overall population (Fig.4). One study specifically compared the CFR among non-pregnant and pregnant females population. It was shown that the CFR of pregnant females was significantly higher than non-pregnant females (11% vs 1.5%, *P*<.01).[96]

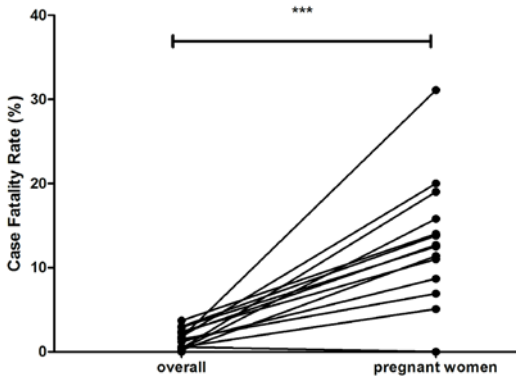

Figure 4. Case Fatality Rates (CFR) of overall population and pregnant women.

In addition to a high CFR among pregnant woman, HEV infection during pregnancy may lead to worse outcome. In HEV outbreak setting, several studies descriptively reported worse pregnancy outcomes such as postpartum haemorrhage, premature delivery, stillbirth, miscarriage and neonatal death.[22, 74, 78] Since these were descriptive studies, the relative contributions of HEV infection to pregnancy-related outcome could not be determined. Gurley ES et al.[22] reported that pregnancies complicated by acute jaundice had an increased risk for miscarriage, stillbirth and neonatal death, as compared to pregnancy without jaundice (OR 2.7; 95% CI 1.2–6.1).

Outbreak settings

Most HEV outbreaks occurred in community-based settings, such as village (rural area), city (urban area) or affecting a large area (one province) (Table 1). Several outbreaks occurred in a more-restricted (closed) settings, such as military units,[18, 26, 30, 49, 51, 98] college,[24] prison,[47] and factory.[106] In recent years, several outbreaks were also reported from refugee camps with a big number of suspected cases.[67, 68, 70, 75, 92] Interestingly, one study reported an HEV outbreak that occurred on a cruise ship.[101]

Table 1. HEV outbreak settings and underlying cause of HEV outbreaks

Outbreak settings and underlying cause (modes of transmission)	References
Outbreak settings	
City (urban area)	[22]; [23]; [27]; [31]; [37]; [38]; [43]; [45]; [46]; [48]; [52-55]; [57]; [59]; [61]; [62]; [65]; [78]; [79]; [93]; [106][5]
Village (rural area)	[12, 36][3]; [17][4]; [19][4]; [40]; [56]; [58]; [60]; [64]; [66]; [91]; [96][4]; [100]; [104, 105][3]
Affect large area (district or province)	[33][2]; [41]; [50][1]; [80-82][3]; [84]
Refugee camps	[67]; [68]; [70, 71][3]; [75]; [83]; [92]
Military units or military camps	[18]; [26]; [30]; [49]; [51]; [98]
Hospital	[28]; [99]
Cruise ship	[101]
Prison	[47]
Factory	[106][5]
College	[24]
Modes of transmission	
Contamination of drinking water	
eakage of water pipeline (broken, poor construction)	[18]; [22]; [31]; [38]; [41]; [45]; [49]; [51]; [53]; [54]; [57-59]; [61]; [64]; [65]
Failure of water treatment	[24]; [27]; [40]; [43]; [45]; [52]; [60]; [70]
Use of untreated water from river, spring	[12]; [17]; [56]; [91]; [96]
Flooding, heavy rainfall	[19]; [31]; [69]; [75]
Leakage of sewage pipelines	[38]; [55]
Food contamination	[101]

[1] Two district affected. [2] One province affected. [3] Refer to one outbreak. [4] Situated along the river. [5] Two outbreaks reported in one study

Risk factors and modes of transmission

Several risk factors were reported as the underlying cause of the outbreak (Table 1). The main mode of transmission reported was water-borne transmission. Leakage of water pipeline due to broken or poor construction was the most reported cause underlying the outbreak. The broken water pipelines lead to faecal or sewage contamination of the drinking water supply. Another underlying cause of the outbreak was failure of water treatment (such as filtration or chlorination). This failure led to the

supply of grossly contaminated drinking water to the household. The use of untreated water from river and spring was also reported as the underlying cause of the outbreak. Several HEV outbreaks occurred following flooding or heavy rainfall,[19, 31, 69, 75] facilitating contamination of water supplies with faeces. One study reported food contamination as the likely cause of the outbreak of HEV aboard a cruise ship.[101]

Role of person-to-person transmission

Several studies investigated the occurrence of person-to-person transmission during HEV outbreaks.[26, 40, 43-45, 58, 63, 81, 94, 104] Most of the studies suggest that there was no or minimal evidence of person-to-person transmission during HEV outbreak. However, there were variations between studies to determine the occurrence of person-to-person transmission. Only one study suggested that person-to-person transmission might be responsible for HEV outbreak in a large and prolonged HEV outbreak in Uganda.[81] This conclusion was supported by several observations: (i) prolonged outbreak, which occurred about 2 years; (ii) HEV was undetectable from the environment (water sources) and the zoonotic sources (pig); (iii) improvement of hygiene (such as chlorination) could not stop the epidemic and (iv) evidence of close contact and time interval between index and secondary cases within household.[81] However, some inquiries have been questioned to argue against the evidence.[107, 108] The relative contribution of person-to-person transmission therefore deserves further investigation, especially in the large and prolonged outbreaks. As HEV transmission occur via faecal-oral route, person-to-person transmission might be possible.

Table 2. Control measures of HEV outbreak

No	Intervention	References
1	Chlorination of the water supply	[26]; [37]; [38]; [40]; [44]; [45]; [54]; [63]; [65]; [77]; [83]
2	Repair of water pipelines	[26]; [45]; [46]; [49]; [53]; [57]; [59]; [61]; [62]; [65]
3	Improving general hygienic precautions (handwashing, boiling water)	[26]; [38]; [65]; [68]; [75]; [83]
4	Provision of alternate water supply	[27]; [30]; [65]
5	Hastening latrine construction.	[68]; [83]
6	Surveillance for additional cases (active case finding)	[26]; [75]
7	Simultaneous closure of of the water supply	[24]; [27]
8	Improving safe drinking water availability	[75]
9	Training of health care workers	[68]
10	Increasing community awareness	[68]

Control measures

To cope with the outbreak, control measures should be taken to prevent more additional cases. However, not all studies described specifically the control measures taken during the outbreaks (Table 2). Chlorination of the water supply was the most reported control measures during HEV outbreaks, followed by repairing of the broken water pipeline. Improving general hygienic precaution

(such as hand washing and boiling of drinking water) is a simple and low cost intervention to prevent HEV transmission during outbreak. Provision of an alternatively safe water supply (such as providing containers of safe drinking water) was reported. Lack of proper facilities for disposal of human faeces is one of the underlying factors responsible for outbreaks, especially in refugee camps. Therefore, hastening of latrine construction was reported as a control measure during HEV outbreaks in the refugee camps.

Table 3. HEV genotype responsible for the outbreak.

Country	Year	HEV Region sequenced	HEV Genotype	Reference
Asia				
India	2008	RNA-dependent RNA polymerase (RdRp gene)	Genotype 1, subtype A	[62]
India	2010	ORF1	Genotype 1, subtype A	[63]
India	1981	RNA polymerase	Genotype 1, subtype A	[109]
India	1975 - 1976	RNA polymerase	Genotype 1, subtype B	[109]
India	1984	RNA polymerase	Genotype 1, subtype A	[109]
India	1990	RNA polymerase	Genotype 1, subtype A	[109]
India	1991	RNA polymerase	Genotype 1, subtype D	[109]
Kyrgyzstan	1987 - 1989	ORF 2 (nt 5972-6319) and ORF 1 (nt 71-353)	Genotype 1	[114]
Bangladesh	2010	ORF2	Genotype 1, subtype A	[23]
Turkmenistan	1985	ORF2	Genotype 1	[33]
Pakistan	1987	Full genome (7195 nt)	Genotype 1, subtype B	[29]; [109]
China	1986 - 1988	Full genome	Genotype 1, subtype B	[21]
Japan	2005	ORF1	Genotype 3	[20]
Africa				
Morocco	1994	nt 5,014 - 7,186 (the 3'-terminal region of ORF1, full length ORF2 and ORF3, and a portion of the 3'-noncoding region)	Genotype 1	[95]
Central African Republic	2002	NS	Genotype 1 and 2	[77]
Sudan and Chad	2004	ORF 2 nucleotides 6,653-7,100	Genotype 1	[76]
Chad	1983 - 1984	ORF2 and ORF3	Genotype 1, subtype C	[89]; [109]
Uganda	2007 - 2009	ORF2	Genotype 1	[80]
Algeria	1986 - 1987	ORF2	Genotype 1	[91]
Algeria	1979 - 1980	ORF2 and ORF3	Genotype 1, subtype C	[89]; [109]
Namibia	1995 - 1996	451 bp region of a subgenomic fragment from the 3' end of the genome in ORF2	Genotype 2	[93]
Europe				
United Kingdom	2008	NS	Genotype 3	[101]
Italy	2011	ORF1 and ORF2	Genotype 4	[102]
America				
Cuba	1999 and 2005	ORF1	Genotype 1	[106]
Mexico	1986	Nearly complete genome (7185 nt)	Genotype 2	[109]; [110]

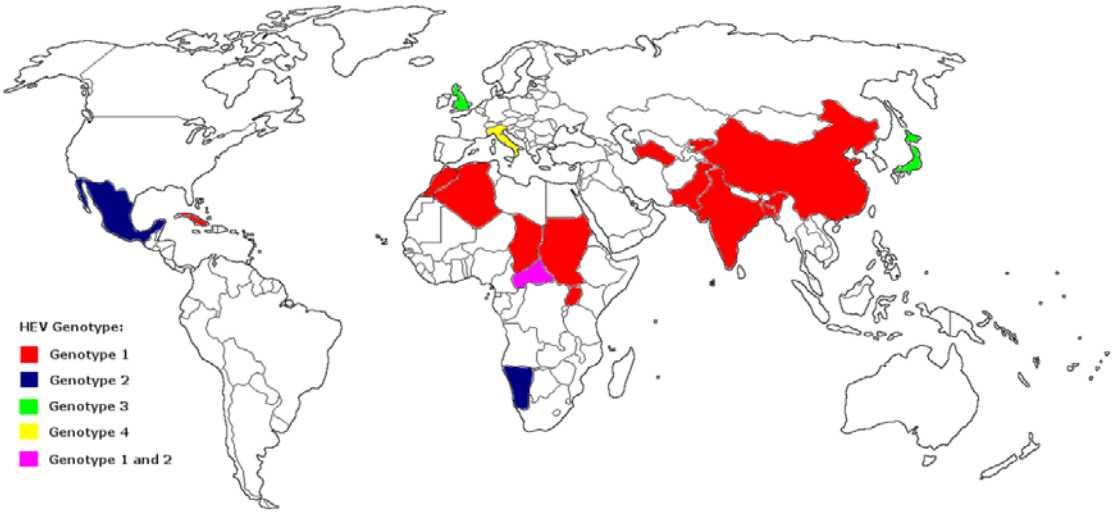

Figure 5. HEV genotype distribution responsible for the outbreaks. (Note: Sudan and South Sudan are regarded as one country.)

HEV genotypes responsible for the outbreak

Data on the genotype responsible for HEV outbreak were available only from limited number of studies (as summarized in Table 3 and shown in Fig.5). The open reading fragment 2 (ORF2) region was the most frequently region sequenced to determine the HEV genotype, followed by ORF 1 region (including RNA polymerase region). In accordance with the global distribution of the HEV genotypes, genotype 1 and 2 were mainly responsible for the outbreaks occurred in developing countries (Asia and Africa), while genotype 3 and 4 were responsible for small outbreaks in the western world (Europe), i.e. UK [101] and Italy.[102] Genotype 2 was responsible for outbreaks in CAR,[77] Namibia,[93] and Mexico.[109, 110] In Asia, all but one outbreak were due to genotype 1. In Asia and Africa, it seems that genotype 1 was more responsible than genotype 2 as the causative agent of HEV outbreaks. Moreover, genotype 1 was also responsible for several large HEV outbreaks, such as in China (1986–1988, with 120,000 suspected cases);[21] India (2008, with 23,915 suspected cases);[62] Turkmenistan (1985, with 16,175 suspected cases);[33] and Uganda (2007–2009, with >10,000 suspected cases).[80] No large HEV outbreaks so far were reported due to genotype 3 and 4.

Discussion

Historically, epidemic of jaundice and hepatitis with high attack rates in young adults and predominant or exclusive deaths among pregnant women was believed to be due to HEV.[9] The first laboratory-confirmed HEV outbreak is Delhi outbreak (1955–1956).[111] Since then, many HEV outbreaks were reported in the literature, especially after the availability of HEV diagnostic assay (HEV serology and RT-PCR). Our data suggest that HEV outbreak occurred repeatedly up to the recent years in many different countries, especially in Asian and African countries. It indicates that HEV outbreak is not new, yet it is a continuous health problem in developing countries. It is highly possible that our data only represent a tip of the iceberg. A higher percentage of HEV outbreaks that have occurred in many (other) countries might be not reported and not well-documented, mainly due to the absence of a surveillance system of HEV infection or lack of serology and PCR confirmation.

For example, about 33 outbreaks of acute viral hepatitis in Cuba were not well-reported and therefore excluded from our analysis.[112] Similarly, reports from 10 different Asian and African countries were not well-documented.[113] We also found a report of an HEV sequence derived from a Kyrgyztan outbreak, but we could not find the outbreak description.[114] Consequently, the actual number of HEV outbreaks should be much higher than what we present in this study. Therefore, the problem of HEV infection should not be underestimated by national and international health agencies.

HEV represents a significant health problem, especially in the developing countries. Acute sporadic form of HEV disease is the most frequent cause of acute viral hepatitis globally.[2] Epidemics of HEV, either in a small or large scale, occur periodically up to this moment, as reported from India.[115, 116] Many large outbreaks of hepatitis E have been reported especially from west and north part of India and thus represent a major health problem in the country (Fig.3). Several outbreaks have also been reported from neighbouring countries such as Bangladesh, Pakistan and Nepal (Fig.2). The Indian subcontinent, therefore, could be the best representation of areas with high endemicity of HEV infection.

In recent years, several large HEV outbreaks reported from refugee settlements. As a result of warfare and conflict in some African countries, displaced populations occupy refugee settlements and this has led to a new epidemic setting for HEV.[67, 68, 70, 75, 92] As the disease is mainly transmitted by faecal contamination of drinking water, the density of the resident population, a limited access to a good quality of drinking water, lack of adequate sanitation and personal hygiene, may predispose to the occurrence of HEV outbreaks in refugee camps.[117] Currently, increasing number of refugee population, resulted from wars, persecution, conflict and human rights violations, imposes one of the most pressing global challenges. This led to a complex humanitarian crisis, partly due to lack access of health service.[118] The most common causes of death in this population are communicable diseases, such as diarrhoeal diseases, measles and malaria.[119] These refugee camps are potential risk settings for water-borne outbreaks including HEV, cholera, hepatitis A virus (HAV), and rotavirus,[120-123] and they deserve the access of more timely, appropriate and quality healthcare services.

Although our data showed a limited number of reported HEV outbreaks in European and American countries, we cannot fully exclude the possibility that HEV could be the future threat in the region. HEV was considered as one of the emerging zoonotic swine pathogens.[124] Autochthonous HEV infection was reported from several countries in Europe, with evidence of zoonotic transmission from pigs.[125] A recent study has reported a small outbreak in China, which is caused by the zoonotic genotype 4 HEV and is related to the food in the company's cafeteria.[126] Therefore, it is highly possible that HEV genotypes 3 and 4 could be the potential cause of small-scale outbreaks in the developed countries in the near future, especially with the lack of transmission route identification and the lack of effective intervention strategies.

During HEV infection, the risk of progression towards fulminant hepatitis is higher among pregnant women as compared to men and non-pregnant women.[127, 128] Several studies during HEV outbreaks demonstrated that HEV infection could result in worse maternal and fetal outcome.[22, 74, 78] Similarly, studies of pregnant women presenting with jaundice due to acute viral hepatitis in hospital-based setting showed that FHF and mortality rate was greater in HEV-infected women than in non-HEV-infected women.[128] HEV-infected pregnant women have also a

significantly higher risk of developing obstetric complications, intrauterine fetal death, preterm delivery and stillbirth as compared to non-HEV-infected pregnant women.[128] It is estimated that HEV is responsible for ~9.8% of pregnancy-associated deaths in Bangladesh and about 10500 of annual maternal death in southern Asia.[129] Some immunological and hormonal factors have been associated with high mortality rate in HEV-infected pregnant women.[130-132] Interventions to prevent the occurrence of HEV infections in this high-risk population are therefore urgently required.[129]

Most studies reported faecal contamination of drinking water as the major route of transmission during HEV outbreak. The most commonly reported underlying cause of this contamination is leakage of water pipeline distribution system, either due to damaged or poor construction. As the water pipelines located close to drain or sewerage system, the damaged facilitate mixing of sewage materials and drinking water supplied to the household, causing water-borne outbreaks such as HEV, HAV, shigellosis and cholera.[133-135] A water-borne outbreak of pesticide poisoning was also reported due to damage of water pipeline distribution system.[136] Therefore, this kind of outbreak could be prevented by proper construction of water pipelines, keeping them away from the drain system, and also by monitoring of pipelines for damage.

Since HEV outbreak is mainly due to contaminated-drinking water, its control would depend upon improved hygiene and sanitation, such as increased access to safe water, provision of soap and chlorine tablets to improve personal hygiene, and proper sewage disposal. During outbreak, it is pivotal to intensively investigate the suspected underlying cause and then initiate targeted intervention to control and stop the outbreak.[83] Mass vaccination of HEV could be another effective strategy to control the outbreaks. Currently, an HEV vaccine has already been licensed for use in China[137] and give an insight that HEV is a vaccine-preventable disease.[111] Comparing the experience with HAV vaccination as an effective measure to control HAV outbreaks, the HEV vaccine holds promises to control large outbreaks. However, it is not known whether the current vaccine works fast enough to effectively protect the exposed population for clinical disease during an HEV outbreak and how long the protection will be afforded. Moreover, it is also not known whether the vaccine is safe and effective in pregnant women, the population in which a high fatality rate was seen during the outbreak.[129] In fact, there is disagreement among the HEV experts whether the current licensed vaccine is necessary to prevent outbreak following the recent earthquake in Nepal.[138-140]

Limitation of the published literature

There are some limitations in the published literature of HEV outbreaks. Firstly, the studies used different criteria to define suspected cases during HEV outbreak. Some studies only used physical symptoms of acute hepatitis (such as jaundice);[27] whereas other studies included laboratory criteria such as liver enzyme (aspartate and alanine aminotransferase).[47, 62] The differences in the criteria may then influences the different calculations of the attack rate. Secondly, the studies on HEV outbreak used different assays and diagnostic methods to confirm the presence of HEV as the causative agent of outbreak. Therefore, it is difficult to compare the validity of the reports. Thirdly, the outbreaks studied varied in the proportion of suspected cases to be tested for HEV. Consequently, the proportion of confirmed HEV cases differs markedly between outbreaks. Moreover, these data also suggest that some of these outbreaks might have been caused not only by a single agent (HEV), but also another agent that may also spread by faecal-oral route, especially HAV. Finally, the

outbreak studies used different epidemiological methods to investigate the outbreaks. Some of those outbreaks were investigated thoroughly, but some of them were not. The full versions of epidemiological investigations of several Indian epidemics were not available, although the outbreaks involved a large scale, in which thousands of people were affected.[13]

Conclusions

The available data suggest that HEV outbreaks occur repeatedly in many developing countries, especially in India and become a significant health problem in Asian and African continent, even before its identification. These outbreaks were mainly due to HEV genotype 1 and 2. Prevention of HEV outbreak in the future is therefore required to reduce the burden of HEV disease. The HEV vaccine, which has been licensed in China, could be potentially used in the control of HEV infection in the future. However, its safety (especially in pregnant women) and efficacy during the outbreak require further investigation. Meanwhile, the preventive measures of HEV outbreak would mainly depend upon improved sanitation and hygiene.

Acknowledgements

The author thank to the Indonesia Endowment Fund for Education (LPDP) for funding PhD fellowship to Mohamad S. Hakim; The Dutch Digestive Foundation (MLDS) for a career development grant (No. CDG 1304), The Daniel den Hoed Foundation for a Centennial Award fellowship and the Erasmus MC Mrace grant to Q. Pan; and the China Scholarship Council for funding PhD fellowship to W. Wang (201303250056).

Supplementary information

http://onlinelibrary.wiley.com/doi/10.1111/liv.13237/abstract

Conflict of Interest

The authors do not have any disclosures to report.

References

1. Kamar N, Bendall R, Legrand-Abravanel F, *et al.* Hepatitis E. *Lancet* 2012; 379: 2477-88.
2. Purcell RH, Emerson SU. Hepatitis E: an emerging awareness of an old disease. *J Hepatol* 2008; 48: 494-503.
3. Teshale EH, Hu DJ. Hepatitis E: Epidemiology and prevention. *World J Hepatol* 2011; 3: 285-91.
4. Kim JH, Nelson KE, Panzner U, Kasture Y, Labrique AB, Wierzba TF. A systematic review of the epidemiology of hepatitis E virus in Africa. *BMC Infect Dis* 2014; 14: 308.
5. Rein DB, Stevens GA, Theaker J, Wittenborn JS, Wiersma ST. The global burden of hepatitis E virus genotypes 1 and 2 in 2005. *Hepatology* 2012; 55: 988-97.
6. Ahmad I, Holla RP, Jameel S. Molecular virology of hepatitis E virus. *Virus Res* 2011; 161: 47-58.
7. Reyes GR, Purdy MA, Kim JP, *et al.* Isolation of a cDNA from the virus responsible for enterically transmitted non-A, non-B hepatitis. *Science* 1990; 247: 1335-9.
8. Tam AW, Smith MM, Guerra ME, *et al.* Hepatitis E virus (HEV): Molecular cloning and sequencing of the full-length viral genome. *Virology* 1991; 185: 120-31.
9. Teo CG. Fatal outbreaks of jaundice in pregnancy and the epidemic history of hepatitis E. *Epidemiol Infect* 2012; 140: 767-87.
10. Wong DC, Purcell RH, Sreenivasan MA. Epidemic and endemic hepatitis in India: Evidence for a non-A, non-B hepatitis virus aetiology. *Lancet* 1980; 2: 876-9.
11. Belabbes EH, Bouguermouh A, Benatallah A, Illoul G. Epidemic non-A, non-B viral hepatitis in Algeria: Strong evidence for its spreading by water. *J Med Virol* 1985; 16: 257-63.
12. Khuroo MS. Study of an epidemic of non-A, non-B hepatitis. Possibility of another human hepatits virus distinct from post-transfusion non-A, non-B type. *Am J Med* 1980; 68: 818-24.
13. Arankalle VA, Chadha MS, Tsarev SA, *et al.* Seroepidemiology of water-borne hepatitis in India and evidence for a third enterically-transmitted hepatitis agent. *Proc Natl Acad Sci U S A* 1994; 91: 3428-32.
14. Viswanathan R. Infectious hepatitis in Delhi (1955-56): a critical study-epidemiology. 1957. *Natl Med J India* 2013; 26: 362-77.
15. Corwin A, Jarot K, Lubis I, *et al.* Two years' investigation of epidemic hepatitis E virus transmission in West Kalimantan (Borneo), Indonesia. *Trans R Soc Trop Med Hyg* 1995; 89: 262-5.
16. Jennings GB, Lubis I, Listiyaningsih E, Burans JP, Hyams KC. Hepatitis E virus in Indonesia. *Trans R Soc Trop Med Hyg* 1994; 88: 57.
17. Sedyaningsih-Mamahit ER, Larasati RP, Laras K, *et al.* First documented outbreak of hepatitis E virus transmission in Java, Indonesia. *Trans R Soc Trop Med Hyg* 2002; 96: 398-404.
18. Uchida T, Aye TT, Ma X, *et al.* An epidemic outbreak of hepatitis E in Yangon of Myanmar: Antibody assay and animal transmission of the virus. *Acta Pathol Jpn* 1993; 43: 94-8.
19. Corwin AL, Khiem HB, Clayson ET, *et al.* A waterborne outbreak of hepatitis E virus transmission in southwestern Vietnam. *Am J Trop Med Hyg* 1996; 54: 559-62.
20. Nakano Y, Yamauchi A, Yano T, *et al.* A diffuse outbreak of hepatitis E in Mie Prefecture, 2005. *Jpn J Infect Dis* 2006; 59: 136-8.
21. Aye TT, Uchida T, Ma XZ, *et al.* Complete nucleotide sequence of a hepatitis E virus isolated from the Xinjiang epidemic (1986-1988) of China. *Nucleic Acids Res* 1992; 20: 3512.
22. Gurley ES, Hossain MJ, Paul RC, *et al.* Outbreak of hepatitis E in urban Bangladesh resulting in maternal and perinatal mortality. *Clin Infect Dis* 2014; 59: 658-65.
23. Harun-Or-Rashid M, Akbar SMF, Takahashi K, *et al.* Epidemiological and molecular analyses of a non-seasonal outbreak of acute icteric hepatitis E in Bangladesh. *J Med Virol* 2013; 85: 1369-76.
24. Iqbal M, Ahmed A, Qamar A, *et al.* An outbreak of enterically transmitted non-A, non-B hepatitis in Pakistan. *Am J Trop Med Hyg* 1989; 40: 438-43.
25. Bryan JP, Tsarev SA, Iqbal M, *et al.* Epidemic hepatitis E in Pakistan: Patterns of serologic response and evidence that antibody to hepatitis E virus protects against disease. *J Infect Dis* 1994; 170: 517-21.
26. Bryan JP, Iqbal M, Tsarev S, *et al.* Epidemic of hepatitis E in a military unit in Abbottabad, Pakistan. *Am J Trop Med Hyg* 2002; 67: 662-8.
27. Rab MA, Bile MK, Mubarik MM, *et al.* Water-borne hepatitis E virus epidemic in Islamabad, Pakistan: A common source outbreak traced to the malfunction of a modern water treatment plant. *Am J Trop Med Hyg* 1997; 57: 151-7.
28. Siddiqui AR, Jooma RA, Smego Jr RA. Nosocomial outbreak of hepatitis E infection in Pakistan with possible parenteral transmission. *Clin Infect Dis* 2005; 40: 908-9.
29. Tsarev SA, Emerson SU, Reyes GR, *et al.* Characterization of a prototype strain of hepatitis E virus. *Proc Natl Acad Sci U S A* 1992; 89: 559-63.
30. Clayson ET, Vaughn DW, Innis BL, Shrestha MP, Pandey R, Malla DB. Association of hepatitis E virus with an outbreak of hepatitis at a military training camp in Nepal. *J Med Virol* 1998; 54: 178-82.
31. Al-Nasrawi KK, Al-Diwan JK, Al-Hadithi TS, Saleh AM. Viral hepatitis E outbreak in Al-Sadr city, Baghdad, Iraq. *East Mediterr Health J* 2010; 16: 1128-32.
32. Sharapov MB, Favorov MO, Yashina TL, *et al.* Acute viral hepatitis morbidity and mortality associated with hepatitis E virus infection: Uzbekistan surveillance data. *BMC Infect Dis* 2009; 9: 35.

33. Albetkova A, Drobeniuc J, Yashina T, *et al.* Characterization of hepatitis E virus from outbreak and sporadic cases in Turkmenistan. *J Med Virol* 2007; 79: 1696-702.
34. Chobe LP, Chadha MS, Banerjee K, Arankalle VA. Detection of HEV RNA in faeces, by RT-PCR during the epidemics of hepatitis E in India (1976-1995). *J Viral Hepat* 1997; 4: 129-33.
35. Sreenivasan MA, Banerjee K, Pandya PG, *et al.* Epidemiological investigations of an outbreak of infectious hepatitis in Ahmedabad city during 1975-76. *Indian J Med Res* 1978; 67: 197-206.
36. Skidmore SJ, Yarbough PO, Gabor KA, Reyes GR. Hepatitis E virus: The cause of a waterbourne hepatitis outbreak. *J Med Virol* 1992; 37: 58-60.
37. Sreenivasan MA, Sehgal A, Prasad SR, Dhorje S. A sero-epidemiologic study of a water-borne epidemic of viral hepatitis in Kolhapur City, India. *J Hyg* 1984; 93: 113-22.
38. Dilawari JB, Singh K, Chawla YK, *et al.* Hepatitis E virus: epidemiological, clinical and serological studies of north Indian epidemic. *Indian J Gastroenterol* 1994; 13: 44-8.
39. Jameel S, Durgapal H, Habibullah CM, Khuroo MS, Panda SK. Enteric non-A, non-B hepatitis: Epidemics, animal transmission, and hepatitis E virus detection by the polymerase chain reaction. *J Med Virol* 1992; 37: 263-70.
40. Arankalle VA, Chadha MS, Mehendale SM, Tungatkar SP. Epidemic hepatitis E: serological evidence for lack of intrafamilial spread. *Indian J Gastroenterol* 2000; 19: 24-8.
41. Risbud AR, Chadha MS, Kushwah SS, Arankalle VA, Rodrigues FM, Banerjee K. Non A non B hepatitis epidemic in Rewa district of Madhya Pradesh. *J Assoc Physicians India* 1992; 40: 262-4.
42. Ray R, Aggarwal R, Salunke PN, Mehrotra NN, Talwar GP, Naik SR. Hepatitis E virus genome in stools of hepatitis patients during large epidemic in north India. *Lancet* 1991; 338: 783-4.
43. Naik SR, Aggarwal R, Salunke PN, Mehrotra NN. A large waterborne viral hepatitis E epidemic in Kanpur, India. *Bull WHO* 1992; 70: 597-604.
44. Aggarwal R, Naik SR. Hepatitis E: Intrafamilial transmission versus waterborne spread. *J Hepatol* 1994; 21: 718-23.
45. Singh V, Singh V, Raje M, Nain CK, Singh K. Routes of transmission in the hepatitis E epidemic of Saharanpur. *Trop Gastroenterol* 1998; 19: 107-9.
46. Singh J, Aggarwal NR, Bhattacharjee J, *et al.* An outbreak of viral hepatitis E: role of community practices. *J Commun Dis* 1995; 27: 92-6.
47. Kar P, Gangwal P, Budhiraja S, *et al.* Analysis of serological evidence of different hepatitis viruses in acute viral hepatitis in prisoners in relation to risk factors. *Indian J Med Res* 2000; 112: 128-32.
48. Aggarwal R, Kumar R, Pal R, Naik S, Semwal SN, Naik SR. Role of travel as a risk factor for hepatitis E virus infection in a disease-endemic area. *Indian J Gastroenterol* 2002; 21: 14-8.
49. Banerjee A, Sahni AK, Rajiva, Nagendra A, Saiprasad GS. Outbreak of viral hepatitis E in a regimental training centre. *Med J Armed Forces India* 2005; 61: 326-9.
50. Kumar S, Ratho RK, Chawla YK, Chakraborti A. Virological investigation of a hepatitis E epidemic in North India. *Singapore Med J* 2006; 47: 769-73.
51. Singh PMP, Handa BSK, Banerjee A. Epidemiological investigation of an outbreak of viral hepatitis. *Med J Armed Forces India* 2006; 62: 332-4.
52. Swain SK, Baral P, Hutin YJ, Rao TV, Murhekar M, Gupte MD. A hepatitis E outbreak caused by a temporary interruption in a municipal water treatment system, Baripada, Orissa, India, 2004. *Trans R Soc Trop Med Hyg* 2010; 104: 66-9.
53. Das P, Adhikary KK, Gupta PK. An outbreak investigation of viral hepatitis E in south Dumdum Municipality of Kolkata. *Indian J Community Med* 2007; 32: 84-5.
54. Sailaja B, Murhekar MV, Hutin YJ, *et al.* Outbreak of waterborne hepatitis E in Hyderabad, India, 2005. *Epidemiol Infect* 2009; 137: 234-40.
55. Sarguna P, Rao A, Sudha Ramana K. Outbreak of acute viral hepatitis due to hepatitis E virus in Hyderabad. *Indian J Med Microbiol* 2007; 25: 378-82.
56. Martolia HCS, Hutin Y, Ramachandran V, Manickam P, Murhekar M, Gupte M. An outbreak of hepatitis E tracked to a spring in the foothills of the Himalayas, India, 2005. *Indian J Gastroenterol* 2009; 28: 99-101.
57. Bali S, Kar SS, Kumar S, Ratho RK, Dhiman RK, Kumar R. Hepatitis E epidemic with bimodal peak in a town of north India. *Indian J Public Health* 2008; 52: 189-93.
58. Rai RR, Nijhawan S, Mathur A, Sharma MP, Udawat HP, Singh N. Seroepidemiology and role of polymerase chain reaction to detect viremia in an epidemic of hepatitis E in Western India. *Trop Gastroenterol* 2008; 29: 202-6.
59. Shankar P, Subrat K, Reddy GMM, Ratho RK, Rajesh K. Investigation of viral hepatitis E outbreak in a town in Haryana. *J Commun Dis* 2008; 40: 249-54.
60. Khuroo MS, Khuroo MS. Seroepidemiology of a second epidemic of hepatitis E in a population that had recorded first epidemic 30 years before and has been under surveillance since then. *Hepatol Int* 2010; 4: 494-9.
61. Chauhan NT, Prajapati P, Trivedi AV, Bhagyalaxmi A. Epidemic investigation of the jaundice outbreak in Girdharnagar, Ahmedabad, Gujarat, India, 2008. *Indian J Community Med* 2010; 35: 294-7.
62. Vivek R, Nihal L, Illiayaraja J, *et al.* Investigation of an epidemic of Hepatitis E in Nellore in south India. *Trop Med Int Health* 2010; 15: 1333-9.
63. Majumdar M, Singh MP, Pujhari SK, Bhatia D, Chawla Y, Ratho RK. Hepatitis E virus antigen detection as an early diagnostic marker: Report from India. *J Med Virol* 2013; 85: 823-7.

64. Tambe MP, Patil SP, Dravid M, Bhagwat VR. Investigation of an outbreak of hepatitis'E' in a rural area of Dhule district in Maharashtra. *J Krishna Ins Med Sciences Univ* 2015; 4: 109-14.
65. Awsathi S, Rawat V, Rawat CM, Semwal V, Bartwal SJ. Epidemiological investigation of the jaundice outbreak in Lalkuan, Nainital district, Uttarakhand. *Indian J Community Med* 2014; 39: 94-7.
66. Shata MT, Daef EA, Zaki ME, *et al.* Protective role of humoral immune responses during an outbreak of hepatitis E in Egypt. *Trans R Soc Trop Med Hyg* 2012; 106: 613-8.
67. Mast EE, Polish LB, Favorov MO, *et al.* Hepatitis E among refugees in Kenya: Minimal apparent person-to-person transmission, evidence for age-dependent disease expression, and new serologic assays. In *Viral Hepatitis and Liver Disease.* Edited by Nishioka K, Suzuki H, Mishiro S, Oda T. Japan: Springer; 1994: 375-8.
68. Ahmed JA, Moturi E, Spiegel P, *et al.* Hepatitis E outbreak, Dadaab refugee camp, Kenya, 2012. *Emerg Infect Dis* 2013; 19: 1010-2.
69. McCarthy MC, He J, Hyams KC, El-Tigani A, Khalid IO, Carl M. Acute hepatitis E infection during the 1988 floods in Khartoum, Sudan. *Trans R Soc Trop Med Hyg* 1994; 88: 177.
70. Guthmann JP, Klovstad H, Boccia D, *et al.* A large outbreak of hepatitis E among a displaced population in Darfur, Sudan, 2004: The role of water treatment methods. *Clin Infect Dis* 2006; 42: 1685-91.
71. Boccia D, Guthmann JP, Klovstad H, *et al.* High mortality associated with an outbreak of hepatitis E among displaced persons in Darfur, Sudan. *Clin Infect Dis* 2006; 42: 1679-84.
72. Anonim. Hepatitis E, Sudan--update. *Wkly Epidemiol Rec* 2004; 79: 341-2.
73. Anonim. Hepatitis E: Chad, Sudan. *Wkly Epidemiol Rec* 2004; 79: 321.
74. Rayis DA, Jumaa AM, Gasim GI, Karsany MS, Adam I. An outbreak of hepatitis E and high maternal mortality at Port Sudan, Eastern Sudan. *Pathog Global Health* 2013; 107: 66-8.
75. Thomson K, Luis Dvorzak J, Lagu J, *et al.* Investigation of hepatitis E outbreak among refugees - Upper Nile, South Sudan, 2012-2013. *Morb Mortal Wkly Rep* 2013; 62: 581-6.
76. Nicand E, Armstrong GL, Enouf V, *et al.* Genetic heterogeneity of hepatitis E virus in Darfur, Sudan, and neighboring Chad. *J Med Virol* 2005; 77: 519-21.
77. Escriba JM, Nakoune E, Recio C, *et al.* Hepatitis E, Central African Republic. *Emerg Infect Dis* 2008; 14: 681-3.
78. Goumba CM, Yandoko-Nakoune ER, Komas NP. A fatal case of acute hepatitis E among pregnant women, Central African Republic. *BMC Res Notes* 2010; 3: 103.
79. Goumba AI, Konamna X, Komas NP. Clinical and epidemiological aspects of a hepatitis E outbreak in Bangui, Central African Republic. *BMC Infect Dis* 2011; 11: 93.
80. Teshale EH, Howard CM, Grytdal SP, *et al.* Hepatitis E epidemic, Uganda. *Emerg Infect Dis* 2010; 16: 126-9.
81. Teshale EH, Grytdal SP, Howard C, *et al.* Evidence of person-to-person transmission of hepatitis E virus during a large outbreak in northern Uganda. *Clin Infect Dis* 2010; 50: 1006-10.
82. Howard CM, Handzel T, Hill VR, *et al.* Novel risk factors associated with hepatitis E virus infection in a large outbreak in Northern Uganda: Results from a case-control study and environmental analysis. *Am J Trop Med Hyg* 2010; 83: 1170-3.
83. Cummings MJ, Wamala JF, Komakech I, *et al.* Hepatitis E in Karamoja, Uganda, 2009-2012: epidemiology and challenges to control in a setting of semi-nomadic pastoralism. *Trans R Soc Trop Med Hyg* 2014; 108: 648-55.
84. Gerbi GB, Williams R, Bakamutumaho B, *et al.* Hepatitis E as a cause of acute jaundice syndrome in northern Uganda, 2010-2012. *Am J Trop Med Hyg* 2015; 92: 411-4.
85. Coursaget P, Krawczynski K, Buisson Y, Nizou C, Molinie C. Hepatitis E and hepatitis C virus infections among French soldiers with non-A,non-B hepatitis. *J Med Virol* 1993; 39: 163-6.
86. Van Cuyck-Gandre H, Caudill JD, Zhang HY, *et al.* Short report: Polymerase chain reaction detection of hepatitis E virus in north African fecal samples. *Am J Trop Med Hyg* 1996; 54: 134-5.
87. Anonim. Hepatitis E, Chad. *Wkly Epidemiol Rec* 2004; 79: 313.
88. Anonim. Outbreak news. *Wkly Epidemiol Rec* 2004; 79: 329-31.
89. Van Cuyck-Gandre H, Zhang HY, Tsarev SA, *et al.* Characterization of hepatitis E virus (HEV) from Algeria and Chad by partial genome sequence. *J Med Virol* 1997; 53: 340-7.
90. Coursaget P, Buisson Y, Enogat N, *et al.* Outbreak of enterically-transmitted hepatitis due to hepatitis A and hepatitis E viruses. *J Hepatol* 1998; 28: 745-50.
91. Grandadam M, Tebbal S, Caron M, *et al.* Evidence for hepatitis E virus quasispecies. *J Gen Virol* 2004; 85: 3189-94.
92. Isaacson M, Frean J, He J, Seriwatana J, Innis BL. An outbreak of hepatitis E in Northern Namibia, 1983. *Am J Trop Med Hyg* 2000; 62: 619-25.
93. Maila HT, Bowyer SM, Swanepoel R. Identification of a new strain of hepatitis E virus from an outbreak in Namibia in 1995. *J Gen Virol* 2004; 85: 89-95.
94. Benjelloun S, Bahbouhi B, Bouchrit N, *et al.* Seroepidemiological study of an acute hepatitis E outbreak in Morocco. *Res Virol* 1997; 148: 279-87.
95. Meng J, Cong M, Dai X, *et al.* Primary structure of open reading frame 2 and 3 of the hepatitis E virus isolated from Morocco. *J Med Virol* 1999; 57: 126-33.
96. Bile K, Isse A, Mohamud O, *et al.* Contrasting roles of rivers and wells as sources of drinking water on attack and fatality rates in a hepatitis E epidemic in Somalia. *Am J Trop Med Hyg* 1994; 51: 466-74.
97. Mushahwar IK, Dawson GJ, Bile KM, Magnius LO. Serological studies of an enterically transmitted non-A, non-B hepatitis in Somalia. *J Med Virol* 1993; 40: 218-21.

98. Tsega E, Krawczynski K, Hansson BG, *et al.* Outbreak of acute hepatitis E virus infection among military personnel in northern Ethiopia. *J Med Virol* 1991; 34: 232-6.
99. Robson SC, Adams S, Brink N, Woodruff B, Bradley D. Hospital outbreak of hepatitis E. *Lancet* 1992; 339: 1424-5.
100. Maurice D, Abassora M, Marcelin NM, Richard N. First documented outbreak of hepatitis E in Northern Cameroon. *Ann Trop Med Public Health* 2013; 6: 682-3.
101. Said B, Ijaz S, Kafatos G, *et al.* Hepatitis E outbreak on cruise ship. *Emerg Infect Dis* 2009; 15: 1738-44.
102. Garbuglia AR, Scognamiglio P, Petrosillo N, *et al.* Hepatitis E virus genotype 4 outbreak, Italy, 2011. *Emerg Infect Dis* 2013; 19: 110-4.
103. Anonim. Enterically transmitted non-A, non-B hepatitis--Mexico. *MMWR Morb Mortal Wkly Rep* 1987; 36: 597-602.
104. Velazquez O, Stetler HC, Avila C, *et al.* Epidemic transmission of enterically transmitted non-A, non-B hepatitis in Mexico, 1986-1987. *J Am Med Assoc* 1990; 263: 3281-5.
105. Favorov MO, Fields HA, Purdy MA, *et al.* Serologic identification of hepatitis E virus infections in epidemic and endemic settings. *J Med Virol* 1992; 36: 246-50.
106. Villalba MDLCM, Lay LDLAR, Chandra V, *et al.* Hepatitis E virus genotype 1, Cuba. *Emerg Infect Dis* 2008; 14: 1320-2.
107. Nishiura H. Household data from the Ugandan hepatitis E virus outbreak indicate the dominance of community infection. *Clin Infect Dis* 2010; 51: 117-8.
108. Aggarwal R. Hepatitis E virus and person-to-person transmission. *Clin Infect Dis* 2010; 51: 477-8; author reply 8-9.
109. Arankalle VA, Paranjape S, Emerson SU, Purcell RH, Walimbe AM. Phylogenetic analysis of hepatitis E virus isolates from India (1976-1993). *J Gen Virol* 1999; 80: 1691-700.
110. Huang CC, Nguyen D, Fernandez J, *et al.* Molecular cloning and sequencing of the Mexico isolate of hepatitis E virus (HEV). *Virology* 1992; 191: 550-8.
111. Aggarwal R. Hepatitis E: Historical, contemporary and future perspectives. *J Gastroenterol Hepatol* 2011; 26 Suppl 1: 72-82.
112. Lay LDLAR, Quintana A, Villalba MCM, *et al.* Dual infection with hepatitis A and E viruses in outbreaks and in sporadic clinical cases: Cuba 1998-2003. *J Med Virol* 2008; 80: 798-802.
113. Favorov MO, Khudyakov YE, Mast EE, *et al.* IgM and IgG antibodies to hepatitis E virus (HEV) detected by an enzyme immunoassay based on an HEV-specific artificial recombinant mosaic protein. *J Med Virol* 1996; 50: 50-8.
114. Lu L, Drobeniuc J, Kobylnikov N, *et al.* Complete sequence of a Kyrgyzstan swine Hepatitis E Virus (HEV) isolated from a piglet thought to be experimentally infected with human HEV. *J Med Virol* 2004; 74: 556-62.
115. Labrique AB, Thomas DL, Stoszek SK, Nelson KE. Hepatitis E: an emerging infectious disease. *Epidemiol Rev* 1999; 21: 162-79.
116. Khuroo MS. Hepatitis E: the enterically transmitted non-A, non-B hepatitis. *Indian J Gastroenterol* 1991; 10: 96-100.
117. Aggarwal R. Hepatitis E: Epidemiology and natural History. *J Clin Exp Hepatol* 2013; 3: 125-33.
118. Langlois EV, Haines A, Tomson G, Ghaffar A. Refugees: towards better access to health-care services. *Lancet* 2016; 387: 319-21.
119. Toole MJ, Waldman RJ. The public health aspects of complex emergencies and refugee situations. *Annu Rev Public Health* 1997; 18: 283-312.
120. Shultz A, Omollo JO, Burke H, *et al.* Cholera outbreak in Kenyan refugee camp: risk factors for illness and importance of sanitation. *Am J Trop Med Hyg* 2009; 80: 640-5.
121. Kaic B, Borcic B, Ljubicic M, Brkic I, Mihaljevic I. Hepatitis A control in a refugee camp by active immunization. *Vaccine* 2001; 19: 3615-9.
122. Nimri LF, Hijazi S. Rotavirus-associated diarrhoea in children in a refugee camp in Jordan. *J Diarrhoeal Dis Res* 1996; 14: 1-4.
123. Mahamud AS, Ahmed JA, Nyoka R, *et al.* Epidemic cholera in Kakuma Refugee Camp, Kenya, 2009: the importance of sanitation and soap. *J Infect Dev Ctries* 2012; 6: 234-41.
124. Uddin Khan S, Atanasova KR, Krueger WS, Ramirez A, Gray GC. Epidemiology, geographical distribution, and economic consequences of swine zoonoses: a narrative review. *Emerg Microbes Infect* 2013; 2: e92.
125. Lewis HC, Wichmann O, Duizer E. Transmission routes and risk factors for autochthonous hepatitis E virus infection in Europe: a systematic review. *Epidemiol Infect* 2010; 138: 145-66.
126. Zhang L, Yan B, Xu A. A hepatitis E outbreak by genotype 4 virus in Shandong province, China. *Vaccine* 2016; 34: 3715-8.
127. Khuroo MS, Teli MR, Skidmore S, Sofi MA, Khuroo MI. Incidence and severity of viral hepatitis in pregnancy. *Am J Med* 1981; 70: 252-5.
128. Patra S, Kumar A, Trivedi SS, Puri M, Sarin SK. Maternal and fetal outcomes in pregnant women with acute hepatitis E virus infection. *Ann Intern Med* 2007; 147: 28-33.
129. Labrique AB, Sikder SS, Krain LJ, *et al.* Hepatitis E, a vaccine-preventable cause of maternal deaths. *Emerg Infect Dis* 2012; 18: 1401-4.
130. Sehgal R, Patra S, David P, *et al.* Impaired monocyte-macrophage functions and defective toll-like receptor signaling in hepatitis E virus-infected pregnant women with acute liver failure. *Hepatology* 2015; 62: 1683-96.
131. Pal R, Aggarwal R, Naik SR, Das V, Das S, Naik S. Immunological alterations in pregnant women with acute hepatitis E. *J Gastroenterol Hepatol* 2005; 20: 1094-101.
132. Navaneethan U, Al Mohajer M, Shata MT. Hepatitis E and pregnancy: Understanding the pathogenesis. *Liver Int* 2008; 28: 1190-9.

133. Rakesh P, Sherin D, Sankar H, Shaji M, Subhagan S, Salila S. Investigating a community-wide outbreak of hepatitis A in India. *J Glob Infect Dis* 2014; 6: 59-64.
134. Saha T, Murhekar M, Hutin YJ, Ramamurthy T. An urban, water-borne outbreak of diarrhoea and shigellosis in a district town in eastern India. *Natl Med J India* 2009; 22: 237-9.
135. Bhunia R, Ramakrishnan R, Hutin Y, Gupte MD. Cholera outbreak secondary to contaminated pipe water in an urban area, West Bengal, India, 2006. *Indian J Gastroenterol* 2009; 28: 62-4.
136. Panda M, Hutin YJ, Ramachandran V, Murhekar M. A fatal waterborne outbreak of pesticide poisoning caused by damaged pipelines, Sindhikela, Bolangir, Orissa, India, 2008. *J Toxicol* 2009; 2009: 692496.
137. Zhu FC, Zhang J, Zhang XF, *et al.* Efficacy and safety of a recombinant hepatitis E vaccine in healthy adults: a large-scale, randomised, double-blind placebo-controlled, phase 3 trial. *Lancet* 2010; 376: 895-902.
138. Cousins S. Experts disagree over necessity of hepatitis E vaccine in Nepal. *BMJ* 2015; 350: h3393.
139. Basnyat B, Dalton HR, Kamar N, *et al.* Nepali earthquakes and the risk of an epidemic of hepatitis E. *Lancet* 2015; 385: 2572-3.
140. Shrestha A, Lama TK, Gupta BP, *et al.* Hepatitis E virus outbreak in postearthquake Nepal: is a vaccine really needed? *J Viral Hepat* 2016.

Part I.

Interferon-stimulated genes (ISGs)-based strategies

Chapter 3

Transcriptional Regulation of Antiviral Interferon-stimulated Genes

Wenshi Wang[1], Lei Xu[1], Junhong Su[2], Maikel P. Peppelenbosch[1] and Qiuwei Pan[1]

[1]Department of Gastroenterology and Hepatology, Erasmus MC-University Medical Center and Postgraduate School Molecular Medicine, Rotterdam, the Netherlands

[2]Medical Faculty, Kunming University of Science and Technology, Kunming, PR China

Trends in Microbiology, 2017, 25(7):573-584

Abstract

Interferon-stimulated genes (ISGs) are a group of gene products that coordinately combat pathogen invasions, in particular viral infections. Transcription of ISGs rapidly occurs upon pathogen invasion, and this is classically provoked via activation of the Janus kinase/signal transducer and activator of transcription (JAK-STAT) pathway, mainly by interferons (IFNs). However, plethoras of recent studies have reported a variety of non-canonical mechanisms regulating ISG transcription. These new studies are extremely important for understanding the quantitative and temporal differences in ISG transcription under specific circumstances. Because these canonical and non-canonical regulatory mechanisms are essential for defining the nature of host defense and associated detrimental pro-inflammatory effects, we comprehensively review the state of this rapidly evolving field and the clinical implications of recently acquired knowledge in this respect.

Outstanding Questions

- Although signaling through the same receptor, there are many type I IFNs in the genome. How the cells dynamically control the production of the particular members of these type I IFNs?
- Upon IFNλ binding, which types of modification (*e.g.* phosphorylation, acetylation) happened to IFNλRs to kick off ISG transcription?
- Generally, HAT activity transforms chromatin into a more relaxed structure, while HDAC activity organizes chromatin into higher order nucleosomes. Counterintuitively, HDAC activity has been reported to be required for ISG transcription. How this mechanistically works?
- How exactly the nucleotide synthesis pathways mediate ISG transcription?
- Will ISG-based antiviral strategy circumvent the issue of side effects caused by IFN treatment, but retain the therapeutic potency in patients?

Trends Box

- Transcriptional regulation of interferon-stimulated genes (ISGs) defines the state of host anti-pathogen defense.
- In light of the recently identified regulatory elements and mechanisms of the IFN-JAK-STAT pathway, new insights have been gained into this classical cascade in regulating ISG transcription.
- A variety of non-canonical mechanisms have been recently revealed that coordinately regulate ISG transcription.
- With regards to the adverse effects of IFNs in clinic, ISG-based antiviral strategy could be the next promising frontier in drug discovery.

Host antiviral defense

IFN-mediated innate immune response forms a forward line of cell-autonomous defense against pathogens. Virus invasion (*e.g.* the presence of single-stranded RNA in endosomes or cytosolic double-stranded RNA) triggers the host cells to recognize the infection through pattern recognition receptors, that in turn mediates production of IFNs [1]. The thus-released IFN molecules bind to cell surface receptors and initiate signal transduction prominently involving the Janus kinase signal transducer and activator of transcription (JAK-STAT) pathway. This activates the transcription of hundreds of so-called IFN-stimulated genes (ISGs) that are the effectors of cell-autonomous antiviral defense. The representative well-studied ISG members in this respect with specific or broad antiviral activities include RIG-I, MDA5, MX2, IRF1, IRF3, IRF7, IRF9, IFITM3, ISG15 and OASL [2]. ISGs act at different stages of the viral life cycle, from entry, replication, assembly to release. This leads to a remarkable antiviral state that provides adequate cellular immunity against positive-, negative-, and double-stranded RNA viruses, DNA viruses, and even intracellular bacteria and parasites.

Although the JAK-STAT pathway plays key roles in regulating ISG transcription, a far more complex cell signaling network with both canonical and non-canonical mechanisms is involved [3]. The signaling strength, kinetics and specificity of regulatory pathways on ISG transcription are modulated at various levels by distinct mechanisms in conjunction. Understanding the different mechanisms of ISG transcription and how their mode-of-action relates to clinically used antiviral medications will reveal new insights of virus-host interactions and provide novel avenues for antiviral drug development. Therefore, we aim to comprehensively review the classical and non-classical mechanisms in regulating ISG transcription and to emphasize their clinical implications.

Classical mechanisms of regulating ISG transcription: the IFN-JAK-STAT pathway

Upon IFN binding to its cognate cell surface receptors, a signal is transmitted through the membrane into the cell via the JAK-STAT pathway, leading to rapid transcriptional activation of ISGs [4]. Decades of dedicated efforts have elucidated this classical regulatory network, as we have outlined here (Figure 1).

IFNs and their receptors-dependent regulation

Genes encoding IFNs and their receptors have been duplicated extensively throughout vertebrate evolution, indicating substantial evolutionary pressure on this system in combating pathogens [5]. Up to now, more than twenty distinct IFN genes/proteins have been identified. Based on the type of receptor through which they signal, the multitude of different IFNs in mammalian genome are classified into three major types: Type I, II and III. In humans, type I IFNs include IFN-α (which can be further subdivided into 13 different subtypes), IFN-β, IFN-δ, IFN-ε, IFN-κ, IFN-ζ and IFN-ω1-3. All type I IFNs bind to a common cell-surface receptor, the type I IFN heterodimeric receptor complexes comprising two subunits: IFN-α receptor 1 (IFNAR1) and IFN-α receptor 2 (IFNAR2). Unlike type I IFNs, there is only one type II IFN, IFN-γ. It has no marked structural homology with type I IFNs. IFN-γ binds to a different cell surface receptor comprised of two subunits: IFNGR1 and IFNGR2.

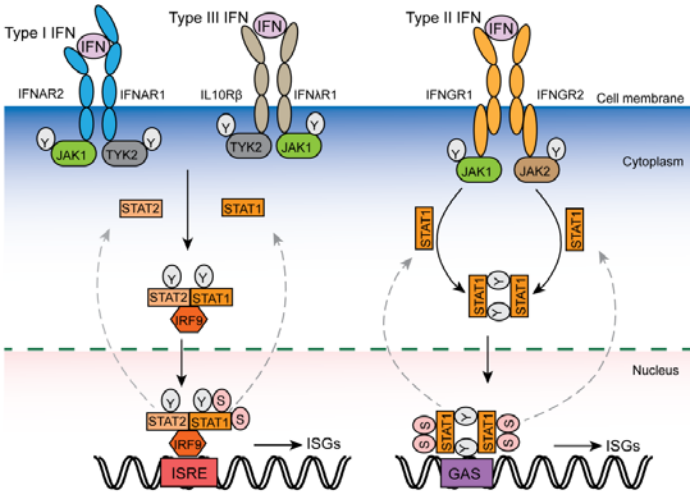

Figure 1. The classical IFN signaling pathways in regulating ISG transcription. The three different classes of IFNs signal through their corresponding receptor complexes, leading to the phosphorylation of preassociated Janus kinases. For type I and III IFNs, the phosphorylated Janus kinase 1 (JAK1) and tyrosine kinase 2 (TYK2) in turn phosphorylate the receptors at specific intracellular tyrosine residues. This leads to the recruitment and phosphorylation of signal transducers and activators of transcription 1 and 2 (STAT1 and STAT2) at specific tyrosine residues. Then, STAT1 and 2 recruits IRF9 to form the IFN-stimulated gene factor 3 (ISGF3). For type II IFNs, the phosphorylated JAK1 and JAK2 tyrosine kinases phosphorylate the receptor chains, leading to tyrosine phosphorylation and homodimerization of STAT1. Both ISGF3 and STAT1 homodimer translocate to the nucleus to get further phosphorylation at specific serine residues of STAT1, achieving fully activation. Consequently, IFN-stimulated genes (ISGs) are transcriptionally activated upon the binding of ISGF3 and STAT1 homodimer to IFN-stimulated response elements (ISRE) and gamma-activated sequence (GAS) promoter elements, respectively. Conversely, the specific phosphatases in the nucleus dephosphorylate STAT1 and STAT2 to avoid excessive and detrimental responses.

Type III IFN family is composed of four genes: IFNλ1 (IL29), IFNλ2 (IL28A), IFNλ3 (IL28B) and IFNλ4 (frameshift variant of IL28B). They signal through the IFNλ receptor (IFNλR) which is composed of two subunits: IFNλR1 (IL28Rα) and IL10Rβ.

Type II IFN signaling leads to STAT1 phosphorylation, followed by homodimerization, nuclear translocation, and DNA binding at gamma-activated sequence (GAS) elements located within promoter regions of IFN-γ-induced genes. While both type I and III IFN signaling activate similar intracellular JAK-STAT pathway forming the transcription complex, ISGF3, to transcribe ISGs, although they utilize distinct receptor complexes for signaling [6]. However, IFNAR is ubiquitously expressed in all nucleated cells; whereas IFNλR1 is only expressed on specific tissues/cells of epithelial origin [7], suggesting a selectivity of type III IFNs compared with type I IFNs.

For optimal activation, signaling through the IFN receptor complex depends on tyrosine phosphorylation, serine phosphorylation and acetylation on IFN receptors (Table 1) [8-10]. Nevertheless, negative regulation is also essential for balancing its beneficial antiviral versus detrimental pro-inflammatory effects. Primarily, this is achieved by (i) phosphorylation induced IFN receptor ubiquitination and degradation [11]; (ii) blocking the interaction between IFNAR and downstream signaling elements, such as the function of USP18, ISG15 and SOCS1 [12-16]; (iii) receptor-mediated ligand internalization/degradation [17]; and (iv) modulating cell surface IFN receptor level [18, 19].

JAK kinases (JAKs)-dependent regulation

The JAKs comprises 4 members, three of them (JAK1, JAK2 and TYK2) function in IFN signaling and are ubiquitously expressed [20]. They are pre-associated with the corresponding IFN receptor. Upon IFN binding to receptor, they become activated through close proximity trans-phosphorylation (JAK1: $Tyr^{1022,1023}$, JAK2: $Tyr^{1007,1008}$ and TYK2: $Tyr^{1054,1055}$). Subsequently, activated JAKs phosphorylate the cytoplasmic regions of the receptor, generating docking sites for SH2-domain containing proteins, in particular STAT1 and STAT2 [21]. Activation of JAK enzymatic activity also triggers negative feedback on antiviral immunity. Phosphatases, including T cell protein tyrosine phosphatase (TCPTP), protein tyrosine phosphatases (PTP) 1B and CD45, are the most important negative regulators [22-25]. The SOCS-1 protein also negatively regulates this process through phosphorylation mediated proteasomal degradation of JAK [26]. The critical function of JAKs in cell signaling has made them ideal targets for controlling a range of autoimmune diseases. Several JAK inhibitors have been approved by the FDA or are in clinical trials for the treatment of rheumatoid arthritis, psoriasis, inflammatory bowel disease and ankylosing spondylitis [27].

Table 1. Classical modification of the IFN-JAK-STAT pathway

	Modification site	Modification type[a]	Signal transduction	References
IFNAR1	Tyr^{466}	Phosphorylation	Activation	[28]
IFNAR1	Tyr^{512} and Tyr^{337}	Phosphorylation	Activation	[29]
IFNAR1	Ser^{535}, Ser^{539}	Phosphorylation	Inactivation	[11]
IFNAR1	Lys^{501}, Lys^{525} and Lys^{526}	Ubiquitination	Inactivation	[11]
IFNAR2	Ser^{364}, Ser^{384}	Phosphorylation	Activation	[9]
IFNAR2	Lys^{399}	Acetylation	Activation	[9]
IFNGR1	Pro^{267}	ND	Activation	[30]
IFNGR1	Tyr^{440}	Phosphorylation	Activation	[31]
IFNGR1	$^{270}LI^{271}$	ND	Inactivation	[17]
IFNGR1	Tyr^{441}	Phosphorylation	Inactivation	[16, 31]
IFNGR2	$^{263}PPSIP^{267}$ and $^{270}IEEYL^{274}$	ND	Activation	[10]
JAK1	$Tyr^{1022,1023}$	Phosphorylation	Activation	[21]
JAK2	$Tyr^{1007,1008}$	Phosphorylation	Activation	[21]
TYK2	$Tyr^{1054,1055}$	Phosphorylation	Activation	[21]
STAT1	Tyr^{701}	Phosphorylation	Activation	[32]
STAT1	Ser^{727}	Phosphorylation	Activation	[32]
STAT1	Ser^{708}	Phosphorylation	Activation	[33]
STAT1	Lys^{703}	SUMO-1 Binding	Inactivation	[34]
STAT2	Tys^{690}	Phosphorylation	Activation	[35]
STAT2	Ser^{287}	Phosphorylation	Inactivation	[35]

[a]ND, not determined.

STAT-dependent regulation

There are seven STAT members in mammals, STAT1, STAT2, STAT3, STAT4, STAT5a, STAT5b and STAT6. STAT1 and STAT2 are the most important STATs with respect to IFN signaling [2]. In response to IFNs, STAT1 is phosphorylated on Tyr^{701}, Ser^{708} and Ser^{727}. These sites are all positively related to

signaling transduction [33, 36]. STAT2 acquires transcriptional activation upon tyrosine phosphorylation (Tyr^{690}). Conversely, serine phosphorylation (Ser^{287}) in STAT2 negatively regulates IFN response [21, 35]. Although JAKs play key role in STAT1 phosphorylation and activation, nevertheless, other cellular factors are also required. Tyrosine kinase non-receptor 1 (TNK1) and retinoic acid-inducible gene I (RIG-I) potentiate dual phosphorylation of STAT1 at Tyr^{701} and Ser^{727} positions [37-39]; Nuclear cyclin-dependent kinase 8 (CDK8) phosphorylates Ser^{727} of STAT1 [40, 41]. Protein kinase C family members, PKC-δ or PKC-ε mediates phosphorylation of STAT1 on Ser^{727} (no effect on STAT1 tyrosine phosphorylation) via its upstream phosphatidylinositol 3-kinase (PI3K)-AKT pathway [42-45]. Interestingly, stress signals can also induce phosphorylation of STAT1 (Ser^{727}) via the p38-MAPK pathway [46]. As p38-MAP kinase inhibitors are well tolerated and safe for humans, it is thus tempting to speculate that such inhibitors may be used to mitigate pro-inflammatory effects following IFN-γ-therapy [47].

Evidently, phosphatase-dependent STAT1 dephosphorylation constitutes an important negative-regulatory event that is central in titrating the IFN response. The functional phosphatases include SHP-2 [48, 49], the nuclear isoform of TCPTP, TC45 [50] and SHPTP1 [51]. Phosphatase dysregulation has been reported in cancers and autoimmune disorders, thus representing potential therapeutic targets [52]. A small ubiquitin-related modifier 1 (SUMO-1) was also reported to conjugate at Lys^{703} of STAT1 to inhibit signaling transduction [34]. Thus, a plethora of molecular mechanisms can balance the IFN response through acting on STAT1.

IRF9 is a main DNA binding component of the ISGF3 complex. IRF9 alone binds to DNA and recognizes the specific promotor elements denoted as interferon-stimulated response elements (ISRE), but has no transcriptional activity. Upon its DNA binding, IRF9 provides specific protein-DNA interaction sites for STAT1 and STAT2. Activated STAT1 and STAT2 bind to the ISRE region together with IRF9 to exert strong pro-transcriptional activity [53]. Theoretically, IRF9 (as part of the ISGF3 complex) only involves in type I and III IFN signaling to regulate ISG transcription. However, IFNγ induced ISG activation and antiviral state were severely impaired in the absence of IRF9, indicating that IRF9 may also be involved in type II IFN signaling [54, 55]. More interestingly, IFNγ pretreatment induces high levels of IRF9, which serves as an important subunit of latent precursor to ISGF3. In this way, IFN-α and IFN-γ synergize to induce the formation of ISGF3 complex, leading to much stronger ISG transcription [56].

Regulation of ISGs at the transcriptional level

In the case of type I and III IFNs, ISGF3 works as the predominant transcriptional factor binding to ISREs within the promoter region of ISGs; whereas for type II IFN, the homodimers or heterodimers of STATs are the determinant binding to GAS elements. However, this is a simplified model and other regulatory elements are also involved (Figure 2).

Chromatin modulators. Histone octamers bind to DNA and organize chromatin into higher order nucleosomes, prohibiting transcription factor binding and gene expression [57]. As a consequence, the induction of ISGs by IFNs requires chromatin remodeling. The condensed chromatin needs to be transformed into a more relaxed structure. In humans, the nucleosome remodeling complex BAF and PBAF prime ISG promoters by utilizing ATP-derived energy to maintain chromatin in a constitutively open conformation, allowing fast and potent induction of ISGs after IFN exposure [58-61]. Histone acetylation and deacetylation are also essential in chromatin modulation.

These reactions are typically catalyzed by enzymes with histone acetyltransferase (HAT) or histone deacetylase (HDAC) activity. HAT activity transforms chromatin into a more relaxed structure, while HDAC activity organizes chromatin into higher order nucleosomes. Therefore, the HAT family members, including p300/CBP and GCN5, are essential for transcriptional activation of ISGs [62, 63]. HATs are positive regulators of transcription in general. However, HDAC activity is also essential for transcriptional induction of ISGs [64-69]. HDAC activity has been reported to be required for recruiting RNA polymerase II to the promoters of ISGs [70], although how HDACs regulate transcriptional activation of ISG remains unclear. In addition, FOXO3 and PI3K/AKT pathway coordinate in chromatin modulation. FOXO3 together with the nuclear co-repressor 2 (NCOR2) and HDAC3 forms a ternary complex to facilitate a closed chromatin structure to limit ISG transcription under basal conditions. However, type I IFN can activate the PI3K/AKT pathway, which in turn leads to FOXO3 degradation and ISG transcription [71].

Co-activators and co-repressors. Particular co-activators or co-repressors mediate the transcription of ISGs via the interaction with ISGF3 or STAT1 homodimers. The co-activators, such as MCM5 (minichromosome maintenance) and MCM3 protein complex [72, 73], N-Myc interactor (NMi) [74] and DRIP150 [75], facilitate the transcriptional activation of ISGs. Conversely, co-repressors, such as TAF-1 [76] and the protein inhibitor of activated STAT proteins (PIAS1 and PIASγ [77, 78], negatively suppress the formation of transcription complex on the ISG promoter to limit transcription. Recently, four previously unrecognized regulatory factors (ETV6, ATF3, LYN and TBK1) of ISG transcription have been identified [79]. These efforts have led to a more comprehensive understanding of ISG transcription.

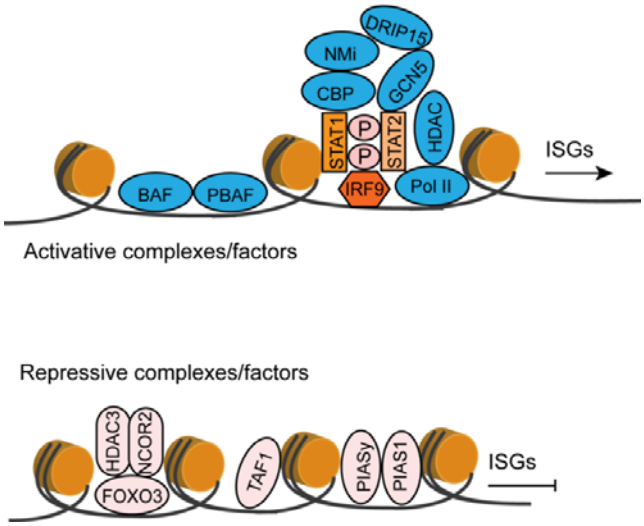

Figure 2. The transcriptional regulation of IFN-stimulated genes (ISGs) involves chromatin remodeling and various co-activators and co-repressors. Upon IFN stimulation, the IFN-stimulated gene factor 3 (ISGF3) or STAT1 homodimer binds to ISG promoter regions, recruiting various chromatin remodeling factors and transcriptional co-activators. These factors include the nucleosome remodeling complex BAF and PBAF, p300/CBP and GCN5 histone acetyltransferase (HAT), histone deacetylase (HDAC), minichromosome maintenance 3 and 5 (MCM3 and MCM5), N-Myc interactor (NMi), DRIP150 (a subunit of the multimeric mediator coactivator complex). Consequently, the condensed chromatin transforms into a more relaxed structure to facilitate the transcription of ISGs. Conversely, the co-repressor factors could inhibit ISG transcription either via the facilitation of a closed chromatin or interference with the recruitment of STAT1 or ISGF3 to the ISG promoter.

Non-canonical regulation of ISG transcription

All three types of IFNs signal through the JAK-STAT pathway to elicit antiviral activity. Yet, type II IFN is thought to do so only through STAT1 homodimers; whereas type I and III IFNs activate both STAT1 and STAT2 to form ISGF3 together with IRF9. However, accumulating evidence highlights a far more complex process of activation and function beyond this classical theory. The heterogeneity of the regulatory mechanisms of ISG transcription has been recently highlighted. A substantial fraction of these cascades have little or no link to STAT1/2 and ISGF3, paralleling the existence of non-canonical mechanisms outside of the JAK-STAT axis [79]. Here, we review both JAK-STAT axis dependent and independent non-canonical mechanisms of ISG transcription (Figure 3).

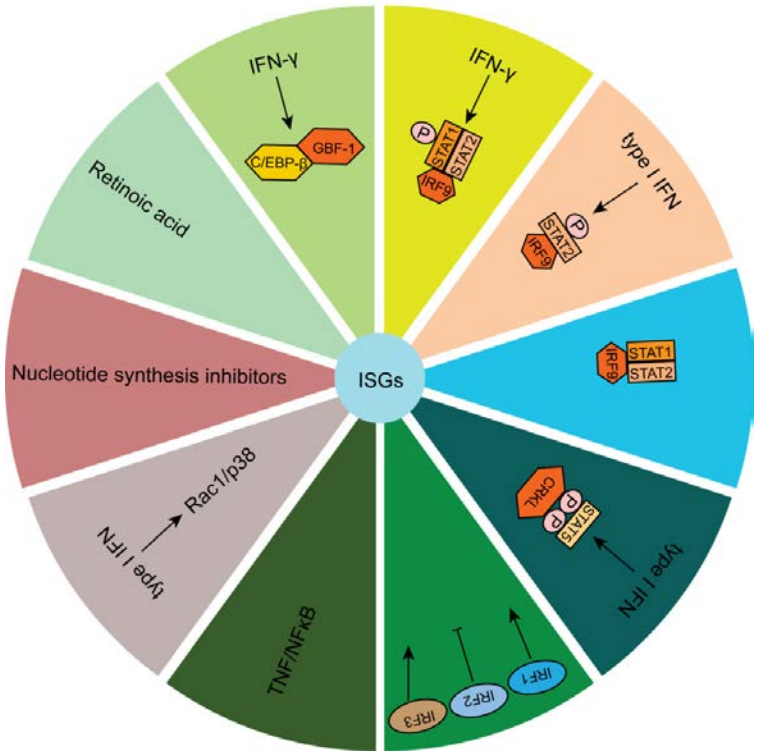

Figure 3. Non-canonical mechanisms in regulating ISG transcription. Non-canonical mechanisms both within and outside of the IFN-JAK-STAT axis were summarized. Together with canonical mechanisms, they coordinately regulate ISG transcription, thus defining the cellular defense status against pathogen invasion.

Non-canonical ISGF3 complex.

Up to date, three different forms of non-canonical ISGF3 complexes have been identified, including ISGF3^{II}, the STAT2-IRF9 complex and unphosphorylated ISGF3 (U-ISGF3). IFN-γ treatment has been reported to induce the formation of a new manifestation of ISGF3 (ISGF3^{II}) containing phosphorylated STAT1, unphosphorylated STAT2 and IRF9 [80]. In the absence of STAT1, STAT2 was found to interact with IRF9 to form an ISGF3-like complex to mediate specific ISG transcription [81]. Finally, continuous exposure to a low level of exogenous IFNs, U-ISGF3 formed by IFN induced IRF9 and unphosphorylated STAT1 and STAT2, can lead to increased expression of a subset of ISGs [82, 83].

STAT5-CrkL complex.

Apart from STAT1 and STAT2, STAT5 is also involved in type I IFN induced ISG transcription. STAT5 interacts constitutively with IFN receptor-associated TYK-2. Upon type I IFN stimulation, STAT5 is phosphorylated on both tyrosine and serine sites, thus acting as a docking site for the SH2 domain of CrkL. CrkL and STAT5 then form a complex that translocates to the nucleus and binds to GAS elements to activate type I IFN-dependent gene transcription [3, 84].

IRFs.

IRF1 has been shown to function as a transcription factor. The DNA sequences (IRF-E site) recognized by IRF1 overlap with the ISRE, and in this way IRF1 induces a subset of ISGs. IRF1 can also enhance the levels of both total and phosphorylated STAT1 to amplify ISG transcription via JAK-STAT pathway [85]. Conversely, IRF2 binds to the same IRF-E site to repress IRF1 induced transcription [86, 87]. Upon virus infection, IRF3 is activated and cooperates with NF-κB and ATF-2/c-Jun to form a transcriptionally active enhanceosome complex on the IFN-β promoter. Newly synthesized IFN binds to cognate receptors to activate ISG transcription via the JAK-STAT pathway. Importantly, IRF3 was also been reported to directly induce a subset of ISGs in an IFN-independent manner through the ISREs element on their promoters [88, 89].

Cross-regulation between TNF and IFN signaling.

It is well documented that when combined with TNF-α, type I or II IFN works cooperatively on antiviral ISG induction and exerts synergistic antiviral effects [90-93]. TNF-α has been reported to inhibit hepatitis C virus (HCV) infection-caused degradation of IFNAR2, thus maintaining IFN signaling and ISG expression [93]. TNF-α alone can already moderately induce the transcription of a subset of ISGs [90, 91]. This is mainly through NF-κB protein complex, a key downstream element of the TNF-α signaling. This may explain the antiviral activity of TNF-α on different virus as documented [92, 94-96].

Rac1/p38 pathway.

Rac1/p38 Map kinase signaling regulates IFN induced ISG transcription. Type I IFN treatment results in activation of Rac1 and its downstream effectors including MAP kinase kinase 3 (MKK3), MAP kinase kinase 6 (MKK6) [97, 98] and cytosolic phospholipase A2 [99, 100]. In turn, these events provoke phosphorylation and activation of the p38 MAP kinase, an important mediator of the inflammatory response [101]. p38 MAP kinase activation leads to downstream MapKapK-2 and MapKapK-3 activation, contributing to type I IFN-dependent transcriptional regulation of ISGs. However, Rac1/p38 Map kinase signaling is not required for IFN-dependent phosphorylation of STAT1 on both sites (Ser^{727} and Tyr^{701}) and has no impact on the formation of ISGF3 complex [102, 103]. Histone phosphorylation and chromatin remodeling are possible mechanisms employed by this cascade [102]. Many immune-relevant gene products are subject to post-transcriptional regulation by this signaling [104], but ISGs have not been investigated in this respect.

IFN-γ-activated response element (GATE).

In response to IFN-γ, two factors bind to a unique IFN-γ-activated response element called GATE, the CCAAT/enhancer binding protein C/EBP-β and the GATE binding factor GBF-1. MEK1, ERK1 and ERK2

are the upstream kinases needed to activate C/EBP-β in response to IFN-γ [105]. This novel IFN-γ-activated pathway promotes ISG expression in STAT1-, but not JAK1-dependent manner.

Nucleotide synthesis inhibitor.

Purine and pyrimidine nucleotides are the major cellular energy carriers and constitute subunits of nucleic acids. Nucleotides can be synthesized de novo through a series of enzymatic reactions or recycled through salvage pathways. Interestingly, purine and pyrimidine synthesis inhibitors (such as ribavirin, mycophenolic acid and brequinar) can efficiently induce ISG expression and exert strong and broad antiviral responses [106-108]. However, this process is independent of the classical JAK-STAT cascade, suggesting a non-canonical mechanism that is independent of IFNs [109]. Ribavirin, an inhibitor of the IMPDH enzyme, was shown to reset a subset of ISG promoters to a "ready to be activated" status, thus potentiating ISG activation [110]. However, the crosstalk of nucleotide synthesis and innate immune response remains to be further elucidated.

Retinoic acid.

Retinoic acid (RA) is a metabolite of vitamin A that mediates the functions of vitamin A required for growth and development. RA activates transcriptional status via retinoic acid receptors (RAR) and retinoid X receptors (RXR) heterodimer, which binds to regions in promoters called retinoic acid response elements (RAREs). Numerous studies have reported antiviral activities of RA against a variety of pathogens [111, 112]. Interestingly, intracellular RA increases ISG expression at basal levels and augments ISG induction in response to IFNs [113]. This is consistent with the clinical observation that RA enhances the response to IFN-based antiviral therapy [112, 114]. Strikingly, a bioinformatics study showed that most ISGs regulatory regions contain RARE sequence [113]. This indicates that RA can induce transcriptional activation of these ISGs containing RAREs, facilitating the binding of additional transcription factors to the promoters of these ISGs. Consequently, RA initiates and works synergistically with IFNs to induce ISG expression.

IFNs and ISGs: clinical implications and future perspective

IFNs have been used in various clinical settings to counteract pathogen-related diseases. Because of its robust and broad antiviral activity, IFN-α represents the standard treatment for chronic hepatitis B virus (HBV) or HCV infections for decades. Its application also extends to other virus infections as off-label treatment, *e.g.* hepatitis E virus [115] and severe acute respiratory syndrome [116]. IFN-λ has been shown to play a crucial role in cancer, autoimmune disease and viral infections [117]. The antitumor and anti-infection activities of IFN-γ have been comprehensively evaluated and used in a variety of clinical indications. It has been approved by FDA to treat chronic granulomatous disease and osteopetrosis and is experimentally used for the treatment of idiopathic pulmonary fibrosis and Friedreich's ataxia [118]. But it is unsuccessful for treating viral infections [119, 120]. IFN-λ has been shown specific antiviral activity in both chronic HBV and HCV patients, not superior as compared to IFN-α therapy but with limited side effects [121, 122]. This is because of the fact that IFNλR1 has a more restricted tissue-specific pattern of expression. IFN-λ has also been shown to determine the intestinal epithelial antiviral host defense against rotavirus infection. It acts synergistically with IL-22 for the induction of ISGs and eventually controls rotavirus infection in animal models [123, 124]. Thus, IFN-λ

might be an attractive option for the treatment of many viral infections. Although the clinical application of IFNs, in particular for HCV, will be limited because of the recent launch of direct-acting antiviral agents, it may extend to other devastating viral diseases such as Ebola, Zika or Dengue virus infections.

Mechanistically, for all three different types of IFNs, ISGs are the ultimate antiviral effectors. Recent studies on the function of individual ISG indicate that different viruses are targeted by unique sets of ISGs. Some ISGs possess broad antiviral but others have specific antiviral effects [125]. Thus, characterization of individual ISG with respect to their antiviral spectrum or specificity provides new avenues for improving current antiviral therapies. Interestingly, several ISGs have been reported to paradoxically enhance the replication of certain viruses, illustrating the complexity of the network of mutual interaction between ISGs and viruses [125]. In pre-clinical or clinical studies, the expression pattern of some specific ISGs have been identified as bio-makers to predict treatment responses, disease progression or outcomes in both infectious (*e.g.* HCV and HIV infections) [126-128] and non-infectious human diseases (*e.g.* Aicardi-Goutieres syndrome and systemic lupus erythematosus) [129, 130]. Some ISGs (*e.g.* TLR3, TLR7, RIG-I and MDA5) belong to pattern recognition receptors (PRRs). Attributing to their key roles in innate immune responses, there is a growing interest in targeting PRRs for the prevention and treatment of cancer, autoimmune diseases and infections. Their specific activators are now undergoing preclinical and clinical evaluation for safety and efficacy [131]. With regards to the adverse effects of IFNs in clinic, ISG-based antiviral strategies could be the next promising frontier in drug discovery.

Concluding Remarks

Decades of research has shaped up a picture of the complex network in regulating ISG transcription. This includes both canonical and non-canonical mechanisms within and outside of the IFN-JAK-STAT axis, coordinately defining the cellular defense status against pathogen invasion. We expect that the spectrum of new elements involved in both canonical and non-canonical regulation of ISG transcription will continue to grow and their mechanism-of-actions will be further clarified (see **Outstanding Questions**). Because of their importance in clinical implication, this knowledge is highly relevant in guiding the development of new therapies that promote the eradication of severe pathogen infections, but avoiding autoimmune diseases and toxic effects to the host.

References

1. Wu, J. and Z.J. Chen, Innate immune sensing and signaling of cytosolic nucleic acids. *Annu Rev Immunol*, 2014. **32**: p. 461-88.
2. Schneider, W.M., M.D. Chevillotte, and C.M. Rice, Interferon-stimulated genes: a complex web of host defenses. *Annu Rev Immunol*, 2014. **32**: p. 513-45.
3. Platanias, L.C., Mechanisms of type-I- and type-II-interferon-mediated signalling. *Nat Rev Immunol*, 2005. **5**(5): p. 375-86.
4. Stark, G.R. and J.E. Darnell, Jr., The JAK-STAT pathway at twenty. *Immunity*, 2012. **36**(4): p. 503-14.
5. Krause, C.D. and S. Pestka, Cut, copy, move, delete: The study of human interferon genes reveal multiple mechanisms underlying their evolution in amniotes. *Cytokine*, 2015. **76**(2): p. 480-95.
6. Kotenko, S.V., IFN-lambdas. *Curr Opin Immunol*, 2011. **23**(5): p. 583-90.
7. Galani, I.E., O. Koltsida, and E. Andreakos, Type III interferons (IFNs): Emerging Master Regulators of Immunity. *Adv Exp Med Biol*, 2015. **850**: p. 1-15.
8. Tang, X., et al., Acetylation-dependent signal transduction for type I interferon receptor. *Cell*, 2007. **131**(1): p. 93-105.

9. New, M., H. Olzscha, and N.B. La Thangue, HDAC inhibitor-based therapies: can we interpret the code? *Mol Oncol*, 2012. **6**(6): p. 637-56.
10. Schroder, K., et al., Interferon-gamma: an overview of signals, mechanisms and functions. *J Leukoc Biol*, 2004. **75**(2): p. 163-89.
11. Kumar, K.G., J.J. Krolewski, and S.Y. Fuchs, Phosphorylation and specific ubiquitin acceptor sites are required for ubiquitination and degradation of the IFNAR1 subunit of type I interferon receptor. *J Biol Chem*, 2004. **279**(45): p. 46614-20.
12. Malakhova, O.A., et al., UBP43 is a novel regulator of interferon signaling independent of its ISG15 isopeptidase activity. *EMBO J*, 2006. **25**(11): p. 2358-67.
13. Zhang, X., et al., Human intracellular ISG15 prevents interferon-alpha/beta over-amplification and auto-inflammation. *Nature*, 2015. **517**(7532): p. 89-93.
14. Fenner, J.E., et al., Suppressor of cytokine signaling 1 regulates the immune response to infection by a unique inhibition of type I interferon activity. *Nat Immunol*, 2006. **7**(1): p. 33-9.
15. Linossi, E.M., et al., Suppression of cytokine signaling: the SOCS perspective. *Cytokine Growth Factor Rev*, 2013. **24**(3): p. 241-8.
16. Starr, R., et al., SOCS-1 binding to tyrosine 441 of IFN-gamma receptor subunit 1 contributes to the attenuation of IFN-gamma signaling in vivo. *J Immunol*, 2009. **183**(7): p. 4537-44.
17. Farrar, M.A. and R.D. Schreiber, The molecular cell biology of interferon-gamma and its receptor. *Annu Rev Immunol*, 1993. **11**: p. 571-611.
18. Bernabei, P., et al., Interferon-gamma receptor 2 expression as the deciding factor in human T, B, and myeloid cell proliferation or death. *J Leukoc Biol*, 2001. **70**(6): p. 950-60.
19. Bach, E.A., et al., Ligand-induced autoregulation of IFN-gamma receptor beta chain expression in T helper cell subsets. *Science*, 1995. **270**(5239): p. 1215-8.
20. Babon, J.J., et al., The molecular regulation of Janus kinase (JAK) activation. *Biochem J*, 2014. **462**(1): p. 1-13.
21. Steen, H.C. and A.M. Gamero, STAT2 phosphorylation and signaling. *JAKSTAT*, 2013. **2**(4): p. e25790.
22. Myers, M.P., et al., TYK2 and JAK2 are substrates of protein-tyrosine phosphatase 1B. *J Biol Chem*, 2001. **276**(51): p. 47771-4.
23. Irie-Sasaki, J., et al., CD45 is a JAK phosphatase and negatively regulates cytokine receptor signalling. *Nature*, 2001. **409**(6818): p. 349-54.
24. Yamada, T., et al., CD45 controls interleukin-4-mediated IgE class switch recombination in human B cells through its function as a Janus kinase phosphatase. *J Biol Chem*, 2002. **277**(32): p. 28830-5.
25. Simoncic, P.D., et al., The T cell protein tyrosine phosphatase is a negative regulator of janus family kinases 1 and 3. *Curr Biol*, 2002. **12**(6): p. 446-53.
26. Ali, S., et al., SHP-2 regulates SOCS-1-mediated Janus kinase-2 ubiquitination/degradation downstream of the prolactin receptor. *J Biol Chem*, 2003. **278**(52): p. 52021-31.
27. O'Shea, J.J., et al., Janus kinase inhibitors in autoimmune diseases. *Ann Rheum Dis*, 2013. **72 Suppl 2**: p. ii111-5.
28. Yan, H., et al., Phosphorylated interferon-alpha receptor 1 subunit (IFNaR1) acts as a docking site for the latent form of the 113 kDa STAT2 protein. *EMBO J*, 1996. **15**(5): p. 1064-74.
29. Zhao, W., et al., A conserved IFN-alpha receptor tyrosine motif directs the biological response to type I IFNs. *J Immunol*, 2008. **180**(8): p. 5483-9.
30. Kaplan, D.H., et al., Identification of an interferon-gamma receptor alpha chain sequence required for JAK-1 binding. *J Biol Chem*, 1996. **271**(1): p. 9-12.
31. Qing, Y., et al., Role of tyrosine 441 of interferon-gamma receptor subunit 1 in SOCS-1-mediated attenuation of STAT1 activation. *J Biol Chem*, 2005. **280**(3): p. 1849-53.
32. Sadzak, I., et al., Recruitment of Stat1 to chromatin is required for interferon-induced serine phosphorylation of Stat1 transactivation domain. *Proc Natl Acad Sci U S A*, 2008. **105**(26): p. 8944-9.
33. Ng, S.L., et al., IkappaB kinase epsilon (IKK(epsilon)) regulates the balance between type I and type II interferon responses. *Proc Natl Acad Sci U S A*, 2011. **108**(52): p. 21170-5.
34. Ungureanu, D., et al., SUMO-1 conjugation selectively modulates STAT1-mediated gene responses. *Blood*, 2005. **106**(1): p. 224-6.
35. Steen, H.C., et al., Identification of STAT2 serine 287 as a novel regulatory phosphorylation site in type I interferon-induced cellular responses. *J Biol Chem*, 2013. **288**(1): p. 747-58.
36. Tenoever, B.R., et al., Multiple functions of the IKK-related kinase IKKepsilon in interferon-mediated antiviral immunity. *Science*, 2007. **315**(5816): p. 1274-8.
37. Ooi, E.L., et al., Novel antiviral host factor, TNK1, regulates IFN signaling through serine phosphorylation of STAT1. *Proc Natl Acad Sci U S A*, 2014. **111**(5): p. 1909-14.
38. Jiang, L.J., et al., RA-inducible gene-I induction augments STAT1 activation to inhibit leukemia cell proliferation. *Proc Natl Acad Sci U S A*, 2011. **108**(5): p. 1897-902.
39. Zhang, F., et al., Hepatitis E genotype 4 virus from feces of monkeys infected experimentally can be cultured in PLC/PRF/5 cells and upregulate host interferon-inducible genes. *J Med Virol*, 2014. **86**(10): p. 1736-44.
40. Staab, J., C. Herrmann-Lingen, and T. Meyer, CDK8 as the STAT1 serine 727 kinase? *JAKSTAT*, 2013. **2**(3): p. e24275.

41. Bancerek, J., et al., CDK8 kinase phosphorylates transcription factor STAT1 to selectively regulate the interferon response. *Immunity*, 2013. **38**(2): p. 250-62.
42. Choudhury, G.G., A linear signal transduction pathway involving phosphatidylinositol 3-kinase, protein kinase Cepsilon, and MAPK in mesangial cells regulates interferon-gamma-induced STAT1alpha transcriptional activation. *J Biol Chem*, 2004. **279**(26): p. 27399-409.
43. Nguyen, H., et al., Roles of phosphatidylinositol 3-kinase in interferon-gamma-dependent phosphorylation of STAT1 on serine 727 and activation of gene expression. *J Biol Chem*, 2001. **276**(36): p. 33361-8.
44. Uddin, S., et al., Protein kinase C-delta (PKC-delta) is activated by type I interferons and mediates phosphorylation of Stat1 on serine 727. *J Biol Chem*, 2002. **277**(17): p. 14408-16.
45. Deb, D.K., et al., Activation of protein kinase C delta by IFN-gamma. *J Immunol*, 2003. **171**(1): p. 267-73.
46. Ramsauer, K., et al., p38 MAPK enhances STAT1-dependent transcription independently of Ser-727 phosphorylation. *Proc Natl Acad Sci U S A*, 2002. **99**(20): p. 12859-64.
47. Branger, J., et al., Inhibition of coagulation, fibrinolysis, and endothelial cell activation by a p38 mitogen-activated protein kinase inhibitor during human endotoxemia. *Blood*, 2003. **101**(11): p. 4446-8.
48. Wu, T.R., et al., SHP-2 is a dual-specificity phosphatase involved in Stat1 dephosphorylation at both tyrosine and serine residues in nuclei. *J Biol Chem*, 2002. **277**(49): p. 47572-80.
49. Xu, D. and C.K. Qu, Protein tyrosine phosphatases in the JAK/STAT pathway. *Front Biosci*, 2008. **13**: p. 4925-32.
50. ten Hoeve, J., et al., Identification of a nuclear Stat1 protein tyrosine phosphatase. *Mol Cell Biol*, 2002. **22**(16): p. 5662-8.
51. David, M., et al., Differential regulation of the alpha/beta interferon-stimulated Jak/Stat pathway by the SH2 domain-containing tyrosine phosphatase SHPTP1. *Mol Cell Biol*, 1995. **15**(12): p. 7050-8.
52. He, R.J., et al., Protein tyrosine phosphatases as potential therapeutic targets. *Acta Pharmacol Sin*, 2014. **35**(10): p. 1227-46.
53. Qureshi, S.A., M. Salditt-Georgieff, and J.E. Darnell, Jr., Tyrosine-phosphorylated Stat1 and Stat2 plus a 48-kDa protein all contact DNA in forming interferon-stimulated-gene factor 3. *Proc Natl Acad Sci U S A*, 1995. **92**(9): p. 3829-33.
54. John, J., et al., Isolation and characterization of a new mutant human cell line unresponsive to alpha and beta interferons. *Mol Cell Biol*, 1991. **11**(8): p. 4189-95.
55. Kimura, T., et al., Essential and non-redundant roles of p48 (ISGF3 gamma) and IRF-1 in both type I and type II interferon responses, as revealed by gene targeting studies. *Genes Cells*, 1996. **1**(1): p. 115-24.
56. Levy, D.E., et al., Synergistic interaction between interferon-alpha and interferon-gamma through induced synthesis of one subunit of the transcription factor ISGF3. *EMBO J*, 1990. **9**(4): p. 1105-11.
57. Bell, O., et al., Determinants and dynamics of genome accessibility. *Nat Rev Genet*, 2011. **12**(8): p. 554-64.
58. Cui, K., et al., The chromatin-remodeling BAF complex mediates cellular antiviral activities by promoter priming. *Mol Cell Biol*, 2004. **24**(10): p. 4476-86.
59. Yan, Z., et al., PBAF chromatin-remodeling complex requires a novel specificity subunit, BAF200, to regulate expression of selective interferon-responsive genes. *Genes Dev*, 2005. **19**(14): p. 1662-7.
60. Huang, M., et al., Chromatin-remodelling factor BRG1 selectively activates a subset of interferon-alpha-inducible genes. *Nat Cell Biol*, 2002. **4**(10): p. 774-81.
61. Ni, Z., et al., Apical role for BRG1 in cytokine-induced promoter assembly. *Proc Natl Acad Sci U S A*, 2005. **102**(41): p. 14611-6.
62. Bhattacharya, S., et al., Cooperation of Stat2 and p300/CBP in signalling induced by interferon-alpha. *Nature*, 1996. **383**(6598): p. 344-7.
63. Paulson, M., et al., IFN-Stimulated transcription through a TBP-free acetyltransferase complex escapes viral shutoff. *Nat Cell Biol*, 2002. **4**(2): p. 140-7.
64. Shakespear, M.R., et al., Histone deacetylases as regulators of inflammation and immunity. *Trends Immunol*, 2011. **32**(7): p. 335-43.
65. Chang, H.M., et al., Induction of interferon-stimulated gene expression and antiviral responses require protein deacetylase activity. *Proc Natl Acad Sci U S A*, 2004. **101**(26): p. 9578-83.
66. Gao, B., et al., Inhibition of histone deacetylase activity suppresses IFN-gamma induction of tripartite motif 22 via CHIP-mediated proteasomal degradation of IRF-1. *J Immunol*, 2013. **191**(1): p. 464-71.
67. Nusinzon, I. and C.M. Horvath, Interferon-stimulated transcription and innate antiviral immunity require deacetylase activity and histone deacetylase 1. *Proc Natl Acad Sci U S A*, 2003. **100**(25): p. 14742-7.
68. Falkenberg, K.J. and R.W. Johnstone, Histone deacetylases and their inhibitors in cancer, neurological diseases and immune disorders. *Nat Rev Drug Discov*, 2014. **13**(9): p. 673-91.
69. Klampfer, L., et al., Requirement of histone deacetylase activity for signaling by STAT1. *J Biol Chem*, 2004. **279**(29): p. 30358-68.
70. Sakamoto, S., R. Potla, and A.C. Larner, Histone deacetylase activity is required to recruit RNA polymerase II to the promoters of selected interferon-stimulated early response genes. *J Biol Chem*, 2004. **279**(39): p. 40362-7.
71. Litvak, V., et al., A FOXO3-IRF7 gene regulatory circuit limits inflammatory sequelae of antiviral responses. *Nature*, 2012. **490**(7420): p. 421-5.
72. Zhang, J.J., et al., Ser727-dependent recruitment of MCM5 by Stat1alpha in IFN-gamma-induced transcriptional activation. *EMBO J*, 1998. **17**(23): p. 6963-71.

73. DaFonseca, C.J., F. Shu, and J.J. Zhang, Identification of two residues in MCM5 critical for the assembly of MCM complexes and Stat1-mediated transcription activation in response to IFN-gamma. *Proc Natl Acad Sci U S A*, 2001. **98**(6): p. 3034-9.
74. Zhu, M., et al., Functional association of Nmi with Stat5 and Stat1 in IL-2- and IFNgamma-mediated signaling. *Cell*, 1999. **96**(1): p. 121-30.
75. Lau, J.F., et al., Role of metazoan mediator proteins in interferon-responsive transcription. *Mol Cell Biol*, 2003. **23**(2): p. 620-8.
76. Kadota, S. and K. Nagata, Silencing of IFN-stimulated gene transcription is regulated by histone H1 and its chaperone TAF-I. *Nucleic Acids Res*, 2014. **42**(12): p. 7642-53.
77. Tahk, S., et al., Control of specificity and magnitude of NF-kappa B and STAT1-mediated gene activation through PIASy and PIAS1 cooperation. *Proc Natl Acad Sci U S A*, 2007. **104**(28): p. 11643-8.
78. Liu, B., et al., A transcriptional corepressor of Stat1 with an essential LXXLL signature motif. *Proc Natl Acad Sci U S A*, 2001. **98**(6): p. 3203-7.
79. Mostafavi, S., et al., Parsing the Interferon Transcriptional Network and Its Disease Associations. *Cell*, 2016. **164**(3): p. 564-78.
80. Morrow, A.N., et al., A novel role for IFN-stimulated gene factor 3II in IFN-gamma signaling and induction of antiviral activity in human cells. *J Immunol*, 2011. **186**(3): p. 1685-93.
81. Fink, K. and N. Grandvaux, STAT2 and IRF9: Beyond ISGF3. *JAKSTAT*, 2013. **2**(4): p. e27521.
82. Cheon, H., et al., IFNbeta-dependent increases in STAT1, STAT2, and IRF9 mediate resistance to viruses and DNA damage. *EMBO J*, 2013. **32**(20): p. 2751-63.
83. Sung, P.S., et al., Roles of unphosphorylated ISGF3 in HCV infection and interferon responsiveness. *Proc Natl Acad Sci U S A*, 2015. **112**(33): p. 10443-8.
84. Fish, E.N., et al., Activation of a CrkL-stat5 signaling complex by type I interferons. *J Biol Chem*, 1999. **274**(2): p. 571-3.
85. Xu, L., et al., IFN regulatory factor 1 restricts hepatitis E virus replication by activating STAT1 to induce antiviral IFN-stimulated genes. *FASEB J*, 2016.
86. Harada, H., et al., Structure and regulation of the human interferon regulatory factor 1 (IRF-1) and IRF-2 genes: implications for a gene network in the interferon system. *Mol Cell Biol*, 1994. **14**(2): p. 1500-9.
87. Ivashkiv, L.B. and L.T. Donlin, Regulation of type I interferon responses. *Nat Rev Immunol*, 2014. **14**(1): p. 36-49.
88. Grandvaux, N., et al., Transcriptional profiling of interferon regulatory factor 3 target genes: direct involvement in the regulation of interferon-stimulated genes. *J Virol*, 2002. **76**(11): p. 5532-9.
89. Collins, S.E., R.S. Noyce, and K.L. Mossman, Innate cellular response to virus particle entry requires IRF3 but not virus replication. *J Virol*, 2004. **78**(4): p. 1706-17.
90. Bartee, E., et al., The addition of tumor necrosis factor plus beta interferon induces a novel synergistic antiviral state against poxviruses in primary human fibroblasts. *J Virol*, 2009. **83**(2): p. 498-511.
91. Wang, W., et al., Convergent Transcription of Interferon-stimulated Genes by TNF-alpha and IFN-alpha Augments Antiviral Activity against HCV and HEV. *Sci Rep*, 2016. **6**: p. 25482.
92. Mestan, J., et al., Antiviral activity of tumour necrosis factor. Synergism with interferons and induction of oligo-2',5'-adenylate synthetase. *J Gen Virol*, 1988. **69 (Pt 12)**: p. 3113-20.
93. Lee, J., et al., TNF-alpha Induced by Hepatitis C Virus via TLR7 and TLR8 in Hepatocytes Supports Interferon Signaling via an Autocrine Mechanism. *PLoS Pathog*, 2015. **11**(5): p. e1004937.
94. Ruby, J., H. Bluethmann, and J.J. Peschon, Antiviral activity of tumor necrosis factor (TNF) is mediated via p55 and p75 TNF receptors. *J Exp Med*, 1997. **186**(9): p. 1591-6.
95. Seo, S.H. and R.G. Webster, Tumor necrosis factor alpha exerts powerful anti-influenza virus effects in lung epithelial cells. *J Virol*, 2002. **76**(3): p. 1071-6.
96. Mestan, J., et al., Antiviral effects of recombinant tumour necrosis factor in vitro. *Nature*, 1986. **323**(6091): p. 816-9.
97. Uddin, S., et al., The Rac1/p38 mitogen-activated protein kinase pathway is required for interferon alpha-dependent transcriptional activation but not serine phosphorylation of Stat proteins. *J Biol Chem*, 2000. **275**(36): p. 27634-40.
98. Li, Y., et al., Activation of mitogen-activated protein kinase kinase (MKK) 3 and MKK6 by type I interferons. *J Biol Chem*, 2005. **280**(11): p. 10001-10.
99. Wu, T., et al., Interferon-gamma induces the synthesis and activation of cytosolic phospholipase A2. *J Clin Invest*, 1994. **93**(2): p. 571-7.
100. Peppelenbosch, M.P., et al., Rac mediates growth factor-induced arachidonic acid release. *Cell*, 1995. **81**(6): p. 849-56.
101. Young, P.R., Perspective on the discovery and scientific impact of p38 MAP kinase. *J Biomol Screen*, 2013. **18**(10): p. 1156-63.
102. Li, Y., et al., Role of p38alpha Map kinase in Type I interferon signaling. *J Biol Chem*, 2004. **279**(2): p. 970-9.
103. Uddin, S., et al., Activation of the p38 mitogen-activated protein kinase by type I interferons. *J Biol Chem*, 1999. **274**(42): p. 30127-31.
104. Lee, Y.B., J.W. Schrader, and S.U. Kim, p38 map kinase regulates TNF-alpha production in human astrocytes and microglia by multiple mechanisms. *Cytokine*, 2000. **12**(7): p. 874-80.

105. Hu, J., et al., ERK1 and ERK2 activate CCAAAT/enhancer-binding protein-beta-dependent gene transcription in response to interferon-gamma. *J Biol Chem*, 2001. **276**(1): p. 287-97.
106. Lucas-Hourani, M., et al., Inhibition of pyrimidine biosynthesis pathway suppresses viral growth through innate immunity. *PLoS Pathog*, 2013. **9**(10): p. e1003678.
107. Pan, Q., et al., Mycophenolic acid augments interferon-stimulated gene expression and inhibits hepatitis C Virus infection in vitro and in vivo. *Hepatology*, 2012. **55**(6): p. 1673-83.
108. Chung, D.H., et al., Discovery of a broad-spectrum antiviral compound that inhibits pyrimidine biosynthesis and establishes a type 1 interferon-independent antiviral state. *Antimicrob Agents Chemother*, 2016.
109. Wang, Y., et al., Cross Talk between Nucleotide Synthesis Pathways with Cellular Immunity in Constraining Hepatitis E Virus Replication. *Antimicrob Agents Chemother*, 2016. **60**(5): p. 2834-48.
110. Testoni, B., et al., Ribavirin restores IFNalpha responsiveness in HCV-infected livers by epigenetic remodelling at interferon stimulated genes. *Gut*, 2016. **65**(4): p. 672-82.
111. Neuzil, K.M., et al., Safety and pharmacokinetics of vitamin A therapy for infants with respiratory syncytial virus infections. *Antimicrob Agents Chemother*, 1995. **39**(5): p. 1191-3.
112. Bocher, W.O., et al., All-trans retinoic acid for treatment of chronic hepatitis C. *Liver Int*, 2008. **28**(3): p. 347-54.
113. Cho, N.E., et al., Retinoid regulation of antiviral innate immunity in hepatocytes. *Hepatology*, 2016. **63**(6): p. 1783-95.
114. Bitetto, D., et al., Vitamin A deficiency is associated with hepatitis C virus chronic infection and with unresponsiveness to interferon-based antiviral therapy. *Hepatology*, 2013. **57**(3): p. 925-33.
115. Debing, Y. and J. Neyts, Antiviral strategies for hepatitis E virus. *Antiviral Res*, 2014. **102**: p. 106-18.
116. Loutfy, M.R., et al., Interferon alfacon-1 plus corticosteroids in severe acute respiratory syndrome: a preliminary study. *JAMA*, 2003. **290**(24): p. 3222-8.
117. Lasfar, A., A. Zloza, and K.A. Cohen-Solal, IFN-lambda therapy: current status and future perspectives. *Drug Discov Today*, 2016. **21**(1): p. 167-71.
118. Miller, C.H., S.G. Maher, and H.A. Young, Clinical Use of Interferon-gamma. *Ann N Y Acad Sci*, 2009. **1182**: p. 69-79.
119. Lau, J.Y., et al., A randomised controlled trial of recombinant interferon-gamma in Chinese patients with chronic hepatitis B virus infection. *J Med Virol*, 1991. **34**(3): p. 184-7.
120. Muir, A.J., P.B. Sylvestre, and D.C. Rockey, Interferon gamma-1b for the treatment of fibrosis in chronic hepatitis C infection. *J Viral Hepat*, 2006. **13**(5): p. 322-8.
121. Chan, H.L., et al., Peginterferon lambda for the treatment of HBeAg-positive chronic hepatitis B: A randomized phase 2b study (LIRA-B). *J Hepatol*, 2016. **64**(5): p. 1011-9.
122. Muir, A.J., et al., A randomized phase 2b study of peginterferon lambda-1a for the treatment of chronic HCV infection. *J Hepatol*, 2014. **61**(6): p. 1238-46.
123. Hernandez, P.P., et al., Interferon-lambda and interleukin 22 act synergistically for the induction of interferon-stimulated genes and control of rotavirus infection. *Nat Immunol*, 2015. **16**(7): p. 698-707.
124. Pott, J., et al., IFN-lambda determines the intestinal epithelial antiviral host defense. *Proc Natl Acad Sci U S A*, 2011. **108**(19): p. 7944-9.
125. Schoggins, J.W., et al., A diverse range of gene products are effectors of the type I interferon antiviral response. *Nature*, 2011. **472**(7344): p. 481-5.
126. Asselah, T., et al., Liver gene expression signature to predict response to pegylated interferon plus ribavirin combination therapy in patients with chronic hepatitis C. *Gut*, 2008. **57**(4): p. 516-24.
127. Dill, M.T., et al., Interferon-gamma-stimulated genes, but not USP18, are expressed in livers of patients with acute hepatitis C. *Gastroenterology*, 2012. **143**(3): p. 777-86 e1-6.
128. Crow, Y.J. and N. Manel, Aicardi-Goutieres syndrome and the type I interferonopathies. *Nat Rev Immunol*, 2015. **15**(7): p. 429-40.
129. Bennett, L., et al., Interferon and granulopoiesis signatures in systemic lupus erythematosus blood. *J Exp Med*, 2003. **197**(6): p. 711-23.
130. Mandl, J.N., et al., Divergent TLR7 and TLR9 signaling and type I interferon production distinguish pathogenic and nonpathogenic AIDS virus infections. *Nat Med*, 2008. **14**(10): p. 1077-87.
131. Mullen, L.M., G. Chamberlain, and S. Sacre, Pattern recognition receptors as potential therapeutic targets in inflammatory rheumatic disease. *Arthritis Res Ther*, 2015. **17**: p. 122.

Chapter 4

Non-canonical Antiviral Mechanisms of ISGs: Dispensability of Interferons

Lei Xu[1], **Wenshi Wang[1]**, Maikel P. Peppelenbosch[1], and Qiuwei Pan[1]

[1]Department of Gastroenterology and Hepatology, Erasmus MC-University Medical Center, Rotterdam, the Netherlands

Trends in Immunology. 2017. 38(1):1-2

Type I interferons (IFNs) have broad antiviral activities through the induction of interferon-stimulated genes (ISGs). It is considered to constitute the first line of antiviral defense, but excessive exposure to IFNs provokes tissue damage and other pathological events. In addition to type I IFNs, however, the body has other innate antiviral defenses as well, which were commandingly reviewed by dr. Paludan in a recent issue of *Trends in Immunology* [1]. The article highlights that type I IFN-independent antiviral mechanisms, including alternative antiviral cytokines (*e.g.* IFN-λ or interleukin 22), or the basal expression of particular ISGs that all can mediate early antiviral defenses without evoking the inflammatory damage associated with production of type I IFNs. However, we feel that, while the constitutively expressed IFN regulatory factors (IRFs) and pattern recognition receptors (PRRs) have been largely examined in the context of the scaling of IFN responses, they also mediate important antiviral mechanisms that are independent of IFN induction and, thus, should also be emphasized.

There are hundreds of ISGs that are usually induced by IFNs. Although they are thought to be the ultimate antiviral effectors, only a small subset of ISGs actually have potent antiviral activity as recently demonstrated by a screening of over 380 human ISGs for their antiviral effects [2, 3]. Some ISGs appear to act on specific viruses; whereas others have potent antiviral activity against a broad spectrum of viruses, especially IRFs (*e.g.* IRF1 and IRF2) and PRRs (*e.g.* cGAS, RIG-I and MDA5) [2, 3]. Classically, the induction or/and activation of these broad antiviral ISGs by viruses or IFNs are thought to enhance further IFN production, in turn inducing strong and broad induction of ISGs capable of combating viral infection through positive feedback loop. However, constitutive expression of particular ISGs may provide necessary antiviral defense without the need for IFN production. Especially the observation that, several ISGs have general antiviral effects in human STAT1 deficient fibroblasts, which are deficient in IFN signal transduction, in our view strongly supports this notion [2].

IRFs are transcription factors that indeed can bind to promoter regions of specific IFN genes to drive their transcription. PRRs can recognize specific components of the viral nucleic acid and trigger IFN production through downstream elements including IRF3 and IRF7 [4]. Thus, IFNs are important mediators of their antiviral action. However, accumulating evidence suggest that these broad antiviral ISGs simultaneously function through IFN-independent pathways, as they are capable of inducing transcription of many ISGs independent of IFN production or signaling [2]. For instance, IRF1 inhibits hepatitis E virus infection through activation of STAT1 transcription and phosphorylation without concomitant IFN production [5]. cGAS can induce a large number of ISGs via a STING-dependent, IRF3-mediated process but functions independent of the canonical IFN signaling [3]. RIG-I has also been demonstrated to induce ISGs by augmenting STAT1 activation but independent of the classical IFN pathway [6]. It has been reported to strengthen STAT1 activation by disruption of the binding of STAT1 to its negative regulator SHP1 [7].

We feel that this idea is further bolstered by the definition of at least some of the other molecular mechanisms that execute type I IFN-independent antiviral defense. RIG-I can directly inhibit viral replication by blocking the binding of viral polymerase to viral RNA [8, 9]. During hepatitis B virus (HBV) infection, RIG-I recognizes and binds the 5'-ε region of the pregenomic viral RNA (pgRNA). It thus prevents the interaction of HBV polymerase with this 5'-ε region, leading to suppression of HBV replication [8]. During influenza A virus infection, RIG-I binds to the nucleocapsids of cytoplasm-invading viruses, resulting in destabilization of the nucleocapsids that hampers viral propagation [9]. Furthermore, RIG-I and MDA5 exert their direct antiviral functions that require intact ATPase activity

and involves displacing viral proteins from their pre-bound positions on dsRNA [10]. In response, viruses have also developed sophisticated strategies to counteract host antiviral defense. For instance, herpesvirus can hijack activated RIG-I to avoid antiviral cytokine production [11]. Hepatitis C virus can prevent physical interaction between viral RNA and host PRRs like RIG-I and MDA5 [12]. Nevertheless, constitutive expression of RIG-I and MDA5 can be expected to provide protection against a variety of viruses.

In line with the review by Paludan highlighting the essential role of IFN-independent antiviral response, we now have extended and emphasized the importance of possible IFN-independent mechanisms of these broad antiviral ISGs. However, these non-canonical antiviral mechanisms are largely elusive, thus deserving further investigation, although the IFN-dependent mechanisms also require further clarification (Figure 1). We would thus call upon the scientific community to devote more attention to this under-investigated subject as it appears to constitute a vital component of the defense of the body against viral challenges.

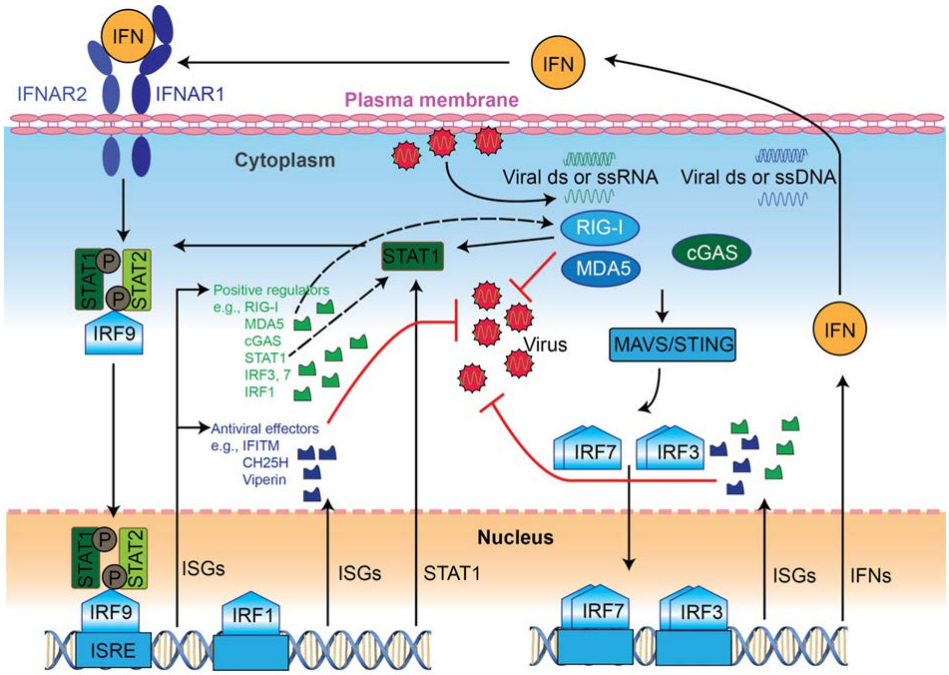

Figure 1. Interferon (IFN)-Dependent and Independent Antiviral Mechanisms of IFN-Stimulated Genes (ISGs). Classically, Type I IFN induces gene expression via the Janus kinase-signal transducer and activator of transcription (JAK-STAT) pathway, resulting in expression of a range of ISGs that can be mainly divided into antiviral effectors and positive regulators. Some positive regulators, such as retinoic-acid inducible gene I (RIG-I), melanoma differentiation associated protein 5 (MDA5), and cyclic GMP-AMP synthase (cGAS), can recognize viral nucleic acid, triggering expression of IFNs through the IFN regulatory factors IRF3 and IRF7. Many of these positive regulators can activate the transcription of ISGs independently of IFN production. In particular, cGAS can induce ISG expression via a stimulator of IFN genes (STING)-dependent, IRF3-mediated process. RIG-I can induce ISG expression by augmenting STAT1 activation. IRF1 can activate ISG expression via STAT1 activation. Of note, RIG-I and MDA5 also directly inhibit viral propagation. Abbreviations: IFNAR1/2, IFN-α receptor 1/2; ISRE, IFN-stimulated response element. The red line with a blunt end indicates antiviral activity.

References

1. Paludan, S.R., Innate Antiviral Defenses Independent of Inducible IFNalpha/beta Production. *Trends Immunol*, 2016. **37**(9): p. 588-96.
2. Schoggins, J.W., et al., A diverse range of gene products are effectors of the type I interferon antiviral response. *Nature*, 2011. **472**(7344): p. 481-5.
3. Schoggins, J.W., et al., Pan-viral specificity of IFN-induced genes reveals new roles for cGAS in innate immunity. *Nature*, 2014. **505**(7485): p. 691-5.
4. Gurtler, C. and A.G. Bowie, Innate immune detection of microbial nucleic acids. *Trends Microbiol*, 2013. **21**(8): p. 413-20.
5. Xu, L., et al., IFN regulatory factor 1 restricts hepatitis E virus replication by activating STAT1 to induce antiviral IFN-stimulated genes. *FASEB J*, 2016. **30**(10): p. 3352-3367.
6. Jiang, L.J., et al., RA-inducible gene-I induction augments STAT1 activation to inhibit leukemia cell proliferation. *Proc Natl Acad Sci U S A*, 2011. **108**(5): p. 1897-902.
7. Zhang, F., et al., Hepatitis E genotype 4 virus from feces of monkeys infected experimentally can be cultured in PLC/PRF/5 cells and upregulate host interferon-inducible genes. *J Med Virol*, 2014. **86**(10): p. 1736-44.
8. Sato, S., et al., The RNA sensor RIG-I dually functions as an innate sensor and direct antiviral factor for hepatitis B virus. *Immunity*, 2015. **42**(1): p. 123-32.
9. Weber, M., et al., Influenza virus adaptation PB2-627K modulates nucleocapsid inhibition by the pathogen sensor RIG-I. *Cell Host Microbe*, 2015. **17**(3): p. 309-19.
10. Yao, H., et al., ATP-Dependent Effector-like Functions of RIG-I-like Receptors. *Mol Cell*, 2015. **58**(3): p. 541-8.
11. He, S., et al., Viral pseudo-enzymes activate RIG-I via deamidation to evade cytokine production. *Mol Cell*, 2015. **58**(1): p. 134-46.
12. Neufeldt, C.J., et al., The Hepatitis C Virus-Induced Membranous Web and Associated Nuclear Transport Machinery Limit Access of Pattern Recognition Receptors to Viral Replication Sites. *PLoS Pathog*, 2016. **12**(2): p. e1005428.

Chapter 5

Convergent Transcription of Interferon-stimulated Genes by TNF-α and IFN-α Augments Antiviral Activity against HCV and HEV

Wenshi Wang[1], Lei Xu[1], Johannes H. Brandsma[2], Yijin Wang[1], Mohamad S. Hakim[1,3], Xinying Zhou[1], Yuebang Yin[1], Gwenny M. Fuhler[1], Luc J. W. van der Laan[4], C. Janneke van der Woude[1], Dave Sprengers[1], Herold J. Metselaar[1], Ron Smits[1], Raymond A. Poot[1], Maikel P. Peppelenbosch[1] and Qiuwei Pan[1]

[1]Department of Gastroenterology and Hepatology, Postgraduate School Molecular Medicine, Erasmus MC-University Medical Center, Rotterdam, 3015 CE, the Netherlands.

[2]Department of Cell Biology, Medical Genetics Cluster, Erasmus MC-University Medical Center, Rotterdam, 3015 CE, the Netherlands.

[3]Department of Microbiology, Faculty of Medicine, Gadjah Mada University, Yogyakarta, Indonesia.

[4]Department of Surgery, Postgraduate School Molecular Medicine, Erasmus MC-University Medical Center, Rotterdam, 3015 CE, The Netherlands.

Scientific Reports. 2016. 6. 25482.

Abstract

IFN-α has been used for decades to treat chronic hepatitis B and C, and as an off-label treatment for some cases of hepatitis E virus (HEV) infection. TNF-α is another important cytokine involved in inflammatory disease, which can interact with interferon signaling. Because interferon-stimulated genes (ISGs) are the ultimate antiviral effectors of the interferon signaling, this study aimed to understand the regulation of ISG transcription and the antiviral activity by IFN-α and TNF-α. In this study, treatment of TNF-α inhibited replication of HCV by 71 ± 2.4% and HEV by 41 ± 4.9%. Interestingly, TNF-α induced the expression of a panel of antiviral ISGs (2-11 fold). Blocking the TNF-α signaling by Humira abrogated ISG induction and its antiviral activity. Chip-seq data analysis and mutagenesis assay further revealed that the NF-κB protein complex, a key downstream element of TNF-α signaling, directly binds to the ISRE motif in the ISG promoters and thereby drives their transcription. This process is independent of interferons and JAK-STAT cascade. Importantly, when combined with IFN-α, TNF-α works cooperatively on ISG induction, explaining their additive antiviral effects. Thus, our study reveals a novel mechanism of convergent transcription of ISGs by TNF-α and IFN-α, which augments their antiviral activity against HCV and HEV.

Introduction

Cytokines orchestrate cellular communication in an autocrine, juxtacrine, or paracrine fashion through binding to distinct families of receptors, triggering specific immune responses against invading pathogens. The interferon (IFN)-mediated innate immune response is probably the most prominent response and provides a robust first defense line. Among different types of interferons, IFN-α (a type I member) has been used for decades to treat chronic hepatitis B or C infection in the clinic [1]. When stimulated by its cognate ligand, interferon receptors respond by the activation of kinases of the Janus family (JAKs), which in turn phosphorylate tyrosine residues in the intracellular tail of the interferon receptors. These phosphotyrosines serve as docking sites for recruitment and phosphorylation of the Signal Transducers and Activators of Transcription (STAT) family, which provokes STAT1 and STAT2 dimerization and subsequent binding to interferon regulatory factor 9 (IRF9) to form the IFN-stimulated gene factor 3 (ISGF3) complex. The ISGF3 complex translocates into the nucleus, and binds to specific promotor elements denoted as interferon signaling response elements (ISREs) and thus mediate the transcription of so-called interferon-stimulated genes (ISGs). ISGs are the ultimate antiviral effectors of the interferon signaling.

It is generally believed that ISGs are predominantly induced by interferons. However, ISGs are still up-regulated in embryonic fibroblasts from IFN alpha/beta receptor knockout mouse upon infection of West Nile virus [2]. These observations suggest the existence of alternative mechanisms of regulating ISG transcription. But these non-canonical mechanisms remain largely unknown.

Tumor necrosis factor alpha (TNF-α) is another important cytokine that mediates host response to infections. TNF-α/TNFR interactions can play decisive roles in the outcome of a number of viral infections, contributing to virus control or immune mediated pathology [3]. Deregulation of TNF-α is associated with many pathological conditions, including various types of arthritis and inflammatory bowel disease (IBD) [4]. TNF-α inhibitors have been successfully used in the clinic to treat these chronic immune-mediated diseases [5]. However, patients receiving TNF-α inhibitors are often at high risk of viral infections [6]. Treatment with TNF-α inhibitors have been reported to increase reactivation of concurrent chronic hepatitis B and potentially increase hepatitis C virus (HCV) replication [7], further supporting the importance of TNF-α in defending the human body against viral infections. Interestingly, several previous studies reported crosstalk between TNF-α and the antiviral interferon signaling and ISG expression in the setting of vesicular stomatitis virus [8], hepatitis C virus (HCV) [9], respiratory virus [10] and poxvirus infections [11].

However, the exact antiviral mechanisms of TNF-α and how it cooperates with the interferon signaling remain largely elusive, thus prompting us to explore their molecular basis. Here we report that TNF-α alone was sufficient to induce the expression of ISGs and to exert antiviral activity against HCV and hepatitis E virus (HEV). This is through the activation of the NF-κB signaling but independent of the canonical interferon pathway. Surprisingly, we found a consensus DNA binding sequence between the NF-κB and ISRE motif with bioinformatics analysis. Functional assays revealed that the NF-κB complex is able to bind to the ISRE motif and directly activates the transcription of antiviral ISGs. Combination of TNF-α with IFN-α further boosts the induction of ISGs and results in augmented antiviral activity against HCV and HEV. Thus, this study identified a non-canonical mechanism of driving antiviral ISG transcription, which provides the molecular basis for the antiviral action of TNF-α and its additive antiviral effect with interferon.

Results

TNF-α activates ISG transcription and exerts antiviral activity against HCV and HEV

TNF-α is involved in host responses to a variety of pathogen invasions, including HCV and HEV infections [9, 12]. To assess the direct effects of TNF-α on HCV and HEV replication, we employed a human hepatocyte cell line, i.e. Huh7, transfected with a HCV or HEV replicon luciferase as reporters. In parallel, Huh7 cells constitutively expressing a non-secreted *firefly* luciferase under control of the human phosphoglycerate kinase (PGK) promoter (LV-PGK-Luc) were also used for normalization of nonspecific effects on luciferase signals. Both HCV and HEV replicon luciferase activity were significantly inhibited by treatment of cells with TNF-α (Fig. 1A, B). For instance, 100 ng/mL TNF-α inhibited HCV to 29 ± 2.4% (n = 5, P < 0.001), HEV to 59 ± 4.9% (n = 5, P < 0.01) at 72 hrs.

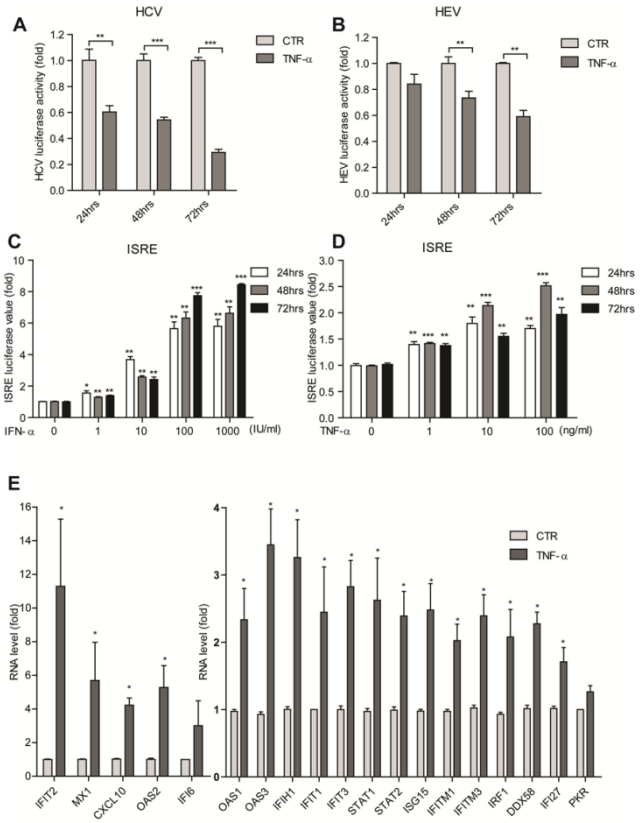

Figure 1. TNF-α activates ISG transcription and exerts antiviral activity against HCV and HEV. (A) In the Huh7 cell-based subgenomic HCV replicon, treatment with recombinant human TNF-α (100 ng/mL) inhibited HCV replication-related luciferase activity as measured at 3 different time points (n = 5). (B) Same as (A) for the Huh7 cell-based subgenomic HEV replicon model. (C) In the Huh7 cell-based ISRE luciferase reporter cells, treatment with IFN-α resulted in a dose-dependent induction of ISRE-related luciferase activity (n = 3 independent experiments with 2 - 3 replicates each). (D) Same as (C) for TNF-α. (E) Expression profile of 20 antiviral ISGs in Huh7 cells as measured by qRT-PCR. Most ISGs were highly up-regulated with TNF-α treatment (n = 5). Data presented as mean ± SD (*P < 0.05; **P < 0.01; ***P < 0.001).

Since TNF-α has been reported to interacts with interferon signaling and ISGs are the ultimate antiviral effectors of the interferon cascade, we thus attempted to investigate whether TNF-α alone has any effect on ISG transcription. Based on the knowledge that interferon induces ISG expression via the activation of the ISRE motifs within the promoters of ISGs, a Huh7 cell line stably harboring a ISRE-driven luciferase reporter was used [13]. As expected, IFN-α treatment induced a strong transactivation of ISRE-driven luciferase value (Fig. 1C). Surprisingly, TNF-α stimulation also provoked a strong transactivation of the ISRE transcription elements (Fig. 1D). This interesting result prompted us to investigate the relative expression level of a panel of well-studied antiviral ISGs by qRT-PCR. Consistently, treatment of TNF-α provoked the induction of most tested ISGs, ranging from 1.7 to 11.3 fold increase (Fig. 1E). These data demonstrate that TNF-α transactivates the ISRE motif, resulting in the induction of ISGs, which in turn mediate the antiviral effects of TNF-α against HCV and HEV.

Activation of ISRE transcription by TNF-α does not require interferon production

The fact that TNF-α can induce ISGs inspired us to investigate the straightforward possibility that TNF-α merely triggers the production of interferons. Interferon regulatory factor 1 (IRF1) was demonstrated to be important in a TNF-α triggered IFN-β autocrine loop in primary macrophage cells [14]. To dissect whether a similar mechanism exist in our experiment system, we first studied the potential involvement of IRF1. Lentiviral vector was used to overexpress IRF1 in Huh7 based ISRE-driven luciferase reporter cells and the successful overexpression of IRF1 was confirmed at both mRNA and protein levels (Fig. 2A, B). IRF1 overexpression significantly increased ISRE-regulated luciferase activity (Fig. 2C). Surprisingly, the combination of IRF1 overexpression and TNF-α induced a strong additive ISRE activation (Fig. 2C). Furthermore, stable IRF1 knockdown by lentiviral RNAi (Fig. 2D, E) had no significant effect on TNF-α induced ISRE activation (Fig. 2F). In addition, the involvement of another interferon regulatory factor, IRF7, was also examined via loss-of-function assay. TNF-α induced ISRE activation was not affected even upon the efficient IRF7 knockdown (Supplementary Figure 1A-C). These results suggest that TNF-α triggered ISRE activation is independent of IRF1 and IRF7.

We next investigated the effects of TNF-α on gene expression of type I interferons. As determined by qRT-PCR, the constitutive expression levels of IFN-α and β1 in Huh7 cells are rather low, compared to the reference genes GAPDH and RP2 (Fig. 2G). Moreover, TNF-α treatment did not significantly increase IFN-α and IFN-β1 mRNA levels (Fig. 2H). This is consistent with a previous study showing that the Huh7 cell line responds to interferon but does not produce interferon [15]. These data collectively indicate that activation of ISRE transcription by TNF-α does not require interferon production in our model system.

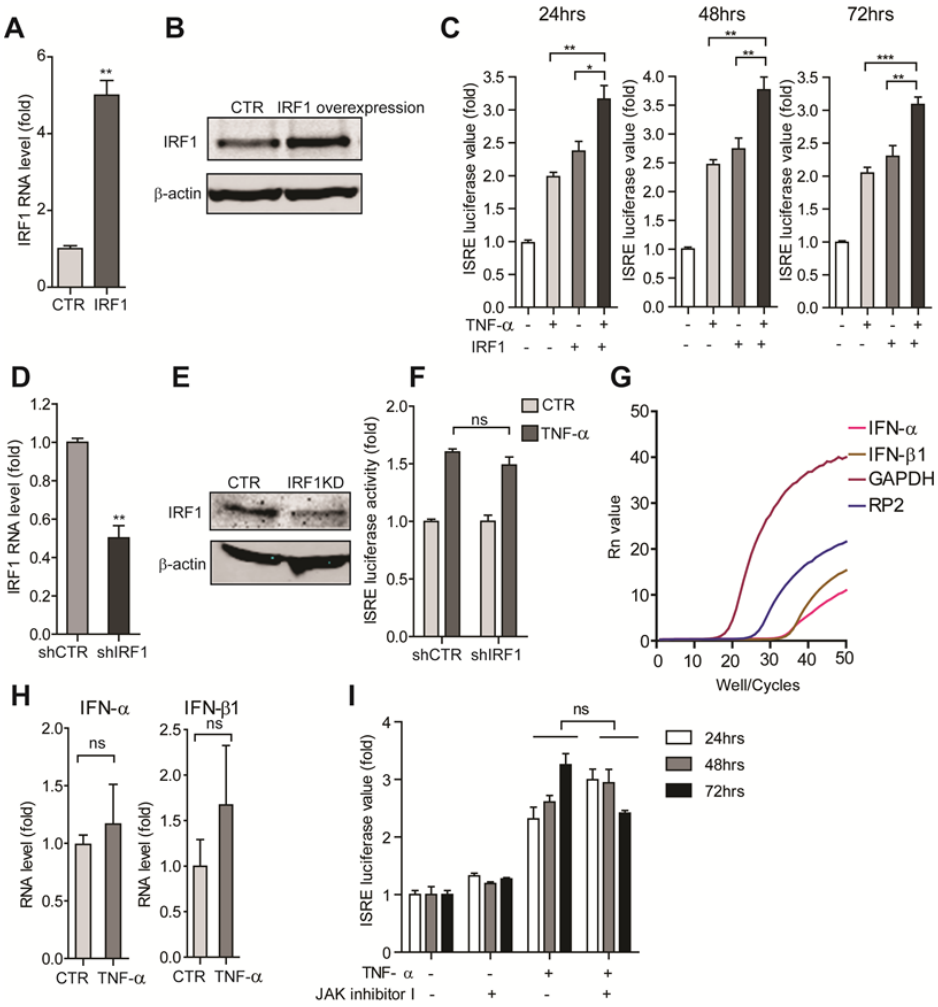

Figure 2: Activation of ISRE transcription by TNF-α does not require interferon production and the JAK-STAT signaling. (A) qRT-PCR analysis of IRF1 overexpression by lentiviral vectors in the Huh7 based ISRE luciferase reporter cells. Compared to the control vector transduced cells, the IRF1 lentiviral vector showed strong IRF1 induction on RNA level. (B) Western blot analysis confirmed the successful overexpression of IRF1 by lentiviral vectors in the Huh7 based ISRE luciferase reporter cells. (C) In the Huh7 cell-based ISRE luciferase reporter cells, the combination of IRF1 overexpression and TNF-α induced a strong additive ISRE activation as measured at 3 different time points (n = 5). (D) qRT-PCR analysis of IRF1 knockdown by lentiviral shRNA vectors in the Huh7 based ISRE luciferase reporter cells. Compared to the control vector transduced cells, the IRF1 shRNA treated clones showed strong reduction of IRF1 RNA levels. (E) Western blot analysis confirmed the successful knockdown of IRF1 by lentiviral shRNA vectors in the Huh7 based ISRE luciferase reporter cells. (F) Knockdown of IRF1 in Huh7 based ISRE luciferase reporter cells did not block TNF-α induced ISRE-related luciferase activation (n = 4). (G) The relative IFN-α and β1 expression levels in Huh7 cells were determined by qRT-PCR. GAPDH and RP2 served as internal reference genes. (H) IFN-α and β1 expression levels in Huh7 cells were not up-regulated upon TNF-α treatment as measured by qRT-PCR (n = 6). (I) JAK inhibitor I (5 μM) did not abrogate TNF-α induced ISRE-related luciferase activation (n = 3 independent experiments with 2 - 3 replicates each). Data presented as mean ± SD (*P < 0.05; **P < 0.01; ***P < 0.001; ns, not significant).

TNF-α induced ISRE activation is independent of the JAK-STAT signaling

Classically, ISGs are induced by interferons via the JAK-STAT signaling. Following receptor activation by interferons, JAK1 phosphorylates STAT1 and Tyrosine kinase 2 (TYK2) phosphorylates STAT2. This provokes STAT1 and STAT2 dimerization and subsequent binding to IRF9 to form the ISGF3 complex. The ISGF3 complex translocates into the nucleus, binds to the ISRE motif [5'-CAGTTTCACTTTCC-3'] and drives the transcription of ISGs (Supplementary Figure 2A). To test whether activation of ISRE by TNF-α require JAK-STAT signaling, we first examined the role of JAKs. Strikingly, neither JAK inhibitor (an inhibitor of JAK1, JAK2, JAK3 and TYK2) nor Bayer-18 (a selective TYK2 inhibitor) abrogated TNF-α induced ISRE activation (Fig. 2I and Supplementary Figure 2B). Consistently, TNF-α induced ISG

expression was not affected by the treatment of JAK inhibitor I (Supplementary Figure 2D). In contrast, both IFN-α induce ISRE activation and ISG expression were largely blocked by JAK inhibitor I (Supplementary Figures 2C and 3A). Interestingly, the selective TYK2 inhibitor, Bayer-18, did not significantly affect IFN-α induced ISRE activation (Supplementary Figure 2C). This is consistent with a previous study, showing that TYK2 plays a restricted role in IFN-α signaling [16].

Furthermore, to see if TNF-α treatment has any effect on STATs activation and translocation, we examined the phosphorylation status of STAT1 at amino acid 701 (Y701P) and STAT2 at amino acid 690 (Y690), which are indispensable signature of STAT1 and STAT2 activation, respectively. WB results showed TNF-α treatment had no effects on the phosphorylation of both STAT1 and STAT2 at indicated sites (Fig. 3A, B). Confocal microscopy analysis also confirmed that IFN-α induced the activation and nuclear translocation of STAT1 and STAT2 via the phosphorylation at indicated sites, while TNF-α had no effects (Fig. 3C, D). To further exclude a role of STAT1 in TNF-α induced ISRE activation, lentiviral RNAi was used to knockdown STAT1. The stable STAT1 knockdown (Fig. 3E, F) had no effect on both TNF-α induced ISRE activation and ISG expression (Fig. 3G, H). Collectively, TNF-α triggered ISRE activation is totally independent of STAT1.

In addition, the role of IRF9 was also verified, which is a key downstream element of interferon pathway. IRF9 was up-regulated and translocated into cell nucleus upon IFN-α stimulation, whereas TNF-α stimulation did not induce the translocation of IRF9 into cell nucleus (Supplementary Figure 3B). These results collectively demonstrate that TNF-α induced ISRE activation is independent of the JAK-STAT signaling.

TNF-α activates ISRE via TNF receptor 1

TNF receptor (TNFR) is the important upstream component in TNF-α induced signaling transduction. TNF acts through two receptors, TNFR1 and TNFR2. TNFR1 is the major signaling receptor for TNF-α and is expressed by all human tissues, while TNFR2 is mostly expressed in immune cells and mediates limited biological responses [17]. In light of the fact that TNF-α is capable of activating ISG transcription, we sought to determine whether this action of TNF-α was mediated via TNFR. For this, the ISRE reporter cell line was transduced with integrating lentiviral RNAi vectors to silence TNFR1, resulting in a profound down-regulation of TNFR1 expression (Fig. 4A). As expected, IFN-α induced ISRE activation was not influenced (Fig. 4B), but TNF-α induced ISRE luciferase activity was largely abrogated in TNFR1 knockdown cells when compared to control cells (Fig. 4C). Consistently, the induction of ISGs by TNF-α was also blocked by TNFR1 knockdown (Supplementary Figure 4A).

To further confirm these results, the clinically widely used drug for rheumatoid arthritis patients and Crohn's disease, Humira (adalimumab), was used. Humira binds specifically to TNF-α and blocks its interaction with TNF receptors. As expected, Humira effectively blocks TNF-α induced activation of NF-κB luciferase activity (Fig. 5A), NF-κB activity being a well-known downstream effect of TNF-α receptor ligation. Importantly, both TNF-α induced ISRE luciferase activity and ISG expression were also abrogated by Humira treatment (Fig. 5B, C). This effect was not limited to Huh7 cells, but also observed in a human lung cell line, A549 (Supplementary Figure 4B). More relevantly, Humira totally abolished TNF-α mediated antiviral effect against HCV and HEV (Fig. 5D, E), providing a possible explanation for the high risk of infection in patients treated with TNF-α inhibitors. Next, we collected serum samples from anti-TNF-α treatment naive Crohn's disease patients and measured

the serum TNF-α levels by ELISA. 3 serum samples with high TNF-α levels were selected to treat Huh7 based ISRE-driven luciferase reporter cells (Fig. 5F). Consistently, all 3 serum samples exerted higher ISRE activity compared to control serum sample (Fig. 5F, right). Furthermore, Humira decreased the serum induced ISRE activity (Supplementary Figure 4C). More interestingly, serum samples with higher TNF-α levels inhibited HCV-related luciferase activity compared to control serum sample (Supplementary Figure 4D). Collectively, these results demonstrate that TNF-α acts via its receptor to activate ISG transcription and exerts antiviral activity, which can be blocked by clinically used TNF-α inhibitor.

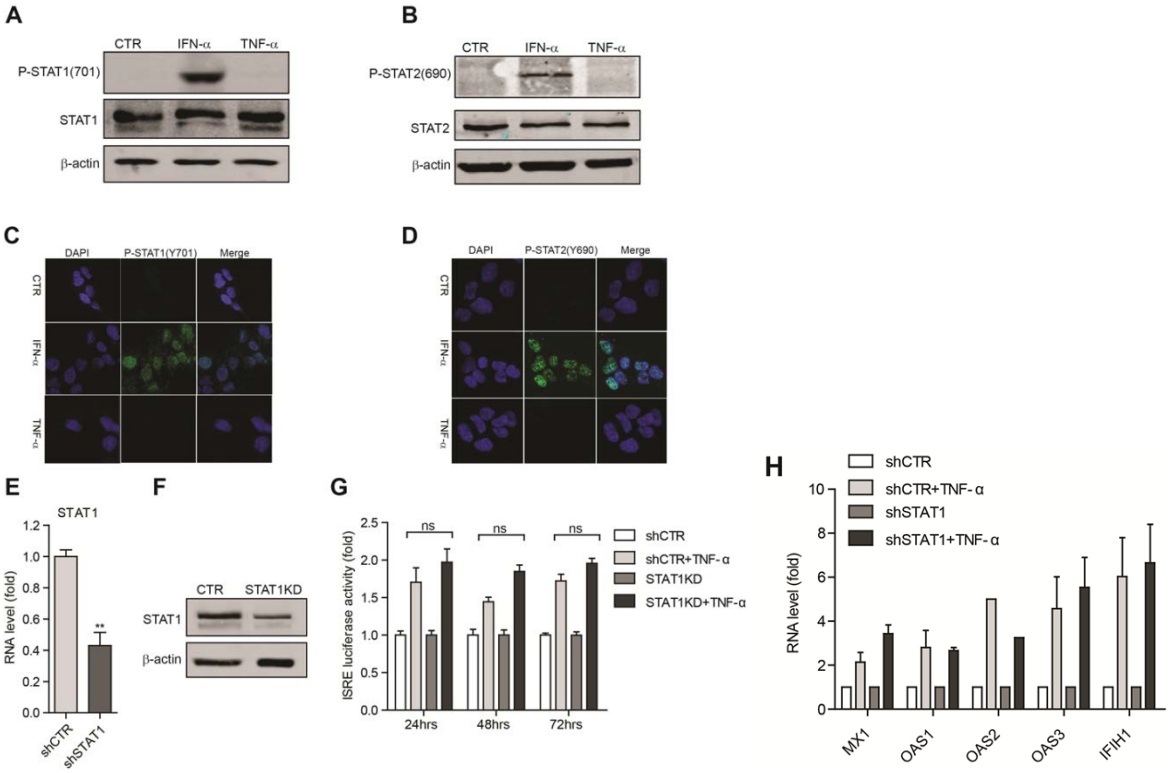

Figure 3: TNF-α activates ISRE in a STAT1 independent manner. (A) Western blot analysis of total STAT1 and phosphorylated STAT1 (Y701P) protein levels under the treatment of TNF-α (100 ng/mL), IFN-α (1000 IU/mL). (B) Same as (A) for the detection of total STAT2 and phosphorylated STAT2 (Y690P) protein levels under the treatment of TNF-α, IFN-α. (C) Confocal microscopy analysis of phosphorylated STAT1 (Y701P) localization in Huh7 cells treated with IFN-α or TNF-α. STAT1 was phosphorylated and translocated to the nucleus upon IFN-α, but not TNF-α treatment. Phosphorylated STAT1 (Y701P) antibody (green). Nuclei were visualized by DAPI (blue). (D) Same as (C) for the detection and localization of phosphorylated STAT2 (Y690P). (E) qRT-PCR confirmed the successful STAT1 knockdown by lentiviral shRNA vectors in the Huh7 based ISRE luciferase reporter cells. (F) Western blot analysis confirmed the successful knockdown of STAT1 by lentiviral shRNA vectors in the Huh7 based ISRE luciferase reporter cells. (G) STAT1 knockdown had no significant influence on TNF-α induced ISRE-related luciferase activation as measured at 3 different time points (n = 3 independent experiments with 2 -3 replicates each). (H) STAT1 knockdown exerts no effect on TNF-α induced ISG expression as measured by qRT-PCR (n = 3).

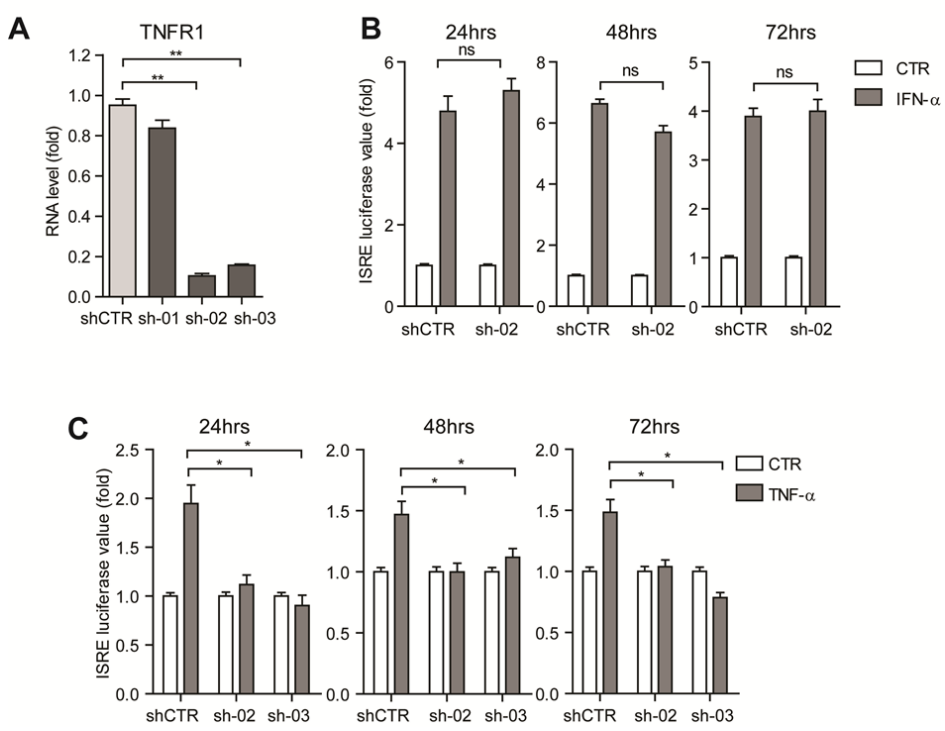

Figure 4: TNF-α activates ISRE via TNF receptor I.

(A) qRT-PCR analysis of TNFR1 knockdown by lentiviral shRNA vectors in the Huh7 based ISRE luciferase reporter cells. Compared to the control vector transduced cells, the two shRNA treated clones (sh-02 and sh-03) showed strong reduction of TNFR1 RNA levels. (B) TNFR1 knockdown had no significant influence on IFN-α induced ISRE-related luciferase activation as measured at 3 different time points (n = 3 independent experiments with 2 - 3 replicates each). (C) TNFR1 knockdown blocked TNF-α induced ISRE-related luciferase activation as measured at 3 different time points (n = 3 independent experiments with 2 - 3 replicates each).

TNF-α mediates the activation of ISRE through NF-κB signaling

Activation of NF-κB signaling is one of the most important canonical responses to the stimulation of TNF-α. Following TNF receptor activation by TNF-α, inhibitor of kappa B (IκB) proteins undergo phosphorylation dependent ubiquitination and degradation, resulting in the activation and translocation of NF-κB dimers into the cell nucleus. In the cell nucleus, NF-κB dimers bind to the specific NF-κB motifs, [5'-GGGAA/CTTTCC-3'], within the promoter regions driving the expression of NF-κB target genes (Supplementary Figure 5A). Because some studies have reported that TNF-α can also increase the transcriptional activity of activator protein-1 (AP-1) in some specific cell types [18, 19], we thus created Huh7 based stable NF-κB or AP-1 driven luciferase reporter cell lines, respectively. As shown in Supplementary Figure 5B, stimulation with TNF-α led to strong activation of NF-κB luciferase activity, but no significant effect on AP-1 activity. Therefore, we only focused on NF-κB signaling for the following investigation.

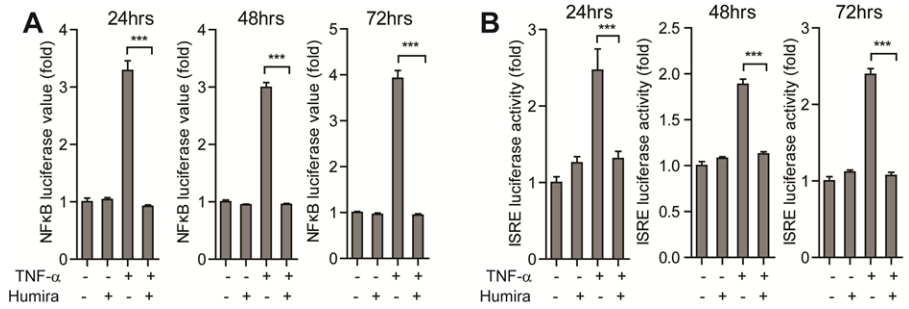

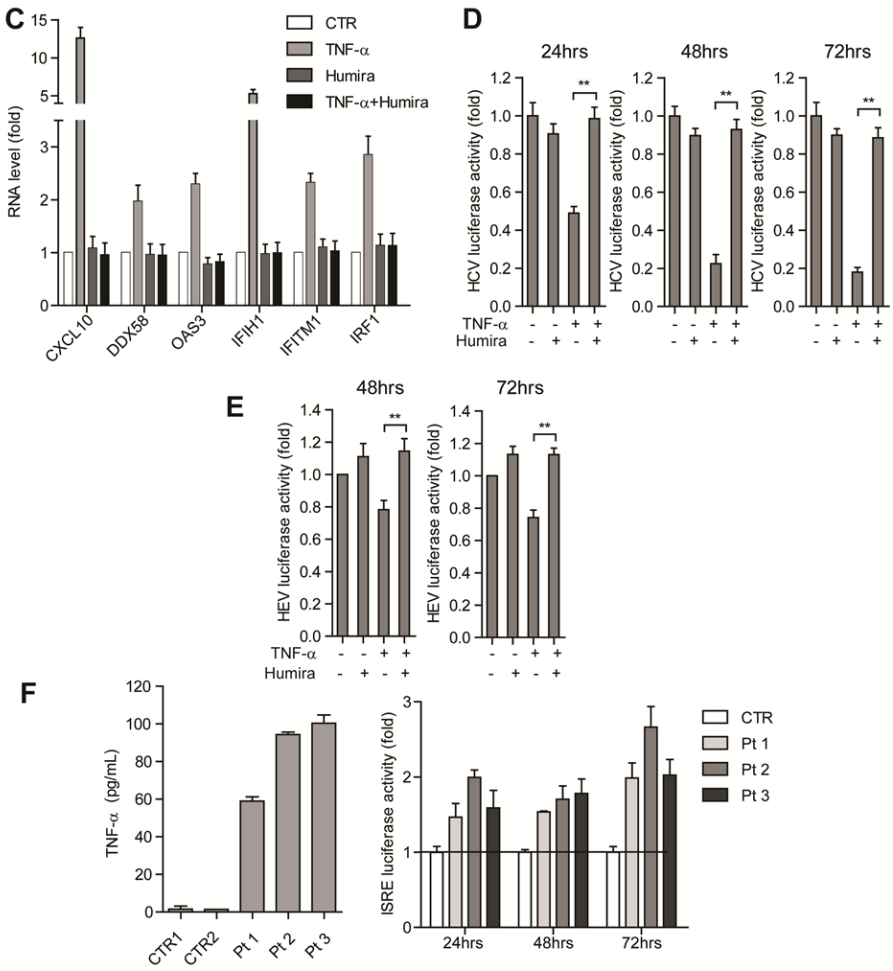

Figure 5: Both TNF-α induced ISG expression and antiviral activity against HCV and HEV were abrogated by its inhibitor Humira. (A) In the Huh7 cell-based NF-κB luciferase reporter cells, the TNF-α inhibitor, Humira, abrogated TNF-α induced NF-κB-related luciferase activation as measured at 3 different time points (n = 3 independent experiments with 2 - 3 replicates each). (B) Same as (A) for the Huh7 cell-based ISRE luciferase reporter cells. (C) In Huh7 cells, the TNF-α inhibitor, Humira, abrogated TNF-α induced ISG expression as measured by qRT-PCR (n = 4). (D) In the Huh7 cell-based subgenomic HCV replicon, Humira abrogated the TNF-α induced anti-HCV effect as measured at 3 different time points (n = 3 independent experiments with 2 - 3 replicates each). (E) Same as (D) for Huh7 cell-based subgenomic HEV replicon. (F) TNF-α levels in serum samples collected from anti-TNF-α treatment naive Crohn's disease patients were measured by ELISA kit (left). Serum samples with higher TNF-α levels showed stronger ISRE-related luciferase activity compared with control serum as measured at 3 different time points. Data presented as mean ± SD. (*P < 0.05; **P < 0.01; ***P < 0.001; ns, not significant).

The NF-κB complex is the endpoint of its signal transduction, which comprises the heterodimeric RelA (P65)-P50 complex. Indeed, unstimulated cells display little nuclear RelA, but the RelA protein level in the cell nucleus was substantially elevated following TNF-α stimulation (Fig. 6A). Thus, to dissect the role of the RelA (P65)-P50 complex in TNF-α induced ISRE activation, the Huh7 ISRE reporter cell line was transduced with integrating lentiviral RNAi vectors to silence RelA (P65), resulting in profound down-regulation of RelA expression (Fig. 6B). Consistently, TNF-α induced ISRE

luciferase activity and ISG expression was largely demolished in RelA knockdown cells when compared with control cells (Fig. 6C, D). On the contrary, IFN-α induced ISRE activation was not affected (Fig. 6E). Thus, NF-κB signaling appears to be essential for TNF-α mediated ISRE activation.

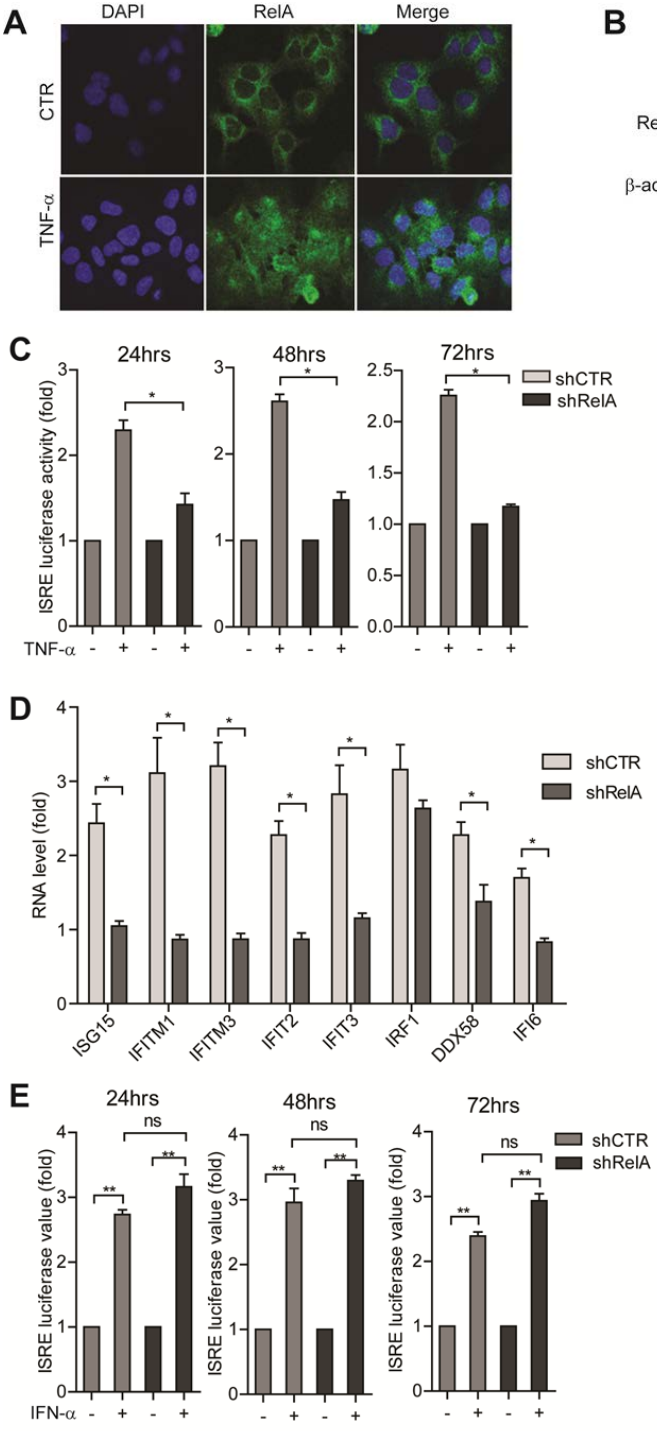

Figure 6: TNF-α mediates the induction of ISRE by activation of the NF-κB signaling. (A) Confocal microscopy analysis of RelA induction and localization in Huh7 cells treated with TNF-α. RelA was induced and translocated to the nucleus upon TNF-α treatment. RelA antibody (green). Nuclei were visualized by DAPI (blue). (B) Western blot analysis confirmed the successful knockdown of RelA by lentiviral shRNA vectors in the Huh7 based ISRE luciferase reporter cells. (C) RelA knockdown largely blocked TNF-α induced ISRE-related luciferase activation as measured at 3 different time points (n = 3 independent experiments with 2 - 3 replicates each). (D) RelA knockdown largely blocked TNF-α induced ISG expression as measured by qRT-PCR (n = 4). (E) RelA knockdown has no significant influence on IFN-α induced ISRE-related luciferase activation as measured at 3 different time points (n = 3 independent experiments with 2 - 3 replicates each). Data presented as mean ± SD (*P < 0.05; **P < 0.01; ***P < 0.001; ns, not significant).

The NF-κB complex directly binds to ISRE and drives its transcriptional activity

Upon TNF-α stimulation and signaling activation, the transcription factor complex, NF-κB, can directly bind to a sequence specific motif [5'-GGGAA/CTTTCC-3'] to promote target gene transcription [13, 20-22]. The puzzling role of NF-κB in the transactivation of ISRE led us to perform an *in silico* analysis

comparing the ISRE motif and the NF-κB DNA binding site. Surprisingly, we identified a partial consensus sequence region in common within these two motifs (Fig. 7A). We thus hypothesized that NF-κB might bind to this consensus sequence within the ISRE motif to drive transcription of corresponding ISGs. To test this hypothesis, we retrieved genome wide RelA and STAT1 (positive control) ChIP-seq data from the ENCODE ChIP-seq Experiment Matrix database. ChIP-seq datasets were processed and analyzed. Confirming our hypothesis, we found that RelA showed a similar genome-wide binding pattern with STAT1. For a large cohort of genes, RelA overlapped with STAT1 in their gene binding site (Fig. 7B, left). To be more specifically, we further analyzed the RelA and STAT1 binding sites that were within 1 kb of a transcription start site. This region is frequently located at the site of the promoter. Consistently, RelA still overlaps with STAT1 in the specific binding sites near gene transcription start sites. Since most genes bound and regulated by STAT1 are ISGs, this indicates that RelA also possesses the ability to bind and regulate a large cohort of ISGs. Then we analyzed RelA binding on a list of well-established antiviral ISGs. Convincingly, RelA shows strong and specific binding on the promoters of indicated ISGs, while the rabbit-IgG (negative control) shows no significant binding (Fig. 7C). To further confirm that NF-κB binds to the consensus sequence within the ISRE motif to drive corresponding ISG transcription, we mutated the consensus nucleotide sequence within the ISRE motif based on the lentiviral transcriptional reporter vector expressing the *firefly* luciferase gene driven by multiple ISREs. In theory, RelA will not be able to bind to this mutant ISRE sequence (Supplementary Figure 6). Huh7 cells were transduced with this vector to create a stable reporter cell line. As expected, TNF-α failed to activate this mutated ISRE (Fig. 7D). Hence, NF-κB can directly bind to the ISRE motif and activate its transcriptional activity.

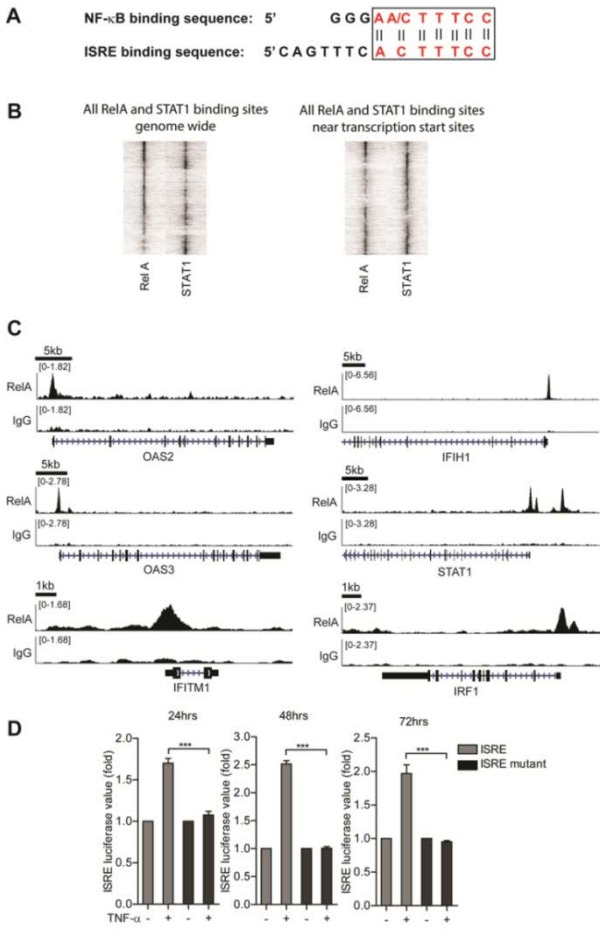

Figure 7: The NF-κB complex directly binds to ISRE and drives its transcriptional activity. (A) NF-κB and ISRE sequence specific binding regions. Their consensus nucleotides are labeled in red color, and the consensus region is enclosed by the rectangular box. (B) Heatmaps display the normalized ChIP-seq reads representing the binding intensity of STAT1 and RelA. Displayed are 8 kb regions centered on the summits of significant STAT1 and/or RelA binding sites. The heatmap are clustered for the STAT1 and RelA binding signal based on the central 0.5 kb of the heatmap. left) Heatmaps of all significant STAT1 and RelA binding sites (n = 13367). right) Heatmap of all significant STAT1 and RelA binding sites that are within 1 kb of a transcription start site (n = 4545). (C) Binding of RelA to the promoters of the indicated ISGs. Sequence reads from anti-RelA ChIP-seq or rabbit-IgG-control were plotted relative to chromosomal position. Genome location of corresponding ISGs is shown beneath the track signaling. RelA shows strong and specific binding on the promoters of indicated ISGs, while the rabbit-IgG, serving as negative control, shows no significant binding. (D) In the Huh7 cell-based mutant ISRE luciferase reporter cells, TNF-α did not induce mutant ISRE related luciferase activation as measured at 3 different time points (n = 3 independent experiments with 2–3 replicates each). Data presented as mean ± SD (*P < 0.05; **P < 0.01; ***P < 0.001; ns, not significant).

TNF-α cooperates with IFN-α in ISG induction and antiviral action

Because of the distinct signaling cascades that finally converge the transcription of antiviral ISGs by TNF-α and interferons, we further investigated the combinatory effects of TNF-α with IFN-α on ISG induction and antiviral action. Thus, we quantified the expression levels of a list of well-known antiviral ISGs in the Huh7 cell line with treatment of TNF-α, IFN-α or a combination thereof. Both TNF-α and IFN-α can induce significant up-regulation of tested ISGs, and their combination resulted in a strong additive induction of ISGs (Fig. 8A).

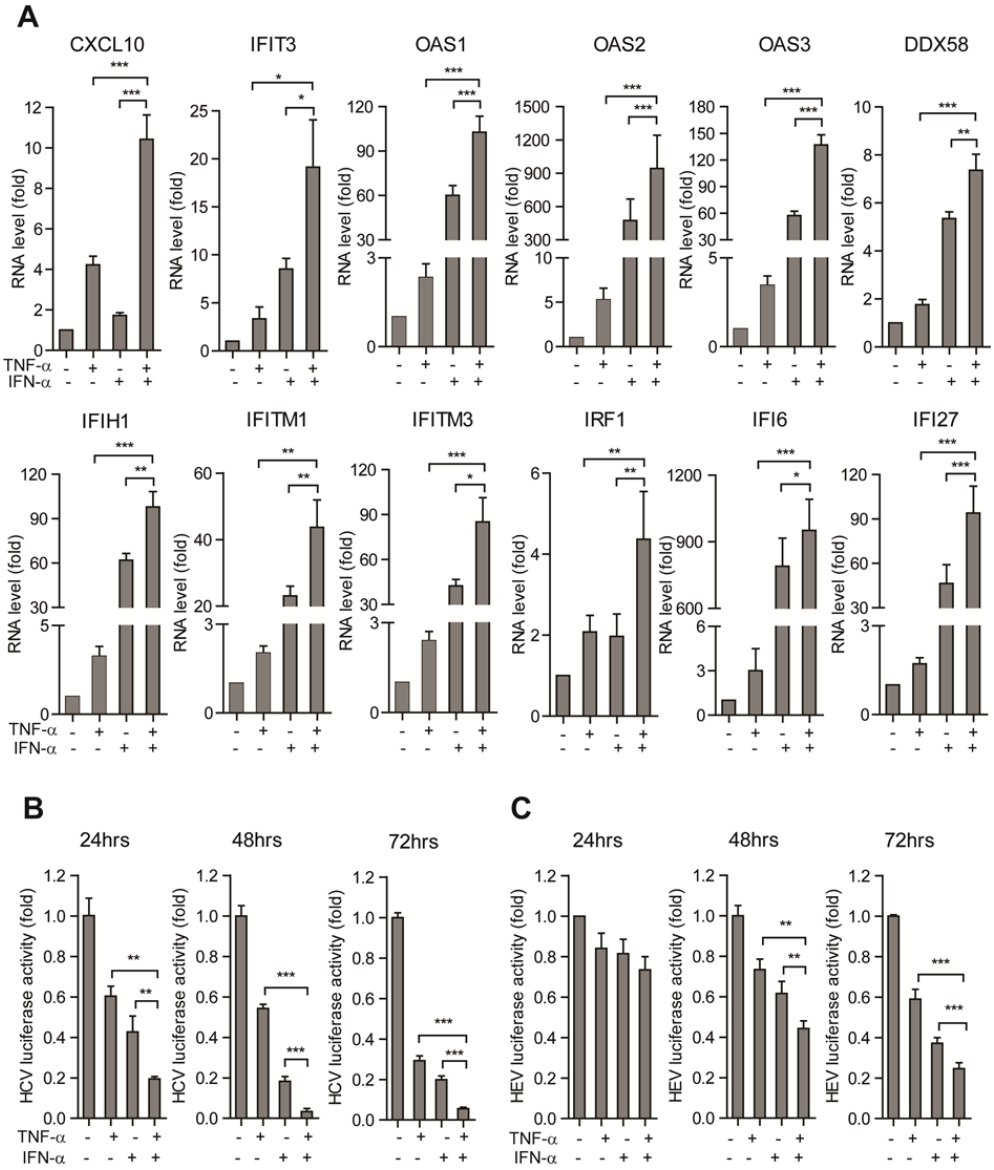

Figure 8: TNF-α cooperates with IFN-α in ISG induction and antiviral action. (A) In the Huh7 cells, the combination of TNF-α and IFN-α induced a strong additive ISG expression compared with treatment of either TNF-α or IFN-α alone as measured by qRT-PCR (n = 6). (B) In the Huh7 cell-based subgenomic HCV replicon model, the combination of TNF-α and IFN-α induced a strong additive anti-HCV effect compared with treatment of either TNF-α or IFN-α alone as measured at 3 different time (n = 3 independent experiments with 2 - 3 replicates each). (C) Same as (B) for the Huh7 cell-based subgenomic HEV replicon model.

Consistent with a previous publication [23], our results of ISG antiviral assay (Supplementary Figure 7) again highlight the important antiviral role of ISGs. Thus, the cooperation in ISG induction

prompted us to test whether an additive antiviral effect can be achieved with the combination of TNF-α and IFN-α. Hence, we employed the Huh7 cell line based HCV or HEV replicon luciferase reporter as the cell models for the test. As shown in Fig. 8B and 8C, the combination of TNF-α and IFN-α resulted in additive antiviral effects in both HCV and HEV replicon models. Thus, TNF-α cooperates with IFN-α in ISG induction, explaining their additive antiviral effects against HCV and HEV as we observed.

Discussion

TNF-α is a cytokine within the TNF superfamily, which acts as a central mediator of inflammation and immune regulations. Although TNF-α was first noted for its role in the killing of tumor cells [24], it has pleiotropic functions that include the inflammatory response and host resistance to pathogens. Indeed, numerous studies have demonstrated the importance of TNF-α in protection against pathogens, including *Mycobacterium tuberculosis, Cryptococcus neoformans*, vesicular stomatitis virus, encephalomyocarditis virus, herpes simplex virus, influenza virus and hepatitis B virus [25-29]. Disordered TNF-α regulation may have a significant negative role in inflammation and pathogenesis. Based on this, TNF-α antagonists have been proven to be highly effective in the treatment of certain inflammatory diseases, such as rheumatoid arthritis [30], psoriatic arthritis [31], juvenile rheumatoid arthritis [32], and Crohn's disease [33]. Several TNF-α inhibitors have been approved for the treatment of these inflammatory illnesses by the US Food and Drug Administration (FDA). Contradictory, many studies have demonstrated an increased risk of opportunistic infections and difficulty in clearing infections once they develop in patients treated with TNF-α inhibitors, such as HBV or HCV infection [34-36]. Our experimental results showing that clinically used anti-TNF-α inhibitors can totally abrogate the antiviral activity of TNF-α appear to support those clinical observations and highlight the primary role of TNF-α in host defense against infections.

As a first line defense, TNF-α and type I interferons are induced by microbial stimuli and mediate innate immune responses. Despite the fact that cells at sites of infection are continuously exposed to both cytokines, the interactions between TNF-α and interferons remain under investigated [37]. Although previous studies have reported that TNF-α interacts with antiviral interferon signaling and regulates ISG expression in the setting of different virus infections [8-10], the molecular mechanisms behind these interactions have not been delineated. In this study, we demonstrated that the activation of NF-κB signaling by TNF-α was able to directly transactivate the ISRE motif, resulting in the induction of antiviral ISGs. This whole process is independent of IFN production and the canonical JAK-STAT cascade, but relies on TNF-α induced NF-κB activity. NF-κB is a homo- or heterodimeric complex formed by the Rel-like domain-containing proteins: RelA (P65), RelB, c-Rel, P50 and P52 and the heterodimeric RelA (P65)-P50 complex appear to be the most abundant one. The dimers bind to the sequence specific NF-κB response element in the promoter region of their target genes to regulate transcription. To our surprise, *in silico* analysis discovered a consensus nucleotide sequence shared by the ISRE motif and NF-κB DNA binding site. ChIP-seq data analysis reveals RelA (P65) can directly bind to the promoter region of a large cohort of ISGs. Our loss-of-function and mutagenesis assay further confirmed that NF-κB could directly drive ISRE-controlled gene transcription. Since NF-κB is also the key downstream effector of most Toll-like

receptors (TLR), this novel mechanism may also partially explain the antiviral activities of TLR agonists in clinic, such as the TLR7 agonists, which are being therapeutically targeted and explored for HCV treatment in clinic trial [38].

More excitingly, TNF-α not only activates antiviral ISGs transcription, but also cooperates with IFN-α, explaining the additive antiviral outcome of their combination. This highlights the important facts that different cytokines orchestrate innate immune responses by activating signaling cascades to protect against infection efficiently.

In conclusion, we revealed a novel antiviral mechanism of TNF-α. TNF-α, via the activation of NF-κB cascade, can drive the transcription of antiviral ISGs through direct binding of ISREs. This antiviral mechanism may provide clues for tackling the high rise of infections caused by TNF-α inhibitor treatment in patients. More interestingly, TNF-α also acts cooperatively with IFN-α in antiviral ISGs induction to exert additive antiviral effects. These findings not only provide new clues for understanding virus-host interactions but also assign a novel function of the canonical NF-κB pathway.

Materials and Methods

The HCV subgenomic replicon comprised Huh7 cells containing a subgenomic HCV bicistronic replicon (1389/NS3-3 V/LucUbiNeo-ET) linked to the *firefly* luciferase reporter gene were maintained with 250 μg/mL G418 (Sigma, Zwijndrecht, the Netherlands). The HEV subgenomic model was based on Huh7 cells containing the subgenomic HEV sequence (Kernow-C1 p6/luc) coupled to a *Gaussia* luciferase reporter gene. Lentiviral pLK.O knockdown vectors (Sigma-Aldrich) targeting IRF1, TNFR1, RelA were obtained from the Erasmus Biomics Center and produced in HEK293T cells as previously described [39]. The use of serum samples from IBD patients was approved by the Medical Ethical Committee of the Erasmus Medical Center (Medisch Ethische Toetsings Commissie Erasmus MC), and the informed consent was obtained from all subjects. All methods were carried out in accordance with the approved guidelines. For more details, see Supplementary Information.

Acknowledgements

The authors gratefully thank Dr. Suzanne U. Emerson (National Institute of Allergy and Infectious Diseases, NIH, USA) for generously providing the plasmids to generate subgenomic HEV genomic RNA; Prof. Ralf Bartenschlager and Dr. Volker Lohmann (University of Heidelberg, Germany) for providing the HCV replicon cells; Prof. Dr. Charles M. Rice (the Rockefeller University) providing the overexpression lentiviral vector. The authors also would like to acknowledge the ENCODE Experiment Matrix for providing the RelA and STAT1 ChIP-seq dataset. This research is supported by the European Association for the Study of the Liver (EASL) for a Sheila Sherlock Fellowship (to Q. Pan), the Netherlands Organization for Scientific Research (NWO/ZonMw) for a VENI grant (No. 916-13-032) (to Q. Pan), the Dutch Digestive Foundation (MLDS) for a career development grant (No. CDG 1304) (to Q. Pan), the Daniel den Hoed Foundation for a Centennial Award fellowship (to Q. Pan), the Erasmus MC Mrace grant (to Q. Pan), the China Scholarship Council for funding PhD fellowships to W. Wang (201303250056), Y. Wang (201207720007), X. Zhou (201206150075), Y. Yin (201307720045)

and L. Xu (201306300027) and Indonesia Endowment Fund for Education (LPDP) PhD fellowship to Mohamad S. Hakim.

Supplementary Materials and Methods

Reagents

Recombinant human TNF-α (Peprotech, USA) and human IFN-α (Thermo Scientific, the Netherlands) was dissolved in PBS. Stocks of JAK inhibitor 1 (Santa Cruz Biotech, CA) and Bayer-18 (Synkinase, China) were dissolved in DMSO with a final concentration of 5 mg/mL. Antibodies phospho-STAT1 (Tyr701) (58D6, #9167), STAT1 (#9172), RelA (P65) (C22B4, #4764), IRF1 (D5E4), IRF7 (D2A1J), Anti-rabbit IgG(H+L), F(ab') 2 Fragment (Alexa Fluor 488 conjugate) and Anti-mouse IgG (H+L), F(ab')2 Fragment (Alexa Fluor® 488 Conjugate) were purchased from Cell Signaling Technology. IRF9 antibody was obtained from LSBio (Life Span BioSciences, Inc.). β-actin, STAT2 (sc-476), phospho-STAT2 (Tyr690) were purchased from Santa Cruz Biotechnology; anti-rabbit or anti-mouse IRDye-conjugated antibodies were used as secondary antibodies for western blotting (Stressgen, Victoria, BC, Canada).

Cell models

The HCV subgenomic replicon comprised Huh7 cells containing a subgenomic HCV bicistronic replicon (1389/NS3-3V/LucUbiNeo-ET) linked to the *firefly* luciferase reporter gene were maintained with 250 μg/mL G418 (Sigma, Zwijndrecht, the Netherlands). The HEV subgenomic model was based on Huh7 cells containing the subgenomic HEV sequence (Kernow-C1 p6/luc) coupled to a *Gaussia* luciferase reporter gene. Luciferase normalization cells (LV-PGK-Luc) were generated by transducing Huh7 cells with a lentiviral vector expressing the *firefly* luciferase gene under control of the human phosphoglycerate kinase (PGK) promoter. ISRE, NF-κB, AP-1 luciferase reporter cells were generated by transducing Huh7 cells with lentiviral vectors expressing the *firefly* luciferase gene under the control of the promoters containing the ISRE, NF-κB, AP-1 motifs, respectively (System Biosciences).

Gene knockdown or overexpression by lentiviral vectors

Lentiviral pLKO.1 knockdown vectors (Sigma-Aldrich) targeting IRF1, IRF7, STAT1, TNFR1, RelA (P65) were obtained from the Erasmus Biomics Center and produced in HEK293T cells. After a pilot study, the shRNA vectors exerting optimal gene knockdown were selected. Stable gene knockdown cells were generated after lentiviral vector transduction and puromycin (2 μg/mL; Sigma) selection. IRF1, IFI6 and DDX58 lentiviral overexpression vectors were a kind gift from Prof. Charles M. Rice, the Rockefeller University [23]. Meanwhile, two control vectors expressing reporter genes *Photinus pyralis* luciferase (Fluc) or Green fluorescent protein (GFP) were also used.

Measurement of luciferase activity

For *Gaussia* luciferase analysis, the activity of secreted luciferase in the cell culture medium was measured by BioLux® *Gaussia* Luciferase Flex Assay Kit (New England Biolabs) according to the

manufacturer's instructions. For *firefly* luciferase, luciferin potassium salt (100 mM; Sigma) was added to cells and incubated for 10 min at 37 °C The luciferase activity was quantified with a LumiStar Optima luminescence counter (BMG Lab Tech, Offenburg, Germany).

Quantitative real-time polymerase chain reaction

RNA was isolated with a Machery-NucleoSpin RNA II kit (Bioke, Leiden, The Netherlands) and quantified using a Nanodrop ND-1000 (Wilmington, DE, USA). cDNA was synthesized from total RNA using a cDNA Synthesis Kit (TAKARA BIO INC). The cDNA of all detected genes was amplified for 50 cycles and quantified with a SYBR-Green-based real-time PCR (Applied Biosystems) according to the manufacturer's instructions. GAPDH and RP2 were considered as reference genes to normalize gene expression. All the primer sequences are included in Supplemental Table 2.

Western Blot Assay

Cultured cells were lysed in Laemmli sample buffer containing 0.1 M DTT and heated 5 mins at 95 °C, followed by loading onto a 10% sodium dodecyl sulfate polyacrylamide gel and separation by electrophoresis. After 90 mins running at 120 V, proteins were electrophoretically transferred onto a polyvinylidene difluoride membrane (Invitrogen) for 1.5 hrs with an electric current of 250 mA. Subsequently, the membrane was blocked with a mixture of 2.5 mL blocking buffer (Odyssey) and 2.5 mL phosphate-buffered saline containing 0.05% Tween 20. It was followed by overnight incubation with primary antibodies (1: 1 000) at 4 °C. The membrane was washed 3 times followed by incubation for 1 h with IRDye-conjugated secondary antibody (1: 5 000). After washing 3 times, protein bands were detected with the Odyssey 3.0 Infrared Imaging System.

Enzyme-linked immunosorbent assay (ELISA)

Serum samples were collected and stored at -80 °C. TNF-α level was measured by an ELISA kit (eBioscience, USA) according to manufacturer's instructions. The absorbance was measured at 450 nm in an automatic microplate reader. Results were calculated based on a standard curve.

Confocal laser electroscope assay

Huh7 cells were seeded on glass coverslips. After 12 hrs, cells were washed with PBS, fixed in 4% PBS-buffered formalin for 10 mins and blocked with tween-milk-glycine medium (PBS, 0.05% tween, 5 g/L skim milk and 1.5 g/L glycine). Samples were incubated with primary antibodies overnight at 4 °C. Subsequently, samples were incubated with 1:1 000 dilutions of the anti-mouse IgG (H+L), F(ab')2 Fragment (Alexa Fluor® 488 Conjugate) or anti-rabbit IgG(H+L), F(ab') 2 Fragment (Alexa Fluor 488 conjugate) secondary antibodies. Nuclei were stained with DAPI (4, 6-diamidino-2-phenylindole; Invitrogen). Images were detected using confocal electroscope.

ChIP-seq data analysis

ChIP-seq datasets for STAT1 in Gm12878 cells and RelA in the TNFα stimulated Gm12878 cells were retrieved from the ENCODE database. ChIP-seq datasets were processed and mapped to hg38

reference genome as described [40]. ChIP-seq datasets with multiple replicates were merged. MACS 1.4.2 was used for peak calling and for the generation of binding profiles [41]. MACS was run with -p 1e-10, using the mock control of TNF-α stimulated cell as control dataset for both the STAT1 and RelA ChIP-seq. Heatmaps were generated based on a unified peak list. If the centers of two binding regions reported by MACS were 100 bp or less apart, they were unified to a single binding region. Heatmaps were normalized for each individual factor by calculating the RPM based on the sum of all reads displayed by the heatmap. RPM was log2 transformed and manhattan clustering was performed. The heatmap images were generated in R. The sequencing profiles were generated in the IGV browser [42].

Construction of mutant ISRE reporter cell line

Based on the sequence specific ISRE motif, a mutant version of ISRE was designed and synthesized (Forward: 5'-*aattc*AGTTTCGTCAAGTCTTTCAGTTTCGTCAAGTCTTTCAGTTTCGTCAAGTCTTTCAGTTTCGTCAAGTCTTT*a*-3'; Reverse: 5'-*ctagt*AAAGACTTGACGAAACTGAAAGACTTGACGAAACTGAAAGACTTGACGAAACTGAAAGACTTGACGAAACT*g*-3'), which shows no consensus sequence with the NF-κB motif. EcoRI and SpeI sites are included (shown in italics) to facilitate directional cloning into the pGreenFire Lenti-Reporter vector (System Biosciences). The recombinant plasmid was verified by restriction enzyme digestion and DNA sequencing. Stable mutant ISRE reporter cells were generated after lentiviral vector transduction and puromycin (2 μg/mL; Sigma) selection.

Statistical analysis

All results were presented as mean ± SD. Comparisons between groups were performed with Mann-Whitney test. Differences were considered significant at a P value less than 0.05.

Ethics Statement

The use of serum samples from IBD patients was approved by the Medical Ethical Committee of the Erasmus Medical Center (Medisch Ethische Toetsings Commissie Erasmus MC). The volunteers or patients agreed to participate by written informed consent.

Supplementary Data

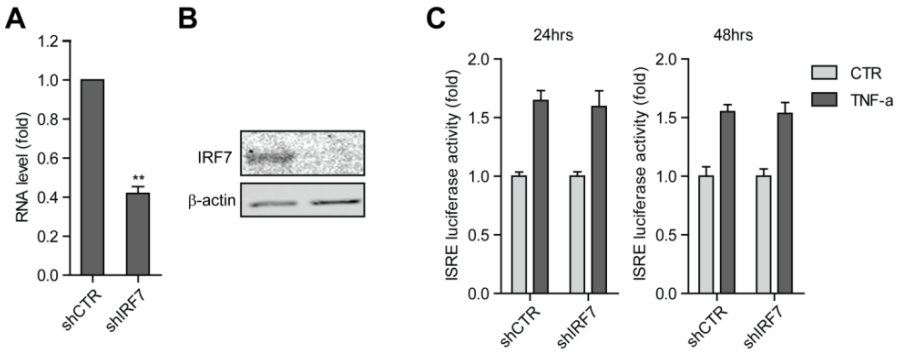

Figure S1. TNF-α induced ISRE activation is independent of IRF7. (A) qRT-PCR analysis of successful IRF7 knockdown by lentiviral shRNA vectors in the Huh7 based ISRE luciferase reporter cells. (B) Western blot analysis confirmed the successful knockdown of IRF7 by lentiviral shRNA vectors in the Huh7 based ISRE luciferase reporter cells. (C) IRF7 knockdown had no significant influence on TNF-α induced ISRE-related luciferase activation as measured at 2 different time points (n = 3 independent experiments with 2 - 3 replicates each).

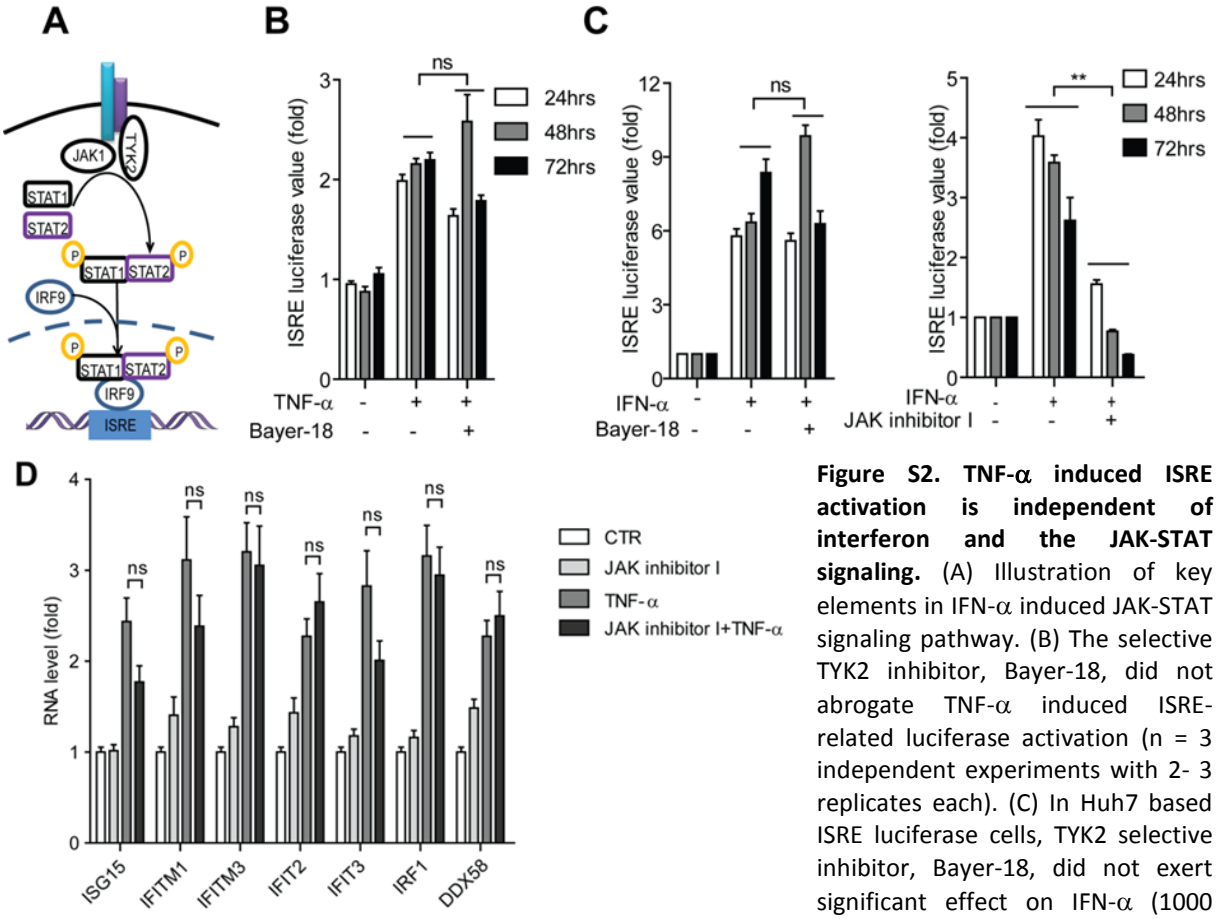

Figure S2. TNF-α induced ISRE activation is independent of interferon and the JAK-STAT signaling. (A) Illustration of key elements in IFN-α induced JAK-STAT signaling pathway. (B) The selective TYK2 inhibitor, Bayer-18, did not abrogate TNF-α induced ISRE-related luciferase activation (n = 3 independent experiments with 2- 3 replicates each). (C) In Huh7 based ISRE luciferase cells, TYK2 selective inhibitor, Bayer-18, did not exert significant effect on IFN-α (1000 IU/mL) induced ISRE-luciferase activity (left), while JAK inhibitor I (10 µM) abrogated IFN-α (1000 IU/mL) induced ISRE luciferase activity as measured at 24, 48 and 72 hrs (n = 3 independent experiments with 2 - 3 replicates each). (D) JAK inhibitor I exerts no significant influence on TNF-α induced ISG expression as measured by qRT-PCR. (n = 4).

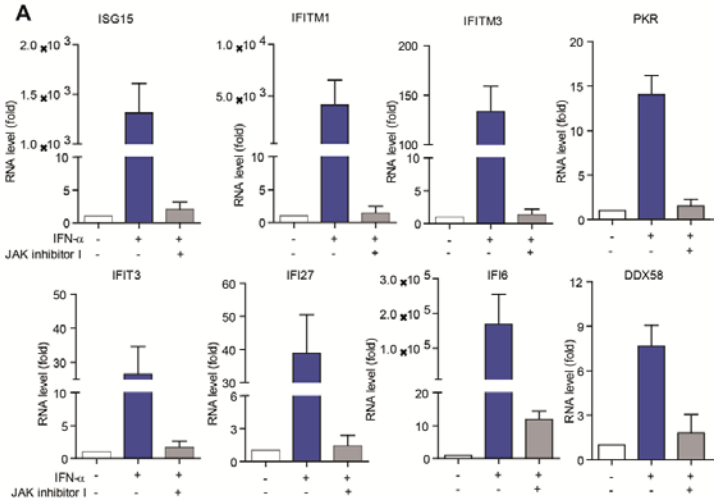

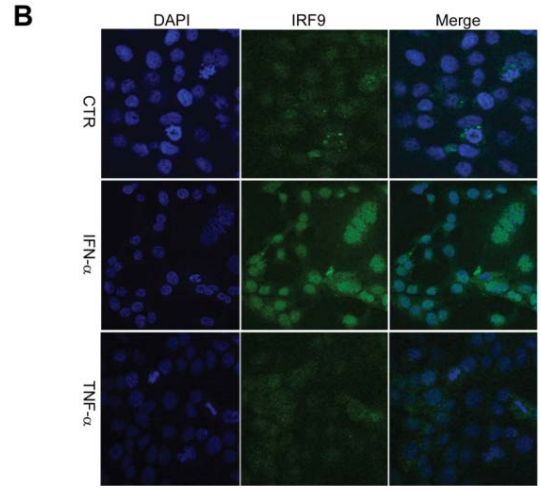

Figure S3. IFN-α induced ISRE activation depends on the JAK-STAT signaling. (A) In Huh7 cells, JAK inhibitor I (10 μM) abrogated IFN-α (1000 IU/mL) induced ISG expression as measured by qRT-PCR. (B) Confocal microscopy analysis of IRF9 localization in Huh7 cells treated with IFN-α or TNF-α. IRF9 was induced and translocated to the nucleus upon IFN-α, but not TNF-α treatment. IRF9 antibody (green). Nuclei were visualized by DAPI (blue).

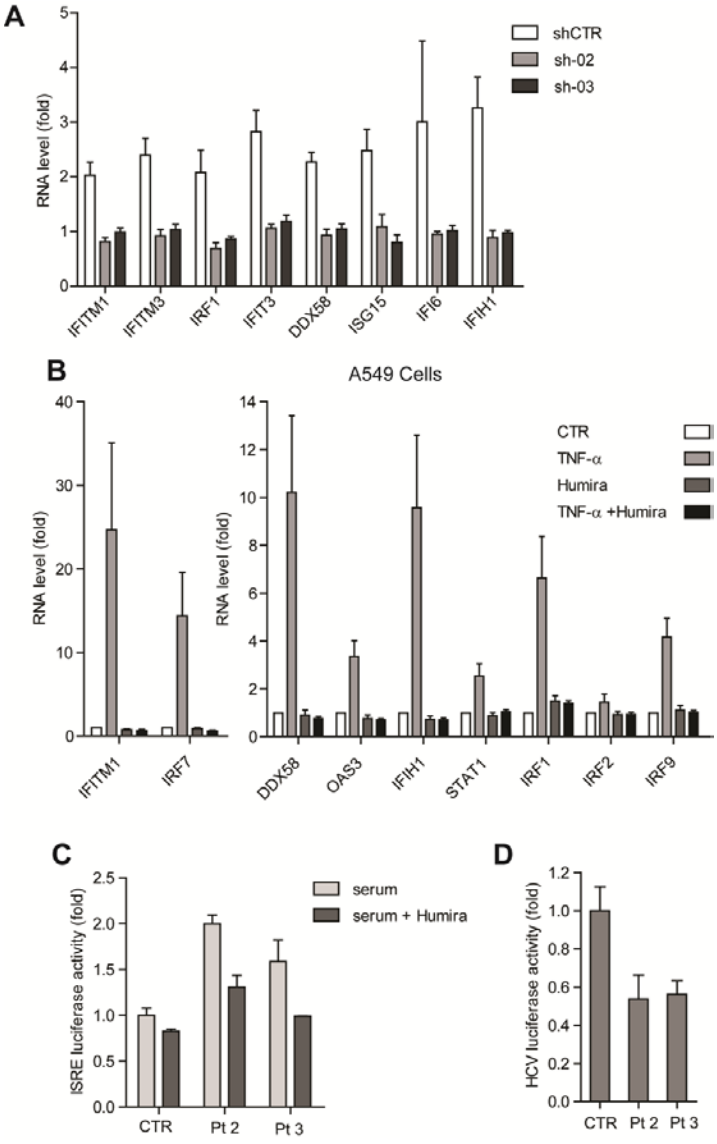

Figure S4. TNF-α activates ISRE via TNF receptor. (A) TNFR1 knockdown blocked TNF-α induced ISG expression as measured by qRT-PCR (n = 4). (B) In A549 cells, TNF-α inhibitor, Humira, abrogated TNF-α induced ISG expression as measured by qRT-PCR (n = 4). (C) Humira decreased serum samples (with higher TNF-α levels) induced ISRE-related luciferase activity. (D) Serum samples with higher TNF-α levels inhibited HCV-related luciferase activity compared with control serum.

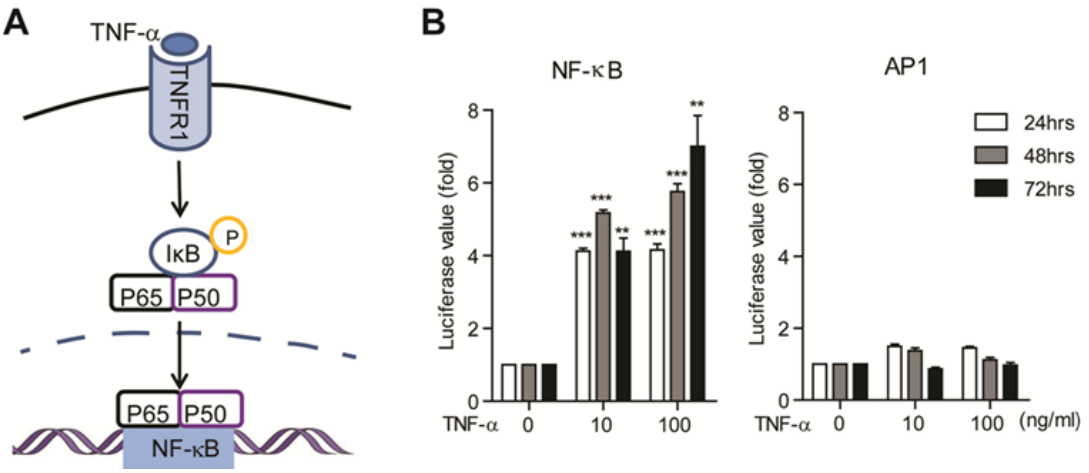

Figure S5. TNF-α efficiently activate NF-κB signaling pathway. (A) Illustration of key elements in TNF-αinduced NF-κB signaling pathway. (B) In the Huh7 cell-based NF-κB or AP1 luciferase reporter cells, TNF-α dose-dependently induced activation of NF-κB-related luciferase activity, while no significant effect on AP1-related luciferase activity as measured at 3 different time points (n = 3 independent experiments with 2 - 3 replicates each).

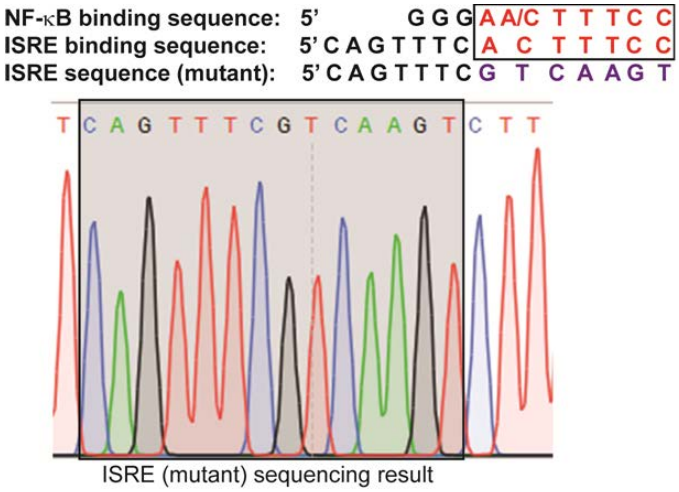

Figure S6. The nucleotide sequence of NF-κB, ISRE and the ISRE mutant binding regions. Their consensus nucleotides are labeled in red color, and the consensus region is marked in a rectangular box. The mutated nucleotides are shown in purple color. The ISRE (mutant) sequencing result is shown in the illustration below.

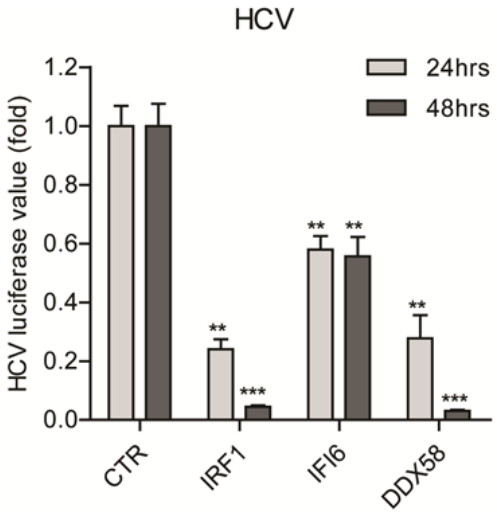

Fig. S7. ISG, *e.g.* IRF1, IFI6 or DDX58 exerts strong antiviral effect against HCV. Huh7 cell based HCV replicon luciferase reporter was transduced with integrating lentiviral vectors to overexpress ISG, *e.g.* IRF1, IFI6 or DDX58, showing strong antiviral potency against HCV.

References

1. Lin, F.C. and H.A. Young, Interferons: Success in anti-viral immunotherapy. *Cytokine Growth Factor Rev*, 2014. **25**(4): p. 369-76.
2. Pulit-Penaloza, J.A., S.V. Scherbik, and M.A. Brinton, Type 1 IFN-independent activation of a subset of interferon stimulated genes in West Nile virus Eg101-infected mouse cells. *Virology*, 2012. **425**(2): p. 82-94.
3. Mbanwi, A.N. and T.H. Watts, Costimulatory TNFR family members in control of viral infection: outstanding questions. *Semin Immunol*, 2014. **26**(3): p. 210-9.
4. Brenner, D., H. Blaser, and T.W. Mak, Regulation of tumour necrosis factor signalling: live or let die. *Nat Rev Immunol*, 2015. **15**(6): p. 362-74.
5. Nielsen, O.H., New strategies for treatment of inflammatory bowel disease. *Front Med (Lausanne)*, 2014. **1**: p. 3.
6. Murdaca, G., et al., Infection risk associated with anti-TNF-alpha agents: a review. *Expert Opin Drug Saf*, 2015. **14**(4): p. 571-82.
7. Pompili, M., et al., Tumor necrosis factor-alpha inhibitors and chronic hepatitis C: a comprehensive literature review. *World J Gastroenterol*, 2013. **19**(44): p. 7867-73.
8. Mestan, J., et al., Antiviral activity of tumour necrosis factor. Synergism with interferons and induction of oligo-2',5'-adenylate synthetase. *J Gen Virol*, 1988. **69 (Pt 12)**: p. 3113-20.
9. Lee, J., et al., TNF-alpha Induced by Hepatitis C Virus via TLR7 and TLR8 in Hepatocytes Supports Interferon Signaling via an Autocrine Mechanism. *PLoS Pathog*, 2015. **11**(5): p. e1004937.
10. Fink, K., et al., IFNbeta/TNFalpha synergism induces a non-canonical STAT2/IRF9-dependent pathway triggering a novel DUOX2 NADPH oxidase-mediated airway antiviral response. *Cell Res*, 2013. **23**(5): p. 673-90.
11. Bartee, E., et al., The addition of tumor necrosis factor plus beta interferon induces a novel synergistic antiviral state against poxviruses in primary human fibroblasts. *J Virol*, 2009. **83**(2): p. 498-511.
12. Devhare, P.B., et al., Analysis of antiviral response in human epithelial cells infected with hepatitis E virus. *PLoS One*, 2013. **8**(5): p. e63793.
13. Colin, L., et al., The AP-1 binding sites located in the pol gene intragenic regulatory region of HIV-1 are important for viral replication. *PLoS One*, 2011. **6**(4): p. e19084.
14. Yarilina, A., et al., TNF activates an IRF1-dependent autocrine loop leading to sustained expression of chemokines and STAT1-dependent type I interferon-response genes. *Nat Immunol*, 2008. **9**(4): p. 378-87.
15. Keskinen, P., et al., Impaired antiviral response in human hepatoma cells. *Virology*, 1999. **263**(2): p. 364-75.
16. Shimoda, K., et al., Tyk2 plays a restricted role in IFN alpha signaling, although it is required for IL-12-mediated T cell function. *Immunity*, 2000. **13**(4): p. 561-71.
17. Tartaglia, L.A., et al., The two different receptors for tumor necrosis factor mediate distinct cellular responses. *Proc Natl Acad Sci U S A*, 1991. **88**(20): p. 9292-6.
18. Westwick, J.K., et al., Tumor necrosis factor alpha stimulates AP-1 activity through prolonged activation of the c-Jun kinase. *J Biol Chem*, 1994. **269**(42): p. 26396-401.
19. Yin, Y., et al., JNK/AP-1 pathway is involved in tumor necrosis factor-alpha induced expression of vascular endothelial growth factor in MCF7 cells. *Biomed Pharmacother*, 2009. **63**(6): p. 429-35.
20. Wan, F. and M.J. Lenardo, Specification of DNA binding activity of NF-kappaB proteins. *Cold Spring Harb Perspect Biol*, 2009. **1**(4): p. a000067.
21. Hess, J., P. Angel, and M. Schorpp-Kistner, AP-1 subunits: quarrel and harmony among siblings. *J Cell Sci*, 2004. **117**(Pt 25): p. 5965-73.
22. Van Lint, C., A. Burny, and E. Verdin, The intragenic enhancer of human immunodeficiency virus type 1 contains functional AP-1 binding sites. *J Virol*, 1991. **65**(12): p. 7066-72.
23. Schoggins, J.W., et al., A diverse range of gene products are effectors of the type I interferon antiviral response. *Nature*, 2011. **472**(7344): p. 481-5.
24. Carswell, E.A., et al., An endotoxin-induced serum factor that causes necrosis of tumors. *Proc Natl Acad Sci U S A*, 1975. **72**(9): p. 3666-70.
25. Flynn, J.L., et al., Tumor necrosis factor-alpha is required in the protective immune response against Mycobacterium tuberculosis in mice. *Immunity*, 1995. **2**(6): p. 561-72.
26. Huffnagle, G.B., et al., Afferent phase production of TNF-alpha is required for the development of protective T cell immunity to Cryptococcus neoformans. *J Immunol*, 1996. **157**(10): p. 4529-36.
27. Mestan, J., et al., Antiviral effects of recombinant tumour necrosis factor in vitro. *Nature*, 1986. **323**(6091): p. 816-9.
28. Seo, S.H. and R.G. Webster, Tumor necrosis factor alpha exerts powerful anti-influenza virus effects in lung epithelial cells. *J Virol*, 2002. **76**(3): p. 1071-6.
29. Tzeng, H.T., et al., Tumor necrosis factor-alpha induced by hepatitis B virus core mediating the immune response for hepatitis B viral clearance in mice model. *PLoS One*, 2014. **9**(7): p. e103008.
30. Furst, D.E., et al., Adalimumab, a fully human anti tumor necrosis factor-alpha monoclonal antibody, and concomitant standard antirheumatic therapy for the treatment of rheumatoid arthritis: results of STAR (Safety Trial of Adalimumab in Rheumatoid Arthritis). *J Rheumatol*, 2003. **30**(12): p. 2563-71.
31. Mease, P.J., et al., Etanercept in the treatment of psoriatic arthritis and psoriasis: a randomised trial. *Lancet*, 2000. **356**(9227): p. 385-90.

32. Lovell, D.J., et al., Etanercept in children with polyarticular juvenile rheumatoid arthritis. Pediatric Rheumatology Collaborative Study Group. *N Engl J Med*, 2000. **342**(11): p. 763-9.
33. Present, D.H., et al., Infliximab for the treatment of fistulas in patients with Crohn's disease. *N Engl J Med*, 1999. **340**(18): p. 1398-405.
34. Kim, S.Y. and D.H. Solomon, Tumor necrosis factor blockade and the risk of viral infection. *Nat Rev Rheumatol*, 2010. **6**(3): p. 165-74.
35. Vigano, M., et al., Anti-TNF drugs in patients with hepatitis B or C virus infection: safety and clinical management. *Expert Opin Biol Ther*, 2012. **12**(2): p. 193-207.
36. Shale, M.J., et al., Review article: chronic viral infection in the anti-tumour necrosis factor therapy era in inflammatory bowel disease. *Aliment Pharmacol Ther*, 2010. **31**(1): p. 20-34.
37. Yarilina, A. and L.B. Ivashkiv, Type I interferon: a new player in TNF signaling. *Curr Dir Autoimmun*, 2010. **11**: p. 94-104.
38. Gearing, A.J., Targeting toll-like receptors for drug development: a summary of commercial approaches. *Immunol Cell Biol*, 2007. **85**(6): p. 490-4.
39. Pan, Q., et al., Combined antiviral activity of interferon-alpha and RNA interference directed against hepatitis C without affecting vector delivery and gene silencing. *J Mol Med (Berl)*, 2009. **87**(7): p. 713-22.
40. Engelen, E., et al., Proteins that bind regulatory regions identified by histone modification chromatin immunoprecipitations and mass spectrometry. *Nat Commun*, 2015. **6**: p. 7155.
41. Zhang, Y., et al., Model-based analysis of ChIP-Seq (MACS). *Genome Biol*, 2008. **9**(9): p. R137.
42. Robinson, J.T., et al., Integrative genomics viewer. *Nat Biotechnol*, 2011. **29**(1): p. 24-6.

Chapter 6

Unphosphorylated ISGF3 Drives Constitutive Expression of Interferon-stimulated Genes to Protect Against Viral Infections

Wenshi Wang[1], Yuebang Yin[1], Lei Xu[1], Junhong Su[2], Fen Huang[2], Yijin Wang[1], Patrick P C Boor[1], Kan Chen[1], Wenhui Wang[1], Wanlu Cao[1], Xinying Zhou[1], Pengyu Liu[1], Luc J. W. van der Laan[3], Jaap Kwekkeboom[1], Maikel P. Peppelenbosch[1] and Qiuwei Pan[1]

[1]Department of Gastroenterology and Hepatology, Postgraduate School Molecular Medicine, Erasmus MC-University Medical Center, Rotterdam, the Netherlands

[2]Medical Faculty, Kunming University of Science and Technology, Kunming, PR China

[3]Department of Surgery, Postgraduate School Molecular Medicine, Erasmus MC-University Medical Center, Rotterdam, the Netherlands

Science Signaling, 2017, 10(476).

Abstract

Interferon-stimulated genes (ISGs) are antiviral effectors that are efficiently induced by interferons (IFNs) via the formation of a tripartite transcription factor ISGF3 (IRF9, phosphorylated STAT1 and STAT2). However, we found that IFN-independent ISG expression was detectable in immortalized cell lines, primary intestinal and liver organoids, and liver tissues. We report that the constitutive expression of ISGs was mediated by the unphosphorylated ISGF3 (U-ISGF3) complex, which was formed by IRF9 together with unphosphorylated STAT1 and STAT2. Under homeostatic conditions, the nuclear localization of endogenous STAT1, STAT2, and IRF9 was observed. Analysis of a chromatin immunoprecipitation–sequencing (ChIP-seq) dataset revealed that STAT1 specifically bound to the promoters of ISGs even in the absence of IFNs. Knockdown of STAT1, STAT2, or IRF9 by RNA interference (RNAi) led to the decreased expression of a range of ISGs in Huh7.5 cells, which was confirmed in mouse embryonic fibroblasts (MEFs) from STAT1-/-, STAT2-/-, or IRF9-/- mice. Furthermore, decreased ISG expression was accompanied by the increased replication of hepatitis C virus (HCV) and hepatitis E virus (HEV). Conversely, simultaneous overexpression of all of the ISGF3 components, but not any single factor, induced the expression of ISGs and inhibited viral replication. However, no phosphorylated STAT1 and STAT2 was detected. Substitution of wild-type STAT1 with a phosphorylation-deficient mutant had comparable effect on IFN-independent expression of ISGs or antiviral activity, suggesting that ISGF3 works in a phosphorylation-independent manner. These data suggest that the U-ISGF3 complex is both necessary and sufficient for constitutive ISG expression and antiviral immunity under homeostatic conditions.

Keywords: U-ISGF3; HCV; HEV; basal ISG; transcription

Introduction

Interferon-stimulated genes (ISGs) are hardwired within genomes and provide a robust first line of defense against invading pathogens. Canonically, following pathogen invasion and interferon (IFN) stimulation, IFN receptors respond with activation of the Janus kinases JAK1 and TYK2, which in turn phosphorylate tyrosine residues in the intracellular tail of the IFN receptors. Subsequently, STAT1 and STAT2 are phosphorylated, which provokes dimerization and subsequent binding to interferon regulatory factor 9 (IRF9) to form the IFN-stimulated gene factor 3 (ISGF3) complex. The ISGF3 complex translocates into the nucleus, and binds to specific promotor elements denoted as IFN-stimulated response elements (ISREs), leading to the rapid transcriptional activation of hundreds of ISGs. This leads to an effective antiviral state against positive-, negative-, and double-stranded RNA viruses, DNA viruses, and intracellular bacteria and parasites [1]. Interestingly, an IFN regulated non-canonical mechanism of ISG transcription was recently reported. When cells are continuously exposed to a low amount of exogenous interferon, unphosphorylated ISGF3 (U-ISGF3), formed by interferon induced IRF9 and unphosphorylated STAT1 and STAT2, leads to steady-state increased expression of a subset of ISGs [2].

In the absence of interferon activation, constitutive ISG expression is also critical in determining cellular susceptibility to viral infection [3]. Inefficient replication of influenza A virus has been reported in human bronchial epithelial cells (BEAS-2B) with a higher expression level of basal ISGs, compared with other respiratory epithelial cell lines [4]. Similar observation was reported with regard to reovirus replication in cardiac myocytes [5, 6]. Conversely, abnormal regulation of basal ISG expression is associated with adverse consequences in patients. Patients with chronic hepatitis C virus (HCV) infection who have abnormally high levels of basal ISG expression in the liver are prone to poor sustained virologic response (SVR) to pegylated IFN-α and ribavirin therapy [7, 8]. Abnormally high expression levels of basal ISGs have been reported to promote tumor growth, and confer resistance to chemotherapy and radiotherapy [9, 10]. Thus, the question as to the mechanisms maintaining and determining the level of constitutive ISG expression is of utmost importance.

Here, we report that under homeostatic status, nuclear localization of endogenous STAT1, STAT2 and IRF9 were observed in cell lines, 3-D cultured primary intestinal and liver organoids, and liver tissues. In the absence of interferons, constitutive ISG expression is mediated by endogenous U-ISGF3 complex, formed by IRF9, and unphosphorylated STAT1 and STAT2. This process is totally independent of IFN production and the upstream elements of IFN signaling, but effectively confers resistance of host cells to HCV and HEV infections. Thus, the endogenous U-ISGF3 complex is both necessary and sufficient for sustaining constitutive ISG transcription and antiviral immunity in host cells under homeostatic condition.

Results

Constitutive ISG transcription is independent of IFN production

The profile of constitutive ISG expression in human liver tissue, 3D-cultured primary human liver and intestinal organoids (fig. S1A), and three different cell lines (Huh7.5, Caco2, and A549) was quantified by quantitative reverse-transcription polymerase chain reaction (qRT-PCR) analysis. ISG expression

was readily detectable in all tested models under homeostatic conditions (Fig. 1, A and B). This finding was further confirmed by the quantification of the gene copy numbers of four representative ISGs, as normalized to the corresponding plasmid template using a standard curve calculation method (Fig. 1C and fig. S1B).

The classical role of IFN in the induction of ISG expression prompted us to investigate the potential involvement of IFN in our system. Thus, we collected conditioned medium from these cultured cells (after 48 hours) and added to a transcriptional reporter system that mimics IFN response with a luciferase reporter gene that was driven by multiple ISREs (ISRE-Luc). Cell culture medium from all three cell lines failed to stimulate any response in the ISRE-luc model(Fig. 1D). Consistently, the conditioned medium failed to stimulate ISG expression in Huh7.5 cells (fig. S1C). In addition, conditioned culture medium was also used to perform a functional assay on the IFN sensitive HCV-replicon model, Huh7.5-HCV-luc; however, we found that the culture media did not affect HCV replication (Fig. 1E). JAK1 is the key upstream component that drives the activation of IFN signaling. IFN-α-stimulated STAT1 phosphorylation and ISG expression were blocked by a pharmacological JAK inhibitor, JAK inhibitor I (fig. S2, A and B). However, JAK inhibitor I did not decrease constitutive ISG expression in Huh7.5, Caco2, or A549 cells (Fig. 1F and fig. S2, C and D). Together, these data suggest that constitutive ISG expression is independent of IFN production.

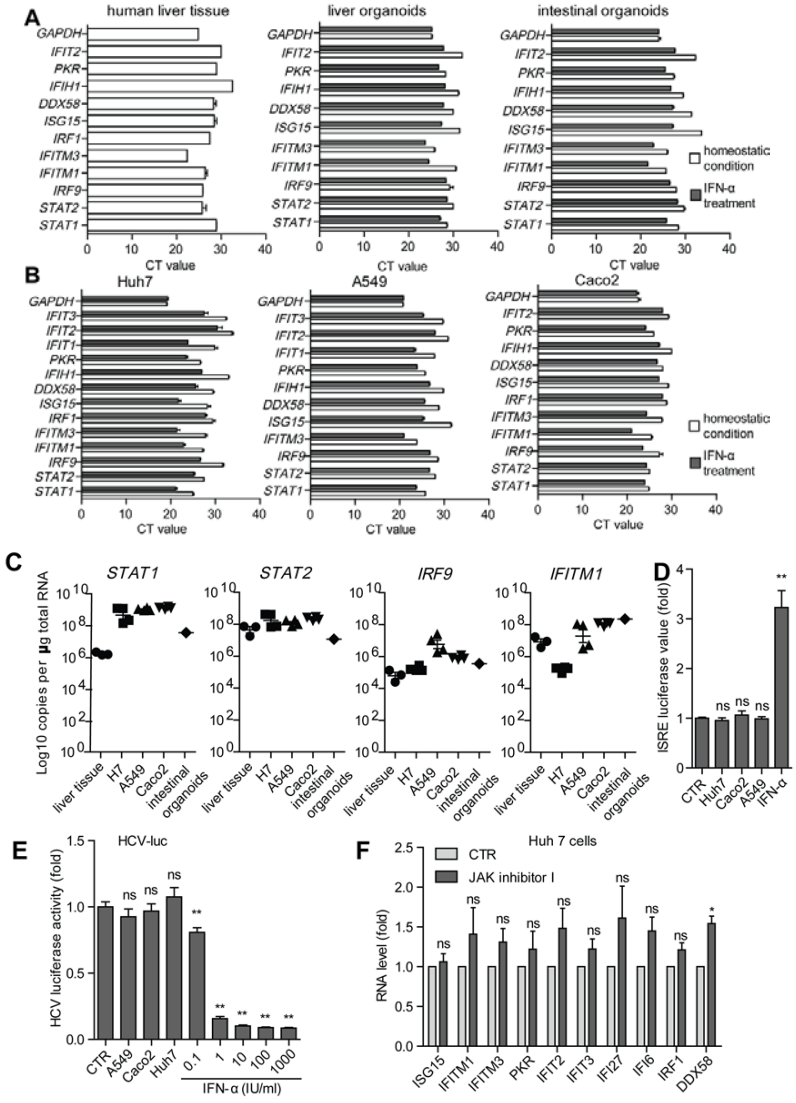

Figure 1. Cell sustains basal ISG transcription independent of interferon production. (A and B) Total RNA was extracted from human liver tissue samples, primary human liver organoids, human intestinal organoids (A), and from Huh7.5 cells, A549 cells, and Caco2 cells (B). The relative abundances of mRNAs of the indicated ISGs were quantified by qRT-PCR. Human liver organoids, intestinal organoids, Huh7.5 cells, A549 cells, and Caco2 cells treated for 24 hours with IFN-α (1000 IU/ml) served as the positive controls for ISG expression. *GAPDH* was used as reference gene. Data are means ± SEM from three independent experiments. (C) The gene copy numbers of the four indicated ISGs were quantified relative to the appropriate plasmid templates using a standard curve calculation method. Data are means ± SEM from three independent experiments. (D) Huh7.5-ISRE-luccells were left untreated or were treated for 24 hours with conditioned medium from Huh7.5, Caco2, or A549 cells or with IFN-α (10 IU/ml) as a positive control. ISRE luciferase values were then measured and the fold-increase in activity relative to that of untreated cells was determined. Data are means ± SEM from three independent experiments. (E) HCV viral replication-related firefly luciferase activity was measured upon the treatment of Huh7.5-HCV-luc cells with conditioned medium from Huh7.5, Caco2, or A549 cells. As a positive control, the cells were treated with the indicated range of concentrations of IFN-α. Data are means ± SEM from three independent experiments. (F) Huh7.5 cells were treated with vehicle (CTR) or with 5 μM JAK inhibitor I for 24 hours before being subjected to qRT-PCR analysis of the relative abundances of the indicated mRNAs. Data are means ± SEM of four independent experiments. **P* < 0.05; ***P* < 0.01; ns, not significant.

STAT1, STAT2, and IRF9 are required for constitutive ISG transcription and they constrain HCV and HEV replication

Upon IFN stimulation, STAT1 is a vital transcription factor to drive ISG transcription. Thus, we first examined the role of STAT1 in basal ISG transcription under homeostatic conditions. Because nuclear localization is a primary determinant for the transcriptional function of STAT1, we investigated the cellular location of endogenous STAT1. We found that the staining of endogenous STAT1 protein in both cytoplasm and nucleus was apparent. in human and mouse liver tissue samples as determined by immunohistochemistry (IHC) (Fig. 2A). Consistently, the cellular localization of STAT1 was similar in primary human liver and intestinal organoids and in three different cell lines (Fig. 2, B to E, fig. S3, A and B). To investigate whether STAT1 in the cell nucleus could bind to the promoter regions of ISGs, we retrieved genome-wide STAT1 ChIP-seq data (GSE31477) from the ENCODE ChIP-seq Experiment Matrix database and Gene Expression Omnibus [11]. The STAT1 ChIP-seq datasets were then processed and analyzed. Even without IFN stimulation, STAT1 showed specific binding peaks on the promoter regions of a large cohort of ISGs (186 out of 350 ISGs analyzed), including IRF1, IRF9, STAT1, and ISG15 (Fig. 2F), whereas rabbit immunoglobulin G (IgG, which was the negative control) showed no specific binding peak.

To further investigate the role of STAT1 in basal ISG expression, Huh7.5 cells were transduced with an integrating lentiviral vector expressing STAT1-specific short hairpin RNA (shRNA), which resulted in a marked decrease in STAT1 abundance (Fig. 3A). Knockdown of endogenous STAT1 led to the decreased expression of 13 out of 14 tested ISGs, with inhibitory efficiency ranging from 30 to 90% (Fig. 3B). In addition, we performed experiments with mouse embryonic fibroblasts (MEFs) from wild-type (WT) and $STAT1^{-/-}$ mice to examine the effect of STAT1 on ISG expression (Fig. 3, C and D). We found that the abundances of ISG mRNAs were reduced in $STAT1^{-/-}$ MEFs compared to those in WT MEFs (Fig. 3E). Furthermore, shRNA mediated STAT1 knockdown increased viral replication of HCV (2.2-fold) (Fig. 3F) and HEV (1.7-fold) (Fig. 3G) compared to its shRNA control in Huh7.5-based HCV-luc and HEV-luc models. In contrast, over-expression of STAT1 did not substantially affect ISG expression or viral replication (Fig. 3, H to J), suggesting that STAT1, although important for such responses, does not work alone.

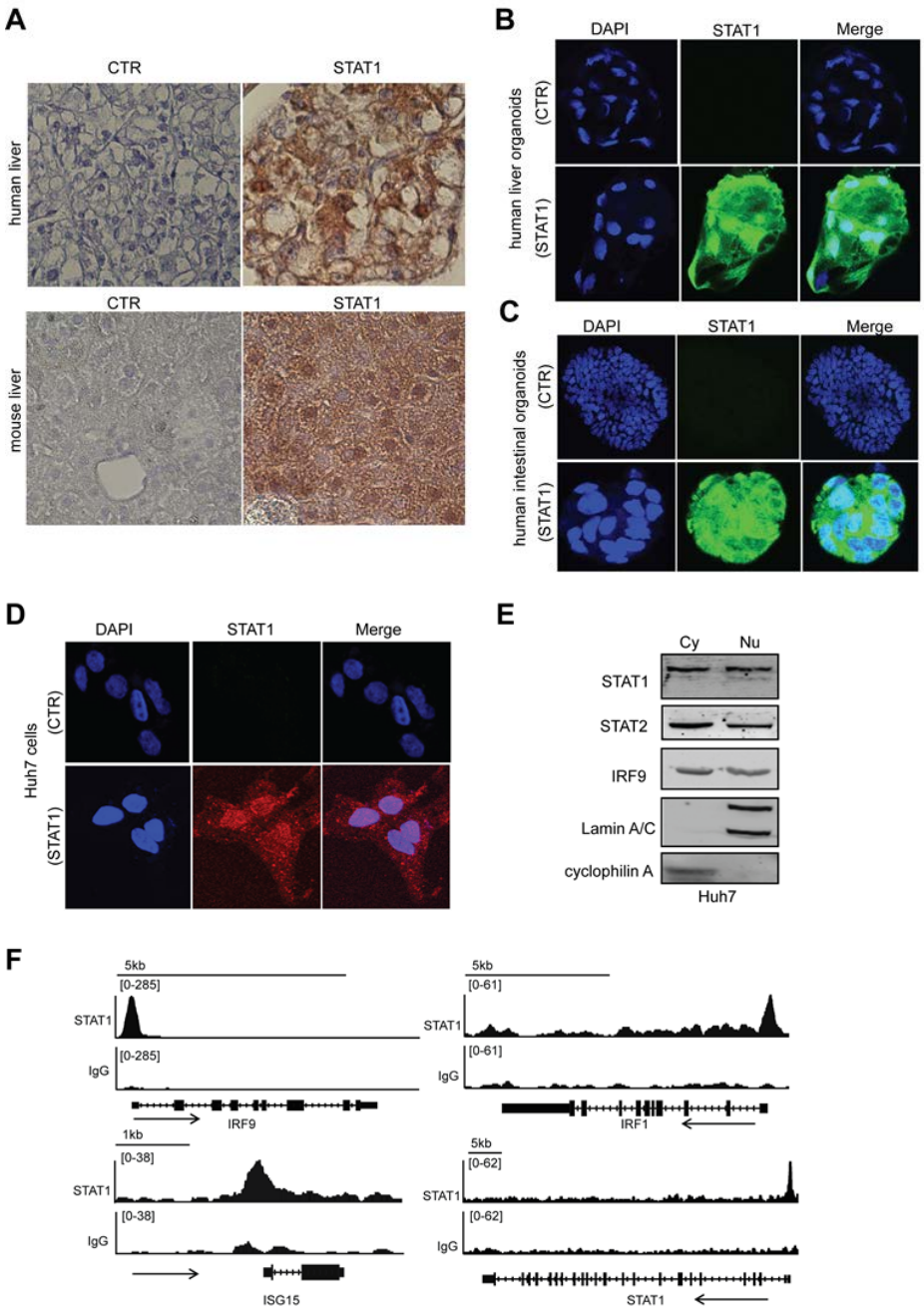

Figure 2. A substantial fraction of endogenous STAT1 is localized in the nucleus and binds to ISG promoters under homeostatic conditions. (A) Representative immunohistochemical staining analysis of the cellular localization of endogenous STAT1 in cells in human (top) and mouse (bottom) liver sections. As a negative control (CTR), primary antibody against STAT1 was replaced with PBS containing 0.05% Tween. Images are representative of three independent experiments. (B to D) Confocal laser electroscope analysis of endogenous STAT1 localization in human liver organoids (B), human intestinal organoids (C), and Huh7.5 cells (D). STAT1 is shown in green in organoids and in red in Huh7.5 cells. Nuclei were visualized by DAPI (blue). As a negative control (CTR), primary antibody against STAT1 was replaced with PBS containing 0.05% Tween. Images are representative of multiple organoids or cells from three independent experiments. (E) Huh7.5 cell lysates were fractionated into cytoplasmic (Cy) and nuclear (Nu) fractions and then were analyzed by Western blotting with antibodies against the indicated proteins. Cyclophilin A and Lamin A/C were used as cytosolic and nuclear markers, respectively. Western blots are representative of three independent experiments. (F) The ChIP-seq dataset for STAT1 (GSE31477) was retrieved from the ENCODE database. Binding profiles of endogenous STAT1 to the promoter regions of the indicated ISGs. Sequence reads from anti-STAT1 antibody or rabbit-IgG-control ChIP-seq data were plotted relative to chromosomal position. The genome locations of the corresponding ISGs are shown beneath the track signaling.

Next, we examined the involvement of STAT2. Under homeostatic conditions, STAT2 was abundantly present in both the cytoplasm and nuclei of human liver tissue, human liver organoids, human intestinal organoids, and cell lines (Fig. 4, A to D). Furthermore, knockdown of STAT2 by lentiviral shRNA (Fig. 4E) led to the decreased expression of ISGs (10 out of 12 tested ISGs), ranging from a 30 to 70% decrease (Fig. 4F). MEFs from STAT2$^{-/-}$ mice (Fig. 4G) had reduced amounts of many ISG mRNAs compared to those in WT MEFs (Fig. 4H). ShRNA mediated STAT2 knockdown increased replication of HCV (1.5-fold) (Fig. 4I) and HEV (1.6-fold) (Fig. 4J) compared to its shRNA control in Huh7.5-based HCV-luc and HEV-luc models. However, overexpression of STAT2 did not affect either ISG expression or viral replication (Fig. 4, K to M), mirroring the results obtained from experiments with overexpressed STAT1.

Finally, the role of IRF9 was also investigated. Substantial nuclear localization of IRF9 was observed in human and mouse liver tissues (Fig. 5A), human liver organoids (Fig. 5B), human intestinal organoids (Fig. 5C), and Huh7.5 cells (Fig. 5D). Knockdown of endogenous IRF9 by lentiviral vector based IRF9-specific shRNA (Fig. 5E) resulted in decreased ISG expression in Huh7.5 cells (Fig. 5F). Consistently, compared with WT MEFs, IRF9$^{-/-}$ MEFs (Fig. 5G) had reduced amounts of ISG mRNAs under homeostatic conditions (Fig. 5H). ShRNA mediated IRF9 knockdown increased replication of both HCV (3.8-fold) (Fig. 5I) and HEV (1.8-fold) (Fig. 5J) compared to its shRNA control in Huh7.5-based HCV-luc and HEV-luc models. Over-expression of IRF9 in Huh7.5 cells had no effect on ISG expression (Fig. 5K). Whereas overexpression of IRF9 in these cells inhibited HCV replication (Fig. 5L), it had no effect on HEV replication (Fig. 5M). The idea that the reduced replication of HCV was ISG-independent was supported by the observation that over-expression of IRF9 in Caco2 cells had no substantial effect on either ISG expression or rotavirus replication (fig. S3, C and D). Together, these results suggest that STAT1, STAT2, and IRF9 are all required and likely cooperate to regulate the basal expression of ISGs.

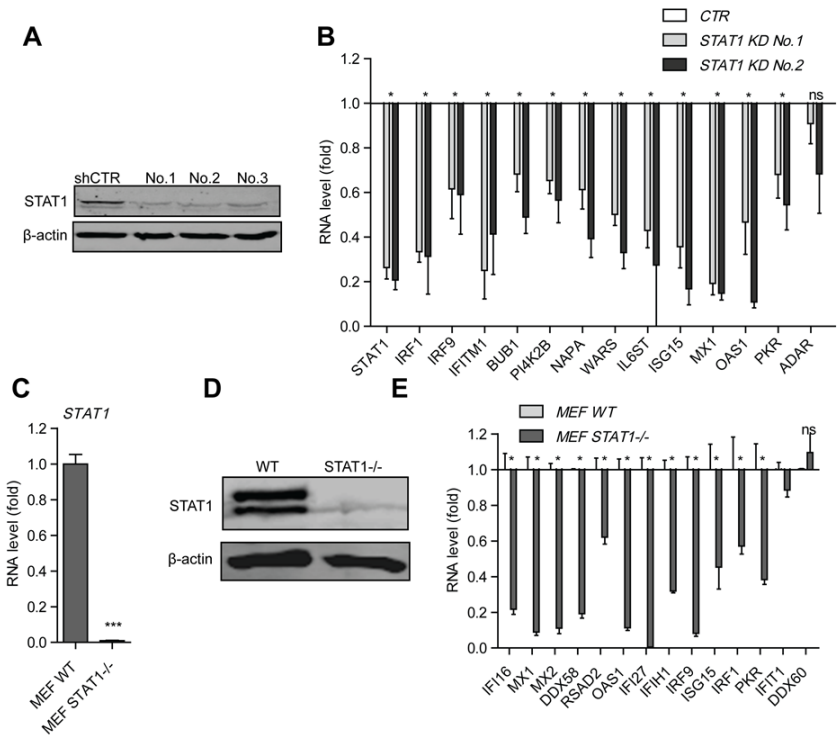

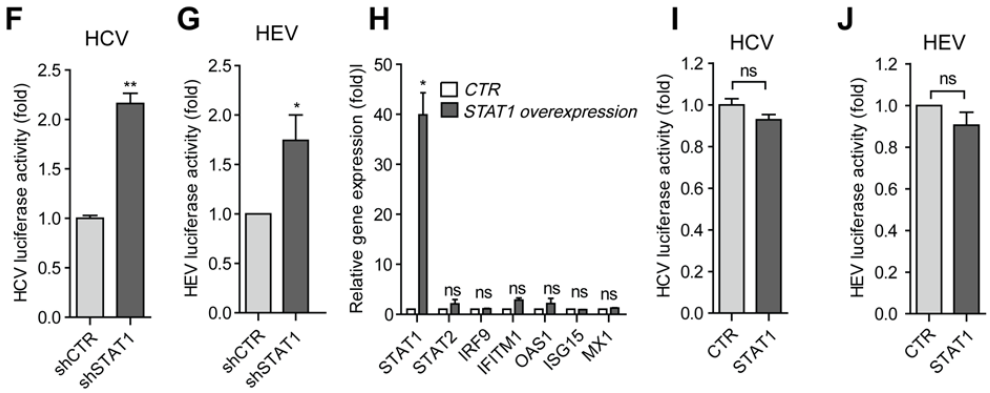

Figure 3. STAT1 is required for sustaining the basal expression of ISGs and constraining viral replication. (A) Huh7.5 cells were transduced with lentiviruses expressing control shRNA (shCTR) or three different STAT1-targeting shRNAs. After the puromycin selection for two weeks, cells were analyzed by Western blotting with antibodies against the indicated proteins. Western blots are representative of three independent experiments. (B) Huh7.5 cells expressing control shRNA or the indicated STAT1-specific shRNAs were analyzed by qRT-PCR to determine the relative abundances of the indicated mRNAs. Data are means ± SEM of four independent experiments. (C) WT and STAT1$^{-/-}$ MEFs were analyzed by qRT-PCR to determine the relative abundance of *STAT1* mRNA. Data are means ± SEM of four independent experiments. (D) WT and STAT1$^{-/-}$ MEFs were analyzed by Western blotting with antibodies against the indicated proteins. Western blots are representative of three independent experiments. (E) WT and STAT1$^{-/-}$ MEFs were subjected to qRT-PCR analysis of the relative abundance of the indicated mRNAs. Data are means ± SEM of three independent experiments. (F) HCV replicon positive Huh7.5 cells were transduced with lentiviruses expressing control or STAT1-specific shRNAs before being subjected to a HCV replication–related luciferase activity. Data are means ± SEM of three independent experiments. (G) HEV replicon positive Huh7.5 cells were transduced with lentiviruses expressing control or STAT1-specific shRNAs before being subjected to a HEV replication–related luciferase activity. Data are means ± SEM of three independent experiments. (H) Huh7.5 cells transduced with lentivirus expressing control or STAT1-specific shRNA were subjected to qRT-PCR analysis of the relative abundances of the indicated mRNAs. Data are means ± SEM of three independent experiments. (I and J) HCV replicon positive (I) and HEV replicon positive (J) Huh7.5 cells transduced with control lentivirus or with lentivirus expressing STAT1 were subjected to qRT-PCR analysis of the relative abundances of the indicated mRNAs. Data are means ± SEM of three independent experiments. **P* < 0.05; ***P* < 0.01; ****P* < 0.001; ns, not significant.

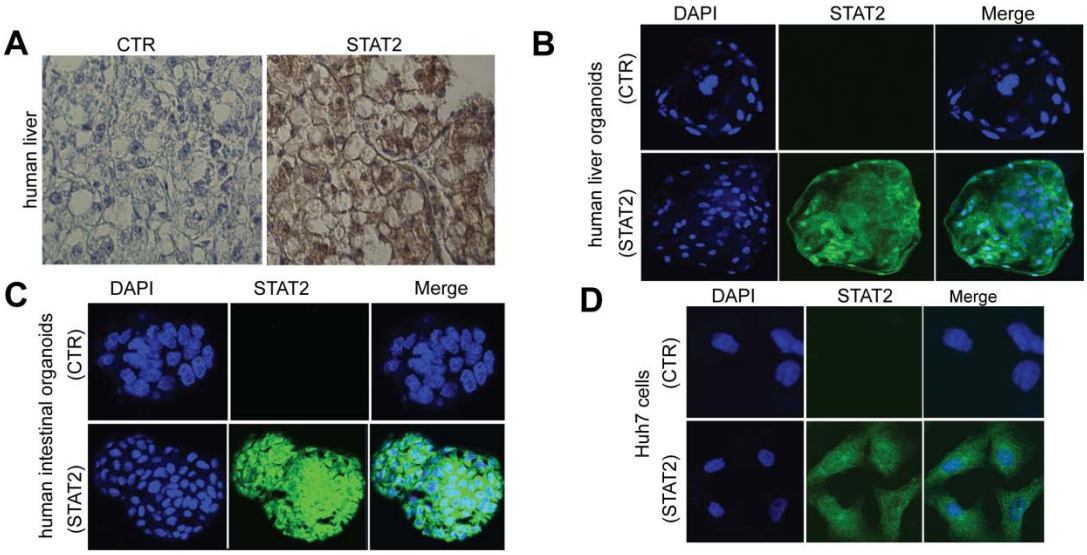

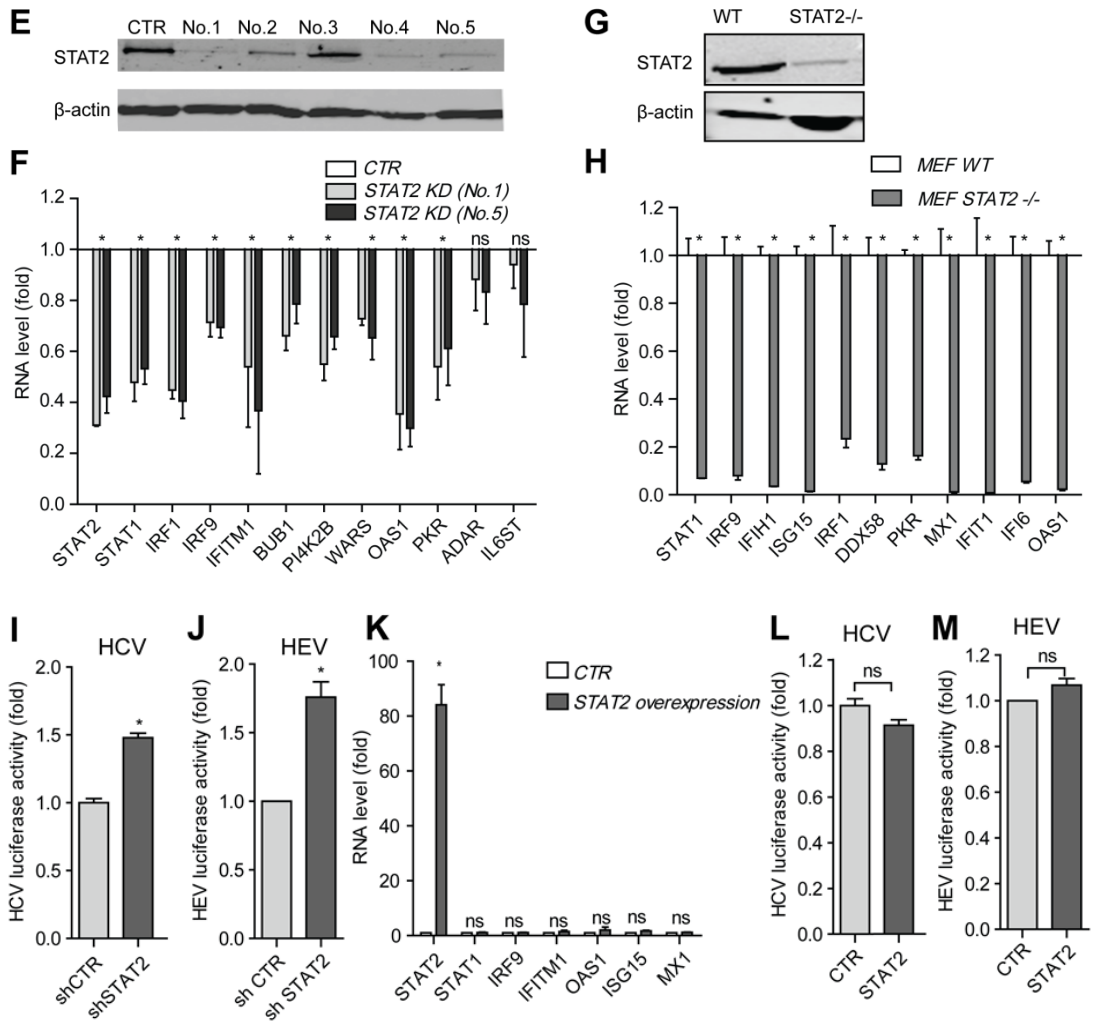

Figure 4. STAT2 is essential for sustaining the basal expression of ISGs and constraining viral replication. (A) Immunohistochemical staining of the cellular localization of endogenous STAT2 in cells from human liver tissue. As a negative control, primary antibody against STAT2 was replaced with PBS containing 0.05% Tween. Images are representative of three independent experiments. (B to D) Confocal laser electroscope analysis of the cellular localization of endogenous STAT2 in human liver organoids (B), human intestinal organoids (C), and Huh7.5 cells (D). STAT2 antibody staining is shown in green, whereas nuclei were visualized by DAPI (blue). As a negative control, primary antibody against STAT2 was replaced with PBS containing 0.05% Tween. Images are representative of multiple organoids or cells from three independent experiments. (E) Huh7.5 cells transduced with lentiviruses expressing control shRNA or the indicated STAT2-specific shRNAs were analyzed by Western blotting with antibodies against the indicated proteins. Western blots are representative of three independent experiments. (F) Huh7.5 cells expressing control shRNA or the indicated STAT2-specific shRNAs were analyzed by qRT-PCR to determine the relative abundances of the indicated mRNAs. Data are means ± SEM of four independent experiments. (G) WT and $STAT2^{-/-}$ MEFs were analyzed by Western blotting with antibodies against the indicated proteins. Western blots are representative of three independent experiments. (H) WT and $STAT2^{-/-}$ MEFs were subjected to qRT-PCR analysis of the relative abundance of the indicated mRNAs. Data are means ± SEM of three independent experiments. (I and J) HCV replicon positive (I) and HEV replicon positive (J) Huh7.5 cells were transduced with lentiviruses expressing control or STAT2-specific shRNAs before being subjected to assays of viral replication–related luciferase activity. Data are means ± SEM of three independent experiments. (K) Huh7.5 cells transduced with control lentivirus or with lentivirus expressing STAT2 were subjected to qRT-PCR analysis of the relative abundances of the indicated mRNAs. Data are means ± SEM of three independent experiments. (L and M) HCV-positive (L) and HEV-positive (M) Huh7.5 cells transduced with control lentivirus or with lentivirus expressing STAT2 were subjected to qRT-PCR analysis of the relative abundances of the indicated mRNAs. Data are means ± SEM of three independent experiments. *P < 0.05; **P < 0.01; ns, not significant.

STAT1, STAT2, and IRF9 function as the U-ISGF3 complex to drive ISG expression and exert antiviral effects against HCV and HEV

Because STAT1, STAT2, and IRF9 alone were all necessary, but not sufficient, to drive constitutive ISG expression, we investigated whether these three factors in combination functioned as the ISGF3 complex independently of activation by exogenous IFN. Thus, we over-expressed STAT1, STAT2, and IRF9 in Huh7.5 cells through lentiviral transduction (Fig. 6 A), which led to a substantial antiviral effect and induction of ISG expression (Fig. 6, B to D), as compared to the over-expression of any one of the three factors alone. These data suggest that the integrity of the ISGF3 complex is necessary for these effects.

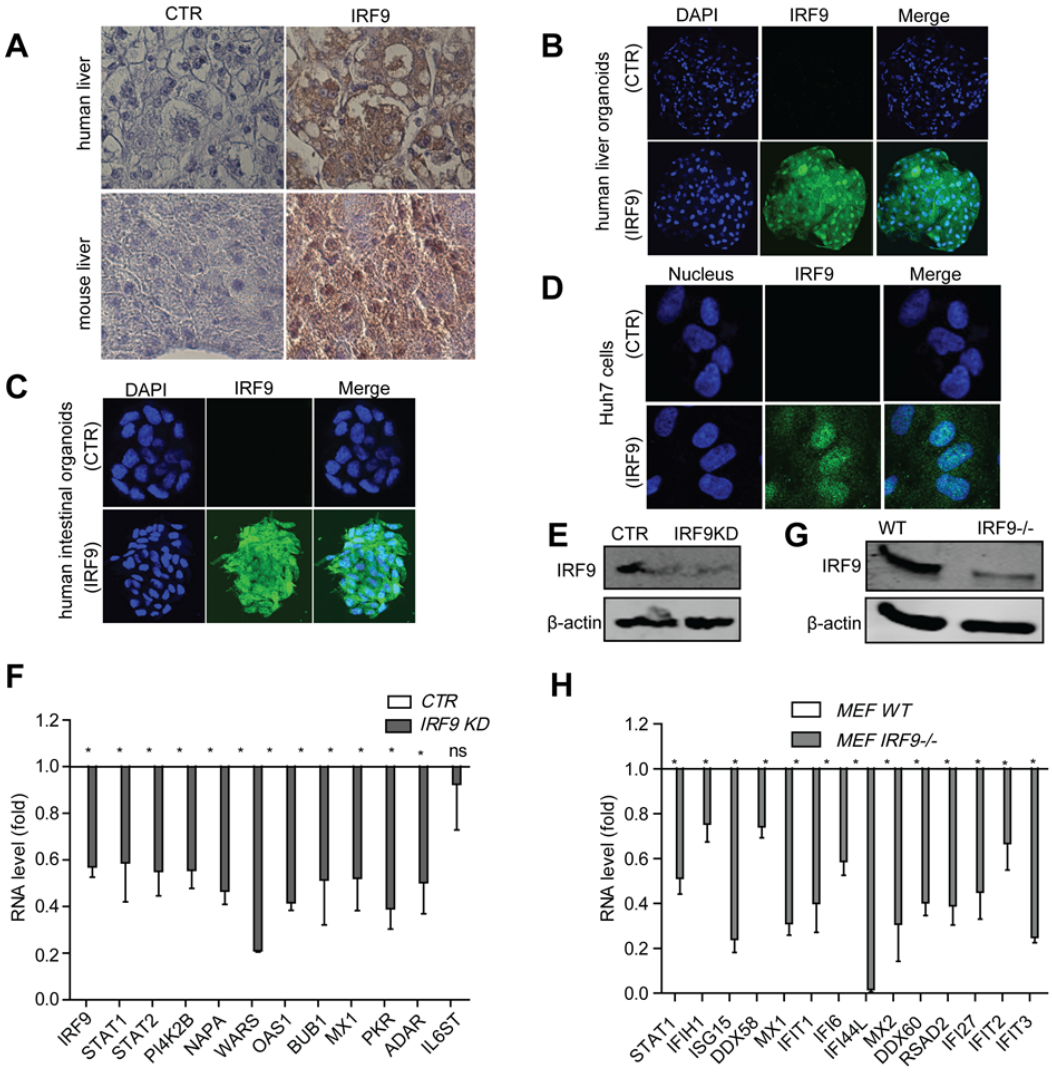

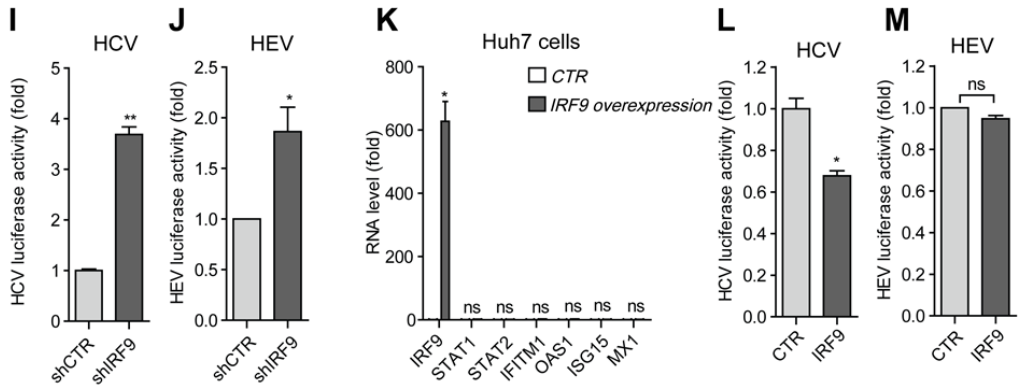

Figure 5. IRF9 is also required for the basal expression of ISGs and for limiting viral replication. (A) Immunohistochemical staining of the cellular localization of endogenous IRF9 in cells from human (top) and mouse (bottom) liver tissue. As a negative control, primary antibody against IRF9 was replaced with PBS containing 0.05% Tween. Images are representative of three independent experiments. (B to D) Confocal laser electroscope analysis of the cellular localization of endogenous IRF9 in human liver organoids (B), human intestinal organoids (C), and Huh7.5 cells (D). IRF9 antibody staining is shown in green, whereas nuclei were visualized by DAPI (blue). As a negative control, primary antibody against IRF9 was replaced with PBS containing 0.05% Tween. Images are representative of multiple organoids or cells from three independent experiments. (E) Huh7.5 cells transduced with lentiviruses expressing control shRNA or IRF9-specific shRNAs were analyzed by Western blotting with antibodies against the indicated proteins. Western blots are representative of three independent experiments. (F) Huh7.5 cells expressing control shRNA or IRF9-specific shRNAs were analyzed by qRT-PCR to determine the relative abundances of the indicated mRNAs. Data are means ± SEM of four independent experiments. (G) WT and $IRF9^{-/-}$ MEFs were analyzed by Western blotting with antibodies against the indicated proteins. Western blots are representative of three independent experiments. (H) WT and $IRF9^{-/-}$ MEFs were subjected to qRT-PCR analysis of the relative abundance of the indicated mRNAs. Data are means ± SEM of three independent experiments. (I and J) HCV-positive (I) and HEV-positive (J) Huh7.5 cells were transduced with lentiviruses expressing control or IRF9-specific shRNAs before being subjected to assays of viral replication–related luciferase activity. Data are means ± SEM of three independent experiments. (K) Huh7.5 cells transduced with control lentivirus or with lentivirus expressing IRF9 were subjected to qRT-PCR analysis of the relative abundances of the indicated mRNAs. Data are means ± SEM of three independent experiments. (L and M) HCV-positive (L) and HEV-positive (M) Huh7.5 cells transduced with control lentivirus or with lentivirus expressing IRF9 were subjected to qRT-PCR analysis of the relative abundances of the indicated mRNAs. Data are means ± SEM of three independent experiments. *$P < 0.05$; **$P < 0.01$; ns, not significant.

To rule out any interference by endogenous WT STAT1 or STAT2 (should any be present in the cells) and to further confirm the role of ISGF3, we overexpressed STAT1, STAT2, and IRF9 in U3A cells (which are STAT1-deficient) and U6A cells (which are STAT2-deficient) (fig. S4, A to D) [12], which led to a substantial induction of ISG expression in both cell types (fig. S4, B and D), mirroring the results observed in Huh7.5 cells. STAT1 phosphorylated at Tyr^{701} (pSTAT1-Tyr^{701}) and STAT2 phosphorylated at Tyr^{690} (pSTAT2-Tyr^{690}) were undetectable even when either protein was overexpressed (Fig. 6A), which suggests that ISGF3 complex occurs through a phosphorylation-independent mechanism. Indeed, no pSTAT1-Tyr^{701} or pSTAT2-Tyr^{690} was detected in either human or mouse liver tissue samples by IHC (Fig. 6E and fig. S4E) or in three individual liver tissue samples that were examined by Western blotting (Fig. 6F). The same observation was also made by examining human liver organoids (Fig. 6G), intestinal organoids (fig. S4, F to H), and Huh7.5 cells (Fig. 6H). Furthermore, overexpression of a mutant STAT1 (Y701F-STAT1), which cannot be phosphorylated at Tyr^{701} [13], together with STAT2 and IRF9 in Huh7.5 cells led to a comparable potency of antiviral effect and ISG induction (Fig. 6, I to K). This was further confirmed in U3A cells (fig. S4, I and J).

In addition to the tyrosine phosphorylation sites in STAT1 and STAT2, phosphorylation of the sites Ser^{708} and Ser^{727} in STAT1 correlates with ISG expression [14, 15]. However, we were unable to detect pSTAT1-Ser^{727} in either Huh7.5 cells (fig. S4K) or human liver tissue samples (fig. S4L). Generally, STAT1 or STAT2 is phosphorylated by specific kinases upon cellular stimulation (for example, by IFNs). Furthermore, pSTAT1 and pSTAT2 proteins undergo dephosphorylation. Thus, the phosphorylation and dephosphorylation processes are coordinated to maintain the phosphorylation states of these proteins to an extent that achieves a balance between their beneficial, antiviral actions and their detrimental, proinflammatory effects. Consequently, the inhibition of phosphatases would alter this balance, resulting in increased amounts of pSTAT1 and pSTAT2 and to the greater induction of ISG expression (fig. S5A) [16]. Thus, we performed experiments with the phosphatase inhibitor NSC87877 (which has IC_{50} values of 0.318 μM for SHP-2, 0.355 μM for SHP-1, and 1.691 μM for PTP1B) to specifically inhibit the key phosphatases involved in pSTAT1 and pSTAT2 dephosphorylation at both tyrosines and serines [16-18]. However, we found that NSC87877 had no effect on basal ISG expression in either Huh7.5 cells or Caco2 cells (Fig. 7A and fig. S5B). NSC87877 also had no effect on ISG expression induced by the simultaneous over-expression of STAT1, STAT2, and IRF9 (Fig. 7B). Together, these data suggest that STAT1, STAT2, and IRF9 function as part of U-ISGF3 to drive ISG expression, which leads to antiviral effects.

The basal expression of particular ISGs is enhanced in chemotherapy-resistant cancer cells and in chronic HCV patients who are resistant to IFN therapy; however, under these conditions, pSTAT1 is almost undetectable [2, 19]. Thus, we overexpressed Y701F-STAT1, STAT2, and IRF9 together in Huh7.5 cells and examined the basal expression of several ISGs that were previously identified as potential makers to predict responsiveness to IFN therapy in patients chronically infected with HCV [7, 8]. As expected, the expression of all of these ISGs was increased upon overexpression of the components of the U-ISGF3 (fig. S5C). Note that IFNs stimulate the expression of antiviral ISGs and of negative regulatory ISGs to avoid excessive IFN responses [20]. We found that the expression of four of five of these negative regulatory ISGs was also enhanced upon overexpression of U-ISGF3 (fig. S5D).

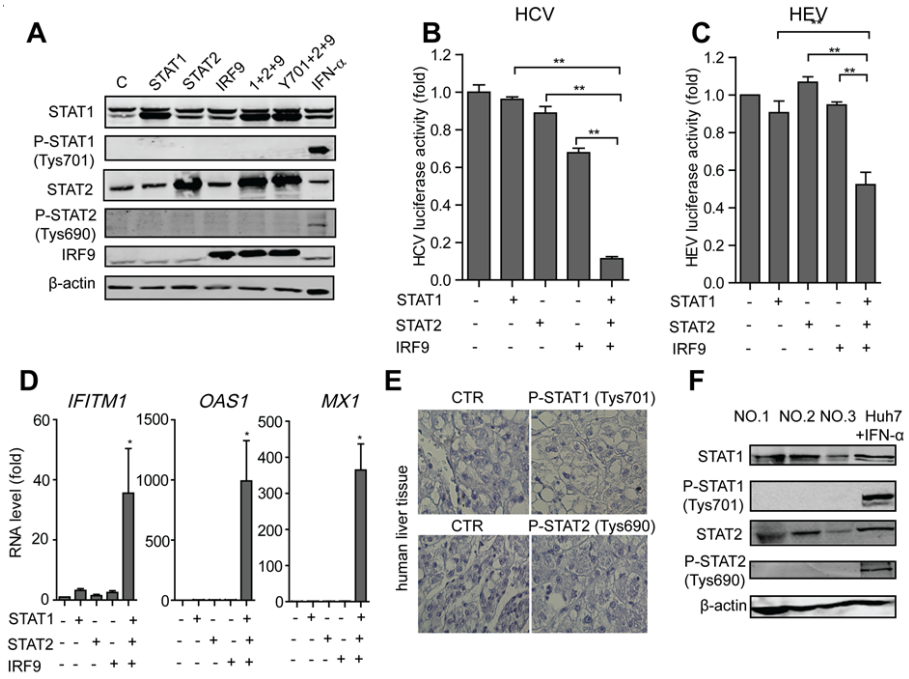

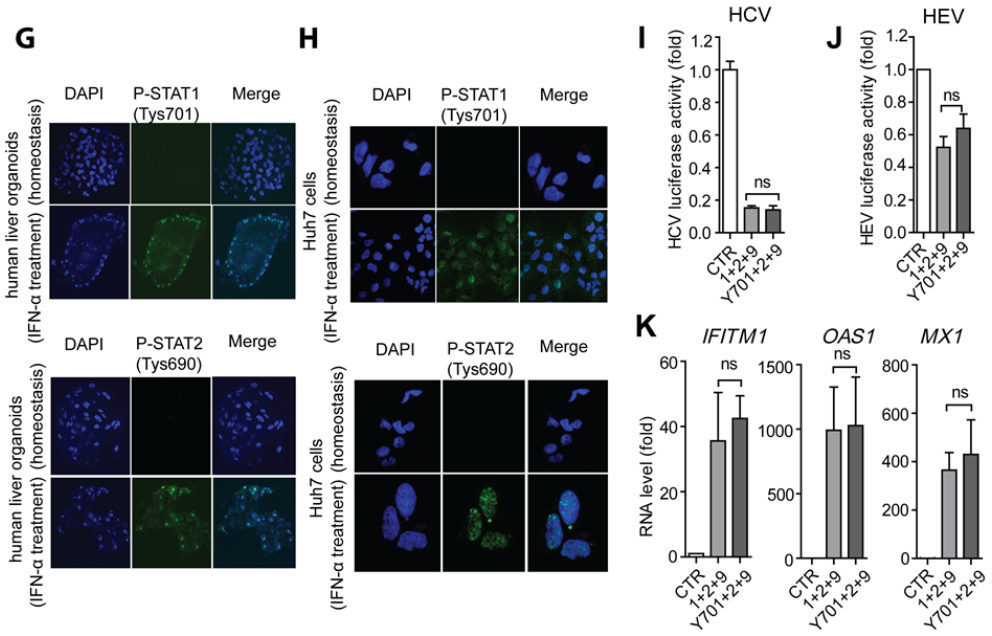

Figure 6. U-ISGF3 stimulates the expression of ISGs and constrains viral replication. Huh7.5 cells were transduced with control lentivirus (C) or with lentiviruses expressing the indicated proteins before being subjected to Western blotting analysis with antibodies against the indicated proteins. As a positive control for the detection of pSTAT1 and pSTAT2, Huh7.5 cells were treated with IFN-α for 30min. Western blots are representative of three independent experiments. (B and C) HCV-positive (B) and HEV-positive (C) Huh7.5 cells were transduced with control lentivirus or with lentiviruses expressing the indicated proteins before being subjected to assays of viral replication–related luciferase activity. Data are means ± SEM of three independent experiments. (D) Huh7.5 cells were transduced with control lentivirus or with lentiviruses expressing the indicated proteins before being subjected to qRT-PCR analysis of the relative abundances of the indicated mRNAs. Data are means ± SEM of three independent experiments. (E) Representative immunohistochemical analysis of pSTAT1-Tyr^{701} and pSTAT2-Tyr^{690} in human liver tissue samples. Neither protein was detected. As negative controls (CTR), the primary antibodies were replaced with PBS containing 0.05% Tween. (F) Samples from three individual human liver samples were analyzed by Western blotting with antibodies against the indicated proteins. As a positive control for pSTAT proteins, Huh7.5 cells were treated with IFN-α for 30 min. Western blots are representative of three independent experiments. (G and H) Confocal laser electroscope analysis of pSTAT1-Tyr^{701} (top) and pSTAT2-Tyr^{690} (bottom) in human liver organoids (G) and Huh7.5 cells (H). The pSTAT1 and pSTAT2 proteins are shown in green, whereas nuclei were visualized by DAPI (blue). Human liver organoids or Huh7.5 cells treated with IFN-α for 30 min served as the corresponding positive controls. Images are representative of multiple organoids or cells from three individual experiments. (I and J) HCV-positive (I) and HEV-positive (J) Huh7.5 cells transduced with control lentivirus or lentiviruses expressing WT or Y701F mutant STAT1 together with STAT2 and IRF9 were subjected to assays of viral replication–related luciferase activity. Data are means ± SEM of three independent experiments. (K) Huh7.5 cells transduced with control lentivirus or lentiviruses expressing WT or Y701F mutant STAT1 together with STAT2 and IRF9 were subjected to qRT-PCR analysis of the relative abundances of the indicated mRNAs. Data are means ± SEM of three independent experiments. *P < 0.05; **P < 0.01; ns, not significant.

U-ISGF3 drives ISG transcription without stimulating IFN production

To further dissect whether the U-ISGF3–induced expression of ISGs was independent of IFN production, we measured the basal abundances of mRNAs of several IFNs, including *IFNA*, *IFNB*, *IFNG*, *IL29*, and *IL28A* (fig. S5E). The abundances of *IFNA* and *IFNB*mRNAs were not statistically significantly increased by the overexpression of STAT1, STAT2, or IRF9 alone or in combination (Fig. 7, C and D), whereas the mRNAs encoding *IFNG*, *IL29*, and *IL28A* were undetectable with or without overexpression of the U-ISGF3 components (fig. S5E). To further confirm the lack of IFN production,

we collected the conditioned medium of these cells (fig. S5F) and performed functional assays. Conditioned culture medium from any of the overexpressing Huh7.5 cells was unable to stimulate an IFN response in an ISRE reporter assay (fig. 7E). Consistently, treatment of Huh7.5 cells with these conditioned media had no effect on ISG expression (fig. S5G). These data suggest that the U-ISGF3–induced expression of ISGs is IFN-independent.

U-ISGF3 drives ISG expression independently of the upstream components of the IFN signaling pathway

IFNs are mainly produced by so-called IFN-producing cells (IPCs). In our study, we included three types of well-known IPCs, human plasmacytoid dendritic cells (pDCs), myeloid dendritic cells (mDCs), and T cells to demonstrate the classical IFN-dependent mechanisms of ISG transcription and antiviral action. As expected, these IPCs produced IFNs to activate the JAK-STAT pathway, drive ISG transcription, and exert antiviral activity. These effects were specifically blocked by JAK inhibitor I (fig. S6). Therefore, upon IFN stimulation, the intact JAK-STAT signaling pathway is a prerequisite for the formation of its downstream transcription factor complex, ISGF3, which drives the expression of ISGs (fig. S7A). To dissect the involvement of its upstream elements in basal ISG transcription, we knocked down either IFN-αR1 or IFN-λR1 in Huh7.5 cells by lentiviral shRNA (Fig. 7F). Efficient knockdown of IFN-αR1 or IFN-λR1 had no effect on constitutive ISG expression (Fig. 7G). In addition, knockdown of endogenous JAK1 in Huh7.5 cells (Fig. 7, H and I) did not inhibit the constitutive expression of ISGs (Fig. 7J). This finding was further confirmed in experiments with Caco2 cells (fig. S7, B to D). Conversely, collective overexpression of STAT1, STAT2, and IRF9 by lentiviral transduction in IFN-αR1-, IFN-λR1-, or JAK1-knockdown Huh7.5 cells showed comparable ISG induction ability compared with control lentiviral vector (Fig. 7K). These results suggest that U-ISGF3 drives the basal expression of ISGs independently of the upstream elements of the IFN signaling pathway.

Discussion

ISGs are the ultimate antiviral effectors of the IFN signaling. They function either by targeting different steps of the viral life cycle or by reinforcing host defense by further activation of ISG expression [1, 21]. Classically, upon IFN stimulation, STAT1 and STAT2 are phosphorylated, leading to the association with IRF9 to form the transcription factor complex ISGF3. Phosphorylated ISGF3 translocates into cell nucleus and binds to the promoter regions of ISGs to activate the transcription of these hundreds of ISGs. However, when cells are continuously exposed to a low level of exogenous interferon, unphosphorylated ISGF3 (U-ISGF3), formed by interferon stimulated IRF9 and unphosphorylated STAT1 and STAT2, can also lead to increased expression of a subset of ISGs [2]. Importantly, both regulatory mechanisms require the activation by IFN.

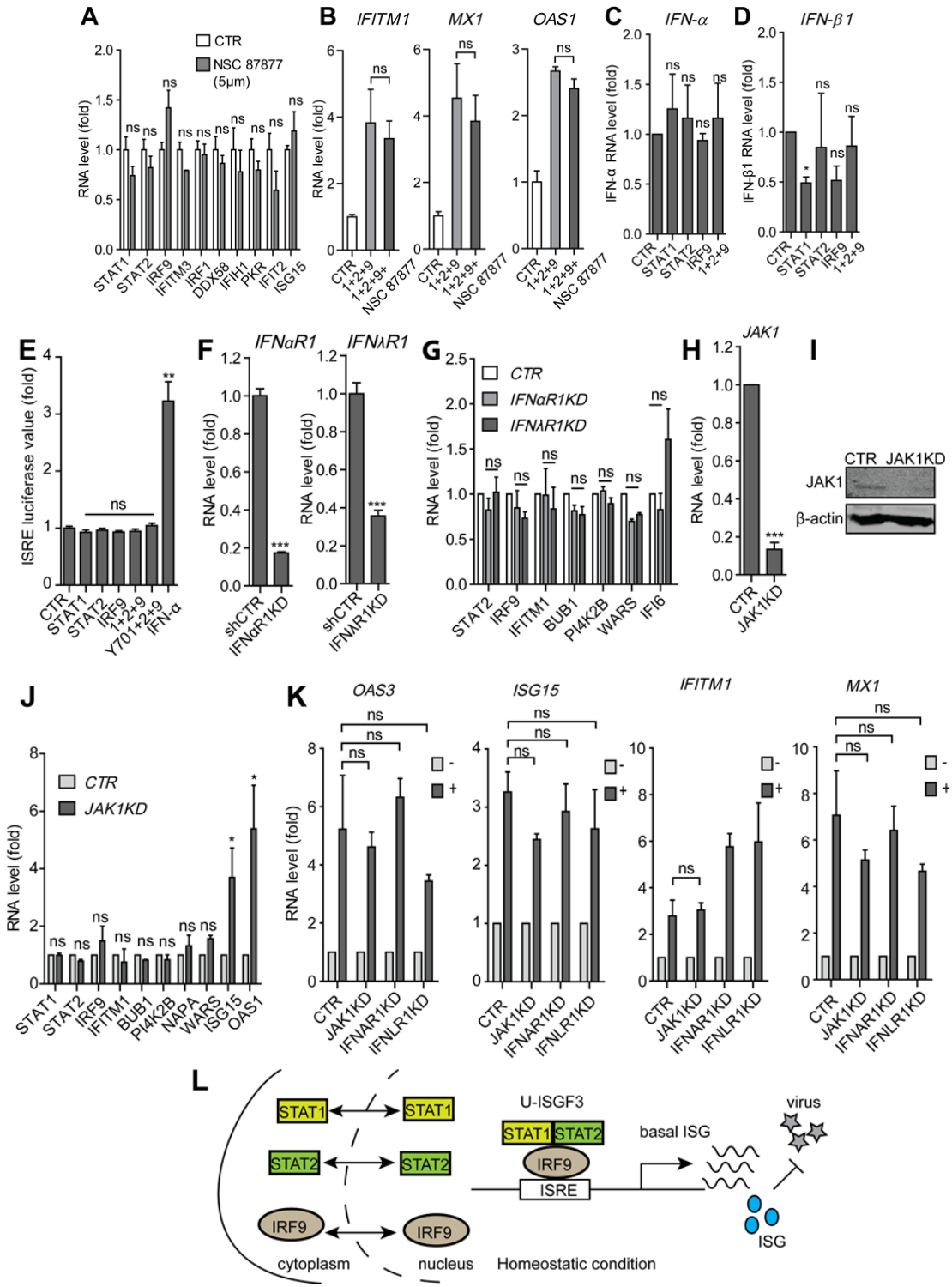

Figure 7. U-ISGF3 stimulates the expression of ISGs independently of IFN production and the upstream elements of the IFN signaling pathway. (A) Huh7.5 cells were left untreated (CTR) or were treated with 5 μM NSC87877 (phosphatase inhibitor) before the cells were subjected to qRT-PCR analysis of the relative abundances of the indicated mRNAs. Data are means ± SEM of three independent experiments. (B to D) Huh7.5 cells were transduced with control lentivirus or with lentiviruses expressing STAT1, STAT2, and IRF9, individually or in combination, before being treated with vehicle or NSC87877. The cells were then subjected to qRT-PCR analysis of the relative abundances of the indicated mRNAs for ISGs (B), *IFNA* (C), and *IFNB* (D). Data are means ± SEM of three independent experiments. (E) Huh7.5 cells transduced with lentiviruses expressing the indicated proteins were cultured for 48 hours before the cell culture medium was collected and used to treat an ISRE luciferase reporter cell line. As a positive control, culture medium was collected from cells treated

with IFN-α (10 IU/ml). Data are means ± SEM of three independent experiments. (F) Huh7.5 cells transduced with lentiviruses expressing control shRNA, *IFNAR1*-specific shRNA, or *IFNLR1*-specific shRNA were analyzed by qRT-PCR to determine the extent of knockdown of the indicated mRNAs. Data are means ± SEM of three independent experiments. (G) Huh7.5 cells transduced with lentiviruses expressing control shRNA, *IFNAR1*-specific shRNA, or *IFNLR1*-specific shRNA were analyzed by qRT-PCR to determine the relative abundances of the indicated mRNAs. Data are means ± SEM of three independent experiments. (H and I) Huh7.5 cells transduced with lentiviruses expressing control or JAK1-specific shRNAs were analyzed by qRT-PCR to determine the extent of knockdown of JAK1 mRNA (H) or by Western blotting with antibodies against the indicated proteins (I). Data in (H) are means ± SEM of three independent experiments. Western blots are representative of three independent experiments. (J) Huh7.5 cells transduced with lentiviruses expressing control or JAK1-specific shRNAs were analyzed by qRT-PCR to determine the relative abundances of the indicated mRNAs. Data are means ± SEM of three independent experiments. (K) Huh7.5 cells were transduced with lentiviruses expressing control shRNA or shRNAs specific for JAK1, IFNAR, or IFNLR. After the puromycin selection, they were not (-) or were (+) transduced with lentiviruses expressing STAT1, STAT2, and IRF9. The cells were then subjected to qRT-PCR analysis of the relative abundances of the indicated mRNAs. Data are means ± SEM of three independent experiments. **P* < 0.05; ***P* < 0.01; ns, not significant. (L) Illustration of the mechanism of basal expression of ISGs under homeostatic conditions. Unphosphorylated STAT1, STAT2, and IRF9 shuttle between the cytoplasm and the nucleus. When these three components are present in the nucleus, they function as the constitutively active transcription factor complex U-ISGF3 to sustain the basal expression of ISGs. The products of these expressed ISGs confer protection to the cell from viral infection.

Classically, IFNs are mainly produced by so-called IFN-producing cells (IPCs) These IPCs produced IFNs to activate the JAK-STAT pathway, drive ISG transcription, and exert antiviral activity. Huh7.5Huh7.5Here, we highlighted the existence of an IFN-independent mechanism that sustains the constitutive expression of IFN-encoding genes. We found that constitutive ISG expression was mediated by the endogenous U-ISGF3 complex. This regulatory mechanism was independent of IFN production and the upstream elements of IFN signaling, but conferred the cells with resistance against viral infections (Fig. 7L). Thus, these data suggest that both IFN-dependent and -independent antiviral mechanisms co-exist and work cooperatively.

As a critical element in determining cellular susceptibility to viral infection, constitutively expressed ISGs also determine the rapid response and intensity of cellular antiviral activity. Because many ISGs are key components of antiviral pathways, their basal expression is necessary for the quick activation of these signaling pathways upon ligand engagement. Taking the JAK-STAT pathway as a typical example, because the key components of this cascade are present in the cell under homeostatic conditions, the synthesis of new protein components of this pathway in response to stimulation with IFN is not required. Therefore, activation of this signaling pathway can rapidly occur, resulting in a timely and effective way of controlling invading pathogens. Furthermore, most of the necessary components of the JAK-STAT pathway are encoded by ISGs.

In particular circumstances, deficiency of a single ISG can lead to compromised immunity following virus infection. Mice genetically deficient for STAT1, STAT2 or IRF9 developed persistent virus infection or even lethal disease in response to virus invasion, including those provoked by choriomeningitis virus, respiratory syndrome coronavirus and vesicular stomatitis virus [22-25]. In contrast, cells maintaining relatively higher levels of baseline ISGs show stronger resistance against virus infection. Nevertheless, the abnormal regulation of constitutive ISG expression is closely associated with treatment outcome in cancer or chronic HCV patients. Chronic hepatitis C patients with abnormally high levels of ISG expression in the liver at baseline poorly respond to pegylated IFN-α/ribavirin therapy [7, 8]. In cancer patients, abnormally high expression of ISGs promotes tumor

growth, metastasis, and confers resistance to chemotherapy and radiation [9, 10]. Thus, constitutive ISGs at requisite levels are vital to prepare the host cells into a "combat ready" or "pre-arming" mode, but also determine the treatment responses in particular diseases in patients. In conclusion, we have demonstrated that endogenous U-ISGF3 function as the constitutive transcription factor to sustain basal ISG transcription, conferring cell resistance against virus infection. In contrast, the absence of U-ISGF3 can lead to decreased ISG expression at baseline, being susceptible to virus infection.

Supplementary Materials and Methods

Study approval

The animal study was approved by the institutional animal ethics committee (Dier Experimenten Commissie). Human intestinal or liver tissues were obtained from patients during surgical resection. The patients agreed to participate by written informed consent, and the study was approved by the Medical Ethical Committee of the Erasmus Medical Center (Medisch Ethische Toetsings Commissie Erasmus MC).

Reagents

Human IFN-α (Thermo Scientific) was dissolved in phosphate-buffered saline (PBS) before use. Antibody against pSTAT1-Tyr^{701} (58D6; rabbit monoclonal; #9167) was obtained from Cell Signaling Technology. Antibodies against STAT1 (rabbit polyclonal; sc-592), STAT2 (rabbit polyclonal; SC-476), pSTAT2-Tyr^{690} (rabbit polyclonal; sc-21689-R), pSTAT1-Ser^{727} (rabbit polyclonal; sc-16570-R), ISGF-3γ p48 (H-143; rabbit polyclonal; sc-365893), and β-actin were purchased from Santa Cruz Biotechnology. Anti-rabbit or anti-mouse IRDye-conjugated secondary antibodies were obtained from LI-COR Biosciences. Stocks of JAK inhibitor 1 and NSC87877 (Santa Cruz Biotechnology) were dissolved in DMSO at a concentration of 10 mM.

3-D primary human intestinal or liver organoids models

Human intestinal crypt isolation and primary human intestinal organoids culture was described previously [26]. Human liver cell isolation and primary human liver organoids culture was described accordingly [27].

Cell models

Huh7.5 cells (a human hepatoma cell line), Caco2 cells (a human epithelial colorectal adenocarcinoma cell line), and A549 cells (a human alveolar basal epithelial cell line) were cultured in Dulbecco's modified Eagle medium (DMEM, Lonza Biowhittaker) complemented with 10% (v/v) fetal calf serum (FCS, Hyclone), 100 IU/ml penicillin, and 100 μg/ml streptomycin. Wild-type (WT) MEFs and MEFs from STAT1$^{-/-}$ [28] and STAT2$^{-/-}$ [29] mice were generously provided by Prof. Andrea Kröger (Helmholtz Centre for Infection Research) and Christian Schindler (Columbia University, NY), respectively. IRF9$^{-/-}$ mice and the corresponding WT MEFs [30] [30] were generously provided by K. Mossman (McMaster University, Canada). STAT1-deficient (U3A) and STAT2-deficient (U6A) cell lines

were kindly provided by G. R. Stark (Lerner Research Institute). Huh7.5 cells expressing the HCV subgenomic replicon containing a subgenomic HCV bicistronic replicon (1389/NS3-3V/LucUbiNeo-ET) linked to the firefly *luciferase* reporter gene were maintained in Dulbecco's modified Eagle medium (DMEM) complemented with 10% (v/v) fetal calf serum, 100 IU/ml penicillin, and 100 µg/ml streptomycin and 250 µg/ml G418 (Sigma) [31]. The HEV subgenomic model: Huh7.5 cells containing the subgenomic HEV sequence (Kernow-C1 p6/luc) coupled to a Gaussia luciferase reporter gene [32, 33]. Luciferase normalization cells (Huh7.5-norm) were generated by transducing Huh7.5 cells with a lentiviral vector expressing the firefly *luciferase* gene under the control of the human *phosphoglycerate kinase* (*PGK*) promoter. For the ISRE reporter model, Huh7.5 cells were transduced with a lentiviral transcriptional reporter system that expressed the firefly *luciferase* gene driven by a promoter containing multiple ISRE promoter elements (SBI Systems Biosciences), and luciferase activity was used as a reporter of ISRE promoter activation [34, 35]. Human plasmacytoid dendritic cells (pDCs), myeloid dendritic cells (mDCs), and T cells were purified from the buffy coats of healthy blood donors and were cultured in round-bottom, 96-well plates [36]. Culture medium of these cells was harvested after 48 hours and served as conditioned medium for further experiments. For simian rotavirus experiments, SA11, a well-characterized and broadly used laboratory strain of the virus, was used to inoculate the Caco2 cell line as a rotavirus infection model [26].

Gene knockdown or overexpression by lentiviral vectors

Lentiviral pLKO knockdown vectors (Sigma-Aldrich) expressing shRNAs targeting IFN-αR1, IFN-λR1, JAK1, STAT1, STAT2, or IRF9 and their appropriate controls were obtained from the Erasmus Biomics Center and were produced in HEK 293T cells. After a pilot study, those shRNA-expressing vectors that exerted optimal gene knockdown were selected. These shRNA sequences are listed in table S1. Stable gene knockdown cells were generated after lentiviral vector transduction and selection in medium containing puromycin (3 µg/ml; Sigma). The pTRIP.CMV.IVSb.ISG.ires.TagRFP–based STAT1, STAT2, and IRF9 overexpression lentiviral vectors were a kind gift from C. M. Rice (Rockefeller University) [37]. Control vectors expressing green fluorescent protein (GFP) was also used. The pLV-tetO-CMV-SV40-Puro-LoxP–based lentiviral vectors expressing WT STAT1 or the Y701F-STAT1 mutant (which cannot be phosphorylated) were kindly provided by G. R. Stark (Lerner Research Institute) [13]. Lentiviral pseudoparticles were generated as described previously [13, 37]. Ultracentrifugation was used to achieve high-titer lentiviruses with superior transduction efficiency.

Measurement of luciferase activity

For *Gaussia* luciferase analysis, the activity of secreted luciferase in the cell culture medium was measured with the BioLux *Gaussia* Luciferase Flex Assay Kit (New England Biolabs) according to the manufacturer's instructions. For firefly luciferase assays, luciferin potassium salt (100 mM; Sigma) was added to the cells and incubated for 10 min at 37°C. Luciferase activity was then quantified with a LumiStar Optima luminescence counter (BMG Lab Tech).

Quantitative RT-PCR analysis

RNA was isolated with a Machery-NucleoSpin RNA II kit (Bioke) and quantified with a Nanodrop ND-1000 spectrophotometer (Wilmington). All RNA samples were adjusted to a concentration of 62.5

ng/µL. RNA (500 ng) was used as template for the generation of complementary DNA (cDNA) with the reverse transcription system (TAKARA BIO INC). The cDNA (10 ng/well) of all detected genes was amplified for 50 cycles and quantified with a SYBRGreen-based real-time PCR system (Applied Biosystems) according to the manufacturer's instructions. *GAPDH* was considered as reference gene to normalize gene expression. Relative gene expression (based on mRNA abundance) was normalized to that of *GAPDH* using the formula: $2^{-\Delta\Delta CT}$ ($\Delta\Delta CT = \Delta CT_{sample} - \Delta CT_{control}$) [38]. All of the primer sequences are included in table S2.

Quantification of gene copy numbers

To generate a template with which to quantify ISG copy number under basal conditions, vectors containing the corresponding ISG genes were used. A series of dilutions, from 10^{-2} to 10^{-10}, were prepared and then were amplified and quantified by qRT-PCR to generate a standard curve. The standard curve was generated by plotting the log of the copy number against the cycle threshold (CT) value (fig. S1A). Copy numbers were calculated with the following equation: Copy number (molecules/µg) = (1 µg/0.01 µg) × [concentration (ng/µL) × 6.022×10^{23} (molecules/mol)] / [length of amplicon × 640 (g/mol) × 10^{9} (ng/g)].

Nuclear extraction and Western blotting analysis

Nuclear and cytoplasmic proteins were extracted with the nuclear and cytoplasmic protein extraction kit (Active Motif) according to the manufacturer's instructions. All samples were lysed in Laemmli sample buffer containing 0.1 M DTT and heated for 5 min at 95°C, which was followed by loading the samples onto a 10% sodium dodecyl sulfate polyacrylamide gel (SDS-PAGE) and separation by electrophoresis. After 90 min running at 120 V, proteins were electrophoretically transferred onto a polyvinylidene difluoride (PVDF) membrane (Invitrogen) for 1.5 hours with an electric current of 250 mA. Subsequently, the membrane was blocked with a mixture of 2.5 ml of blocking buffer (Odyssey) and 2.5 ml of PBS containing 0.05% Tween 20. This was followed by overnight incubation with the appropriate primary antibody (at a 1:1000 dilution) at 4°C. The membrane was washed three times, which was followed by incubation for 1 hour with IRDye-conjugated secondary antibody (1: 5000). After the membrane was washed three times, protein bands were detected with the Odyssey 3.0 Infrared Imaging System.

IFN production assay

Huh7.5 cells were seeded into 6-well plates at a density of 10×10^{4} cells per well and then were transduced with lentiviruses expressing STAT1, STAT2, or IRF9 singly or in combination at 37°C. Forty-eight hours later, the lentiviral particles were removed and the cells were washed three times with PBS. The culture medium was refreshed and the transduced cells were cultured for another 48 hours. The culture medium was subsequently collected and added to an ISRE luciferase reporter cell line that is sensitive to IFNs. The conditioned medium was also used to treat Huh7.5 cells for 24 hours, which was followed by quantification of ISG expression by qRT-PCR analysis.

Confocal laser electroscope assay

Cells were seeded on glass coverslips. After 12 hours, the cells were washed with PBS, fixed in 4% PBS-buffered formalin for 10 min, and blocked with Tween-milk-glycine medium [PBS, 0.05% Tween, skim milk (5 g /L), and glycine (1.5 g/L)]. Samples were incubated with primary antibodies overnight at 4 °C. The samples were then incubated with anti-mouse IgG (H+L), F(ab')2 Fragment (Alexa Fluor 488 conjugate), or anti-rabbit IgG(H+L), F(ab') 2 Fragment (Alexa Fluor 488 conjugate) secondary antibodies (each at a 1:1000 dilution). Nuclei were stained with DAPI (4,6-diamidino-2-phenylindole; Invitrogen). Images were detected with confocal electroscope (lens: 40 ×, software: ZenLightEdition).

Immunohistochemistry (IHC)

Paraffin-embedded liver tissue sections were deparaffinized in xylene, rehydrated in graded alcohols, and rinsed once in PBS containing 0.05% Tween. After antigen retrieval, 1.5% H_2O_2 was used to block endogenous peroxidase for 10 min at room temperature. The slides were incubated in 5% milk blocking solution, which was followed by overnight incubation with primary antibody at a 1:200 dilution before the tissue sections were then counterstained with hematoxylin. As a negative control, the primary antibody was replaced with PBS containing 0.05% Tween.

ChIP-seq data analysis

The ChIP-seq dataset for STAT1 (GSE31477) was retrieved from the ENCODE database. ChIP-seq datasets were processed and mapped to the hg19 reference genome as described previously [11]. ChIP-seq datasets with multiple replicates were merged. MACS 1.4.2 software was used for peak-calling and for the generation of binding profiles [39]. If the centers of two binding regions reported by MACS were 100 bp or less apart, then they were unified to a single binding region. The sequencing profiles were generated in the IGV browser [40].

Statistical analysis

All results were presented as means ± SEM. Comparisons between groups were performed with the Mann-Whitney test. Differences were considered to be statistically significant when $P < 0.05$.

Supplementary Figures

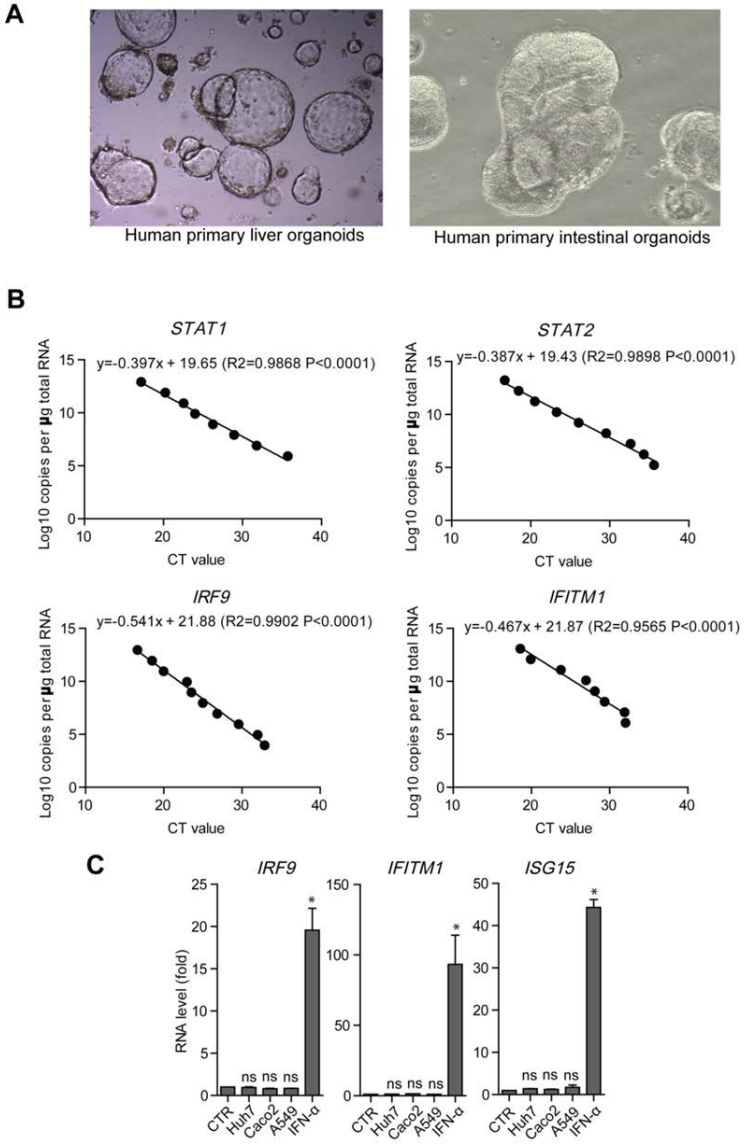

Fig. S1. Cells sustain basal ISG expression under homeostatic conditions. (A) Representative microscopy image of cultured human primary liver organoids (left) and intestinal organoids (right). (B) Standard curve for quantifying ISG genes copy numbers. Plasmids containing the corresponding ISG genes (*STAT1*, *STAT2*, *IRF9*, and *IFITM1*) were used. The plasmids were extracted, followed by a series of dilutions, from 10^{-2} to 10^{-10}, were prepared and then were amplified and quantified by qRT-PCR. Standard curve was generated by plotting the cycle threshold (CT) value with regard to the log copy number. (C) With the treatment of Huh7, Caco2, A549 conditioned medium or IFN-α (10 IU/ml, positive control) for 24 hours, the expression levels of *IRF9*, *IFITM1*, and *ISG15* in Huh7 cells were quantified by qRT-PCR (n = 3 independent experiments). **P* < 0.05; ***P* < 0.01; ns, not significant.

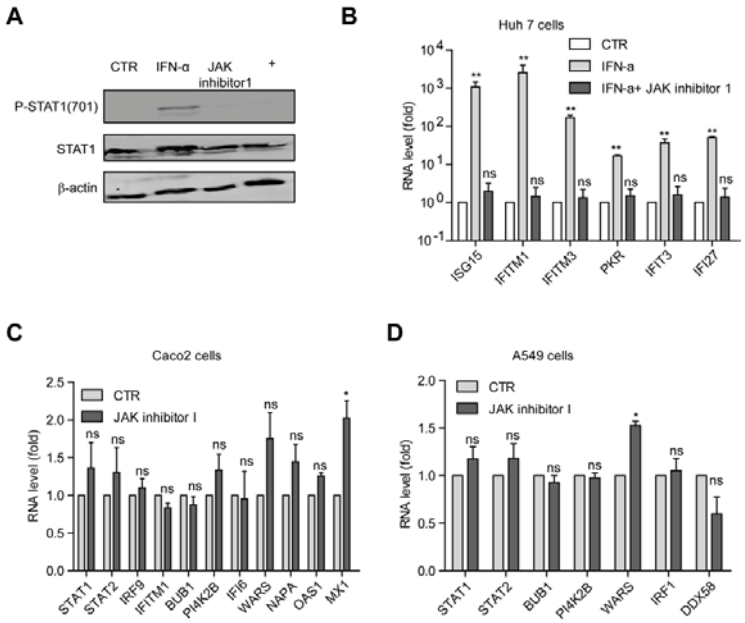

Fig. S2. Sustained basal ISG expression is independent of IFN production. (A) Representative Western blotting analysis (from three experiments) of total STAT1 and pSTAT1 (Tyr701) protein levels under the treatment of IFN-α (1000IU/ml), JAK inhibitor I (5uM) or the combination. (B) Huh7.5 cells were treated with IFN-α (1000IU/ml), 5 μM JAK inhibitor I or their combination for 24 hours before being subjected to qRT-PCR analysis of the relative abundances of the indicated mRNAs. (n = 3 independent experiments). (C) Caco2 cells were treated with 5 μM JAK inhibitor I for 24 hours before being subjected to qRT-PCR analysis of the relative abundances of the indicated mRNAs (n = 3 independent experiments). (D) Same as (C) for A549 cells (n = 3 independent experiments).

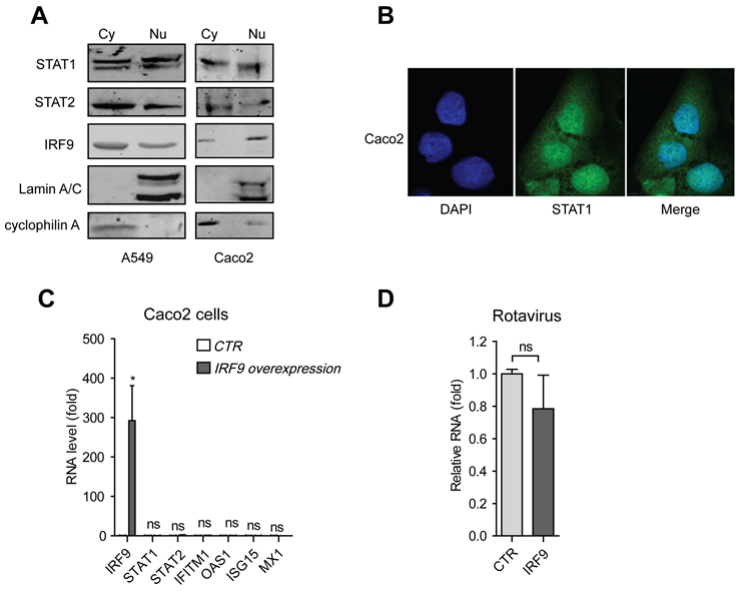

Fig. S3. STAT1, STAT2, and IRF9 are required for constitutive ISG expression.

(A) A549 and Caco2 cell lysates were fractionated into cytoplasmic (Cy) and nuclear (Nu) fractions and then were analyzed by Western blotting with antibodies against the indicated proteins. Cyclophilin A and Lamin A/C were used as cytosolic and nuclear markers, respectively. Western blots are representative of three independent experiments. (B) Confocal laser electroscope analysis of endogenous STAT1 localization in Caco2 cells. STAT1 is shown in green. Nuclei were visualized by DAPI (blue). Images are representative of multiple cells from three independent experiments.. (C) Caco2 cells transduced with control lentivirus or with lentivirus expressing IRF9 were subjected to qRT-PCR analysis of the relative abundances of the indicated mRNAs. (n = 3 independent experiments). (D) Rotavirus positive Caco2 cells transduced with control lentivirus or with lentivirus expressing IRF9 were subjected to qRT-PCR analysis of the relative abundances of the indicated mRNAs. (n = 3 independent experiments). *$P < 0.05$; **$P < 0.01$; ns, not significant.

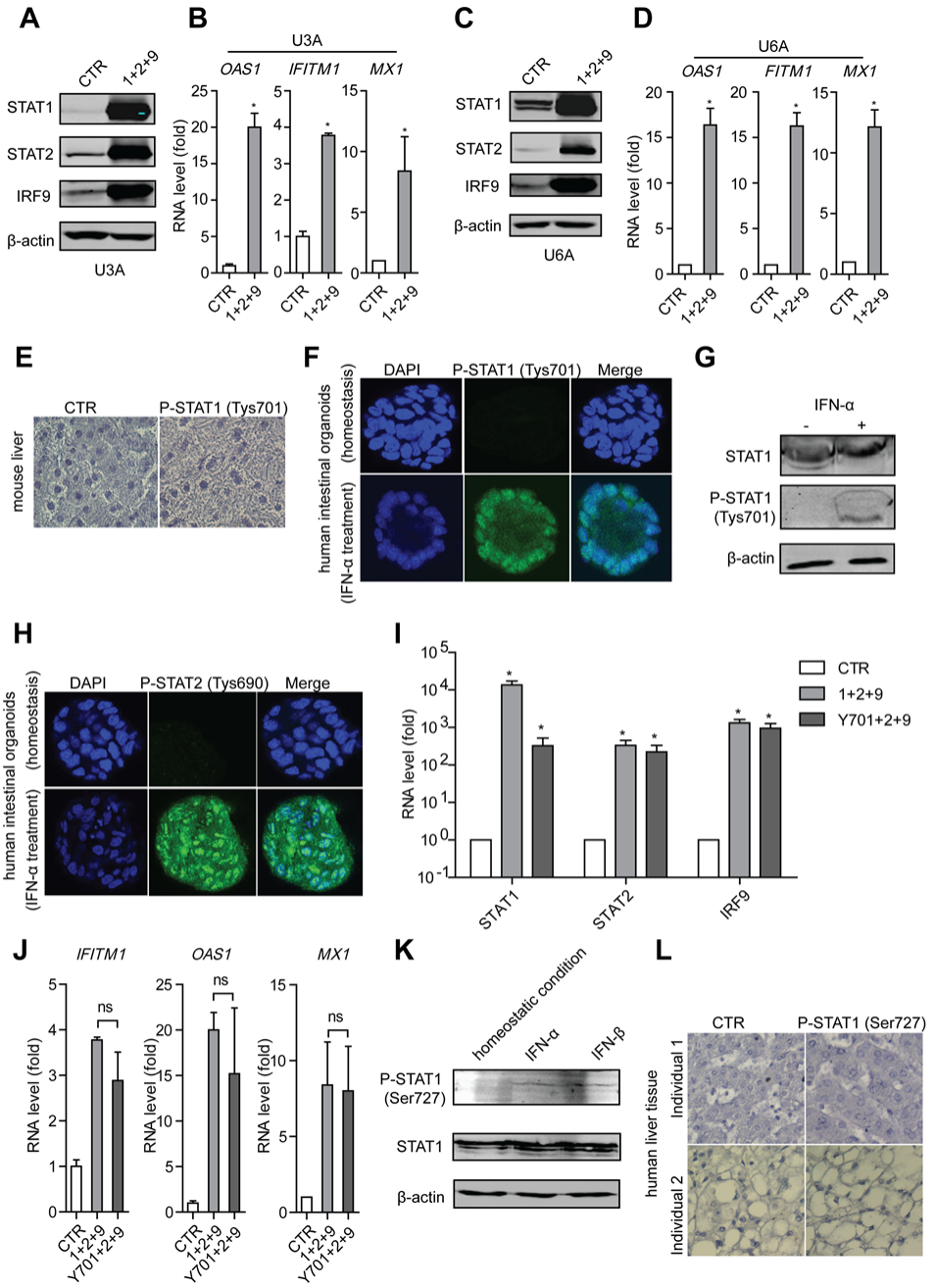

Fig. S4. The overexpression of U-ISGF3 leads to increased ISG expression. (A) STAT1 mutant cells (U3A) were transduced with control lentivirus or with lentivirus expressing STAT1, STAT2 and IRF9 before being subjected to Western blotting analysis with antibodies against the indicated proteins. Western blots are representative of three independent experiments.Western blotting (B) U3A cells were transduced with control lentivirus or with lentiviruses expressing the indicated proteins before being subjected to qRT-PCR analysis of the relative abundances of the indicated mRNAs. Data are means ± SEM of three independent experiments. (C) Same as (A) for U6A cells. (D) Same as (B) for U6A cells. (E) Representative immunohistochemical analysis of pSTAT1-Tyr^{701} in mouse liver tissue samples. As negative control, primary antibody against pSTAT1-Tyr^{701} was replaced with PBS plus Tween 0.05%. (F and G) Confocal laser electroscope analysis (F) and Western blotting analysis (G) of pSTAT1-Tyr^{701} in human intestinal organoids (from three experiments). Human intestinal organoids treated with IFN-α for 30 min served as the corresponding positive control. (H) Confocal laser electroscope analysis of pSTAT2-Tyr^{690}) in human intestinal organoids. Human intestinal organoids treated with IFN-α for 30 min served as the positive control. Images are representative of multiple organoids from three individual experiments. (I) RT-PCR confirmed the successful over-expression of STAT1, Y701F-STAT1, STAT2 or IRF9 in U3A cells (n = 3 independent experiments). (J) In U3A cells, over-expression of Y701F-STAT1 together with STAT2 and IRF9 led to a comparable ISG induction compared with its wild type (n = 3 independent experiments). (K)

Representative Western blotting analysis (from three experiments) of pSTAT1 (Ser^{727}) in Huh7 cells under the homeostatic condition. Huh7 cells treated with IFN-α, IFN-β (100IU/ml, 16 hours) served as positive controls. (L) Representative immunohistochemical staining (from three experiments) analysis of pSTAT1 (Ser^{727}) in human liver tissue samples from two individuals. Neither of them was detected. As negative control, primary antibody against pSTAT1 (Ser^{727}) was replaced with PBS plus Tween 0.05%. *P < 0.05; **P < 0.01; ns, not significant.

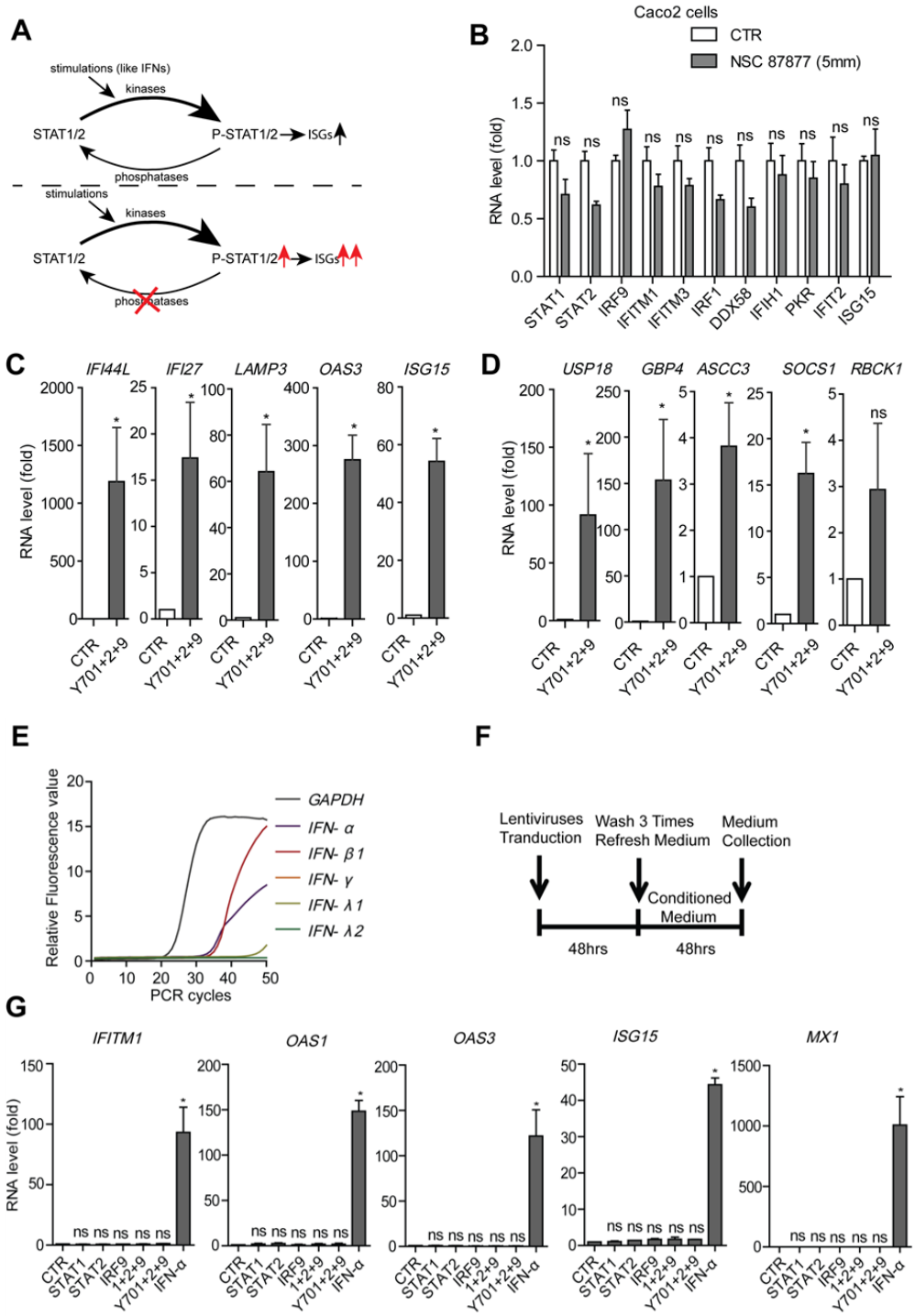

Fig. S5. U-ISGF3 stimulates ISG expression independently of IFN production. (A) The regulation of phosphorylation process of STAT1/2 was illustrated. Upon stimulations (e.g. by IFNs), STAT1/2 get phosphorylated by specific kinases. Importantly, phosphorylated STAT1/2 undergo dephosphorylation process. Thus, the phosphorylation and dephosphorylation process coordinate to maintain the phosphorylation level at a balanced state, which balances its beneficial antiviral versus detrimental proinflammatory effects. Consequently, the inhibition of phosphatases will alter the balanced state, leading to higher levels of

phosphorylated STAT1/2 and a much stronger induction of ISGs. (B) Caco2 cells were left untreated (CTR) or were treated with 5 µM NSC87877 (phosphatase inhibitor) before the cells were subjected to qRT-PCR analysis of the relative abundances of the indicated mRNAs. (n = 3 independent experiments). (C) and (D) Huh7.5 cells transduced with control lentivirus or with lentivirus expressing Y701F-STAT1, STAT2 and IRF9 were subjected to qRT-PCR analysis of the relative abundances of the indicated mRNAs. (n = 3 independent experiments). (E) The basal expression levels of several interferons, including *IFNA, IFNB1, IFNG, IL29*, *IL28A*, and the reference gene (*GAPDH*) were evaluated by qRT-PCR. (F) Schematic illustration of the production of conditioned medium (supernatant). (G) Huh7.5 cells were treated with conditioned medium from Huh7.5 cells with over-expression of STAT1, STAT2, IRF9 or their combination were subjected to qRT-PCR analysis of the relative abundances of the indicated mRNAs. IFN-α (10 IU/ml) serves as positive control (n = 3 independent experiments).

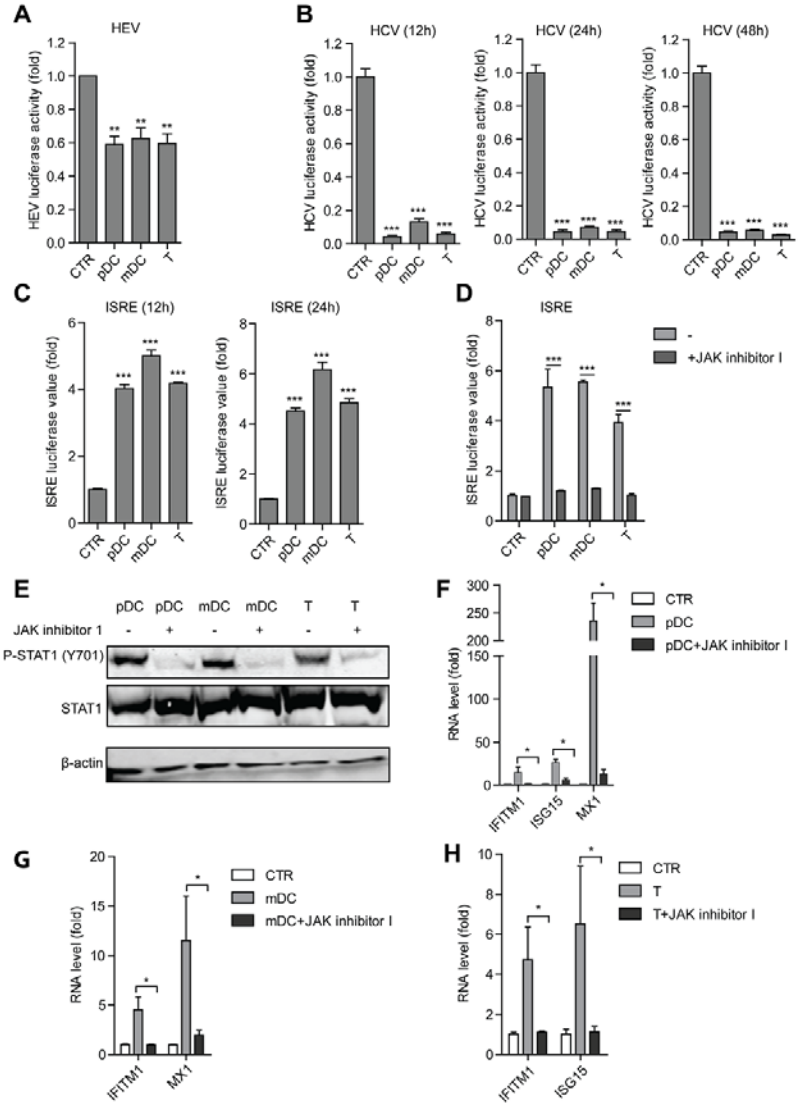

Fig. S6. IPCs produce IFNs to activate the JAK-STAT pathway, thus stimulating ISG expression and antiviral activity. (A) HEV viral replication-related firefly luciferase activity was measured upon the treatment of conditioned medium from pDC, mDC and T cells for 48 hours Data are means ± SEM of two or three replicates from three independent experiments. (B) HCV viral replication-related firefly luciferase activity was measured at 3 different time points (12 hours, 24 hours and 48 hours) upon the treatment of conditioned medium from pDC, mDC and T cells Data are means ± SEM of two or three replicates from three independent experiments. (C) ISRE luciferase value was measured at 2 different time points (12 hours and 24 hours) after the treatment of conditioned medium from pDC, mDC and T cells Data are means ± SEM of two or three replicates from three independent experiments. (D) Huh7.5-ISRE-luc cells were treated with conditioned medium from pDC, mDC and T cells without (-) or with JAK inhibitor I (5 µM) for 24 hours ISRE luciferase values were then measured and the fold-increase in activity relative to that of untreated cells was determined. Data are means ± SEM of two or three replicates from three independent experiments. (E) Representative Western blotting analysis

(from three experiments) of total STAT1 and pSTAT1(Tyr701) in Huh7.5 cells treated with conditioned medium (from pDC, mDC and T cells). (F) Huh7.5 cells were treated with conditioned medium (from pDC) without or with JAK inhibitor I (5 µM) for 24 hours before subjected to qRT-PCR analysis of the relative abundances of the indicated mRNAs. (n = 3 independent experiments). (G and H) Same as (F) for conditioned medium from mDC (G) and T (H) cells. *$P < 0.05$; **$P < 0.01$; ***$P < 0.001$; ns, not significant.

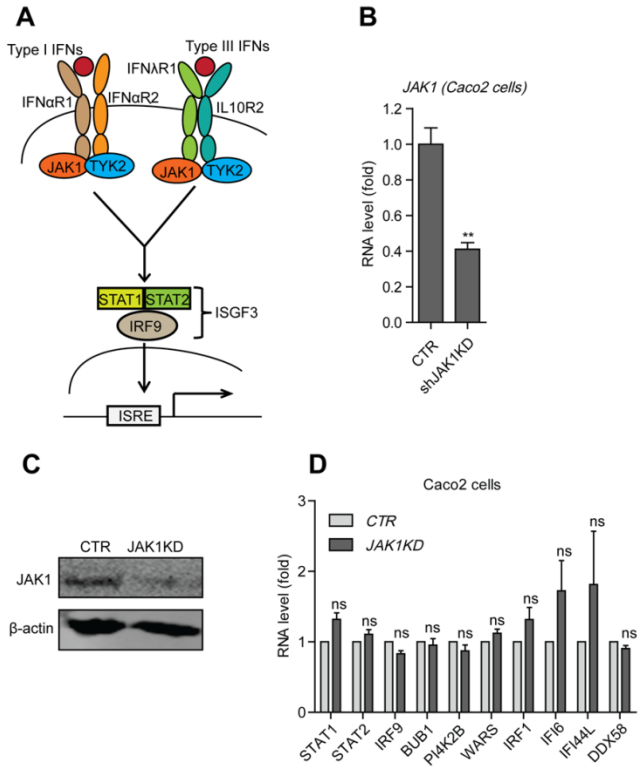

Fig. S7. U-ISGF3 stimulates ISG expression independently of upstream elements of the IFN signaling pathway. (A) Illustration of type I and III IFN signaling pathways. (B and C) Caco2 cells transduced with lentiviruses expressing control or JAK1-specific shRNAs were analyzed by qRT-PCR to determine the extent of knockdown of JAK1 mRNA (B) or by Western blotting with antibodies against the indicated proteins (C). Data in (B) are means ± SEM of three independent experiments. Western blots are representative of three independent experiments. (D) Caco2 cells transduced with lentiviruses expressing control or JAK1-specific shRNAs were analyzed by qRT-PCR to determine the relative abundances of the indicated mRNAs. Data are means ± SEM of three independent experiments. (n = 3 independent experiments). *$P < 0.05$; **$P < 0.01$; ns, not significant.

Acknowledgments

The authors gratefully thank S. U. Emerson (National Institute of Allergy and Infectious Diseases, NIH, USA) for generously providing the plasmids to generate subgenomic HEV genomic RNA; R. Bartenschlager and V. Lohmann (University of Heidelberg, Germany) for providing the HCV replicon cells; C. M. Rice (Rockefeller University) for providing the STAT1, STAT2, and IRF9 lentiviral vectors; G. R. Stark (Lerner Research Institute) for providing the WT STAT1 and Y701F-STAT1 lentiviral vectors and the U3A and U6A cells; A. Kröger (Helmholtz Centre for Infection Research) for providing the WT and STAT1$^{-/-}$ MEFs; C. Schindler (Columbia University, NY) for providing STAT2$^{-/-}$ MEFs; and K. Mossman (McMaster University, Canada) for providing primary WT and IRF9$^{-/-}$ MEFs. The authors also would like to acknowledge the ENCODE Experiment Matrix for providing the STAT1 ChIP-seq dataset.

Funding sources

This research was supported by The Netherlands Organization for Scientific Research (NWO/ZonMw) for VENI grant No. 916-13-032 to Q.P., the Dutch Digestive Foundation (MLDS) for a career development grant (No. CDG 1304) to Q.P., the Daniel den Hoed Foundation for a Centennial Award fellowship (to Q.P.), the European Association for the Study of the Liver (EASL) for a Sheila Sherlock Fellowship (to Q.P.), and the China Scholarship Council for funding Ph.D. fellowships to W.W. (201303250056), Y.Y. (201307720045), L.X. (201306300027), Y.W. (201207720007), and X.Z. (No. 201206150075).

References

1. Schneider, W.M., M.D. Chevillotte, and C.M. Rice, Interferon-stimulated genes: a complex web of host defenses. *Annu Rev Immunol*, 2014. **32**: p. 513-45.
2. Cheon, H., et al., IFNbeta-dependent increases in STAT1, STAT2, and IRF9 mediate resistance to viruses and DNA damage. *EMBO J*, 2013. **32**(20): p. 2751-63.
3. Cho, H., et al., Differential innate immune response programs in neuronal subtypes determine susceptibility to infection in the brain by positive-stranded RNA viruses. *Nat Med*, 2013. **19**(4): p. 458-64.
4. Seng, L.G., et al., High basal expression of interferon-stimulated genes in human bronchial epithelial (BEAS-2B) cells contributes to influenza A virus resistance. *PLoS One*, 2014. **9**(10): p. e109023.
5. Zurney, J., K.E. Howard, and B. Sherry, Basal expression levels of IFNAR and Jak-STAT components are determinants of cell-type-specific differences in cardiac antiviral responses. *J Virol*, 2007. **81**(24): p. 13668-80.
6. Stewart, M.J., et al., Basal and reovirus-induced beta interferon (IFN-beta) and IFN-beta-stimulated gene expression are cell type specific in the cardiac protective response. *J Virol*, 2005. **79**(5): p. 2979-87.
7. Dill, M.T., et al., Interferon-induced gene expression is a stronger predictor of treatment response than IL28B genotype in patients with hepatitis C. *Gastroenterology*, 2011. **140**(3): p. 1021-31.
8. Sarasin-Filipowicz, M., et al., Interferon signaling and treatment outcome in chronic hepatitis C. *Proc Natl Acad Sci U S A*, 2008. **105**(19): p. 7034-9.
9. Khodarev, N.N., B. Roizman, and R.R. Weichselbaum, Molecular pathways: interferon/stat1 pathway: role in the tumor resistance to genotoxic stress and aggressive growth. *Clin Cancer Res*, 2012. **18**(11): p. 3015-21.
10. Luszczek, W., et al., Combinations of DNA methyltransferase and histone deacetylase inhibitors induce DNA damage in small cell lung cancer cells: correlation of resistance with IFN-stimulated gene expression. *Mol Cancer Ther*, 2010. **9**(8): p. 2309-21.
11. Consortium, E.P., An integrated encyclopedia of DNA elements in the human genome. *Nature*, 2012. **489**(7414): p. 57-74.
12. McKendry, R., et al., High-frequency mutagenesis of human cells and characterization of a mutant unresponsive to both alpha and gamma interferons. *Proc Natl Acad Sci U S A*, 1991. **88**(24): p. 11455-9.
13. Cheon, H. and G.R. Stark, Unphosphorylated STAT1 prolongs the expression of interferon-induced immune regulatory genes. *Proc Natl Acad Sci U S A*, 2009. **106**(23): p. 9373-8.
14. Perwitasari, O., et al., Inhibitor of kappaB kinase epsilon (IKK(epsilon)), STAT1, and IFIT2 proteins define novel innate immune effector pathway against West Nile virus infection. *J Biol Chem*, 2011. **286**(52): p. 44412-23.
15. Ooi, E.L., et al., Novel antiviral host factor, TNK1, regulates IFN signaling through serine phosphorylation of STAT1. *Proc Natl Acad Sci U S A*, 2014. **111**(5): p. 1909-14.
16. Wu, T.R., et al., SHP-2 is a dual-specificity phosphatase involved in Stat1 dephosphorylation at both tyrosine and serine residues in nuclei. *J Biol Chem*, 2002. **277**(49): p. 47572-80.
17. Myers, M.P., et al., TYK2 and JAK2 are substrates of protein-tyrosine phosphatase 1B. *J Biol Chem*, 2001. **276**(51): p. 47771-4.
18. Eriksen, K.W., et al., Deficient SOCS3 and SHP-1 expression in psoriatic T cells. *J Invest Dermatol*, 2010. **130**(6): p. 1590-7.
19. Sung, P.S., et al., Roles of unphosphorylated ISGF3 in HCV infection and interferon responsiveness. *Proc Natl Acad Sci U S A*, 2015. **112**(33): p. 10443-8.
20. Porritt, R.A. and P.J. Hertzog, Dynamic control of type I IFN signalling by an integrated network of negative regulators. *Trends Immunol*, 2015. **36**(3): p. 150-60.
21. Schoggins, J.W. and C.M. Rice, Interferon-stimulated genes and their antiviral effector functions. *Curr Opin Virol*, 2011. **1**(6): p. 519-25.
22. Hofer, M.J., et al., Mice deficient in STAT1 but not STAT2 or IRF9 develop a lethal CD4+ T-cell-mediated disease following infection with lymphocytic choriomeningitis virus. *J Virol*, 2012. **86**(12): p. 6932-46.
23. Li, W., et al., IRF7-dependent type I interferon production induces lethal immune-mediated disease in STAT1 knockout mice infected with lymphocytic choriomeningitis virus. *J Virol*, 2014. **88**(13): p. 7578-88.

24. Zornetzer, G.A., et al., Transcriptomic analysis reveals a mechanism for a prefibrotic phenotype in STAT1 knockout mice during severe acute respiratory syndrome coronavirus infection. *J Virol*, 2010. **84**(21): p. 11297-309.
25. Meraz, M.A., et al., Targeted disruption of the Stat1 gene in mice reveals unexpected physiologic specificity in the JAK-STAT signaling pathway. *Cell*, 1996. **84**(3): p. 431-42.
26. Yin, Y., et al., Modeling rotavirus infection and antiviral therapy using primary intestinal organoids. *Antiviral Res*, 2015. **123**: p. 120-31.
27. Huch, M., et al., Long-term culture of genome-stable bipotent stem cells from adult human liver. *Cell*, 2015. **160**(1-2): p. 299-312.
28. Nandakumar, R., et al., Hepatitis C virus replication in mouse cells is restricted by IFN-dependent and -independent mechanisms. *Gastroenterology*, 2013. **145**(6): p. 1414-23 e1.
29. Park, C., et al., Immune response in Stat2 knockout mice. *Immunity*, 2000. **13**(6): p. 795-804.
30. Kimura, T., et al., Essential and non-redundant roles of p48 (ISGF3 gamma) and IRF-1 in both type I and type II interferon responses, as revealed by gene targeting studies. *Genes Cells*, 1996. **1**(1): p. 115-24.
31. Pan, Q., et al., Combined antiviral activity of interferon-alpha and RNA interference directed against hepatitis C without affecting vector delivery and gene silencing. *J Mol Med (Berl)*, 2009. **87**(7): p. 713-22.
32. Shukla, P., et al., Adaptation of a genotype 3 hepatitis E virus to efficient growth in cell culture depends on an inserted human gene segment acquired by recombination. *J Virol*, 2012. **86**(10): p. 5697-707.
33. Shukla, P., et al., Cross-species infections of cultured cells by hepatitis E virus and discovery of an infectious virus-host recombinant. *Proc Natl Acad Sci U S A*, 2011. **108**(6): p. 2438-43.
34. Wang, W., et al., Convergent Transcription of Interferon-stimulated Genes by TNF-alpha and IFN-alpha Augments Antiviral Activity against HCV and HEV. *Sci Rep*, 2016. **6**: p. 25482.
35. Pan, Q., et al., Mycophenolic acid augments interferon-stimulated gene expression and inhibits hepatitis C Virus infection in vitro and in vivo. *Hepatology*, 2012. **55**(6): p. 1673-83.
36. Pedroza-Gonzalez, A., et al., Tumor-infiltrating plasmacytoid dendritic cells promote immunosuppression by Tr1 cells in human liver tumors. *Oncoimmunology*, 2015. **4**(6): p. e1008355.
37. Schoggins, J.W., et al., A diverse range of gene products are effectors of the type I interferon antiviral response. *Nature*, 2011. **472**(7344): p. 481-5.
38. Livak, K.J. and T.D. Schmittgen, Analysis of relative gene expression data using real-time quantitative PCR and the 2(-Delta Delta C(T)) Method. *Methods*, 2001. **25**(4): p. 402-8.
39. Zhang, Y., et al., Model-based analysis of ChIP-Seq (MACS). *Genome Biol*, 2008. **9**(9): p. R137.
40. Robinson, J.T., et al., Integrative genomics viewer. *Nat Biotechnol*, 2011. **29**(1): p. 24-6.

Chapter 7

RIG-I Is a Key Antiviral Interferon-Stimulated Gene Against Hepatitis E Virus Dispensable of Interferon Production

Lei Xu[1], **Wenshi Wang[1]**, Yunlong Li[2], Xinying Zhou[1], Yuebang Yin[1], Yijin Wang[1], Robert A. de Man[1], Luc J. W. van der Laan[3], Fen Huang[2], Nassim Kamar[4,5,6], Maikel P. Peppelenbosch[1] and Qiuwei Pan[1]

[1]Department of Gastroenterology and Hepatology, Postgraduate School Molecular Medicine, Erasmus MC-University Medical Center, Rotterdam, the Netherlands

[2]Medical Faculty, Kunming University of Science and Technology, Kunming, China

[3]Department of Surgery, Postgraduate School Molecular Medicine, Erasmus MC-University Medical Center, Rotterdam, the Netherlands

[4]Department of Nephrology and Organ Transplantation, CHU Rangueil, Toulouse, France.

[5]INSERM U1043, IFR-BMT, CHU Purpan, Toulouse, France

[6]University Toulouse III-Paul Sabatier, Toulouse, France

Hepatology, 2017, 65(6): 1823-1839

Abstract

Interferons (IFNs) are broad antiviral cytokines that exert their function by inducing the transcription of hundreds of IFN-stimulated genes (ISGs). However, little is known about the antiviral potential of these cellular effectors on hepatitis E virus (HEV) infection, the leading cause of acute hepatitis globally. In this study, we profiled the antiviral potential of a panel of important human ISGs on HEV replication in cell culture models by overexpression of an individual ISG. The mechanism of action of the key anti-HEV ISG was further studied. We identified retinoic acid–inducible gene I (RIG-I), melanoma differentiation–associated protein 5, and IFN regulatory factor 1 (IRF1) as the key anti-HEV ISGs. We found that basal expression of RIG-I restricts HEV infection. Pharmacological activation of the RIG-I pathway by its natural ligand 5'-triphosphate RNA potently inhibits HEV replication. Overexpression of RIG-I activates the transcription of a wide range of ISGs. RIG-I also mediates but does not overlap with IFN-a-initiated ISG transcription. Although it is classically recognized that RIG-I exerts antiviral activity through the induction of IFN production by IRF3 and IRF7, we reveal an IFNindependent antiviral mechanism of RIG-I in combating HEV infection. We found that activation of RIG-I stimulates an antiviral response independent of IRF3 and IRF7 and regardless of IFN production. However, it is partially through activation of the Janus kinase (JAK)–signal transducer and activator of transcription (STAT) cascade of IFN signaling. RIG-I activated two distinct categories of ISGs, one class of JAK-STAT-dependent and the other of JAK-STAT-independent, which coordinately contribute to the anti-HEV activity. Conclusion: We identified RIG-I as an important anti-HEV ISG that can be pharmacologically activated; activation of RIG-I stimulates the cellular innate immunity against HEV regardless of IFN production but partially through the JAK-STAT cascade of IFN signaling.

Keyword: HEV; ISG; Retinoic acid-inducible gene I; JAK-STAT pathway

Introduction

Hepatitis E virus (HEV) infection is the most common cause of acute viral hepatitis worldwide [1]. As a single-strand RNA virus, HEV has been divided into 4 genotypes (gt) [1]. Although acute HEV infections are mostly self-limiting, gt1 HEV infection during pregnancy may lead to high mortality up to 30% [2]. In immunosuppressed patients, such as organ transplant recipients, gt3 HEV infection can cause chronic hepatitis [2]. For those chronic patients, monotherapy or the combination of ribavirin or/and pegylated Interferon-α (PegIFN-α) have been used as off-label treatment [1]. The observation that different populations with different status of their immune system have distinct outcomes of HEV infection highlights the importance of studying HEV-host interactions.

The innate immune response plays an essential role in defending viral infections. Patients with genetic deficiencies in the innate immune system are often pro to viral infection and develop more severe symptoms [3, 4]. In response to viral infection, host cells produce virus-induced cytokines including interferons (IFNs), particularly type I IFN (IFN-α and -β), which have potent antiviral activity against a broad spectrum of viruses [5]. Type I IFNs promote an antiviral state in an autocrine or paracrine manner by transcriptional induction of hundreds of interferon-stimulated genes (ISGs) [6]. However, excessive accumulation of type I IFNs may evoke pathological effects to the organism [7]. Recently, emerging studies have described the type I IFNs independent innate antiviral defense [8, 9]. These IFN-independent antiviral mechanisms including the production of alternative antiviral cytokines (*e.g.* IFN-λ or interleukin 22) and the basal expression of direct antiviral ISGs [9]. The basal expression of these ISGs may be attributed to tonic IFN signaling and this establishes a cell-autonomous antiviral status of the host, but independent of virus-triggered IFN production. Therefore, ISGs play important roles in both IFN-dependent and -independent antiviral mechanisms.

As the ultimate antiviral effectors, ISGs are transcriptionally induced through the Janus kinase/signal transducers and activators of transcription (JAK-STAT) pathway by tonic or exogenous IFNs. In previous studies, more than 380 individual human ISGs have been tested for their antiviral effects on a wide species of viruses including many important human and animal viruses [10, 11]. Surprisingly, only small subsets of ISGs exert antiviral activities against either a specific or broad spectrum of viruses. Unexpectedly, a few ISGs even promote the replication of certain viruses [10, 11]. Given the fact that IFN-α has anti-HEV activity *in vitro* and is probably also effective in chronic patients [12-14], this strongly suggests that ISGs may play a vital role in IFN-mediated HEV clearance. Furthermore, a genome-wide transcriptome profiling has identified the up-regulation of 30 genes in blood cells of chronic HEV patients, of which 25 are ISGs [15].

Because the function of ISGs during HEV infection remains largely elusive, we have profiled the effects of a panel of ISGs that are known to have anti- or pro-viral effects on certain viruses [10, 11]. We found most of these ISGs only have minor but some have potent anti-HEV effects. Among those ISGs, RIG-I is a key member that effectively restricts HEV replication. Furthermore, biological or pharmacological activation of RIG-I exerts potent anti-HEV effects. Mechanistically, it robustly activates the innate cellular antiviral response, unexpectedly dispensable of IFN production, but requiring the key elements of the JAK-STAT signaling.

Materials and Methods

HEV cell culture models

Multiple cell lines were used for supporting HEV replication, including Huh7.5 cells: a RIG-I defective hepatoma cell line that derived from Huh7 cells; A549 cells: a human lung epithelial carcinoma cell line that widely used for supporting HEV replication [16]. HepaRG cells: a hepatic cell line which retains many characteristics of primary human hepatocytes that also permissive for HEV replication. For the full-length HEV model, a plasmid construct containing the full-length HEV genome (Kernow-C1 p6 clone, GenBank Accession Number: JQ679013) was linearized at a 3' terminal MluI. Capped HEV viral RNA transcripts were generated by the Ambion *mMESSAGE* mMACHINE® *in vitro* RNA transcription Kit (Thermo Fisher Scientific Life Sciences) [16]. Huh7.5 cells, A549 cells and HepaRG cells were electroporated using the Bio-Rad's electroporation systems (240 V, pulse length 0.5, number 1 and cuvette 4 mm) with full-length HEV viral RNA to generate consecutive HEV-infected cell models, Huh7.5-p6, A549-p6 and HepaRG-p6. Briefly, cells were collected and washed with 5 mL Opti-MEM (Thermo Fisher Scientific Life Sciences) for three times. The cell pellet was resuspended with 100 µL Opti-MEM and mixed with 10 µg p6 full-length HEV RNA and then subjected to electroporation. To generate the subgenomic (p6-Luc) HEV model, a construct containing subgenomic HEV was also used. This plasmid has an HEV sequence in which the 5' portion of HEV ORF2 was replaced with the in-frame *Gaussia princeps* luciferase reporter gene to generate subgenomic (p6-Luc) [16]. The luciferase has a signal sequence that let it secreted into medium, and therefore, measurement of secreted luciferase activity represents HEV replication levels. Huh7.5 cells were electroporated as described above with HEV subgenomic RNA to generate subgenomic HEV replication model, Huh7.5-p6-Luc.

HEV reinfection assays

Supernatant that contains HEV viral particles were collected from the full-length HEV infectious cells (Huh7.5-p6) that cultured for 96 h. The supernatant was filtered by 0.45 µm filter to get rid of dead cell and then was centrifuged for 30 min (10 000 rpm) to remove cell debris. Next, 2 h ultracentrifugation (22 000 rpm) was used to purify and concentrate HEV virus particles (SW28 rotor; Beckman Coulter, Brea CA, USA). Subsequently, the collected pellet was resuspended and was diluted to 1×10^7 HEV viral RNA copies/mL and then stored at -80 °C as described previously [17]. For HEV infection assay, Huh7.5 and A549 cells were seeded into 12-well plates at a density of 7×10^4 cells per well. The next day, for each well, 400 µL HEV stock that contains 1×10^7 viral RNA copies/mL HEV was incubated with target cells at 37 °C for 6 h. Next, the HEV inoculum was removed and cell layers were washed 3 times with 1 mL PBS followed by adding 1 mL fresh medium to each well. For 6-well plates, cells were seeded at a density of 1.4×10^5 per well. The next day, for each well, target cells were incubated with 800 µL HEV stock at 37 °C for 6 h. Then, the HEV inoculum was removed and washed as usual and then added 2 mL fresh medium.

Lentivirus production and transduction assays

pTRIP.CMV.IVSb.ISG.ires.TagRFP based ISG overexpression vectors were kind gifts from Prof. Charles M. Rice (the Rockefeller University) [10]. Two vectors expressing *Photinus pyralis* luciferase (Fluc) or GFP as reporter genes were used as a control. Lentiviral pseudoparticles were generated in 293T cells by co-transfection of ISG expression plasmid (pTRIP.CMV.IVSb.ISG.ires.TagRFP), HIV gag-pol and VSV-G in a ratio of 1: 0.8: 0.2 as described and lentiviral stocks were stored at -80 °C [10]. For transduction assays, cells were seeded into 24-well plates at a density of 5×10^4 cells per well and transduced with lentiviral pseudoparticles at 37 °C. pLKO.1 based shRNA lentiviral vectors (Biomics Center in Erasmus Medical Center) targeting RIG-I was used to knockdown RIG-I gene expression and scrambled control vector (shSCR) was used as a control. Lentiviral pseudoparticles were generated as described previously [17]. To obtain stable gene knockdown cell line, cells were transduced with shRNA lentiviral particles for 3 days and selected by puromycin (Sigma-Aldrich, Zwijndrecht, the Netherlands) at a concentration of 2.5 μg/mL. After selection, optimal knockdown cell lines were chosen. The shRNA sequences are listed in Table S1 in Supporting Information.

Statistical analysis

GraphPad Prism 5 software was used for data analysis using a Mann-Whitney test. All results were presented as mean ± standard errors of the means (SEM). P values of less than 0.05 (single asterisks in figures) were considered statistically significant; whereas P values less than 0.01 (double asterisks) and 0.001 (triple asterisks) were considered highly significant. Further details are provided in the Supporting Information.

Results

Identification of antiviral ISGs against HEV replication

To identify key ISGs that regulate HEV replication, 25 important human ISGs which are known to have anti- or pro-viral effects on certain viruses [10] were tested in two Huh7.5 cells based HEV models (Huh7.5-p6-Luc and Huh7.5-p6). Huh7.5 is an RIG-I defective hepatoma cell line derived from Huh7 cells, which was widely used for supporting viral infections (Supporting Fig. S1A) [18]. These ISGs include MAP3K14, IFI44L, RIG-I (also known as DDX58), HPSE, RTP4, NAMPT (also known as PBEF1), IRF1, IFITM1, IFITM2, IFITM3, C6orf150 (also known as cGAS), UNC84B (also known as SUN2), IRF2, IRF7, IRF9, IFI6, OASL, DDX60, MOV10, TREX1, MDA5 (also known as IFIH1), ADAR, FAM46C, LY6E and MCOLN2 [10].

Ectopic overexpression of each ISG was delivered by a bicistronic lentiviral vector co-expressing the ISG and a red fluorescent protein (TagRFP). Two vectors that express a *Photinus pyralis* luciferase (Fluc) gene or a green fluorescent protein (GFP) gene were used as controls [10]. The successful overexpression of each ISG was confirmed by flow cytometry analysis to measure the expression of TagRFP (Supporting Fig. S1B-S1F). Transient transfection was used to overexpression ISG when lentiviral stocks failed to achieve high-level transduction [10]. Before profiling on HEV, each ISG was first tested for the ability to inhibit HCV replication in Huh7.5 cell-based HCV luciferase replicon model [10]. Similar to the previous study, most ISGs inhibit HCV replication to some extent; whereas several genes (IRF1, IRF2 and RIG-I) have strong anti-HCV effects (Supporting Fig. S1G). Next, all ISGs were tested for their anti-HEV ability in a subgenomic HEV model (Huh7.5-p6-Luc). At 24 h

after lentivirus transduction, most genes inhibited HEV-related luciferase activity to some extent (Fig. 1A). One gene named RIG-I was found to have strong anti-HEV activity at 48 h post transduction (Fig. 1B). More anti-HEV ISGs were identified 72 h after transduction, including IRF1, MDA5 and RIG-I (Fig. 1C). These genes could inhibit HEV-related luciferase activity by almost 50% compared to control. To further validate the antiviral ability, those ISGs were also tested in the full-length infectious HEV model (Huh7.5-p6). A similar inhibition pattern was obtained in this model (Fig. 1D). At 48 h after transduction, IRF1, MDA5 and RIG-I potently decreased HEV viral RNA level; whereas most of the other genes showed minor effects.

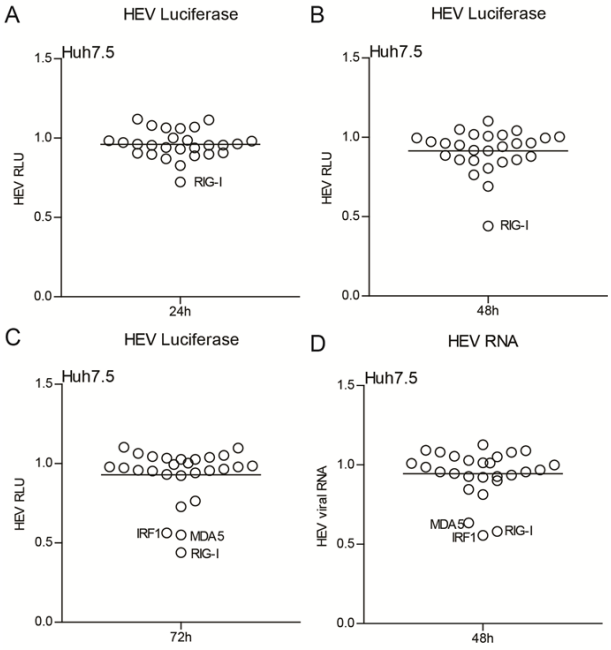

FIG. 1. Identification of ISGs that inhibit HEV replication.

Luciferase activity analysis of HEV-related *Gaussia* luciferase activity in Huh7.5-p6-Luc cells transduced with ISG overexpression or Fluc vector for 24 h (A), 48 h (C) or 72 h (C) (n = 4 independent experiments with each of 2 replicates). RLU: relative luciferase unit. (D) qRT-PCR analysis of HEV viral RNA level in Huh7.5-p6 cells transduced with ISG overexpression or Fluc vector for 48 h (n = 4). Data were normalized to the Fluc control (set as 1) and presented in dot plots.

RIG-I is a key anti-HEV ISG

Among these three potent anti-HEV ISGs, we have previously demonstrated that IRF1 inhibits HEV replication by stimulating antiviral ISG expressions [17]. Both RIG-I and MDA5 are pattern recognition receptors (PRRs) that sense viral RNA in the cytoplasm [19]. In this study, we mainly focused on the antiviral potential of RIG-I. To validate the anti-HEV activity of RIG-I, we performed additional independent experiments in two Huh7.5-based HEV models (Huh7.5-p6 and Huh7.5-p6-Luc). Lentiviral transduced RIG-I overexpression was confirmed in Huh7.5-p6 cells by qRT-PCR and immunoblotting (Fig. 2A). In both models, RIG-I overexpression inhibited HEV replication to an extent similar to a high dose of IFN-α treatment (Fig. 2B). Next, we confirmed the anti-HEV ability of RIG-I in different cell models: a human lung epithelial cell line A549 that is widely used for HEV propagation and a human hepatic progenitor cell-derived cell line HepaRG. Both of them are capable of supporting long-term HEV replication (A549-p6 and HepaRG-p6) [17]. As shown in Fig. 2C and 2D, RIG-I overexpression also significantly inhibited HEV replication in both HepaRG and A549 based HEV models.

To further explore the role of basal RIG-I in constraining HEV infection, RNAi approach was used to silence RIG-I gene expression. HEV RNA level was significantly increased in RIG-I silenced A549 cells (Fig. 2E and 2F). As expected, in RIG-I defective Huh7.5 cells, RIG-I knockdown did not

affect HEV infection (Supporting Fig. S2A and S2B) and we indeed observed that RIG-I defected Huh7.5 cell are more permissive for supporting HEV infection (Supporting Fig. S2C). These results have demonstrated that RIG-I has potent anti-HEV ability and the basal expression of RIG-I plays important role in defending HEV infection.

Pharmacological activation of RIG-I stimulates an antiviral response that inhibits HEV replication

To explore the antiviral response induced by RIG-I pathway, the natural ligand of RIG-I 5'pppRNA was used to activate the RIG-I signaling [20]. Different concentrations of RIG-I agonist were used to induce an antiviral response in A549 cells, a model with functional RIG-I expression (Supporting Fig. S1A). As shown in Fig. 3A, gene expression of type I IFN (IFN-β)
and type III IFN (IFN-λ) was significantly induced by RIG-I agonist 48 h or 72 h after treatment. Concurrently, the expression of many ISGs including STAT1, IFIH1, PKR, TRAIL, RANTES and RIG-I were also significantly induced by 5'pppRNA treatment (Fig. 3A).

Correspondingly, treatment with RIG-I agonist has resulted in a significant reduction of HEV replication in A549-p6 cells. With 1000 ng/mL 5'pppRNA treatment, the HEV viral RNA were inhibited by 67.8% ± 8.1% (mean ± SEM) (n = 7; P < .01), 90.0% ± 8.6% (n = 6; P < .01) at 48 h and 72 h after treatment, respectively (Fig. 3B). Since Huh7.5 cells are RIG-I defected cells (Supporting Fig. S1A), RIG-I agonist was unable to induce any antiviral response as expected (Supporting Fig. S2D).

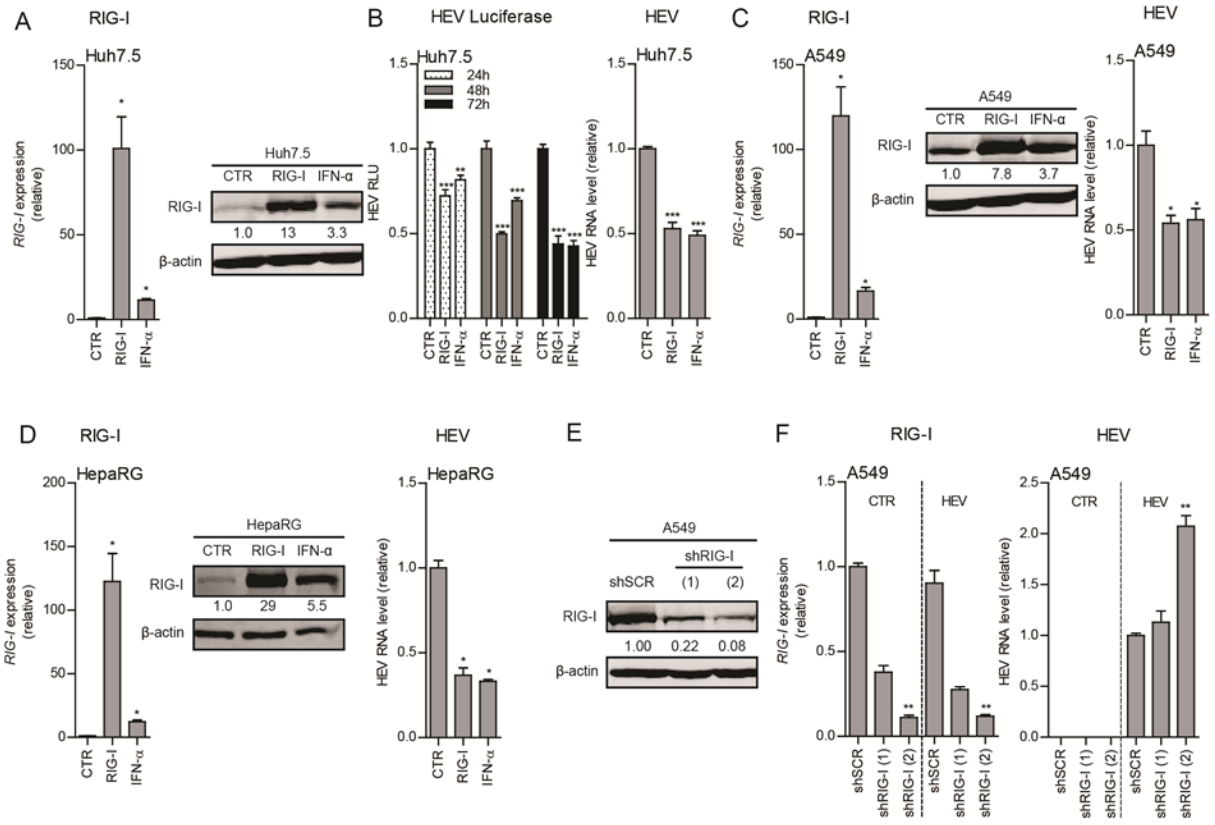

FIG. 2. RIG-I inhibits HEV replication in multiple cell models. qRT-PCR analysis and immunoblot analysis of RIG-I expression in Huh7.5-p6 cells (A), A549-p6 cells (C) and HepaRG-p6 cells (D) transduced with RIG-I, Fluc vector or treated with IFN-α (1000 IU/mL) for 48 h (qRT-PCR: n = 4). (B) Analysis of HEV-related *Gaussia* luciferase activity in Huh7.5-p6-Luc cells transduced with RIG-I, Fluc vector or treated with IFN-α (1000 IU/mL) for 24 h, 48 h or 72 h (n = 4 independent experiments with each of 3 - 4 replicates) and qRT-PCR analysis of HEV viral

RNA level in Huh7.5-p6 cells transduced with RIG-I vector or treated with IFN-α (1000 IU/mL) for 48 h (qRT-PCR: n = 8). RLU: relative luciferase unit. qRT-PCR analysis of HEV viral RNA level in A549-p6 cells (C) and HepaRG-p6 cells (D) transduced with RIG-I, Fluc vector or treated with IFN-α (1000 IU/mL) for 48 h (n = 4). (E) Immunoblot analysis of RIG-I expression in A549 cells transduced with lentiviral shRNA vector targeting RIG-I (shRIG-I(1) and shRIG-I(2)) or scrambled control (shSCR). Stable RIG-I knockdown or shSCR control A549 cells were infected with HEV. RIG-I expression level and HEV viral RNA level (F) were analyzed by qRT-PCR 72 h after HEV infection. Data were normalized to the Fluc control (CTR, set as 1, A-D) or to the scrambled control (shSCR, set as 1, F). Data are means ± SEM. *P < 0.05; **P < 0.01; ***P < 0.001; NS, not significant. For immunoblot results (A, C, D and E), band intensity of each lane was quantified by Odyssey Software. Immunoblot quantification results were normalized to β-actin expression and control was set as 1.

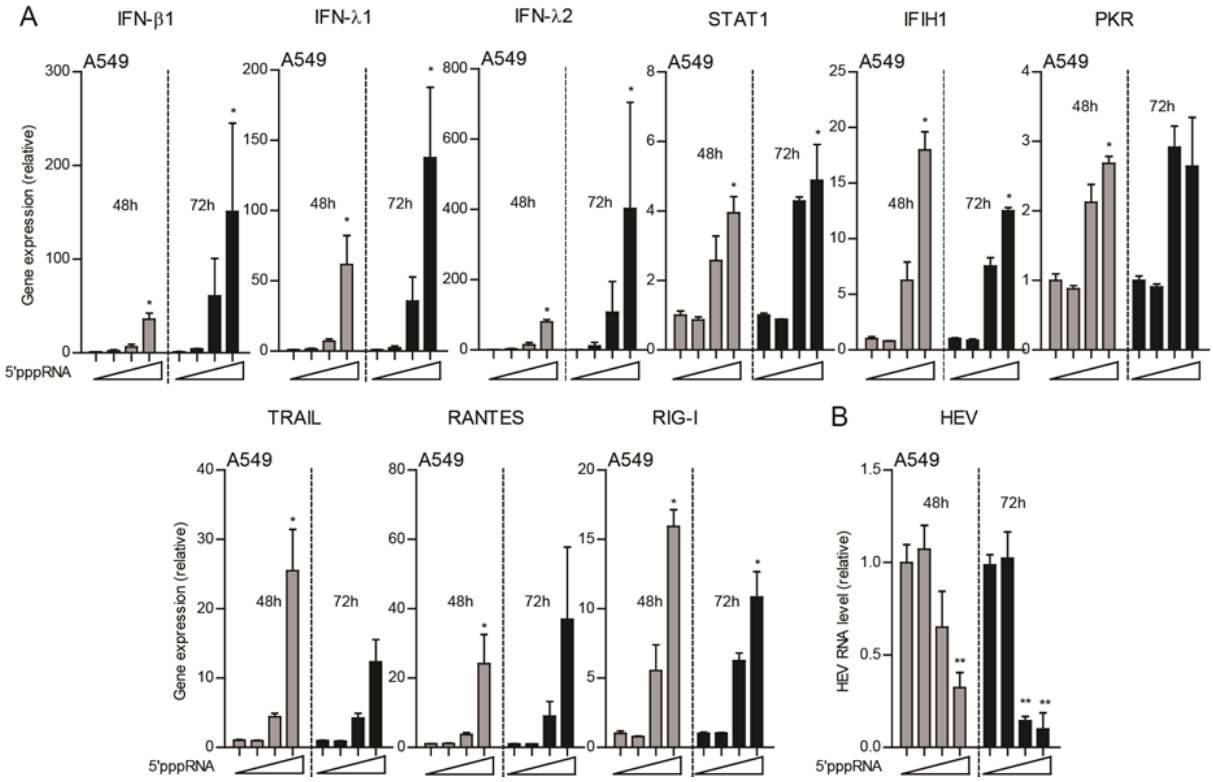

FIG. 3. 5'pppRNA stimulates an antiviral response that inhibits HEV. A549-p6 cells were transfected with various concentrations of 5'pppRNA (10 ng/mL, 100 ng/mL and 1000 ng/mL), IFN gene mRNA levels, ISG mRNA levels (A) and HEV viral RNA level (B) were analyzed by real-time qRT-PCR 48 h or 72 h after transfection (A: n = 3-5; B: n = 6-8). Data were normalized to a control that was transfected with PEI-Mix but without 5'pppRNA at each time point (48 h and 72 h, both set as 1), respectively. Data are means ± SEM. *P < 0.05; **P < 0.01; ***P < 0.001; NS, not significant.

To clarify whether the antiviral activity of 5'pppRNA exclusively relies on RIG-I pathway, we employed wild-type mouse embryonic fibroblasts (MEF) cells (WT, RIG-I$^{+/+}$) and RIG-I deficient MEF cells (RIG-I$^{-/-}$). These two MEF cell lines were transfected with different concentrations of 5'pppRNA. 1000 ng/mL 5'pppRNA treatment induced mouse IFN genes (mouse IFN-β, mIFN-β; mouse IFN-λ, mIFN-λ) more than 1000-fold at 24 h after stimulation (Supporting Fig. S3A). In contrast, no IFN gene was induced in RIG-I$^{-/-}$ MEF, indicating that this is exclusively dependent on the RIG-I signaling (Supporting Fig. S3A). Meanwhile, 5'pppRNA activated the expression of many mouse ISGs, including mMX1, mIRF9, mIFIH1, mSTAT1, mIRF1, mPML, mXAF, mIRF7, mISG15 and mRIG-I in RIG-I$^{+/+}$ MEF cells (Supporting Fig. S3A). After 48 h treatment, IFN gene and ISG expression was significantly induced by 5'pppRNA, although, to a less extent compared to 24 h after treatment (Supporting Fig. S3B). Hence, the anti-HEV activity of 5'pppRNA was specifically via RIG-I. We now demonstrated that

pharmacological activation of RIG-I stimulates an antiviral response that inhibits HEV replication specifically via RIG-I.

RIG-I activates the transcription of a wide range of ISGs

RIG-I has been shown to trigger STAT1 activation and ISG expression [21]. In general, the activation of STAT1 leads to the formation and nuclear translocation of IFN-stimulated gene factor 3 (ISGF3). This complex further binds to the IFN-stimulated response element (ISRE) motifs in the genome DNA and drives the transcription of ISGs. A recent study has reported that RIG-I overexpression stimulates ISRE promoter activity [22]. Thus, we employed a transcriptional reporter system that mimics IFN response with a reporter luciferase gene that was driven by multiple ISREs (ISRE-Luc). As shown in Fig. 4A, RIG-I significantly increased the ISRE-related luciferase activity. The activation of ISRE element usually leads to the transcription of ISGs that contain this element in their promoter regions. Therefore, we measured gene expression of a wide range of important antiviral ISGs. As shown in Fig. 4B-4D, RIG-I overexpression stimulated the expression of a large number of ISGs in Huh7.5, A549 and HepaRG cells. Interestingly, the ISG expression pattern induced by RIG-I was different from IFN-α treatment (Supporting Fig. S4A-S4C). The induction of some important ISGs was further confirmed by immunoblotting at protein levels (Fig. 4E and 4F).

RIG-I mediates IFN-α-induced antiviral ISG transcription

Gene expression profile analysis in the previous study revealed that 5'pppRNA treatment induced a distinct transcriptome compared to IFN-α treatment [20]. Besides, as a nucleic acid sensor, RIG-I is also an ISG that can be induced by IFN-α treatment and we already demonstrated that RIG-I activates the expression of many ISGs (Fig. 4). Therefore, we hypothesized that RIG-I may reinforce the IFN-α initiated ISG induction. We thus investigated the association of RIG-I expression with the response to IFN-α treatment. Indeed, in RIG-I overexpressed Huh7.5 cells, IFN-α induced ISG expression was significantly enhanced (Fig. 5A). Similarly, IFN-α induced ISG expression was also enhanced in RIG-I transduced A549 cells (Fig. 5B).

To further determine the role of RIG-I in IFN-α-activated cell signaling, the RIG-I knockdown A549 cell line and RIG-I deficient MEF cell line (RIG-I$^{-/-}$) were employed. In A549 cells, RIG-I deficiency significantly attenuated the ISG induction ability of IFN-α (Fig. 5C). Consistently, in RIG-I deficient MEF cells (RIG-I$^{-/-}$), the ISG induction ability of mIFN-α (mouse IFN-α) was also significantly reduced (Fig. 5D). In contrast, the ISG induction ability of mIFN-α was not affected in IRF3/7$^{-/-}$ or NFκB$^{-/-}$ MEF cells (Supporting Fig. S5A and S5B). Taken together, these results demonstrated that RIG-I functionally contributes to the antiviral ISG induction ability of IFN-α.

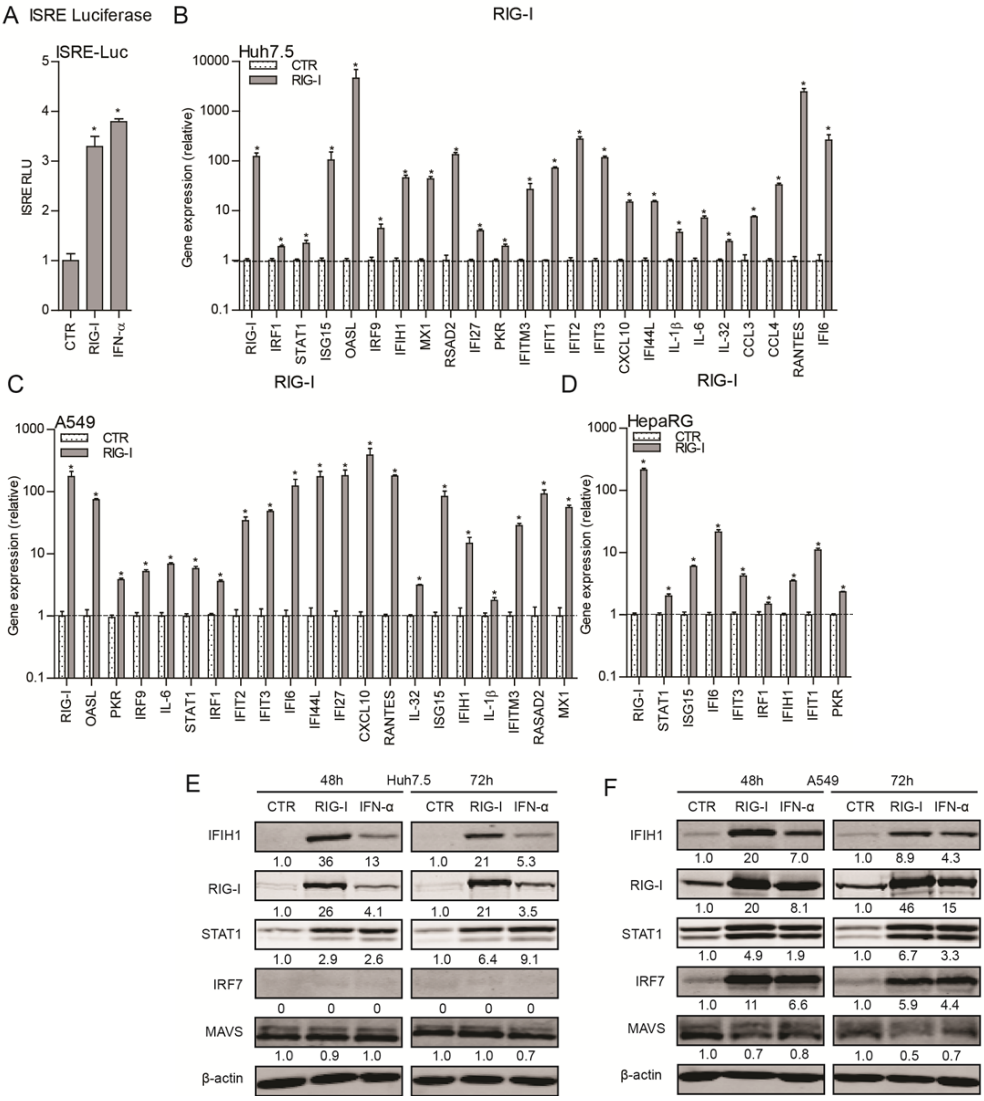

FIG. 4. RIG-I activates the transcription of a wide range of ISGs. (A) Analysis of ISRE related *firefly* luciferase activity in Huh7-ISRE-Luc cells transduced with RIG-I vector or treated with IFN-α (1000 IU/mL) for 48 h (n = 3 independent experiments with each of 1-2 replicates). qRT-PCR analysis of ISG mRNA levels in Huh7.5-p6 cells (B), A549-p6 cells (C) and HepaRG-p6 cells (D) transduced with RIG-I or Fluc vector for 48 h (n = 6). Immunoblot analysis of ISG protein levels in Huh7.5-p6 cells (E) and A549-p6 cells (F) transduced with RIG-I or Fluc vector for 48 h or 72 h. Date in (A) were normalized to the untreated Fluc control (CTR, set as 1). Data in (B-D) were normalized to the Fluc control (CTR, set as 1). Data are means ± SEM. *P < 0.05; **P < 0.01; ***P < 0.001; NS, not significant. For immunoblot results (E and F), band intensity of each lane was quantified by Odyssey Software. Immunoblot quantification results were normalized to β-actin expression and control was set as 1.

RIG-I activates the innate anti-HEV immune response dispensable of interferon production

RIG-I is a cytosolic nucleic acid sensor and the binding of viral RNA to RIG-I leads to the activation of downstream pathways that eventually triggers IFN gene expression via IRF3 and IRF7 [19]. In turn, the secreted IFNs establish antiviral response in infected and surrounding cells by stimulating the expression of ISGs. To further study the ISG induction ability of RIG-I pathways, the activator of RIG-I 5'pppRNA were transfected in IRF3/7 double knockout MEF cells (IRF3/7$^{-/-}$). Indeed, 5'pppRNA failed to induce IFN-β expression in the IRF3/7$^{-/-}$ cells (Fig. 6A). Strikingly, 5'pppRNA is still capable of

inducing ISGs in the absent of IRF3/7 and IFN-β expression (Fig. 6B). These results indicate RIG-I could also stimulate ISG transcription in IFN- independent manners. Next, we determined the mRNA expression levels of IFN genes in RIG-I overexpressed Huh7.5 cell line, a cell line that unable to produce any IFNs [23]. We found that the mRNA expression level of IFN genes was very low and no IFN gene (IFN-α, -β and -λ) was induced by RIG-I overexpression in Huh7.5-p6 cells (Fig. 6C, Supporting Fig. S6A). Furthermore, no IFN gene was up-regulated in HepaRG-p6 cells by RIG-I overexpression (Supporting Fig. S6B-S6C). To confirm the lack of IFN production in these RIG-I overexpressed cells, conditioned medium (supernatant) from the RIG-I transduced Huh7.5-p6 cells was collected (Fig. 6D). Two IFN sensitive assays were performed: an IFN functional assay and an HCV replicon-based bioassay. The IFN functional assay was based on a transcriptional reporter system that mimics IFN response as used above (Fig. 4A). As shown in Fig. 6E, conditioned medium collected from RIG-I overexpressed Huh7.5-p6 cells was not able to induce ISRE activation. Furthermore, this conditioned medium did not affect HCV-related luciferase activity (Fig. 6F). Similarly, conditioned medium collected from HepaRG cells also failed to activate ISRE-related luciferase activity (Supporting Fig. S6D). These results suggest that ectopic overexpression of RIG-I did not trigger IFN expression and production. Thus, we demonstrated that RIG-I could activate innate immune response dispensable of IFN production.

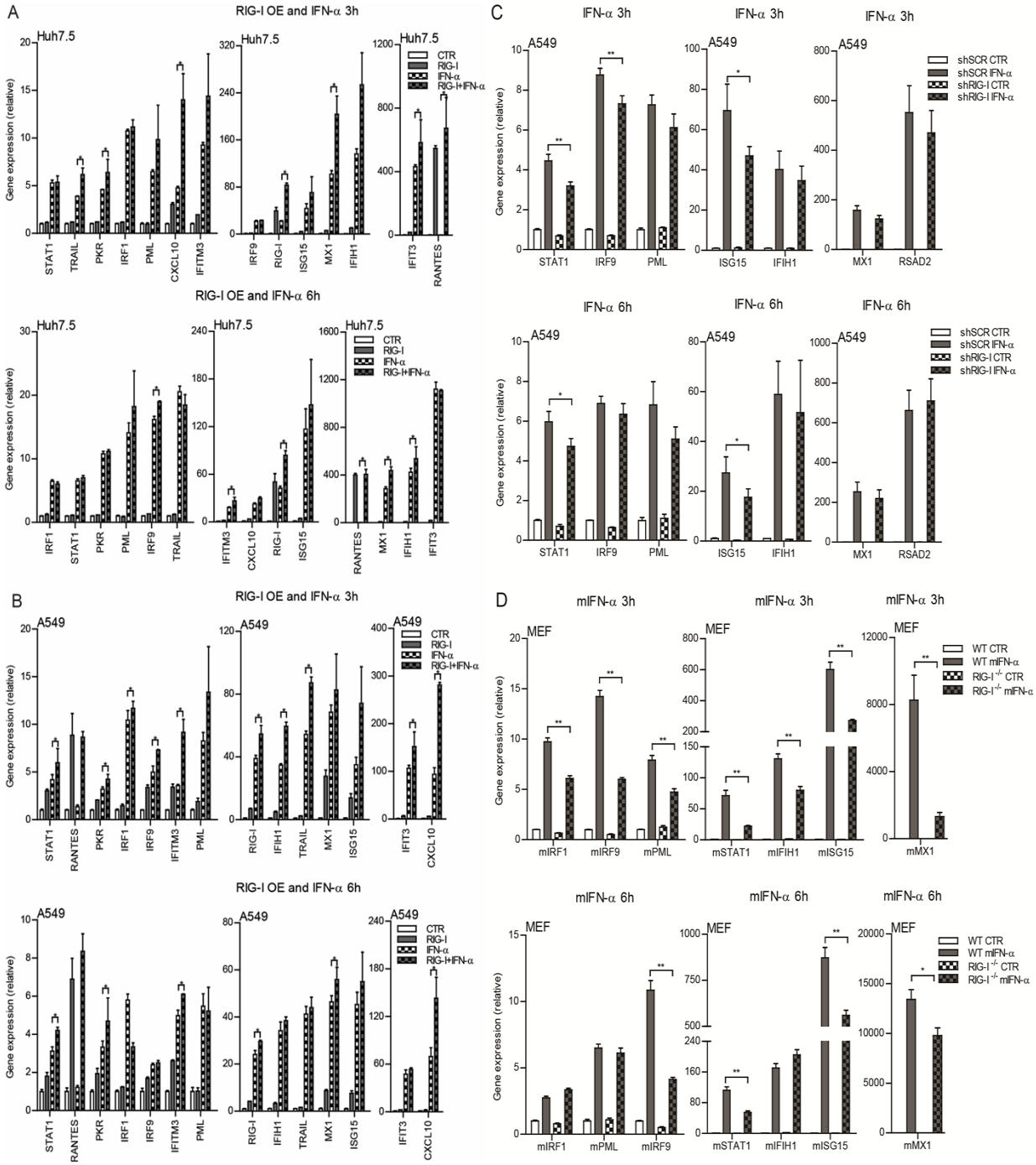

FIG. 5. RIG-I mediates IFN-α-induced antiviral ISG transcription. qRT-PCR analysis of ISG mRNA expression levels. Huh7.5 cells were transduced with RIG-I or Fluc vector, at 48 h post-transduction cells were treated with IFN-α (1000 IU/mL) for 3 h or 6 h (A) (n = 4). A549 cells were transduced with RIG-I or Fluc vector, at 48 h post-transduction cells were treated with IFN-α (1000 IU/mL) for 3 h or 6 h (B) (n = 4). Data in (A and B) were normalized to untreated the Fluc control (CTR, set as 1). A549 cells were transduced with lentiviral shRNA vectors targeting RIG-I or scrambled control (shSCR). The stable RIG-I knockdown and control A549 cells were treated with IFN-α (1000 IU/mL) for 3 h or 6 h (C). ISG mRNA levels were analyzed by qRT-PCR (n = 6). qRT-PCR analysis of mouse ISG mRNA levels in WT and RIG-I$^{-/-}$ MEF cells treated with mouse IFN-α (mIFN-α, 1000 IU/mL) for 3 h or 6 h (D) (n = 6). Data in (C) were normalized to the untreated scrambled control (shSCR CTR, set as 1). Data in (D) were normalized to untreated WT MEF cells (WT CTR, set as 1). Data are means ± SEM. *P < 0.05; **P < 0.01; ***P < 0.001; NS, not significant.

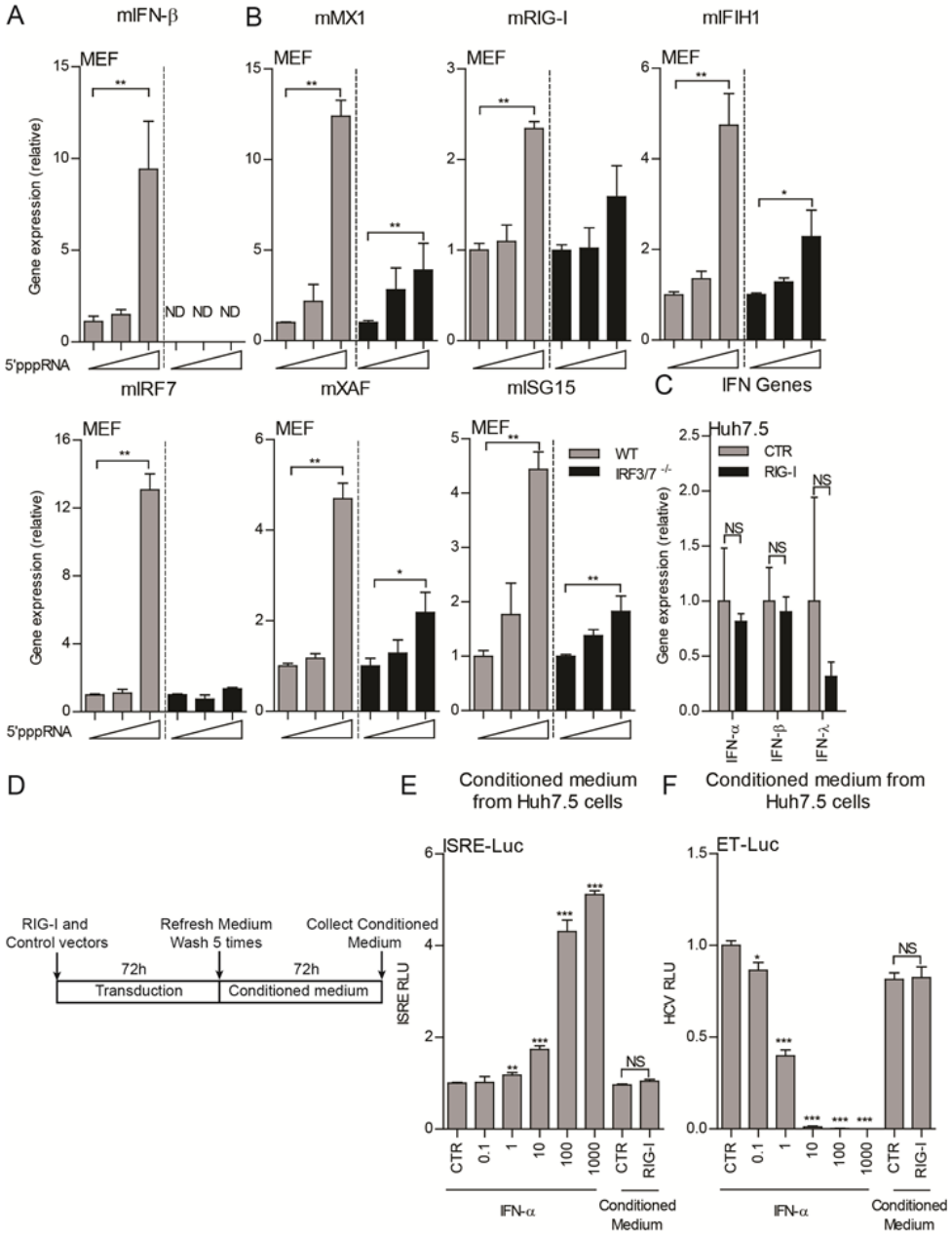

FIG. 6. RIG-I activates an immune response dispensable of interferon production. WT and IRF3 and IRF7 double deficient (IRF3/7$^{-/-}$) mouse embryonic fibroblasts (MEF) cells were transfected with various concentrations of 5'pppRNA (100 ng/mL and 1000 ng/mL), mouse IFN-β (mIFN-β) (A) and mouse ISG (B) mRNA levels were analyzed by qRT-PCR 24 h after transfection (n = 6). (C) qRT-PCR analysis of IFN gene mRNA levels in Huh7.5-p6 cells transduced with RIG-I or Fluc vector for 48 h (n = 4). (D) Production of conditioned medium (supernatant). Cells were transduced with RIG-I or GFP (CTR) vector for 72 h and then the cells were washed 5 times and medium was refreshed. Cells were cultured for another 72 h and supernatant was collected as conditioned medium. Analysis of ISRE-related *firefly* luciferase activity in Huh7-ISRE-Luc cells (E) or HCV-related *firefly* luciferase activity in Huh7.5-ET-Luc cells (F) that treated with conditioned medium from Huh7.5 cells or various concentrations of IFN-α for 48 h (n = 3 independent experiments with each of 3 - 4 replicates). Data in (A) and (B) were normalized to a control that transfected with PEI-Mix but without 5'pppRNA in each cell line (WT and IRF3/7$^{-/-}$, both set as 1), respectively. Data in (C) was normalized to the Fluc control (CTR, set as 1). Data in (E) and (F) were normalized to the untreated GFP control (CTR, set as 1). Data are means ± SEM. *P < 0.05; **P < 0.01; ***P < 0.001; NS, not significant.

RIG-I mediated ISG transcription and anti-HEV activity partially through activation of JAK-STAT pathway.

The previous study has demonstrated that RIG-I can augment STAT1 activation, which is a key element of JAK-STAT cascade within the IFN pathway [21]. Consistent with these results, we also observed that RIG-I overexpression induced the phosphorylation of STAT1 at 701 site in Huh7.5-p6 cells, which is an indispensable marker of JAK-STAT pathway activation (Fig. 7A).

To elucidate whether the ISG induction and anti-HEV abilities of RIG-I are through the activation of STAT1, we used a JAK inhibitor named CP-690550 (Tofacitinib) to pharmacologically block the JAK-STAT pathway. In Huh7.5-p6 cells, RIG-I and IFN-α induced STAT1 phosphorylation were totally blocked by CP-690550 (Fig. 7B). Meanwhile, lentiviral-delivered RIG-I overexpression was not affected by this inhibitor (Fig. 7B and 7C). Surprisingly, we found that RIG-I-induced ISRE activation was not totally diminished by this inhibitor; whereas IFN-α triggered ISRE activation was totally blocked (Fig. 7C). These results suggest that RIG-I-induced ISRE activation partially independent of its STAT1 phosphorylation ability. Next, we tested the mRNA expression level of 23 RIG-I inducible ISGs in RIG-I overexpressed Huh7.5-p6 cells treated with JAK inhibitor CP-690550. Surprisingly, among these 23 tested RIG-I inducible ISGs, only 10 genes were affected by CP-690550 treatment, but the others were not affected at all (Fig. 7D and 7E). As a positive control, the expression level of all these 23 genes that induced by IFN-α was totally diminished by this inhibitor (Supporting Fig. S7A and S7B). Consequently, the anti-HEV ability of RIG-I was only partially blocked by CP-690550; whereas the anti-HEV effects of IFN-α were totally abolished (Fig. 7F). To further confirm these results, another JAK inhibitor named JAK inhibitor 1 was used to treat RIG-I transduced Huh7.5-p6 cells. As expected, similar results were obtained (Supporting Fig. S8). To explore whether this is a common mechanism in different cell lines, we also used this JAK inhibitors 1 to treat RIG-I overexpressed HepaRG-p6 cells and similar results were obtained (Supporting Fig. S9).

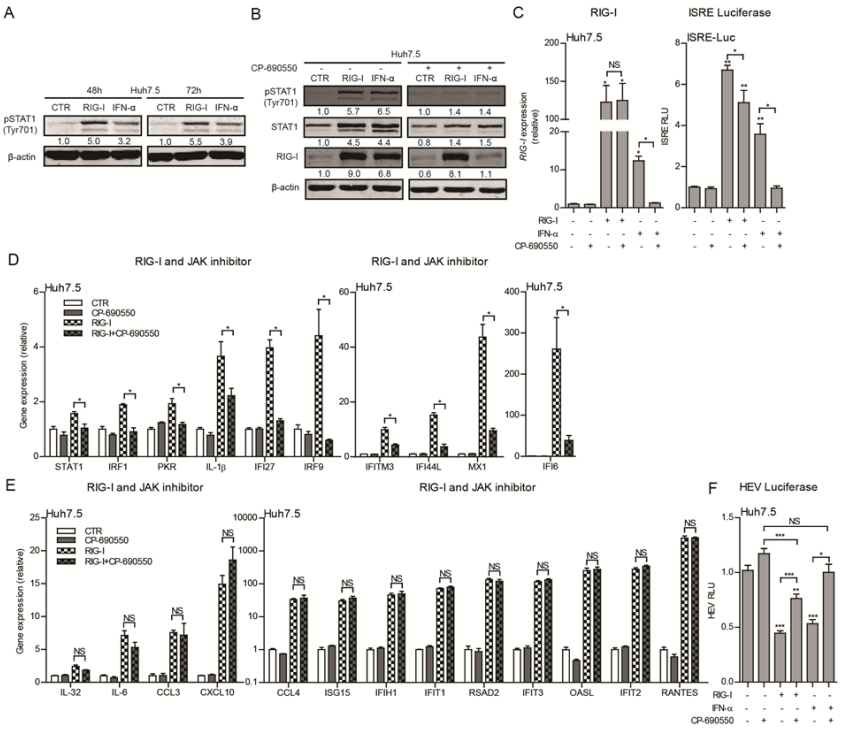

FIG. 7. JAK inhibitor CP-690550 partially diminishes RIG-I-induced ISG transcription and anti-HEV activity. (A) Immunoblot analysis of p-STAT1 (Tyr^{701}) expression in Huh7.5 cells transduced with RIG-I vector or treated with IFN-α (1000 IU/mL) for 48 h or 72 h. (B) Immunoblot analysis of ISG protein levels in Huh7.5 cells transduced with RIG-I vector or treated with IFN-α (1000 IU/mL) or CP-690550 (1000 ng/mL) for 48 h. qRT-PCR analysis of RIG-I mRNA level in Huh7.5-p6 cells and analysis of ISRE-related *firefly* luciferase activity in Huh7-ISRE-Luc cells (C) transduced with RIG-I vector or treated with IFN-α (1000 IU/mL) or CP-690550 (1000 ng/mL) for 48 h (qRT-PCR: n = 4; ISRE: n = 3 independent experiments with each of 2 replicates). (D and E) qRT-PCR analysis of ISG mRNA levels in Huh7.5 cells transduced with RIG-I vector or treated with CP-690550 (1000 ng/mL) for 48 h (n =5-6). (F) Analysis of HEV related *Gaussia* luciferase activity in Huh7-p6-Luc cells transduced with RIG-I vector or treated with IFN-α (1000 IU/mL) or CP-690550 (1000 ng/mL) for 72 h. (n = 4 independent experiments with each of 3 - 4 replicates). For immunoblot results (A and B), band intensity of each lane was quantified by Odyssey Software. Immunoblot quantification results were normalized to β-actin expression and control was set as 1. Data in (C left panel, D and E) were normalized to the untreated Fluc control (CTR, set as 1). Date in (C right panel and F) were normalized to the untreated GFP control (CTR, set as 1). Data are means ± SEM. *P < 0.05; **P < 0.01; ***P < 0.001; NS, not significant.

To further confirm the ISG induction ability of RIG-I is not totally dependent on the JAK-STAT pathway, we overexpressed RIG-I in STAT1 deficient human (STAT1$^{-/-}$) fibrosarcoma cells [24]. In STAT1$^{-/-}$ cell, RIG-I failed to induce STAT1 phosphorylation (Fig. 8A). A similar ISG induction pattern was also observed in RIG-I overexpressed STAT1$^{-/-}$ cells. Some genes such as STAT1, IRF9 and IFI6 can only be induced in WT cell but not in STAT1$^{-/-}$ cells by RIG-I, although RIG-I overexpression level was similar in both cell lines (Fig. 8B and 8C). Meanwhile, another group includes genes that can be activated in both WT and STAT1$^{-/-}$ cells such as IFIT1, RANTES and CXCL10 (Fig. 8D). As a control, IFN-α induced ISG transcription was totally abolished in STAT1$^{-/-}$ cells (Supporting Fig. S10A). Together, these results demonstrated that RIG-I activates ISG transcription and exerts its anti-HEV activity partially through the activation of the JAK-STAT pathway.

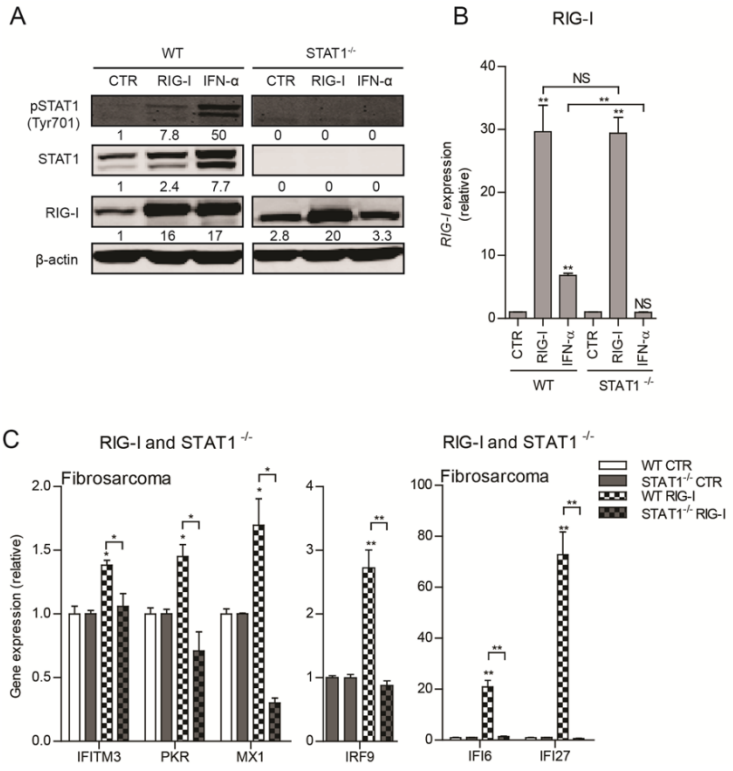

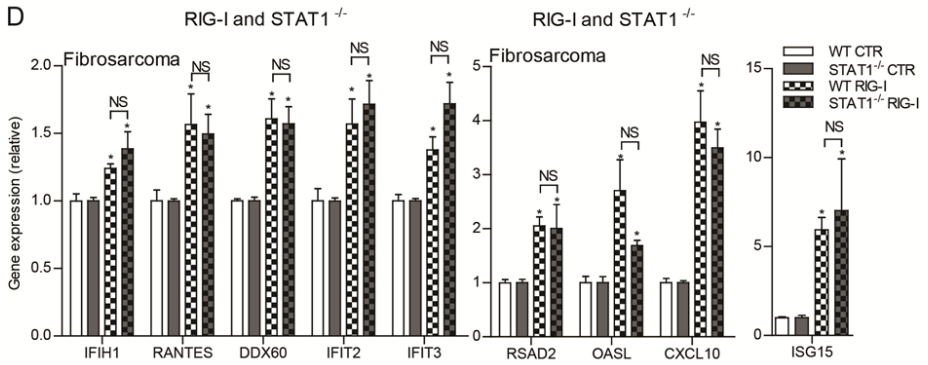

FIG. 8. The ISG induction ability of RIG-I is partially diminished in STAT1 deficient cells. (A) Immunoblot analysis of ISG protein levels in WT and STAT1 deficient ($STAT1^{-/-}$) fibrosarcoma cells transduced with RIG-I vector or treated with IFN-α (1000 IU/mL) for 48 h. (B) qRT-PCR analysis of RIG-I mRNA level in WT and $STAT1^{-/-}$ cells transduced with RIG-I vector or treated with IFN-α (1000 IU/mL) for 48 h (n =4-5). (C and D) qRT-PCR analysis of ISG mRNA levels in WT and $STAT1^{-/-}$ cells transduced with RIG-I or Fluc vector for 48 h (n = 4-5). For immunoblot results (A), band intensity of each lane was quantified by Odyssey Software. Immunoblot quantification results were normalized to β-actin expression and control was set as 1. Data in (C) were normalized to the untreated Fluc control (CTR, set as 1). Date in (D) and (E) were normalized to untreated WT and $STAT1^{-/-}$ cells, respectively (both set as 1). Data are means ± SEM. *P < 0.05; **P < 0.01; ***P < 0.001; NS, not significant.

Discussion

Currently, IFNs in particular IFN-α have been approved for treating viral infections including chronic hepatitis B (HBV) and C virus (HCV) infections [6]. In some cases, IFN-α has been used as an off-label drug to treat chronic HEV infection [12, 25]. *In vitro* study also showed the inhibition of HEV replication by IFN-α treatment [13, 14, 26]. IFN-α exerts its antiviral ability through the induction of ISGs, but how these ISGs affect HEV replication are still largely unknown. This study comprehensively profiled the antiviral ability of many important human ISGs described previously [10]. We found that most of these ISGs showed minor anti-HEV effect. In contrast, several previously reported broad antiviral ISGs including MDA5, IRF1 and RIG-I were identified as strong anti-HEV ISGs. Previously, we have demonstrated that IRF1 inhibits HEV replication by activating antiviral ISGs [17]. RIG-I is a pattern recognition receptor (PRR) and numerous studies have demonstrated that it plays important roles in defending a wide spectrum of virus infections such as HCV [10, 20], HBV [27] and influenza virus [28]. Here, in this study we comprehensively investigated the antiviral potential of RIG-I and its mechanism-of-action.

RIG-I, as a PPR, senses the viral RNA in the cytoplasm during infection. Binding of RIG-I with its ligand such as 5'-triphosphorylated RNA activates the downstream signaling pathway through the adaptor proteins mitochondrial antiviral signaling protein (MAVS). Classically, the aggregation of MAVS in mitochondrial subsequently leads to the production of type I and III IFNs through the phosphorylation of IRF3 and IRF7. The produced IFN proteins subsequently activate ISG expression in infected and bystander cells to eradicate the virus and prevent further infections. In this study, we observed overexpression of RIG-I activated transcription and expression of a wide range of ISGs, and many of them are known to have strong antiviral activities [10, 11, 17, 20, 29-32].

Although working as a cytosolic nucleic acid sensor that triggers IFN production, RIG-I itself is also an ISG regulated by IFN-initiated JAK-STAT cascade. This feedback amplification loop is able to enhance the responsiveness of host cells to infection. It has been shown that 5'pppRNA treatment

induced a broader transcriptome compared to IFN-α treatment. Consistently, we found that a combinatorial action of IFN-α treatment and RIG-I overexpression in ISG induction and anti-HEV activity. Conversely, IFN-α induced ISG transcription was attenuated when RIG-I was deleted (Fig. 5). These results suggest that RIG-I partially mediates the ISG transcription activity of IFN-α.

Classically, the main antiviral function of RIG-I is believed via the induction of IFN production upon sensing cytosolic viral nucleic acid. However, we found that RIG-I overexpression in our models doesn't induce the production of IFNs, but triggers the transcription of a wide range of genes including ISGs, chemokines and cytokines, without the activation of downstream MAVS pathway (Fig. 4E). In fact, emerging recent studies have proposed additional antiviral mechanisms of RIG-I that are partially dependent or independent of IFNs [27, 28, 33].

It has been demonstrated that induction of ISGs and antiviral ability by RIG-I activation were only partially reduced in the absence of IFN-α/β receptors [20]. Additionally, RIG-I can exert broad antiviral activity in the models that have defected IFN signaling [10]. We now observed that in cells that lacking of the key downstream components of RIG-I pathway (IRF3 and IRF7), the RIG-I activator 5'pppRNA is still able to induce ISG expression (Fig. 6A) without activating IFN genes. In line with this, we also observed that in Huh7.5 cells (a cell line which could not produce any IFN protein), RIG-I overexpression induces ISG transcription and exerts potent anti-HEV activity (Fig. 2). Together with recent reports, our observations strongly support that RIG-I can also execute its antiviral action via IFN-independent mechanisms. However, these IFN-dispensable actions are diverse and their exact mechanisms remain largely elusive.

Typically, the activation of RIG-I will trigger the activation of IRF3/7 and NF-κB through the MAVS antiviral singling.[20, 34] Activation of NF-κB pathway leads to the transcription of many pro-inflammatory genes including IFN genes. Our previous study also revealed that the NF-κB complex can directly bind to ISRE and drives its transcription of some ISGs.[35] Interestingly, many of the pro-inflammatory genes are regulated by both the NF-κB and JAK-STAT pathways. For instance, the transcription of CXCL10 is positively regulated by ISRE and NF-κB during viral infection.[36] It has been reported that MEF cells with a defected NF-κB pathway were more sensitive to the antiviral action of type I IFN.[37] We also observed that the IFN induced expression of some ISGs was enhanced in NF-κB KO MEF cells; whereas the expression of other genes was lower or unaffected (Supporting Fig. S5). Furthermore, a subset of RIG-I induced ISGs were unaffected when JAK-STAT pathway was blocked (Fig 7E), indicating the involvement of additional regulatory mechanisms. Thus, RIG-I and its down downstream pathways form a large complex web. Besides JAK-STAT cascade, other pathways such as NF-κB may also involve the regulation of RIG-I mediated ISG induction and antiviral activity.

A previous study demonstrated that RIG-I overexpression triggers STAT1 activation and ISG expression independent of its canonical MAVS pathway [21]. We now confirmed that overexpression of RIG-I activated STAT1 phosphorylation at 701 site (Fig. 7A) without the involvement of IFNs. We further addressed the contribution of STAT1 phosphorylation to the anti-HEV action of RIG-I. By using pharmacological inhibitors to block the JAK-STAT pathway, we demonstrated that RIG-I induced ISG transcription and anti-HEV activity is only partially but IFN-α mediated effect are totally dependent on this cascade. Furthermore, in a JAK-STAT deficient cell model, only a small proportion of RIG-I inducible ISGs were affected upon RIG-I overexpression. We thus classified these RIG-I inducible ISGs into two categories. One group, including STAT1, IRF1 and IRF9, is completely dependent on RIG-I-induced STAT1 phosphorylation. The other group, including IFIT1, IFIH1 and RANTES, is induced

independently of JAK-STAT pathway. Of note, both subsets may contribute to the anti-HEV ability of RIG-I, since the anti-HEV action of RIG-I was only partially attenuated by blocking JAK-STAT pathway (Fig. 7E). Recently, accumulating evidence unrevealed direct antiviral action of RIG-I independent of its downstream IFN production effect [27, 28, 33]. However, whether RIG-I has the direct anti-HEV effect is still unknown and need further investigation.

IFN-α and ribavirin have been used as monotherapy or combination for treating chronic HEV patients. Ribavirin monotherapy appears effective in many patients but failed in a substantial proportion of cases probably due to the development of drug resistance mutations in the viral genome [38-40]. IFN-α seems also effective but is associated with organ rejection, since most of the chronic HEV patients are immunocompromised organ recipients [41]. It is also well-known that excessive exposure to IFNs can result in pathogenesis to the host, and treatment of IFN-α is associated with various severe side effects in patients [42]. Therefore, dissecting the antiviral and the pathogenic mechanisms is necessary for developing specific antiviral strategies while avoiding unnecessary side effects. Our identification of RIG-I as a key anti-HEV ISG and its activation by the natural ligand 5'pppRNA exerting potent anti-HEV activity have provided proof-of-concept for designing such specific anti-HEV approach. Several RIG-I agonists (ImOl-100, Rigontec; MCT-465, Multicell Technologies; SB-9200, Spring Bank Pharmaceuticals) are at various stages of pre-clinical or clinical development for treating viral infections [43]. Thus, the possibility of using these RIG-I agonists in treating HEV infection deserves further evaluations.

In conclusion, we have identified RIG-I as a key anti-HEV ISG that inhibit HEV replication. Biological or pharmacological activation of the RIG-I pathway potently inhibit HEV replication. We further observed ectopic overexpression of RIG-I activated the transcription of many antiviral ISGs to establish an anti-HEV status. This is dispensable of IFN production but partially through the activation of JAK-STAT cascade. Thus, this study revealed new insights of HEV-host interactions, and provided novel avenues for antiviral drug development.

Funding Information

This research is supported by the European Association for the Study of the Liver (EASL) for a Sheila Sherlock Fellowship (to Q. Pan), the Netherlands Organization for Scientific Research (NWO/ZonMw) for a VENI grant (No. 916-13-032) (to Q. Pan), the Dutch Digestive Foundation (MLDS) for a career development grant (No. CDG 1304) (to Q. Pan), the Daniel den Hoed Foundation for a Centennial Award fellowship (to Q. Pan), the Erasmus MC Mrace grant (to Q. Pan) and the China Scholarship Council for funding PhD fellowships to L. Xu (201306300027), W. Wang (201303250056), X. Zhou (No. 201206150075), Y. Yin (201307720045) and Y. Wang (201207720007).

Acknowledgements

The authors gratefully thank Dr. Charles M. Rice (the Rockefeller University) for generously providing the overexpression lentiviral vector, Dr. Suzanne U. Emerson (National Institute of Allergy and Infectious Diseases, NIH, USA) for generously providing the plasmids to generate subgenomic and full-length HEV genomic RNA, Dr. Ralf Bartenschlager and Dr. Volker Lohmann (University of Heidelberg, Germany) for providing the HCV replicon cells., Dr. Sanna M. Mäkelä (National Institute for Health and Welfare Viral Infections Unit, Helsinki, Finland) for providing WT and RIG-I$^{-/-}$ MEF cells

generated by Dr. Michael J. Gale (Department of Immunology University of Washington) and WT, IRF3/7$^{-/-}$ and NFκB$^{-/-}$ MEF cells generated by Dr. A. Hoffmann (Signaling Systems Lab, Los Angeles, CA). We also thank Dr. George R. Stark (Lerner Research Institute) for providing WT and STAT1$^{-/-}$ human fibrosarcoma cells.

Abbreviations

HEV, hepatitis E virus; ISGs, interferon stimulated genes; IFN, interferon; IFN-α, interferon-α; mIFN-α, mouse interferon-α; RIG-I, retinoic acid-inducible gene I; MDA5, melanoma differentiation-Associated protein 5; JAK1, janus kinase 1; STAT1, signal transducers and activators of transcription 1; Fluc, *Photinus pyralis* luciferase; IRF1/2/7/9, interferon regulatory factor 1/2/7/9; PRRs, pattern recognition receptors; ISRE, IFN-stimulated response element; ISGF3, IFN-stimulated gene factor 3; MEF, mouse embryonic fibroblasts; TagRFP, red fluorescent protein; FCS, fetal calf serum; qRT-PCR, quantitative RT-PCR; GFP, green fluorescent protein; shRNA, short hairpin RNA; MTT, 3-(4,5-dimethylthiazol-2-yl)-2,5-diphenyltetrazolium bromide; RP2, human retinitis pigmentosa 2; GAPDH, glyceraldehyde 3-phosphate dehydrogenase.

Supplemental Materials and Methods

Reagents

Human IFN-α (Thermo Fisher Scientific, Life Sciences, the Netherlands) was dissolved in PBS. Mouse IFN-α (mIFN-α) was obtained from Thermo Fisher Scientific (#121001, Life Sciences). CP-690550 (Tofacitinib) was obtained from Santa Cruz Biotechnology and dissolved in DMSO. JAK inhibitor 1 (CAS 457081-03-7) was also obtained from Santa Cruz Biotechnology and dissolved in DMSO at a final concentration of 5 mg/mL. Dimethyl sulfoxide (DMSO, Sigma, Zwijndrecht, the Netherlands) was used as vehicle control at different concentrations. 5'ppp-dsRNA was purchased from InvivoGen (#tlrl-3prna, InvivoGen, CA, USA). Phospho-STAT1 (Tyr^{701}) (58D6, Rabbit mAb, #9167), STAT1 (Rabbit mAb, #9172), MDA5 (IFIH1) (D74E4, Rabbit mAb, #5321) and IRF7 (D2A1J, Rabbit mAb, #13014) antibodies were obtained from Cell Signaling Technology (Danvers, MA, USA). MAVS antibody (E-3, Mouse mAb, #sc-166583), RIG-I antibody (H-300, Rabbit polyclonal, #sc-98911) and β-actin antibody (C-4, Mouse mAb, #sc-47778) were obtained from Santa Cruz Biotechnology (Santa Cruz, CA, USA). 800CW Goat anti-Rabbit IgG (H + L) or 680RD Goat anti-Mouse IgG (H + L) IRDye®-conjugated secondary antibodies were obtained from Li-COR Biosciences (Lincoln, NE, USA).

Cell culture

Huh7.5 cells, 293T cells and A549 cells were grown in Dulbecco's modified Eagle medium (DMEM) (Lonza Biowhittaker, Verviers, Belgium) supplemented with 10% (v/v) fetal calf serum (FCS) (Hyclone, Lonan, Utah) and antibiotics. HepaRG cell line was maintained in William's medium (Thermo Fisher Scientific Life Sciences) as described previously [17]. Hepatitis C virus (HCV) luciferase replication models (ET-Luc) was based Huh7.5 cells coupled with a subgenomic HCV bicistronic replicon (I389/NS3-3V/LucUbiNeo-ET). Huh7.5-ET-Luc cells were grown in DMEM with 250 μg/mL G418

(Sigma Aldrich, Zwijndrecht, the Netherlands). ISRE (IFN-stimulated response element) activation reporter model (Huh7-ISRE-Luc) was based on Huh7 cells that expressing the *firefly* luciferase reporter gene driven by a promoter containing multiple ISRE elements (SBI Systems Biosciences, Mountain View, CA). Luciferase activity represents ISRE promoter activation level and this cell line was maintained in DMEM with 10% FCS and antibiotics.

Mouse embryonic fibroblast cells (MEFs) were grown in DMEM with 10% FCS, 0.6 μg/mL penicillin, 60 μg/mL streptomycin, 2 mM L-glutamine and 20 mM HEPES as described previously [29]. WT and RIG-I$^{-/-}$ MEF cells were generated by Dr. Michael J. Gale (Department of Immunology University of Washington). WT, IRF3/7$^{-/-}$ and NFκB$^{-/-}$ MEF cells were generated by Dr. A. Hoffmann (Signaling Systems Lab, Los Angeles, CA). All these MEF cells were kindly provided by Dr. Sanna M. Mäkelä (National Institute for Health and Welfare Viral Infections Unit, Helsinki, Finland) with the permission of Dr. Michael J. Gale and Dr. A. Hoffmann [29]. WT (fTGH) and STAT1 deficient (U3A, STAT1$^{-/-}$) human fibrosarcoma cells were grown in DMEM with 10% FCS and antibiotics. WT and STAT1$^{-/-}$ fibrosarcoma cells were kind gifts of Prof. George R. Stark (Lerner Research Institute) [44].

RNA and DNA transfection

Polyethylenimine (PEI, Sigma-Aldrich, Zwijndrecht, the Netherlands) was used for transfection of 5'pppRNA in A549 and MEF cells. Cells were seeded in 96-well plates at a density of 1×10^4 cells per well. The next day, the medium was removed and cell layer was washed by Opti-MEM. Different concentrations of 5'pppRNA were transfected with PEI in a total volume of 100 μL Opti-MEM. After 5 h, the medium was changed to normal medium. For lentiviral stocks failed to reach high-level transduction efficacy, DNA-transfection-based overexpression approach was used. Briefly, 7×10^4 Huh7.5 cells were seeded into 24-well plates per well. After cells adhered to the plate, 400 ng lentiviral ISG plasmids were transfected with PEI (Sigma-Aldrich, Zwijndrecht, the Netherlands) in a total volume of 1 mL Opti-MEM per well. After 5 h, the medium was changed to normal DMEM medium that contains 10% FBS.

Measurement of luciferase activity

Measurement of secreted *Gaussia* luciferase activity was conducted by using *BioLux*® *Gaussia* Luciferase Flex Assay Kit (New England Biolabs, Ipswich, MA, USA) according to the manufacturer's instructions. Luminescence signal was monitored by using a LumiStar Optima luminescence counter (BMG Lab Tech, Offenburg, Germany). Measurement of *firefly* luciferase activity was conducted by adding luciferin potassium salt (Sigma-Aldrich, Zwijndrecht, the Netherlands) to cells at a final concentration of 0.1 mM. 10 min after incubation, luciferase activity was measured.

Interferon production bioassay

10×10^4 cells per well were seeded into 6-well plates. Cells were transduced with control or RIG-I lentiviral pseudoparticles at 37 °C as described above. 72 h later, lentiviral particles were removed and cell layer was washed 3 times with PBS. Next, the medium wad refreshed and cultured for another 72 h to let the produced cytokines secreted into the medium. Subsequently, the supernatant (conditioned medium) was collected and then filtered by a 0.45 μm filter. To detect the secreted IFN

proteins in conditioned medium, two luciferase reporter models which are extremely sensitive to interferon treatments were used. Huh7.5-ET-Luc luciferase model is an HCV replicon which the HCV-related *firefly* luciferase activity can be potently inhibited by low concentration of IFN-α treatments. Huh7-ISRE-Luc is a luciferase reporter model in which the *firefly* luciferase gene was driven by a promoter containing multiple ISRE elements. In this model, the *firefly* luciferase activity can be potently induced by low concentration of IFN-α treatment. Therefore, these two luciferase models can be used to sensitively assess the presence of IFN proteins in the conditioned medium.

Real-time Quantitative RT-PCR (Real-time qRT-PCR)

RNA was isolated from cells using the Machery-NucleoSpin RNA II kit (Bioke, Leiden, Netherlands). RNA concentration was quantified by a Nanodrop ND-1000 Spectrophotometer (Thermo, DE, USA). 500 ng RNA was reverse transcribed to cDNA by using Takara cDNA Synthesis Kit with random hexamer primers according to manufacturer's instructions (Takara Bio, Inc., Shiga, Japan). Host gene expression and intracellular HEV level were quantified by SYBR-Green-based (Applied Biosystems® SYBR® Green PCR Master Mix, Thermo Fisher Scientific Life Sciences) real-time PCR on the StepOnePlus™ System (Thermo Fisher Scientific Life Sciences). For all human cell lines, two genes GAPDH and RP2 (Human retinitis pigmentosa 2) were used as housekeeping genes and expression level of target genes was normalized to GAPDH and RP2 by the $2^{-\Delta\Delta CT}$ method. For all mouse cell lines, one gene mGAPDH was used as housekeeping genes and expression level of target genes was normalized to mGAPDH by the $2^{-\Delta\Delta CT}$ method. Primers sets used for this study were listed in Table S2 and Table S3 in Supporting Information.

Quantification of HEV replication

Huh7.5-p6 and Huh7.5-p6-Luc are two well-established HEV models that could stably support HEV replication for a long term. In these two cell models, HEV-related *Gaussia* luciferase activity and HEV viral RNA level were measured over 3 months after electroporation when the HEV replication level was stable as described above. Lentivirus transduction and HEV RNA quantification were performed 2 weeks and 4 weeks after HEV RNA electroporation in A549-p6 and HepaRG-p6 models, respectively. WT and RIG-I$^{-/-}$ cells were infected with HEV virus stock as described in reinfection assays for 24 h. 3 days after HEV infection, cells were transfected with 5'pppRNA and HEV viral RNA was quantified 48 h after transfection. Intracellular HEV viral RNA was isolated from cellular lysates. The cells were lysed by using 350 mL RA1 buffer (Bioke, Leiden, The Netherlands) followed by RNA isolation as described above. Primer sequences for detecting HEV viral RNA were 5'-ATCGGCCAGAAGTTGGTTTTTAC-3' (sense) and 5'-CCGTGGCTATAACTGTGGTCT-3' (antisense). qRT-PCR was performed as follows: 10 min at 95 °C, 40 cycles of 15 s at 95 °C, 30 s at 58 °C, and 30 s at 72 °C.

Immunoblot analyses

Whole cell lysates were suspended in SDS sample buffer and heated at 95 °C for 5 min. Proteins were separated in 10% sodium dodecyl sulphate-polyacrylamide (SDS-PAGE) gel and were transferred onto a PVDF membrane (InvitroGen). Membranes were blocked for 1h at room temperature and then

were probed with primary antibodies overnight at 4 °C. Rabbit anti-p-STAT1 (1: 1000), anti-STAT1 (1: 1000), anti-IRF7 (1: 1000), anti-MDA5 (1: 1000), anti-RIG-I (1: 1000) antibodies or mouse anti-MAVS (1: 1000) and anti-β-actin (1: 1000) were used. Membranes were incubated at room temperature with goat anti-rabbit or goat anti-mouse IRDye®-conjugated secondary antibodies (Li-COR Biosciences, Lincoln, USA) (1: 5000). β-actin was served as loading control. Antibody signals were detected by Odyssey Infrared Imaging System and were visualized by Odyssey 3.0 software. Band intensity was quantified by Odyssey Software and normalized to the β-actin signal. The quantification result was showed below each band.

MTT assay

Cells were seeded in 96-well plates and cell viability was determined by adding 10 mM 3-(4,5-Dimethylthiazol-2-yl)-2,5-Diphenyltetrazolium Bromide (MTT) (Sigma, Zwijndrecht, the Netherlands). After 3 h, the medium was replaced with 100 µL of DMSO and was incubated for another 50 min. Absorbance was measured by absorbance reader (Bio-Rad, CA, USA) at a wavelength of 490 nm.

Flow cytometry analysis

The positive percentage of cells transduced with lentivirus was determined by directly detect TagRFP protein expression level. Cells were analyzed on a FACSAria™ flow cytometer (BD Biosciences) equipped with a 561-nm laser.

Supplementary Tables

Supplementary Table 1. Lentiviral shRNA sequences.

No.	Gene	ACCESSION	Sequences	Target Sequence
shRIG-I(1)	DEAD (Asp-Glu-Ala-Asp) box polypeptide 58	NM_014314.3	CCGGCCAGAGAAACTTGCCAGTTATCTCGAGATAACTGGCAAGTTTCTCTGGTTTTTTG	CCAGAGAAACTTGCCAGTTAT
shRIG-I(2)	DEAD (Asp-Glu-Ala-Asp) box polypeptide 58	NM_014314.3	CCGGCCAGAATTATCCCAACCGATACTCGAGTATCGGTTGGGATAATTCTGGTTTTTTG	CCAGAATTATCCCAACCGATA

Supplementary Table 2. Primer sequences for human cells.

Gene	F-Sequences (5' to 3')	R-Sequences (5' to 3')
ADAR	TCCGTCTCCTGTCCAAAGAAGG	TTCTTGCTGGGAGCACTCACAC
CCL3	ACTTTGAGACGAGCAGCCAGTG	TTTCTGGACCCACTCCTCACTG
CCL4	GCTTCCTCGCAACTTTGTGGTAG	GGTCATACACGTACTCCTGGAC
CXCL10	GGTGAGAAGAGATGTCTGAATCC	GTCCATCCTTGGAAGCACTGCA
DDX60	GGTGTTTTCACCAGGGAGTATCG	CCAGTTTTGGCGATGAGGAGCA
GAPDH	TGTCCCCACCCCCAATGTATC	CTCCGATGCCTGCTTCACTACCTT
IFI27	CGTCCTCCATAGCAGCCAAGAT	ACCCAATGGAGCCCAGGATGAA
IFI44L	TGCACTGAGGCAGATGCTGCG	TCATTGCGGCACACCAGTACAG
IFI6	TGATGAGCTGGTCTGCGATCCT	GTAGCCCATCAGGGCACCAATA
IFIH1(MDA5)	GCTGAAGTAGGAGTCAAAGCCC	CCACTGTGGTAGCGATAAGCAG
IFIT1	GCCTTGCTGAAGTGTGGAGGAA	ATCCAGGCGATAGGCAGAGATC
IFIT2	GGAGCAGATTCTGAGGCTTTGC	GGATGAGGCTTCCAGACTCCAA
IFIT3	CCTGGAATGCTTACGGCAAGCT	GAGCATCTGAGAGTCTGCCCAA
IFITM3	CTGGGCTTCATAGCATTCGCCT	AGATGTTCAGGCACTTGGCGGT
IFN-α	TGGGCTGTGATCTGCCTCAAAC	CAGCCTTTTGGAACTGGTTGCC
IFN-β1	CTTGGATTCCTACAAAGAAGCAGC	TCCTCCTTCTGGAACTGCTGCA
IFN-λ1	GGAAGACAGGAGAGCTGCAACT	AACTGGGAAGGGCTGCCACATT
IFN-λ2	TCGCTTCTGCTGAAGGACTGCA	CCTCCAGAACCTTCAGCGTCAG
IL-1β	CCACAGACCTTCCAGGAGAATG	GTGCAGTTCAGTGATCGTACAGG
IL-32	TCAAAGAGGGCTACCTGGAGAC	TCTGTTGCCTCGGCACCGTAAT
IL-6	AGACAGCCACTCACCTCTTCAG	TTCTGCCAGTGCCTCTTTGCTG
IRF1	GAGGAGGTGAAAGACCAGAGCA	TAGCATCTCGGCTGGACTTCGA
IRF2	TAGAGGTGACCACTGAGAGCGA	CTCTTCATCGCTGGGCACACTA
IRF9	CCACCGAAGTTCCAGGTAACAC	AGTCTGCTCCAGCAAGTATCGG
ISG15	CTCTGAGCATCCTGGTGAGGAA	AAGGTCAGCCAGAACAGGTCGT
JAK1	GAGACAGGTCTCCCACAAACAC	GTGGTAAGGACATCGCTTTTCCG
MX1	GGCTGTTTACCAGACTCCGACA	CACAAAGCCTGGCAGCTCTCTA
NAMPT	CTCCACCAGAACCGAAGGCAAT	AGGGTTACAAGTTGCTGCCACC
OASL	GTGCCTGAAACAGGACTGTTGC	CCTCTGCTCCACTGTCAAGTGG
PKR	GAAGTGGACCTCTACGCTTTGG	TGATGCCATCCCGTAGGTCTGT
PML	CCGTCATAGGAAGTGAGGTCTTC	GTTTTCGGCATCTGAGTCTTCCG
RANTES	CCTGCTGCTTTGCCTACATTGC	ACACACTTGGCGGTTCTTTCGG
RIG-I	CACCTCAGTTGCTGATGAAGGC	GTCAGAAGGAAGCACTTGCTACC
RP2	CCCATTAAACTCCAAGGCAA	AAGCTGAGGATGCTCAAAGG
RSAD2	CCAGTGCAACTACAAATGCGGC	CGGTCTTGAAGAAATGGCTCTCC
STAT1	ATGGCAGTCTGGCGGCTGAATT	CCAAACCAGGCTGGCACAATTG
STAT2	CAGGTCACAGAGTTGCTACAGC	CGGTGAACTTGCTGCCAGTCTT
TRAIL	TGGCAACTCCGTCAGCTCGTTA	AGCTGCTACTCTCTGAGGACCT

Supplementary Table 3. Primer sequences for mouse cells.

Gene	F-Sequences (5' to 3')	R-Sequences (5' to 3')
mIFIH1	TGCGGAAGTTGGAGTCAAAGCG	TGCGGAAGTTGGAGTCAAAGCG
mIFN-β	AAGAGTTACACTGCCTTTGCCATC	CACTGTCTGCTGGTGGAGTTCATC
mIFN-λ	CCAGTGGAAGCAAAGGATTGCC	GCACCTCATGTCCTTCTCAAGC
mIRF1	TCCAAGTCCAGCCGAGACACTA	ACTGCTGTGGTCATCAGGTAGG
mIRF7	CCTCTGCTTTCTAGTGATGCCG	CGTAAACACGGTCTTGCTCCTG
mIRF9	CAACATAGGCGGTGGTGGCAAT	GTTGATGCTCCAGGAACACTGG
mISG15	CATCCTGGTGAGGAACGAAAGG	CTCAGCCAGAACTGGTCTTCGT
mMX1	TGGACATTGCTACCACAGAGGC	TGGACATTGCTACCACAGAGGC
mPML	GTCTAAGACCCAACCTGTGGCT	CTTCATGGAGCCGACTGTCTGA
mRIG-I	AGCCAAGGATGTCTCCGAGGAA	ACACTGAGCACGCTTTGTGGAC
mSTAT1	GCCTCTCATTGTCACCGAAGAAC	TGGCTGACGTTGGAGATCACCA
mXAF	CTGCGCTTCATAGTCCTTTGCC	AGGGTGCTGTTGGCTTTCCTTG

Supplementary Figures

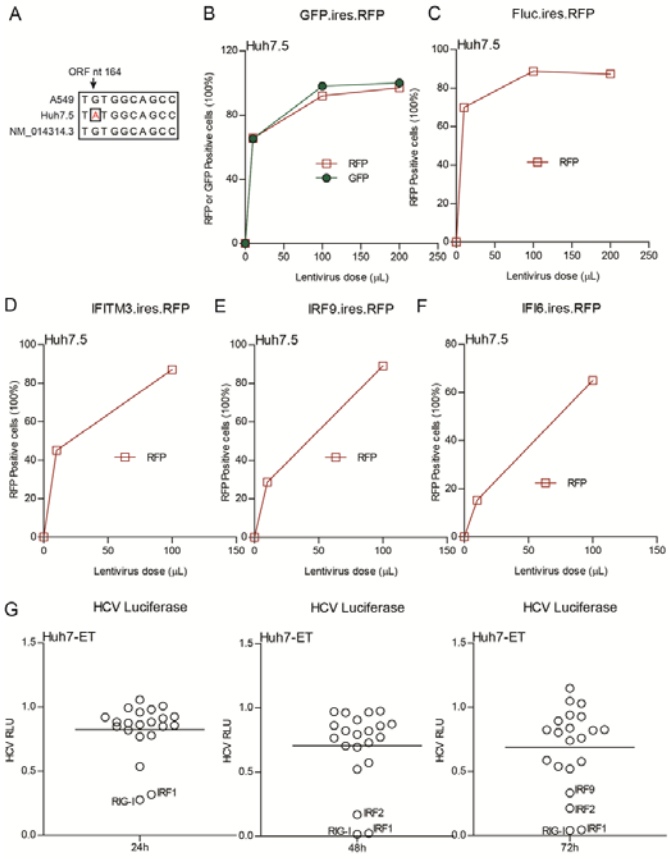

Figure S1. ISG-coupled TagRFP overexpression and the validation of their anti-HCV activities. (A) Sequencing analysis of RIG-I mutation in Huh7.5 and A549 cells. The mutation of RIG-I in ORF nt 164 in Huh7.5 cells was indicated as red. (B) Flow cytometry analysis of GFP or RFP positive cells in Huh7.5 cells transduced with GFP vector at the indicated doses for 48 h. (C-F) Flow cytometry analysis of RFP positive cells in Huh7.5 cells transduced with ISG.ires.RFP and Fluc vector at the indicated doses for 48 h. (G) Analysis of HCV related *firefly* luciferase activity in Huh7.5-ET-Luc cells transduced with ISG or GFP vector for 24 h, 48 h or 72 h (n = 4 independent experiments with each of 2 replicates). RLU: relative luciferase unit. Data in (G) were normalized to the GFP control (set as 1) and presented in dot plots.

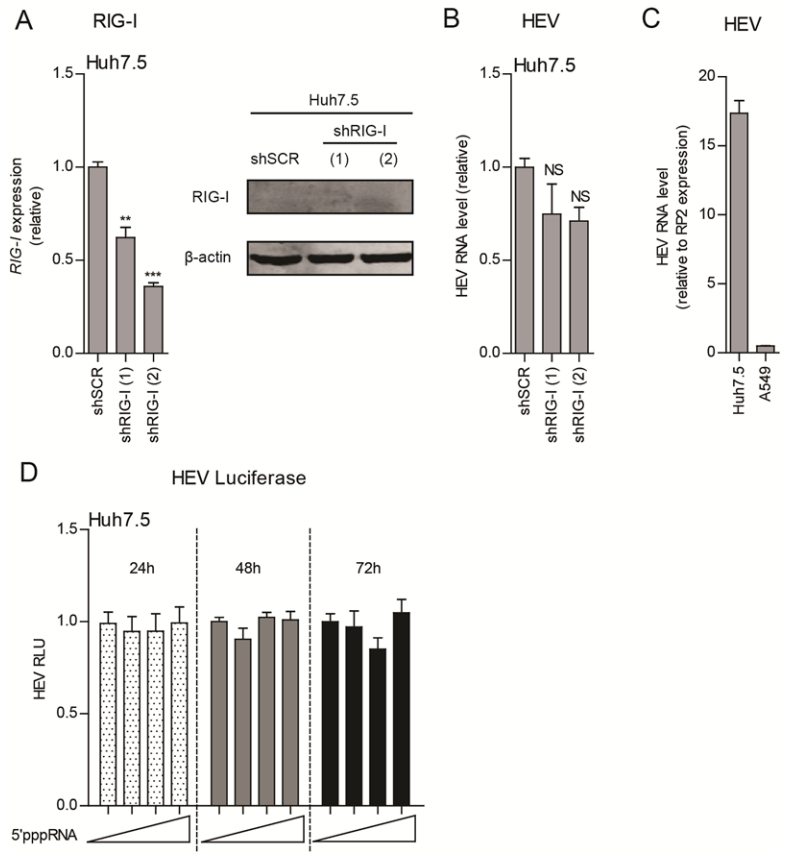

Figure S2. Gene knockdown of RIG-I in Huh7.5 cells does not affect HEV infection and 5'pppRNA does not stimulate an antiviral response in this cells. qRT-PCR analysis and immunoblot analysis of RIG-I expression in Huh7.5 cells transduced with lentiviral shRNA vectors targeting RIG-I (shRIG-I(1) and shRIG-I(2)) or scrambled control (shSCR). (B) Stable RIG-I knockdown or scrambled control (shSCR) Huh7.5 cells were infected with HEV and HEV viral RNA level was analyzed by qRT-PCR 72 h after infection. (C) Huh7.5 cells and A549 cells were infected with HEV and HEV viral RNA level was analyzed by qRT-PCR 72 h after infection. Date in (A) and (B) were normalized to the scrambled control (shSCR, set as 1). Date in (C) were normalized with one housekeeping gene RP2 and presented relative to RP2 expression. (D) Huh7.5-p6-Luc cells were transfected with various concentrations of 5'pppRNA (10 ng/mL, 100 ng/mL and 1000 ng/mL). HEV related *Gaussia* luciferase activity was analyzed at 24 h, 48 h or 72 h after transfection (n = 2 independent experiments with each of 2 - 3 replicates). RLU: relative luciferase unit. Data were normalized to a control that transfected with PEI-Mix but without 5'pppRNA at each time point (24 h, 48 h and 72 h, all set as 1), respectively.

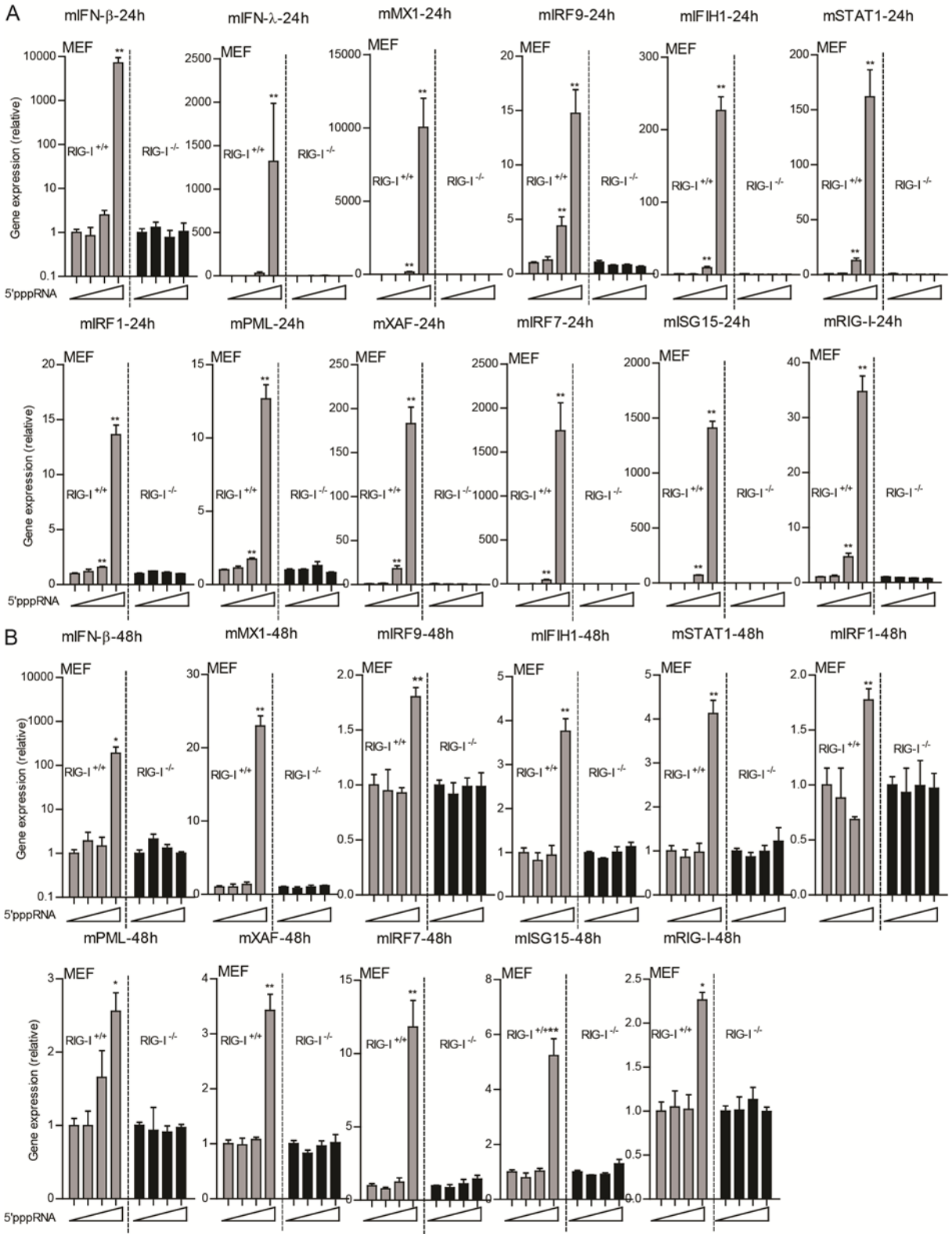

Figure S3. The antiviral ability of 5'pppRNA is dependent on functional RIG-I signaling. WT (RIG-I$^{+/+}$) and RIG-I deficient (RIG-I$^{-/-}$) mouse embryonic fibroblasts (MEF) cells were transfected with various concentrations of 5'pppRNA (10 ng/mL, 100 ng/mL and 1000 ng/mL), mouse IFN genes (mIFN-β and mIFN-λ) and mouse ISGs including mMX1, mIRF9, mIFIH1, mSTAT1, mIRF1, mPML, mXAF, mIRF7, mISG15 and mRIG-I mRNA level was analyzed by qRT-PCR 24 h (A) or 48 h (B) after transfection (n = 6). Data were normalized to a control that transfected with PEI-Mix but without 5'pppRNA at each cell line (RIG-I$^{+/+}$ and RIG-I$^{-/-}$, both set as 1), respectively. Data are means ± SEM. *P < 0.05; **P < 0.01; ***P < 0.001; NS, not significant.

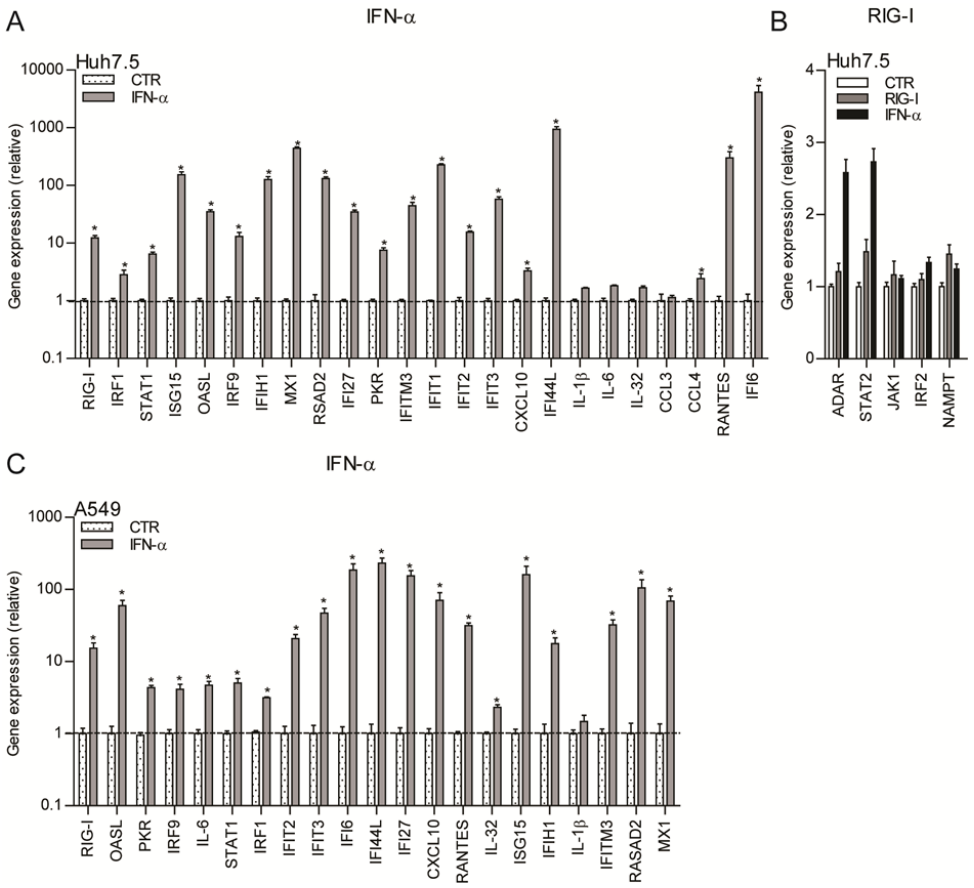

Figure S4. IFN-α activates ISG transcription in different cell lines. qRT-PCR analysis of ISG mRNA levels in Huh7.5-p6 cells (A) and A549-p6 cells (C) treated with IFN-α (1000 IU/mL) for 48 h (n = 4). (B) qRT-PCR analysis of ISG mRNA levels in Huh7.5-p6 cells transduced with RIG-I or Fluc vector or treated with IFN-α (1000 IU/mL) for 48 h (n = 2 - 3). Data were normalized to the untreated Fluc control (CTR, set as 1). Data are means ± SEM. *P < 0.05; **P < 0.01; ***P < 0.001; NS, not significant.

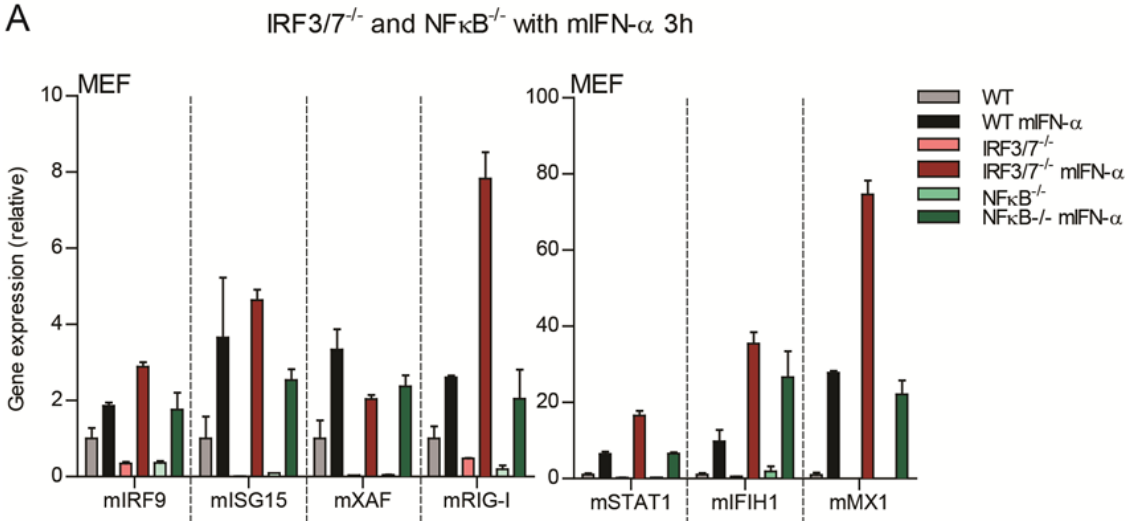

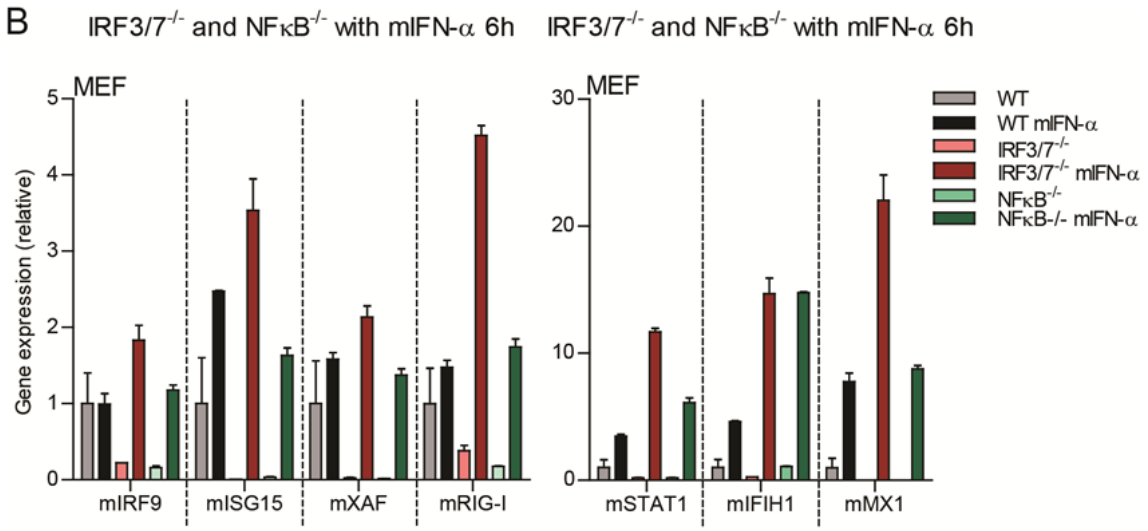

Figure S5. The ISG induction ability of mIFN-α is not attenuated in IRF3/7$^{-/-}$ and NFκB$^{-/-}$ cells. qRT-PCR analysis of mouse ISG mRNA levels in WT, IRF3/IRF7 double deficient (IRF3/7$^{-/-}$) or NFκB deficient (NFκB$^{-/-}$) mouse embryonic fibroblasts (MEF) cells treated with mouse IFN-α (mIFN-α, 1000 IU/mL) for 3 h (A) or 6 h (B) (n = 3). Data in (A) were normalized to the untreated Fluc control (CTR, set as 1). Data in (B) and (C) were normalized to untreated WT MEF cells (WT CTR, set as 1). Data are means ± SEM. *P < 0.05; **P < 0.01; ***P < 0.001; NS, not significant.

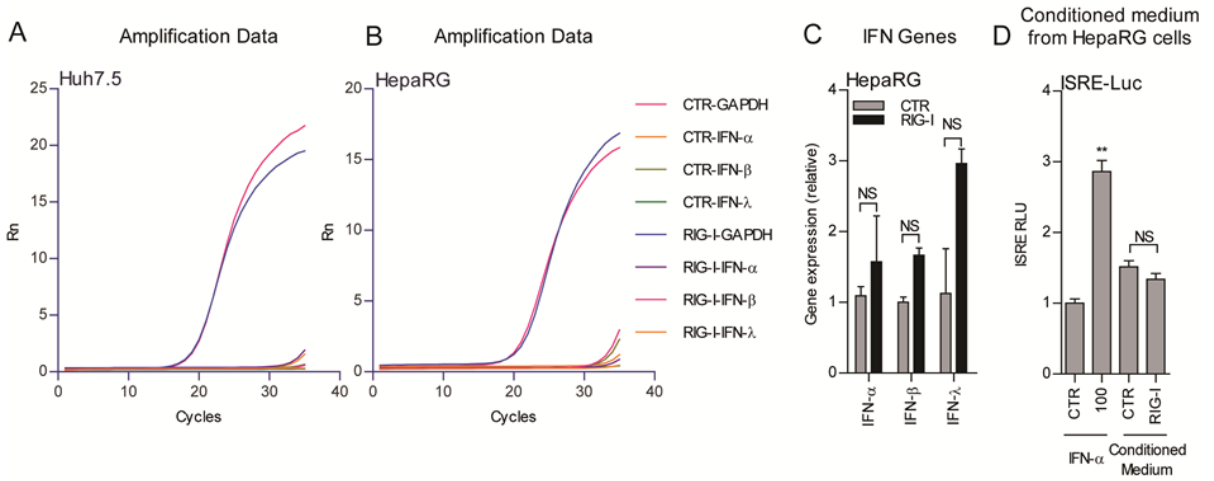

Figure S6. RIG-I overexpression does not trigger ISG production in HepaRG cells. Plot of qRT-PCR analysis of IFN gene expression in Huh7.5-p6 (A) and HepaRG-p6 cells (B) transduced with RIG-I or Fluc (CTR) vector for 48 h. Rn: Fluorescence signal from the reporter dye normalized to that from the negative control. (C) qRT-PCR analysis of IFN gene mRNA levels in HepaRG-p6 cells transduced with RIG-I or Fluc vector for 48 h (n = 4). (D) Analysis of ISRE-related firefly luciferase activity in Huh7-ISRE-Luc cells treated with conditioned medium from HepaRG cells or IFN-α (100 IU/mL) for 48 h (n = 2 independent experiments with each of 2 - 3 replicates). Data in (C) were normalized to the Fluc control (CTR, set as 1). Data in (D) were normalized to the untreated GFP control (CTR, set as 1). Data are means ± SEM. *P < 0.05; **P < 0.01; ***P < 0.001; NS, not significant.

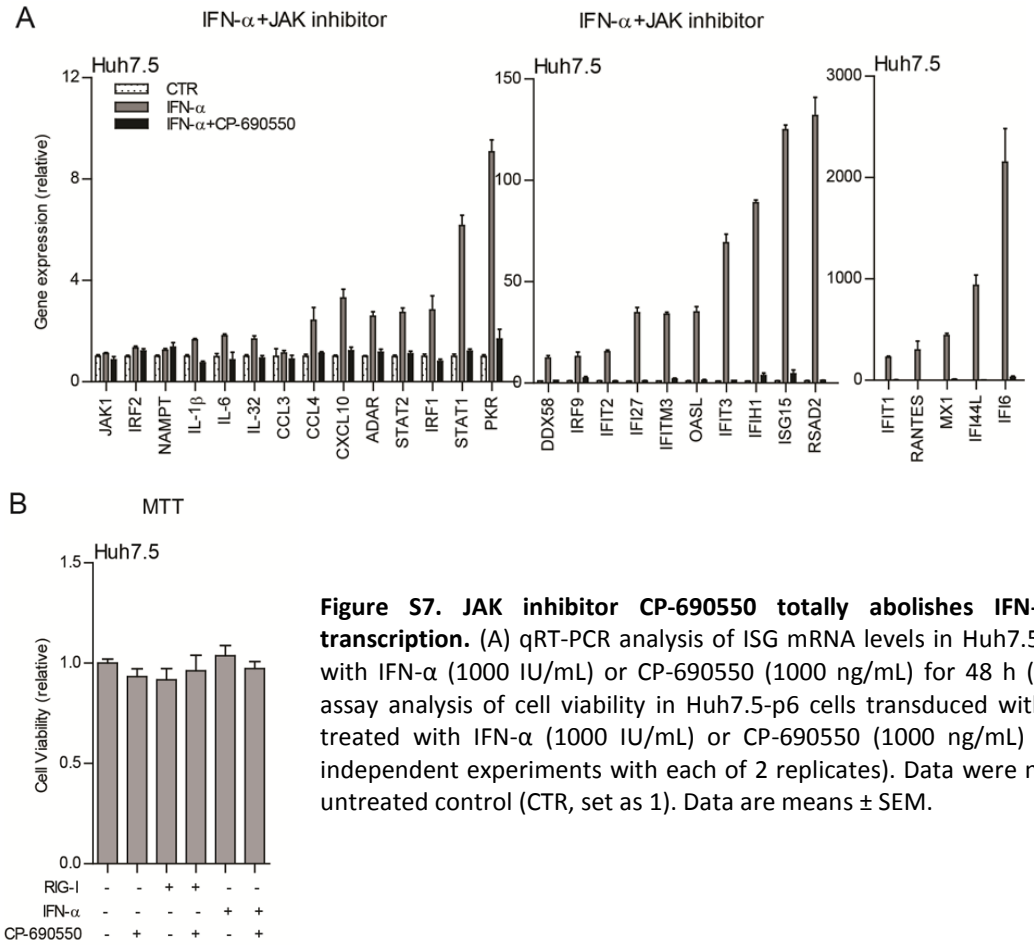

Figure S7. JAK inhibitor CP-690550 totally abolishes IFN-α induced ISG transcription. (A) qRT-PCR analysis of ISG mRNA levels in Huh7.5-p6 cells treated with IFN-α (1000 IU/mL) or CP-690550 (1000 ng/mL) for 48 h (n =5-6). (B) MTT assay analysis of cell viability in Huh7.5-p6 cells transduced with RIG-I vector or treated with IFN-α (1000 IU/mL) or CP-690550 (1000 ng/mL) for 48 h (n = 2 independent experiments with each of 2 replicates). Data were normalized to the untreated control (CTR, set as 1). Data are means ± SEM.

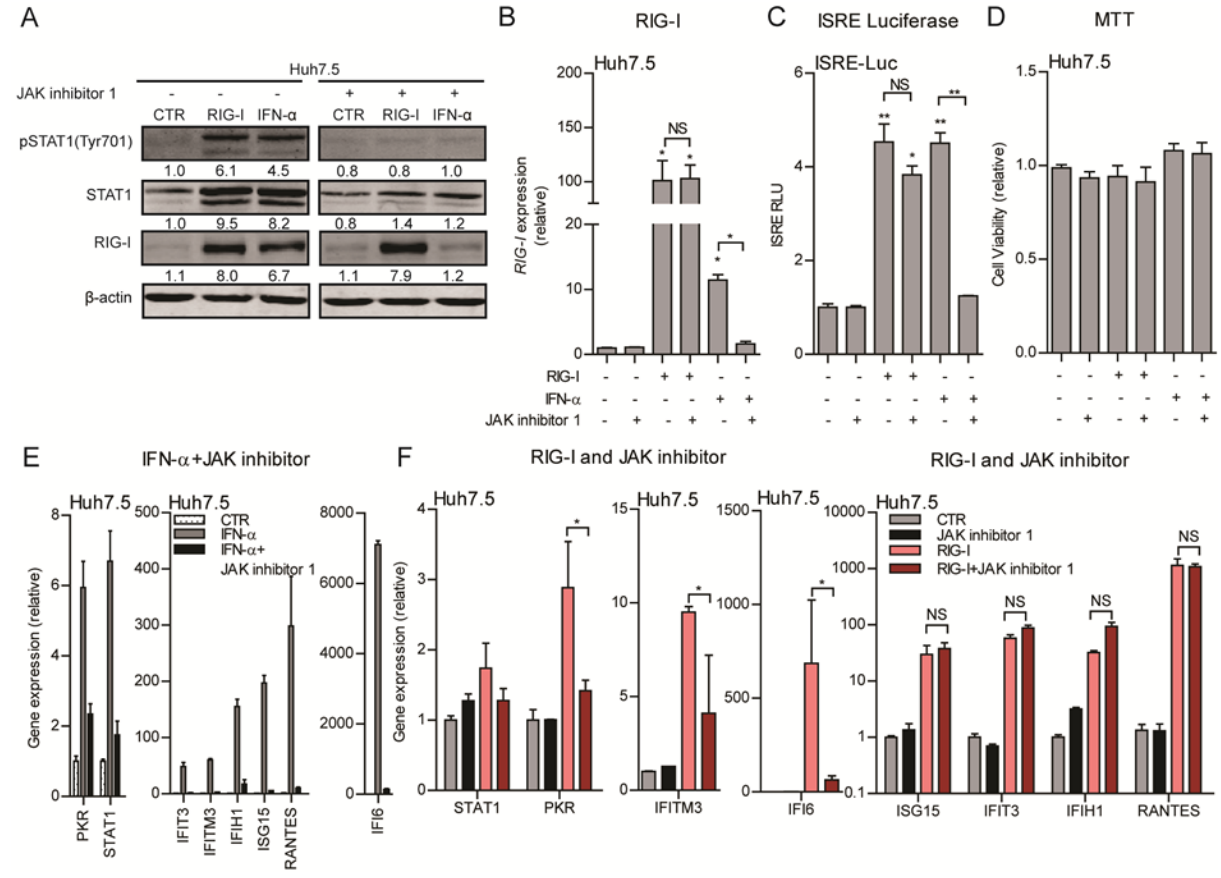

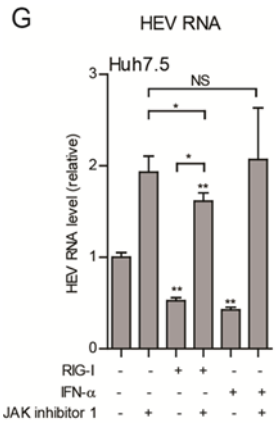

Figure S8. JAK inhibitor 1 partially diminishes RIG-I-induced ISG transcription and anti-HEV activity. (A) Immunoblot analysis of ISG protein levels in Huh7.5 cells-p6 transduced with RIG-I vector or treated with IFN-α (1000 IU/mL) or JAK inhibitor 1 (10 μM) for 48 h. qRT-PCR analysis of RIG-I mRNA level in Huh7.5-p6 cells (B), analysis of ISRE-related *firefly* luciferase activity in Huh7-ISRE-Luc cells (C) and MTT assay analysis of cell viability in Huh7.5 cells (D) transduced with RIG-I vector or treated with IFN-α (1000 IU/mL) or JAK inhibitor 1 (10 μM) for 48 h (qRT-PCR: n = 4; ISRE-Luc: n = 3 independent experiments with each of 2 replicates; MTT: 2 independent experiments with each of 2 replicates). (E) qRT-PCR analysis of ISG mRNA levels in Huh7.5-p6 cells treated with IFN-α (1000 IU/mL) or JAK inhibitor 1 (10 μM) for 48 h (n =3). (F) qRT-PCR analysis of ISG mRNA levels in Huh7.5-p6 cells transduced with RIG-I vector or treated with JAK inhibitor 1 (10 μM) for 48 h (n = 4). (G) qRT-PCR analysis of HEV viral RNA level in Huh7.5-p6 cells transduced with RIG-I vector or treated with IFN-α (1000 IU/mL) or JAK inhibitor 1 (10 μM) for 48 h (n = 6). For immunoblot results (A), band intensity of each lane was quantified by Odyssey Software. Immunoblot quantification results were normalized to β-actin expression and control was set as 1. Data in (B, E, F and G) were normalized to the untreated Fluc control (CTR, set as 1). Date in (C and D) were normalized to the untreated GFP control (CTR, set as 1). Data are means ± SEM. *P < 0.05; **P < 0.01; ***P < 0.001; NS, not significant.

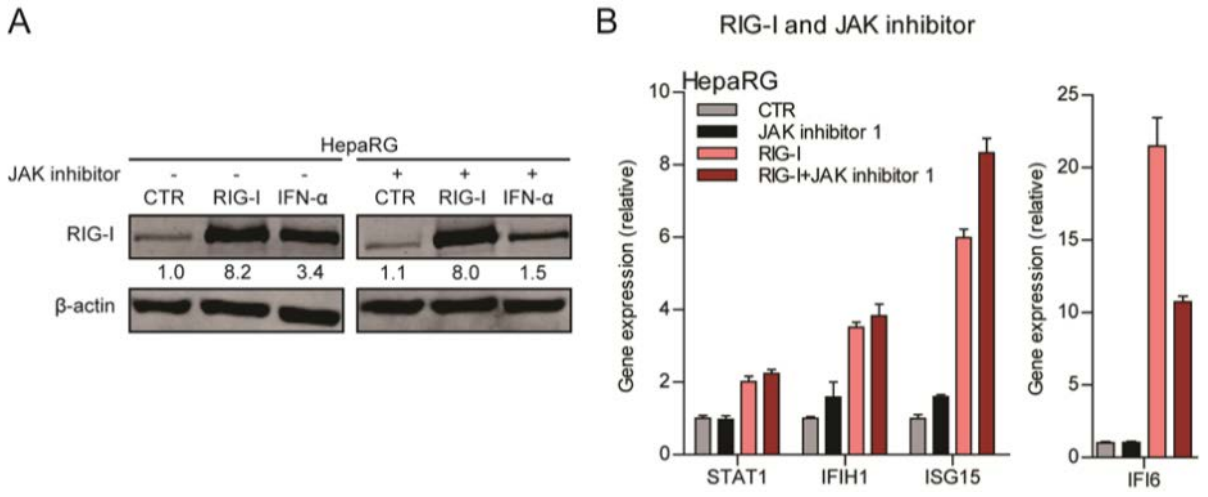

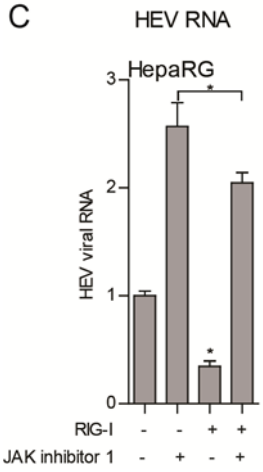

Figure S9. JAK inhibitor 1 partially diminishes RIG-I-induced ISG transcription and anti-HEV activity in HepaRG cells. (A) Immunoblot analysis of RIG-I mRNA level in HepaRG-p6 cells transduced with RIG-I vector or treated with IFN-α (1000 IU/mL) or JAK inhibitor 1 (10 μM) for 48 h. qRT-PCR analysis of ISG mRNA levels (B) and HEV viral RNA (C) level in HepaRG-p6 cells transduced with RIG-I vector or treated with JAK inhibitor 1 (10 μM) for 48 h. Immunoblot quantification results were normalized to β-actin expression and control was set as 1. Data in (B and C) were normalized to the untreated Fluc control (CTR, set as 1). Data are means ± SEM. *P < 0.05; **P < 0.01; ***P < 0.001; NS, not significant.

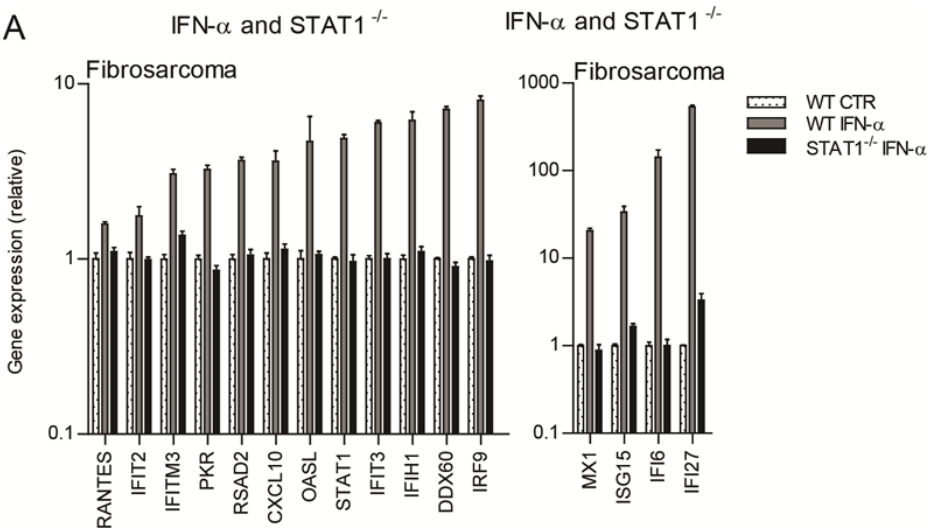

Figure S10. IFN-α does not induce ISG expression in STAT1 deficient cells. (A) qRT-PCR analysis of ISG mRNA levels in WT and STAT1 deficient (STAT1$^{-/-}$) fibrosarcoma cells treated with IFN-α (1000 IU/mL) for 48 h (n = 4). Date were normalized to untreated WT and STAT1$^{-/-}$ cells, respectively (both set as 1). Data are means ± SEM.

References

1. Debing, Y., et al., Update on Hepatitis E Virology:Implications for Clinical Practice. *J Hepatol*, 2016. **65**(1): p. 200-12.
2. Kamar, N., et al., Hepatitis E. *Lancet*, 2012. **379**(9835): p. 2477-88.
3. Andersen, L.L., et al., Functional IRF3 deficiency in a patient with herpes simplex encephalitis. *J Exp Med*, 2015. **212**(9): p. 1371-9.
4. Ciancanelli, M.J., et al., Infectious disease. Life-threatening influenza and impaired interferon amplification in human IRF7 deficiency. *Science*, 2015. **348**(6233): p. 448-53.
5. Borden, E.C., et al., Interferons at age 50: past, current and future impact on biomedicine. *Nat Rev Drug Discov*, 2007. **6**(12): p. 975-90.
6. Schneider, W.M., M.D. Chevillotte, and C.M. Rice, Interferon-stimulated genes: a complex web of host defenses. *Annu Rev Immunol*, 2014. **32**: p. 513-45.
7. Santiago-Raber, M.L., et al., Type-I interferon receptor deficiency reduces lupus-like disease in NZB mice. *J Exp Med*, 2003. **197**(6): p. 777-88.
8. Iversen, M.B., et al., An innate antiviral pathway acting before interferons at epithelial surfaces. *Nat Immunol*, 2016. **17**(2): p. 150-8.
9. Paludan, S.R., Innate Antiviral Defenses Independent of Inducible IFNalpha/beta Production. *Trends Immunol*, 2016. **37**(9): p. 588-96.
10. Schoggins, J.W., et al., A diverse range of gene products are effectors of the type I interferon antiviral response. *Nature*, 2011. **472**(7344): p. 481-5.
11. Schoggins, J.W., et al., Pan-viral specificity of IFN-induced genes reveals new roles for cGAS in innate immunity. *Nature*, 2014. **505**(7485): p. 691-5.
12. Kamar, N., et al., Pegylated interferon-alpha for treating chronic hepatitis E virus infection after liver transplantation. *Clin Infect Dis*, 2010. **50**(5): p. e30-3.
13. Zhou, X., et al., Disparity of basal and therapeutically activated interferon signalling in constraining hepatitis E virus infection. *J Viral Hepat*, 2016. **23**(4): p. 294-304.
14. Todt, D., et al., Antiviral activity of different interferon (sub-) types against hepatitis E virus replication. *Antimicrob Agents Chemother*, 2016.
15. Moal, V., et al., Chronic hepatitis E virus infection is specifically associated with an interferon-related transcriptional program. *J Infect Dis*, 2013. **207**(1): p. 125-32.
16. Shukla, P., et al., Adaptation of a genotype 3 hepatitis E virus to efficient growth in cell culture depends on an inserted human gene segment acquired by recombination. *J Virol*, 2012. **86**(10): p. 5697-707.
17. Xu, L., et al., IFN regulatory factor 1 restricts hepatitis E virus replication by activating STAT1 to induce antiviral IFN-stimulated genes. *FASEB J*, 2016. **30**(10): p. 3352-3367.
18. Sumpter, R., Jr., et al., Regulating intracellular antiviral defense and permissiveness to hepatitis C virus RNA replication through a cellular RNA helicase, RIG-I. *J Virol*, 2005. **79**(5): p. 2689-99.
19. Cao, X., Self-regulation and cross-regulation of pattern-recognition receptor signalling in health and disease. *Nat Rev Immunol*, 2015. **16**(1): p. 35-50.

20. Goulet, M.L., et al., Systems analysis of a RIG-I agonist inducing broad spectrum inhibition of virus infectivity. *PLoS Pathog*, 2013. **9**(4): p. e1003298.
21. Jiang, L.J., et al., RA-inducible gene-I induction augments STAT1 activation to inhibit leukemia cell proliferation. *Proc Natl Acad Sci U S A*, 2011. **108**(5): p. 1897-902.
22. Kane, M., et al., Identification of Interferon-Stimulated Genes with Antiretroviral Activity. *Cell Host Microbe*, 2016. **20**(3): p. 392-405.
23. Keskinen, P., et al., Impaired antiviral response in human hepatoma cells. *Virology*, 1999. **263**(2): p. 364-75.
24. Rabbani, M.A., et al., Identification of IFN-stimulated gene (ISG) proteins that inhibit human parainfluenza virus type 3. *J Virol*, 2016.
25. Haagsma, E.B., et al., Treatment of chronic hepatitis E in liver transplant recipients with pegylated interferon alpha-2b. *Liver Transpl*, 2010. **16**(4): p. 474-7.
26. Debing, Y., et al., Ribavirin inhibits in vitro hepatitis E virus replication through depletion of cellular GTP pools and is moderately synergistic with alpha interferon. *Antimicrob Agents Chemother*, 2014. **58**(1): p. 267-73.
27. Sato, S., et al., The RNA sensor RIG-I dually functions as an innate sensor and direct antiviral factor for hepatitis B virus. *Immunity*, 2015. **42**(1): p. 123-32.
28. Weber, M., et al., Influenza virus adaptation PB2-627K modulates nucleocapsid inhibition by the pathogen sensor RIG-I. *Cell Host Microbe*, 2015. **17**(3): p. 309-19.
29. Makela, S.M., et al., RIG-I Signaling Is Essential for Influenza B Virus-Induced Rapid Interferon Gene Expression. *J Virol*, 2015. **89**(23): p. 12014-25.
30. Lucas, T.M., J.M. Richner, and M.S. Diamond, The Interferon-Stimulated Gene Ifi27l2a Restricts West Nile Virus Infection and Pathogenesis in a Cell-Type- and Region-Specific Manner. *J Virol*, 2016. **90**(5): p. 2600-15.
31. Mboko, W.P., et al., Interferon regulatory factor 1 restricts gammaherpesvirus replication in primary immune cells. *J Virol*, 2014. **88**(12): p. 6993-7004.
32. Reynaud, J.M., et al., IFIT1 Differentially Interferes with Translation and Replication of Alphavirus Genomes and Promotes Induction of Type I Interferon. *PLoS Pathog*, 2015. **11**(4): p. e1004863.
33. Yao, H., et al., ATP-Dependent Effector-like Functions of RIG-I-like Receptors. *Mol Cell*, 2015. **58**(3): p. 541-8.
34. Ramos, H.J. and M. Gale, Jr., RIG-I like receptors and their signaling crosstalk in the regulation of antiviral immunity. *Curr Opin Virol*, 2011. **1**(3): p. 167-76.
35. Wang, W., et al., Convergent Transcription of Interferon-stimulated Genes by TNF-alpha and IFN-alpha Augments Antiviral Activity against HCV and HEV. *Sci Rep*, 2016. **6**: p. 25482.
36. Brownell, J., et al., Direct, interferon-independent activation of the CXCL10 promoter by NF-kappaB and interferon regulatory factor 3 during hepatitis C virus infection. *J Virol*, 2014. **88**(3): p. 1582-90.
37. Pfeffer, L.M., et al., Role of nuclear factor-kappaB in the antiviral action of interferon and interferon-regulated gene expression. *J Biol Chem*, 2004. **279**(30): p. 31304-11.
38. Debing, Y., et al., Hepatitis E virus mutations associated with ribavirin treatment failure result in altered viral fitness and ribavirin sensitivity. *J Hepatol*, 2016. **65**(3): p. 499-508.
39. Todt, D., et al., In vivo evidence for ribavirin-induced mutagenesis of the hepatitis E virus genome. *Gut*, 2016. **65**(10): p. 1733-43.
40. Debing, Y., et al., A mutation in the hepatitis E virus RNA polymerase promotes its replication and associates with ribavirin treatment failure in organ transplant recipients. *Gastroenterology*, 2014. **147**(5): p. 1008-11 e7; quiz e15-6.
41. Peters van Ton, A.M., T.J. Gevers, and J.P. Drenth, Antiviral therapy in chronic hepatitis E: a systematic review. *J Viral Hepat*, 2015. **22**(12): p. 965-73.
42. Manns, M.P., H. Wedemeyer, and M. Cornberg, Treating viral hepatitis C: efficacy, side effects, and complications. *Gut*, 2006. **55**(9): p. 1350-9.
43. Junt, T. and W. Barchet, Translating nucleic acid-sensing pathways into therapies. *Nat Rev Immunol*, 2015. **15**(9): p. 529-44.
44. Cheon, H. and G.R. Stark, Unphosphorylated STAT1 prolongs the expression of interferon-induced immune regulatory genes. *Proc Natl Acad Sci U S A*, 2009. **106**(23): p. 9373-8.

Part II.

Drug-based strategies

Chapter 8

Targeting Viral Polymerase for Treating Hepatitis E Infection: How Far Are We?

Wenshi Wang, Maikel P. Peppelenbosch and Qiuwei Pan

Department of Gastroenterology and Hepatology, Postgraduate School Molecular Medicine, Erasmus MC-University Medical Center, Rotterdam, the Netherlands

Gastroenterology, 2016, 150(7):1690

Dear Editor: We read with great interest the paper by Dao Thi et al[1] reporting that sofosbuvir inhibits hepatitis E virus (HEV) infection and results in an additive effect when combined with ribavirin in vitro. This observation emphasizes the potential of sofosbuvir as an add-on therapy to ribavirin for the treatment of HEV infected patients.

Sofosbuvir is a direct-acting antiviral drug against hepatitis C virus (HCV) by targeting the NS5B RNA-dependent RNA polymerase. RNA-dependent RNA polymerase is responsible for initiating and catalyzing viral RNA synthesis. Sofosbuvir metabolizes to a pharmacologically active uridine analog triphosphate (GS-461203) upon entry into cells. This active form then binds to NS5B and is incorporated into the viral RNA, leading to the termination of viral RNA synthesis.[2] Because of a high curative rate, modest side effect profile, and a temporally reduced therapy, sofosbuvir has achieved great success for the treatment of chronic HCV infection. Both HCV and HEV are single-stranded RNA virus that have characteristics in common with respect to hepatocyte tropism, life-cycle, and requirement of RNA polymerase for replication. Although hepatitis E has evolved into a global health issue, there is no proven medication available. The strategy employed by Dao Thi et al to discover potential anti-HEV drugs from existing approved antiviral medications is highly relevant and cost effective. A successful analogous example of this strategy is the use of lamivudine for the treatment of both chronic hepatitis B and human immunodeficiency virus (HIV)/AIDS. Lamivudine is an analogue of cytidine. It can inhibit both HIV (type 1 and 2) and hepatitis B virus reverse transcriptase, leading to the termination of DNA synthesis, which provides a rational explanation to its clinical efficacy.

Intriguingly, earlier study has documented the high specificity of sofosbuvir for inhibiting HCV. It lacks efficacy to a number of HCV-related viruses of the Flaviviridae family, including West Nile virus and yellow fever virus. In apparent agreement, no effect of sofosbuvir was observed on unrelated viruses including hepatitis B virus, HIV and influenza virus A.[3] In fact, HCV and HEV are only distantly related. HCV belongs to the genus Hepacivirus within the family Flaviviridae, whereas HEV is classified as a member of the genus Orthohepevirus in the Hepeviridae family. It is thus truly remarkable that Dao Thi et al now have reported the anti-HEV effects of sofosbuvir in cell culture models. With a most sensitive model of a genotype 3 HEV subgenomic replicon, a median inhibition concentration of 1.2mmol/L was reported, and an additive anti-HEV effect was observed when combined with ribavirin. However, in a widely used genotype 3 replicon with a luciferase reporter (p6/luc),[4] only approximately 50% of inhibitory effect was observed even with treatment of 10 mmol/L of sofosbuvir. Strikingly, no antiviral activity was observed in a genotype 1 (Sar55/S17/luc) replicon system.

As a potent HCV polymerase inhibitor, the median effective concentration values of sofosbuvir against fulllength replicons of HCV from genotypes 1a, 1b, 2a, 3a, and 4a, and chimeric 1b replicons encoding NS5B from genotype 2b, 5a, or 6a have been reported to range from 0.014 to 0.11 mmol/L. Similarly, we observed a median effective concentration of 0.018 mmol/L against HCV replication when using Huh7-based replicon containing a subgenomic HCV bicistronic replicon (1389/NS3-3V/LucUbiNeo-ET) linked to the firefly luciferase reporter gene. In contrast, we only observed very limited effect of sofosbuvir on HEV (100 mmol/L inhibited luciferase activity by only 10%) by using the HEV genotype 3 (Kernow-C1, P6) replicon cell model containing a luciferase reporter.4

These distinct effects of sofosbuvir on HCV and HEV suggest a rather low affinity toward the HEV polymerase, if any exists. We interpret these data that sofosbuvir is likely not a candidate ready for the treatment of hepatitis E. Nevertheless, sofosbuvir may represent as a starting point for the development of bona fide HEV polymerase inhibitors, but this will require knowledge on the crystallographic structure of the HEV polymerase.

References

1. Dao Thi VL, et al. Gastroenterology 2016;150:82–85.
2. Summers BB, et al. J Pharm Pharmacol 2014; 66:1653–1666.
3. Lam AM, et al. Antimicrob Agents Chemother 2010; 54:3187–3196.
4. Shukla P, et al. J Virol 2012;86:5697–5707.

Chapter 9

Distinct Antiviral Potency of Sofosbuvir Against Hepatitis C and E Viruses

Wenshi Wang[1#], Mohamad S. Hakim[1,2#], Vidya P. Nair[3], Petra E. de Ruiter[4], Dave Sprengers[1], Luc J. W. Van Der Laan[4], Maikel P. Peppelenbosch[1], Milan Surjit[3], Qiuwei Pan[1]

[1]Department of Gastroenterology and Hepatology, Erasmus MC-University Medical Center and Postgraduate School Molecular Medicine, Rotterdam, the Netherlands

[2]Department of Microbiology, Faculty of Medicine, Gadjah Mada University, Yogyakarta, Indonesia

[3]Virology Laboratory, Vaccine and Infectious Disease Research Centre, Translational Health Science and Technology Institute, NCR Biotech Science Cluster, Faridabad, Haryana, India

[4]Department of Surgery, Erasmus MC-University Medical Center and Postgraduate School Molecular Medicine, Rotterdam, the Netherlands

[#]Both authors contributed equally

Modified from

Gastroenterology, 2016, 151(6):1251-1253

Abstract

There is a pressing need for discovering effective antiviral treatment for hepatitis E virus (HEV) infection. A recent study reported that sofosbuvir, an anti-hepatitis C virus (HCV) drug that targets its RNA-dependent RNA polymerase (RdRp), has potent anti-HEV effect in cell culture. Given the important potential clinical implications, this study has comparatively assessed the antiviral efficacy of sofosbuvir in both HCV and HEV models. In contrast to HCV, we found that HEV was not sensitive to inhibition by sofosbuvir. In coinfection models of HCV and HEV, sofosbuvir markedly inhibited HCV, but not HEV. Furthermore, sofosbuvir did not inhibit HEV RdRp activity in vitro. Our study suggests that sofosbuvir is likely not valuable in the treatment of HEV or HEV/HCV coinfected patients.

Keywords: Antiviral; Sofosbuvir; Hepatitis E Virus; Hepatitis C Virus

Introduction

Hepatitis E virus (HEV) infection is emerging as a global health issue. HEV genotypes 1 and 2 are prevalent in developing countries in which they cause both epidemic and sporadic hepatitis. HEV genotypes 3 and 4 are zoonotic viruses which infect both human and animal species.[1] HEV infection is generally self-limiting and asymptomatic with consequent of low mortality rates. However, in immunocompromised patients, such as patients receiving organ transplantation, more than 60% of HEV-infected patients will develop chronic disease and quickly progress towards severe liver complications such as fibrosis and cirrhosis. Since there are no approved clinical drugs for HEV, the management of chronic HEV patients mostly depends on manipulation of immunosuppression drugs, either dose-reduction or even withdrawal of these drugs (if possible).[2] Moreover, ribavirin, pegylated interferon-α, or combination of both drugs have been used as off-label antiviral drugs with varying success rate. However, HEV mutations associated with ribavirin treatment failure have been reported. [3,4] Therefore, the development of more effective antiviral drugs for HEV is urgently required. The search for new anti-HEV drugs based on clinically available antiviral medicine is a costeffective and highly relevant approach in the clinical settings. In this context, sofosbuvir (SOF), the direct-acting anti-hepatitis C virus (HCV) drug (targeting HCV RdRp; RNA-dependent RNA polymerase), has been recently reported to be a potential anti-HEV drug candidate.[5] However, we believe that the anti-HEV and anti-HCV potency of SOF should be comparatively assessed, before proposing its clinical application for treating HEV-infected patients.

Results and Discussion

In this study, the potential anti-HEV effect of SOF was investigated in HEV replication models with concentrations ranging from 0.01 μM to 10 μM (Supplementary Figure 1A), which is comparable to the previous study.[5] In this model, human hepatoma Huh7 cells were transfected with a subgenomic construct of HEV coding sequence derived from genotype 1 (Sar55/S17/luc) and genotype 3 (Kernow-C1, p6-luc), in which the 5' portion of open reading frame 2 (ORF2) coding sequence was replaced with a gene encoding a secreted form of Gaussia luciferase. To normalize for non-specific effects of SOF on luciferase signals, Huh7 cells stably expressing a non-secreted firefly luciferase under control of the human phosphoglycerate kinase (PGK) promotor (PGK-Luc) was used. In addition, Huh7 cells harboring a subgenomic HCV bicistronic replicon (I389/NS3- 3V/LucUbiNeo-ET; Huh7-ET) was used as control of anti-HCV activity.[6] We demonstrated that SOF significantly reduced and even eliminated HCV-driven luciferase activity at 24 and 48 hours of treatments, but did not affect the PGK-driven luciferase activity. However, an antiviral effect of SOF was not observed in both HEV genotype 1- and genotype 3-based subgenomic replicon either at 24 and 48 hours of treatment (Figure 1A).

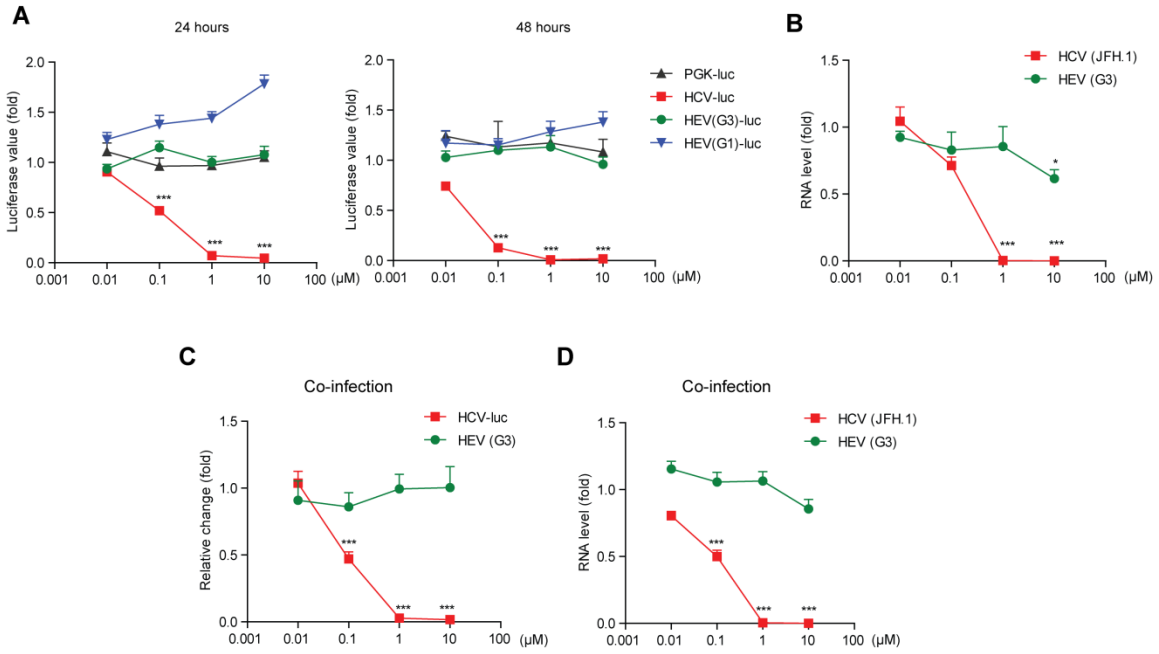

Figure 1. The antiviral effect of sofosbuvir (SOF) was investigated on various hepatitis E virus (HEV) and hepatitis C virus (HCV) models. (A) In the Huh7 cell-based subgenomic HCV replicon, treatment with SOF dose-dependently decreased and even eliminated HCV replication-related luciferase activity. Although SOF exerted no effects on HEV replication in both HEV genotype 1-based and genotype 3-based subgenomic replicon either at 24 and 48 hours of treatment. PGK-Luc was used to assess nonspecific effects of SOF on luciferase signals (n=3 independent experiments with 2–3 replicates each). (B) SOF strongly inhibited HCV in Huh7 based full-length JFH1-infectious model, whereas a modest effect on HEV was observed in the full-length p6 infectious models after the treatment of SOF at the highest concentration (10 mmol/L) for 48 hours (n=2 independent experiments with 2 replicates each). (C) Huh7 cell-based subgenomic HCV replicon was infected with infectious HEV p6 particles. SOF exerted no significant anti-HEV effect, while retained its strong effect against HCV replication (measured at 48 hours; n=4). (D) Huh7 cells were coinfected with both infectious HEV (p6) and HCV (JFH.1) particles. SOF led to the elimination of HCV at a concentration of 1 mmol/L, while exerting no significant effect on HEV (measured at 48 hours; n=4).

We further evaluated anti-HEV effect of SOF in the full-length (Kernow-C1, p6) infectious models of HEV genotype 3. The infectious HCV model, containing full-length JFH1-derived genome, was used as the control of antiviral activity.[7] In this model, only a modest effect was observed after the treatment of SOF at the highest concentration (10 μM) for 48 hours (Figure 1B). In contrast, SOF strongly inhibited HCV in HCV infectious model. At concentration of 1 μM, SOF completely eliminated HCV RNA replication (Figure 1B). These results showed the highly specific effect of SOF against HCV replication.

We then examined whether SOF could directly inhibit the activity of HEV RNA-dependent RNA polymerase enzyme. An in vitro RdRp assay[8] was conducted to evaluate the effect of SOF on HEV RdRp activity. Huh7 purified RdRp-Flag was used in the presence of increasing dose of SOF. As template, an in vitro transcribed RNA containing 130 bases from 5'-end and 210 bases from 3'-end of HEV genotype 1 was employed. Addition of SOF at any of the concentrations tested did not inhibit HEV RdRp activity as measured by the level of double stranded RNA intermediate level (680 bases) (Supplementary Figure 1B).

Acute and chronic HEV patients may develop extra-hepatic manifestations such as neurological and kidney complications.[1] Therefore, we established HEV genotype 3-based infectious and replication models in human embryonic kidney epithelial cell line HEK 293T cells and human

glioblastoma cell line U-87 MG cells. We then explored the anti-HEV potential of SOF in these cell lines. In line with the results observed in Huh7-based HEV replication model, we did not observe any effect of SOF on both HEK 293T and U-87 MG based HEV replication models (Supplementary Figure 1C). Furthermore, in both HEK 293T cell and U-87 MG cell based HEV infectious models, only a moderate effect was observed after the treatment of SOF at the highest concentration (10 μM) for 48 hours (Supplementary Figure 1D). This is consistent with the result in Huh7 based HEV infectious model. The similar results we obtained from both hepatic and extra-hepatic cell lines further emphasized the highly specific effect of SOF against HCV relative to HEV.

In clinical settings, coinfection of HCV and HEV could be found.[9] To clarify whether SOF could inhibit viral replication of both viruses in this specific setting, Huh7-ET cells infected with infectious HEV particles (Kernow-C1, p6) were used as an in vitro HCV and HEV coinfection model. Surprisingly, SOF lost its modest effect on HEV, while retained its strong antiviral viral effect against HCV replication (Figure 2A). This observation was further supported by the coinfection of both infectious HEV (Kernow-C1, p6) and HCV particles (JFH.1) in Huh7 cells. In this model, SOF led to the elimination of HCV virus at the concentration of 1 μM/mL, while exerting no significant effect on HEV even at the concentration of 10 μM (Figure 2B). This results underscored the highly specific anti-viral effect of SOF againts HCV.

Based on evaluation in chronic HCV patients, the geometric mean steady state of SOF concentration was 828 ng•hr/mL when coadministered with ribavirin.[10] The concentration was much lower than the concentration of SOF we used in vitro at which SOF showed modest effect on HEV (10 μM of SOV is equivalent to 5294.5 ng/mL). Therefore, we suggest that SOF is likely not valuable to be used in the clinical settings for treating HEV-infected patients. Nevertheless, targeting HEV polymerase is a potential strategy to develop new antiviral drugs against HEV.

Acknowledgements

The authors would like to thank Dr. Suzanne U. Emerson (National Institute of Allergy and Infectious Diseases, National Institutes of Health, Bethesda, MD) for kindly providing the plasmids to generate subgenomic and full-length HEV genotype 1 and 3 cell culture system; Prof. Takaji Wakita (National Institute of Infectious Diseases, Japan) for providing the full-length JFH1-derived infectious HCV replicon; Prof. Ralf Bartenschlager and Dr. Volker Lohmann (University of Heidelberg, Germany) for generously providing the Huh7 subgenomic HCV replicon cells.

References

1. Kamar N, et al. Lancet 2012; 379: 2477-2488.
2. Zhou X, et al. Rev Med Virol 2013; 23: 295-304.
3. Debing Y, Ramiere C, et al. J Hepatol 2016; 65: 499-508.
4. Debing Y, Gisa A, et al. Gastroenterology 2014; 147: 1008-1011.
5. Dao Thi VL, et al. Gastroenterology 2016; 150: 82-85.
6. Frese M, et al. Hepatology 2002; 35: 694-703.
7. Wakita T, Pietschmann T, et al. Nat Med 2005; 11: 791-796.
8. Nair VP, et al. PLoS Pathog 2016; 12: e1005521.
9. Wu KT, et al. J Med Virol 2009; 81: 1734-1742.
10. Summers BB, et al. J Pharm Pharmacol 2014; 66: 1653-1666.

Supplementary Materials and Methods

Anti-viral Agents

Sofosbuvir (SOF) was purchased from Selleckchem (Houston, TX). Stocks of SOF were dissolved in dimethyl sulfoxide (DMSO) at a concentration of 10 mM.

Cell Culture

Human hepatoma cell line Huh7, human embryonic kidney epithelial cell line HEK 293T cells, and human glioblastoma cell line U-87 MG cells were cultured in Dulbecco's modified Eagle medium (Invitrogen, Carlsbad, CA) supplemented with 10% fetal bovine serum, 100 IU/mL penicillin and 100 IU/mL streptomycin.

Stable luciferase expressing cells were generated by transducing naïve Huh7 with a lentiviral vector expressing the firefly luciferase gene under control of the human phosphoglycerate kinase (PGK) promotor (LV-PGK-Luc). LV-PGK-Luc was used as household luciferase activity for normalization and to determine the specific effects on viral replication-related luciferase activity.

Hepatitis E Virus (HEV) Cell Culture Models

A plasmid construct containing the full-length HEV genome (Kernow-C1 p6 clone, GenBank Accession Number JQ679013) and a construct containing subgenomic HEV sequence coupled with a Gaussia luciferase reporter gene (p6-Luc) were used to generate HEV genomic RNA by using the Ambion mMESSAGE mMACHINE in vitro RNA transcription Kit (Life Technologies Corporation, Carlsbad, CA).[1,2] For HEV genotype 1, we used Sar55/S17/luc subgenomic replicons coupled with a Gaussia luciferase reporter gene.

The Huh7 cells, HEK 293T cells, and U-87 MG cells were collected and centrifuged for 5 min, 1500 rpm, 4 ^{o}C. Supernatant was removed and washed with 4 mL Optimem by centrifuging for 5 min, 1500 rpm, 4 ^{o}C. The cell pellet was re-suspended in 100 µL Optimem and mixed with p6 full-length HEV RNA or p6-Luc subgenomic RNA. Electroporation was performed to generate infectious or replication models, respectively.

Hepatitis C Virus (HCV) Cell Culture Models

HCV subgenomic replicon model (Huh7-ET) was based on Huh7 cells containing a subgenomic HCV bicistronic replicon (I389/NS3-3V/LucUbiNeo-ET) which contains the non-structural coding sequence of HCV and the firefly luciferase gene. Huh7-ET cells were cultured in the presence of 250 µg/mL G418 (Sigma).[3] As an infectious model, Huh7 cells harboring the full-length JFH-1 derived HCV genome was used.[4]

Measurement of Luciferase Activity

To quantify the HEV replication models, the activity of secreted gaussia luciferase in the cell culture medium was measured using BioLux Gaussia Luciferase Flex Assay Kit (New England Biolabs, Ipswich, MA). Huh7-ET and PGK-Luc firefly luciferase activity was quantified by adding luciferin potassium salt (100 mM, Sigma) to the cells and then incubating for 30 minutes at 37 ^{o}C. Both gaussia and firefly

luciferase activities were quantified with a LumiStar Optima luminescence counter (BMG labTech, Offenburg, Germany).

Quantitative Real-Time Polymerase Chain Reaction

RNA was isolated with a Machery-NucleoSpin RNA II kit (Bioke, Leiden, The Netherlands) and quantified using a Nanodrop ND-1000 (Wilmington, DE, USA). cDNA was prepared from total RNA using a cDNA Synthesis Kit (Takara Bio Inc). The cDNA of HEV, HCV, glyceraldehyde-3-phosphate dehydrogenase (GAPDH), and human retinitis pigmentosa 2 (RP2) were amplified by 50 cycles and quantified with a SYBRGreen-based real-time PCR (MJ Research Opticon, Hercules, CA, USA) according to the manufacturer's instructions. GAPDH and RP2 were considered as reference genes to normalize gene expression. The qPCR primer sequences listed as follows: HEV-F 5'-ATTGGCCAGAAGTTGGTTTTCAC-3'; HEV-R 5'-CCGTGGCTATAATTGTGGTCT-3'; HCV-F 5'-GTCTAGCCATGGCGTTAGTATGAG-3'; HCV-R 5'-AGATGTTCAGGCACTTGGCGG-3'; GAPDH-F 5'-TGTCCCCACCCCCAATGTATC-3'; GAPDH-R 5'-CTCCGATGCCTGCTTCACTACCTT-3'; RP2-F 5'-GTCAGAGACAGAAGAGCAGCGA-3'; RP2-R 5'- GGACACTTCCTTTGTCTGAACTAG-3'

MTT assays

10 mM 3-(4,5-dimethylthiazol-2-yl)-2,5-diphenyltetrazolium bromide (MTT) (Sigma) was added to cells seeded in 96-well plates. The cells was incubated at 37 ^{o}C with 5% CO2 for 3 h. The culture medium was then removed and 100 µl of DMSO was added to each well. The absorbance of each well was read on the microplate absorbance readers (BIO-RAD) at wavelength of 490 nm. All measurements were performed in triplicates.

HEV RNA-dependent RNA-polymerase (RdRp) Assay

HEV RdRp assay was performed as described previously.[5] SOF was added to the reaction mixture at the indicated final concentrations (1, 10, 100 µM).

Statistical Analysis

Statistical analysis was performed using the nonpaired, nonparametric test (Mann-Whitney test; GraphPad Prism software, GraphPad Software Inc., La Jolla, CA). P values <.05 were considered statistically significant.

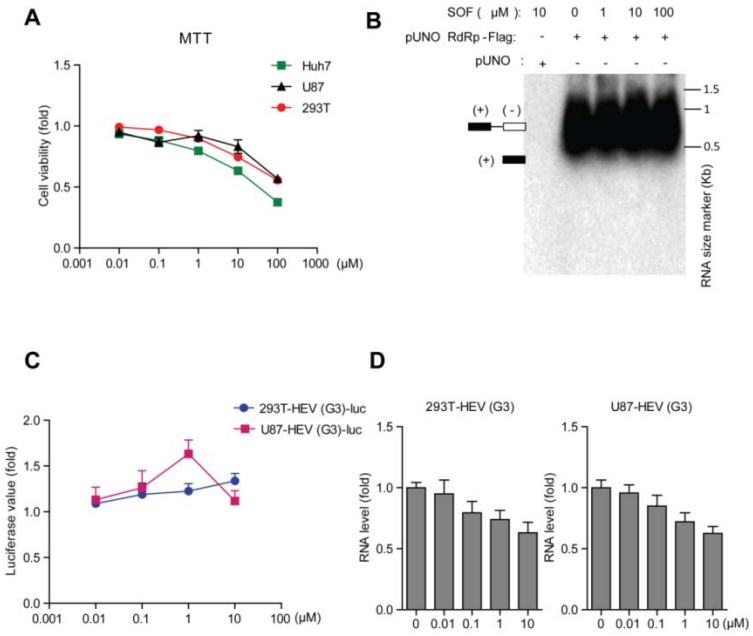

Supplementary figure 1. The antiviral effect of SOF was evaluated on extra-hepatic cell based HEV models. (A) The effects of SOF on hepatic and extra-hepatic cell lines were determined by MTT assay. SOF showed relatively strong cytotoxicity at the concentration of 100 µM. (B) Effect of SOF on HEV RdRp activity in vitro. RdRp assay was performed using purified HEV RdRp and a 340 base HEV RNA template. Schematic illustrates the position of dsRNA (+,-) and ssRNA. (C) SOF exerted no antiviral effect on both HEK 293T and U-87 MG based HEV replication models (n = 3 independent experiments with 2–3 replicates each). (D) In both HEK 293T cell and U-87 MG cell based HEV infectious models, a moderate anti-HEV effect was observed after the treatment of SOF for 48 hours (n = 2 independent experiments with 2 replicates each).

References

1. Shukla P, Nguyen HT, et al. Proc Natl Acad Sci U S A 2011; 108: 2438-2443.
2. Shukla P, Nguyen HT, et al. J Virol 2012; 86: 5697-5707.
3. Frese M, et al. Hepatology 2002; 35: 694-703.
4. Wakita T, Pietschmann T, et al. Nat Med 2005; 11: 791-796.
5. Nair VP, et al. PLoS Pathog 2016; 12: e1005521

Chapter 10

Direct-acting antiviral therapy for hepatitis E virus?

Nassim Kamar[1], **Wenshi Wang[2]**, Harry R. Dalton[3], Qiuwei Pan[2]

[1]Departments of Nephrology and Organ Transplantation, CHU Rangueil, INSERM U1043, IFR-BMT, Université Paul Sabatier, Toulouse, France.

[2]Department of Gastroenterology and Hepatology, Erasmus MC-University Medical Center, Rotterdam, the Netherlands

[3]Royal Cornwall Hospital; European Centre for Environment and Human Health, University of Exeter, Truro, UK

Modified from

The Lancent Gastroenterology & Hepatology, 2017, 2(3):154-155.

As highlighted by an Editorial in the December, 2016, issue of *The Lancet Gastroenterology & Hepatology*,[1] many gaps still exist in our knowledge of hepatitis E virus (HEV). Genotypes 3 and 4 infections can cause chronic hepatitis, cirrhosis that develops quite rapidly after infection, and extra-hepatic manifestations such as neurological symptoms and kidney injuries. Ribavirin monotherapy is effective for treating chronic HEV and HEV-associated glomerular disease, with sustained virological responses (SVRs) of 85–90%. For patients who relapse, retreatment with ribavirin for a longer period—eg, 6 months instead of 3 months—achieves viral clearance in some. However, for a few patients, ribavirin treatment fails. Mutations in HEV RNA polymerase have been noted before or during therapy in patients who relapse. However, the clinical relevance of such mutations in treatment failure is uncertain since findings from in-vitro studies show that some of these mutations facilitate HEV replication but paradoxically seem to increase ribavirin sensitivity. Effective antiviral therapy is therefore needed for HEV-infected patients with ribavirin treatment failure.

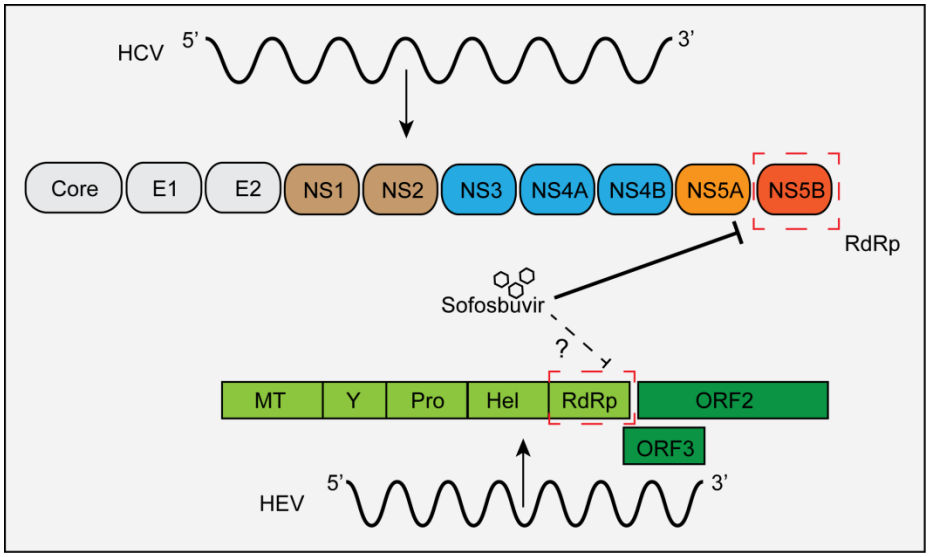

Figure 1. Both HCV and HEV are single-standard RNA viruses that primary infect the liver and cause hepatitis. Both have the RNA-dependent RNA polymerase (RdRp) that is responsible for the replication of the viral genome. Sofosbuvir is a potent inhibitor of HCV RdRp that effectively cure chronic hepatitis C patients. It is an intriguing question whether sofosbuvir is also an inhibitor of HEV RdRp, and can be used to treat hepatitis E patients? (MT, Methyltransferase; Y, Y-domain; Pro, protease; Hel, helicase; RdRp, RNA-dependent RNA polymerase).

In-vitro data suggest that sofosbuvir, a direct-acting antiviral (DAA) agent against hepatitis C virus (HCV), can inhibit HEV replication and exert an additive effect when combined with ribavirin.[2] Sofosbuvir is a specific and potent inhibitor that targets the HCV NS5B RNA-dependent RNA polymerase (Figure 1). Although both HCV and HEV are single-standard RNA viruses requiring RNA polymerase for replication, the in-vitro efficacy of sofosbuvir against HEV reported in this study[2] is modest, even at high concentrations, and varies among diff erent model types of HEV replication or infection.[2] Findings from another study showed that sofosbuvir was effective at inhibiting HCV replication, but was much less efficacious against HEV in cell culture models of both monoinfection and HCV–HEV co-infection.[3]

van de Walk and colleagues[4] reported a case of a patient who had received stem-cell transplantation and was infected with HEV, who relapsed after ribavirin cessation. When retreated

with ribavirin, no decrease in HEV RNA was noted. Hence, sofosbuvir was added to ribavirin, which led to a reduction in HEV viral load. Viral clearance was achieved after two flareups but a relapse occurred after treatment cessation.[4] In another study,[5] a patient who had received a liver transplantation and who was chronically co-infected with HCV and HEV was given sofosbuvir and daclatasvir (without ribavirin) for 12 weeks. HCV SVR was achieved but no effect was noted on HEV viral load or on specific anti-HEV T-cell responses.[5]

These in-vitro and in-vivo data suggest that sofosbuvir is unlikely to be the drug of choice for patients who do not clear HEV with ribavirin. No data are available for the anti-HEV activity of other DAAs that are used to treat HCV; however, it would be unsurprising if they were also ineffective since they were specifically designed and optimized for targeting HCV viral proteins. To develop effective DAAs for HEV, it is essential to gain more insight into the crystallographic structures of the viral proteins, particularly the HEV polymerase.

References

1. The Lancet Gastroenterology & Hepatology. Hepatitis E: a neglected virus. *Lancet Gastroenterol Hepatol* 2016; 1: 261.
2. Dao Thi VL, Debing Y, Wu X, et al. Sofosbuvir inhibits hepatitis E virus replication in vitro and results in an additive eff ect when combined with ribavirin. *Gastroenterology* 2016; 150: 82–85.
3. Wang W, Hakim MS, Nair VP, et al. Distinct antiviral potency of sofosbuvir against hepatitis C and E viruses. *Gastroenterology* 2016; 151: 1251–53.
4. van der Valk M, Zaaijer HL, Kater AP, Schinkel J. Sofosbuvir shows antiviral activity in a patient with chronic hepatitis E virus infection. *J Hepatol* 2017; 66: 242–43.
5. Donnelly MC, Imlach SN, Abravanel F, et al. Sofosbuvir and daclatasvir anti-viral therapy fails to clear HEV viremia and restore reactive T cells in a HEV/HCV co-infected liver transplant recipient. *Gastroenterology* 2017; 152: 300–01.

Chapter 11

Nucleoside analogue 2'-C-methylcytidine inhibits hepatitis E virus replication but antagonizes ribavirin

Changbo Qu, Lei Xu, Yuebang Yin, Maikel P. Peppelenbosch, Qiuwei Pan, and **Wenshi Wang***

Department of Gastroenterology and Hepatology, Erasmus MC-University Medical Center, Rotterdam, The Netherlands.

Archive of Virology. 2017. 162(10):2989-2996..

Abstract

Hepatitis E virus (HEV) infection has emerged as a global health issue; whereas no approved medication is available. The nucleoside analogue 2'-C-methylcytidine (2CMC), a viral polymerase inhibitor, has been shown to inhibit the infection of a variety of viruses, including hepatitis C virus (HCV). Here, we report that 2CMC significantly inhibits the replication of HEV in a subgenomic replication and a full-length infectious models. Importantly, long-term treatment with 2CMC did not attenuate its antiviral potency, indicating a high barrier to drug resistance development. However, the combination of 2CMC with ribavirin, an off-label treatment for HEV, exerts antagonistic effects. Our results indicate that 2CMC serves as a potential antiviral drug against HEV infection.

Key words: 2’-C-methylcytidine, hepatitis E virus, replication, antiviral drug, nucleoside analogue

Introduction

Hepatitis E virus (HEV) is a single-stranded, positive-sense RNA virus, and its genome consists of three open reading frames (ORFs). ORF1 encodes a polyprotein that has all the nonstructural proteins needed for HEV replication. ORF2 encodes the capsid protein of the HEV virion. ORF3 encodes a small multifunctional protein with a molecular mass of 13kDa [11]. HEV was initially thought to only cause acute infection confined only to developing countries. However, over the last decade, hepatitis E cases are frequently reported in developed countries, and have been recognized mainly as autochthonous cases rather than an imported disease [11, 12]. Generally, HEV infection is self-limiting and asymptomatic with a consequence of low mortality rate; whereas it can cause high mortality in pregnant women. However, in immunocompromised patients receiving organ transplantation, more than 60% of HEV-infected patients will develop chronic disease and quickly progress towards severe liver complications such as fibrosis and cirrhosis [20]. Besides hepatitis, this virus has been associated with a broad range of extra-hepatic manifestations, in particular renal and neurological injuries [14, 21]. Therefore, the development of specific antiviral drugs for HEV infection is urgently required.

Nucleoside analogues have been used in clinic for almost 50 years and represent as cornerstones for treating patients with cancer or viral infection. Ribavirin (RBV) has been used as an off-label antiviral drug showing high efficacy in many chronic HEV patients, but HEV mutations associated with ribavirin treatment failure have been reported [4, 7]. Sofosbuvir (SOF), a potent direct-acting agent (DAA) against hepatitis C virus (HCV) [2], has been recently suggested to inhibit HEV replication in cell culture and exert an additive effect when combined with ribavirin [4]. However, other *in vitro* and clinical studies have demonstrated that sofosbuvir is not very effective against HEV infection [8, 18, 19], suggesting that this drug might not a promising candidate for the treatment of chronic HEV patients.

2'-C-methylcytidine (2CMC) was initially identified as a competitive inhibitor of the HCV RNA-dependent RNA polymerase (RdRp). Besides HCV, it has been shown to inhibit the replication of a variety of other viruses (*e.g.* dengue virus and norovirus) [13, 15]. It also has been reported to inhibit cutthroat trout virus, a non-pathogenic fish virus, which is remarkable similar to HEV [6]. In this study, we have demonstrated that 2CMC efficiently inhibit HEV replication, thus serves as a potential candidate for anti-HEV drug development.

Materials and Methods

Reagents and Antibodies

2CMC, RBV, Guanosine triphosphate (GTP) and Cytidine 5’-Triphosphate (CTP) were purchased from Sigma-Aldrich, and were dissolved in dimethyl sulfoxide (DMSO) (Sigma-Aldrich, St Louis, MO). The HEV-specific antibody was purchased from EMD Millipore (MAB8002).

HEV Cell Culture Models

Multiple cell lines were employed in this study, including human hepatoma cell line (Huh7 and PLC/PRF/5), human embryonic kidney cell line (HEK293), human primary glioblastoma cell line (U87),

human fetal lung fibroblast cell line (MRC5). Huh7 and U87 cell lines were kindly provided by Professor Bart Haagmans from Department of Viroscience, Erasmus Medical Center. Human embryonic kidney 293 cell line, PLC/PRF/5 and MRC5 were originally obtained from ATCC (www.atcc.org). These cells were cultured in Dulbecco's modified Eagle medium (Lonza Biowhittaker, Verviers, Belgium) supplemented with 10% fetal bovine serum, 100 IU/ml penicillin, and 100 µg/ml streptomycin. For the full-length HEV model, a plasmid construct containing the full-length HEV genome (Kernow-C1 p6 clone; GenBank Accession Number JQ679013) was employed to generate HEV genomic RNA by using the Ambion mMessage mMachine *in vitro* RNA transcription Kit (Thermo Fisher Scientific Life Sciences) [16]. Huh7, PLC/PRF/5, HEK293, U87 and MRC5 cells were electroporated with full-length HEV genome RNA to generate consecutive HEV-infected cell models (Huh7-p6, PLC/PRF/5-p6, HEK293-p6, U87-p6 and MRC5-p6). To generate the subgenomic (p6-Luc) HEV model, a plasmid construct containing subgenomic HEV was used. This plasmid has an HEV sequence in which the 5' portion of HEV ORF2 was replaced with the in-frame *Gaussia princeps* luciferase reporter gene [16]. Huh7, U87 and HEK293 cells were electroporated with HEV subgenomic RNA to generate HEV subgenomic models (Huh7-p6-Luc, U87-p6-Luc, and HEK293-p6-Luc). To normalize non-specific effects of 2CMC on the luciferase signal, Huh7 cells stably expressing a non-secreted firefly luciferase under control of the human phosphoglycerate kinase (PGK) promotor (PGK-Luc) were used [18]. In addition, Huh7 cells harboring a subgenomic HCV bicistronic replicon (I389/NS3-3V/LucUbiNeo-ET) (Huh7-HCV-Luc) were used as positive control of antiviral activity.

Quantification of HEV Replication

For Gaussia luciferase, the secreted luciferase activity in the cell culture medium was measured by BioLux® Gaussia Luciferase Flex Assay Kit (New England Biolabs). Gaussia luciferase activity was quantified with a LumiStar Optima luminescence counter (BMG LabTech, Offenburg, Germany). For the full-length infectious models (HEV-p6), intracellular viral RNA was quantified. RNA was isolated with a Machery-Nucleo Spin RNA II kit (Bioke, Leiden, The Netherlands) and quantified using a Nanodrop ND-1000 (Wilmington, DE, USA). cDNA was prepared from total RNA using a cDNA Synthesis Kit (TAKARA BIO INC). HEV RNA level was quantified with a SYBR Green-based real-time PCR (Applied Biosystems® SYBR® Green PCR Master Mix, Life technologies, CA, USA) according to the manufacturer's instructions. PCR steps consisted of a 10 min holding stage (95 ℃) followed by 40 cycles of 15 s at 95 ℃, 30 s at 58 ℃, and 30 s at 72 ℃. Glyceraldehyde-3-phosphate dehydrogenase (GAPDH) was considered as reference gene to normalize gene expression. Relative gene expression was normalized to GAPDH using the formula $2^{-\Delta\Delta CT}$ ($\Delta\Delta CT = \Delta CT_{sample} - \Delta CT_{control}$). The HEV primer sequences were as followed: HEV-F 5'-ATTGGCCAGAAGTTGGTTTTCAC-3'; HEV-R 5'-CCGTGGCTATAATTGTGGTCT-3'; GAPDH-F 5'-TGTCCCCACCCCCAATGTATC-3'; GAPDH-R 5'CTCCGATGCCTGCTTCACTACCTT-3'.

MTT assay

The cells were seeded in 96-well and 10 mM 3-(4,5-dimethylthiazol-2-yl)-2,5 diphenyltetrazolium bromide (MTT) (Sigma) was added to cells. Subsequently, the cells were incubated at 37 ℃ with 5% CO_2 for 3 h. The culture medium was then removed and 100 µl of DMSO was added to each well. The

absorbance of each well was read on the microplate absorbance readers (BIO-RAD) at wavelength of 490 nm.

Long-term treatment assay

For the long-term treatment assay of subgenomic model (Huh7-p6-luc), the cells were seeded into 96 wells with 5000 cells per well. The cells of CTR or 2CMC treatment groups were passaged and seeded with the same cell numbers every 3 days (d), meanwhile maintaining the cell incubated with vehicle (non-treatment) or 2CMC (10 μM) respectively throughout the entire incubation period. For the long-term treatment assay of infectious model (Huh7-p6), the cells were seeded into 48 wells with 2×10^4 cells per well. The cells of CTR or 2CMC treatment groups were passaged and seeded with the same cell numbers every 3 days, meanwhile maintaining the cell incubated with vehicle (non-treatment) or 2CMC (10 μM) respectively throughout the entire incubation period.

Western blot assay

Cultured cells were lysed in Laemmli sample buffer containing 0.1 M DTT and heated 5 mins at 95 ℃, followed by loading onto a 10 % sodium dodecyl sulfate polyacrylamide gel and separation by electrophoresis. After 90 mins running at 120 V, proteins were electrophoretically transferred onto a polyvinylidene difluoride membrane (Invitrogen) for 1.5 h with an electric current of 250 mA. Subsequently, the membrane was blocked with a mixture of 2.5 ml blocking buffer (Odyssey) and 2.5 ml phosphate-buffered saline containing 0.05% Tween 20. It was followed by overnight incubation with anti-HEV capsid protein primary antibodies (1:1000) at 4 ℃. The membrane was then washed 3 times followed by incubation for 1 h with goat anti-mouse IRDye-conjugated secondary antibody (Li-COR Biosciences, Lincoln, USA) (1:5000). After washing 3 times, protein bands were detected with the Odyssey 3.0 Infrared Imaging System.

IC50 and CC50 calculation

50% inhibition concentration (IC50) value and 50% cytotoxic concentration (CC50) were calculated based on model Y¼Bottom þ (Top-Bottom)/ (1 þ 10^((LogIC50-X)*HillSlope)) by using GraphPad Prism 5 software (GraphPad Prism 5; GraphPad Software Inc., La Jolla, CA, USA).

Statistical Analysis

Statistical analysis was performed using the nonpaired, nonparametric test with Mann-Whitney test and one-way ANOVA with Tukey's Multiple Comparison post-test (GraphPad Prism version 5.01; GraphPad Software). P values <0.05 were considered statistically significant.

Results

In this study, the potential anti-HEV effect of 2CMC was investigated in HEV replication models with concentrations ranging from 0.1 μM to 10 μM. We demonstrated that 2CMC significantly reduced HEV-driven luciferase activity, and the anti-HEV activity was even comparable with its anti-HCV effect at the concentration of 10 μM (Fig. 1A). IC50 value of 2CMC against HEV replication was 1.64 μM, CC50 of 2CMC to Huh7 cells was 111.2 μM and selectivity index (SI, CC50/IC50) was 67.8 (Fig. 1B).

The anti-HEV effect of 2CMC was further confirmed in the full-length (Kernow-C1, p6) infectious model of HEV genotype 3 by both RT-PCR assay (Fig. 1C) and western blot assay (Fig. 1D).

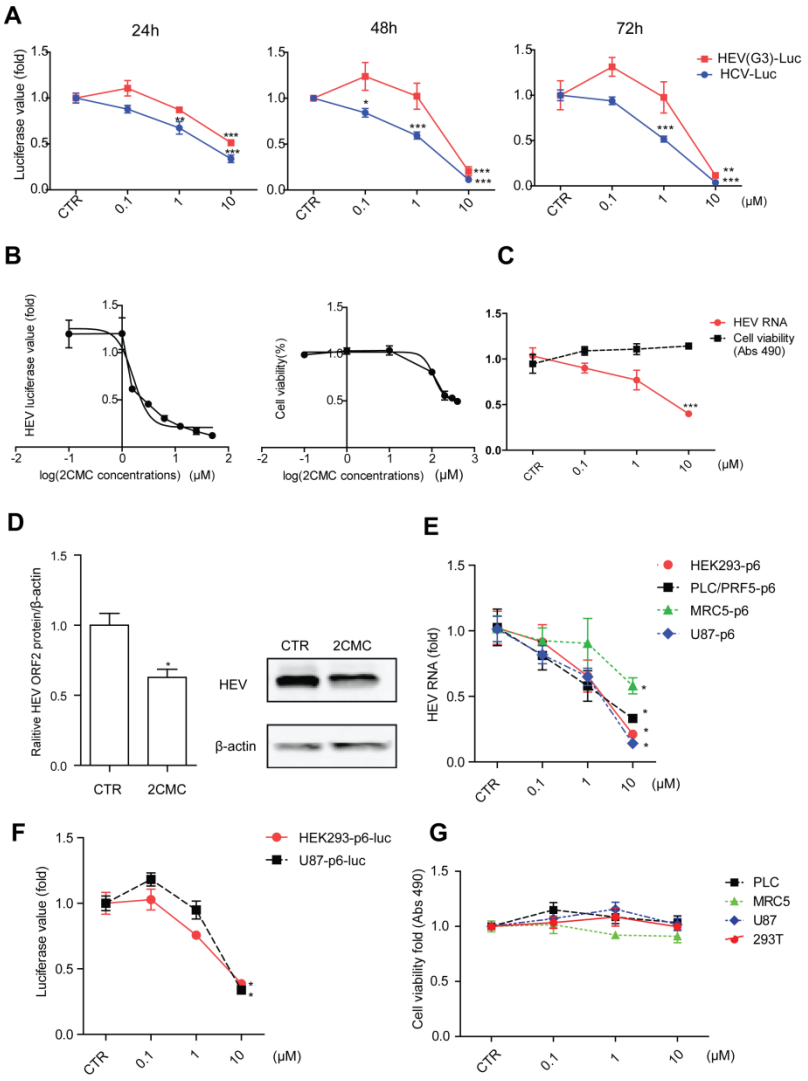

Figure 1. 2CMC exerts potent anti-HEV effect. (A) Huh7-p6-Luc cells and Huh7-HCV-Luc cells were treated with indicated concentrations of 2CMC for 24h, 48h, or 72h, and the untreated (CTR) group serves as control. Luciferase value was measured at indicated time points. Data are means ± SEM of four independent experiments; CTR means the non-treatment control. *P < 0.05; **P < 0.01; ***P < 0.001. (B) Huh7-p6-Luc cells were treated with 10 μM 2CMC for 48 h. 50% inhibition concentration (IC50) and 50% cytotoxic concentration (CC50) of 2CMC against HEV replication were calculated using GraphPad Prism 5 software. (C) Huh7-p6 cells were treated with indicated concentrations of 2CMC for 48 h. RT-PCR analysis of HEV RNA or Cell viability analysis were performed. Data are means ± SEM of four independent experiments; CTR means the non-treatment control. Abs 490 means absorption at 490 nm. ***P < 0.001. (D) Immunoblot analysis of HEV ORF2 protein level in Huh7 cell based HEV infectious cell model (Huh7-p6) treated with 2CMC (10 μM) for 48 h. Data are means ± SEM of four independent experiments; CTR means the non-treatment control. *P < 0.05. (E) Hepatic and extra-hepatic cells were treated with indicated concentrations of 2CMC for 48 h. RT-PCR analysis of HEV RNA was performed. Data are means ± SEM of four independent experiments; CTR means the non-treatment control. (F) HEK293T-p6-luc and U87-p6-luc cells were treated with indicated concentrations of 2CMC for 48 h and then were subjected to luciferase activity analysis. Data are means ± SEM of three independent experiments; CTR means the non-treatment control. *P < 0.05. (G) Indicated cells were treated with 2CMC for 48 h and then the cells were subjected to cell viability analysis using MTT assay.

Since HEV related extra-hepatic manifestations have been reported [12], we extended our study to some other hepatic and extra-hepatic cell lines. HEV infectious or replication models were established in HEK293, PLC/PRF/5, MRC5 and U87 cells. The anti-HEV potential of 2CMC in these cell lines was tested. In line with the results observed in Huh7-based HEV replication and infectious models, we observed similar anti-HEV effect of 2CMC in all these cell models without affecting the cell viability (Fig. 1E to G).

Drug resistance is a main factor that limits the effectiveness of the antiviral treatment. To characterize 2CMC in this respect, we performed experiments in which both HEV replication and

infectious models were constantly exposed to 2CMC (10 µM). Interestingly, 2CMC retained its anti-HEV activity in both models even after long-term exposure (Fig. 2A and B). Furthermore, the negative control retained high levels of luciferase activity after long-term incubation with 2CMC, excluding the loss of cell viability during the experimental period (Fig. 2C). Taken together, 2CMC displays a high barrier for drug resistance development.

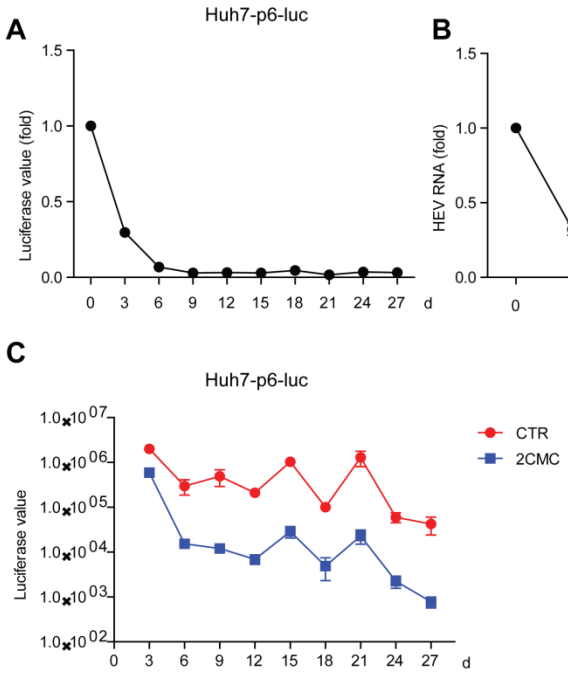

Figure 2. 2CMC retains anti-HEV effect in Huh7-p6-luc and Huh7-p6 models after long-term treatment. (A) Treatment of 2CMC in the Huh7-p6-luc model for 27 days. The cells were passaged every 3 days, and were incubated with vehicle (non-treatment) or 2CMC (10 µM) throughout the entire period. Data are means ± SEM of four independent experiments; CTR means the non-treatment control. (B) Treatment of 2CMC in the Huh7-p6 model for 15 days. The cells were passaged every 3 days, and were incubated with vehicle (non-treatment) or 2CMC (10 µM) throughout the entire period. Data are means ± SEM of four independent experiments. (C) Treatment of 2CMC in the Huh7-p6-luc model for 27 days. The absolute luciferase values of Huh7-p6-luc cells are measured at indicated time points.

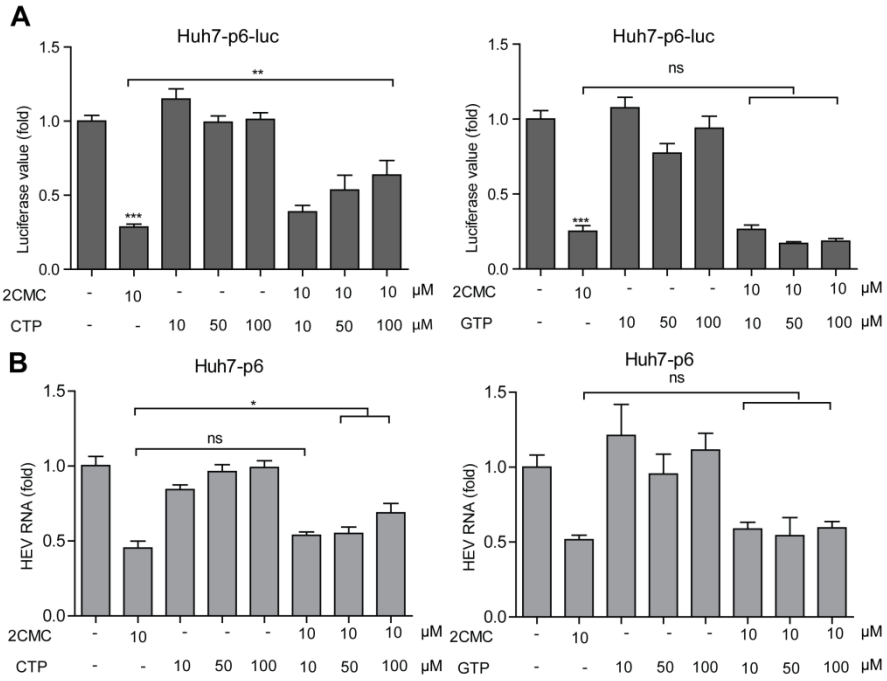

Figure 3. Combination of CTP and GTP with 2CMC in Huh7-p6-luc model (A) and Huh7-p6 (B) cell models. The cells were treated with 2CMC, CTP or GTP, alone or in combination for 72 h before measurement of luciferase activity. Data are means ± SEM of four to six independent experiments. *P < 0.05; **P < 0.01; ***P < 0.001; ns, not significant.

Figure 4. 2CMC antagonizes ribavirin in the Huh7-p6-luc model. (A) The Huh7-p6-Luc cells were treated with 2CMC and ribavirin, alone or in combination, for 72 h before analysis of luciferase activity. Untreated group

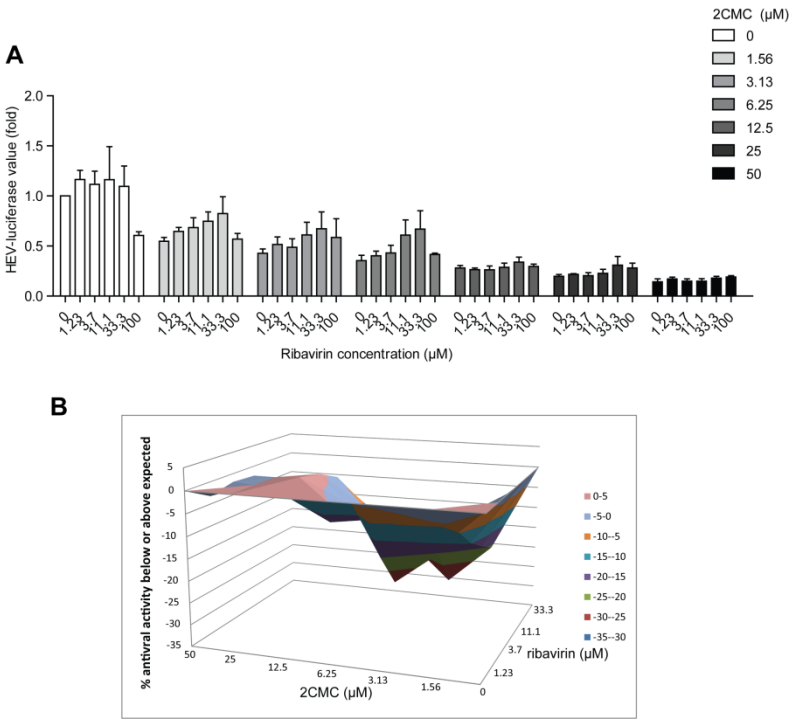

serves as control. (B) The combinatory effect of 2CMC and ribavirin on HEV replication was analyzed using the mathematical model MacSynergy. The three-dimensional surface plot represents the differences (within 95% confidence interval) between actual experimental effects and theoretical additive effects of the combination at various concentrations of the two compounds. Data are means ± SEM of three independent experiments.

Theoretically, nucleoside/nucleotide analogs serve as potential direct-acting antivirals because they bind to the viral RNA polymerase active site to block viral replication. To evaluate the inhibitory specificity of 2CMC against HEV replication, we performed a competition assay employing the substrate cytidine triphosphate (CTP) as an analogous competitor of 2CMC. Our results indicated that the CTP dose-dependently reversed the inhibitory effects of 2CMC on HEV replication activity. In contrast, guanosine triphosphate (GTP) exerted no effect, implying the inhibitory specificity of 2CMC against HEV replication (Fig. 3A and B). Another nucleoside analogue, ribavirin, has been used as an off-label treatment for HEV infection in clinic. Thus, its combination with 2CMC was tested related to their anti-HEV effects. Interestingly, a moderate antagonistic effect (-36.93 μM^2 %) was observed, implying a similar antiviral mechanism they employed (Fig. 4A and B).

Discussion

Nucleoside analogue has been used against a variety of viruses due to its broad spectrum of antiviral effects and its high barrier to drug resistance development. Ribavirin, an guanosine analogue, is the choice for treating most of the chronic HEV patients. However, treatment failure has been observed in some cases. Sofosbuvir, a prodrug of a uridine nucleoside analogue that is very effective against HCV, has been recently investigated for its anti-HEV potency. However, debates have been sparked regarding its potency against HEV [9, 17]. 2CMC, a cytidine nucleoside analogue, has been shown to inhibit the infection of a variety of viruses, including HCV and HIV [5]. In this study, we have demonstrated that 2CMC potently inhibits HEV replication in different cell models, even though a slight difference between these different cell models (Fig 1A and C). The possible explanation is that these models recapitulate the different steps of the HEV life cycle. The full-length infectious clone (Huh7-p6) models the entire cycle of HEV infection; whereas the subgenomic model (Huh7-p6-luc) only mimics viral replication due to lacking of ORF2 and ORF3.

Encouragingly, the anti-HEV activity was even comparable with its anti-HCV effect at particular concentrations. More importantly, In the long-term treatment experiment, 2CMC displays

a high barrier to resistance development. Furthermore , we have extensively demonstrated that it is a specific anti-HEV effect, but not due to cytotoxicity. It has been suggested that after absorbed into the cells, 2CMC is converted to its 5'-triphosphates (2CMC-CTP) which serves as active molecule that compete with natural substrate CTP. Consistently, our results have demonstrated that CTP but not GTP reverses the anti-HEV effect of 2CMC, revealing a potential mechanism-of-action of 2CMC against HEV.

Since ribavirin has been widely used to treat chronic HEV patients, a combined therapy of ribavirin with 2CMC might be envisaged. To test this, the combinatory effects of both drugs were investigated. Unexpectedly, an antagonistic effect was observed. These findings are in agreement with the earlier observation of the combinatory effects of ribavirin and 2CMC on HCV and HIV [3].

Of note, the potential adverse effects of 2CMC should be carefully evaluated in future studies. The clinical applications of nucleoside analogues have been limited in some cases due to the off target effects. Mitochondrial DNA polymerase is an important off target for many nucleoside analogues. It has been reported that the nucleoside analogue containing 2-C-methyl (2-CM) could reduce mitochondrial transcription and oxidative phosphorylation, resulting in dysfunction of cell metabolism [1, 10]. Therefore, efforts for the future anti-HEV drug development are proposed to focus on the design of less toxic agents based on the main chemical structure of 2CMC.

In conclusion, 2CMC exerts potent anti-HEV effects in well-established cell culture models, and serves as a potential backbone for anti-HEV drug design. To achieve better efficacy and less side effects, future research is still required for drug optimization based on the chemical structure of 2CMC.

Acknowledgments

The authors would like to thank Dr. Suzanne U. Emerson (National Institute of Allergy and Infectious Diseases, National Institutes of Health, Bethesda, MD) for kindly providing the plasmids to generate subgenomic and full-length HEV genotype 3 cell culture systems; Prof. Ralf Bartenschlager and Dr. Volker Lohmann (University of Heidelberg, Germany) for generously providing the Huh7 subgenomic HCV replication cells. The authors also thank the Dutch Digestive Foundation (MLDS) for a career development grant (No. CDG 1304), the Daniel den Hoed Foundation for a Centennial Award grant (to Q. Pan), and the China Scholarship Council for funding PhD fellowships for C. Qu (No.201509110121), L. Xu (No.201306300027), Y. Yin (No.201307720045) and W. Wang (No. 201303250056).

Compliance with ethical standards

This article does not contain any studies with human participants or animals performed by any of the authors and is in compliance with ethical standards for research.

Conflict of interest

The authors declare no conflict of interest.

References

1. Arnold JJ, Sharma SD, Feng JY, Ray AS, Smidansky ED, Kireeva ML, Cho A, Perry J, Vela JE, Park Y, Xu Y, Tian Y, Babusis D, Barauskus O, Peterson BR, Gnatt A, Kashlev M, Zhong W, Cameron CE (2012) Sensitivity of mitochondrial transcription and resistance of RNA polymerase II dependent nuclear transcription to antiviral ribonucleosides. PLoS Pathog 8:e1003030
2. Cholongitas E, Papatheodoridis GV (2014) Sofosbuvir: a novel oral agent for chronic hepatitis C. Ann Gastroenterol 27:331-337
3. Coelmont L, Paeshuyse J, Windisch MP, De Clercq E, Bartenschlager R, Neyts J (2006) Ribavirin antagonizes the in vitro anti-hepatitis C virus activity of 2'-C-methylcytidine, the active component of valopicitabine. Antimicrob Agents Chemother 50:3444-3446
4. Dao Thi VL, Debing Y, Wu X, Rice CM, Neyts J, Moradpour D, Gouttenoire J (2016) Sofosbuvir Inhibits Hepatitis E Virus Replication In Vitro and Results in an Additive Effect When Combined With Ribavirin. Gastroenterology 150:82-85 e84
5. De Clercq E (2007) The design of drugs for HIV and HCV. Nat Rev Drug Discov 6:1001-1018
6. Debing Y, Winton J, Neyts J, Dallmeier K (2013) Cutthroat trout virus as a surrogate in vitro infection model for testing inhibitors of hepatitis E virus replication. Antiviral Res 100:98-101
7. Debing Y, Gisa A, Dallmeier K, Pischke S, Bremer B, Manns M, Wedemeyer H, Suneetha PV, Neyts J (2014) A mutation in the hepatitis E virus RNA polymerase promotes its replication and associates with ribavirin treatment failure in organ transplant recipients. Gastroenterology 147:1008-1011 e1007; quiz e1015-1006
8. Donnelly MC, Imlach SN, Abravanel F, Ramalingam S, Johannessen I, Petrik J, Fraser AR, Campbell JD, Bramley P, Dalton HR, Hayes PC, Kamar N, Simpson KJ (2017) Sofosbuvir and Daclatasvir Anti-Viral Therapy Fails to Clear HEV Viremia and Restore Reactive T Cells in a HEV/HCV Co-Infected Liver Transplant Recipient. Gastroenterology 152:300-301
9. Eyer L, Zouharova D, Sirmarova J, Fojtikova M, Stefanik M, Haviernik J, Nencka R, de Clercq E, Ruzek D (2017) Antiviral activity of the adenosine analogue BCX4430 against West Nile virus and tick-borne flaviviruses. Antiviral Res 142:63-67
10. Feng JY, Xu Y, Barauskas O, Perry JK, Ahmadyar S, Stepan G, Yu H, Babusis D, Park Y, McCutcheon K, Perron M, Schultz BE, Sakowicz R, Ray AS (2016) Role of Mitochondrial RNA Polymerase in the Toxicity of Nucleotide Inhibitors of Hepatitis C Virus. Antimicrob Agents Chemother 60:806-817
11. Fujiwara S, Yokokawa Y, Morino K, Hayasaka K, Kawabata M, Shimizu T (2014) Chronic hepatitis E: a review of the literature. J Viral Hepat 21:78-89
12. Kamar N, Bendall R, Legrand-Abravanel F, Xia NS, Ijaz S, Izopet J, Dalton HR (2012) Hepatitis E. Lancet 379:2477-2488
13. Lee JC, Tseng CK, Wu YH, Kaushik-Basu N, Lin CK, Chen WC, Wu HN (2015) Characterization of the activity of 2'-C-methylcytidine against dengue virus replication. Antiviral Res 116:1-9
14. Pischke S, Hartl J, Pas SD, Lohse AW, Jacobs BC, Van der Eijk AA (2017) Hepatitis E virus: Infection beyond the liver? J Hepatol 66:1082-1095
15. Rocha-Pereira J, Jochmans D, Dallmeier K, Leyssen P, Cunha R, Costa I, Nascimento MS, Neyts J (2012) Inhibition of norovirus replication by the nucleoside analogue 2'-C-methylcytidine. Biochem Biophys Res Commun 427:796-800
16. Shukla P, Nguyen HT, Faulk K, Mather K, Torian U, Engle RE, Emerson SU (2012) Adaptation of a genotype 3 hepatitis E virus to efficient growth in cell culture depends on an inserted human gene segment acquired by recombination. J Virol 86:5697-5707
17. Todt D, Gisa A, Radonic A, Nitsche A, Behrendt P, Suneetha PV, Pischke S, Bremer B, Brown RJ, Manns MP, Cornberg M, Bock CT, Steinmann E, Wedemeyer H (2016) In vivo evidence for ribavirin-induced mutagenesis of the hepatitis E virus genome. Gut 65:1733-1743
18. van der Valk M, Zaaijer HL, Kater AP, Schinkel J (2017) Sofosbuvir shows antiviral activity in a patient with chronic hepatitis E virus infection. J Hepatol 66:242-243
19. Wang W, Hakim MS, Nair VP, de Ruiter PE, Huang F, Sprengers D, Van Der Laan LJ, Peppelenbosch MP, Surjit M, Pan Q (2016) Distinct Antiviral Potency of Sofosbuvir Against Hepatitis C and E Viruses. Gastroenterology 151:1251-1253
20. Zhou X, de Man RA, de Knegt RJ, Metselaar HJ, Peppelenbosch MP, Pan Q (2013) Epidemiology and management of chronic hepatitis E infection in solid organ transplantation: a comprehensive literature review. Rev Med Virol 23:295-304
21. Zhou X, Huang F, Xu L, Lin Z, de Vrij FM, Ayo-Martin AC, van der Kroeg M, Zhao M, Yin Y, Wang W, Cao W, Wang Y, Kushner SA, Peron JM, Alric L, de Man RA, Jacobs BC, van Eijk JJ, Aronica EM, Sprengers D, Metselaar HJ, de Zeeuw CI, Dalton HR, Kamar N, Peppelenbosch MP, Pan Q (2017) Hepatitis E virus infects neurons and brains. J Infect Dis

Part III.

Virus-host interation-based strategies

Chapter 12

Biological or pharmacological activation of protein kinase C alpha constrains hepatitis E virus replication

Wenshi Wang[1], Yijin Wang[1], Yannick Debing[2], Xinying Zhou[1], Yuebang Yin[1], Lei Xu[1], Elena Herrera Carrillo[3], Johannes H Brandsma[4], Raymond A. Poot[4], Ben Berkhout[3], Johan Neyts[2], Maikel P. Peppelenbosch[1] and Qiuwei Pan[1]

[1]Department of Gastroenterology and Hepatology, Erasmus MC-University Medical Center, Rotterdam, The Netherlands.

[2]Department of Microbiology and Immunology, Rega Institute for Medical Research, KU Leuven, Leuven, Belgium.

[3]Laboratory of Experimental Virology, Department of Medical Microbiology, Center for Infection and Immunity Amsterdam (CINIMA) Academic Medical Center of the University of Amsterdam, Amsterdam, The Netherlands;

[4]Department of Cell Biology, Medical Genetics Cluster, Erasmus MC, Rotterdam, The Netherlands.

Antiviral Research, 2017, 140: 1-12.

Abstract

Although hepatitis E has emerged as a global health issue, there is limited knowledge of its infection biology and no FDA-approved medication is available. Aiming to investigate the role of protein kinases in hepatitis E virus (HEV) infection and to identify potential antiviral targets, we screened a library of pharmacological kinase inhibitors in a cell culture model, a subgenomic HEV replicon containing luciferase reporter. We identified protein kinase C alpha (PKCα) as an essential cell host factor restricting HEV replication. Both specific inhibitor and shRNA-mediated knockdown of PKCα enhanced HEV replication. Conversely, over-expression of the activated form of PKCα or treatment with its pharmacological activator strongly inhibited HEV replication. Interestingly, upon the stimulation by its activator, PKCα efficiently activates its downstream Activator Protein 1 (AP-1) pathway, leading to the induction of antiviral interferon-stimulated genes (ISGs). This process is independent of the JAK-STAT machinery and interferon production. However, PKCα induced HEV inhibition appears independent of the AP1 cascade. The discovery that activated PKCα restricts HEV replication reveals new insight of HEV-host interactions and provides new target for antiviral drug development.

Keywords: PKCα, hepatitis E virus, PMA, AP-1, ISG

Introduction

Hepatitis E virus (HEV) is one of the most common causes of acute viral hepatitis in the world. Although the mortality rate is < 1% among the general population, pregnant women can have a fatality rate of up to 30% (1). Additionally, chronic hepatitis E has become a significant clinical problem in immunocompromised patients. Up to date, there is still no proven medication available and its infection biology is poorly understood.

Protein kinases are principal components of the machineries that orchestrate immune response against diverse pathogenic entities, including viruses, by subsequent stimulation of specific signal transduction cascades (2). However, kinase controlled pathways employed by the host cells to stimulate antiviral immunity remain largely obscure. Knowledge of such pathways could prove exceedingly useful for the rational design of therapeutic avenues against HEV infection.

Encouragingly, numerous pharmacological kinase inhibitors or activators have been developed to target particular kinases. Among those, several are approved drugs in particular for treating cancer (3), and many are currently at various stages of preclinical and clinical development. These compounds have broad implications for treating various diseases, including cancer, inflammation, diabetes and viral infections (4, 5).

Thus, this study aims to comprehensively profile kinase-mediated cascades in cell–autonomous antiviral immunity starting from screening a library of pharmacological kinase inhibitors in Huh7 based HEV replication cell model. We identified protein kinase C alpha (PKCα) as an important anti-HEV mediator. Concurrently, we also revealed a novel function of PKC-Activator Protein 1 (AP-1) pathway, serving as a non-canonical pathway to activate transcription of antiviral interferon-stimulated genes (ISGs).

Materials and Methods

Reagents and Antibodies

Stocks of phorbol 12-myristate 13-acetate (PMA) (Sigma-Aldrich, St Louis, MO) and JAK inhibitor I (Santa Cruz Biotech, Santa Cruz, CA) were dissolved in dimethyl sulfoxide (DMSO) (Sigma-Aldrich, St Louis, MO) to concentrations of 100 μg/ml and 20 mM, respectively. Antibodies including phospho-PKCα/β (#9375), phospho-STAT1 (58D6, #9167), c-Fos (9F6, #2250), RelA (C22B4, #4764), Anti-rabbit IgG(H+L),F(ab') 2 Fragment (Alexa Fluor 488 conjugate) and Anti-mouse IgG (H+L), F(ab')2 Fragment (Alexa Fluor® 488 Conjugate) were purchased from Cell Signaling Technology, the Netherlands. Anti-rabbit or anti-mouse IRDye-conjugated antibodies were used as secondary antibodies for western blotting (Stressgen, Victoria, BC, Canada).

Viruses and cell culture models

Hepatocellular carcinoma cells Huh7 were kindly provided by Professor Bart Haagmans from Department of Viroscience, Erasmus Medical Center. Human Embryonic Kidney 293 cells were originally obtained from ATCC (www.atcc.org). The HEV infectious model (Huh7-P6) was based on Huh7 cells containing the full-length HEV genome (Kernow-C1 p6 clone, GenBank Accession Number JQ679013) (6). Infectious HEV particles are generated and secreted into cell culture medium, which

can be collected and used for secondary infection (7-10). The HEV subgenomic model was based on Huh7 cells containing the subgenomic HEV sequence (Kernow-C1 p6/luc) coupled to a Gaussia luciferase reporter gene. HEV replication defective model was based on Huh7 cells transfected with *in vitro* transcribed RNA from MluI-linearized plasmids p6-luc-GAD (kindly provided by Suzanne U. Emerson). A mutation in the HEV polymerase results in defect of viral replication. ISRE, NF-κB, AP-1 luciferase reporter cells were generated by transducing Huh7 cells with lentiviral vectors expressing the firefly luciferase gene under the control of ISRE, NF-κB, AP-1 promoters, respectively (System Biosciences). For simian rotavirus, SA11, a well-characterized and broadly used laboratory strain, was used to inoculate the Caco2 cell line as a rotavirus infection model. Murine norovirus 1 (MNV-1) was used to infect RAW 264.7 cells as a norovirus infection model (11). The HIV virus production model was based on 293T cells transfected with HIV-1 molecular clone pLAI and pRL. The HIV single cycle entry model was based on TZM-bl cells infected with HIV clone Plai (12). For influenza virus, multicycle replication curves were generated by inoculating A549 cells at a multiplicity of infection (MOI) of 0.01 50 percent tissue culture infectious doses ($TCID_{50}$) of A/Netherlands/246/1978(A/H3N2) or A/Netherlands/602/09 (A/H1N1) in duplicate. Supernatants were sampled at 0, 6, 12, 24, 48 and 72 hours post inoculation, and virus titers in these supernatants were determined by means of end-point titration in MDCK cells as described previously (13).

Screen of pharmacological kinase inhibitors

The kinase inhibitor library used for the screening was made available by the KU Leuven Centre for Drug Design & Development (www.cd3.eu). Huh7 cells were seeded in 96-well plates at 7.5×10^3 cells per well in 100 µl of DMEM with10% FBS and were incubated at 37°C. After 24 hrs, cell layers were washed and transfected with capped p6/luc RNA (100 ng per well [each]) by use of DMRIE-C reagent (0.2 µl per well) according to the manufacturer's instructions. Plates were incubated at 37°C for 4 hrs. Afterwards, the transfection medium was removed. Cell layers were washed twice with PBS and 100 µl of compound (diluted to a final concentration of 100, 20, 4 and 0.8 µM, respectively, in DMEM with 10% FBS) was added to each well. For control wells, the compound was omitted. After incubation for 3 days, HEV replicon – related Gaussia luciferase values were measured accordingly (14). Cell viability (CV) caused by compound-specific side effects were also analyzed after 3 days by using the CellTiter 96 AQ_{ueous} nonradioactive cell proliferation (monotetrazolium salt [MTS]) assay (Promega) (15). HEV replicon - related luciferase values were normalized with the following formula: $Luc\ (Norm) = (Luc_{replicon + compound} - Luc_{replicon + control}) / (CV_{replicon + compound} - CV_{replicon + control})$

Gene knockdown or over-expression by lentiviral vectors

Lentiviral pLKO knockdown vectors (Sigma–Aldrich) targeting PKCα, PKCβ, IRF9, RelA, c-Fos or control were obtained from the Erasmus Biomics Center and produced in HEK293T cells as previously described (16). After a pilot study, the shRNA vectors exerting optimal gene knockdown were selected. These shRNA sequences are listed in Supplementary Table 2. Stable gene knockdown cells were generated after lentiviral vector transduction and puromycin (2.5µg/ml; Sigma) selection. wtPKCα and caPKCα overexpression lentivral vectors were a kind gift from Dr. Lin from the University of Minnesota. To create stable over-expression cell lines, GFP positive cells were sorted by cell sorter after lentiviral vectors transduction.

Reinfection assays

Reinfection assay was performed accordingly (17). Supernatant (containing infectious HEV particles) was collected from Huh7-P6 HEV model and purified by ultracentrifugation. The supernatant was first filtered through 0.45 mm filter followed by centrifugation at 10,000 rpm for 30 min to remove cell debris and then 22,000 rpm for 2 hrs to pellet HEV virus (SW 28 rotor). The pellet was suspended and diluted to 1×10^7 HEV viral RNA copies/ml. The diluted HEV virus stock was stored at −80°C. For HEV infection, cells were seeded into 12-well plates at a density of 7×10^4 cells per well and incubated for 24 hrs. Next, cells were incubated with 400 µl HEV stock (1×10^7 viral RNA copies/ml) per well at 37°C for 6 hrs. Then, the inoculum was removed, and cell layers were washed 3 times with PBS, and 1 ml fresh medium was added to each well.

Measurement of luciferase activity

For Gaussia luciferase, the secreted luciferase activity in the cell culture medium was measured by BioLux® Gaussia Luciferase Flex Assay Kit (New England Biolabs). For firefly luciferase, luciferin potassium salt (100 mM; Sigma) was added to cells and incubated for 30 min at 37 °C. Both Gaussia and firefly luciferase activity was quantified with a LumiStar Optima luminescence counter (BMG LabTech, Offenburg, Germany).

Quantitative real-time polymerase chain reaction

RNA was isolated with a Machery-NucleoSpin RNA II kit (Bioke, Leiden, The Netherlands) and quantified using a Nanodrop ND-1000 (Wilmington, DE, USA). cDNA was synthesized from total RNA using a cDNA Synthesis Kit (TAKARA BIO INC). The cDNA of all target genes was amplified for 50 cycles and quantified with a SYBRGreen-based real-time PCR (Applied Biosystems) according to the manufacturer's instructions. GAPDH was considered as a reference gene to normalize gene expression. Relative gene expression was normalized to GAPDH using the formula $2^{-\Delta\Delta CT}$ ($\Delta\Delta CT = \Delta CT_{sample} - \Delta CT_{control}$). All the primer sequences are included in Supplementary Table 3.

Western blot assay

Cultured cells were lysed in Laemmli sample buffer containing 0.1 M DTT and heated 5 mins at 95 °C, followed by loading onto a 10% sodium dodecyl sulfate polyacrylamide gel and separation by electrophoresis. After 90 mins running at 120 V, proteins were electrophoretically transferred onto a polyvinylidene difluoride membrane (Invitrogen) for 1.5 hrs with an electric current of 250 mA. Subsequently, the membrane was blocked with a mixture of 2.5 ml blocking buffer (Odyssey) and 2.5 ml phosphate-buffered saline containing 0.05% Tween 20. It was followed by overnight incubation with primary antibodies (1:1000) at 4 °C. The membrane was washed 3 times followed by incubation for 1 hr with IRDye-conjugated secondary antibody (1:5000). After washing 3 times, protein bands were detected with the Odyssey 3.0 Infrared Imaging System.

Confocal laser electroscope assay

Huh7 cells were seeded on glass coverslips. After 12 hrs, cells were washed with PBS, fixed in 4% formalin for 10 mins and blocked with tween-milk-glycine medium (PBS, 0.05% tween, 5g/L skim milk

and 1.5g/L glycine). Samples were incubated with primary antibodies overnight at 4 °C. Subsequently, samples were incubated with 1:1000 dilutions of the anti-mouse IgG (H+L), F(ab')2 Fragment (Alexa Fluor® 488 Conjugate) or anti-rabbit IgG(H+L), F(ab') 2 Fragment (Alexa Fluor 488 conjugate) secondary antibodies. Nuclei were stained with DAPI (4,6-diamidino-2-phenylindole; Invitrogen). Images were detected using confocal electroscope.

Creation of mutant ISRE reporter cell line

Based on the sequence specific ISRE motif, a mutant version of ISRE was designed and synthesized (Forward: 5'-*aattc*AGTCACGTCTTCCCTTTCAGTCACGTCTTCCCTTTCAGTCACGTCTTCCCTTTCAGTCACGTCTTCCCTTT*a*-3'; Reverse: 5'-*ctagt*AAAGGGAAGACGTGACTGAAAGGGAAGACGTGACTGAAAGGGAAGACGTGACTGAAAGGGAAGACGTGACT*g*-3'), which shows no consensus sequence with AP-1 motif. EcoRI and SpeI sites are included (shown in italics) to facilitate directional cloning into the pGreenFire Lenti-Reporter vector (System Biosciences). The recombinant plasmid was verified by restriction enzyme digestion and DNA sequencing. Stable mutant ISRE reporter cells were generated after the lentiviral vector transduction and puromycin (2.5µg/ml; Sigma) selection.

C-Fos ChIP-seq data analysis

The c-Fos ChIP-seq data set with accession number GSM754332 was retrieved from the Gene Expression Omnibus. Sequence reads with low complexity that are unlikely to map uniquely to the genome were removed from the dataset using prinseq-lite with the dust method with 7 as threshold (18, 19). Bases on 5' and 3' end of the reads with a quality score below 28 were trimmed also using prinseq-lite. Trimmed reads were required to have a minimum length of 20 bases. The remaining sequences with a Phred score <70 were mapped to the hg38 reference genome using Bowtie v0.12.7 (20), where we used a seed length of 36 in which we allowed a maximum of 2 mismatches. If a read had multiple alignments, only the best matching read was reported. Duplicated reads were removed. MACS v1.4.2 was used for peak calling using default settings. The sequencing profiles of c-Fos were created in the IGV browser (21).

MTT assay

Cells were seeded in 96-well plates and cultured at 37 °C with 5% CO_2 for 24, 48, 72 hrs, respectively. Then 10 mM 3-(4,5-dimethylthiazol-2-yl)-2,5-diphenyltetrazolium bromide (MTT) (Sigma) was added to cells and incubated for 4 hrs. Subsequently, medium was removed and 100 µl of DMSO was added to each well. The absorbance of each well was read on a microplate absorbance readers (BIO-RAD) at a wavelength of 490 nm. All measurements were performed in triplicate.

Statistical analysis

All results were presented as mean ± SEM. Comparisons between groups were performed with Mann-Whitney test. Differences were considered significant at a P value less than 0.05.

Results

A screening for kinases identifies conventional PKCs as cell-autonomous anti-HEV elements

Protein kinases are pivotal mediators of signal transduction and identifying kinases involved in biological responses can shed important light on kinase associated virus-host interactions. The lack of understanding as to which signal pathways mediate cell-autonomous antiviral immunity against HEV thus prompted us to execute a screening of kinase inhibitors with respect to their effects in antiviral responses. To this end, we employed a hepatocyte cell line, i.e. Huh7, transfected with a HEV replicon luciferase reporter as a platform for the screening of 132 pharmacological kinase inhibitors with known specificity profile (14) (Fig. S1A and Table S1). We arbitrarily set the control luciferase value to 1 and identified 40 inhibitors (normalized value $\geqslant$ 1.2) that increase and 42 compounds (normalized value $\leqslant$ 0.8) that inhibit luciferase activity in this assay system (Fig. 1A and Table S2). Inhibition of luciferase activity might be due to non-specific effects not related to the scientific question at hand (*e.g.* effects on translation or cell survival). Strikingly, stimulation of luciferase activity likely relates to the inhibition of signaling elements involved in constraining viral replication and hence we concentrated on luciferase enhancing compounds in our search for elements involved in antiviral immunity. Go6976, a fairly specific inhibitor of the conventional PKCs (PKCα, PKCβI, PKCβII, and PKCγ) (22), has increased HEV luciferase activity. Subsequent western blot analysis for the phosphorylation state of PKC isoforms confirmed the inhibition of PKCα and PKCβ by Go6976 in our experimental system (Fig.1B). HEV promoting activity of Go6976 was further confirm in two independent cell culture models: a subgenomic HEV containing luciferase reporter and a full-length HEV infectious cell culture system (Fig. 1C, D and Fig. S1B). Go6976 showed inhibitory effect on host cell growth (Fig. S1C), which is expected because of the crucial roles of PKCs in cell physiology. Interestingly, Go6976 is also indicated as a potential inhibitor of protein kinase D (PKD), although with relatively lower sensitivity compared with PKCα and PKCβ1. Therefore, we also tested the role of PKD in Go6976 induced HEV replication. CID 755673, a selective PKD inhibitor (IC_{50}: 0.182 – 0.227μM) was tested in both HEV cell culture systems. However, CID 755673 showed no significant effect on HEV replication (Fig. S1D and E). Therefore, the effect of Go6976 on HEV is likely independent of PKD. Collectively, these data demonstrated that conventional PKCs are important antiviral elements, at least with respect to HEV infection.

PKCα is the key anti-HEV isoform

The observation that conventional PKCs constrain HEV replication raises questions as to the role of different PKC isoforms. To dissect the effects of individual PKC isoforms, we silenced the expression of *PRKCA* (the gene coding for PKCα) and *PRKCB* (that gives rise to PKCβI and PKCβII) in Huh7 cells using lentiviral-mediated RNAi. Since PKCγ has been shown to be specifically expressed in neuronal tissue (23), we ruled it out for further research. Western blot and qRT-PCR confirmed successful down-regulation of PKC isoforms (Fig. 2A and B) at protein and RNA levels. Subsequently, cells were inoculated with infectious HEV particles and cellular HEV RNA was quantified by qRT-PCR after 48 hrs. Knockdown of PKCα led to a 2.25 ± 0.3 fold ($n = 4$, $p < 0.05$) increase of HEV RNA; whereas PKCβ

knockdown resulted in no significant effect (Fig. 2C), suggesting that PKCα is the relevant isoform here.

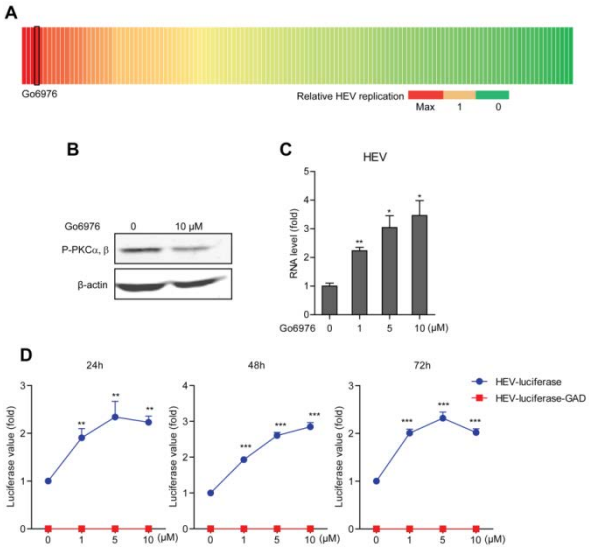

Fig 1. Conventional PKCs function as cell-autonomous antiviral elements against HEV. (A) Heatmap summary of the screening results. The Huh7 cell line transfected with a subgenomic HEV luciferase reporter replicon was used. Compared to control, relative HEV luciferase activity depicted in red to green for each inhibitor. Red means that the signal is higher than control; whereas green means lower than control. See also Table S1. (B) Go6976 (10 μM) treatment inhibited phosphorylation of PKCα and PKCβ protein levels in Huh7 cells as determined by western blot. (C) qRT-PCR analysis of HEV RNA in Huh7 cells harboring full-length HEV infectious genome. Treatment with Go6976 increased cellular HEV RNA (n = 3). (D) In the Huh7 cell-based subgenomic HEV replicon model, treatment with different doses of Go6976 increased HEV replication-related luciferase activity. Cells transfected with replicon defective control (HEV-luciferase-GAD) RNA were also treated with Go6976 (n = 3 independent experiments with 2 - 3 replicates each). Data presented as mean ± SEM (**, P < 0.05; **, P < 0.01; ***, P<0.001;* ns, not significant).

PKCα maintains its inactive state via an inhibitory region within the effector binding domain of the kinase. Its pseudosubstrate site mediates this inhibition by binding to the active site and preventing substrate interaction (24). A constitutively active PKCα (caPKCα) is available in which a glutamic acid present in this region is substituted for alanine. (Fig. 2D). This form dramatically increases effector-independent kinase activity, compared to the wild-type PKCα (wtPKCα) (25). Huh7 cells were transduced with integrating lentiviral vectors co-expressing GFP and caPKCα or wtPKCα (Fig. S1F). Cell cytometry confirmed transgene expression by measuring GFP and positive cells were sorted and expanded for further experimentation (Fig. S1G). Huh7 cells expressing caPKCα or wtPKCα were inoculated with infectious HEV particles and relative viral RNA level was quantified 48 hrs post-inoculation. Consistent with PKCα knockdown (Fig. 2C), expression of caPKCα significantly decreased HEV RNA by 49% (n = 4, p < 0.05), while wtPKCα over-expression showed no effect on HEV compared to control sample (Fig. 2E).

This promising result prompted us to investigate the potential role of the classical PKC pharmacological activator, PMA, also commonly known as 12-*O*-Tetradecanoylphorbol-13-acetate (TPA). PMA, structurally analogous to diacylglycerol, is commonly used to activate PKC. It is also a promising drug candidate, currently under a Phase II clinical trial for the treatment of patients with relapsed/refractory acute myelogenous leukemia (NCT01009931). As expected, PMA exerted strong anti-HEV effects in both HEV subgenomic and full-length infectious models (Fig. 3A, B and Fig. S2A, B); while no clear effect on cell growth and viability was observed (Fig. S2C). This result prompted us to assess the combined antiviral effect of PMA with the off-label anti-HEV drugs IFN-α or ribavirin (14, 26, 27). Although PMA and IFN-α showed comparable anti-HEV capacity, they failed to exert further combined effect (Fig. 3C and E). The combination of PMA with ribavirin showed strong additive anti-HEV effect (Fig. 3D and F). These data collectively indicate that activated PKCα plays an important role in cell-autonomous anti-HEV immunity.

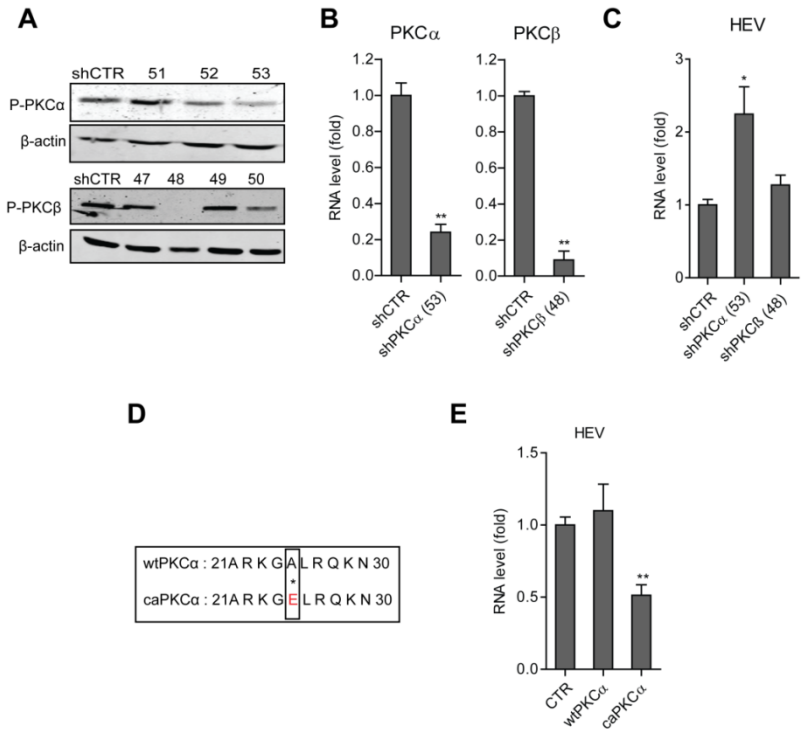

Fig 2. PKCα is the key antiviral isoform against HEV. (A) Western blot analysis of PKCα and PKCβ knockdown by lentiviral shRNA vectors. Compared with the control vector transduced cells, the shPKCα clone 53 and shPKCβ clone 48 exert potent silencing capability shown at protein levels. Blots depict phosphorylated PKCα, PKCβ and β-actin. (B) qRT-PCR analysis of PKCα and PKCβ knockdown by lentiviral shRNA vectors. Compared to the control vector transduced cells, the no.53 and 48 clones of shPKCα and PKCβ, respectively, exert a potent silencing capability shown at RNA levels (n = 3). (C) Cellular HEV RNA level in PKCα or PKCβ knockdown cells was determined by qRT-PCR 48 hrs post-inoculation with HEV particles. Knockdown of PKCα led to a 2.25 ± 0.3 fold increase of HEV RNA; whereas PKCβ knockdown resulted in no significant increase (n = 4). (D) The change in amino acid sequence between wtPKCα and caPKCα is shown in the rectangular frame. (E) qRT-PCR analysis of cellular HEV RNA level in CTR, wtPKCα or caPKCα over-expressing cells after inoculation of infectious HEV particles for 72 hrs. caPKCα over-expression inhibited HEV RNA by 49%. Data presented as mean ± SEM (**, P < 0.05; **, P < 0.01; ***, P<0.001;* ns, not significant).

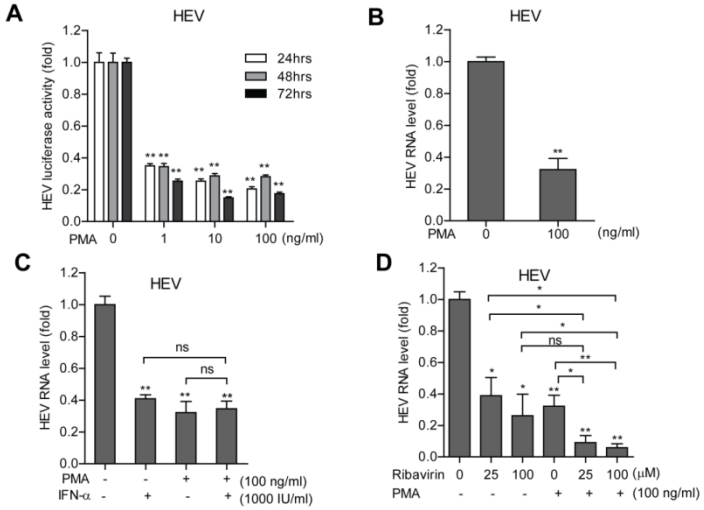

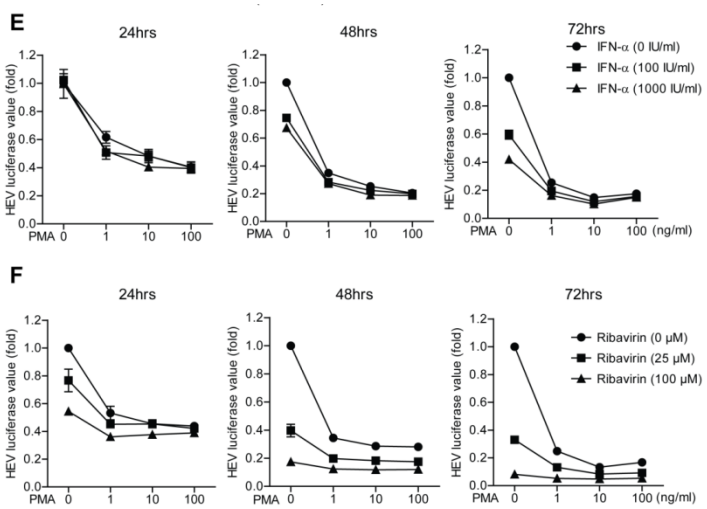

Fig 3. PKC specific activator PMA exerts strong antiviral activity against HEV. (A) In the Huh7 cell-based subgenomic HEV replicon model, treatment with different doses of PMA inhibited HEV replication-related luciferase activity (n = 3 independent experiments with2 - 3 replicates each). (B) qRT-PCR analysis of HEV RNA derived from Huh7 cells harboring the full-length HEV infectious genome. Treatment with PMA (100 ng/ml) for 48 hrs significantly inhibited cellular HEV RNA by 68% (n = 9). (C) Huh7 cells harboring the full-length HEV infectious genome were treated with different doses of IFN-α, PMA or a combination of both for 48 hrs. Cellular HEV RNA level was determined by qRT-PCR. PMA and IFN-α showed comparable anti-HEV capacity, but they failed to exert further combined effect (n = 4). (D) Same as (C) for ribavirin, PMA or a combination of both. The combination of PMA with ribavirin showed strong additive anti-HEV effect (n = 4). (E) The Huh7 cell-based subgenomic HEV replicon was treated with PMA, IFN-α or a combination of both. Their combination showed no additive effect. Luciferase values were measured at 24, 48 and 72 hrs. (n = 3 independent experiments with 2 – 3 replicates each). (F) Same as (E) for PMA, ribavirin or a combination of both. Their combination showed additive anti-HEV activity. (n = 3 independent experiments with 2 – 3 replicates each). Data presented as mean ± SEM (**, P < 0.05; **, P < 0.01; ***, P<0.001;* ns, not significant).

PKCα provokes transcriptional activation of ISGs, independent of the IFN-JAK-STAT pathway

We extended our study on a list of other viruses (rotavirus, murine norovirus, HIV-1 and influenza virus). Although no significant antiviral effects on HIV-1 and influenza virus, PMA significantly inhibited rotavirus and murine norovirus 1 infection (Fig. S2B - G). The relative broad antiviral efficacy induced by PMA prompted us to investigate its potential link to the function of IFNs, which possess broad antiviral effects via efficient induction of ISGs.

Following interferon stimulation and interferon receptor activation, STAT1 and STAT2 are phosphorylated and form heterodimers, which subsequently bind to IRF9 leading to the formation of the so-called IFN-stimulated gene factor 3 (ISGF3) complex. ISGF3 translocates to the nucleus and binds to the DNA specific sequence motif [5'-CAGTTTCACTTTCC-3'], ISREs, to drive the expression of ISGs, which are the ultimate antiviral effectors of the interferon cascade (Fig. 4A) (28). As expected, employing a Huh7 stably transfected ISRE-driven luciferase reporter cell line (29), we observed the induction of luciferase activity with IFN-α stimulation (Fig. 4A). Surprisingly, forced activation of PKC, using the PMA stimulus, also provokes transactivation of ISRE elements (Fig. 4B). Further confirmation was obtained by quantification of a panel of well-known antiviral ISGs (Fig. 4C). Importantly, when the ISRE reporter cell line was transduced with integrating lentiviral vectors expressing shRNA specifically targeting PKCα, β or a control shRNA (shCTR), PKCα silencing resulted in a significant decrease of ISRE luciferase activity compared with shCTR control; whereas PKCβ

knockdown did not significantly affect ISRE activity (Fig. 4D). These data demonstrate that PMA activates PKCα to mediate the transcriptional activity of ISRE, resulting in the induction of antiviral ISGs.

Signal transduction of the IFN-α/β receptor appears kaleidoscopic in that multiple discrete signaling cassettes are activated. An important effector is phosphatidylinositol-3OH-kinase (PI3) kinase, a major regulator of cellular signaling. Activation of PI3 kinase in turn leads to the activation of various effector pathways in different cell types, including 3-phosphoinositide dependent protein kinase (PDK), Protein kinase B (PKB), mechanistic target of rapamycin (mTOR) and PKC (Fig. S3B) (30). As PI3 kinase signaling and other signaling cassettes downstream of the interferon receptors may (in)directly crosstalk with PKCα, we investigated possible effects of IFN-α on PKC activation. As determined by western blot, PKC α/β are not activated upon IFNα challenge (1000 IU/ml; Fig. S3C). Thus, PKCα activation is not the downstream effect of the IFN receptor.

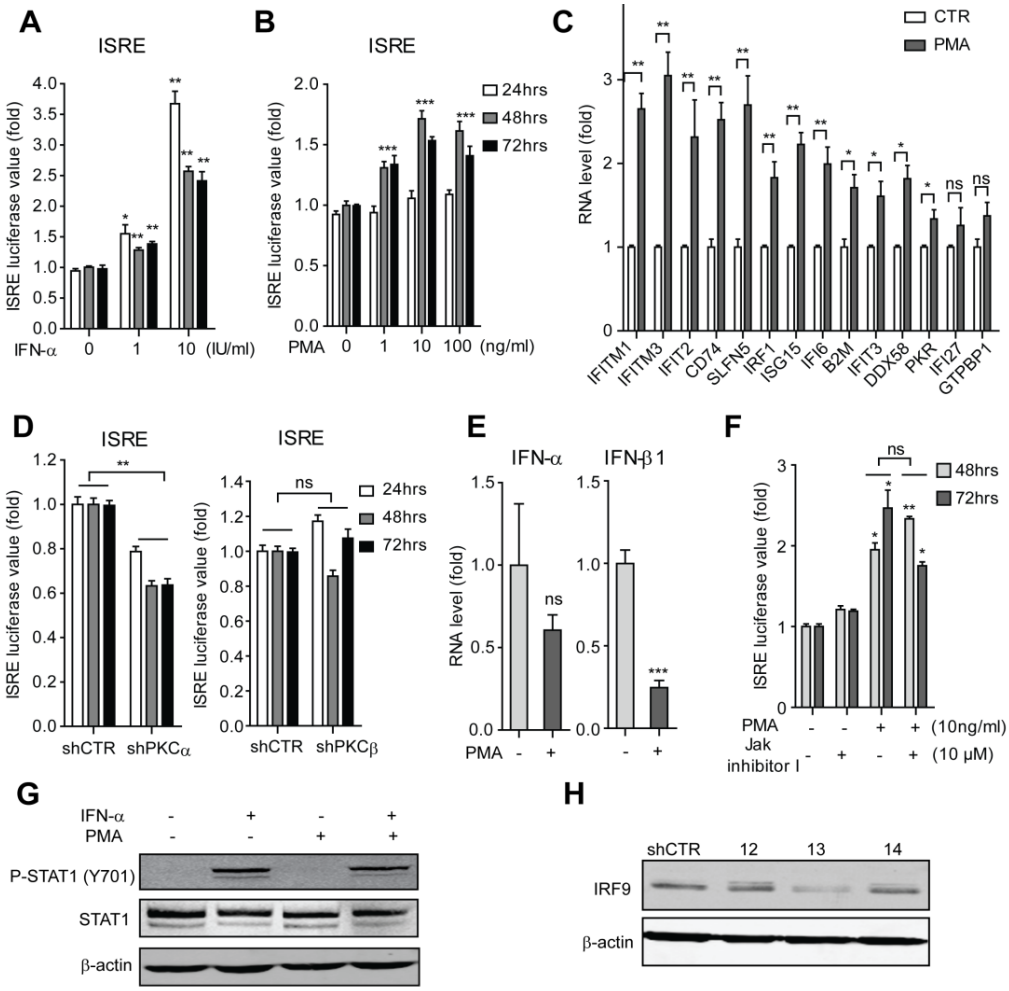

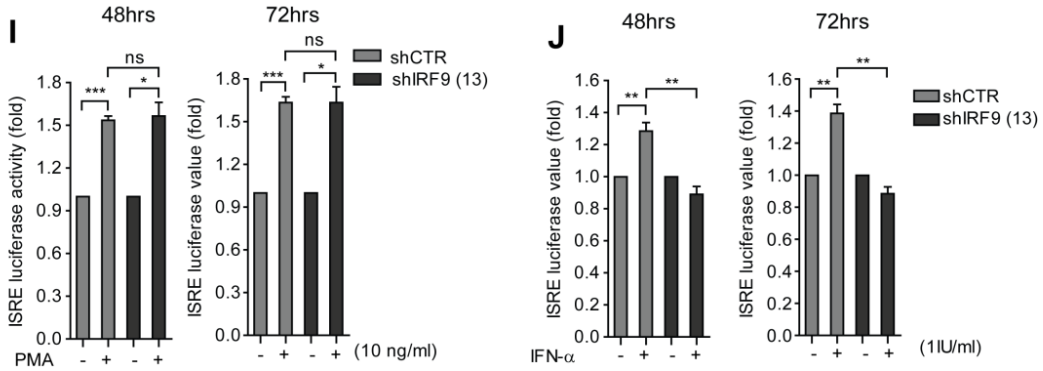

Fig 4. PKCα provokes transcriptional activation of ISGs, independent of IFN-JAK-STAT pathway. (A) In Huh7 based ISRE luciferase reporter cells, treatment with IFN-α resulted in a dose-dependent induction of ISRE-related luciferase activity (n = 3 independent experiments with 2 – 3 replicates each). (B) Same as (A) for PMA. (C) After PMA (100 ng/ml) treatment, expression profile of 14 different ISGs in Huh7 cells was quantified by qRT-PCR. Except for IFI27 and GTBP1, other ISGs were significantly induced (n = 6). (D) Knockdown PKCα by lentiviral shRNA vector (No. 48) in Huh7 based ISRE luciferase reporter cells resulted in significant inhibition of ISRE-related luciferase activity; while PKCβ knockdown (No. 53) had no significant effect (n = 3 independent experiments with 2 – 3 replicates each). (E) qRT-PCR analysis of IFN-α and β1 expression levels in Huh7 cells treated with PMA (100 ng/ml) (n = 3). (F) ISRE luciferase activity was measured, after treatment with JAK inhibitor I, PMA or a combination of both for 48 and 72 hrs (n = 3 independent experiments with 2 – 3 replicates each). (G) Phosphorylated STAT1 protein level was detected by western blot, after treatment with IFN-α (1000 IU/ml), PMA (100 ng/ml) or a combination of both. (H) Western blot analysis of IRF9 knockdown by lentiviral shRNA vectors in the Huh7 based ISRE luciferase reporter cells. Compared to the control vector transduced cells, the clone NO.13 of shIRF9 exerts strong silencing capability shown at protein levels. Blots depict IRF9 and β-actin. (I) Knockdown of IRF9 in Huh7 based ISRE luciferase reporter cells has no effect on PMA induced ISRE-related luciferase activation, as measured at 48 and 72 hrs (n = 3 independent experiments with 2 – 3 replicates each). (J) Knockdown of IRF9 in the Huh7 based ISRE luciferase reporter cells blocks IFN-α (1 IU/ml) induced ISRE-related luciferase activation, as measured at 48 and 72 hrs (n = 3 independent experiments with 2 – 3 replicates each). Date presented as mean ± SD (**, P < 0.05; **, P < 0.01; ***, P<0.001;* ns, not significant).

To further investigate whether PKCα activation results in direct ISRE activation or whether indirect autocrine/paracrine mechanisms are responsible, we investigated possible PMA effects on the expression of type I interferons. PMA treatment did not increase IFN-α mRNA but even slightly decreased IFN-β1 expression (Fig. 4E). In apparent agreement, incubation with the *pan*-JAK inhibitor I abrogated STAT1 phosphorylation and the induction of ISRE-regulated luciferase activity in Huh7 cells even following high dose IFN-α treatment (1000 IU/ml) (Fig. S3D and E), but did not diminish PMA-induced ISRE activation (Fig. 4F). Furthermore, PMA did not affect STAT1 phosphorylation or IFN-α induced STAT1 activation at amino acid 701 (Y701P), which is an indispensable signature of STAT1 activation (Fig. 4G). We further examined the role of IRF9, a key downstream element antiviral effector of the interferon pathway. As expected, PMA-induced ISRE luciferase activity was not affected in IRF9 knockdown cells compared to the shCTR control (Fig. 4H and I); whereas IFN-α induced activation was clearly impaired (Fig. 4J and S3F). These results collectively indicate that PKCα-induced ISRE activation is independent of the classical interferon pathway.

PKCα mediated ISG transcriptional activation and anti-HEV effect is independent of the NF-κB pathway

NF-κB signaling is a central pathway involved in cellular innate immune response. PMA can activate NF-κB signaling via the phosphorylation of NF-κB/p65 by PKCα (31-33). Thus, we investigated the potential involvement of NF-κB pathway. To this end, we used a lentiviral transcriptional reporter system expressing the firefly luciferase gene under the control of NF-κB responsive promoter. Huh7 cells were transduced with the vector to create a stable NF-κB reporter cell line. As expected, stimulation with PMA led to the strong activation of NF-κB luciferase activity (Fig. 5A) and thus a role of NF-κB signaling cannot be ruled out. Thus, the Huh7 cell line was transduced with integrating lentiviral shRNA vectors to silence RelA (P65), an essential subunit of the NF-κB transcription complex, resulting in profound down-regulation of RelA expression (Fig. 5B and C). These cells, however, still showed ISRE-driven luciferase activation (Fig. 5D). Consistently, PMA induced anti-HEV effect was not abrogated in RelA knockdown cells (Fig. 5E). Thus, NF-κB signaling appears not to be involved in PKCα mediated ISG transcriptional activation and anti-HEV effect.

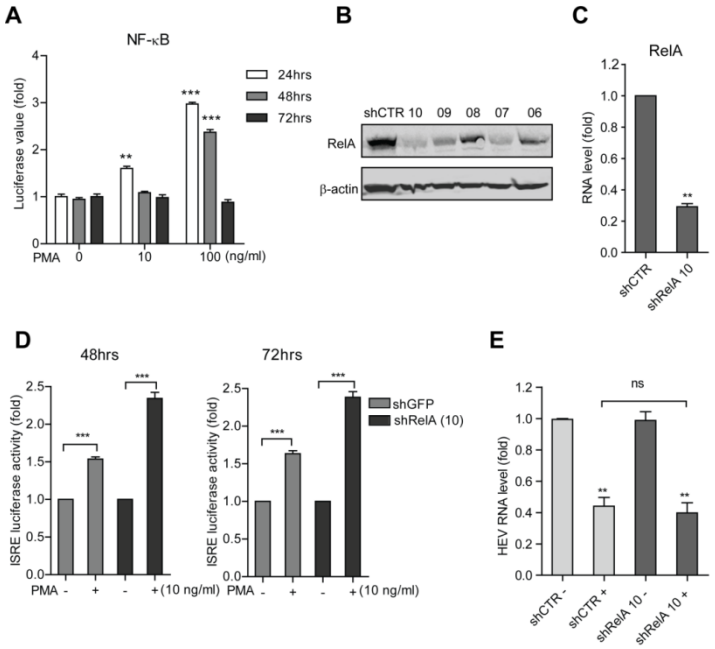

Fig 5. PKCα mediated anti-HEV activity is independent of NF-κB signaling. (A) In Huh7 based NF-κB luciferase reporter cells, treatment with PMA resulted in a dose-dependent induction of NF-κB related luciferase activity (n = 3 independent experiments with 2 – 3 replicates each). (B) Western blot analysis of RelA knockdown by lentiviral shRNA vectors in Huh7 cells. Blots depict RelA and β-actin. (C) qRT-PCR analysis of RelA knockdown by lentiviral shRNA vectors at RNA level (n = 3). (D) Knockdown of RelA in Huh7 based ISRE luciferase reporter cells did not block PMA induced ISRE-related luciferase activation measured at 48 and 72 hrs (n = 3 independent experiments with 2 – 3 replicates each). (E) Knockdown of RelA did not block PMA induced anti-HEV activity as determined by qRT-PCR 48 hrs post-inoculation with HEV particles (n = 4). Data presented as mean ± SEM (**, P < 0.05; **, P < 0.01; ***, P<0.001;* ns, not significant).

PKCα/AP1 represents a non-canonical mechanism of activating ISG transcription, but is dispensable for PKCα-mediated anti-HEV activity

AP-1 signaling is another important pathway involved in cellular innate immune response. PMA can also activate AP1 signaling via the activation of PKCα (34, 35). Indeed, PMA stimulation provokes a strong induction of c-Fos, an essential subunit of the AP1 transcription complex (Fig. 6A). Accordingly, unstimulated cells displayed hardly detectable c-Fos protein, but c-Fos was substantially induced and translocated to nucleus following PMA stimulation (Fig. 6B). Convincingly, we also used a lentiviral

transcriptional reporter system expressing the firefly luciferase gene under control of an AP-1 responsive promoter. Huh7 cells were transduced with the vector to create a stable AP-1 reporter cell line. As shown in Fig. 6C, stimulation with PMA led to the strong activation of AP-1 luciferase activity. Thus, to determine the role of AP-1 activation, Huh7 cells were transduced with integrating lentiviral RNAi vectors to silence *c*-Fos (Fig. 6D and E). Surprisingly, PMA induced ISRE activation was abrogated in c-Fos knockdown cells (Fig. 6F). Consistently, the induction of ISGs by PMA was also sensitive to c-Fos knockdown (Fig. 6G). Thus, AP-1 appears essential for PKCα-mediated ISRE activation.

Upon signaling activation, the transcription factor, AP-1, can bind to the sequence specific palindromic AP-1 site [5'-(A/T)T(G/T)(A/C)(G/C)TCA(G/C/A)-3'] to promote gene transcription (36, 37). The puzzling role of AP-1 in the transactivation of the ISRE led us to perform an *in silico* analysis comparing the ISRE motif and the AP-1 DNA binding site and surprisingly revealed a consensus sequence of these two motifs (Fig. 6H). We thus hypothesized that AP-1 might bind to this consensus sequence within the ISRE motif to drive its transcription. To test this hypothesis, we retrieved genome wide c-Fos ChIP-Seq data from GEO database (GSM754332) and analyzed the data set using Integrative Genomics Viewer (IGV) (Fig. S4A) (21, 38, 39). Confirming our hypothesis, we found c-Fos binding to the promoter regions of a list of ISGs (Fig. S5). To further confirm this notion, we mutated the consensus nucleotide sequence within the ISRE motif based on the lentiviral transcriptional reporter vector expressing the firefly luciferase gene driven by multiple ISREs, resulting in a mutant ISRE luciferase reporter vector that should not be capable of AP-1 binding. (Fig. S4B). Huh7 cells were transduced with this vector to create a stable reporter cell line. As expected, PMA failed to activate this mutated ISRE (Fig. 6J). Hence, AP-1 is capable of direct transactivation of the ISRE. Surprisingly, PMA mediated anti-HEV activity was not abrogated in c-Fos knockdown cells (Fig. 5K), even though the ISRE activation and ISG induction was blocked. Thus, AP-1 mediated ISG induction appears not essential for PKCα-mediated anti-HEV activity.

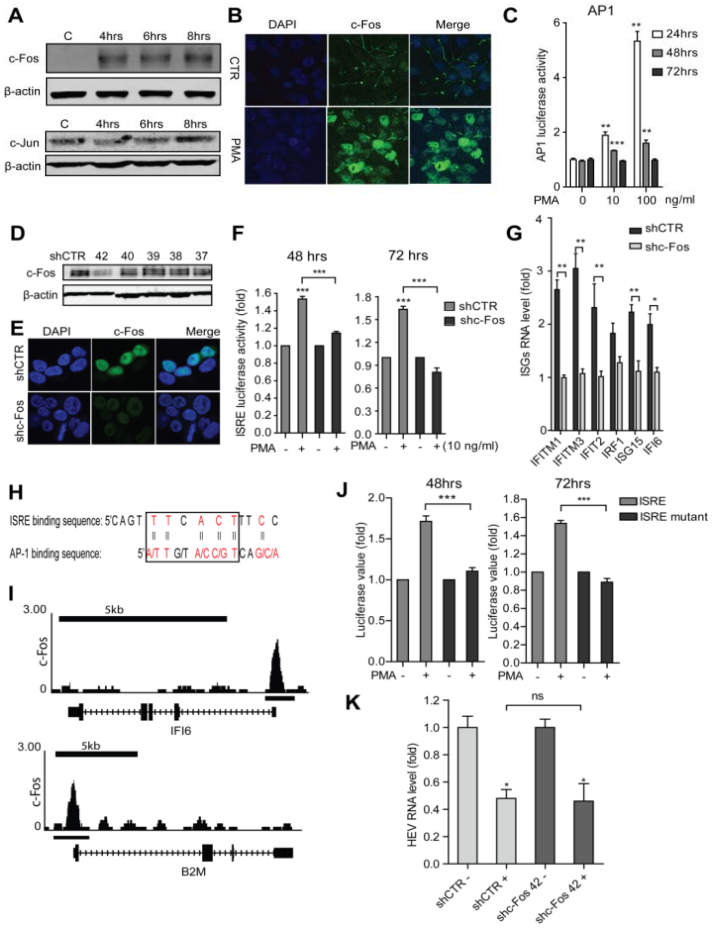

Fig 6. PKCα/AP1 serves as a non-canonical mechanism to mediate ISG transcription, but is not essential for PKCα-mediated anti-HEV activity. (A) Western blot analysis of c-Fos and c-Jun protein levels in Huh7 cells treated with PMA (100 ng/ml) for 4, 6 and 8 hrs. PMA stimulation provokes strong induction of c-Fos. (B) Confocal microscopy analysis of c-Fos localization in Huh7 cells treated with PMA for 4 hrs. c-Fos was induced and translocated to nucleus upon PMA stimulation. c-Fos antibody (green). Nuclei were visualized by DAPI (blue). (C) In Huh7 based AP-1 luciferase reporter cells, treatment with PMA resulted in dose-dependent induction of AP-1-related luciferase activity (n = 3 independent experiments with 2 – 3 replicates each). (D) Western blot analysis of c-Fos knockdown by lentiviral shRNA vectors. Compared to the control vector transduced cells, the NO.42 clone of shc-Fos exerts potent silencing capability shown at protein levels. Blots depict c-Fos and β-actin. (E) Confocal microscopy analysis confirmed profound down-regulation of c-Fos after knockdown by lentiviral shRNA vectors. C-Fos antibody (green). Nuclei were visualized by DAPI (blue). (F) Knockdown of c-Fos in Huh7 based ISRE luciferase reporter cells demolished PMA induced ISRE-related luciferase activation, as measured at 48 and 72 hrs (n = 3 independent experiments with 2 – 3 replicates each). (G) qRT-PCR analysis confirmed that the induction of ISGs by PMA was largely abrogated after c-Fos knockdown (n = 3). (H) ISRE and AP-1 sequence specific binding regions. Their consensus nucleotides are labeled in red color, and the consensus region is enclosed by the rectangular box. (I) Examples of two ISG genes with c-Fos binding to their promoter regions. The normalized binding signals were used as the input data. Binding peak detection was performed with PeakSeq v1.01 for identifying and ranking peak regions in ChIP-Seq data analysis. The Y axis value represents the binding signaling value; the black bar in the right corner represent the scale (5k bp). (J) Huh7 cells carrying the ISRE mutated luciferase reporter showed demolished activation upon PMA stimulation, as measured at 48 and 72 hrs (n = 3 independent experiments with 2 – 3 replicates each). (K) Knockdown of c-Fos in Huh7 cells did not abrogate PMA induced anti-HEV activity as determined by qRT-PCR 48 hrs post inoculation with HEV particles (n = 4). Data presented as mean ± SEM (**, P < 0.05; **, P < 0.01; ***, P<0.001;* ns, not significant).

Discussion

Protein kinases play pivotal roles in regulating immune responses either positively or negatively via regulating protein functions, signal transduction or other cellular processes.(40-42). This study comprehensively profiled kinase-mediated cascades in cell–autonomous antiviral immunity via screening a library of pharmacological kinase inhibitors on Huh7 based HEV replication cell model. We identified PKCα as an important antiviral host factor and a targetable host factor for antiviral drug development. Both functional over-expression and pharmacological activation showed strong and comparable anti-HEV activity compared to IFN-α.

PMA, as a phorbol ester, binds to the C1 domain in the regulatory region of PKCs to promote their activation (43). Although PMA was reported to have a potential tumor-promoting role in experimental skin cancer mouse models (44), its anti-cancer activity in fact has been extensively investigated in the clinic, including in patients with hematological malignancy, squamous cell carcinoma, renal cell carcinoma, ovarian teratocarcinoma, subcutaneous adenocarcinoma and prostate cancer (45). Cancer patients often suffer from depressed white blood cell and neutrophil counts because of chemotherapeutic drugs. PMA treatment has been shown to increase white blood cell and neutrophil counts towards a normal range with only mild and reversible side effects observed (46). A Phase I trial of treating hematologic cancer or bone marrow disorder with PMA has been successfully conducted at The State University of New Jersey (NCT00004058). The same institute is currently pursuing a Phase II trial plus dexamethasone & choline magnesium trisalicylate in the treatment of patients with relapsed/refractory acute myelogenous leukemia (NCT01009931). An interesting link is that patients with leukemia or other cancers are prone to virus infections, including HEV (47-49). The potential clinical prospects of PMA or its derivatives may be of achieving “one stone two birds” effects: simultaneously combating cancer and virus.

An interesting point of this study is the discovery of a new mechanism in transcription of antiviral ISGs, although moderately. Classically, ISG induction was known to be initiated predominantly by the IFN-JAK-STAT pathway in cell-autonomous defense against viral infection. Upon phosphorylation, STAT1 and STAT2 forming a complex with IRF9, this ISGF3 complex translocates to the nucleus and binds to the ISRE to drive ISG transcription. Here, we demonstrated that activation of the PKCα/AP-1 cascade was able to moderately drive ISG transcription as well. This action is independent of IFN production and the canonical JAK-STAT machinery. AP-1 is a transcription complex mainly composed of c-Jun and c-Fos proteins forming a heterodimers through their leucine-zipper domains. The AP-1 dimers recognize the sequence specific response elements via the basic domain and regulate target genes involved in cell proliferation, differentiation and apoptosis (50). Surprisingly, we observed consensus sequence between the ISRE and the AP-1 DNA binding site. Using ChIP-Seq data analysis and loss-of-function mutagenesis assays, we firmly demonstrated that AP-1 could directly drive gene transcription through binding to the ISRE on the ISG promoter region. Of note, the ISG induction effect induced by the PKCα/AP1 pathway is moderate, this may explain its non-essential role for PKCα-mediated anti-HEV activity.

In conclusion, we identified PKCα as an important cell-autonomous antiviral factor against HEV in host defense. In addition, we also revealed a non-canonical mechanism in transcriptional activation of ISGs, although this is dispensable for PKCα-mediated antiviral activity. These results provide valuable antiviral target and shed new insights of virus-host interactions.

Conflict of interest statement

The authors have declared that no conflict of interest exists.

Acknowledgements

The authors gratefully thank Dr. Patrick Chaltin and Arnaud Marchand for the availability of the cell kinase inhibitors; Dr. Suzanne U. Emerson (National Institute of Allergy and Infectious Diseases, NIH, USA) for generously providing the plasmids to generate subgenomic and full-length HEV genomic RNA; Dr. Herbert W. Virgin (Washington University School of Medicine, USA) for providing the mouse norovirus strain; Dr. Hong-Yiou Lin (University of Minnesota) providing the over-expression PKC□ lentiviral vector. Dr. Miranda de Graaf (Department of Viroscience, Erasmus Medical Center, Netherlands) for the help with influenza replication curves. The authors also would like to acknowledge the ENCODE Consortium and the ENCODE production laboratory(s) generating the c-Fos ChIP-Seq dataset (GSM754332). This research is supported by the Netherlands Organization for Scientific Research (NWO/ZonMw) for a VENI grant (No. 916-13-032 to Q. P.), the Dutch Digestive Foundation (MLDS) for a career development grant (No. CDG 1304 to Q. P.), the Daniel den Hoed Foundation for a Centennial Award fellowship (to Q. P.), European Association for the Study of the Liver (EASL) for a Sheila Sherlock Fellowship (to Q. P.) and the China Scholarship Council for funding PhD fellowships (201303250056 to W. W.), (201207720007 to Y. W.), (201206150075 to X. Z.), (201307720045 to Y. Y.) and (201306300027 to L. X.). Y. Debing is a fellow of the Research Foundation – Flanders (FWO).

Supplementary data

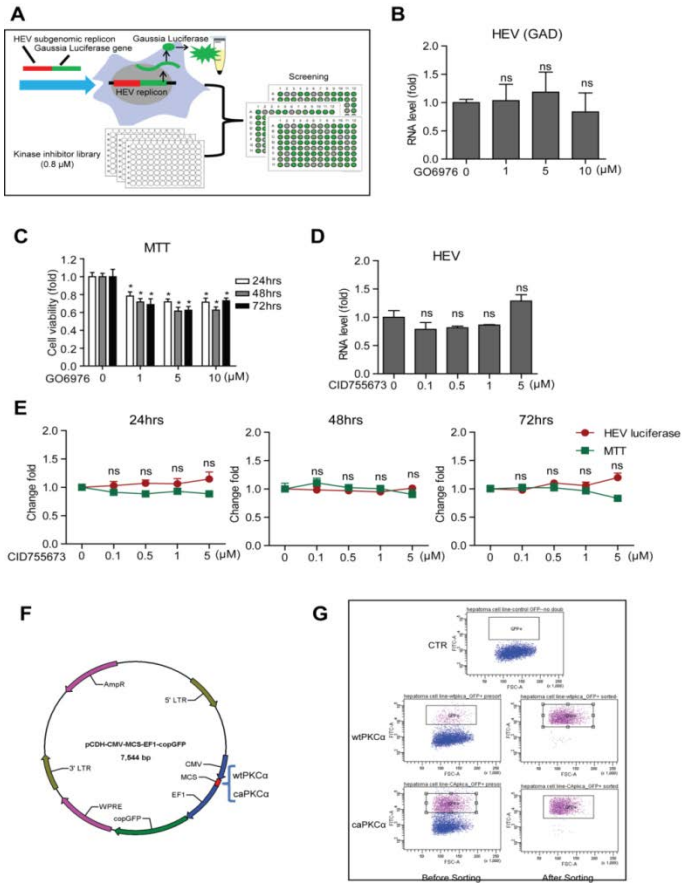

Fig. S1. Conventional PKCs function as cell-autonomous antiviral elements against HEV. (A) Diagram of screening a library of pharmacological kinase inhibitors in HEV subgenomic replicon. (B) Huh7 cells transfected with HEV replication-defective control (GAD) RNA were treated for 48 hours with Go6976. qRT-PCR analysis showed that Go6976 exerted no significant effect on HEV replication-defective control (GAD) RNA level. (C) MTT assay of Go6976 on Huh7 cell line. (D) qRT-PCR analysis of HEV RNA in Huh7 cells harboring full-length HEV infectious genome. Treatment with PKD inhibitor, CID755673 exerted no significant effect on cellular HEV RNA level (n = 3). (E) In the Huh7 cell-based subgenomic HEV replicon model, treatment with PKD inhibitor, CID755673 exerted no effect on HEV replication-related luciferase activity. MTT results of CID755673 on Huh7 cells were also included. (F) Illustration of plasmid map of wtPKCα and caPKCα. (G) Cell cytometry sorting result of wtPKCα and caPKCα positive cells based on the GFP tag. Date presented as mean ± SD (**, P < 0.05; **, P < 0.01; ***, P<0.001;* ns, not significant).

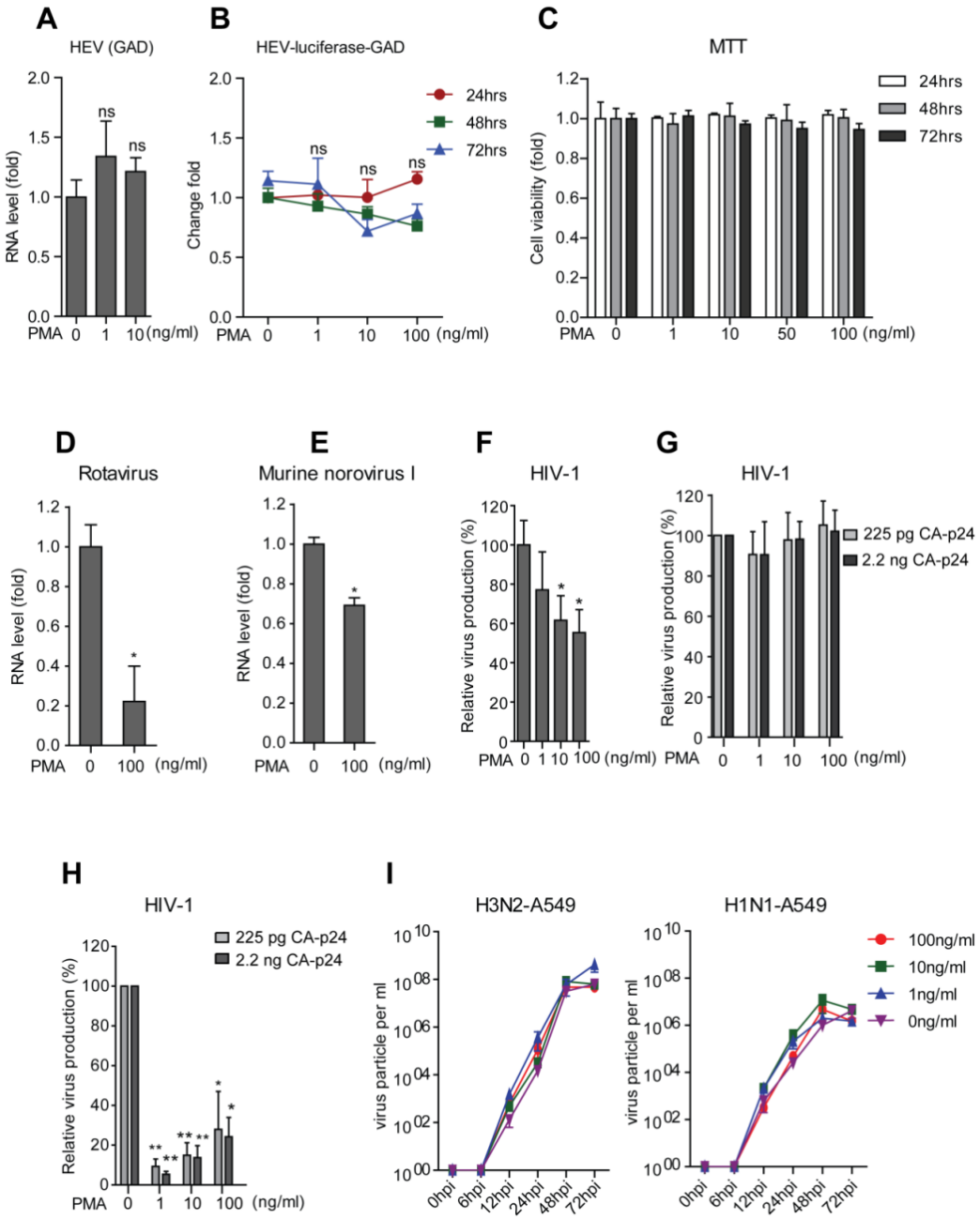

Fig. S2. The PKC specific activator PMA (TPA) exerts relative broad antiviral activity. (A) Huh7 cells transfected with HEV replication-defective control (GAD) RNA were treated for 48 hours with PMA. qRT-PCR analysis showed that PMA exerted no significant effect on HEV replication-defective control (GAD) RNA level. (B) Huh7 cells transfected with replicon defective control (HEV-luciferase-GAD) RNA were treatment with PMA. It exerted no effect on HEV (GAD) replication-related luciferase activity. (C) MTT assay of PMA on Huh7 cell line. PMA exerts no clear cell toxicity. (D) Rotavirus RNA derived from Caco2 cells was detected by qRT-PCR. Treatment with PMA (100 ng/ml) for 48 hrs significantly inhibited rotavirus RNA level by 78% (n = 3). (E) Treatment with PMA (100 ng/ml) for 48 hrs inhibited murine norovirus 1 RNA level by 31% in RAW264.7 cells as determined by qRT-PCR (n = 6). (F) HIV-1 virus production was measured in DNA-transfected 293T cells. HEK293T cells were co-transfected with 250 ng HIV-1 molecular clone pLAI and 1 ng of pTK-Renilla. CA-p24 levels in the culture supernatant and renilla luciferase expression in cells were measured at 2 days post-transfection. Normalized CA-p24 expression without PMA (only DMSO) was set at 100% (n = 4). (G) Single cycle HIV-1 entry assay. The TZM-bl cells were first infected with HIV-1 LAI (225 pg or 2.2 ng CA-p24) for 2 hrs, subsequently washed with PBS and then fresh PMA-containing medium was added. Infected cells without PMA (only DMSO) were included as control. (n = 2 independent experiments with 4 replicates each). (H) Single cycle HIV-1 entry assay. The TZM-bl cells were first pretreated with PMA for 2 hrs and subsequently infected with LAI (225 pg or 2.2 ng CA-p24) for an additional 2 hrs. Subsequently fresh PMA-containing medium was added.

Infected cells without PMA (only DMSO) were included as control (n = 2 independent experiments with 4 replicates each). (I) PMA exerts no antiviral effect on influenza virus (A/H3N2 and A/H1N1). A549 cells infected with A/H3N2 and A/H1N1 at a multiplex of infectivity of 0.01. Samples were harvested 0, 6, 12, 24, 48 and 72 hours post infection. Geometric mean titers were calculated from two independent experiments, error bars indicate standard deviations. Date presented as mean ± SD (**, P < 0.05; **, P < 0.01; ***, P<0.001;* ns, not significant).

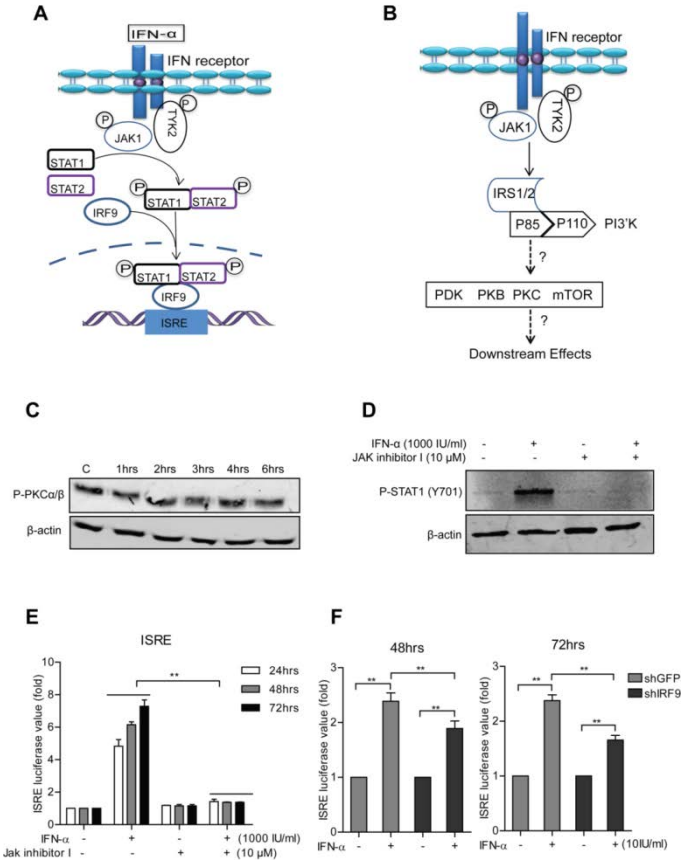

Fig. S3. PKCα induced ISRE activation is independent of interferon signaling. (A) Illustration of key regulatory molecules in the IFN-α induced JAK-STAT signaling pathway. P, phosphorylation. (B) Illustration of key regulatory molecules in PI3'K signaling pathway induced by IFN receptors. (C) IFN-α (1000 IU/ml) stimulation exerts no effect on phosphorylated PKCα/β proteins as measured at different time points by western blot. (D) Western blot analysis of Huh7 cells treated with IFN-α (1000 IU/ml), JAK inhibitor I (10 μM) or combination. Incubation with the *pan*-JAK inhibitor I abrogated STAT1 phosphorylation in Huh7 cells following IFN-α treatment. Blots depict phosphorylated STAT1 and β-actin. (E) In Huh7 based ISRE luciferase cells, JAK inhibitor I (10 μM) abrogated IFN-α (1000 IU/ml) induced ISRE-related luciferase activity as measured at 24, 48 and 72 hrs (n = 3 independent experiments with 2 – 3 replicates each). (F) IFN-α induced ISRE luciferase activity was partly abolished in IRF9 knockdown cells, compared to the shCTR control as measured at 48 and 72 hrs (n = 3 independent experiments with 2 – 3 replicates each). All data presented as mean ± SD (**, P < 0.05; **, P < 0.01; ***, P<0.001;* ns, not significant).

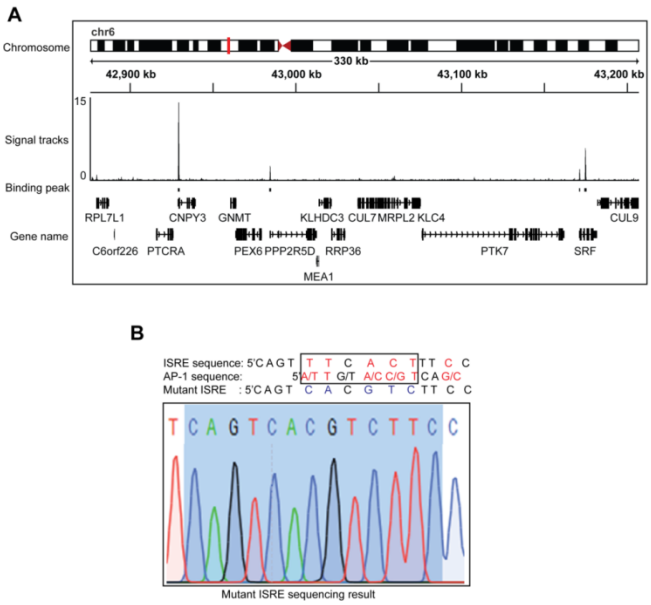

Fig. S4. PKCα / AP1 serves as a non-canonical mechanism of activating ISG transcription. (A) Integrative Genomics Viewer (IGV) analysis of genome wide c-Fos ChIP-Seq data from GEO database (GSM754332). Example shown depicts locus on chromosome harboring the genes. Signal tracks record the c-Fos binding ability to relevant genes listed below. The positive binding was marked with binding peak based on the calculation of signal tracks. (B) The nucleotide sequence of AP-1, ISRE and the ISRE mutant binding regions. Their consensus nucleotides are labeled in red color, and the consensus region is marked in a rectangular box. The mutated nucleotides are shown in blue color. The ISRE (mutant) sequencing result is shown in the illustration below.

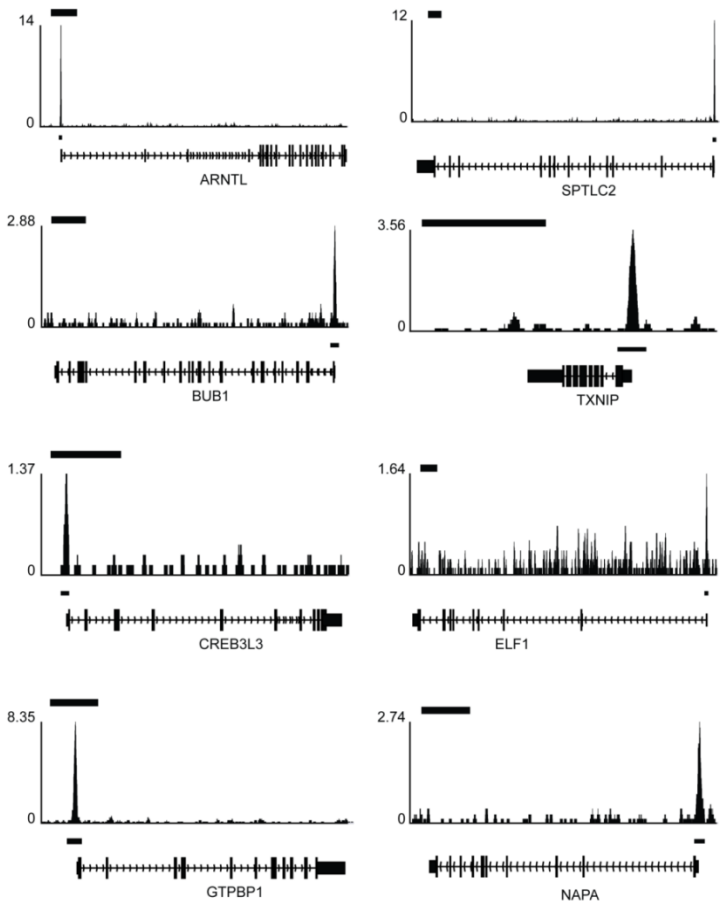

Fig. S5. Examples of ISG genes with c-Fos binding to their promoter regions. The normalized binding signals were used as the input data. Binding peak detection was performed with PeakSeq v1.01 for identifying and ranking peak regions in ChIP-Seq data analysis. The Y axis value represents the binding signaling value; the black bar in the right corner represent the scale (5kb).

Supplementary Tables

Table S1 and S2

http://www.sciencedirect.com/science/article/pii/S0166354216306283?via%3Dihub#appsec1

Table S3. shRNA sequences

Name	Oligo Sequences
shPKCα-51	CCGGCTTTGGAGTTTCGGAGCTGATCTCGAGATCAGCTCCGAAACTCCAAAGTTTTT
shPKCα-52	CCGGCGAGCTATTTCAGTCTATCATCTCGAGATGATAGACTGAAATAGCTCGTTTTT
shPKCα-53	CCGGCATGGAACTCAGGCAGAAATTCTCGAGAATTTCTGCCTGAGTTCCATGTTTTT
shPKCβ-47	CCGGCGTCCTTCATTTCTGTCATTCCTCGAGGAATGACAGAAATGAAGGACGTTTTTTG
shPKCβ-48	CCGGGCCATGAATTTGTCACATTCTCTCGAGAGAATGTGACAAATTCATGGCTTTTTTG
shPKCβ-49	CCGGGAAACAAAGATGGTTGTATTCCTCGAGGAATACAACCATCTTTGTTTCTTTTTTG
shPKCβ-50	CCGGGACGACCTGCTTTGATTTAACCTCGAGGTTAAATCAAAGCAGGTCGTCTTTTTTG
shIRF9-12	CCGGGAGACTTGGTCAGGTACTTTCCTCGAGGAAAGTACCTGACCAAGTCTCTTTTTG
shIRF9-13	CCGGCTCAGTAGTTGTCCGTGATAACTCGAGTTATCACGGACAACTACTGAGTTTTTG
shIRF9-14	CCGGTTCAAGGCCTGGGCAATATTTCTCGAGAAATATTGCCCAGGCCTTGAATTTTTG
shRelA-06	CCGGGCCTTAATAGTAGGGTAAGTTCTCGAGAACTTACCCTACTATTAAGGCTTTTT
shRelA-07	CCGGCGGATTGAGGAGAAACGTAAACTCGAGTTTACGTTTCTCCTCAATCCGTTTTT
shRelA-08	CCGGGCAGGCTATCAGTCAGCGCATCTCGAGATGCGCTGACTGATAGCCTGCTTTTT
shRelA-09	CCGGCACCATCAACTATGATGAGTTCTCGAGAACTCATCATAGTTGATGGTGTTTTT
shRelA-10	CCGGCCTGAGGCTATAACTCGCCTACTCGAGTAGGCGAGTTATAGCCTCAGGTTTTT
shc-Fos-37	CCGGGCTGGTAGTTAGTAGCATGTTCTCGAGAACATGCTACTAACTACCAGCTTTTT
shc-Fos-38	CCGGGCGGAGACAGACCAACTAGAACTCGAGTTCTAGTTGGTCTGTCTCCGCTTTTT
shc-Fos-39	CCGGCACTGCTTACACGTCTTCCTTCTCGAGAAGGAAGACGTGTAAGCAGTGTTTTT
shc-Fos-40	CCGGGTGGAACAGTTATCTCCAGAACTCGAGTTCTGGAGATAACTGTTCCACTTTTT
shc-Fos-42	CCGGGCGGAGACAGACCAACTAGAACTCGAGTTCTAGTTGGTCTGTCTCCGCTTTTTG

Table S4. Primer sequences

Name	Oligo Sequences (Forward)	Oligo Sequences (Reverse)
HEV	5’-ATTGGCCAGAAGTTGGTTTTCAC-3’	5’-CCGTGGCTATAATTGTGGTCT-3’
HEV-ORF1	5’-CAAAAAGCCCCGCAACAAGA-3’	5’-GAGGGTAAGGGGCACAGATG-3’
PKCα	5'-GCCTATGGCGTCCTGTTGTATG-3'	5'-GAAACAGCCTCCTTGGACAAGG-3'
PKCβ	5'-GAGGGACACATCAAGATTGCCG-3'	5'-CACCAATCCACGGACTTCCCAT-3'
Rotavirus	5'-TGGTTAAACGCAGGATCGGA-3'	5'-AACCTTTCCGCGTCTGGTAG-3'
IFITM1	5'-GGCTTCATAGCATTCGCCTACTC-3'	5'-AGATGTTCAGGCACTTGGCGGT-3'
IFITM3	5'-CTGGGCTTCATAGCATTCGCCT-3'	5'-AGATGTTCAGGCACTTGGCGGT-3'
IFIT2	5'-GGAGCAGATTCTGAGGCTTTGC-3'	5'-GGATGAGGCTTCCAGACTCCAA-3'
IRF1	5'-GAGGAGGTGAAAGACCAGAGCA-3'	5'-TAGCATCTCGGCTGGACTTCGA-3'
ISG15	5'-CTCTGAGCATCCTGGTGAGGAA-3'	5'-AAGGTCAGCCAGAACAGGTCGT-3'
IFI6	5'-TGATGAGCTGGTCTGCGATCCT-3'	5'-GTAGCCCATCAGGGCACCAATA-3'
IFIT3	5'-CCTGGAATGCTTACGGCAAGCT-3'	5'-GAGCATCTGAGAGTCTGCCCAA-3'
DDX58	5'-CACCTCAGTTGCTGATGAAGGC-3'	5'-GTCAGAAGGAAGCACTTGCTACC-3'
PKR	5'-GAAGTGGACCTCTACGCTTTGG-3'	5'-TGATGCCATCCCGTAGGTCTGT-3'
IFI27	5'-CGTCCTCCATAGCAGCCAAGAT-3'	5'-ACCCAATGGAGCCCAGGATGAA-3'
IFNα	5'-GACTCCATCTTGGCTGTGA-3'	5'-TGATTTCTGCTCTGACAACCT-3'
IFNβ1	5'-CTTGGATTCCTACAAAGAAGCAGC-3'	5'-TCCTCCTTCTGGAACTGCTGCA-3'
SLFN5	TTCTGCTGTGCGGTGTTTGCCA	CTGGAGAACCATCTCAGGACAC
CD74	AAGCCTGTGAGCAAGATGCGCA	AGCAGGTGCATCACATGGTCCT
B2M	CCACTGAAAAAGATGAGTATGCCT	CCAATCCAAATGCGGCATCTTCA
GTPBP1	CCTTCATCGACTTGGCTGGTCA	CCAGGTGTTCTTTGGTCATCCC
GAPDH	5’-TGTCCCCACCCCCAATGTATC-3’	5’-CTCCGATGCCTGCTTCACTACCTT-3’
RP2	5’- AAGCTGAGGATGCTCAAAGG-3’	5’-CCCATTAAACTCCAAGGCAA-3’

References

1. Hakim MS, Wang W, Bramer WM, Geng J, Huang F, de Man RA, Peppelenbosch MP, et al. The Global Burden of Hepatitis E Outbreaks: A Systematic Review. Liver Int 2016.
2. Lupberger J, Zeisel MB, Xiao F, Thumann C, Fofana I, Zona L, Davis C, et al. EGFR and EphA2 are host factors for hepatitis C virus entry and possible targets for antiviral therapy. Nat Med 2011;17:589-595.
3. Llovet JM, Ricci S, Mazzaferro V, Hilgard P, Gane E, Blanc JF, de Oliveira AC, et al. Sorafenib in advanced hepatocellular carcinoma. N Engl J Med 2008;359:378-390.
4. Zhang BB, Zhou G, Li C. AMPK: an emerging drug target for diabetes and the metabolic syndrome. Cell Metab 2009;9:407-416.
5. Rask-Andersen M, Zhang J, Fabbro D, Schioth HB. Advances in kinase targeting: current clinical use and clinical trials. Trends Pharmacol Sci 2014;35:604-620.
6. Wang W, Hakim MS, Nair VP, de Ruiter PE, Huang F, Sprengers D, Van Der Laan LJ, et al. Distinct Antiviral Potency of Sofosbuvir Against Hepatitis C and E Viruses. Gastroenterology 2016;151:1251-1253.
7. Shukla P, Nguyen HT, Faulk K, Mather K, Torian U, Engle RE, Emerson SU. Adaptation of a genotype 3 hepatitis E virus to efficient growth in cell culture depends on an inserted human gene segment acquired by recombination. J Virol 2012;86:5697-5707.
8. Shukla P, Nguyen HT, Torian U, Engle RE, Faulk K, Dalton HR, Bendall RP, et al. Cross-species infections of cultured cells by hepatitis E virus and discovery of an infectious virus-host recombinant. Proc Natl Acad Sci U S A 2011;108:2438-2443.
9. Wang YJ, Zhou XY, Debing Y, Chen K, Van der Laan LJW, Neyts J, Janssen HLA, et al. Calcineurin Inhibitors Stimulate and Mycophenolic Acid Inhibits Replication of Hepatitis E Virus. Gastroenterology 2014;146:1775-1783.
10. Zhou XY, Wang YJ, Metselaar HJ, Janssen HLA, Peppelenbosch MP, Pan QW. Rapamycin and everolimus facilitate hepatitis E virus replication: Revealing a basal defense mechanism of PI3K-PKB-mTOR pathway. Journal of Hepatology 2014;61:746-754.
11. Wobus CE, Karst SM, Thackray LB, Chang KO, Sosnovtsev SV, Belliot G, Krug A, et al. Replication of Norovirus in cell culture reveals a tropism for dendritic cells and macrophages. PLoS Biol 2004;2:e432.
12. van Bel N, Das AT, Cornelissen M, Abbink TE, Berkhout B. A short sequence motif in the 5' leader of the HIV-1 genome modulates extended RNA dimer formation and virus replication. J Biol Chem 2014;289:35061-35074.
13. Schrauwen EJ, Bestebroer TM, Rimmelzwaan GF, Osterhaus AD, Fouchier RA, Herfst S. Reassortment between Avian H5N1 and human influenza viruses is mainly restricted to the matrix and neuraminidase gene segments. PLoS One 2013;8:e59889.
14. Debing Y, Emerson SU, Wang Y, Pan Q, Balzarini J, Dallmeier K, Neyts J. Ribavirin inhibits in vitro hepatitis E virus replication through depletion of cellular GTP pools and is moderately synergistic with alpha interferon. Antimicrob Agents Chemother 2014;58:267-273.
15. de Wilde AH, Jochmans D, Posthuma CC, Zevenhoven-Dobbe JC, van Nieuwkoop S, Bestebroer TM, van den Hoogen BG, et al. Screening of an FDA-approved compound library identifies four small-molecule inhibitors of Middle East respiratory syndrome coronavirus replication in cell culture. Antimicrob Agents Chemother 2014;58:4875-4884.
16. Pan QW, Henry SD, Metselaar HJ, Scholte B, Kwekkeboom J, Tilanus HW, Janssen HLA, et al. Combined antiviral activity of interferon-alpha and RNA interference directed against hepatitis C without affecting vector delivery and gene silencing. Journal of Molecular Medicine-Jmm 2009;87:713-722.
17. Xu L, Zhou X, Wang W, Wang Y, Yin Y, Laan LJ, Sprengers D, et al. IFN regulatory factor 1 restricts hepatitis E virus replication by activating STAT1 to induce antiviral IFN-stimulated genes. FASEB J 2016;30:3352-3367.
18. Schmieder R, Edwards R. Fast identification and removal of sequence contamination from genomic and metagenomic datasets. PLoS One 2011;6:e17288.
19. Wang W, Xu L, Brandsma JH, Wang Y, Hakim MS, Zhou X, Yin Y, et al. Convergent Transcription of Interferon-stimulated Genes by TNF-alpha and IFN-alpha Augments Antiviral Activity against HCV and HEV. Sci Rep 2016;6:25482.
20. Langmead CJ, Jha SK. Symbolic approaches for finding control strategies in Boolean Networks. J Bioinform Comput Biol 2009;7:323-338.
21. Robinson JT, Thorvaldsdottir H, Winckler W, Guttman M, Lander ES, Getz G, Mesirov JP. Integrative genomics viewer. Nat Biotechnol 2011;29:24-26.
22. Martiny-Baron G, Kazanietz MG, Mischak H, Blumberg PM, Kochs G, Hug H, Marme D, et al. Selective inhibition of protein kinase C isozymes by the indolocarbazole Go 6976. J Biol Chem 1993;268:9194-9197.
23. Martiny-Baron G, Fabbro D. Classical PKC isoforms in cancer. Pharmacol Res 2007;55:477-486.
24. House C, Kemp BE. Protein-Kinase-C Contains a Pseudosubstrate Prototype in Its Regulatory Domain. Science 1987;238:1726-1728.
25. Pears CJ, Kour G, House C, Kemp BE, Parker PJ. Mutagenesis of the Pseudosubstrate Site of Protein-Kinase-C Leads to Activation. European Journal of Biochemistry 1990;194:89-94.
26. Todt D, Francois C, Anggakusuma, Behrendt P, Engelmann M, Knegendorf L, Vieyres G, et al. Antiviral Activities of Different Interferon Types and Subtypes against Hepatitis E Virus Replication. Antimicrob Agents Chemother 2016;60:2132-2139.
27. Zhou X, Xu L, Wang W, Watashi K, Wang Y, Sprengers D, de Ruiter PE, et al. Disparity of basal and therapeutically activated interferon signalling in constraining hepatitis E virus infection. J Viral Hepat 2016;23:294-304.

28. Ohmori Y, Hamilton TA. Cooperative interaction between interferon (IFN) stimulus response element and kappa B sequence motifs controls IFN gamma- and lipopolysaccharide-stimulated transcription from the murine IP-10 promoter. J Biol Chem 1993;268:6677-6688.
29. Pan QW, Tilanus HW, Janssen HL, van der Laan LJ. Impdh Inhibitors Mycophenolic Acid and Ribavirin Promote the Expression of Interferon-Stimulated Genes by Potentiating the Activity of Interferon Response Element. Hepatology 2011;54:1103a-1103a.
30. Kaur S, Uddin S, Platanias LC. The PI3' kinase pathway in interferon signaling. J Interferon Cytokine Res 2005;25:780-787.
31. Chang MS, Chen BC, Yu MT, Sheu JR, Chen TF, Lin CH. Phorbol 12-myristate 13-acetate upregulates cyclooxygenase-2 expression in human pulmonary epithelial cells via Ras, Raf-1, ERK, and NF-kappa B, but not p38 MAPK, pathways. Cellular Signalling 2005;17:299-310.
32. Mut M, Amos S, Hussaini IM. PKC alpha phosphorylates cytosolic NF-kappaB/p65 and PKC delta delays nuclear translocation of NF-kappaB/p65 in U1242 glioblastoma cells. Turk Neurosurg 2010;20:277-285.
33. Jiang R, Teng Y, Huang Y, Gu J, Li M. Protein kinase C-alpha activation induces NF-kB-dependent VCAM-1 expression in cultured human umbilical vein endothelial cells treated with sera from preeclamptic patients. Gynecol Obstet Invest 2010;69:101-108.
34. Hwang YP, Yun HJ, Kim HG, Han EH, Lee GW, Jeong HG. Suppression of PMA-induced tumor cell invasion by dihydroartemisinin via inhibition of PKCalpha/Raf/MAPKs and NF-kappaB/AP-1-dependent mechanisms. Biochem Pharmacol 2010;79:1714-1726.
35. Langlet C, Springael C, Johnson J, Thomas S, Flamand V, Leitges M, Goldman M, et al. PKC-alpha controls MYD88-dependent TLR/IL-1R signaling and cytokine production in mouse and human dendritic cells. Eur J Immunol 2010;40:505-515.
36. Colin L, Vandenhoudt N, de Walque S, Van Driessche B, Bergamaschi A, Martinelli V, Cherrier T, et al. The AP-1 binding sites located in the pol gene intragenic regulatory region of HIV-1 are important for viral replication. PLoS One 2011;6:e19084.
37. Hess J, Angel P, Schorpp-Kistner M. AP-1 subunits: quarrel and harmony among siblings. J Cell Sci 2004;117:5965-5973.
38. Thorvaldsdottir H, Robinson JT, Mesirov JP. Integrative Genomics Viewer (IGV): high-performance genomics data visualization and exploration. Brief Bioinform 2013;14:178-192.
39. Consortium EP. An integrated encyclopedia of DNA elements in the human genome. Nature 2012;489:57-74.
40. Georgel P, Schuster C, Zeisel MB, Stoll-Keller F, Berg T, Bahram S, Baumert TF. Virus-host interactions in hepatitis C virus infection: implications for molecular pathogenesis and antiviral strategies. Trends Mol Med 2010;16:277-286.
41. Lupberger J, Duong FH, Fofana I, Zona L, Xiao F, Thumann C, Durand SC, et al. Epidermal growth factor receptor signaling impairs the antiviral activity of interferon-alpha. Hepatology 2013;58:1225-1235.
42. Li Q, Zhang YY, Chiu S, Hu Z, Lan KH, Cha H, Sodroski C, et al. Integrative functional genomics of hepatitis C virus infection identifies host dependencies in complete viral replication cycle. PLoS Pathog 2014;10:e1004163.
43. Ono Y, Fujii T, Igarashi K, Kuno T, Tanaka C, Kikkawa U, Nishizuka Y. Phorbol ester binding to protein kinase C requires a cysteine-rich zinc-finger-like sequence. Proc Natl Acad Sci U S A 1989;86:4868-4871.
44. Furstenberger G, Berry DL, Sorg B, Marks F. Skin tumor promotion by phorbol esters is a two-stage process. Proc Natl Acad Sci U S A 1981;78:7722-7726.
45. Schaar D, Goodell L, Aisner J, Cui XX, Han ZT, Chang R, Martin J, et al. A phase I clinical trial of 12- O-tetradecanoylphorbol-13-acetate for patients with relapsed/refractory malignancies. Cancer Chemother Pharmacol 2006;57:789-795.
46. Han ZT, Tong YK, He LM, Zhang Y, Sun JZ, Wang TY, Zhang H, et al. 12-O-Tetradecanoylphorbol-13-acetate (TPA)-induced increase in depressed white blood cell counts in patients treated with cytotoxic cancer chemotherapeutic drugs. Proc Natl Acad Sci U S A 1998;95:5362-5365.
47. Pfefferle S, Frickmann H, Gabriel M, Schmitz N, Gunther S, Schmidt-Chanasit J. Fatal course of an autochthonous hepatitis E virus infection in a patient with leukemia in Germany. Infection 2012;40:451-454.
48. Motte A, Roquelaure B, Galambrun C, Bernard F, Zandotti C, Colson P. Hepatitis E in three immunocompromized children in southeastern France. J Clin Virol 2012;53:162-166.
49. Geng Y, Zhang H, Huang W, T JH, Geng K, Li Z, Wang Y. Persistent hepatitis e virus genotype 4 infection in a child with acute lymphoblastic leukemia. Hepat Mon 2014;14:e15618.
50. Zenz R, Eferl R, Scheinecker C, Redlich K, Smolen J, Schonthaler HB, Kenner L, et al. Activator protein 1 (Fos/Jun) functions in inflammatory bone and skin disease. Arthritis Res Ther 2008;10:201.

Chapter 13

Crosstalk between Nucleotide Synthesis Pathways with Cellular Immunity in Constraining Hepatitis E Virus Replication

Yijin Wang[1], **Wenshi Wang[1]**, Lei Xu[1], Xinying Zhou[1], Ehsan Shokrollahi[2], Krzysztof Felczak[3], Luc J. W. van der Laan[4], Krzysztof W. Pankiewicz[3], Dave Sprengers[1], Nicolaas J. H. Raat[2], Herold J. Metselaar[1], Maikel P. Peppelenbosch[1], Qiuwei Pan[1]

[1]Department of Gastroenterology and Hepatology, Erasmus MC-University Medical Center, Rotterdam, The Netherlands.

[2]Department of Anesthesiology, Laboratory of Experimental Anesthesiology, Erasmus MC-University Medical Center, Rotterdam, The Netherlands.

[3]Center for Drug Design, University of Minnesota, Minneapolis, USA.

[4]Department of Surgery, Erasmus MC-University Medical Center, Rotterdam, The Netherlands.

Antimicrobial Agents and Chemotherapy, 2016; 60(5):2834-48.

Abstract

Viruses are solely dependent on host cells to propagate, therefore understanding virus-host interaction is important for antiviral drug development. Since *de novo* nucleotide biosynthesis is essentially required for both host cell metabolism and viral replication, specific catalytic enzymes of these pathways have been explored as potential antiviral targets. In this study, we investigated the role of different enzymatic cascades of nucleotides biosynthesis in hepatitis E virus (HEV) replication. By profiling various pharmacological inhibitors of nucleotides biosynthesis, we found that targeting the early steps of the purine biosynthesis pathway led to enhancement of HEV replication; whereas targeting the later step resulted in potent antiviral activity via depletion of purine nucleotide. Furthermore, inhibition of pyrimidine pathway resulted in potent anti-HEV activity. Interestingly, all these inhibitors with anti-HEV activity concurrently triggered the induction of antiviral interferon-stimulated genes (ISGs). Although ISGs are commonly induced by interferons via the JAK-STAT pathway, their induction by nucleotides synthesis inhibitors is completely independent of this classical mechanism. In conclusion, this study revealed an unconventional novel mechanism as to a crosstalk between nucleotide biosynthesis pathways and cellular antiviral immunity in constraining HEV infection. Targeting particular enzymes in nucleotide biosynthesis represents a viable option for antiviral drug development against HEV.

Author Summary

HEV is the most common cause of acute viral hepatitis worldwide and is also associated with chronic hepatitis, especially in immunocompromised patients. Although often an acute and self-limiting infection in the general population, HEV can cause severe morbidity and mortality in certain patients, a problem compounded by the lack of FDA-approved anti-HEV medication available. In this study, we have investigated the role of nucleotide synthesis pathway in HEV infection and its potential for antiviral drug development. We show that targeting the later but not the early steps of purine synthesis pathway exert strong anti-HEV activity. In particular, IMPDH is the most important anti-HEV target of this cascade. Importantly, the clinically used IMPDH inhibitors, including mycophenolic acid and ribavirin, have potent anti-HEV activity. Furthermore, targeting pyrimidine synthesis pathway also exerts potent antiviral activity against HEV. Interestingly, antiviral effects of nucleotide synthesis pathway inhibitors appear to depend on medication-induced transcription of antiviral interferon-stimulated genes. Thus, this study reveals an unconventional novel mechanism as to how nucleotide synthesis pathway inhibitors can counteract HEV replication.

Introduction

Hepatitis E virus (HEV) is a single-stranded positive-sense RNA virus, which mainly infects the liver. It is the most common cause of acute viral hepatitis worldwide. In general, HEV infection is a self-limiting disease and associated with low mortality, but epidemics of hepatitis E occur periodically throughout the developing world, resulting in 70,000 death yearly [1]. In western countries, HEV primarily affects immunocompromised patients, in particular organ transplant recipients, as well as hematopoietic stem cell transplant [2-5]. More than 60% of organ recipients infected with HEV develop chronic hepatitis with rapid progression to cirrhosis [2]. Despite an emerging global health issue, no FDA-approved anti-HEV therapy is currently available, only interferon-α, ribavirin or a combination have been occasionally used as off-label treatment. Thus, further research aimed at understanding its infection biology and developing effective antiviral treatment is urgently required.

Cellular nucleotides, including purines and pyrimidines, are the basic building blocks that form the nucleic acids RNA and DNA. Nucleotides are the fundamental components that are required for cell metabolism, such as genome replication. *In vivo*, nucleotides can be synthesized *de novo* through a series of enzymatic reactions or recycled through salvage pathways. Since viral replication heavily relies on the host cells to supply nucleosides, targeting nucleotide biosynthesis pathway thus represents an attractive strategy for antiviral drug development. The nucleotide biosynthesis pathways have been well-studied for decades [6-8]. Numerous compounds have been developed and well-characterized to target particular enzymes of this pathway to inhibit viral infections by depletion or causing imbalance of nucleotide pools [9-18]. Among them, inhibitors of inosine monophosphate dehydrogenase (IMPDH), a key enzyme of the purine synthesis pathway, have been successfully used in the clinic for decades. These drugs including ribavirin and mycophenolic acid (MPA), used as antiviral or immunosuppressive medication respectively, have been demonstrated to have broad antiviral activity against a spectrum of viruses, including dengue virus, yellow fever virus (YFV), hepatitis B, hepatitis C and hepatitis E virus [14, 15, 18-21]. Likewise, Brequinar and Leflunomide, the inhibitors of dihydroorotate dehydrogenase (DHODH), an essential enzyme of pyrimidine nucleotide synthesis, have been shown to inhibit human polyomavirus type BK (BKV), YFV and dengue virus [12, 22].

Besides their function as building blocks of genetic material, free nucleotides also play important roles in cell signalling. We and others have previously reported the potential interaction of nucleotide deprivation and cellular antiviral immune response, such as provoking the expression of interferon-stimulated genes (ISGs) [19, 23]. Given that the liver is a major site for nucleotide synthesis, we comprehensively profiled the role of purine and pyrimidine synthesis pathways in HEV cell culture models, aimed at identifying potential antiviral drug targets and understanding the crosstalk with cellular antiviral immunity against HEV infection.

Materials and Methods

Reagents

Guanosine (CAS: 118-00-3), Adenosine (CAS: 58-61-7), Uridine (CAS: 58-96-8), 6-TG (CAS: 154-42-7), Lometrexol hydrate (CAS: 106400-81-1), MTX hydrate (CAS: 133073-73-1), FA phosphate (CAS: 75607-67-9), BQR sodium salt hydrate (MDL: MFCD21363375), LFM (CAS: 75706-12-6) and 6-AU (CAS:

461-89-2) were purchased from sigma. 23 IMPDH specific inhibitors were kindly provided by Center for Drug Design, University of Minnesota. All the reagents were dissolved in dimethylsulfoxide (DMSO). The effects of these de novo nucleotide biosynthesis inhibitors on host cell viability were determined by MTT assay (Supplementary Figure 7). Stocks of JAK inhibitor 1 (CAS 457081-03-7, Santa Cruz Biotech, CA) was dissolved in DMSO with a final concentration of 5 mg/mL. Stocks of CP-690550 (Tofacitinib) (Santa Cruz Biotech, CA) were dissolved in DMSO with a final concentration of 10 mg/mL.

Cell culture models

Human hepatoma cell line Huh7 and human embryonic kidney epithelial cell line 293T cells were cultured in Dulbecco's modified Eagle medium (DMEM) (Invitrogen) supplemented with 10% fetal bovine serum, 100IU/mL penicillin and 100IU/mL streptomycin. HEV replication model with subgenomic HEV sequence coupled with a Gaussia luciferase reporter gene and HEV infection model containing the full-length HEV genome were used in our study. The construction of two models has been described previously [18]. Besides, Huh7 cells constitutively expressing the firefly luciferase reporter gene driven by the human PGK promoter were used as household luciferase activity for normalizing nonspecific effects on luciferase Activity [11]. Huh7 cells transduced with lentiviral transcriptional reporter system expressing the firefly luciferase gene under control of a promoter containing multiple ISRE promoter elements (SBI Systems Biosciences, Mountain View, CA) was established and luciferase activity represents ISRE promoter activation.

Quantification of HEV replication and infection

The details for exanimating HEV replication and infection were described before [18]. Briefly, For the HEV replication model (p6-Luc), the activity of secreted gaussia luciferase in the cell culture medium was measured using BioLux® *Gaussia* Luciferase Flex Assay Kit (New England Biolabs), as quantification of viral replication, which was normalized by firefly luciferase expression. For full-length HEV infectious model, SYBR Green based qRT-PCR was used to quantify the newly formed viral genomic RNA after cell lysis and the HEV primer sequences were shown in supplementary Table 2.

Gene knockdown by lentiviral vector delivered short hairpin RNA (shRNA)

Lentiviral vectors, targeting PPAT, GART, ATIC, DHODH, were produced in 293T cells as previously described [11]. To generate stable gene knockdown cells, Huh7 cells were transduced with lentiviral vectors. Since the vectors also express a puromycin resistance gene, transduced cells were subsequently selected by adding 2.5 μg/ml puromycin (Sigma) in the cell culture medium. After pilot study, the shRNA vectors (Supplementary Figure 1 and Supplementary Table 3) exerting optimal gene knockdown were selected by qPCR with the corresponding primers shown in supplementary Table 2. Meanwhile, shRNA vector expressing Green fluorescent protein (GFP) was used as control (shCTR). The amount of HEV were assessed after 3 days of infectious HEV medium post-infecting shGFP cells and knockdown cells. For the experiment comparing the activity of compounds between shGFP and knockdown cells, infectious HEV cells were directly transduced with lentiviral shRNA vectors and selected by puromycin.

Statistical analysis

Statistical analysis was performed using the nonpaired, nonparametric test (Mann–Whitney test; GraphPad Prism software). P values less than 0.05 were considered as statistically significant.

Results

Exogenous guanosine, but not uridine, stimulates HEV replication

Purine and pyrimidine nucleotides are the major cellular energy carriers and constitute the defining subunits of nucleic acids. Two distinct pathways are responsible for the biosynthesis of these two types of nucleotides (Figure 1A and 2A). Their fundamental role in cellular biochemistry raises the possibility that modifying flux through nucleotide biosynthesis pathways would profoundly influence the course of viral infection. Thus we decided to assess the overall impact of either purine or pyrimidine synthesis on HEV infection. A first indication that such effects might exist came from experiments in which we arbitrarily increased the purine and pyrimidine content by supplementation of exogenous guanosine (Figure 1A) and uridine (Figure 2A) in human hepatoma cell line (Huh7)-based HEV cell culture models. Guanosine, a purine nucleoside containing guanine attached to a ribose, can be converted to guanosine monophosphate (GMP) through purine salvage synthesis pathway, subsequently replenishes purine nucleotide pool (Figure 1A). Mechanistically, the cleavage of exogenous guanosine was catalysed by purine nucleoside phosphorylase (PNP) to form guanine. In the presence of hypoxanthine/guanine phosphoribosyl transferase (HGPRT), guanine was converted to GMP by addition of ribose 5-phosphate from phosphoribosyl pyrophosphate (PRPP). Supplementation of guanosine dose-dependently enhanced HEV replication-related luciferase activity in the subgenomic replicon (p6-Luc) model and increased cellular viral RNA in the full-length (p6) infectious model (Figure 1B). Likewise, uridine, which is a pyrimidine nucleoside consisting of uracil binding to ribose, commonly presents as uridine monophosphate (UMP) to rescue cells from pyrimidine nucleotide depletion (Figure 2A). In contrast, supplementation of exogenous uridine had no effect on HEV replication (Figure 2B). Thus interaction between at least some of the pathways involved in nucleotide biosynthesis and the HEV infectious process might exist.

Targeting the catalytic steps leading to the primary purine nucleotide synthesis (inosine monophosphate ; IMP), stimulates HEV replication

Given the clear pro-viral effect of exogenous guanosine, we were encouraged to explore potential anti-HEV strategies targeting the different enzymes that are involved in purine nucleotide synthesis. *De novo* purine is mainly synthesized in the liver, which begins with the starting material 5-phosphoribosyl-1-pyrophosphate, PRPP. The first fully-formed nucleotide IMP is catalyzed through ten reactions by six enzymes (Figure 1A). We first selectively targeted three key enzymes of this cascade, including amido phosphoribosyltransferase (APRTase), glycinamide ribonucleotide trasnformylase (GART) and 5-aminoimidazole-4-carboxamide ribonucleotide formyltransferase (AICARFT) through 6-thioguanine (6-TG), lometrexol and methotrexate (MTX), respectively. Somewhat counterintuitively, all three compounds increased HEV replication in both cell culture models (Figure 3). To further clarify the role of their targets, lentiviral-mediated RNAi was used for

knockdown of these three genes PPAT, GART and ATIC that encode the corresponding enzymes APRTase, GART and AICARTF, respectively (Figure 4A). Consistent with the pharmacological results, down-regulation of these enzymes enhanced HEV replication (Figure 4B). Furthermore, the pro-viral effects of the pharmacological inhibitors were largely absent in a context in which their targets were silenced, suggesting that pharmacological effects are not due to off-target effects (Figure 4C).

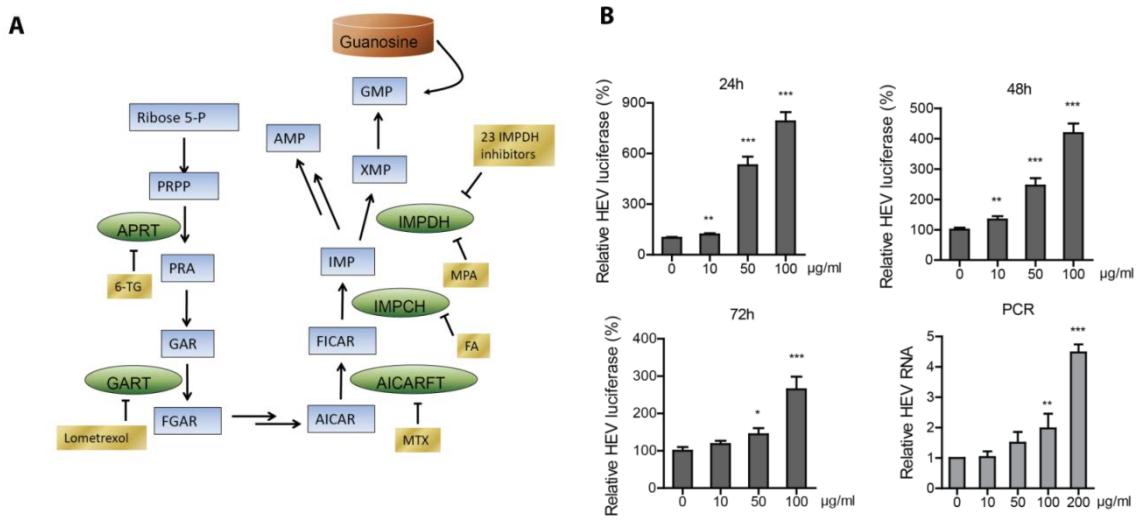

Figure 1. Exogenous guanosine stimulated HEV replication. (A) Schematic overview of de novo biosynthesis of purine nucleotide. PRPP, 5-phosphoribosyl-1-pyrophosphate; PRA, 5-phosphoribosylamine; GAR, glycinamide ribonucleotide; FGAR, formyl-GAR; AICAR, 5-aminoimidazole-4-carboxamide ribonucleotide. (B) Huh7 cell-based subgenomic HEV replicons containing the luciferase reporter gene were treated for 24 h, 48 h, and 72 h with a dose range of guanosine (n = 4). Data are presented as meansstandard errors of the means (SEM). Meanwhile, Huh7 cells with the infectious HEV containing the full-length p6 genome were treated for 48 h with a dose range of guanosine (n = 5). Data were normalized to two housekeeping genes (GAPDH and RP2) and are presented relative to the control (CTR) (set as 1). Data represent means ± SEM. *, P < 0.05; **, P <0.01; ***, P 0.001.

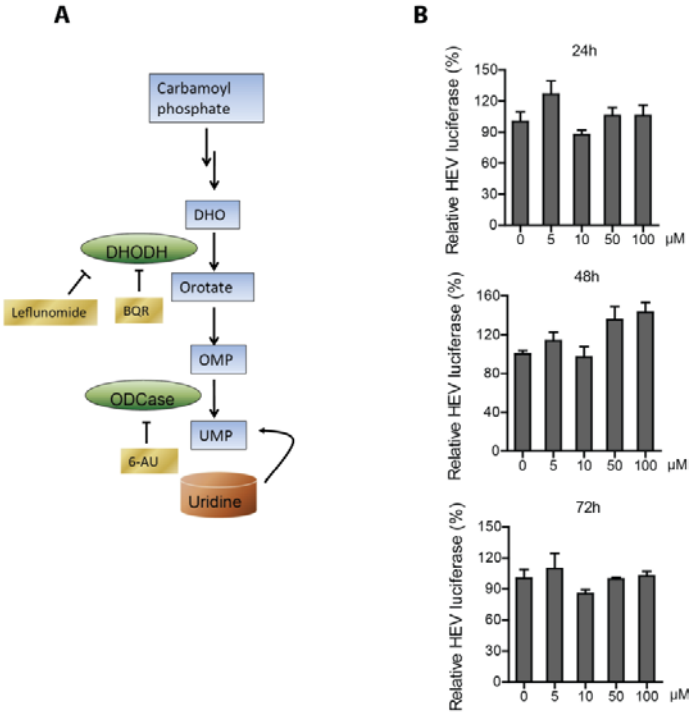

Figure 2. Exogenous uridine does not affect HEV replication. (A) Schematic overview of de novo biosynthesis of pyrimidine nucleotide. (B) Huh7 cell based subgenomic HEV replicon containing the luciferase reporter gene was treated for 24 h, 48 h, and 72 h with a dose range of uridine (n = 5). Data are presented as means ± SEM.

As a bifunctional enzyme, the N-terminal domain of ATIC has AICARFT activity, and the C-terminal domain has IMP cyclohydrolase (IMPCH) activity. FA, an IMPCH inhibitor, also promoted HEV replication but exerted cytotoxicity concurrently (Supplementary Figure 2). Thus these results highlight the interaction of nucleotide biosynthesis and the HEV infection process, but also show that rational design of therapy aimed at exploiting the nucleotide biosynthesis pathway for treatment of HEV is not straightforward.

IMPDH inhibition counteracts HEV replication by depleting the purine nucleotide pool

As a branching point in purine synthesis, IMP is converted to either AMP or XMP/GMP (Figure 1A). IMPDH, an enzyme consisting two isoforms (IMPDH1 and IMPDH2) in human, catalyses the reaction of IMP into XMP for further conversion to GMP. We have previously demonstrated that MPA, an clinically used immunosuppressant preferentially inhibiting IMPDH2, has anti-HEV activity [18]. To further explore the potential of targeting this enzyme, a panel of 23 inhibitors were customized designed and synthesized with variable affinities in inhibiting IMPDH1 or IMPDH2 (Supplementary Table 1). As shown in Figure 5A, HEV replication was inhibited by all of the 23 IMPDH inhibitors at concentration of 10 μM measured by luciferase activity. Accordingly, 21 of the 23 inhibitors also supressed HEV infection as assessed by full-length HEV genome quantification by qRT-PCR (Figure 5B). The anti-HEV activity was also observed at 2 μM of 20 IMPDH inhibitors (Supplementary Figure 3) . To further characterize, we selected three representative compounds with anti-HEV activity in both models. Similar to ribavirin and MPA, guanosine supplementation abrogated the anti-HEV activity of these compounds (Figure 5C), suggesting that depletion of the purine nucleotide pool is responsible for their antiviral action. Thus inhibitors with anti-HEV potential exert their action in this respect through targeting nucleotide synthesis.

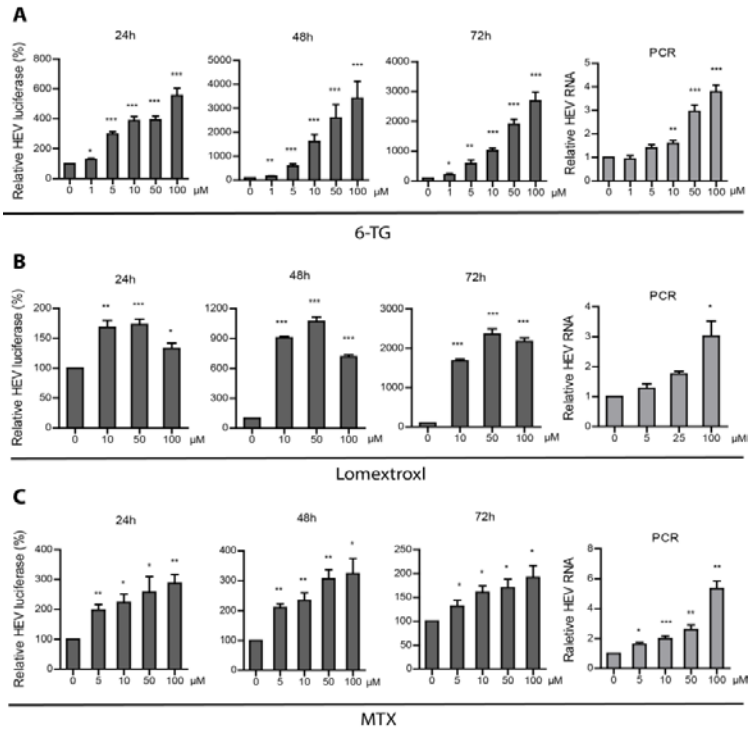

Figure 3. Inhibitors of IMP synthesis cascade stimulate HEV replication. The Huh7 cells containing subgenomic HEV replicons with luciferase reporter genes were incubated with increasing doses of 6-TG (A), lometrexol (B), andMTX(C). The luciferase activity was determined at 24 h, 48 h, and 72 h. Accordingly,Huh7 cells infected with full-length HEV were treated with increasing doses of 6-TG (A), lometrexol (B), and MTX (C). The HEV RNA level was quantified by qRT-PCR after 48 h. Data were normalized to two housekeeping genes and are presented relative to the control (CTR) (set as 1). Data represent means SEM from five to eight experiments. *, $P < 0.05$; **, $P < 0.01$; ***, $P < 0.001$.

Targeting pyrimidine biosynthesis inhibit HEV replication

Even though supplementation of exogenous uridine has no effect on HEV, inhibitors of pyrimidine synthesis have been widely reported to inhibit infection of a broad spectrum of other viruses, prompting further exploration of the role of pyrimidine biosynthesis in HEV replication. We thus selected two catalytic enzymes involved in *de novo* pyrimidine synthesis for further study. Dihydroorotate dehydrogenase (DHODH), which localises to the mitochondria, is a critical enzyme that converts dihydroorotate to orotate. Brequinar (BQR) and leflunomide (LFM) are well-known clinically tested DHODH inhibitors. Treatment with BQR (10 - 500 nM) results in a significant reduction of HEV replication-related luciferase activity in the subgenomic replicon assay system (Figure 6A). Concordantly, BQR also dose-dependently inhibits cellular viral RNA in our infectious HEV model. Treatment with 500 nM BQR for 48 hours resulted in 78 ± 17% (Mean ± SD, n = 7, $P < 0.001$) inhibition of HEV genomic RNA level (determined by qRT-PCR), compared with the control (Figure 6A). Similar results were observed with treatment of LMF (Figure 6B). The specificity of these effects was confirmed in experiments in which we examined by lentiviral RNAi-mediated silencing of the cognate target of these inhibitors, DHODH. Consistently, knockdown of DHODH inhibited HEV replication and abrogated the anti-HEV effect of BQR (Figure 7) and this enzyme does emerges as a relevant target in anti-HEV therapy.

To further identify potential anti-HEV targets, we also examined Orotidine-5'-monophosphate decarboxylase (ODCase), the downstream enzyme of DHODH that catalyses

decarboxylation of OMP to UMP. To this end we employed 6-azauracil (6-AU), a potent inhibitor of ODCase. As shown in Figure 6C, HEV replication was dose-dependently inhibited by 6-AU. Conversely, supplementation with uridine fully restored the HEV infectious potential despite the presence of BQR, LMF or 6-AU (Figure.8). In conjunction, these results show that depletion of pyrimidine nucleotide pool is a powerful anti-HEV strategy.

Inhibitors of purine and pyrimidine synthesis provoke cellular antiviral immune responses through nucleotide depletion

We previously has demonstrated that the IMPDH inhibitor, MPA, can induce the expression of interferon-stimulated genes (ISGs) to combat hepatitis C virus (HCV) infection, although the underlying mechanism remained unclear [19]. ISGs are the ultimate antiviral effectors and are generally assumed to be induced solely through the action of antiviral cytokines, especially interferons. In HEV infection models, we observed that MPA as well as other (three selected) IMPDH inhibitors were able to induce the expression of a panel of antiviral ISGs (Figure 9A), challenging this dogma. The induction of ISGs by IMPDH inhibitors was associated with purine nucleotide depletion, since supplementation of guanosine at least partly abrogated the induction of ISGs (Figure 9B).

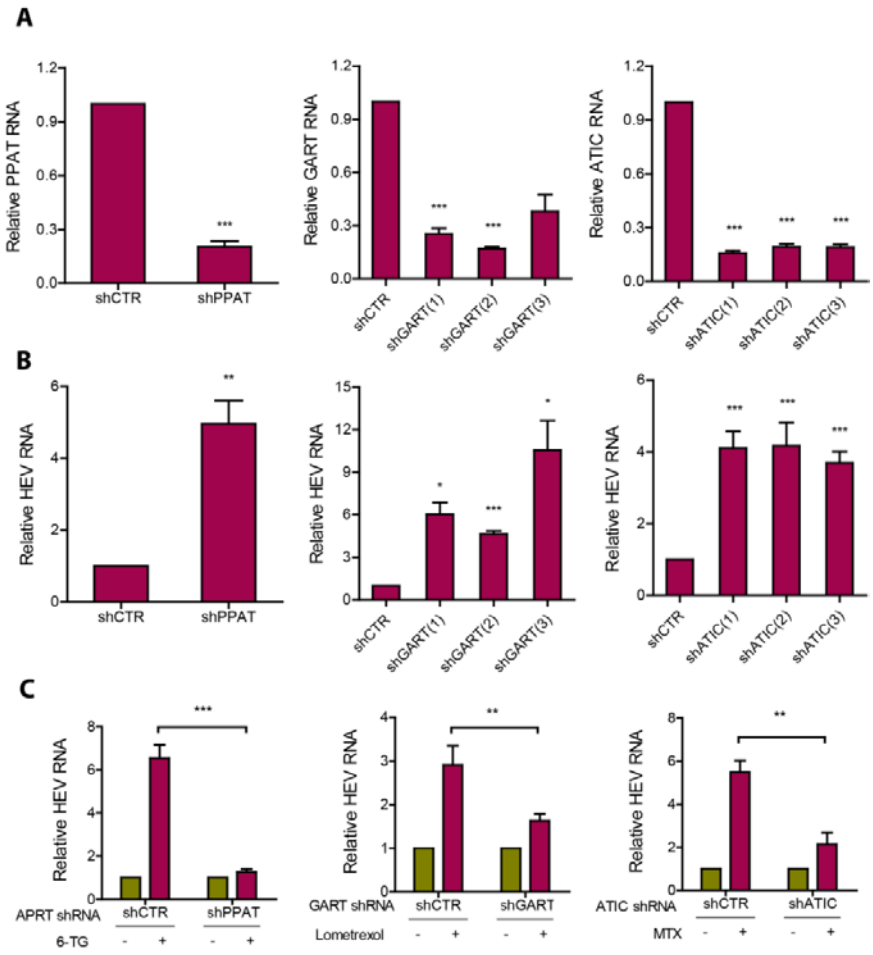

Figure 4. Silencing of enzymes involved in IMP synthesis cascade facilitates HEV replication. (A) Huh7 cells were transduced with lentiviral shRNAs to stably silence the corresponding genes for PPAT, GART, and ATIC (a set of independent shRNA clones targeting each gene was used). Huh7 cells transduced with lentiviral shRNA targeting GFP (shCTR) were used as a control. The efficiency of gene knockdown was analyzed by qRT-PCR. (B) Silencing of PPAT, GART, and ATIC resulted in significant elevation of viral RNA upon inoculation of HEV. HEV RNA levels were determined 72 h after inoculation. (C) Silencing of PPAT, GART, and ATIC abrogated the pro-HEV effects of 6-TG, lometrexol, and MTX. Data were normalized to that for cells without treatment with the three compounds (green bar; set as 1). All data were normalized to two housekeeping genes and are presented relative to the control (CTR) (set as 1) (means ± SEM from four to eight experiments). *, $P < 0.05$; **, $P < 0.01$; ***, $P < 0.001$.

In parallel, we also investigated the effects of pyrimidine synthesis inhibitors. We employed an interferon response reporter that Huh7 cells are stalely integrated with an interferon-stimulated response element (ISRE)-driven luciferase gene that measures ISG transcription upon interferon stimulation. BQR potently induces luciferase activity in this reporter assay, and triggers expression of a panel of ISGs (Supplementary Figure 4 and Figure 10A). Supplementation of uridine completely abrogated these effects on ISG transcription (Figure 10B and Supplementary Figure 4). Similar results were also observed with another pyrimidine synthesis inhibitor, 6-AU, targeting ODCase (Figure 10C). Thus, both purine and pyrimidine synthesis pathways can interact with cellular antiviral immune response, providing a rational explanation as to their antiviral effects.

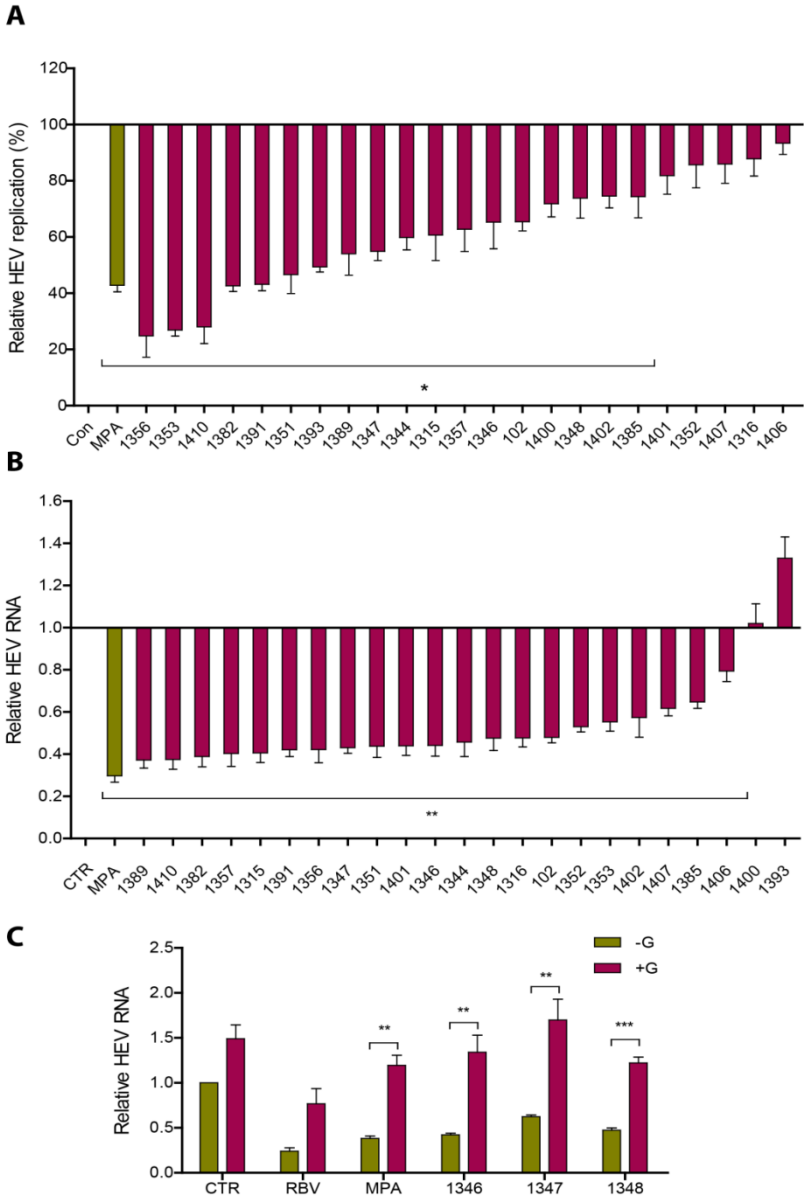

Figure 5. IMPDH inhibitors potently inhibit HEV replication by depletion of the purine nucleotide pool. (A) Huh7 HEV replicon luciferase cells were treated with 23 specific IMPDH inhibitors (10 M) with MPAas a positive control. Luciferase activity was quantified at 24 h after treatment (n = 3) (B) Huh7 cells harbouring full-length HEV were treated with 23 specific IMPDH inhibitors with MPA as a positive control. HEV RNA levels were measured by qRT-PCR at 48 h after treatment (n = 5). (C) Supplementation of guanosine abrogated the anti-HEV effects of 3 representative IMPDH inhibitors (1346, 1347, and 1348) (n = 5). Ribavirin (RBV) and MPA served as positive controls. Data were normalized to two housekeeping genes and are presented relative to the control (CTR) (set as 1) (means ± SEM). *, $P < 0.05$; **, $P < 0.01$; ***, $P < 0.001$.

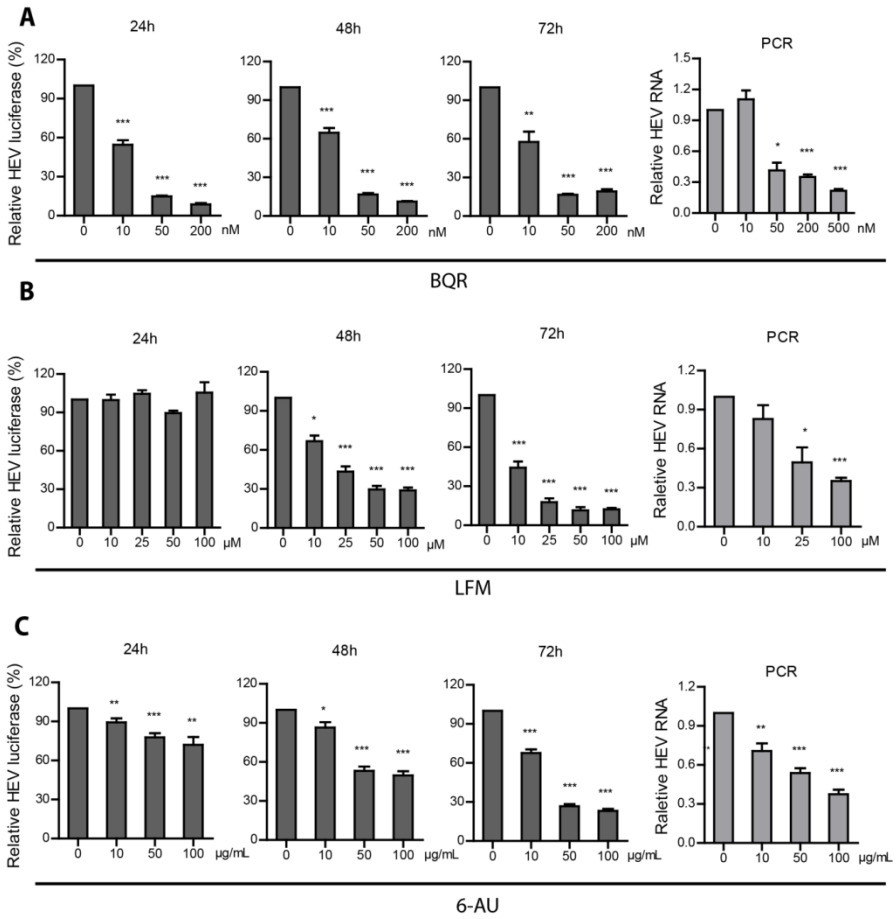

Figure 6. Inhibition of pyrimidine nucleotide synthesis suppresses HEV replication. Huh7 cells containing subgenomic HEV replicons with luciferase report genes were treated with increasing doses of BQR (A), LFM (B), and 6-AU (C). The luciferase activity was determined after 24 h, 48 h, and 72 h. Accordingly, Huh7 cells harboring infectious HEV also were treated with increasing doses of BQR (A), LFM (B), and 6-AU (C). HEV RNA was quantified by qRT-PCR after 48 h of treatment. Data were normalized to two housekeeping genes and are presented relative to the control (CTR) (set as 1). Data represent means ± SEM from four to seven experiments. *, P < 0.05; **, P 0.01; ***, P < 0.001.

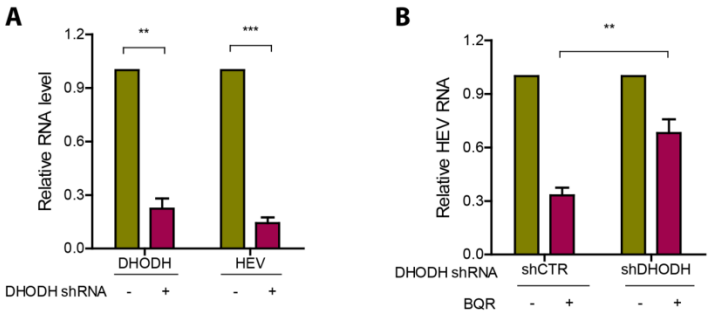

Figure 7. Anti-HEV activity by BQR can be attributed to the inhibition of its target DHODH. (A) Huh7 cells were transduced with lentiviral shRNA to stably silent DHODH (DHODH shRNA+). Huh7 cells transduced with lentiviral shRNA targeting GFP were used as control (DHODH shRNA-). DHODH knockdown was assessed by qRT-PCR (n = 3). DHODH knockdown resulted in significant inhibition of HEV replication. HEV viral RNA were determined 72h after HEV inoculation (n = 6). (B) DHODH knockdown abrogated the anti-HEV effect of BQR (n = 7). Data were normalized to cells without BQR treatment (green bar, set as 1). All data were normalized to two housekeeping genes and presented relative to the control (shCTR) (set as 1) (mean ± SEM). **P <0.01; ***P < 0.001.

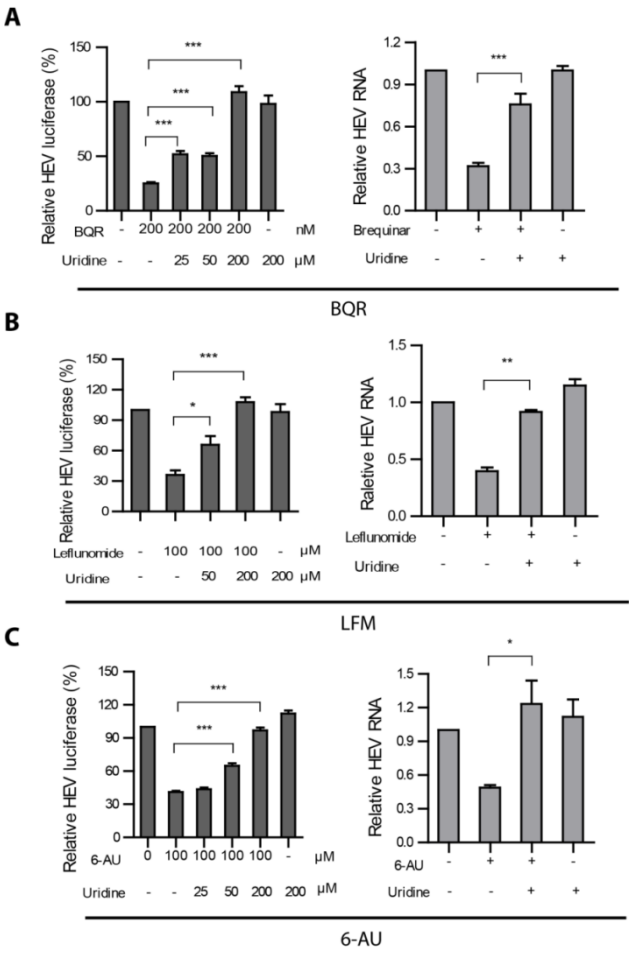

Figure 8. Uridine reverses the anti-HEV activity mediated by pyrimidine inhibition. The Huh7 subgenomic HEV replicon was incubated with BQR (A), LFM (B) and 6-AU (C), supplemented with increasing dose of uridine. After 72h, luciferase activity was determined. Accordingly, Huh7 cells harbouring full-length HEV RNA were treated with BQR (A), LFM (B) and 6-AU (C), and supplemented with 200 µM uridine. HEV viral RNA was assessed by qRT-PCR 48h after treatment. Data were normalized to two housekeeping genes and presented relative to the control (CTR) (set as 1). Data represent mean ± SEM of four to seven experiments. ∗P < 0.05; ∗∗P <0.01; ∗∗∗P < 0.001.

The induction of ISGs by nucleotide synthesis inhibitors is independent of the JAK-STAT machinery

Classically, ISGs are thought only to be induced by interferons through activation of the JAK-STAT pathway. Briefly, the binding of interferons to their receptors leads to activation of Janus activated kinase 1 (JAK1), resulting in tyrosine phosphorylation of downstream substrates, including signal transducer and activator of transcription 1 (STAT1) and STAT2. The complex of STAT1–STAT2–IRF9 (IFN-regulatory factor 9) enters nucleus and binds to the IFN-stimulated response elements (ISRE) motifs in the target gene, subsequently regulating ISG transcription and thus mediating the innate anti-viral immune response.

To assess whether the induction of ISGs by nucleotide synthesis inhibitors also occurs via this classical pathway, we blocked JAK-STAT cascade by employing the pharmacological JAK inhibitors, JAK inhibitor 1 or CP-690550, which were conceivably identified to impair the expression ISGs triggered by IFN-α (Supplementary Figure 5). Surprisingly, the induction of ISGs as well as the anti-HEV effects of these inhibitors were not affected (Figure 11). These results revealed that targeting nucleotide synthesis provokes ISG induction via a non-canonical mechanism that is independent of the classical interferon signalling.

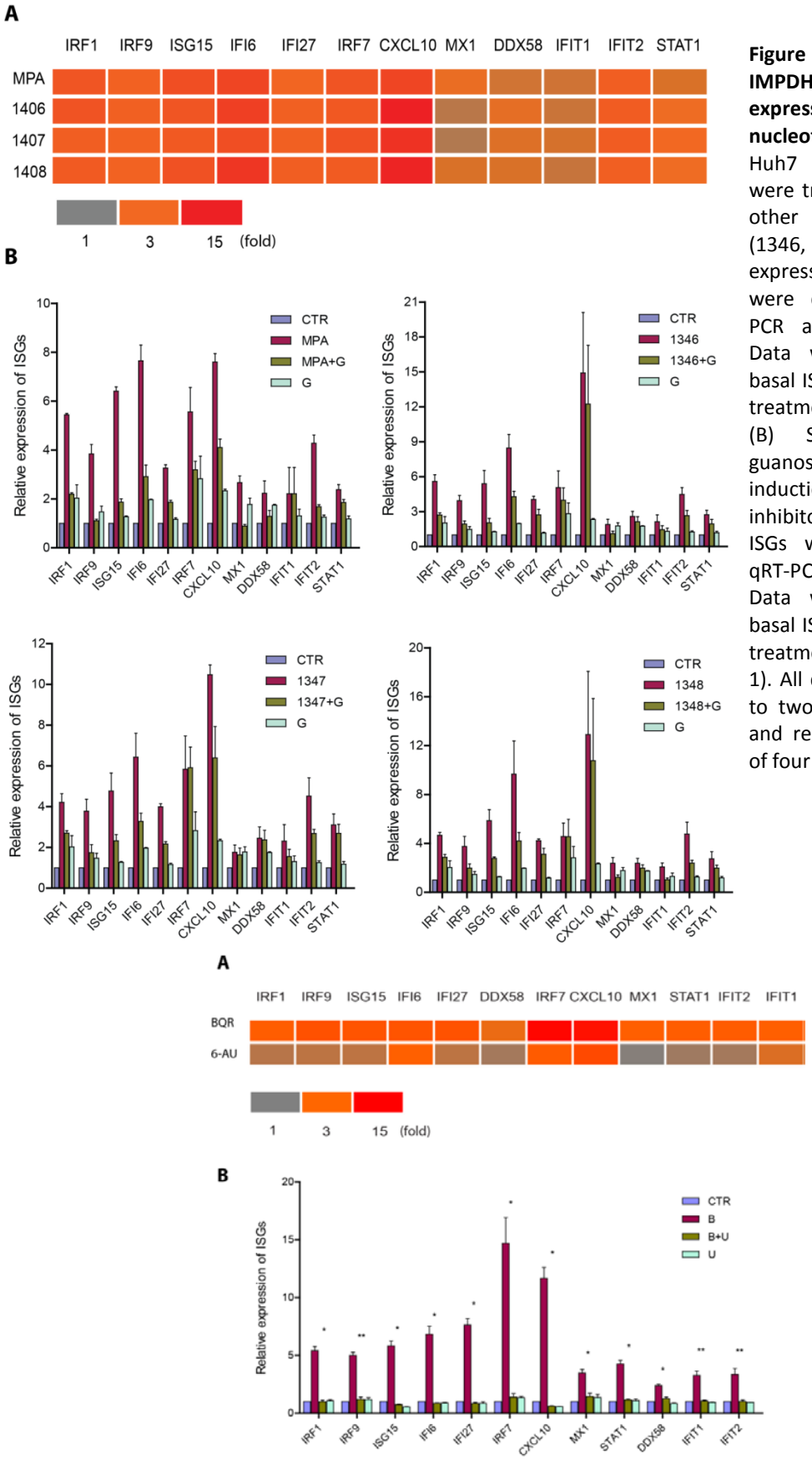

Figure 9. Inhibition of IMPDH stimulates ISG expression through purine nucleotide deprivation. (A) Huh7 cells infected HEV were treated with MPA or 3 other IMPDH inhibitors (1346, 1347 and 1348). The expression of a panel of ISGs were determined by qRT-PCR after 48h treatment. Data were normalized to basal ISG expression without treatment (grey bar, set as 1). (B) Supplementation of guanosine abrogated the induction of ISGs by IMPDH inhibitors. The expression of ISGs were determined by qRT-PCR 48h after treatment. Data were normalized to basal ISG expression without treatment (purple bar, set as 1). All data were normalized to two housekeeping genes and represent mean ± SEM of four experiments.

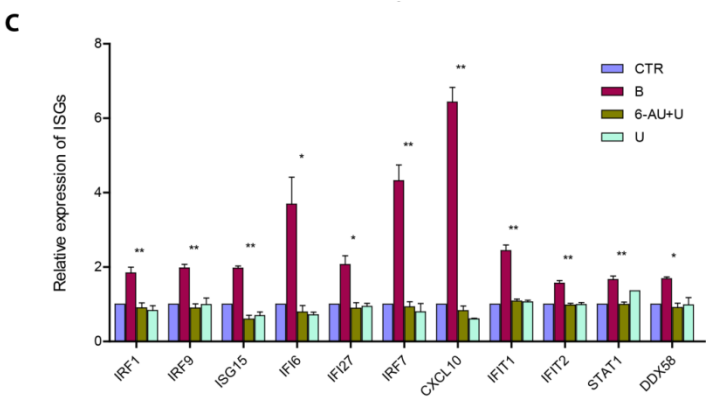

Figure 10. Inhibition of pyrimidine synthesis stimulates ISG expression through pyrimidine nucleotide depletion. (A) Huh7 cells infected with HEV were treated with BQR or 6-AU. After 48h, the expression of a panel of ISGs were determined by qRT-PCR. Data were normalized to basal ISG expression without treatment (grey bar, set as 1). (B) Supplementation of uridine completely abrogated the induction of ISGs by BQR (B) or 6-AU (C).The expression of ISGs were determined by qRT-PCR at 48h after treatment. Data were normalized to basal ISG expression without treatment (purple bar, set as 1). All data were normalized to two housekeeping genes and represent mean ± SEM of five experiments. ∗P < 0.05; ∗∗P <0.01.

Discussion

Nucleotides are key components involved in host cell metabolism and virus infection. Most of the inhibitors targeting de novo nucleotide biosynthesis have been well-characterized by many studies and their efficacy in inhibiting nucleotide synthesis have been thoroughly demonstrated [16, 17, 24-31]. Based on that, we profiled and established the effects and mechanism-of-action of inhibiting *de novo* nucleotides biosynthesis on HEV replication. Unexpectedly, targeting the early steps of the purine nucleotide synthesis pathway (before the primary purine IMP formed) leads to enhancement of HEV replication, whereas targeting later steps (IMPDH enzyme) results in potent antiviral activity against HEV, an effect apparently relating to purine nucleotide depletion. Inhibition of pyrimidine nucleotide synthesis pathway also inhibits HEV replication. Mechanistically, these effects are related to an unconventional interaction with cell-autonomous antiviral immunity dependent on very strong induction of antiviral ISGs.

It is counterintuitive that targeting the upstream enzymes of the purine pathway (before IMP formed) by pharmacological inhibitors facilitates HEV replication, but the specificity became evident from silencing genes encoding the enzymes involved. Supplementation with exogenous purine nucleotides (adenosine or guanosine) in culture medium in presence of these purine synthesis inhibitors were not capable of abrogating the stimulation of HEV replication, suggesting these pro-viral effects may only partly relate to the nucleotide synthesis pathway (Supplementary Figure 6A-C). It is worth noting that targeting the early stage of purine synthesis result in depletion of ATP and/or GTP pool. Cellular energy metabolism mediated by ATP might be important for the host cells to defend virus infection [32, 33]. Therefore, insufficient ATP level might facilitate HEV infection by escaping from host cellular immunity. However, how the ATP levels regulate virus infection deserves further investigation. Similarly, a previous study reported pro-viral activity by nucleotides biosynthesis inhibitors, LFM and FK778, in hepatitis B virus model, although these two compounds are generally antiviral against other viruses [17]. Thus, the question whether the pro-HEV effects of targeting the early steps of the purine pathway are specific to this virus or a general phenomenon in virus biology remains unanswered.

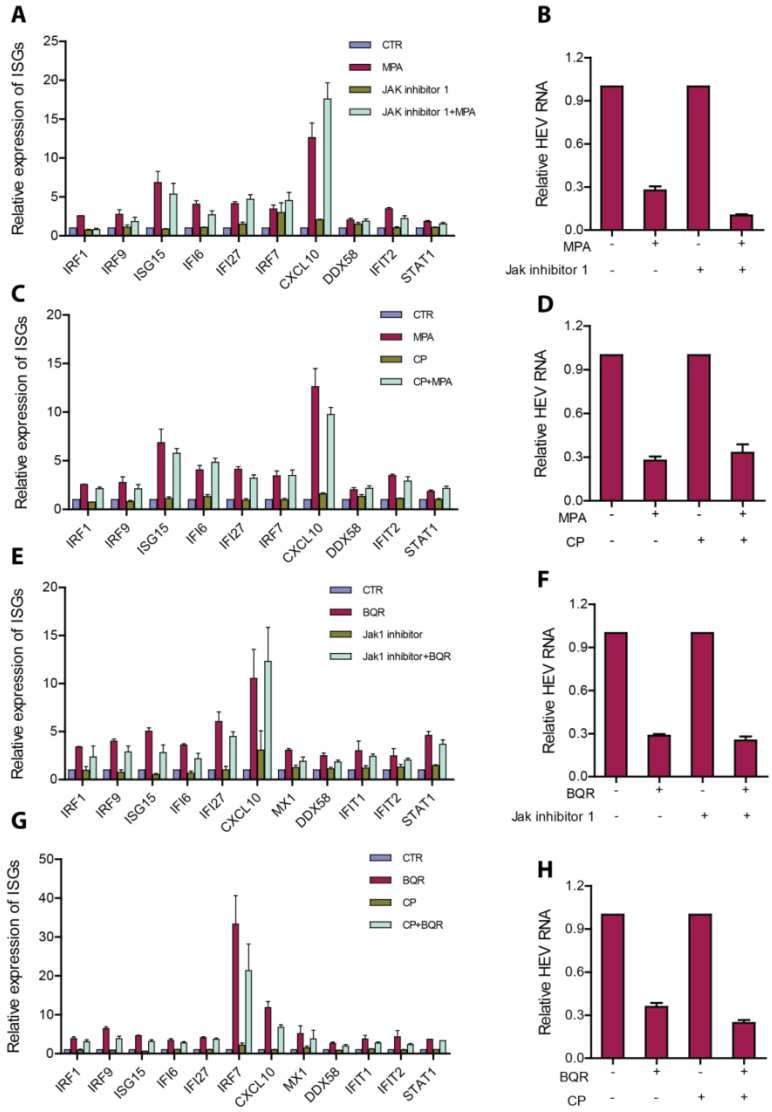

Figure 11. ISGs induction and the anti-HEV activity triggered by nucleotide synthesis inhibitors are independent of the JAK-STAT signalling pathway. The induction of ISGs (A, C) and the anti-HEV effects (B,D) by MPA were quantified in presence or absence of JAK inhibitor 1 (A, B)/CP-690550 (CP) (C, D); The induction of ISGs were normalized to basal ISG expression without MPA treatment (purple bar, set as 1). The relative HEV RNA levels were normalized to cells without treatment of MPA (set as 1). Similarly, the induction of ISGs (E, G) and the anti-HEV effects (F, H) mediated by BQR were quantified in presence or absence of JAK inhibitor 1 (E, F)/CP (G, H). The induction of ISGs were normalized to basal ISG expression without BQR treatment (purple bar, set as 1). The relative HEV RNA levels were normalized to cells without BQR treatment (set as 1). Data were normalized to two housekeeping genes and represent mean ± SEM of three to four experiments.

IMPDH, as a target for antiviral drug development for a broad spectrum of viruses, has been widely investigated. We previously have demonstrated that the IMPDH inhibitors ribavirin and MPA inhibit HEV replication *in vitro* [18, 20]. This study further validated this notion by showing the anti-HEV potential of 23 specifically designed IMPDH inhibitors. The efficacy of 23 IMPDH inhibitors on HEV infection were consistent but with variable degree, which might be due to the different ability and variable affinities in inhibiting IMPDH1 and IMPDH2. As a competitive IMPDH inhibitor, ribavirin has been used in the clinic to treat chronic hepatitis C for decades. However, ribavirin monotherapy hardly has detectable effect on HCV viral load reduction [34], but only when combined with IFN-α, it doubles the response rate, compared with IFN-α alone [35]. In contrast, ribavirin monotherapy as off-label treatment appears very effective for treating chronic HEV infection in that viral clearance was observed in the majority of the patients as reported by a recent large retrospective multicentre study [36], although prospective randomized trials are still required to confirm the findings. Of note that in addition to IMPDH inhibition, ribavirin also possesses pleiotropic biological properties, including immunomodulation, inhibition of gene translation, and interaction with viral RNA-dependent RNA polymerase (RdRp) and mutation of virus [37-39]. Thus, the exact anti-HEV mechanism by ribavirin

remains to be further elucidated, but the present study provides evidence that answer may lie in its relation to nucleotide biosynthesis.

As a non-competitive IMPDH inhibitor, MPA has been used as an immunosuppressant to prevent allograft rejection following organ transplantation [40]. Despite of the opposing effects of inhibitors targeting early or later steps of purine synthesis cascade on HEV, we demonstrated that the anti-HEV action of MPA was independent of those early step enzymes (Supplementary Figure 6D) Interestingly, clinical evidence appears to support our experimental observation that the use of immunosuppressive treatments containing mycophenolate mofetil (the pro-drug of MPA) may lead to more frequent HEV clearance in heart transplant recipients [41]. Nevertheless, because of limited patient number, it is still not sufficient to draw solid conclusion regarding the *in vivo* effect of MPA. A recent cohort study reported the anti-HEV activity by ribavirin was not affected by MPA in patients, but they didn't analyse the direct effect of MPA on HEV infection [42].

The three inhibitors used in our study interfering pyrimidine synthesis have been described in many previous studies [16, 29-31]. Adding to the previous knowledge that pyrimidine synthesis inhibitors, such as BQR and LFM, have broad antiviral activity against a spectrum of viruses [16, 23, 43], we now report their potent anti-HEV activity. Both BQR and LFM are immunosuppressive agents, although whether the mechanism of action is solely via pyrimidine inhibition remains controversially unclear [44-46]. The efficacy of BQR against graft rejection has been extensively investigated in preclinical models [47-49]; whereas LFM has been proposed as off-label immunosuppressive therapy in bone marrow [11] and renal [50] transplantation. In addition, DHODH inhibitors have been explored to treat various other diseases, including malaria, autoimmune and inflammatory diseases, cancer, rheumatoid arthritis and psoriasis [51-55]. Given the bifunctional effects of antiviral and immunosuppressive of BQR and LFM, these regimens may hold the potential to treat HEV-infected organ recipients.

Interestingly, nucleotide synthesis interacts with cellular antiviral immune responses. Here we demonstrated a direct effect of depletion of nucleotide pools on the transcription of antiviral ISGs. ISGs are ultimate antiviral effectors that are thought to be induced by interferons only. Although hundreds of ISGS have been identified, recent functional studies of individual ISG have surprisingly found out that only a small subset of ISGs actually have potent or broad antiviral activities, which include IRF1, DDX58 and IRF7 [56, 57]. It is these antiviral ISGs that are induced in our HEV models upon treatment with nucleotide synthesis inhibitors. Consistently, previous studies in HCV models reported that induction of IRF1 or IRF7 was associated with the antiviral activity of MPA [19] or ribavirin[58], respectively. Furthermore, the antiviral activity of inhibitors of pyrimidine biosynthesis against measles virus, chikungunya virus and West Nile virus was also associated with the induction of ISGs [23].

For now the mechanistic details as to inhibitors of nucleotide biosynthesis can induce ISGs remain obscure. Classically, transcription of ISGs is initiated from the binding of interferons to their receptors, which subsequently drives the activation of JAK-STAT cascade [56]. Inhibition of JAK1 to phosphorylate STAT1, the key event of interferon signalling transduction, often results in complete blockage of antiviral interferon responses [59]. However, exceptions also exist in that ISGs can be induced in the absence of JAK1 or STAT1 activation [60, 61]. Here, we found that induction of ISGs and the anti-HEV effects by nucleotide synthesis inhibitors are independent of the classical JAK-STAT cascade, suggesting the involvement of a non-canonical mechanism that is independent of

interferons and identification of these mechanisms should have substantial value for our understanding of antiviral immunity.

In conclusion, selectively targeting host enzymes involved in *de novo* nucleotide biosynthesis potently inhibits HEV replication. Furthermore, nucleotide biosynthesis pathways interact with cellular immune response that all the pharmacological inhibitors exerting anti-HEV activity are capable of triggering antiviral ISG transcription. Thus, targeting nucleotide biosynthesis represents a viable option for antiviral drug development against HEV.

Supplementary Materials

Supplementary Table 1. Information of 23 specific IMPDH inhibitors

CDD-KP-#	IMPDH I Ki in nM	IMPDH 2 Ki in nM
102	330	250
1316	82.10	55,70
1315	0.60	13.90
1401	2553	231.1
1344	162.80	102.40
1346	859.1	243.9
1347	703.4	230.1
1348	1725	365,7
1351	618.40	185.90
1352	136.20	93.01
1353	1255	364.70
1356	70.12	65.69
1410-L-ABC	N/D	N/D
1357	1813	552.50
1389	11274	297.90
1391	4221	2160
1393	5556	2398
1400	9138	367.7
1402	2203	146.7
1406	N/D	N/D
1407	N/D	N/D
1382	1815	2154
1385	521.80	487.40

Inhibitory constant (Ki) on IMPDH1 and IMPDH2 of 23 specific IMPDH inhibitors. First 3 compounds in the table are insoluble in DMSO. Other compounds are soluble in DMSO. Compounds 1406 and 1407 do not inhibit IMPDH but if converted in the cell into their corresponding NAD analogues should show some inhibition of the enzymes. Ki of 1410-L-ABC, 1406 and 1407 was not determined (ND). Chemical structures of the IMPDH inhibitors will be published somewhere else.

Supplementary Table 2. Primer sequences

Gene	Sequences 5' to 3' **(Forward)**	**Sequences 5' to 3' (Reverse)**
HEV	ATTGGCCAGAAGTTGGTTTTCAC	CCGTGGCTATAATTGTGGTCT
DDX58	CACCTCAGTTGCTGATGAAGGC	GTCAGAAGGAAGCACTTGCTACC

ISG15	CTCTGAGCATCCTGGTGAGGAA	AAGGTCAGCCAGAACAGGTCGT
STAT1	ATGGCAGTCTGGCGGCTGAATT	CCAAACCAGGCTGGCACAATTG
IFI27	CGTCCTCCATAGCAGCCAAGAT	ACCCAATGGAGCCCAGGATGAA
IRF1	GAGGAGGTGAAAGACCAGAGCA	TAGCATCTCGGCTGGACTTCGA
IRF9	CCACCGAAGTTCCAGGTAACAC	AGTCTGCTCCAGCAAGTATCGG
IFIT1	GCCTTGCTGAAGTGTGGAGGAA	ATCCAGGCGATAGGCAGAGATC
IFIT2	GGAGCAGATTCTGAGGCTTTGC	GGATGAGGCTTCCAGACTCCAA
IFI6	TGATGAGCTGGTCTGCGATCCT	GTAGCCCATCAGGGCACCAATA
IRF7	CCACGCTATACCATCTACCTGG	GCTGCTATCCAGGGAAGACACA
CXCL10	GGTGAGAAGAGATGTCTGAATCC	GTCCATCCTTGGAAGCACTGCA
MX1	GGCTGTTTACCAGACTCCGACA	CACAAAGCCTGGCAGCTCTCTA
APRT	GCGATTGAAGCACCTGTGGATG	CGGTTTTTACACAGCACCTCCAC
GART	GCACATCTCTGCCTGTTTGGCT	CATGGAACACCTCCAGTCCTAG
ATIC	CCGAGAGTAAGGACACCTCCTT	GGCATCTGAGATACGCCTTTGC
DHODH	GAGGACATTGCCAGTGTGGTCA	TTCCCACTCAGCCCTCCTGTTT

Supplementary Table 3. shRNA sequences

Gene	Sequences
PPAT (3)	CCGGCCCTTCGTTGTTGAAACACTTCTCGAGAAGTGTTTCAACAACGAAGGGTTTTTG
GART (1)	CCGGGCCCAGGAGTTTGACTTACAACTCGAGTTGTAAGTCAAACTCCTGGGCTTTTTG
GART (2)	CCGGGCACAGTCTCATCATGTCAAACTCGAGTTTGACATGATGAGACTGTGCTTTTTG
GART (3)	CCGGCCCTAACTGTTGTCATGGCAACTCGAGTTGCCATGACAACAGTTAGGGTTTTTG
ATIC (1)	CCGGGCCTTGACAATACTTTCCAAACTCGAGTTTGGAAAGTATTGTCAAGGCTTTTTG
ATIC (2)	CCGGGCAATCTCTATCCCTTTGTAACTCGAGTTACAAAGGGATAGAGATTGCTTTTTG
ATIC (3)	CCGGGCTGGAATCCTAGCTCGTAATCTCGAGATTACGAGCTAGGATTCCAGCTTTTTG
DHODH (5)	CCGGGTGAGAGTTCTGGGCCATAAACTCGAGTTTATGGCCCAGAACTCTCACTTTTT

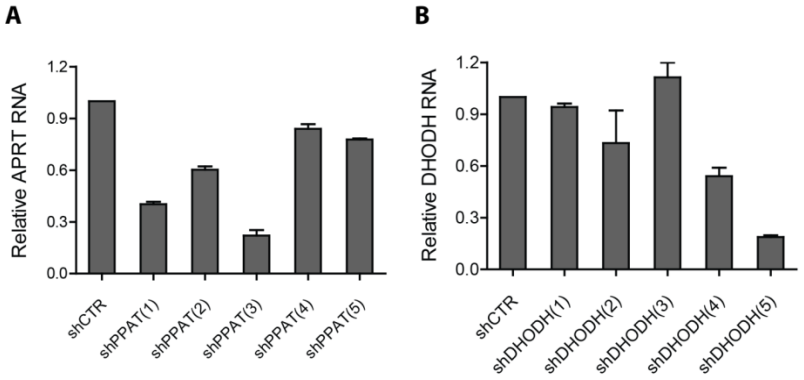

Figure S1. Gene knockdown of PPAT and DHODH with different shRNA lentiviral vectors. Huh7 cells were transduced with lentiviral shRNAs targeting at PPAT (A) and DHODH (B) using a set of 5 different independent shRNA preparations for each gene knockdown. Huh7 cells transduced with lentiviral shRNA targeting GFP (shCTR) were used as control. The efficiency of knockdown of the 2 genes were analysed by qRT-PCR using specific primers. Data were normalized to GAPDH and presented relative to control (set as 1).

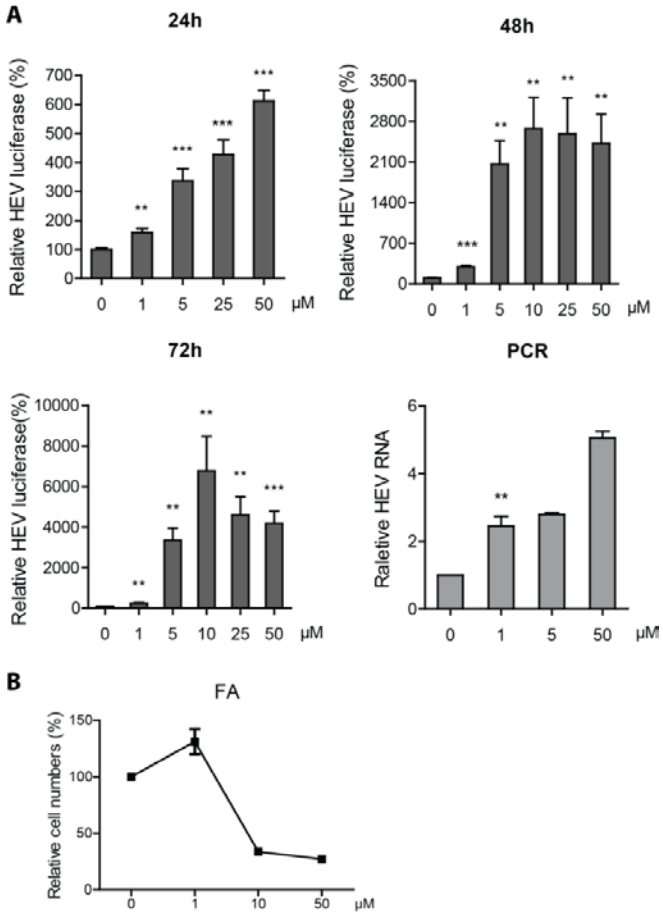

Figure S2. Fludarabine enhances HEV replication. (A) Huh7 cell-based subgenomic HEV replicon containing the luciferase reporter gene were treated for 24h, 48h and 72h with a dose-range of FA. Data presented as mean ± SEM. Meanwhile, Huh7 cells with the infectious HEV containing the full-length p6 genome were treated for 48h with a dose-range of FA. Data were normalized to GAPDH and presented relative to results from untreated cells (set as 1). (B) Huh7 cells were incubated with dose-range of FA. After 72h, MTT assay was performed to determine cytotoxicity of FA.

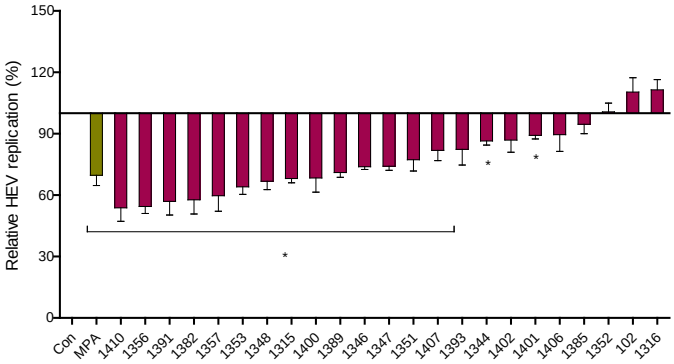

Figure S3. 2 μM IMPDH inhibitors moderately inhibit HEV replication. Huh7 HEV replicon luciferase cells were treated with 23 specific IMPDH inhibitors (2μM) with MPA as a positive control. Luciferase activity was quantified at 24h after treatment (n = 3).

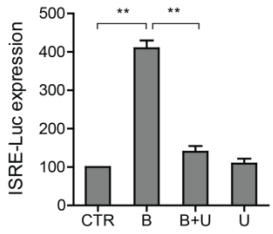

Figure S4. BQR stimulates ISRE transcription through pyrimidine depletion. Huh7-ISRE-Luc cells were incubated with BQR (B) in presence or absence of Uridine (U). ISRE promoter-related firefly luciferase activity was quantified 72h after culture.

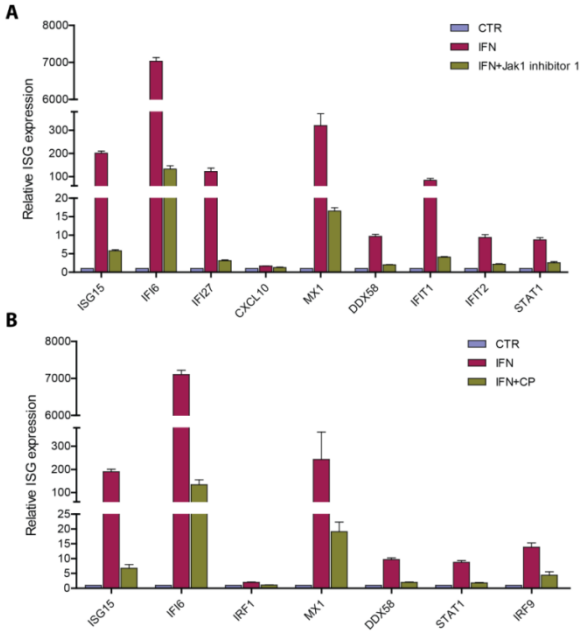

Figure S5. JAK inhibitors diminish IFNα stimulated ISG expression. (A) Huh7 cells infected with HEV were incubated with IFNα in presence or absence of Jak inhibitor 1. After 48h, the expression of ISGs were assessed by qRT-PCR. (B) Same experiment was performed with another JAK inhibitor, CP-690550 (CP). Data were normalized to basal ISG expression without IFNα treatment (purple bar, set as 1). All data were normalized to two housekeeping genes and experiments were performed two to five times.

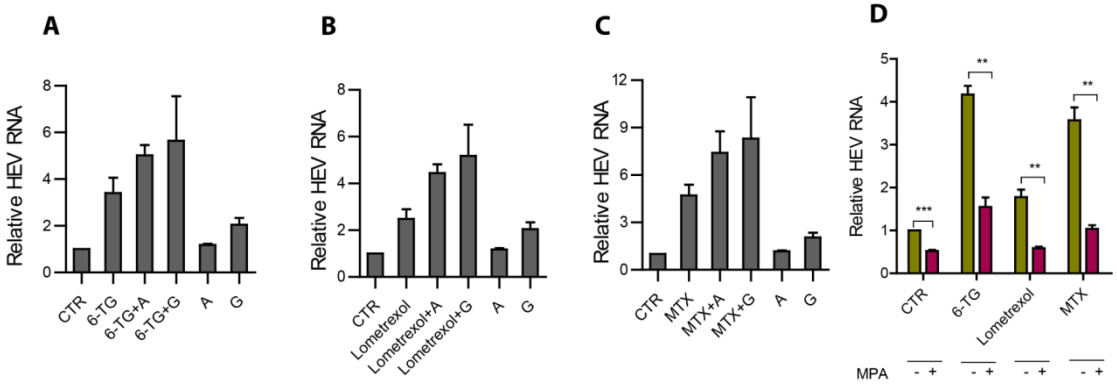

Figure S6. Inhibition of IMP synthesis enhanced HEV replication independent of purine depletion and does not affect the anti-HEV activity of MPA. Huh7 cells infected HEV were treated with 6-TG (A), lometrexol (B) and MTX (C), respectively, in the presence or absence of guanosine (G)/adenosine (A). The HEV RNA was assessed by qRT-PCR 48h after treatment. (D) Huh7 cells infected HEV were treated with 6-TG, lometrexol and MTX, respectively, in the presence or absence of MPA. The HEV RNA was assessed by qRT-PCR 48h after

treatment. Data were normalized to two housekeeping genes and presented relative to the control (CTR) (set as 1). Experiments were performed two to five times.

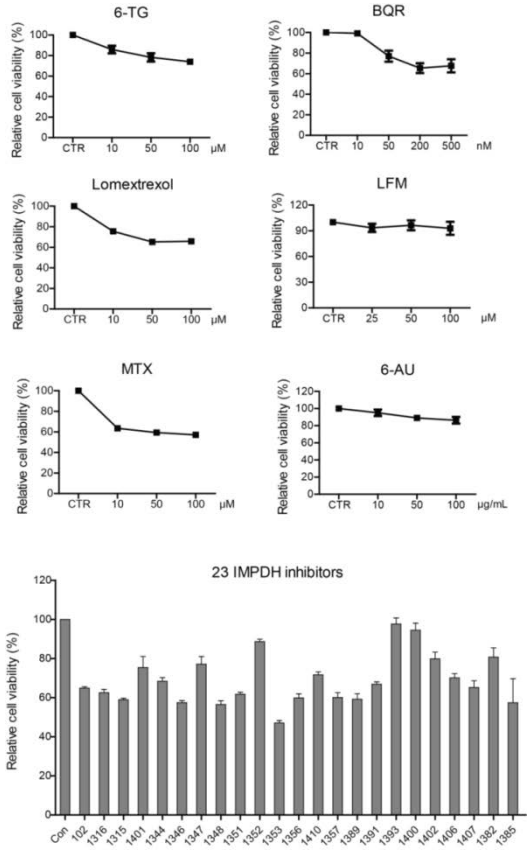

Figure S7. The effects of nucleotide synthesis inhibitors on Huh7 cells viability. Huh7 cells were incubated with a dose-range of 6-TG, lometrexol, MTX, BQR, LFM or 6-AU for 72h treatment. Huh-7 cells were incubated with 23 IMPDH inhibitors at 10 μM for 48h. MTT assay was performed to determine cytotoxicity of these compounds.

Reference

1. Kamar N, Bendall R, Legrand-Abravanel F, Xia NS, Ijaz S, Izopet J, Dalton HR. 2012. Hepatitis E. Lancet 379:2477-2488.
2. Kamar N, Selves J, Mansuy JM, Ouezzani L, Peron JM, Guitard J, Cointault O, Esposito L, Abravanel F, Danjoux M, Durand D, Vinel JP, Izopet J, Rostaing L. 2008. Hepatitis E virus and chronic hepatitis in organ-transplant recipients. N Engl J Med 358:811-817.
3. Zhou X, de Man RA, de Knegt RJ, Metselaar HJ, Peppelenbosch MP, Pan Q. 2013. Epidemiology and management of chronic hepatitis E infection in solid organ transplantation: a comprehensive literature review. Rev Med Virol 23:295-304.
4. Kamar N, Garrouste C, Haagsma EB, Garrigue V, Pischke S, Chauvet C, Dumortier J, Cannesson A, Cassuto-Viguier E, Thervet E, Conti F, Lebray P, Dalton HR, Santella R, Kanaan N, Essig M, Mousson C, Radenne S, Roque-Afonso AM, Izopet J, Rostaing L. 2011. Factors associated with chronic hepatitis in patients with hepatitis E virus infection who have received solid organ transplants. Gastroenterology 140:1481-1489.
5. van der Eijk AA, Pas SD, Cornelissen JJ, de Man RA. 2014. Hepatitis E virus infection in hematopoietic stem cell transplant recipients. Curr Opin Infect Dis 27:309-315.
6. Lane AN, Fan TW. 2015. Regulation of mammalian nucleotide metabolism and biosynthesis. Nucleic Acids Res 43:2466-2485.
7. Moffatt BA, Ashihara H. 2002. Purine and pyrimidine nucleotide synthesis and metabolism. Arabidopsis Book 1:e0018.
8. Blakley RL, Vitols E. 1968. The control of nucleotide biosynthesis. Annu Rev Biochem 37:201-224.
9. Christopherson RI, Lyons SD, Wilson PK. 2002. Inhibitors of de novo nucleotide biosynthesis as drugs. Acc Chem Res 35:961-971.

10. Fried MW, Shiffman ML, Reddy KR, Smith C, Marinos G, Goncales FL, Jr., Haussinger D, Diago M, Carosi G, Dhumeaux D, Craxi A, Lin A, Hoffman J, Yu J. 2002. Peginterferon alfa-2a plus ribavirin for chronic hepatitis C virus infection. N Engl J Med 347:975-982.
11. Avery RK, Bolwell BJ, Yen-Lieberman B, Lurain N, Waldman WJ, Longworth DL, Taege AJ, Mossad SB, Kohn D, Long JR, Curtis J, Kalaycio M, Pohlman B, Williams JW. 2004. Use of leflunomide in an allogeneic bone marrow transplant recipient with refractory cytomegalovirus infection. Bone Marrow Transplant 34:1071-1075.
12. Farasati NA, Shapiro R, Vats A, Randhawa P. 2005. Effect of leflunomide and cidofovir on replication of BK virus in an in vitro culture system. Transplantation 79:116-118.
13. Chong AS, Zeng H, Knight DA, Shen J, Meister GT, Williams JW, Waldman WJ. 2006. Concurrent antiviral and immunosuppressive activities of leflunomide in vivo. Am J Transplant 6:69-75.
14. Takhampunya R, Ubol S, Houng HS, Cameron CE, Padmanabhan R. 2006. Inhibition of dengue virus replication by mycophenolic acid and ribavirin. J Gen Virol 87:1947-1952.
15. Ying C, Colonno R, De Clercq E, Neyts J. 2007. Ribavirin and mycophenolic acid markedly potentiate the anti-hepatitis B virus activity of entecavir. Antiviral Res 73:192-196.
16. Wang QY, Bushell S, Qing M, Xu HY, Bonavia A, Nunes S, Zhou J, Poh MK, Florez de Sessions P, Niyomrattanakit P, Dong H, Hoffmaster K, Goh A, Nilar S, Schul W, Jones S, Kramer L, Compton T, Shi PY. 2011. Inhibition of dengue virus through suppression of host pyrimidine biosynthesis. J Virol 85:6548-6556.
17. Hoppe-Seyler K, Sauer P, Lohrey C, Hoppe-Seyler F. 2012. The inhibitors of nucleotide biosynthesis leflunomide, FK778, and mycophenolic acid activate hepatitis B virus replication in vitro. Hepatology 56:9-16.
18. Wang Y, Zhou X, Debing Y, Chen K, Van Der Laan LJ, Neyts J, Janssen HL, Metselaar HJ, Peppelenbosch MP, Pan Q. 2014. Calcineurin inhibitors stimulate and mycophenolic acid inhibits replication of hepatitis E virus. Gastroenterology 146:1775-1783.
19. Pan Q, de Ruiter PE, Metselaar HJ, Kwekkeboom J, de Jonge J, Tilanus HW, Janssen HL, van der Laan LJ. 2012. Mycophenolic acid augments interferon-stimulated gene expression and inhibits hepatitis C Virus infection in vitro and in vivo. Hepatology 55:1673-1683.
20. Debing Y, Emerson SU, Wang Y, Pan Q, Balzarini J, Dallmeier K, Neyts J. 2014. Ribavirin inhibits in vitro hepatitis E virus replication through depletion of cellular GTP pools and is moderately synergistic with alpha interferon. Antimicrob Agents Chemother 58:267-273.
21. Leyssen P, De Clercq E, Neyts J. 2006. The anti-yellow fever virus activity of ribavirin is independent of error-prone replication. Mol Pharmacol 69:1461-1467.
22. Qing M, Zou G, Wang QY, Xu HY, Dong H, Yuan Z, Shi PY. 2010. Characterization of dengue virus resistance to brequinar in cell culture. Antimicrob Agents Chemother 54:3686-3695.
23. Lucas-Hourani M, Dauzonne D, Jorda P, Cousin G, Lupan A, Helynck O, Caignard G, Janvier G, Andre-Leroux G, Khiar S, Escriou N, Despres P, Jacob Y, Munier-Lehmann H, Tangy F, Vidalain PO. 2013. Inhibition of pyrimidine biosynthesis pathway suppresses viral growth through innate immunity. PLoS Pathog 9:e1003678.
24. Nelson JA, Carpenter JW, Rose LM, Adamson DJ. 1975. Mechanisms of action of 6-thioguanine, 6-mercaptopurine, and 8-azaguanine. Cancer Res 35:2872-2878.
25. Beardsley GP, Moroson BA, Taylor EC, Moran RG. 1989. A new folate antimetabolite, 5,10-dideaza-5,6,7,8-tetrahydrofolate is a potent inhibitor of de novo purine synthesis. J Biol Chem 264:328-333.
26. Pizzorno G, Moroson BA, Cashmore AR, Beardsley GP. 1991. (6R)-5,10-Dideaza-5,6,7,8-tetrahydrofolic acid effects on nucleotide metabolism in CCRF-CEM human T-lymphoblast leukemia cells. Cancer Res 51:2291-2295.
27. Budzik GP, Colletti LM, Faltynek CR. 2000. Effects of methotrexate on nucleotide pools in normal human T cells and the CEM T cell line. Life Sci 66:2297-2307.
28. Carr SF, Papp E, Wu JC, Natsumeda Y. 1993. Characterization of human type I and type II IMP dehydrogenases. J Biol Chem 268:27286-27290.
29. Silva HT, Jr., Cao W, Shorthouse RA, Loffler M, Morris RE. 1997. In vitro and in vivo effects of leflunomide, brequinar, and cyclosporine on pyrimidine biosynthesis. Transplant Proc 29:1292-1293.
30. Greene S, Watanabe K, Braatz-Trulson J, Lou L. 1995. Inhibition of dihydroorotate dehydrogenase by the immunosuppressive agent leflunomide. Biochem Pharmacol 50:861-867.
31. Lopez JM, Marks CL, Freese E. 1979. The decrease of guanine nucleotides initiates sporulation of Bacillus subtilis. Biochim Biophys Acta 587:238-252.
32. Seo JY, Yaneva R, Hinson ER, Cresswell P. 2011. Human mtt
33. megalovirus directly induces the antiviral protein viperin to enhance infectivity. Science 332:1093-1097.
34. Rawling DC, Fitzgerald ME, Pyle AM. 2015. Establishing the role of ATP for the function of the RIG-I innate immune sensor. Elife 4.
35. Pawlotsky JM, Dahari H, Neumann AU, Hezode C, Germanidis G, Lonjon I, Castera L, Dhumeaux D. 2004. Antiviral action of ribavirin in chronic hepatitis C. Gastroenterology 126:703-714.
36. Poynard T, Marcellin P, Lee SS, Niederau C, Minuk GS, Ideo G, Bain V, Heathcote J, Zeuzem S, Trepo C, Albrecht J. 1998. Randomised trial of interferon alpha2b plus ribavirin for 48 weeks or for 24 weeks versus interferon alpha2b plus placebo for 48 weeks for treatment of chronic infection with hepatitis C virus. International Hepatitis Interventional Therapy Group (IHIT). Lancet 352:1426-1432.
37. Kamar N, Izopet J, Tripon S, Bismuth M, Hillaire S, Dumortier J, Radenne S, Coilly A, Garrigue V, D'Alteroche L, Buchler M, Couzi L, Lebray P, Dharancy S, Minello A, Hourmant M, Roque-Afonso AM, Abravanel F, Pol S,

Rostaing L, Mallet V. 2014. Ribavirin for chronic hepatitis E virus infection in transplant recipients. N Engl J Med 370:1111-1120.
38. Tam RC, Lau JY, Hong Z. 2001. Mechanisms of action of ribavirin in antiviral therapies. Antivir Chem Chemother 12:261-272.
39. Paeshuyse J, Dallmeier K, Neyts J. 2011. Ribavirin for the treatment of chronic hepatitis C virus infection: a review of the proposed mechanisms of action. Curr Opin Virol 1:590-598.
40. Feld JJ, Hoofnagle JH. 2005. Mechanism of action of interferon and ribavirin in treatment of hepatitis C. Nature 436:967-972.
41. Manzia TM, De Liguori Carino N, Orlando G, Toti L, De Luca L, D'Andria D, Cardillo A, Anselmo A, Casciani CU, Tisone G. 2005. Use of mycophenolate mofetil in liver transplantation: a literature review. Transplant Proc 37:2616-2617.
42. Pischke S, Stiefel P, Franz B, Bremer B, Suneetha PV, Heim A, Ganzenmueller T, Schlue J, Horn-Wichmann R, Raupach R, Darnedde M, Scheibner Y, Taubert R, Haverich A, Manns MP, Wedemeyer H, Bara CL. 2012. Chronic hepatitis e in heart transplant recipients. Am J Transplant 12:3128-3133.
43. Kamar N, Lhomme S, Abravanel F, Cointault O, Esposito L, Cardeau-Desangles I, Del Bello A, Dorr G, Lavayssiere L, Nogier MB, Guitard J, Ribes D, Goin AL, Broue P, Metsu D, Saune K, Rostaing L, Izopet J. 2015. An Early Viral Response Predicts the Virological Response to Ribavirin in Hepatitis E Virus Organ Transplant Patients. Transplantation 99:2124-2131.
44. Hoffmann HH, Kunz A, Simon VA, Palese P, Shaw ML. 2011. Broad-spectrum antiviral that interferes with de novo pyrimidine biosynthesis. Proc Natl Acad Sci U S A 108:5777-5782.
45. Chong AS, Rezai K, Gebel HM, Finnegan A, Foster P, Xu X, Williams JW. 1996. Effects of leflunomide and other immunosuppressive agents on T cell proliferation in vitro. Transplantation 61:140-145.
46. Xu X, Williams JW, Shen J, Gong H, Yin DP, Blinder L, Elder RT, Sankary H, Finnegan A, Chong AS. 1998. In vitro and in vivo mechanisms of action of the antiproliferative and immunosuppressive agent, brequinar sodium. J Immunol 160:846-853.
47. Cherwinski HM, Cohn RG, Cheung P, Webster DJ, Xu YZ, Caulfield JP, Young JM, Nakano G, Ransom JT. 1995. The immunosuppressant leflunomide inhibits lymphocyte proliferation by inhibiting pyrimidine biosynthesis. J Pharmacol Exp Ther 275:1043-1049.
48. Makowka L, Sher LS, Cramer DV. 1993. The development of Brequinar as an immunosuppressive drug for transplantation. Immunol Rev 136:51-70.
49. Cramer DV, Chapman FA, Makowka L. 1993. The use of brequinar sodium for transplantation. Ann N Y Acad Sci 696:216-226.
50. Cramer DV, Chapman FA, Jaffee BD, Jones EA, Knoop M, Hreha-Eiras G, Makowka L. 1992. The effect of a new immunosuppressive drug, brequinar sodium, on heart, liver, and kidney allograft rejection in the rat. Transplantation 53:303-308.
51. Chon WJ, Josephson MA. 2011. Leflunomide in renal transplantation. Expert Rev Clin Immunol 7:273-281.
52. Boa AN, Canavan SP, Hirst PR, Ramsey C, Stead AM, McConkey GA. 2005. Synthesis of brequinar analogue inhibitors of malaria parasite dihydroorotate dehydrogenase. Bioorg Med Chem 13:1945-1967.
53. Leban J, Vitt D. 2011. Human dihydroorotate dehydrogenase inhibitors, a novel approach for the treatment of autoimmune and inflammatory diseases. Arzneimittelforschung 61:66-72.
54. Baumann P, Mandl-Weber S, Volkl A, Adam C, Bumeder I, Oduncu F, Schmidmaier R. 2009. Dihydroorotate dehydrogenase inhibitor A771726 (leflunomide) induces apoptosis and diminishes proliferation of multiple myeloma cells. Mol Cancer Ther 8:366-375.
55. Herrmann ML, Schleyerbach R, Kirschbaum BJ. 2000. Leflunomide: an immunomodulatory drug for the treatment of rheumatoid arthritis and other autoimmune diseases. Immunopharmacology 47:273-289.
56. Norman P. 2013. Evaluation of WO2013076170: the use of a dihydroorotate dehydrogenase inhibitor for the treatment of psoriasis. Expert Opin Ther Pat 23:1391-1394.
57. Schoggins JW, Wilson SJ, Panis M, Murphy MY, Jones CT, Bieniasz P, Rice CM. 2011. A diverse range of gene products are effectors of the type I interferon antiviral response. Nature 472:481-485.
58. Schoggins JW, MacDuff DA, Imanaka N, Gainey MD, Shrestha B, Eitson JL, Mar KB, Richardson RB, Ratushny AV, Litvak V, Dabelic R, Manicassamy B, Aitchison JD, Aderem A, Elliott RM, Garcia-Sastre A, Racaniello V, Snijder EJ, Yokoyama WM, Diamond MS, Virgin HW, Rice CM. 2014. Pan-viral specificity of IFN-induced genes reveals new roles for cGAS in innate immunity. Nature 505:691-695.
59. Thomas E, Feld JJ, Li Q, Hu Z, Fried MW, Liang TJ. 2011. Ribavirin potentiates interferon action by augmenting interferon-stimulated gene induction in hepatitis C virus cell culture models. Hepatology 53:32-41.
60. Stewart CE, Randall RE, Adamson CS. 2014. Inhibitors of the interferon response enhance virus replication in vitro. PLoS One 9:e112014.
61. Leaman DW, Pisharody S, Flickinger TW, Commane MA, Schlessinger J, Kerr IM, Levy DE, Stark GR. 1996. Roles of JAKs in activation of STATs and stimulation of c-fos gene expression by epidermal growth factor. Mol Cell Biol 16:369-375.
62. Shresta S, Sharar KL, Prigozhin DM, Snider HM, Beatty PR, Harris E. 2005. Critical roles for both STAT1-dependent and STAT1-independent pathways in the control of primary dengue virus infection in mice. J Immunol 175:3946-3954.

Chapter 14

The RNA genome of hepatitis E virus robustly triggers antiviral interferon response

Wenshi Wang[1], Yijin Wang[2], Changbo Qu[1], Shan Wang[2], Jianhua Zhou[1,3], Wanlu Cao[1], Lei Xu[1], Buyun Ma[1], Mohamad S. Hakim[1,4], Yuebang Yin[1], Tiancheng Li[5], Maikel P. Peppelenbosch[1], Jingmin Zhao[2#],Qiuwei Pan[1#]

[1]Department of Gastroenterology and Hepatology, Postgraduate School Molecular Medicine, Erasmus MC-University Medical Center, Rotterdam, the Netherlands

[2]Department of Pathology and Hepatology, Beijing 302 Hospital, Beijing, P.R. China

[3]State Key Laboratory of Veterinary Etiological Biology, Lanzhou Veterinary Research Institute, Chinese Academy of Agricultural Sciences, Lanzhou, Gansu, P.R. China

[4]Department of Microbiology, Faculty of Medicine, Universitas Gadjah Mada, Yogyakarta, Indonesia

[5]Department of Virology II, National Institute of Infectious Diseases, Gakuen 4-7-1, Musashi-murayama, Tokyo 208-0011, Japan

Hepatology,2018 (in press)

Abstract

The outcomes of hepatitis E virus (HEV) infection are diverse, ranging from asymptomatic carrier, self-limiting acute infection, fulminant hepatitis to persistent infection. This is closely associated with the immunological status of the host. This study aims to understand the innate cellular immunity as the first-line defense mechanisms in response to HEV infection. Phosphorylation of STAT1, a hallmark of the activation of antiviral interferon (IFN) response, was observed in the liver tissues of majority of HEV infected patients, but not in the liver of uninfected individuals. In cultured cell lines and primary liver organoids, we found that HEV RNA genome potently induced IFN production and antiviral response. This mechanism is conserved among different HEV strains, including genotype 1, 3 and 7 as tested. Interestingly, the single-stranded HEV RNA (ssRNA) is sufficient to trigger the antiviral response, without requirement of viral RNA synthesis and the generation of RNA replicative form or replicative intermediate. Surprisingly, the m^7G cap and poly A tail are not required, although both are the key features of HEV genome. Mechanistically, this antiviral response occurs in a RIG-I-, MDA5-, MAVS- and β-catenin-independent, but IRF3 and IRF7-dependent manner. Furthermore, the integrity of the JAK-STAT pathway is essentially required. In conclusion, HEV infection elicits an active IFN-related antiviral response in vitro and in patients. It is triggered by the viral RNA and mediated by IRF3/7 and the JAK-STAT cascade. These findings have revealed new insights on HEV-host interactions and provided the basis for understanding the pathogenesis and outcome of HEV infection.

Keywords: hepatitis E virus; viral RNA; interferon; IRF3/7; JAK-STAT

Introduction

Over the last decade, hepatitis E virus (HEV) infection has emerged as a global health issue. It is one of the most common causes of acute viral hepatitis in the world. Although the infection is generally self-limiting, severe complications and high mortality rates have been reported in special populations, including pregnant women, immunocompromised patients, or patients with pre-existing liver disease (1-3). HEV outbreaks periodically occur throughout the resource limited countries including the large ongoing outbreak in Niger, resulting in heavy clinical burden with high mortality rate in pregnant women (4, 5). Unfortunately, there is no FDA-approved medication available and its infection biology is poorly understood.

Virus infections universally evoke active interactions between the virus and host. Host cells are equipped with mechanisms that rapidly detect and respond to virus invasion. These defense mechanisms largely rely on receptors that monitor the cytosol for the presence of atypical nucleic acids from the virus. DExD/H-box RNA helicases of the RIG-I like receptor (RLR) family have been identified as essential intracellular sensors of RNA viruses. Two of the RLR family members, retinoic acid-inducible gene-I protein (RIG-I) and melanoma differentiation-associated protein 5 (MDA5) are ubiquitously expressed, which enable the detection of viral infection in almost all cell types. Upon the detection of viral RNA ligand, RIG-I or MDA5 interacts with a mitochondrion-anchored adaptor protein, MAVS, to initiate downstream signaling that eventually leads to the transcription and production of interferons (IFNs). Once secreted, IFNs create a state of antiviral alertness by inducing the expression of hundreds of IFN-stimulated genes (ISGs). RIG-I has been reported to be essential for IFN production in the setting of Newcastle disease virus, vesicular stomatitis virus, influenza, and Japanese encephalitis virus infections (6, 7). IFN production is impaired in MDA5 deficient cells infected with Picornaviridae, murine norovirus 1 and the murine hepatitis virus (8-10). Some viruses such as West Nile virus and Dengue virus are recognized by both RIG-I and MDA5 (11, 12). Other intricate viral RNA sensor systems outside the RLR family have also been implicated in eliciting IFN response to virus infection, including DDX3 (13), DHX9 (14), DDX1-DDX21-DHX36 complex (15), NLR NOD2 (nucleotide-binding oligomerization domain 2) (16) and LRRFIP1 (17). It is believed that these intricate RNA sensors act independently or cooperatively to mediate innate immune response upon virus invasion.

HEV is a single-stranded positive-sense RNA virus within the family of *Hepeviridae*. The genome contains short 5′- and 3′-noncoding regions (NCRs), 5′-m^7G cap, 3′-poly A tail and three open reading frames (ORF1, ORF2 and ORF3) (18). In patients, in particular in case of acute infection with severe hepatitis, active virus-host interactions is likely the cause of pathogenesis but also the process of combating the infection (19). In this study, we found the phosphorylation of STAT1 (Y701), a hallmark of IFN-related antiviral response, in the liver of HEV infected patients. Since viral nucleic acid is the main pathogen-associated molecular patterns (PAMPs) recognized by host innate immune system, we delivered *in vitro* generated HEV genomic RNA into host cells to investigate the host response. Consistently, HEV RNA potently induce IFN production and antiviral response in both cell lines and 3D cultured primary liver organoids. Surprisingly, the single-stranded HEV RNA (ssRNA) is sufficient to trigger the host response. This occurs in a RIG-I-, MDA5-, MAVS- and β-catenin-independent, but IRF3 and IRF7-dependent manner. Importantly, the integrity of the JAK-STAT

cascade is required for the antiviral response triggered by HEV. These results have provided novel insights into HEV-host interactions.

Results

Activation of STAT1 phosphorylation in the liver of HEV infected patients

To investigate whether HEV infection activates host antiviral response in patients, the expression of phosphorylated STAT1 (Y701), a hallmark of IFN-related antiviral response, was stained in the liver biopsies (Fig.1A). The staining of HEV viral protein ORF2 and phosphorylated STAT1 (P-STAT1) was scored independently based on the proportion of positive cells (Fig.1B). Up to 89% of HEV infected patients showed a positive staining of phosphorylated STAT1 in the liver; whereas no staining was observed in the liver tissues from uninfected individuals (Fig.1C and Table S1). These results indicated that HEV infection elicits an active IFN-related antiviral responses in patients.

HEV genomic RNA potently induces antiviral IFN response

Upon HEV invasion, HEV-derived components, like viral capsid protein or viral genomic RNA can be sensed as “non-itself” by host innate immunity. Therefore, the potential role of HEV protein ORF2 and ORF3 in IFN response was evaluated firstly. HEK293 cells were transfected with control, ORF2 or ORF3-expressing vectors. The expression of ORF2 or ORF3 protein (sFig. 1A and B) has no significant effect on IFN expression as well as the subsequent ISG induction (sFig.1C and D). To further investigate whether any functional IFNs are produced, we collected the conditioned medium from the transfected cells (supernatant) (sFig.1E) and performed an ISRE-based IFN reporter assay, and a highly IFN-sensitive HCV-replicon based bioassay. Consistently, no IFN production was detected in both models (sFig. 1F and G).

We next examined whether HEV viral RNA is the trigger of host innate immune response. *In vitro* generated HEV genomic RNA was used to efficiently deliver into host cells. Upon transfection of genotype 3 (Gt3) HEV RNA (Kernow-C1, P6) into the human liver hepatoma Huh7.5 cells (named Huh7.5-P6), the viral protein ORF2 was subsequently detected by immunofluorescent assay (sFig.2A). The anti-HEV effects of IFN-α and ribavirin were confirmed in these cells (sFig.2B). After inoculation with conditioned cell culture medium derived from Huh7.5-P6 cells, viral protein was also detected in HEK293 cells (sFig.2C). Therefore, Gt3 HEV RNA generated *in vitro* is functional to initiate the essential steps of HEV life cycle.

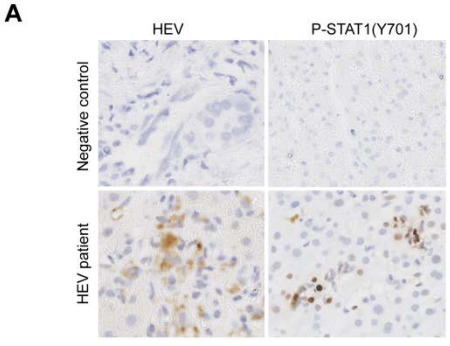

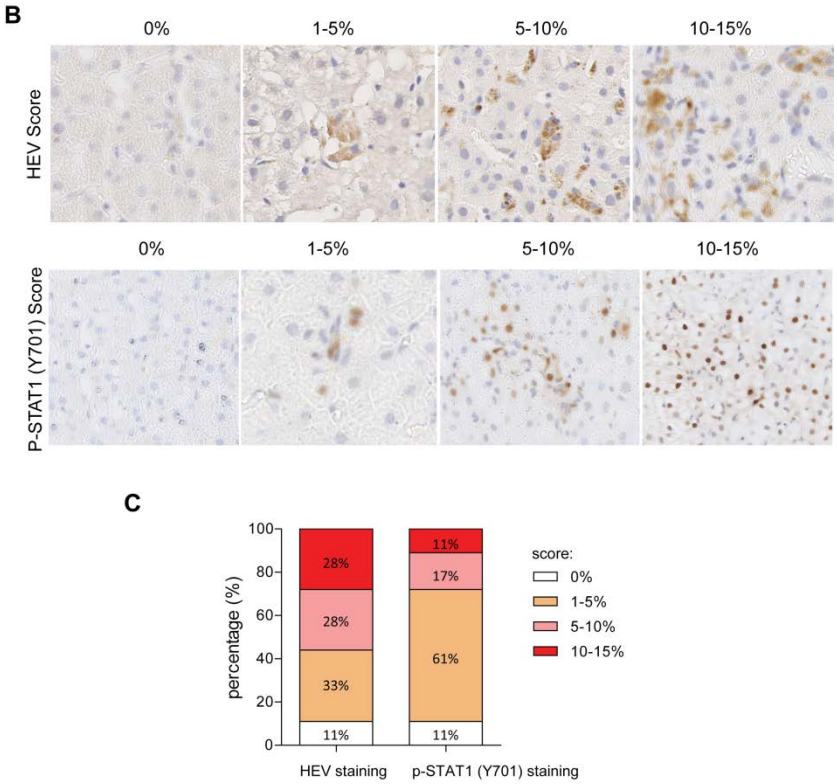

Figure 1. Immunohistochemistry showed the positive staining of P-STAT1 in liver tissues of HEV patients. (A) Representative staining of HEV and P-STAT1 in liver tissue of HEV patients or negative control individuals. (B) Representative staining indicating variable levels of HEV and P-STAT1 on liver tissues. (C) The distribution of HEV and P-STAT1 score among liver tissues.

Importantly, transfection of Gt3 HEV RNA strongly induced IFN response in an dose-dependent manner; while no response was observed in the negative controls, transfection of a GFP vector or cellular RNA. Specifically, the expression of IFNβ (type I IFN), IFNλ1 and IFNλ2 (type III IFN) was strongly induced (Fig. 2A), although no significant change in the levels of IFNα (type I IFN) and IFNγ (type II IFN) (sFig.2D). To examine whether functional IFNs are produced, we collected the conditioned medium from the transfected cells (supernatant) (sFig.1E) and performed an ISRE-based IFN reporter assay, and a highly IFN-sensitive HCV-replicon based bioassay. As shown in Fig. 2B, supernatant from HEK293 cells transfected with Gt3 HEV RNA strongly induced ISRE coupled luciferase activity. Consistently, HCV replicon-related luciferase activity was decreased upon the same treatment (Fig. 2C). Since Interferon-stimulated genes (ISGs) are the downstream antiviral effectors of IFN signaling, thus a list of well-known antiviral ISGs were quantified. The expression levels of these ISGs were significantly up-regulated upon transfection of Gt3 HEV RNA (Fig. 2D). Correspondingly, HEV replicon-related luciferase activity was decreased in HEK293 cells (Fig. 2E). In addition, HEV induced IFN response was further confirmed by the employment of *in vitro* generated genotype 1 (Gt1) HEV and dromedary camel hepatitis E virus (DcHEV; Gt7) (20) (Fig. 2F – I, sFig. 2F). Therefore, in HEK293 cells, HEV could potently induce antiviral IFN response upon viral RNA entry into the cytoplasm.

HEV infection was reported to cause both hepatic and extra-hepatic manifestations, thus we extended our study to hepatic cell lines (Huh7.5 and HepaRG) as well as other extra-hepatic cell line (U87, a neural cell line). Consistently, transfection of HEV RNA led to strong IFN production and IFN response in Huh7.5 (sFig.3), HepaRG (Fig. 3A and B) and U87 cells (Fig. 3C - E). Recently, three dimensional (3-D) cultured primary liver organoids have emerged as innovative models for studying liver physiology and pathology. They contain various types of cells and recapitulate most if not all aspects of *in vivo* liver tissue architecture (21). We further validated that transfection of HEV RNA lead to strong IFN expression and subsequent ISG induction in primary liver organoids cultured from mouse or human liver tissues (Fig. 3F - J).

HEV RNA triggered host response is independent of the m7G cap and poly A tail

HEV genome is a ~ 7.2 kb single stranded RNA with 5' terminal capped (m^7G cap) and 3' terminal polyadenylated (Fig. 4A). The m^7G cap is essential for the HEV infectivity both *in vivo* and *in vitro* (22, 23). The poly A tail is crucial for viral RNA dependent RNA polymerase (RDRP) binding to the 3' UTR (24). Since host cells specifically recognize certain features of the viral nucleic acids, we investigated whether m^7G cap and poly A tail are required for HEV triggered IFN response. Thus, Gt3 HEV RNA lacking m^7G cap or poly A tail were generated *in vitro* and transfected in both HEK293 and Huh7.5 cells. Interestingly, compared with the wild type form, HEV RNA lacking of m^7G cap or poly A tail retains a comparable potency to induce IFN response (Fig.4B and C, sFig.4A - C). These data indicated that HEV triggers IFN response independent of m^7G cap and poly A tail.

The single-stranded HEV RNA (ssRNA) is sufficient to trigger the antiviral response

Upon transfection of HEV RNA genome, the virus replicates and produces different RNA species including ssRNA, viral RNA replicative form (double-stranded RNA, dsRNA) and replicative intermediate. To clarify whether IFN response induced by HEV depend on viral RNA replication and which specific RNA species is involved, two mutant forms of Gt3 HEV RNA (G1634R, G1634K) (Fig. 4A) were transcribed *in vitro*. These two mutant forms have comparable ribavirin sensitivity to the wild type HEV but possessed an enhanced replication fitness *in vitro* (25, 26). However, they exerted comparable activity in inducing IFN response in both HEK293 and Huh7.5 cells when compared with the wild type form (Fig.4D and E, sFig.5A - D). These results imply that the replication of HEV RNA may not be important in this process. To confirm this notion, a replication defective Gt3 HEV replicon (GAD) carrying an alanine substitution in the polymerase active site was used (27, 28). Consistently, compared with wild type form, transfection of Gt3 HEV replicon (GAD) RNA induced strong and comparable IFN response in both HEK293 and Huh7.5 cells (Fig.4F and G, sFig.5E - G). More convincingly, the IFN induction ability of Gt3 HEV replicon (GAD) was also confirmed in other 2-D cultured cell models (*e.g.* HepaRG and U87) (Fig.5A - E) as well as 3-D mouse and human primary liver organoids (Fig.5F - H). Collectively, these results indicate that HEV ssRNA is the specific RNA species involved in triggering IFN response, and this process is independent of viral replication.

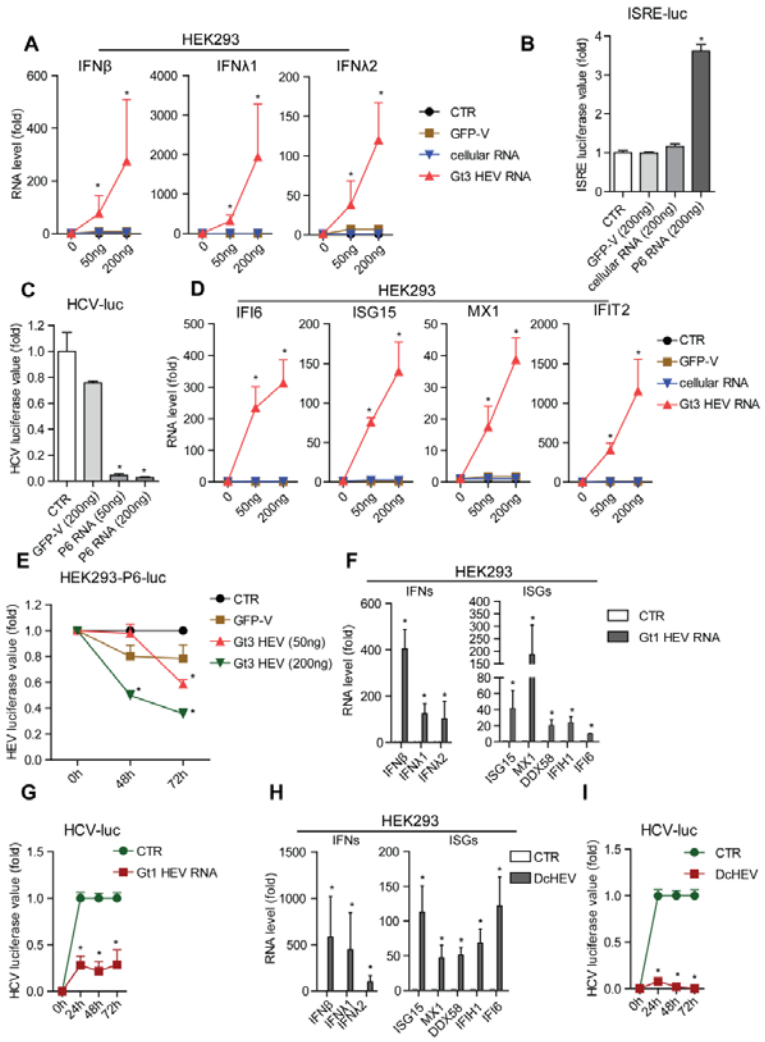

Figure 2. Transfection of HEV RNA potently induces IFN production and IFN response in HEK293 cells. HEK293 cells were transfected with control (transfection reagent only, CTR), GFP-vector (plasmid, GFP-V), cellular RNA or Gt3 HEV RNA. The expression levels of indicated IFNs (A) and ISGs (D) were quantified at 48h.p.t. by qRT-PCR (n = 4). (B) ISRE luciferase value was measured (at 48h) after the treatment of conditioned medium from HEK293 cells transfected with CTR, GFP-V, cellular RNA or Gt3 HEV RNA (n = 6). (C) HCV viral replication-related firefly luciferase activity was measured after the treatment of conditioned medium from HEK293 cells transfected with CTR, GFP-V or Gt3 HEV RNA (n = 4). (E) HEV viral replication-related firefly luciferase activity was measured after the transfection of CTR, GFP-V or Gt3 HEV RNA in HEK293-P6-luc cells (n = 4). HEK293 cells were transfected with CTR, Gt1 HEV RNA (F) or DcHEV RNA (H). The expression levels of indicated IFNs and ISGs were quantified at 48h.p.t. by qRT-PCR (n = 4). HCV viral replication-related firefly luciferase activity was measured after the treatment of conditioned medium from HEK293 cells transfected with Gt1 HEV RNA (G) or DcHEV RNA (I). (n = 4).

It is independent of RIG-I and MDA5

Pattern recognition receptors (PRRs) are the primary sensors detecting viral RNA and subsequently activate antiviral IFN response. They are generally categorized into two major classes depending on their subcellular location, membrane-bound PRRs (*e.g.* Toll-like receptors) and intracellular PRRs (*e.g.* RIG-I-like receptors) (29). Membrane-bound PRRs are predominantly expressed in immune cells, such as macrophages and dendritic cells. Intracellular PRRs are ubiquitously expressed. Our previous study have demonstrated that overexpression of the intracellular PRRs, MDA5 or RIG-I exerts anti-HEV

effects (30). Therefore, we investigated whether these two molecules mediate HEV RNA triggered IFN response.

Interestingly, overexpression of MDA5 triggered IFN production and subsequent IFN response in both HEK293 and Huh7.5 cells (sFig.6A - L). A similar response was observed in HEK293 cells upon the overexpression of RIG-1 (sFig.7A - F), but Huh7.5 cells are defective of RIG-I (30). Consistently, the transfection of 5'-ppp RNA, a specific RIG-I agonist, was unable to induce any IFN responses in Huh7.5 cells (sFig.8A-C). Thus, the fact that HEV triggers IFN response in Huh7.5 cells upon the transfection of viral RNA (sFig. 2C - H) indicates a RIG-I-independent mechanism. To further confirm this notion, wild type (WT) and RIG-I knockout (RIG-I-/-) mouse embryonic fibroblasts (MEF) was employed. The efficient knockout of RIG-I was confirmed by both 5'-ppp RNA transfection assay and western blot assay (sFig.8D and E). Transfection of Gt3 HEV RNA strongly induced IFNβ and representative ISG expression in RIG-I-/- MEF cells (Fig.6A and B, left and right panels). In addition, the conditioned medium was collected from RIG-I-/- MEF cells transfected with Gt3 HEV RNA. Incubation of conditioned medium efficiently induced STAT1 phosphorylation, a key feature of IFN signaling pathway activation. Collectively, HEV initiates IFN production and IFN response independent of RIG-I.

Next, we examined the involvement of MDA5. The efficient knockout of MDA5 (MDA5-/-) was confirmed by western blot assay (sFig. 8F). Strikingly, transfection of HEV RNA in MDA5-/- MEF cells can also strongly induce IFN production and IFN response (Fig.6C), indicating a MDA5 - independent mechanism. Some viruses such as West Nile virus and Dengue virus are recognized by both MDA5 and RIG-I to initiate IFN response (11, 12). This forced us to clarify whether HEV induced IFN response require both MDA5 and RIG-I. Therefore, HEV RNA was transfected in RIG-I and MDA5 double knockout (RIG-I and MDA5-/-) MEF cells (sFig.8E and F). However, IFN production and IFN response were still efficiently initiated (Fig.6D). On the contrary, transfection of a commonly used RIG-I/MDA5 agonist, poly (I;C) only induced IFNβ and ISGs expression in WT, while not RIG-I and MDA5-/- MEF cells (sFig.8G). Thus, HEV RNA triggered IFN response is independent of both MDA5 and RIG-I.

HEV RNA triggered antiviral response is independent of MAVS and β-catenin, but requiring IRF3 and IRF7

In addition to RIG-I and MDA5, other proteins have been implicated in cytosolic sensing of viral RNA to trigger IFN response. They include DDX3 (13), DHX9 (14), DDX1-DDX21-DHX36 complex (15), and NLR NOD2 (nucleotide-binding oligomerization domain 2) (16). Importantly, similar with RIG-I and MDA5, these proteins are thought to sense viral RNA and induce IFN expression in a MAVS-dependent manner. Surprisingly, in MAVS knock out (MAVS-/-) MEFs, IFN response was strongly induced after the transfection of HEV RNA (Fig.6E). Notably, the cytosolic nucleic acid sensor LRRFIP1 has been reported to sense DNA and RNA viruses, thus mediating IFN response via a MAVS-independent, but β-catenin-dependent pathway (17). Therefore, the involvement of β-catenin was investigated by employing β-catenin-/- MEF cells (sFig.8H). Remarkably, the transfection of HEV RNA initiated strong IFN response in β-catenin-/- MEF cells (sFig. 8I). These results indicated that HEV RNA is most likely recognized by a currently undefined or unknown cytosolic nucleic acid sensor to activate antiviral IFN response via MAVS- and β-catenin-independent mechanisms.

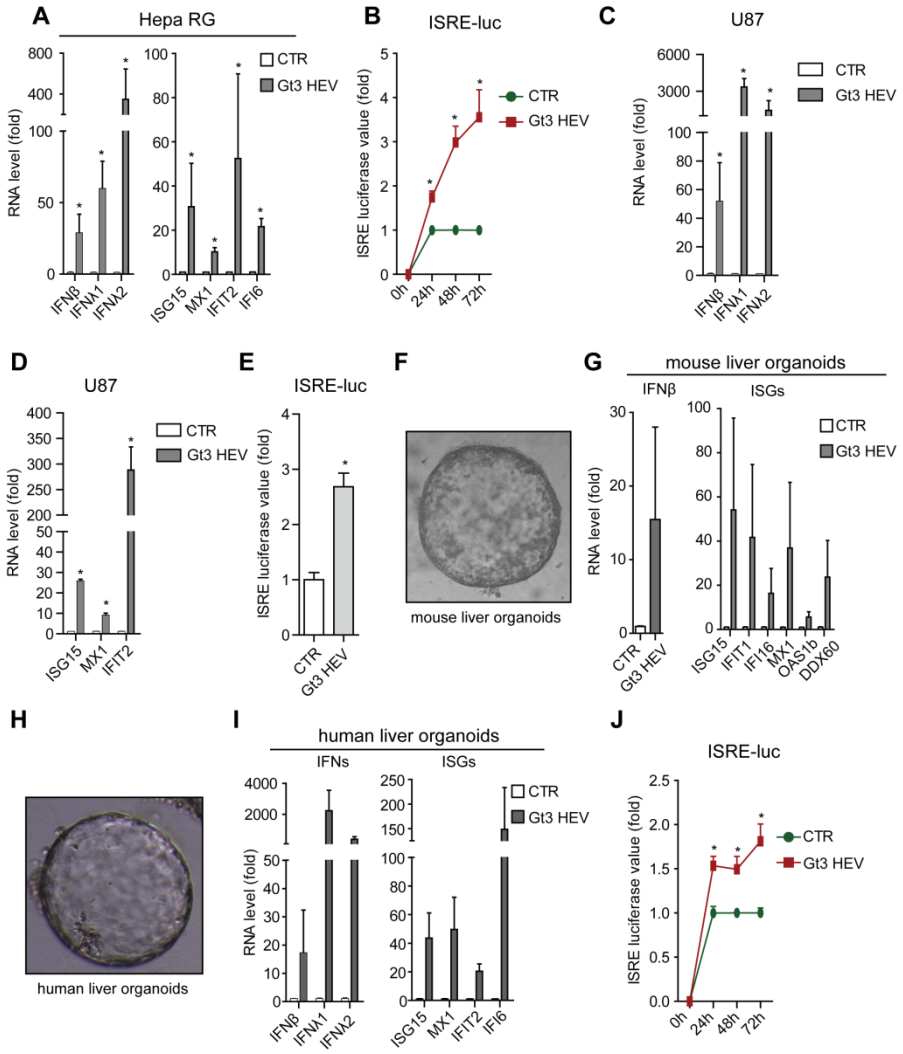

Figure 3. Transfection of HEV RNA induces antiviral response in both 2-D and 3-D cell culture models. (A) HepaRG cells were transfected with CTR, GFP-V or Gt3 HEV RNA (200 ng / well) in 96-well plates. The expression levels of indicated IFNs and ISGs were quantified at 48h.p.t. by qRT-PCR (n = 4). (B) ISRE luciferase value was measured after the treatment of conditioned medium from HepaRG cells transfected with CTR, GFP-V or Gt3 HEV RNA (n = 5). (C) and (D) Same as (A) for U87 cells. (E) Same as (B) for U87 conditioned medium measured at 24h. Representative microscopy image of 3-D cultured mouse (F) and human (H) primary liver organoids. (G) After the transfection of Gt3 HEV RNA in mouse liver organoids, the expression levels of IFNβ and indicated ISGs were quantified at 48h.p.t. by qRT-PCR (n = 4). (I) Same as (G) for human liver organoids (n = 4). (H) Same as (B) for human liver organoids (n = 5).

Given the essential role of two transcription factors, IRF3 and IRF7, in the production of IFNs, we investigated whether these two factors are required. Transfection of HEV RNA failed to stimulate any IFNβ and ISG expression in IRF3 and IRF7 knock out MEFs (Fig.6F, left and right panel). Correspondingly, incubation of conditioned medium (supernatant, IRF3 and IRF7-/- MEFs transfected with HEV RNA) has no effect on STAT1 phosphorylation (Fig.6F,middle panel). Therefore, HEV induces IFN responses in an IRF3 and IRF7-dependent manner. Since HEV ssRNA is the specific RNA species involved in IFN responses, the replication defective Gt3 HEV replicon (GAD) RNA was tested as well. Consistent with its wild type, Gt3 HEV replicon (GAD) RNA induces IFN response in a RIG-I-, MDA5-, MAVS- and β-catenin-independent, but IRF3 and IRF7-dependent manner (Fig.7A - F, sFig.8J).

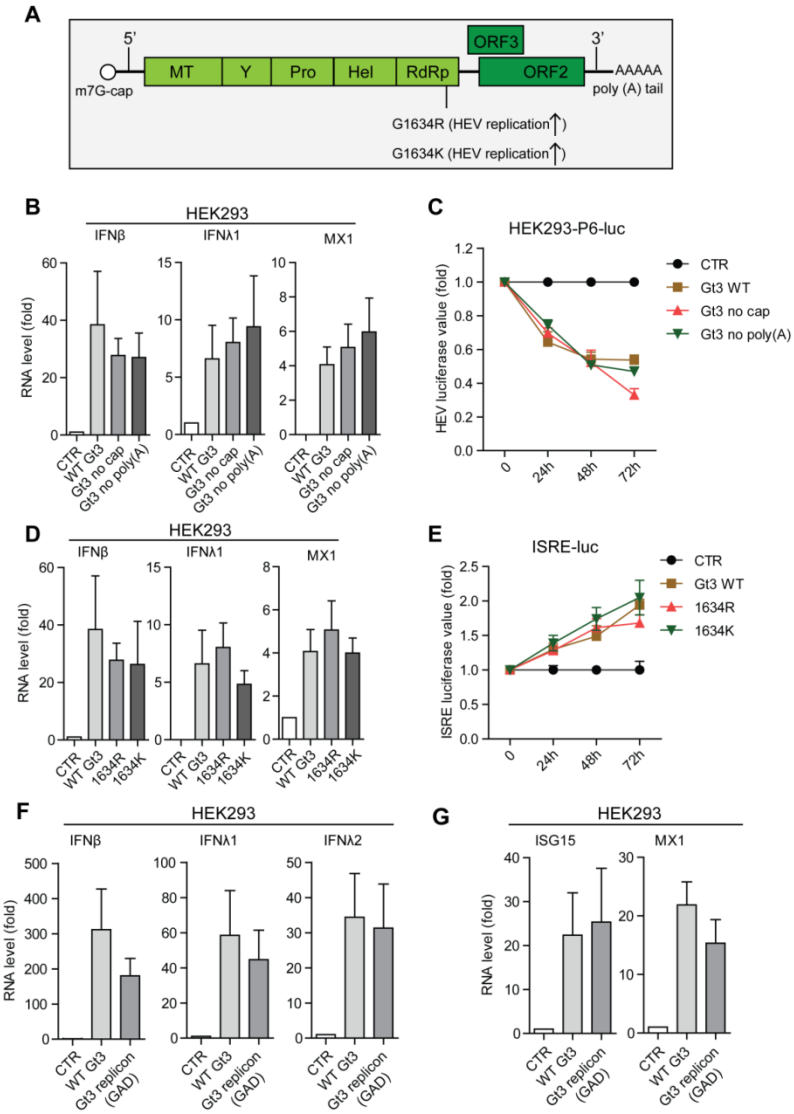

Figure 4. HEV ssRNA is sufficient to trigger IFN response, while independent of viral RNA m^{7}G cap and poly A tail. (A) The illustration of HEV RNA genome (MT, Methyltransferase; Y, Y-domain; Pro, protease; Hel, helicase; RdRp, RNA-dependent RNA polymerase). (B) HEK293 cells were transfected with CTR, wild type (WT), no m^{7}G cap or no poly A tail Gt3 HEV RNA (200ng / well) in 96-well plates. The expression levels of indicated IFNs and ISGs were quantified at 48h.p.t. by qRT-PCR (n = 3). (C) HEV viral replication-related firefly luciferase activity was measured after the same transfection indicated in (B) in HEK293-P6-luc cells (n = 4). (D) HEK293 cells were transfected with CTR, WT, 1634R mutant or 1634K mutant Gt3 HEV RNA (200ng / well) in 96-well plates. The expression levels of indicated IFNs and ISGs were quantified at 48h.p.t. by qRT-PCR (n = 3). (E) ISRE luciferase value was measured after the treatment of conditioned medium from HEK293 cells transfected with CTR, WT, 1634R mutant or 1634K mutant Gt3 HEV RNA (n = 4). HEK293 cells were transfected with CTR, WT or replication defective Gt3 HEV replicon (GAD) RNA (n = 4). The expression levels of indicated IFNs (F) and ISGs (G) were quantified at 48h.p.t. by qRT-PCR.

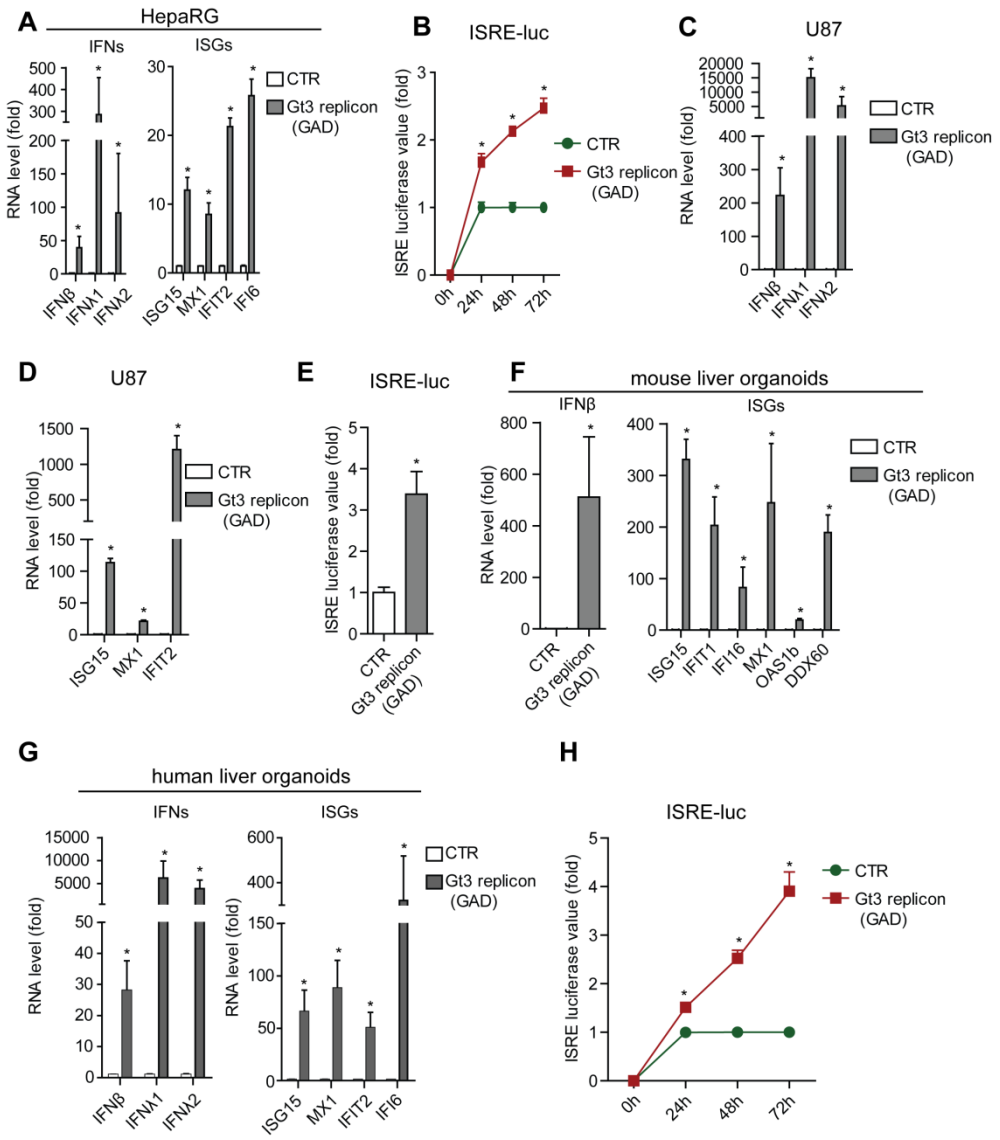

Figure 5. HEV ssRNA triggers IFN response in both 2-D and 3-D cell culture models. (A) HepaRG cells were transfected with Gt3 HEV replicon (GAD) RNA (200ng / well) in 96-well plates. The expression levels of indicated IFNs and ISGs were quantified at 48h.p.t. by qRT-PCR (n = 4). (B) ISRE luciferase value was measured after the treatment of conditioned medium from HepaRG cells transfected with Gt3 HEV replicon (GAD) RNA (n = 5). (C) and (D) Same as (A) for U87 cells. (E) Same as (B) for conditioned medium from U87 cells. (F) Same as (A) for mouse liver organoids (n = 4). (G) Same as (A) for human liver organoids (n = 4). (H) Same as (B) for human liver organoids (n = 5).

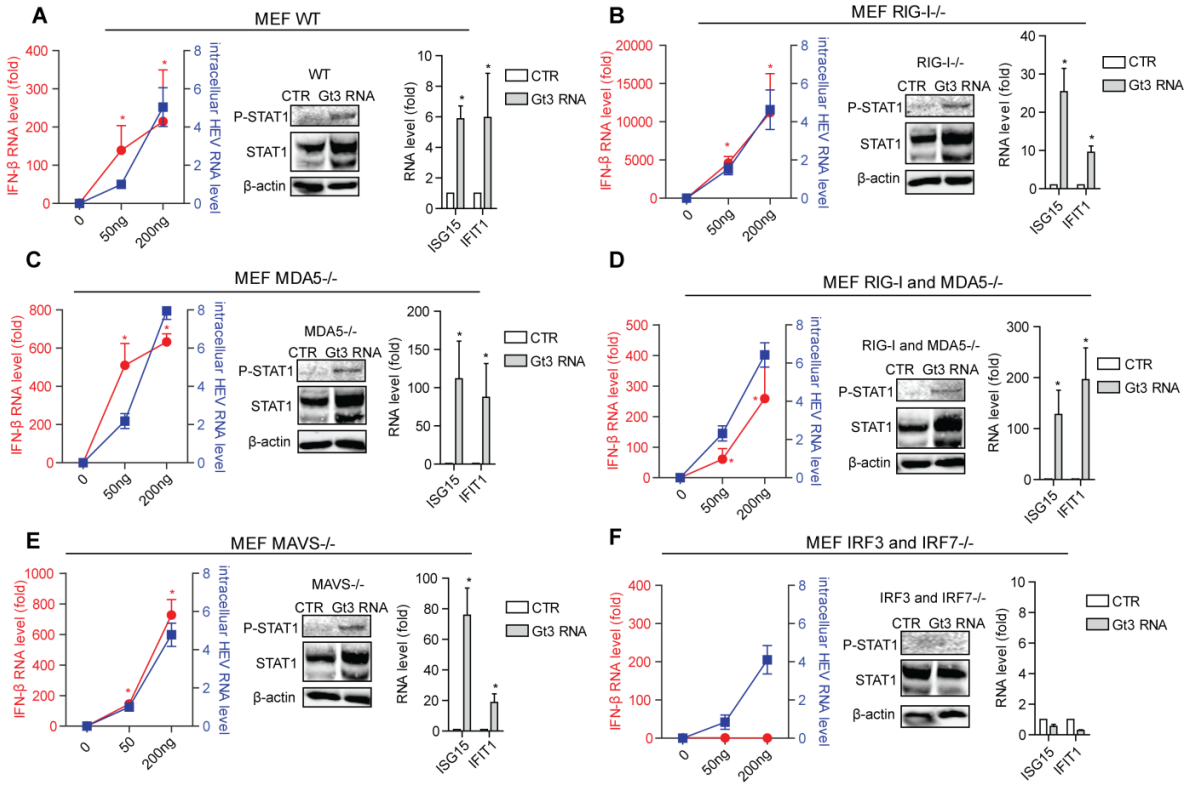

Figure 6. HEV triggers IFN response in a RIG-I-, MDA5- and MAVS-independent but IRF3/IRF7-dependent manner. The transfection of Gt3 HEV RNA (200ng / well) was performed in WT (A), RIG-I-/- (B), MDA5-/- (C), RIG-I and MDA5-/- (D), MAVS-/- (E) and IRF3/IRF7-/- (F) MEFs in 96-well plates. The levels of IFNβ (red line) and the relative intracellular HEV RNA (blue line) were quantified at 48h.p.t. by qRT-PCR (n = 4) (left panel). The MEF cells were treated with conditioned medium collected from indicated cells for 24h. The protein levels of total and phosphorylated (Y701) STAT1 were detected by WB (middle panel). The expression levels of representative ISGs (ISG15 and IFIT1) were quantified at 48h.p.t. by qRT-PCR (n = 4) (right panel).

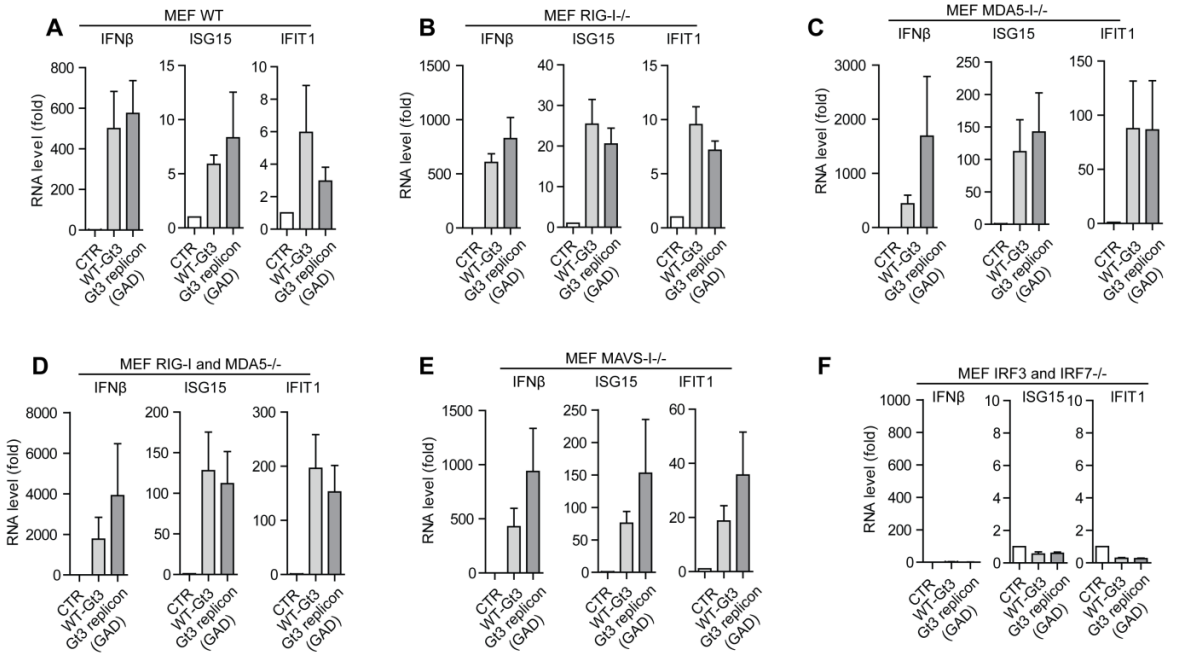

Figure 7. HEV ssRNA triggers IFN response in a MAVS-independent but IRF3/IRF7-dependent manner. The transfection of WT or Gt3 HEV replicon (GAD) RNA was performed in WT (A), RIG-I-/- (B), MDA5-/- (C), RIG-I and MDA5-/- (D), MAVS-/- (E) and IRF3/IRF7-/- (F) MEFs. The levels of IFNβ and the indicated ISGs were quantified at 48h.p.t. by qRT-PCR (n = 4).

The integrity of the JAK-STAT cascade is essential for the antiviral response

Upon IFN production, the thus-released IFN molecules bind to cell-surface receptors and initiate signal transduction prominently via the Janus kinase/signal transducer and activator of transcription (JAK–STAT) pathway. This activates the transcription of hundreds of ISGs that are the effectors of cell-autonomous antiviral defense (31). The transfection of HEV RNA in U3A cells (which are STAT1-deficient) or U6A cells (which are STAT2-deficient) achieved much lower expression levels of ISGs compared with their wild type (Fig. 8A). Strikingly, the expression of IFNs was also largely demolished (Fig. 8B). This was further supported by the use of JAK inhibitor I, a pharmacological JAK inhibitor to block JAK–STAT signal transduction (sFig.8K). JAK inhibitor I sufficiently blocked HEV RNA induced ISG and IFN expression in both HEK293 and Huh7.5 cells (Fig.8C - I). Therefore, the integrity of JAK–STAT pathway is essential for HEV induced IFN response and (in turn) IFN production.

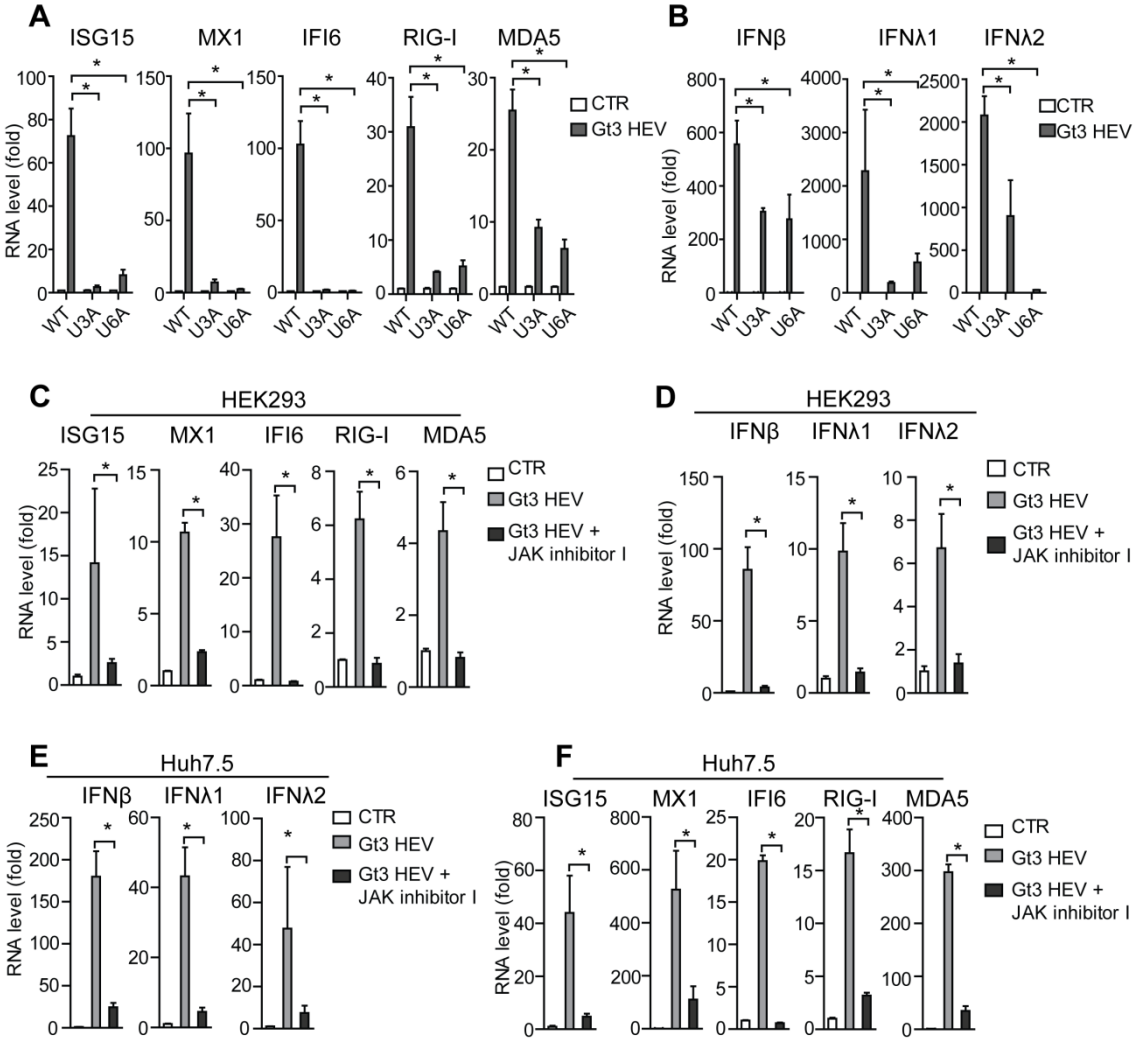

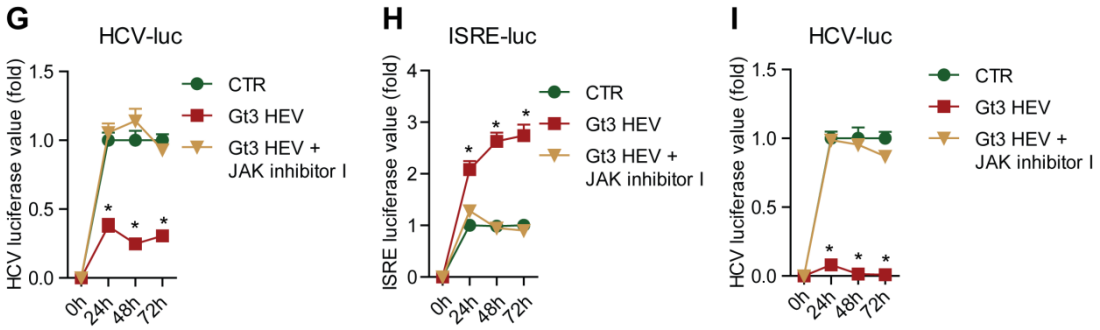

Figure 8. The integrity of JAK–STAT pathway is essential for HEV induced antiviral response.
Gt3 HEV RNA was transfected in WT, U3A (STAT1 deficient) and U6A (STAT2 deficient) cells. The levels of ISGs (A) and IFNs (B) were quantified at 48h.p.t. by qRT-PCR (n = 4). Gt3 HEV RNA was transfected in HEK293 cells with or without JAK inhibitor I (10μm). The levels of ISGs (C) and IFNs (D) were quantified at 48h.p.t. by qRT-PCR (n = 4).(E) Same as (C) for Huh7.5 cells. (F) Same as (D) for Huh7.5 cells. (G) HCV viral replication-related firefly luciferase activity was measured after the treatment of conditioned medium from HEK293 cells transfected with Gt3 HEV RNA with or without JAK inhibitor I (n = 4). (H) ISRE luciferase value was measured after the treatment of conditioned medium from Huh7.5 cells transfected with Gt3 HEV RNA with or without JAK inhibitor I (n = 4). (I) Same as (G) for Huh7.5 cells.

Discussion

The innate immune system is a major host defense machinery triggered by viral infections. One prominent characteristic is the rapid and efficient detection of invading pathogens through recognition of the PAMPs by host PRRs. After specific ligand recognition, host PRRs initiate distinct signaling transduction that lead to the production and secretion of IFNs. IFNs transcriptionally stimulate hundreds of ISGs via the JAK–STAT pathway, thus creating an antiviral state. IFNs in particular IFN-α have been approved for treating viral infections in clinic for decades, including chronic hepatitis B (HBV) and C virus (HCV) infections. IFN-α has also been used as an off-label drug to treat chronic HEV infection (2). Therefore, identifying the cellular innate immune response during virus infection has attracted much attention in recent years. In this study, we found that HEV infection could elicit an active IFN-related antiviral responses in most patients. Mechanistically, we found that HEV RNA could potently induce IFN production and antiviral response upon entry into the cytoplasm. This observation was captured in two dimensional culture of hepatic and extra-hepatic cell lines as well as three dimensional culture of mouse and human primary liver organoids.

HEV genome is a positive-stranded RNA with 5' terminal capped (m^7G cap) and 3' terminal polyadenylated. The m^7G cap structure was critical for efficient infectivity in cell culture models (23). Furthermore, the intrahepatic inoculation of uncapped transcripts failed to initiate HEV infection in chimpanzees even followed for 20 weeks (22). The 3' end of HEV genome could bind specifically to the viral RdRp, directing the synthesis of complementary-strand RNA (24). However, these key features are not essential for HEV triggered IFN response.

After HEV RNA genome entering into host cells, viral replication was initiated. Therefore, different viral RNA species are produced and co-exist, including ssRNA, dsRNA and replicative intermediate. With respect to different viruses, host PRRs recognize different specific PAMPs to initiate IFN productions. For most viruses, like dengue virus, Japanese encephalitis virus or picornavirus, viral replicative form (dsRNA) serves as an IFN inducer (8, 32). However, for some viruses, like respiratory syncytial virus and influenza A virus, ssRNA could induce IFN production (16,

29). In our study, we found that HEV ssRNA is sufficient in inducing IFN response, independent of viral replication. This suggests that host cells are capable to immediately sense HEV invasion before the starting of viral replication.

In the cytosol, RLR helicase subfamily (*e.g.* RIG-I and MDA5) serve as essential immune sensors to detect viral nucleic acids. Upon ligand binding and recognition, RIG-I and MDA5 undergo conformational changes that activate the signaling partner MAVS on the mitochondrial and peroxisomal membranes. MAVS can signal to downstream signaling pathways by activating the serine/threonine-protein kinase IKK and TBK-1 kinases, leading to the induction of IFNs. In our study, overexpression of either RIG-I or MDA5 could efficiently initiate IFN production and subsequent IFN response in particular cell lines. In addition to RLRs, other RNA sensor-related pathways have been implicated in the IFN response to viruses. They include DDX3 (13), DHX9 (14), DDX1-DDX21-DHX36 complex (15), NLR NOD2 (nucleotide-binding oligomerization domain 2) (16) and LRRFIP1-β-catenin pathways (17). With respect to the fact that host cells may encounter a wide variety of intracellular virus infections, these diversified RNA sensors may act both independently and/or cooperatively with the classical RLRs to more efficiently mediate antiviral response. Strikingly, we found that HEV ssRNA induced IFN response is largely independent of the classical RLRs as well as the other RNA sensing pathways as mentioned. However, it is via an IRF3- and IRF7-dependent manner, which is consistent with the essential role of these two transcription factors in IFN production. Therefore, our present study strongly indicates that HEV RNA is likely recognized by a undefined or unknown cytosolic RNA-sensing systems, which deserves further investigation. An unbiased biochemical screen or a genome-wide CRISPR-based screen represents the state-of-art tools to identify and investigate uncharacterized host factors possessing PRRs function.

IFN-mediated innate immune response forms a first line of cell-autonomous defense against pathogens. IFN activates the JAK–STAT pathway, leading to the induction of a wide array of ISGs. Functionally, they are divided into three groups: antiviral effector, negative regulator and positive regulator. ISGs, such as MX1 and ISG15, are antiviral effectors. They control infection by directly targeting pathways and functions essential for pathogen life cycles. some ISGs (*e.g.* SOCS, USP18) are negative regulators. They help resolve the IFN–induced state and return to cellular homeostasis. ISGs, including RIG-I, MDA5, IRFs and STAT1/2, serve as positive regulators to reinforce IFN response. In our study, when the integrity of JAK–STAT pathway was compromised, the expression levels of ISGs induced by HEV were largely blocked. They include antiviral effector (e.g. MX1, ISG15) as well as positive regulators (e.g. RIG-I and MDA5) (Fig. 7). This in turn lead to the attenuation of IFN expression and production. Therefore, the integrity of JAK-STAT cascade is essentially required for HEV-triggered antiviral IFN response.

Our findings that the host cells can rapidly recognize the income HEV genomic ssRNA and evolve potent antiviral response may explain the asymptomatic infection in the general population. A subset of patients with acute hepatitis eventually clear the infection through active virus-host interactions, although pregnant women bear high risk to develop fulminant hepatitis with mortality rate reaching up to 25% (18). In immunocompromised patients, chronic infection has been widely reported, which is conceivably attributed to compromised innate and adaptive immunity (33, 34). Consistently, a recent study have reported that persistent HEV infection in cell culture does not activate type I IFN, although companied by a type III IFN response (35). In our study, we found that HEV RNA activates both type I and III IFN responses, resulting in potent antiviral effects, which more

likely reflected the infection phase with active virus-host interactions in HEV patients. Of note, other elements of the virus, in particular the HEV viral proteins, are also capable of modulating antiviral response (36-39), thus collectively determine the eventual infection course and clinical outcome.

In summary, we have demonstrated that HEV infection elicit an active antiviral interferon response triggered by the viral genome. The incoming genomic ssRNA is the specific viral RNA species to trigger the response. This occurs in a RLRs-, MAVS- and β-catenin- independent, but IRF3 and IRF7-dependent manner. Important, the integrity of JAK-STAT pathway is required for the host antiviral response. These findings have revealed new insights on HEV-host interactions and may provide new avenues for antiviral drug development.

Materials and Methods

Patient materials

Eighteen liver biopsies from patients (2010 – 2017) diagnosed of acute or chronic hepatitis E were retrieved at Beijing 302 hospital, China. The use of patient materials was approved by the medical ethical committee of Beijing 302 hospital. The expression of P-STAT1 (Y701) was stained. Five liver biopsies from hepatic hemangioma patients were collected as negative control. These patient information was shown in Table S1.

Immunohistochemistry (IHC) staining

Immunohistochemistry staining of HEV ORF2 viral protein or P-STAT1 (Y701) was performed to validate HEV infection and visualize phosphorylated-STAT1. In detail, the liver biopsies were fixed in 10% formalin for 1.5 h at room temperature, processed for paraffin embedding, and sectioned at a thickness of 4 μm. The sections were deparaffinized in xylene and rehydrated through graded ethanol treatment, followed by high pressure in citrate buffer (pH 6.0) for 3 min for antigen retrieval. Then they were blocked with 3% H_2O_2 in TBS for 15 min and further blocked with goat serum for 1 hour. The sections were incubated with anti-HEV ORF2 viral protein (Millipore,1:600) or anti-P-STAT1 (Cell signaling,1:800) monoclonal antibody overnight at 4 °C, and incubated with goat anti-mouse/rabbit secondary antibody (ZSGB-BIO,KIT-5030) for 15 min at 37°C. Subsequently, the sections were developed with diaminobenzidine (DAB) (ZSGB-BIO, ZLI-9018), followed by counterstaining hematoxylin. Immunostained sections were scanned using Leica DFC400 digital camera and Leica Application Suite software (Leica Microsystems).

Plasmids and Reagents

The plasmids constructs containing the full-length Gt1 HEV genome (Sar55/S17, GenBank Accession Number: AF444002), Gt3 HEV genome (Kernow-C1 P6 clone, GenBank Accession Number: JQ679013) and HEV replication defective genome (GAD) were kindly provided by Suzanne U. Emerson (National Institute of Allergy and Infectious Diseases, National Institutes of Health, Bethesda, MD). The plasmid containing the full-length dromedary camel HEV genome (GenBank Accession: KJ496144) was kindly provided by Tian-Cheng Li (National Institute of Infectious Diseases, Japan). The plasmids constructs containing the full-length HEV genome (Kernow-C1 P6 clone) with 1634R or 1634K mutations were generated accordingly (25). Plasmid pLVX-ORF2-IRES-zsGrenn1 was

kindly provided by Alexander Ploss (Princeton University) (40). Plasmid pEGFP-C1-ORF3 was constructed in our lab. pTRIP.CMV.IVSb.ISG.ires.TagRFP based RIG-I and MDA5 expression vectors were a kind gift from Prof. Charles M. Rice, the Rockefeller University (41). Human IFN-α (Thermo Fisher Scientific, Life Sciences, the Netherlands) was dissolved in PBS. 5'ppp-dsRNA was purchased from InvivoGen (#tlrl-3prna, InvivoGen, CA, USA). FuGENE® HD Transfection reagent (E2311) was purchased from Promega, USA. Stocks of JAK inhibitor I was dissolved in DMSO at a concentration of 10 mM. Antibodies including phospho-STAT1 (58D6, #9167), RIG-I (D14G6, #3743), MDA5 (D74E4, #5321), β-catenin (6B3, #9582), anti-rabbit IgG(H+L),F(ab') 2 Fragment (Alexa Fluor 488 conjugate) and anti-mouse IgG (H+L), F(ab')2 Fragment (Alexa Fluor® 488 Conjugate) were purchased from Cell Signaling Technology, the Netherlands. Hepatitis E Monoclonal Antibody was purchased from EMD Millipore Corporation, USA. Anti-rabbit or anti-mouse IRDye-conjugated antibodies were used as secondary antibodies for western blotting (Stressgen, Victoria, BC, Canada).

Additional procedures are described in detail in *Supplementary Materials and Methods.*

Acknowledgements

The authors gratefully thank S. U. Emerson (National Institute of Allergy and Infectious Diseases, NIH, USA) for generously providing the plasmids to generate Gt 1, Gt3 HEV genomic RNA and HEV replication defective genome (GAD) RNA; G. R. Stark (Lerner Research Institute) for providing the U3A and U6A cells;. C. M. Rice (the Rockefeller University) for providing pTRIP.CMV.IVSb.ISG.ires.TagRFP based RIG-I and MDA5 expression vectors; S. M. Mäkelä (National Institute for Health and Welfare Viral Infections Unit, Helsinki, Finland) for providing MEF cells (WT, RIG-I-/-, MDA5-/-, RIG-I and MDA5-/-, MAVS-/-, IRF3/7-/-); K. Basler (University of Zürich) for providing β-catenin-/- MEF cells.

References

1. Blasco-Perrin H, Abravanel F, Blasco-Baque V, Peron JM. Hepatitis E, the neglected one. Liver Int 2016;36 Suppl 1:130-134.
2. Dalton HR, Kamar N. Treatment of hepatitis E virus. Curr Opin Infect Dis 2016;29:639-644.
3. Hakim MS, Wang W, Bramer WM, Geng J, Huang F, de Man RA, Peppelenbosch MP, et al. The global burden of hepatitis E outbreaks: a systematic review. Liver Int 2017;37:19-31.
4. Azman AS, Bouhenia M, Iyer AS, Rumunu J, Laku RL, Wamala JF, Rodriguez-Barraquer I, et al. High Hepatitis E Seroprevalence Among Displaced Persons in South Sudan. Am J Trop Med Hyg 2017;96:1296-1301.
5. Rayis DA, Jumaa AM, Gasim GI, Karsany MS, Adam I. An outbreak of hepatitis E and high maternal mortality at Port Sudan, Eastern Sudan. Pathog Glob Health 2013;107:66-68.
6. Loo YM, Fornek J, Crochet N, Bajwa G, Perwitasari O, Martinez-Sobrido L, Akira S, et al. Distinct RIG-I and MDA5 signaling by RNA viruses in innate immunity. J Virol 2008;82:335-345.
7. Kato H, Takeuchi O, Mikamo-Satoh E, Hirai R, Kawai T, Matsushita K, Hiiragi A, et al. Length-dependent recognition of double-stranded ribonucleic acids by retinoic acid-inducible gene-I and melanoma differentiation-associated gene 5. J Exp Med 2008;205:1601-1610.
8. Feng Q, Hato SV, Langereis MA, Zoll J, Virgen-Slane R, Peisley A, Hur S, et al. MDA5 detects the double-stranded RNA replicative form in picornavirus-infected cells. Cell Rep 2012;2:1187-1196.
9. McCartney SA, Thackray LB, Gitlin L, Gilfillan S, Virgin HW, Colonna M. MDA-5 recognition of a murine norovirus. PLoS Pathog 2008;4:e1000108.
10. Roth-Cross JK, Bender SJ, Weiss SR. Murine coronavirus mouse hepatitis virus is recognized by MDA5 and induces type I interferon in brain macrophages/microglia. J Virol 2008;82:9829-9838.
11. Fredericksen BL, Keller BC, Fornek J, Katze MG, Gale M, Jr. Establishment and maintenance of the innate antiviral response to West Nile Virus involves both RIG-I and MDA5 signaling through IPS-1. J Virol 2008;82:609-616.
12. Goubau D, Deddouche S, Reis e Sousa C. Cytosolic sensing of viruses. Immunity 2013;38:855-869.
13. Oshiumi H, Sakai K, Matsumoto M, Seya T. DEAD/H BOX 3 (DDX3) helicase binds the RIG-I adaptor IPS-1 to up-regulate IFN-beta-inducing potential. Eur J Immunol 2010;40:940-948.

14. Zhang Z, Yuan B, Lu N, Facchinetti V, Liu YJ. DHX9 pairs with IPS-1 to sense double-stranded RNA in myeloid dendritic cells. J Immunol 2011;187:4501-4508.
15. Zhang Z, Kim T, Bao M, Facchinetti V, Jung SY, Ghaffari AA, Qin J, et al. DDX1, DDX21, and DHX36 helicases form a complex with the adaptor molecule TRIF to sense dsRNA in dendritic cells. Immunity 2011;34:866-878.
16. Sabbah A, Chang TH, Harnack R, Frohlich V, Tominaga K, Dube PH, Xiang Y, et al. Activation of innate immune antiviral responses by Nod2. Nat Immunol 2009;10:1073-1080.
17. Yang P, An H, Liu X, Wen M, Zheng Y, Rui Y, Cao X. The cytosolic nucleic acid sensor LRRFIP1 mediates the production of type I interferon via a beta-catenin-dependent pathway. Nat Immunol 2010;11:487-494.
18. Panda SK, Varma SP. Hepatitis e: molecular virology and pathogenesis. J Clin Exp Hepatol 2013;3:114-124.
19. Friedman LS, Lee SR, Nelson SB, Masia R. Case 36-2016. A 50-Year-Old Man with Acute Liver Injury. N Engl J Med 2016;375:2082-2092.
20. Li TC, Zhou X, Yoshizaki S, Ami Y, Suzaki Y, Nakamura T, Takeda N, et al. Production of infectious dromedary camel hepatitis E virus by a reverse genetic system: Potential for zoonotic infection. J Hepatol 2016;65:1104-1111.
21. Huch M, Gehart H, van Boxtel R, Hamer K, Blokzijl F, Verstegen MM, Ellis E, et al. Long-term culture of genome-stable bipotent stem cells from adult human liver. Cell 2015;160:299-312.
22. Emerson SU, Zhang M, Meng XJ, Nguyen H, St Claire M, Govindarajan S, Huang YK, et al. Recombinant hepatitis E virus genomes infectious for primates: importance of capping and discovery of a cis-reactive element. Proc Natl Acad Sci U S A 2001;98:15270-15275.
23. Emerson SU, Nguyen H, Graff J, Stephany DA, Brockington A, Purcell RH. In vitro replication of hepatitis E virus (HEV) genomes and of an HEV replicon expressing green fluorescent protein. J Virol 2004;78:4838-4846.
24. Agrawal S, Gupta D, Panda SK. The 3' end of hepatitis E virus (HEV) genome binds specifically to the viral RNA-dependent RNA polymerase (RdRp). Virology 2001;282:87-101.
25. Debing Y, Gisa A, Dallmeier K, Pischke S, Bremer B, Manns M, Wedemeyer H, et al. A mutation in the hepatitis E virus RNA polymerase promotes its replication and associates with ribavirin treatment failure in organ transplant recipients. Gastroenterology 2014;147:1008-1011 e1007; quiz e1015-1006.
26. Todt D, Gisa A, Radonic A, Nitsche A, Behrendt P, Suneetha PV, Pischke S, et al. In vivo evidence for ribavirin-induced mutagenesis of the hepatitis E virus genome. Gut 2016;65:1733-1743.
27. Shukla P, Nguyen HT, Torian U, Engle RE, Faulk K, Dalton HR, Bendall RP, et al. Cross-species infections of cultured cells by hepatitis E virus and discovery of an infectious virus-host recombinant. Proc Natl Acad Sci U S A 2011;108:2438-2443.
28. Wang W, Wang Y, Debing Y, Zhou X, Yin Y, Xu L, Herrera Carrillo E, et al. Biological or pharmacological activation of protein kinase C alpha constrains hepatitis E virus replication. Antiviral Res 2017;140:1-12.
29. Chan YK, Gack MU. Viral evasion of intracellular DNA and RNA sensing. Nat Rev Microbiol 2016;14:360-373.
30. Xu L, Wang W, Li Y, Zhou X, Yin Y, Wang Y, de Man RA, et al. RIG-I Is A Key Antiviral Interferon-Stimulated Gene Against Hepatitis E Virus Dispensable Of Interferon Production. Hepatology 2017.
31. Wang W, Xu L, Su J, Peppelenbosch MP, Pan Q. Transcriptional Regulation of Antiviral Interferon-Stimulated Genes. Trends Microbiol 2017.
32. Uchida L, Espada-Murao LA, Takamatsu Y, Okamoto K, Hayasaka D, Yu F, Nabeshima T, et al. The dengue virus conceals double-stranded RNA in the intracellular membrane to escape from an interferon response. Sci Rep 2014;4:7395.
33. Moal V, Textoris J, Ben Amara A, Mehraj V, Berland Y, Colson P, Mege JL. Chronic hepatitis E virus infection is specifically associated with an interferon-related transcriptional program. J Infect Dis 2013;207:125-132.
34. Gerolami R, Moal V, Colson P. Chronic hepatitis E with cirrhosis in a kidney-transplant recipient. N Engl J Med 2008;358:859-860.
35. Yin X, Li X, Ambardekar C, Hu Z, Lhomme S, Feng Z. Hepatitis E virus persists in the presence of a type III interferon response. PLoS Pathog 2017;13:e1006417.
36. Nan Y, Ma Z, Wang R, Yu Y, Kannan H, Fredericksen B, Zhang YJ. Enhancement of interferon induction by ORF3 product of hepatitis E virus. J Virol 2014;88:8696-8705.
37. Nan Y, Yu Y, Ma Z, Khattar SK, Fredericksen B, Zhang YJ. Hepatitis E virus inhibits type I interferon induction by ORF1 products. J Virol 2014;88:11924-11932.
38. Huang F, Yang C, Yu W, Bi Y, Long F, Wang J, Li Y, et al. Hepatitis E virus infection activates signal regulator protein alpha to down-regulate type I interferon. Immunol Res 2016;64:115-122.
39. Dong C, Zafrullah M, Mixson-Hayden T, Dai X, Liang J, Meng J, Kamili S. Suppression of interferon-alpha signaling by hepatitis E virus. Hepatology 2012;55:1324-1332.
40. Ding Q, Heller B, Capuccino JM, Song B, Nimgaonkar I, Hrebikova G, Contreras JE, et al. Hepatitis E virus ORF3 is a functional ion channel required for release of infectious particles. Proc Natl Acad Sci U S A 2017;114:1147-1152.
41. Schoggins JW, Wilson SJ, Panis M, Murphy MY, Jones CT, Bieniasz P, Rice CM. A diverse range of gene products are effectors of the type I interferon antiviral response. Nature 2011;472:481-485.

Supplementary data

Supplementary Materials and Methods

Cell culture models

Human hepatoma cells Huh7.5 were kindly provided by Professor Bart Haagmans from Department of Viroscience, Erasmus Medical Center. STAT1-deficient (U3A) and STAT2-deficient (U6A) cell lines were kindly provided by G. R. Stark (Lerner Research Institute). Human liver progenitor cell line HepaRG was purchased from Thermofisher Scientific. Human embryonic kidney 293 cells (HEK293), h human glioblastoma cells U87 were originally obtained from ATCC (www.atcc.org). Huh7.5, HEK293 and U87 cells were grown in Dulbecco's modified Eagle medium (DMEM) (Lonza Biowhittaker, Verviers, Belgium) supplemented with 10% (v/v) fetal calf serum (FCS) (Hyclone, Lonan, Utah) and antibiotics. HepaRG cell line was maintained in William's medium (Thermo Fisher Scientific Life Sciences) as described previously (1). The HEV replicon model was based on Huh7.5 (Huh7.5-P6-luc) or HEK293 (HEK293-P6-luc) cells containing the subgenomic HEV sequence (Kernow-C1 p6/luc) coupled to a Gaussia luciferase reporter gene. ISRE luciferase reporter cells were generated by transducing Huh7.5 cells with lentiviral vectors expressing the firefly luciferase gene under the control of ISRE promoter (2). The HCV subgenomic replicon comprised Huh7.5 cells containing a subgenomic HCV bicistronic replicon (1389/NS3-3V/LucUbiNeo-ET) linked to the firefly luciferase reporter gene were maintained with 250 µg/ml G418 (Sigma, Zwijndrecht, the Netherlands). MEF cells (WT, RIG-I-/-, MDA5-/-, RIG-I and MDA5-/-, MAVS-/-, IRF3/7-/-) were kindly provided by Dr. Sanna M. Mäkelä (National Institute for Health and Welfare Viral Infections Unit, Helsinki, Finland). β-catenin knockout MEF cells were kindly provided by Prof. Konrad Basler (University of Zürich). Mouse or human liver cell isolation and primary liver organoids culture were described accordingly (3).

Measurement of luciferase activity

For *Gaussia* luciferase analysis, the activity of secreted luciferase in the cell culture medium was measured by BioLux® *Gaussia* Luciferase Flex Assay Kit (New England Biolabs) according to the manufacturer's instructions. For firefly luciferase, luciferin potassium salt (100 mM; Sigma) was added to cells and incubated for 20 min at 37 °C The luciferase activity was quantified with a LumiStar Optima luminescence counter (BMG Lab Tech, Offenburg, Germany).

Quantitative real-time polymerase chain reaction

RNA was isolated with a Machery-NucleoSpin RNA II kit (Bioke, Leiden, The Netherlands) and quantified using a Nanodrop ND-1000 (Wilmington, DE, USA). All RNA samples were adjusted to the concentration of 62.5ng/µl. 500 ng of RNA was used as template for cDNA preparation with the reverse transcription system(TAKARA BIO INC). The cDNA (10ng/well) of all detected genes was amplified for 50 cycles and quantified with a SYBRGreen-based real-time PCR (Applied Biosystems) according to the manufacturer's instructions. GAPDH was considered as reference genes to

normalize gene expression. Relative gene expressions were normalized to GAPDH using the formula $2^{-\Delta\Delta CT}$ ($\Delta\Delta CT = \Delta CT_{sample} - \Delta CT_{control}$). All the primer sequences are included in Table S2 and S3.

In Vitro RNA Synthesis

Capped viral RNA was *in vitro* transcribed from linearized plasmid DNA with the Ambion mMESSAGE mMACHINE® in vitro RNA transcription Kit (Thermo Fisher Scientific Life Sciences). Un-capped viral RNA was in vitro generated by NEB T7 High Yield RNA Synthesis Kit (E2040S). Nucleic acid concentrations were determined by spectroscopy (Nanodrop ND-1000; Thermo Fischer Scientific, Waltham, MA).

Transfection assay

FuGENE® HD Transfection Reagent was used for transfection assays. Cells were seeded in 96-well plates at a density of 1×10^4 cells per well. After 24h, the medium was removed and cell layer was washed by Opti-MEM. Different concentrations of RNA or plasmid constructs were transfected with FuGENE® HD Transfection Reagent in a total volume of 100 µL Opti-MEM according to the protocol. After 6 h, the medium was changed back to normal medium.

Interferon production assay

10×10^4 cells per well were seeded into 6-well plates. Cells were transfected with corresponding RNA or plasmid constructs as described above. 6h later, medium was removed and cell layer was washed 3 times. Then, the medium wad refreshed and cultured for another 48 h to let the produced cytokines secreted into the medium. Subsequently, the supernatant (conditioned medium) was collected. To detect the secreted IFN proteins in conditioned medium, two luciferase reporter models (Huh7.5-HCV-luc and Huh7.5-ISRE-luc, described above) were used, which are extremely sensitive to interferon treatments.

Confocal laser electroscope assay

Cells were seeded on glass coverslips. After 12 hours, cells were washed with PBS, fixed in 4% PBS-buffered formalin for 10 mins and blocked with tween-milk-glycine medium (PBS, 0.05% tween, 5g/L skim milk and 1.5g/L glycine). Samples were incubated with primary antibodies overnight at 4 °C. Subsequently, samples were incubated with 1:1000 dilutions of the anti-mouse IgG (H+L), F(ab')2 Fragment (Alexa Fluor® 488 Conjugate) or anti-rabbit IgG(H+L), F(ab') 2 Fragment (Alexa Fluor 488 conjugate) secondary antibodies. Nuclei were stained with DAPI (4,6-diamidino-2-phenylindole; Invitrogen). Images were detected using confocal electroscope.

Statistical analysis

All results were presented as mean ± SEM. Data analysis were performed with Mann-Whitney test. Differences were considered significant at a p-value less than 0.05 (single asterisks in figures).

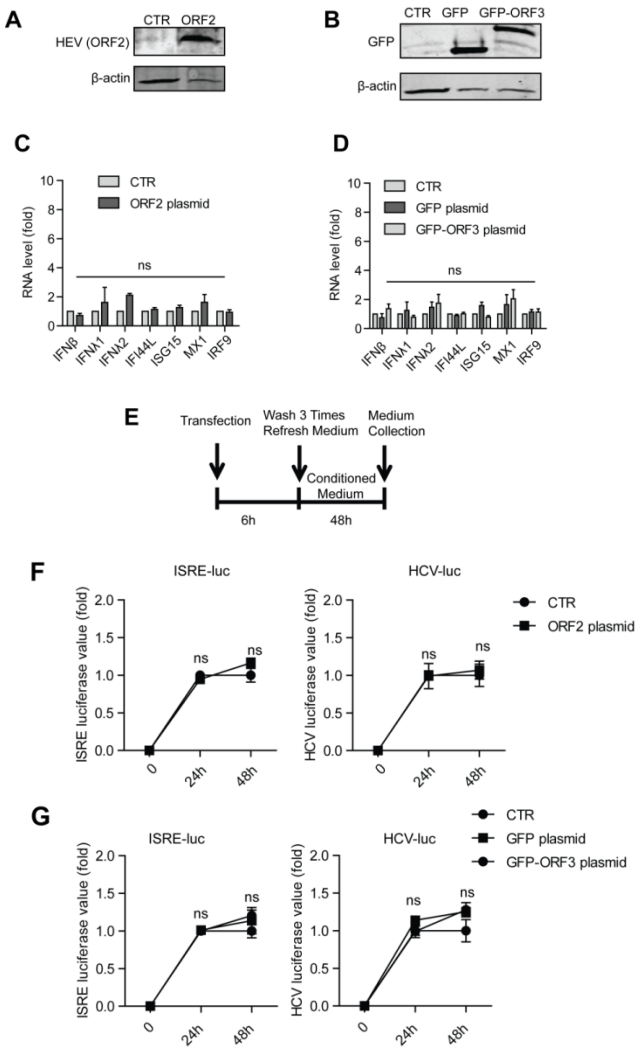

sFig.1 Expression of HEV viral protein ORF2 and ORF3 failed to elicit IFN production and antiviral responses. (A) Western blot analysis of HEK 293 cells transfected with control or ORF2- expressing plasmid. (B) Western blot analysis of HEK 293 cells transfected with control, GFP or GFP-ORF3- expressing plasmid. (C) HEK293 cells were transfected with control or ORF2- expressing plasmid. The expression levels of indicated IFNs and ISGs were quantified at 48h.p.t. by qRT-PCR (n = 4). (D) Same as (C) for ORF3 protein. (E) Schematic illustration of the production of conditioned medium (supernatant). (F) ISRE luciferase value (left) and HCV viral replication-related firefly luciferase activity (right) were measured after the treatment of conditioned medium from HEK293 cells transfected with CTR or ORF2- expressing plasmid (n = 4). (G) Same as (F) for ORF3.

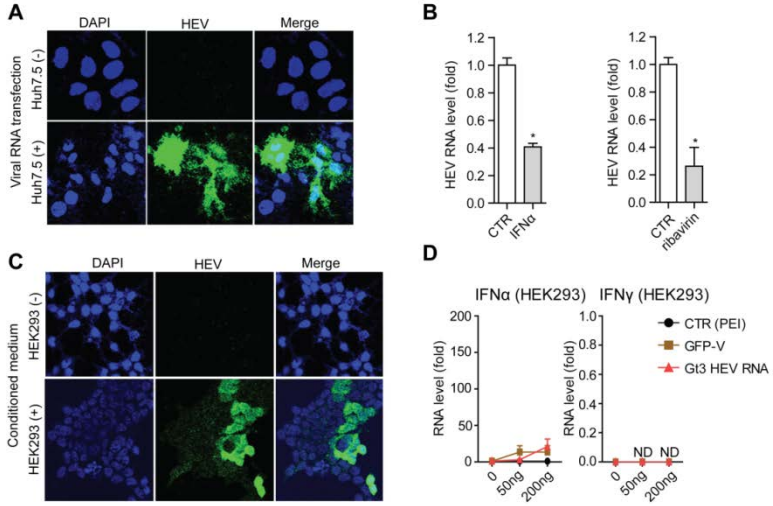

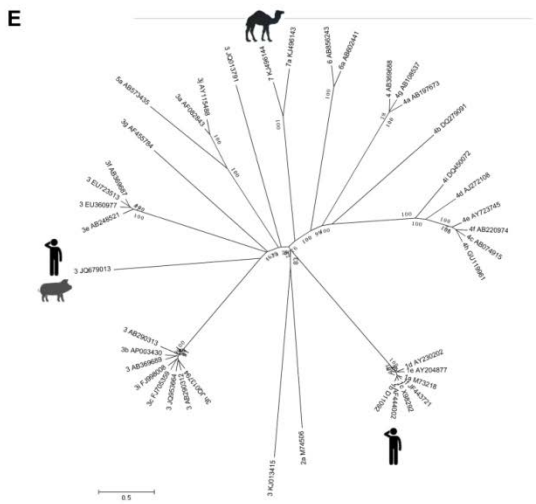

sFig 2. HEV RNA generated *in vitro* is functional to initiate the essential steps of HEV life cycle. (A) Confocal microscopy was used to detect HEV viral protein ORF2 in Huh7.5 cells transfected with CTR or Gt3 HEV RNA. ORF2 antibody (green). Nuclei were visualized by DAPI (blue). (B) Huh7.5 cells transfected with Gt3 HEV RNA were treated with IFNα (1000 IU/ml) or ribavirin (100 μm) for 48h. The intracellular HEV RNA level was quantified by qRT-PCR (n = 4). (C) HEK293 cells were inoculated with conditioned medium from Huh7.5 cells transfected with CTR or Gt3 HEV RNA. Confocal microscopy was used for the detection of HEV viral protein ORF2 in HEK293 cells. ORF2 antibody (green). Nuclei were visualized by DAPI (blue). (D) HEK293 cells were transfected with CTR, GFP-V or Gt3 HEV RNA. The expression levels of indicated IFNs were quantified at 48h.p.t. by qRT-PCR (ND, not detected; n = 3). (E) Phylogenetic tree of HEV complete genome sequences. Three representative HEV strains (GenBank Accession Number: AF444002, JQ679013, KJ496144) employed in this study were indicated.

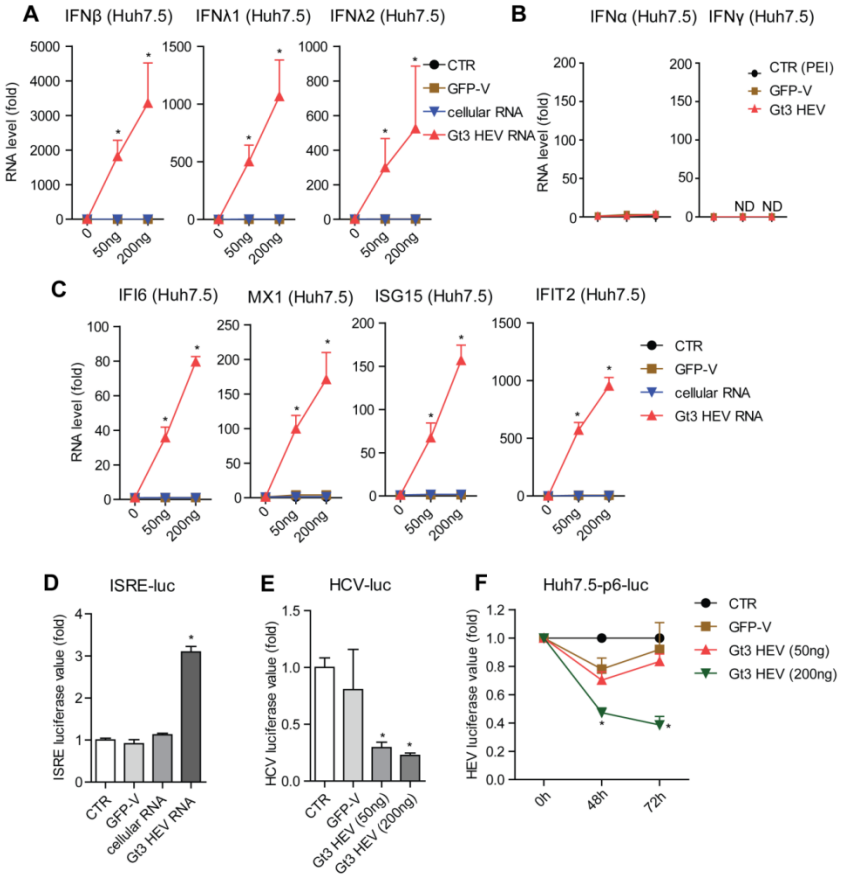

sFig.3. Transfection of HEV RNA induces IFN production and antiviral responses. Huh7.5 cells were transfected with CTR, GFP-V, cellular RNA or Gt3 HEV RNA. The expression levels of indicated IFNs (A and B) and ISGs (C) were quantified at 48h.p.t. by qRT-PCR (n = 3). (D) ISRE luciferase value was measured (at 48h) after the treatment of conditioned medium from Huh7.5 cells transfected with CTR, GFP-V, cellular RNA or Gt3 HEV RNA (n = 6). (E) HCV viral replication-related firefly luciferase activity was measured after the treatment of conditioned medium from Huh7.5 cells transfected with CTR, GFP-V or Gt3 HEV RNA (n = 4). (F) HEV viral replication-related firefly luciferase activity was measured after the transfection of CTR, GFP-V or Gt3 HEV RNA in Huh7.5-P6-luc cells (n = 4).

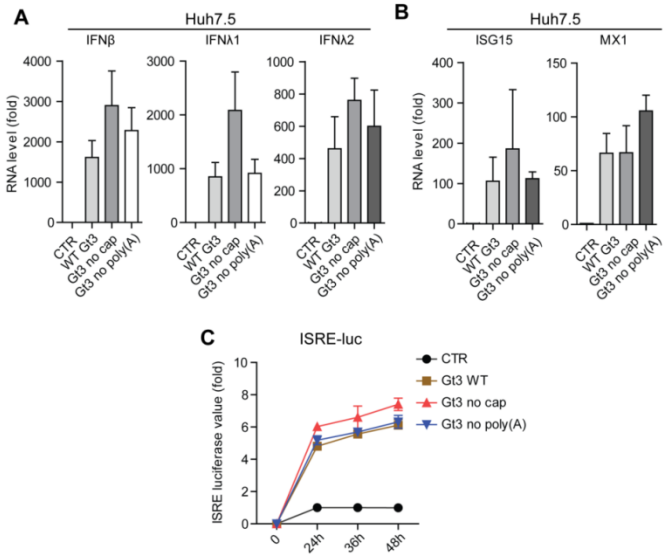

sFig.4. HEV RNA triggers antiviral responses independent of m^{7}G cap and poly A tail. Huh7.5 cells were transfected with CTR, wild type (WT), no m^{7}G cap or no poly A tail Gt3 HEV RNA (200ng / well) in 96-well plates. The expression levels of indicated IFNs (A) and ISGs (B) were quantified at 48h.p.t. by qRT-PCR (n = 3). (C) ISRE luciferase value was measured after the treatment of conditioned medium from Huh7.5 cells transfected with CTR, wild type (WT), no m^{7}G cap or no poly A tail Gt3 HEV RNA (n = 4).

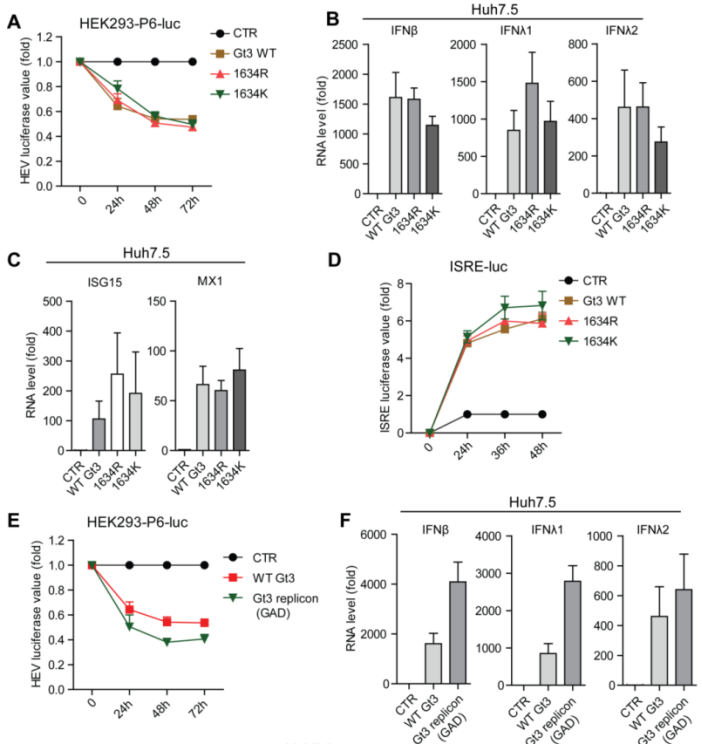

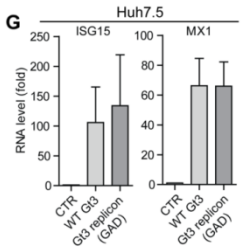

sFig.5. HEV RNA triggers antiviral responses independent of viral replication. (A) HEV viral replication-related firefly luciferase activity was measured after the transfection of CTR, WT, 1634R mutant or 1634K mutant Gt3 HEV RNA in HEK293-P6-luc cells (n = 4). Huh7.5 cells were transfected with CTR, WT, 1634R mutant or 1634K mutant Gt3 HEV RNA. The expression levels of indicated IFNs (B) and ISGs (C) were quantified at 48h.p.t. by qRT-PCR (n = 3). (D) ISRE luciferase value was measured after the treatment of conditioned medium from Huh7.5 cells transfected with CTR, WT, 1634R mutant or 1634K mutant Gt3 HEV RNA (n = 4). (E) HEV viral replication-related firefly luciferase activity was measured after the transfection of Gt3 HEV WT or replicon defective (GAD) RNA in HEK293-P6-luc cells (n = 4). Huh7.5 cells were transfected with CTR, WT or replication defective (GAD) Gt3 HEV RNA (n = 3). The expression levels of indicated IFNs (F) and ISGs (G) were quantified at 48h.p.t. by qRT-PCR.

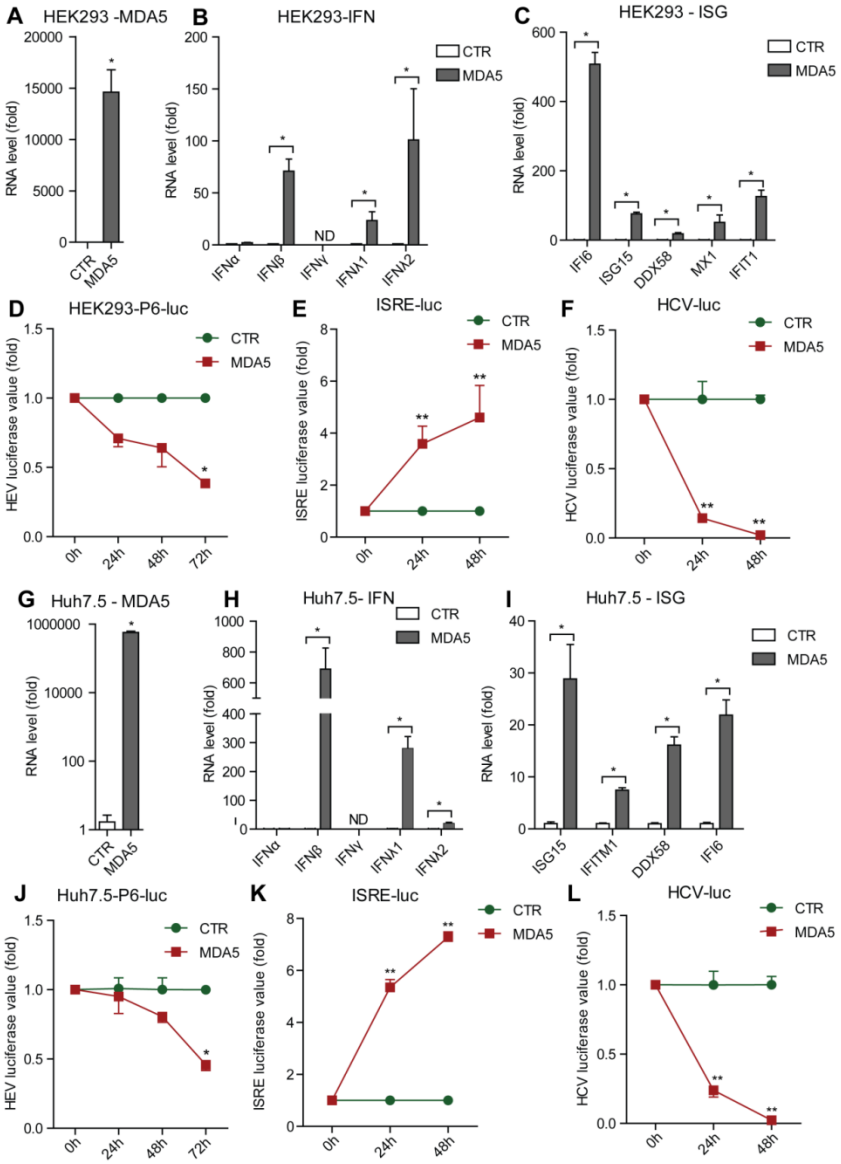

sFig.6. The overexpression of MDA5 potently induces IFN production and antiviral responses in both HEK293 and Huh7.5 cells. HEK293 cells were transfected with MDA5-expression plasmid (200ng / well) in 96 well-

plates. The expression levels of MDA5 (A), IFNs (B) and ISGs (C) were quantified at 48h.p.t. by qRT-PCR (n = 3). (D) HEV viral replication-related firefly luciferase activity was measured after the transfection of MDA5-expression plasmid in HEK293-P6-luc cells (n = 4). (E) ISRE luciferase value was measured after the treatment of conditioned medium from HEK293 cells transfected with MDA5-expression plasmid (n = 4). (F) HCV viral replication-related firefly luciferase activity was measured after the same treatment indicated in (E) (n = 4). Huh7.5 cells were transfected with MDA5-expression plasmid. The expression levels of MDA5 (G), IFNs (H) and ISGs (I) were quantified at 48h.p.t. by qRT-PCR (n = 3). (J) Same as (D) for MDA5 in Huh7.5-P6-luc (n = 4). (K) Same as (E) for conditioned medium from Huh7.5 cells transfected with MDA5 (n = 4). (L) Same as (F) for conditioned medium from Huh7.5 cells transfected with MDA5 (n = 4).

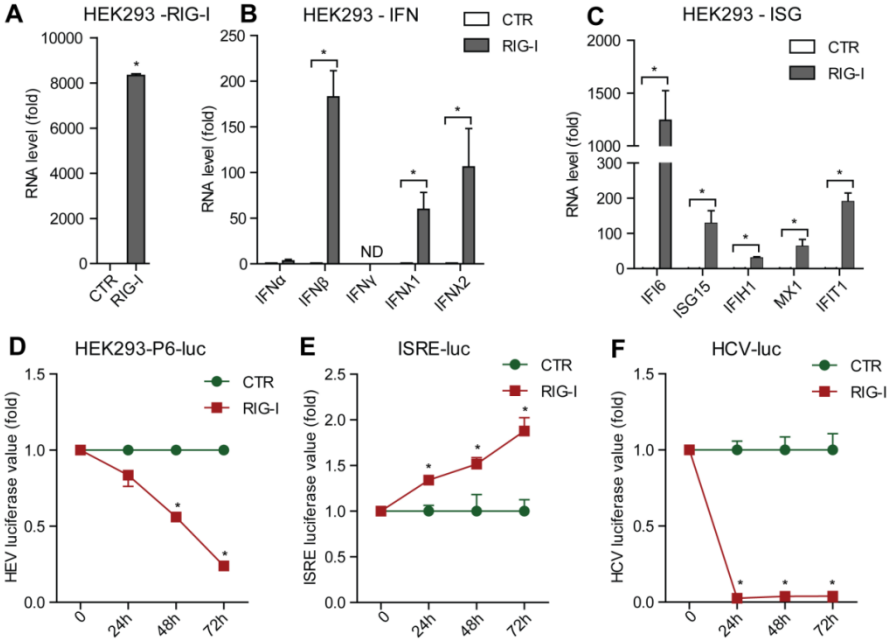

sFig.7. The overexpression of RIG-I potently induces IFN production and antiviral responses in HEK293 cells. HEK293 cells were transfected with RIG-I-expression plasmid (200ng / well) in 96-well plates. The expression levels of MDA5 (A), IFNs (B) and ISGs (C) were quantified at 48h.p.t. by qRT-PCR (n = 3). (D) HEV viral replication-related firefly luciferase activity was measured after the transfection of RIG-I -expression plasmid in HEK293-P6-luc cells (n = 4). (E) ISRE luciferase value was measured after the treatment of conditioned medium from HEK293 cells transfected with RIG-I-expression plasmid (n = 4). (F) HCV viral replication-related firefly luciferase activity was measured after the same treatment indicated in (E) (n = 4).

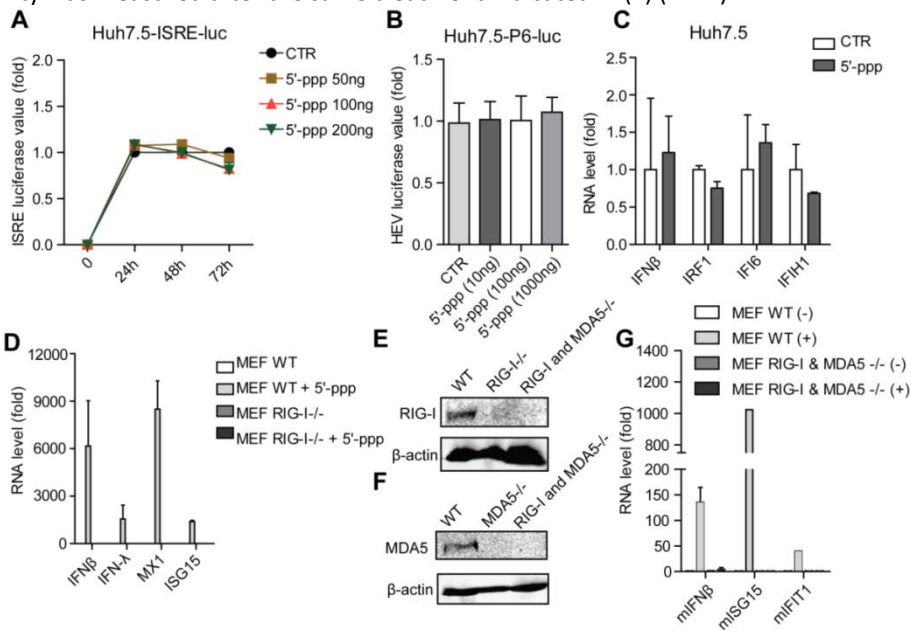

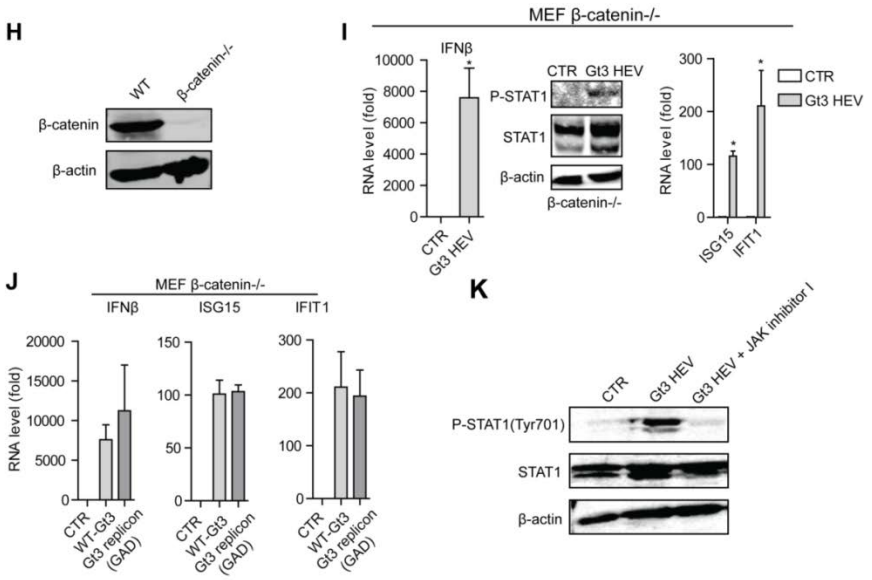

sFig.8. HEV ssRNA triggers IFN response in a MAVS- and β-catenin-independent but IRF3 and IRF7-dependent manner. (A) ISRE luciferase value was measured after the transfection of 5'pppRNA in Huh7.5-ISRE-luc cells (n = 5). (B) HEV viral replication-related firefly luciferase activity was measured after the transfection of 5'pppRNA in Huh7.5-P6-luc cells (n = 4). (C) Huh7.5 cells were transfected with 5'pppRNA. The expression levels of representative IFN and ISG were quantified at 48h.p.t. by qRT-PCR (n = 3). (D) MEF WT or RIG-I-/- cells were transfected with 5'pppRNA. The expression levels of indicated IFNs and ISGs were quantified at 48h.p.t. by qRT-PCR (n = 3). (E) The RIG-I protein level was detected in WT, RIG-I-/-, RIG-I and MDA5-/- MEF cells by western blot analysis. (F) Same as (E) for the detection of MDA5 protein. (G) The transfection of Poly (I:C) was performed in WT or RIG-I and MDA5-/- MEF cells. The expression levels of IFNβ and the representative ISGs were quantified at 48h.p.t. by qRT-PCR (n = 4). (H) The β-catenin protein level was detected in WT and β-catenin-/- MEF cells (I) The transfection of Gt3 HEV RNA (200ng / well) was performed in β-catenin-/- MEF cells in 96-well plates. The expression levels of IFNβ (left panel) and the representative ISGs (ISG15 and IFIT1) (right panel) were quantified at 48h.p.t. by qRT-PCR (n = 3). Conditioned medium was collected from β-catenin-/- MEF cells transfected with CTR or Gt3 HEV RNA. The MEF cells were treated with the corresponding conditioned medium for 24h. The expression levels of total and phosphorylated (Y701) STAT1 proteins were measured by western blot (middle panel). (J) The transfection of WT or Gt3 HEV replicon (GAD) RNA was performed in β-catenin-/- MEF cells. The levels of IFNβ and the indicated ISGs were quantified at 48h.p.t. by qRT-PCR (n = 3). (K) Conditioned medium was collected from HEK293 cells transfected with Gt3 HEV RNA with or without JAK inhibitor I. Then the corresponding conditioned medium was added in HEK293 cells for 24h. The expression levels of total and phosphorylated (Y701) STAT1 proteins were measured by western blot.

Table S1. Patient information

	patient number	Gender	Age	diagnosis	HEV-IgG	HEV-IgM	HEV staining	P-STAT1 (Y701) staining
HEV patients	1	Female	38	acute non-icteric HEV	-	+	1-5%	1-5%
	2	Female	58	acute icteric HEV	weak +	-	5-10%	1-5%
	3	Male	42	acute icteric HEV	-	+	5-10%	1-5%
	4	Male	24	acute icteric HEV	+	+	5-10%	1-5%
	5	Male	20	acute icteric HEV	+	-	10-15%	10-15%
	6	Male	38	acute icteric HEV	weak +	+	10-15%	1-5%
	7	Female	58	acute icteric HEV	+	+	0%	1-5%
	8	Male	58	acute icteric HEV	-	weak +	1-5%	0%
	9	Male	1,5	acute HEV	-	+	1-5%	1-5%
	10	Male	3	acute HEV	-	+	0%	1-5%
	11	Female	61	acute icteric HEV	+	+	1-5%	1-5%
	12	Male	55	acute HEV	+	weak +	10-15%	1-5%
	13	Male	35	HEV	+	-	5-10%	5-10%
	14	Male	19	HEV	+	-	1-5%	10-15%
	15	Female	66	acute HEV	+	-	1-5%	5-10%
	16	Male	52	HEV	+	-	10-15%	5-10%
	17	Male	11	acute non-icteric HEV	+	+	5-10%	0%
	18	Male	36	chronic HEV	+	+	10-15%	1-5%
Negative controls	19	Female	40	hepatic hemangioma	-	-	0%	0%
	20	Female	44	hepatic hemangioma	-	-	0%	0%
	21	Male	49	hepatic hemangioma	-	-	0%	0%
	22	Female	48	hepatic hemangioma	-	-	0%	0%
	23	Female	43	hepatic hemangioma	-	-	0%	0%

+, postive. -, negative.

Table S2. qRT-PCR primer sequences (human)

Gene	F-Sequences (5' - 3')	R-Sequences (5' - 3')
IFNα	GACTCCATCTTGGCTGTGA	TGATTTCTGCTCTGACAACCT
IFNβ	CTTGGATTCCTACAAAGAAGCAGC	TCCTCCTTCTGGAACTGCTGCA
IFNγ	GAGTGTGGAGACCATCAAGGAAG	TGCTTTGCGTTGGACATTCAAGTC
IFNλ1	GGAAGACAGGAGAGCTGCAACT	AACTGGGAAGGGCTGCCACATT
IFNλ2	TCGCTTCTGCTGAAGGACTGCA	CCTCCAGAACCTTCAGCGTCAG
IFI6	TGATGAGCTGGTCTGCGATCCT	GTAGCCCATCAGGGCACCAATA
DDX58	CACCTCAGTTGCTGATGAAGGC	GTCAGAAGGAAGCACTTGCTACC
MX1	GGCTGTTTACCAGACTCCGACA	CACAAAGCCTGGCAGCTCTCTA
ISG15	CTCTGAGCATCCTGGTGAGGAA	AAGGTCAGCCAGAACAGGTCGT
IFITM1	GGCTTCATAGCATTCGCCTACTC	AGATGTTCAGGCACTTGGCGGT
IFIT2	GGAGCAGATTCTGAGGCTTTGC	GGATGAGGCTTCCAGACTCCAA
IFIH1	GCTGAAGTAGGAGTCAAAGCCC	CCACTGTGGTAGCGATAAGCAG
IRF1	GAGGAGGTGAAAGACCAGAGCA	TAGCATCTCGGCTGGACTTCGA
GAPDH	TGTCCCCACCCCCAATGTATC	CTCCGATGCCTGCTTCACTACCTT

Table S3. qRT-PCR primer sequences (mouse)

Gene	F-Sequences (5' - 3')	R-Sequences (5' - 3')
IFNβ	AAGAGTTACACTGCCTTTGCCATC	CACTGTCTGCTGGTGGAGTTCATC
ISG15	CATCCTGGTGAGGAACGAAAGG	CTCAGCCAGAACTGGTCTTCGT
IFIT1	TACAGGCTGGAGTGTGCTGAGA	CTCCACTTTCAGAGCCTTCGCA
IFI16	CCAGTCACCAATACTCCACAGC	CTCTGAGTGGAGAACAGCACCT
MX1	TGGACATTGCTACCACAGAGGC	TTGCCTTCAGCACCTCTGTCCA
OAS1b	CTGTGCTGACCTCAGAGAAGTC	TGCCCTTGAGTGTGGTGCCTTT
DDX60	CGCAAGCCAGACAGTCCTACAA	AAACATCGCCCTGTCTCACGGA
GAPDH	CATCACTGCCACCCAGAAGACTG	ATGCCAGTGAGCTTCCCGTTCAG

References

1. Xu L, Wang W, Li Y, Zhou X, Yin Y, Wang Y, de Man RA, et al. RIG-I Is A Key Antiviral Interferon-Stimulated Gene Against Hepatitis E Virus Dispensable Of Interferon Production. Hepatology 2017.
2. Wang W, Xu L, Brandsma JH, Wang Y, Hakim MS, Zhou X, Yin Y, et al. Convergent Transcription of Interferon-stimulated Genes by TNF-alpha and IFN-alpha Augments Antiviral Activity against HCV and HEV. Sci Rep 2016;6:25482.
3. Huch M, Gehart H, van Boxtel R, Hamer K, Blokzijl F, Verstegen MM, Ellis E, et al. Long-term culture of genome-stable bipotent stem cells from adult human liver. Cell 2015;160:299-312.

Chapter 15

Hepatitis E virus activates STAT3 to facilitate viral replication

Wenshi Wang[1*], Yijin Wang[2], Changbo Qu[1], Shan Wang[2], Wanlu Cao[1], Lei Xu[1], Buyun Ma[1], Jingmin Zhao[2], Maikel P. Peppelenbosch[1], ,Qiuwei Pan[1*]

[1] Department of Gastroenterology and Hepatology, Postgraduate School Molecular Medicine, Erasmus MC-University Medical Center, Rotterdam, the Netherlands

[2] Department of Pathology and Hepatology, Beijing 302 Hospital, Beijing, P.R. China

Gut (under revision).

Abstract

Hepatitis E virus (HEV) is the most common cause of acute viral hepatitis globally, but the mechanisms by which it corrupts hepatocyte cellular machinery to facilitate its replication remain only partially understood. STAT3 is a vital transcription factor centrally involved in cell signaling pathways to exert diverse cellular responses. Here, we demonstrate that HEV potently activates STAT3 phosphorylation in the liver of hepatitis E patients and in cell cultures. This corresponded to a concomitant increase in STAT3-related transcriptional activity. Mechanistically, HEV-mediated STAT3 activation is independent of classical humoral IL-6 and interferon signaling but involves hijacking of Janus kinases (JAKs) and Src kinases via the active viral infection. Importantly, genetic or pharmacological inhibition of STAT3 activation constrained HEV replication. Conversely, over-expression of the activated form of STAT3 increased HEV replication. In conclusion, our results revealed a previously undescribed function of STAT3 as a pro-HEV host factor. HEV-induced STAT3 phosphorylation in turn create a favorable environment to facilitate HEV replication. Therefore, STAT3 serves as a promising target for the development of antivirals against HEV .

Introduction

Hepatitis E virus (HEV) is the most common causes of acute viral hepatitis around the world. It yearly causes around 20 million infections, resulting in around 3 million illnesses and 70,000 deaths worldwide. Epidemics of hepatitis E occur periodically throughout the developing world, resulting in fulminant hepatitis and high mortality in pregnant women (1, 2). In developed countries, persistent HEV infection is also emerging in immunocompromised patients (3, 4). However, there is no FDA-approved medication available. The fundamental and translational research related to virus-host interaction remains largely elusive.

HEV is a single-stranded non-enveloped virus particle. Its genome encodes three viral proteins. ORF1 is a multifunctional nonstructural protein, ORF2 is the viral capsid protein, and ORF3 is a small protein involved in virus secretion (5). Like most viruses, HEV is obligate intracellular parasite that needs to corrupt the host cell machinery to accomplish their life-cycle. However, for HEV, knowledge about host factors needed for virus life cycle is largely unknown. This hampers the development of effective anti-HEV therapy.

The signal transducer and activator of transcription (STAT) family members are transcription factors that play crucial roles in mediating signaling in virtually all cytokine pathways. They become activated through tyrosine phosphorylation typically via cytokine receptor associated kinases, the Janus kinase (JAK) (6). Of all the STAT members, STAT3 is known to exert diverse cellular responses that are highly dependent on cell types and different physiological settings (7). STAT3 is activated by phosphorylation at tyrosine 705 in its C-terminal domain and more than 40 different ligands are known to cause STAT3 activation, including interleukin (IL)-6, IL-10, leukemia inhibitory factor, interferons (IFNs). Upon activation, phosphorylated STAT3 undergoes homodimerization and nucleus translocation, binding to specific DNA response elements in the promoter regions of target genes and regulating their transcription (8). As a vital host protein, STAT3 was reported to play a key role in regulating host immune and inflammatory responses (9). Its role in viral infection appears to be complex. It serves as a proviral factor in some viral infections and antiviral factor in others (6) (10, 11). Correspondingly, STAT3 is either positively or negatively regulated in a range of viral infections depending on the specific virus involved. All these facts highlight the significant role of STAT3 in the complex interplay between viruses and their hosts.

In this study, we found that STAT3 was activated by HEV infection in the liver of hepatitis E patients and in cell cultures. Functionally, STAT3 activation following HEV infection appears an essential step in viral replication. Hence pharmacological inhibition of STAT3 activation constitutes an important novel target to combat the HEV infection.

Results

HEV potently activates STAT3 phosphorylation in the liver of HEV patients and in cultured cell lines

To investigate a possible relationship between STAT3 and HEV, the expression of phosphorylated STAT3 (Y705) was detected in paraffin-embedded liver tissues from 21 HEV patients (Fig.1A). The staining of HEV and P-STAT3 were scored independently based on the proportion of positive cells

(Fig.1B). Up to 86% of HEV infected patients showed a positive staining of P-STAT3; while no staining was observed in five negative controls (Fig.1C). This result indicates that HEV infection induces STAT3 activation in patients.

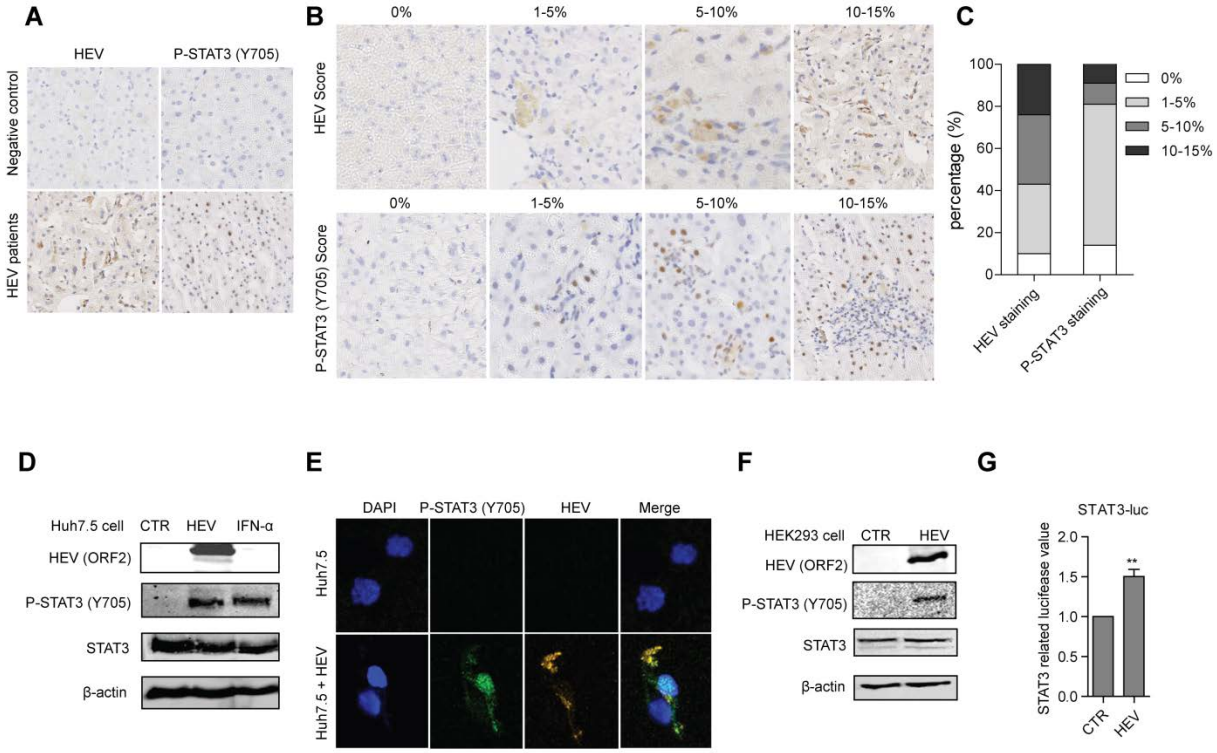

Figure 1. HEV potently activates STAT3 phosphorylation in the liver of HEV patients and in cultured cell lines. (A) Representative staining of HEV or P-STAT3 in liver tissue of HEV patients or negative control individuals. HEV mainly localized within cytoplasm, while P-STAT3 in cell nucleus. (B) Representative staining indicated variable levels of HEV and P-STAT3. The proportion of positive cells were scored from 0% - 15%. (C) The distribution of HEV and P-STAT3 score among all liver tissues tested. (D) Huh7.5 cells infected with HEV or treated with IFN-α (1000IU/ml, 30min) were analyzed with indicated antibodies. HEV infection specifically activates STAT3 phosphorylation at site Y705, while no effect on the protein level of total STAT3 . IFN-α served as a positive control. (E) Confocal laser electroscope analysis of the cellular localization of P-STAT3 and HEV in mock or HEV infected Huh7.5 cells. HEV mainly located in cytoplasm, while HEV-induced P-STAT3 mainly in cell nucleus. (F) Western blotting analysis of P-STAT3 in mock or HEV infected HEK293 cells. (G) Mock or HEV infected HEK293 cells were transiently transfected with STAT3-luc and TK-Renilla (used to normalize the transfection efficiency). The luciferase activity was determined 48 hours post-transfection. HEV infection significantly increased STAT3 promoter-related transcriptional activity.

This interesting observation from HEV patients encouraged us to further investigate in cell culture models. Consistently, the inoculation of HEV activated STAT3 phosphorylation in hepatic cell line, i.e. Huh7.5 (Fig. 1D and E). The level of P-STAT3 induced by HEV is robust, which is even comparable to that elicited by a high dose of IFN alpha (IFN-α, 1000IU/ml) treatment (served as a positive control). On the contrary, uninfected Huh7.5 cells did not show any detectable P-STAT3. Of note, HEV infection did not alter the protein level of total STAT3, suggesting a specific effect on STAT3 phosphorylation rather than a general effects on gene transcription. The clinical observations that HEV infection causes both hepatic and extra-hepatic manifestations prompts us to extend our study to extra-hepatic cell line, i.e. HEK293. Consistently, HEV could also induce STAT3 phosphorylation in HEK293 cells (Fig. 1F), indicating a general mechanism in HEV infection. Based on the fact that STAT3 is a transcriptional factor, its transcriptional activity was also measured upon HEV infection. HEV significantly increased STAT3-related transcriptional activity, correlating with the

activation of STAT3 phosphorylation (Fig. 1G). Collectively, these *in vivo* and *in vitro* results demonstrate that HEV potently activates STAT3 phosphorylation.

Active viral infection determines STAT3 activation

The activation of STAT3 by HEV infection could be caused by incoming virions, viral replication products or active virus infection. To test the possible involvement of HEV viral replication in STAT3 activation, the status of P-STAT3 was detected in the HEV subgenomic replicon model. This model was based on Huh7.5 cells containing the subgenomic HEV sequence (ORF1 region,Kernow-C1, P6-luc) coupled to a Gaussia luciferase reporter gene. Although active HEV replication was confirmed by the measurement of replication-related luciferase value (Fig. 2A), no detectable P-STAT3 was observed (Fig. 2B). Two vectors encoding the corresponding viral proteins (ORF2 or ORF3) were transfected, respectively. This strategy resulted in substantial expression of the relevant viral proteins, but failed to elicit the phosphorylation of STAT3 (Fig. 2C and D). Levels of P-STAT3, however, showed positive correlation with the levels of HEV (Fig. 2E), while same amounts of UV-inactivated virus failed to induce STAT3 activation (Fig. 2F). Thus, active HEV infection results in enhanced phosphorylation of STAT3.

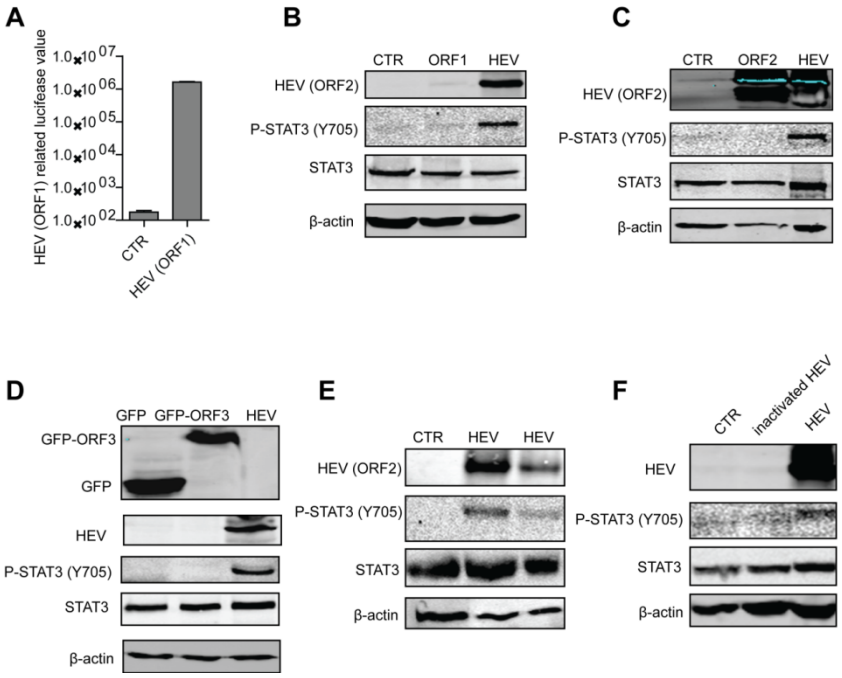

Figure 2. Active HEV infection determines STAT3 activation. (A) The HEV subgenomic replicon model was based on Huh7.5 cells containing the subgenomic HEV sequence (ORF1 region,Kernow-C1, P6-luc) coupled to a Gaussia luciferase reporter gene. The luciferase activity was measured 48 hours post-transfection. (B) The status of P-STAT3 was detected in Huh7.5 cells (CTR) or HEV subgenomic replicon model. Huh7.5 cells infected with HEV served as a positive control. (C) HEK 293 cells were transfected with plasmid pLVX-ORF2-IRES-zsGrenn1. HEV ORF2 protein exerted no effect on STAT3 activation. Cells infected with HEV served as a positive control. (D) Same as (C) for the transfection of plasmid pEGFP-C1-ORF3. HEV ORF3 protein exerted no effect on STAT3 activation. Cells infected with HEV served as a positive control. (E) Western blotting analysis of Huh7.5 cells infected with different doses of HEV. The levels of P-STAT3 positively correlate with the replication levels of HEV. (F) Huh7.5 cells were inoculated with the same dose of UV-inactivated or infectious HEV particles. Western blotting analysis indicated that only the infectious HEV could induce STAT3 activation.

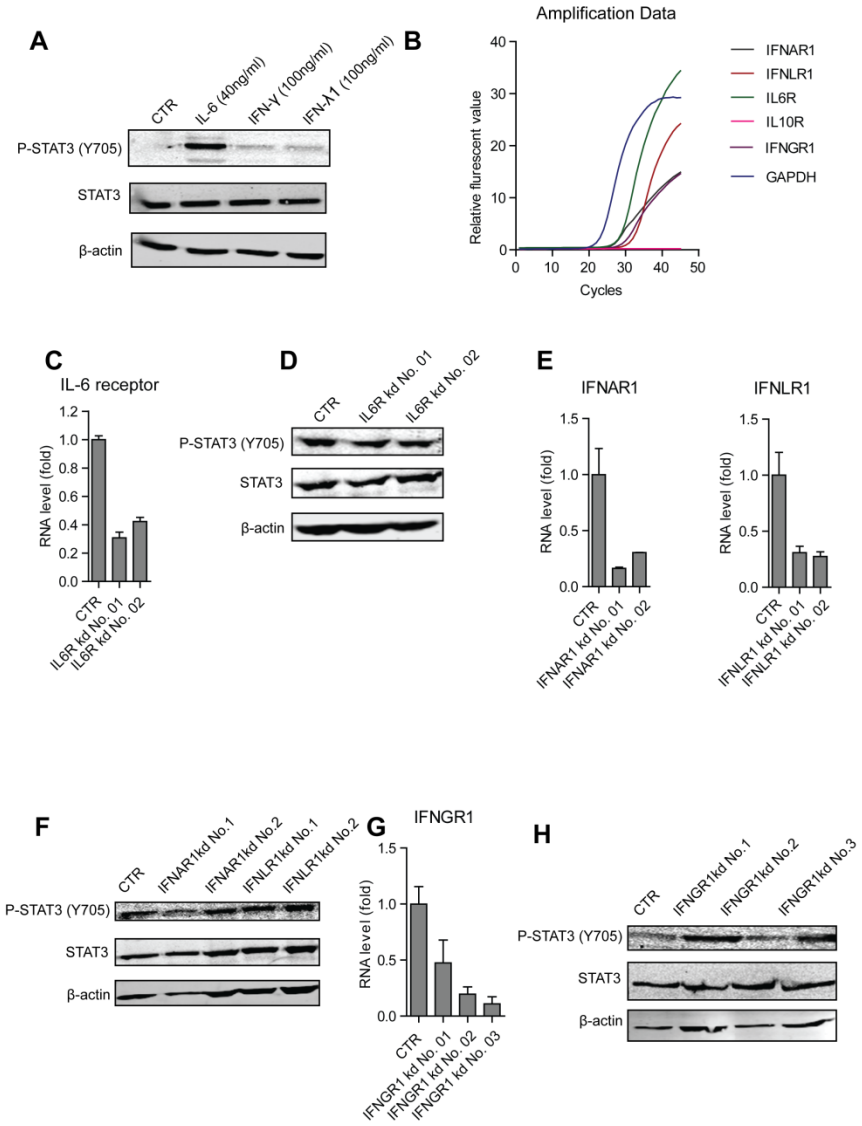

Figure 3. HEV induced STAT3 activation occurs independent of IL-6 and IFNs signaling. (A) Huh7.5 cells were treated with IL-6 (40 ng/ml), IFN-γ (100 ng/ml) and IFN-λ1 (100 ng/ml) for 30 min. The levels of P-STAT3 were analyzed by western blotting. (B) The expression levels of IFNAR1, IFNLR1, IFNGR1, IL6R and IL10R in Huh7.5 cells were analyzed by qRT-PCR. All receptors except IL-10 receptor are expressed in Huh7.5 cells. (C) Huh7.5 cells were transduced with lentiviruses expressing control shRNA (CTR) or two IL-6 receptor –targeting shRNAs. qRT-PCR analysis confirmed the efficient knockdown of IL-6 receptor. (D) CTR or IL-6 receptor knockdown cells were infected with HEV. Western blotting analysis showed that HEV induced comparable levels of P-STAT3 in IL-6 receptor knockdown cells compared with their controls. (E) Same as (C) for the knockdown of IFNAR1 or IFNLR1. (F) Same as (D) for IFNAR1 or IFNLR1 knockdown. (G) Same as (C) for the knockdown of IFNGR1. (H) Same as (D) for IFNGR1 knockdown.

HEV induced STAT3 activation occurs independent of humoral IL-6 and IFN signaling

Depending on cell types and different physiological settings, multiple ligands, including IL-6, IL-10 and IFNs, are known to trigger STAT3 activation. In our model system, IFN-α,IL-6, IFN-γ and IFN-λ1 are capable of inducing STAT3 phosphorylation (Fig. 3A). Therefore, to dissect whether HEV induced STAT3 activation depends on IL or IFN related signaling, the expression status of their corresponding receptors were detected. All the receptors except IL-10 receptor can be easily detected (Fig. 3B), thus

potential HEV-provoked production of these humoral factors constitutes a possible mechanism to mediate HEV associated STAT3 activation. However, lentiviral-based shRNA-mediated knock down of either the IL-6 receptor (Fig. 3C), the IFNAR1, the IFNLR1 (Fig. 3E) or the IFNGR1 (Fig. 3G) does not influence the capacity of HEV to induce STAT3 activation (Fig. 3D, F and H). Therefore, HEV induced STAT3 activation is independent of production of humoral cytokines by the infected cells.

HEV highjacks JAKs and Src to induce STAT3 activation

JAKs (JAK1, JAK2, JAK3 and Tyk2) are cytoplasmic tyrosine protein kinases. Upon signal transduction, STATs are thought to become phosphorylated by JAKs on a tyrosine residue near the C terminus that is conserved in all STAT family members (8). Therefore, the JAK kinases might be the primary candidates to mediate HEV induced STAT3 activation. Although HEV infection provoked no substantial effect on the levels of phosphorylated and total JAKs (Fig. 4A), HEV-mediated STAT3 activation is impaired by the pharmacological JAK inhibitor, JAK inhibitor I (Fig. 4B and C) as well as other JAK inhibitors (AG490, CP690,550 and Bay-18; Fig. 4D-G). Similarly, STAT3 phosphorylation status can also be controlled by Src family protein kinases (12). While HEV infection exerts no major effect on Src levels and phosphorylation status, inhibition of Src substantially impacts HEV-dependent STAT3 activation (Fig. 4H). In contrast, however, inhibition of the *bona-fide* STAT3 activators FGF receptor family does not impact HEV mediated STAT3 activation (Fig. 4I) (13, 14). Collectively, HEV infection corrupts JAK and Src kinases to mediate STAT3 phosphorylation.

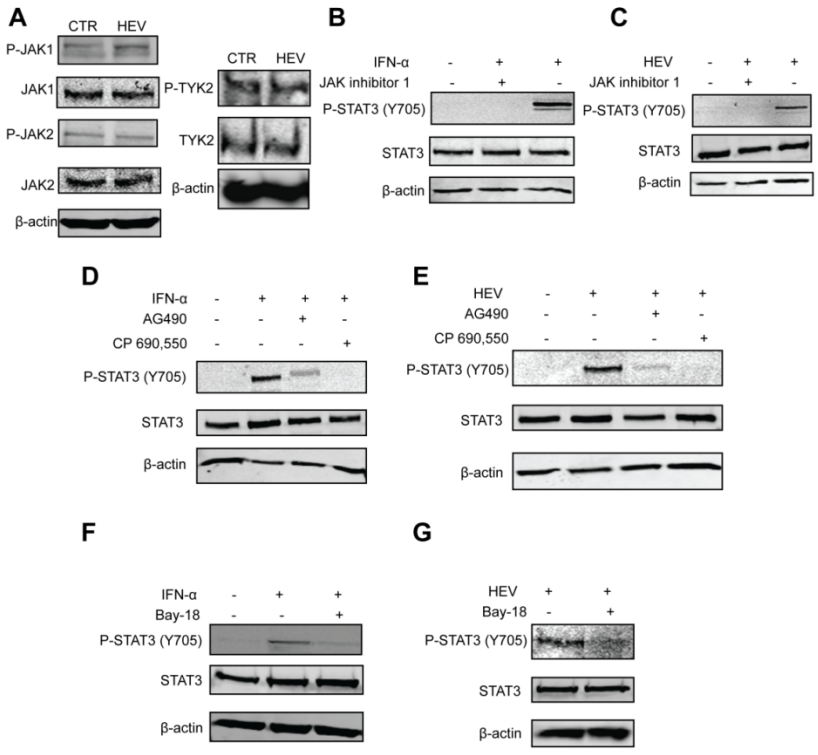

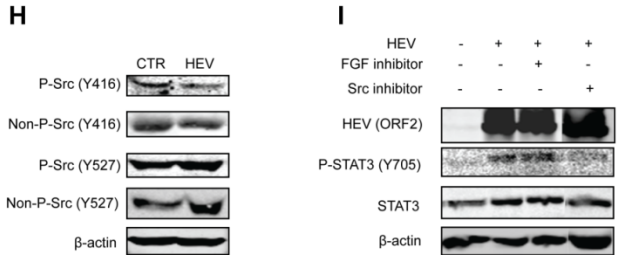

Figure 4. HEV highjacks JAKs and Src to induce STAT3 activation. (A) Western blotting analysis of mock or HEV infected Huh7.5 cells with indicated antibodies. HEV infection exerted no significant effect on the phosphorylated and total levels of JAK kinases. (B) Huh7.5 cells were treated with IFN-α (1000IU/ml) or the combination with JAK inhibitor I (5μm). Western blotting analysis showed that JAK inhibitor I abrogated IFN-α induced STAT3 phosphorylation. (C) Same as (B) for HEV infection. (D) Same as (B) for JAK inhibitors AG490 and CP 690,550. (E) Same as (C) for JAK inhibitors AG490 and CP 690,550. (F) Same as (B) for JAK inhibitor, Bay-18. (G) Same as (C) for JAK inhibitor, Bay-18. (H) Same as (A) for detection of the phosphorylated and un-phosphorylated Src kinases. (I) Huh7.5 cells infected with HEV were treated with control, FGF inhibitor (10μm) or Src inhibitor I (10μm). Western blotting analysis showed that Src inhibitor I decreased HEV induced STAT3 phosphorylation, while FGF inhibitor has no significant effect.

Upon signaling transduction, STATs gets phosphorylated by specific kinases. Meanwhile, P-STATs undergoes dephosphorylation process by specific phosphatase. Thus, the level of P-STAT3 is coordinately determined by phosphorylation and dephosphorylation process (sFig. 1A). Hence it is possible that HEV-induced STAT3 activation occurs via blocking the expression of STAT3-related phosphatases. Seven out of twelve STAT3-related phosphatases can be detected in our model system (sFig. 1B). However, HEV infection exerts no significant effects on the levels of phosphatases measured either by qRT-PCR or western blotting assays (sFig. 1C and D).

STAT3 is essential for efficient HEV replication

To evaluate the importance of STAT3 activation for the HEV infectious process, wild type, STAT3 knockout (STAT3-/-) and STAT3 constitutively activated (STAT3-C) mouse embryonic fibroblasts (MEF) cells were used. HEV replication is decreased in STAT3-/- cells compared with its wild type. Conversely, STAT3-C cells display increased virus replication (Fig. 5A). Therefore, STAT3 serves as a proviral host factor to facilitate HEV replication.

IFN-α induces a wide spectrum of anti-viral mediators, the so-called interferon–stimulated genes (ISGs) via the JAK-STAT pathway (15). STAT1 and STAT2 are well characterized to counteract viral infection through upregulation of ISG expression. Even though STAT3 is also activated by IFN-α, its role in antiviral ISG induction is controversial. Some studies indicated that STAT3 negatively regulates the type I IFN-mediated antiviral response, while a positive regulatory effect has also been reported (16-18). Hence it is possible that STAT3-mediated stimulation of HEV replication involves the IFN pathway. However, this notion was not supported when constitutive expression of IFN-α, IFN-β and representative ISGs were studied in wild type and STAT3-/- cells (Fig. 5B and C). In addition, STAT3-/- cells are comparable to STAT3 proficient controls with respect to the levels of phosphorylated STAT1, phosphorylated STAT2 and ISGs following IFN-α treatment (Fig. 5D and E). Therefore, STAT3 is a proviral host factor for HEV, functionally independent of IFN pathway.

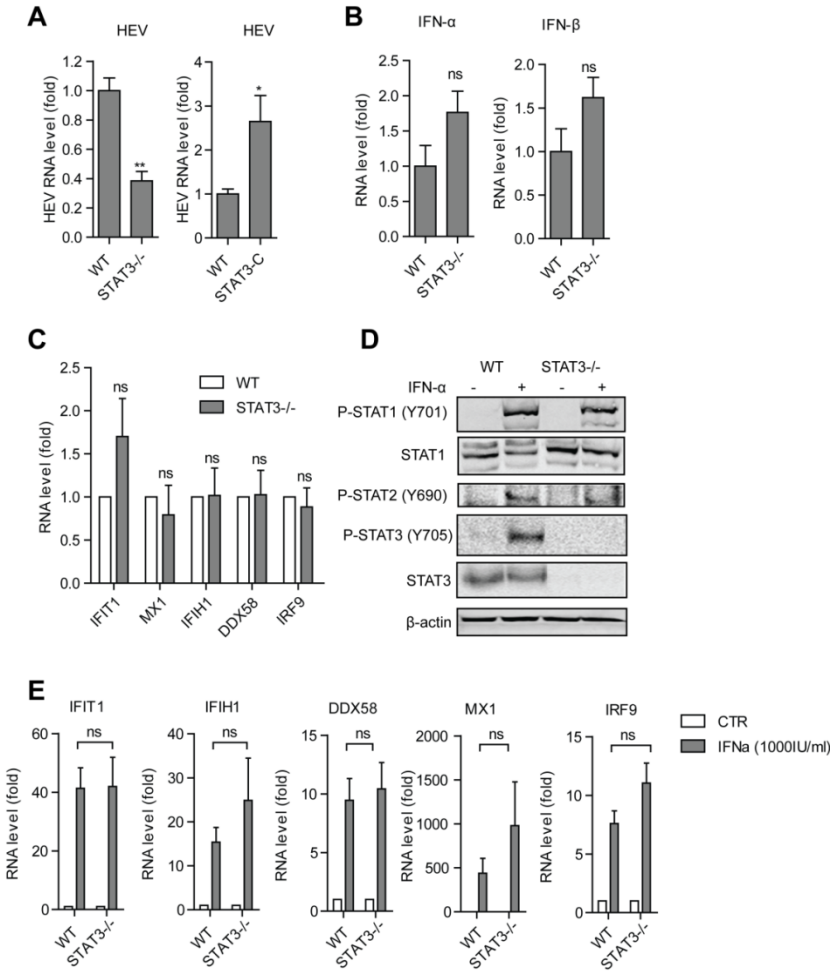

Figure 5. HEV serves as a proviral host factor to promote HEV replication, independent of IFN pathway. (A) Wild type (WT), STAT3 knockout (STAT3-/-) and STAT3 constitutively activated (STAT3-C) MEFs were infected with HEV for 48 hours. qRT-PCR analysis indicated that HEV replication was inhibited in STAT3-/- cells compared with its wild type. Conversely, virus replication was increased in STAT3-C cells. (B) and (C) qRT-PCT analysis of the constitutive expression levels of IFN-α, IFN-β and the representative ISGs in WT and STAT3-/- MEFs. STAT3 knockout exerted no significant effect on the expression levels of IFN-α, IFN-β and representative ISGs. (D) WT and STAT3-/- MEFs were treated with IFN-α (1000IU/ml, 15 min). The protein levels of P-STAT1(Y701), total STAT1, P-STAT2(Y690), P-STAT3 (Y705) and STAT3 were analyzed by western blotting. (E) WT and STAT3-/- MEFs were treated with IFN-α (1000IU/ml, 15 min). The expression levels of indicated ISGs were analyzed by qRT-PCR.

Pharmacological blockage of STAT3 activation constrains HEV replication

Finally, we evaluated the therapeutic potential of targeting STAT3 for combating HEV infection. We investigated the commercially available STAT3 inhibitor, S3I-201, on HEV infection. S3I-201 specifically blocks STAT3 phosphorylation induced by IFN-α or HEV (Fig. 6A). Importantly, S31-201 leads to significant inhibition of HEV replication in our HEV subgenomic model (P6-luc), while no significant cell toxicity is observed at the indicated concentrations (Fig. 5C). Of note, the anti-HEV effect of S3I-201 at the concentration of 20 μm is comparable to that of treatment with IFN-α. Consistent with these observations, the anti-HEV effect of the inhibitor was also observed in three different human hepatic cell lines (Huh7.5, HepaRG and PLC/PRF/5) and two extra-hepatic cell lines (HEK293 and MRC5). harboring full-length HEV genome (Fig. 6C and D). Therefore, pharmacological blockage of STAT3 activation represents a novel strategy for constraining HEV replication.

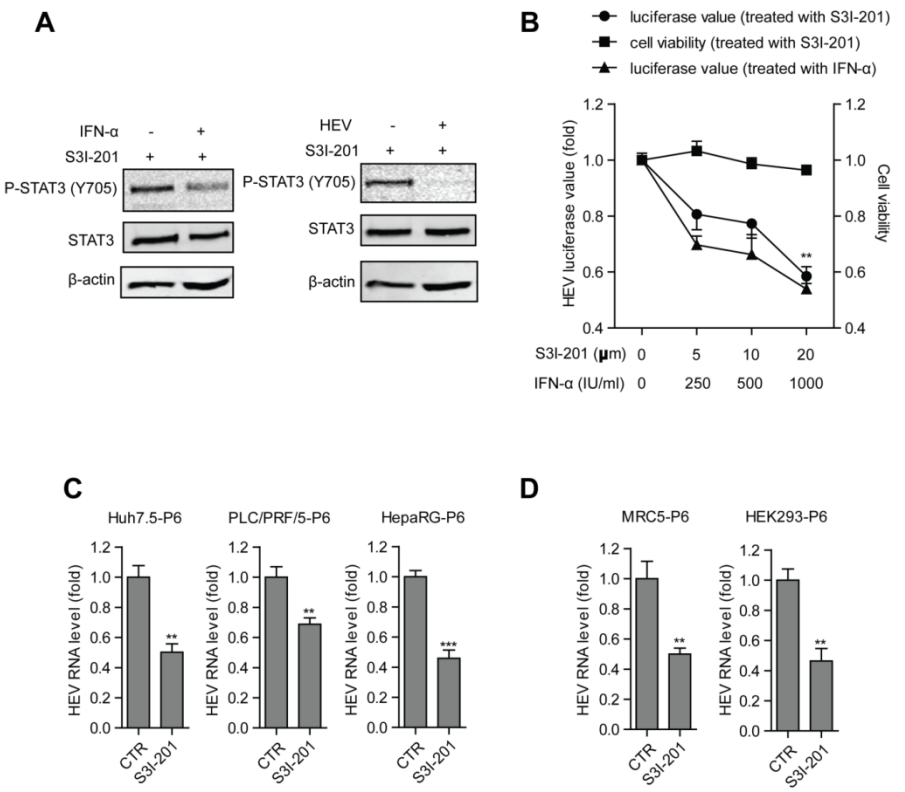

Figure 6. Pharmacological blockage of STAT3 activation constrains HEV replication. (A) Huh7.5 cells were treated with IFN-α (1000IU/ml), infected with HEV or the combination with STAT3 inhibitor, S3I-201 (20 μm). Western blotting analysis showed that S3I-201 decreased IFN-α or HEV induced STAT3 phosphorylation. (B) HEV subgenomic replicon model (Huh7.5-P6-luc) were treated with control or S3I-201 for 48 hours. S3I-201 significantly inhibited HEV-related luciferase activity, while no significant cytotoxicity was observed. IFN-α served as a positive control. (C) and (D) Five HEV infectious cell models (named Huh7.5-P6, PLC/PRF/5-P6, HepaRG-P6, MRC5-P6 and HEK293-P6) were treated with control or S3I-201(20 μm) for 48 hours. qRT-PCR analysis indicated that S3I-201 significantly inhibited HEV replication in all five different cell models.

IFN-α and ribavirin have been used as off-label treatment for chronic HEV infection. Mycophenolic acid (MPA), an immunosuppressive medication used in the clinic for decades, has been demonstrated to exert potent antiviral effect against HEV (19). To evaluate any potential combinatory anti-HEV effect for STAT3 inhibitor and these three drugs, MacSynergy 2 combination analysis was performed (20). The combination of S3I-201 with IFN-α, ribavirin or MPA showed no significant antagonistic or synergistic effect with respect to their anti-HEV ability (sFig. 2A-C).

Discussion

HEV infection is emerging as a global health issue. HEV outbreaks periodically occur throughout the resource limited countries, resulting in heavy health burden with high mortality rate in pregnant women (1). In industrialized regions, persistent infection has also been frequently reported in immunocompromised patients (3). However, the optimal treatment for HEV infection remains to be defined. HEV relies on host machinery to accomplish its full life-cycle, including entry, viral replication and egress. However, the studies related to the identification of host factors that regulate the HEV life cycle are limited.

STAT3 is a vital transcription factor, with clear links to the acute phase response, chronic inflammation, autoimmunity, metabolism and cancer progression (21). The highly pleiotropic nature

of STAT3 signaling suggests that its impact on virus replication will be multifactorial and complex. Indeed, both pro- and antiviral roles of STAT3 have been reported (6). In this study, we find that HEV infection elicit phosphorylation and activation of STAT3 in patients and *in vitro* cell culture models. This in turn created a favorable environment to facilitate HEV replication. Since STAT3 has been studied extensively as a transcription factor, it is plausible that the up-regulation of STAT3-dependent target genes would assist in creating a cellular environment to facilitate HEV replication. However, little is known about the proviral potential of these STAT3 target genes and this evidently requires future investigation. Alternatively, STAT3 itself may interact directly with viral proteins to enhance HEV replication. As expression of viral proteins does not impact STAT3 activation, this indicates an indirect relationship between STAT3 and HEV. Furthermore, STAT3 may regulate the host antiviral responses. STAT3 has been reported to act either as a positive or negative regulator of type I IFN responses, thus influencing ISGs (16-18). However, our results indicated that the pro-HEV effect of STAT3 is independent of IFN pathway. Thus we feel that expression of specific STAT3-dependent genes is the most likely explanation for our finding that STAT3 is essential for HEV replication, and identification of these STAT3 target genes constitutes an urgent task for future research.

Activated STAT3 has been reported to positively regulate microtubules stabilization (22). The microtubule network could be utilized as the transport system to facilitate virus replication and the release of mature virus (23, 24). Therefore, it might be interesting to investigate the possible involvement of microtubules in HEV replication. Recently, the finding that STAT3 also localizes to mitochondria has opened a new area to discover its functions (25, 26). Mitochondrial STAT3 serves as a regulator of the electron transport chain (ETC) and mitochondrial production of ATP and reactive oxygen species (ROS) (27, 28), which may be conceivable linked to the HEV infectious process. Based on the fact that STAT3 is a multi-functional regulator, it is likely that STAT3 may exert its pro-HEV effect in a multifaceted manner.

Constitutive STAT3 activation has been associated with malignant transformation. A large number of studies have been undertaken for the investigation of STAT3 as a cancer drug target, and several pharmacological inhibitors are at various stages of preclinical and clinical development (29). Interestingly, chronic HEV infection has been recently reported to be associated with the development of liver cancer (30). Therefore, the future clinical use of STAT3 inhibitors as anti-cancer drug will provide as an off-label therapy against HEV infection.

Materials and Methods

Additional procedures are described in detail in *SI Materials and Methods.*

Reagents and antibodies

Stocks of JAK inhibitor I (Santa Cruz Biotech, Santa Cruz, CA, 20), CP690550 (tofacitinib) and AG490 (Santa Cruz Biotech, Santa Cruz, CA), Bayer-18 (Synkinase, China) were dissolved in dimethyl sulfoxide (DMSO) (Sigma-Aldrich, St Louis, MO) to concentration of 10 mg/ml. FGF Receptor Tyrosine Kinase Inhibitor and Src Kinase Inhibitor I (Merck Chemicals BV) were dissolved in DMSO to concentration of 10 mM. STAT3 Inhibitor VI, S3I-201 (Santa Cruz Biotech, Santa Cruz, CA) were dissolved in DMSO to concentration of 20 mM. phospho-STAT1(Y701) (58D6, #9167), phospho-STAT3

(Y705) (D3A7, #9145), STAT3 (79D7, #4904), Anti-rabbit IgG(H+L),F(ab') 2 Fragment (Alexa Fluor 488 conjugate) and Anti-mouse IgG (H+L), F(ab')2 Fragment (Alexa Fluor® 488 Conjugate) antibodies were purchased from Cell Signaling Technology. STAT1 (rabbit polyclonal; sc-592), phosphor-STAT2 (Y690) (rabbit polyclonal; sc-21689-R) and β-actin were purchased from Santa Cruz Biotechnology. Hepatitis E Monoclonal Antibody (ORF2) was purchased from EMD Millipore Corporation, USA.

Patient materials

Twenty-one liver biopsies from patients (2010 – 2017) diagnosed of acute or chronic hepatitis E were retrieved at Beijing 302 hospital, China. The use of patient materials was approved by the medical ethical committee of Beijing 302 hospital. The expression of P-STAT3 (Y705) was stained. Five liver biopsies from hepatic hemangioma patients were collected as negative control. These patient information was shown in Table S1.

References

1. Azman AS*, et al.* (2017) High Hepatitis E Seroprevalence Among Displaced Persons in South Sudan. *Am J Trop Med Hyg* 96(6):1296-1301.
2. Rayis DA, Jumaa AM, Gasim GI, Karsany MS, & Adam I (2013) An outbreak of hepatitis E and high maternal mortality at Port Sudan, Eastern Sudan. *Pathog Glob Health* 107(2):66-68.
3. Kamar N*, et al.* (2008) Hepatitis E virus and chronic hepatitis in organ-transplant recipients. *N Engl J Med* 358(8):811-817.
4. Hakim MS*, et al.* (2017) The global burden of hepatitis E outbreaks: a systematic review. *Liver Int* 37(1):19-31.
5. Panda SK & Varma SP (2013) Hepatitis e: molecular virology and pathogenesis. *J Clin Exp Hepatol* 3(2):114-124.
6. Kuchipudi SV (2015) The Complex Role of STAT3 in Viral Infections. *J Immunol Res* 2015:272359.
7. Li Y, de Haar C, Peppelenbosch MP, & van der Woude CJ (2012) New insights into the role of STAT3 in IBD. *Inflamm Bowel Dis* 18(6):1177-1183.
8. Yu H, Lee H, Herrmann A, Buettner R, & Jove R (2014) Revisiting STAT3 signalling in cancer: new and unexpected biological functions. *Nat Rev Cancer* 14(11):736-746.
9. Yu H, Pardoll D, & Jove R (2009) STATs in cancer inflammation and immunity: a leading role for STAT3. *Nat Rev Cancer* 9(11):798-809.
10. Waris G, Turkson J, Hassanein T, & Siddiqui A (2005) Hepatitis C virus (HCV) constitutively activates STAT-3 via oxidative stress: role of STAT-3 in HCV replication. *J Virol* 79(3):1569-1580.
11. McCartney EM*, et al.* (2013) Signal transducer and activator of transcription 3 is a proviral host factor for hepatitis C virus. *Hepatology* 58(5):1558-1568.
12. Versteeg HH, Peppelenbosch MP, & Spek CA (2003) Tissue factor signal transduction in angiogenesis. *Carcinogenesis* 24(6):1009-1013.
13. Dudka AA, Sweet SM, & Heath JK (2010) Signal transducers and activators of transcription-3 binding to the fibroblast growth factor receptor is activated by receptor amplification. *Cancer Res* 70(8):3391-3401.
14. Haura EB (2006) SRC and STAT pathways. *J Thorac Oncol* 1(5):403-405.
15. Wang W, Xu L, Su J, Peppelenbosch MP, & Pan Q (2017) Transcriptional Regulation of Antiviral Interferon-Stimulated Genes. *Trends Microbiol* 25(7):573-584.
16. Mahony R*, et al.* (2017) A novel anti-viral role for STAT3 in IFN-alpha signalling responses. *Cell Mol Life Sci* 74(9):1755-1764.
17. Ho HH & Ivashkiv LB (2006) Role of STAT3 in type I interferon responses. Negative regulation of STAT1-dependent inflammatory gene activation. *J Biol Chem* 281(20):14111-14118.
18. Wang WB, Levy DE, & Lee CK (2011) STAT3 negatively regulates type I IFN-mediated antiviral response. *J Immunol* 187(5):2578-2585.
19. Wang Y*, et al.* (2014) Calcineurin inhibitors stimulate and mycophenolic acid inhibits replication of hepatitis E virus. *Gastroenterology* 146(7):1775-1783.
20. Dang W*, et al.* (2017) Inhibition of calcineurin or IMPDH exerts moderate to potent antiviral activity against norovirus replication. *Antimicrob Agents Chemother*.
21. Levy DE & Lee CK (2002) What does Stat3 do? *J Clin Invest* 109(9):1143-1148.
22. Ng DC*, et al.* (2006) Stat3 regulates microtubules by antagonizing the depolymerization activity of stathmin. *J Cell Biol* 172(2):245-257.
23. Henry Sum MS (2015) The involvement of microtubules and actin during the infection of Japanese encephalitis virus in neuroblastoma cell line, IMR32. *Biomed Res Int* 2015:695283.

24. Wolk B, Buchele B, Moradpour D, & Rice CM (2008) A dynamic view of hepatitis C virus replication complexes. *J Virol* 82(21):10519-10531.
25. Wegrzyn J*, et al.* (2009) Function of mitochondrial Stat3 in cellular respiration. *Science* 323(5915):793-797.
26. Gough DJ*, et al.* (2009) Mitochondrial STAT3 supports Ras-dependent oncogenic transformation. *Science* 324(5935):1713-1716.
27. Yang R & Rincon M (2016) Mitochondrial Stat3, the Need for Design Thinking. *Int J Biol Sci* 12(5):532-544.
28. Mantel C*, et al.* (2012) Mouse hematopoietic cell-targeted STAT3 deletion: stem/progenitor cell defects, mitochondrial dysfunction, ROS overproduction, and a rapid aging-like phenotype. *Blood* 120(13):2589-2599.
29. Yue P & Turkson J (2009) Targeting STAT3 in cancer: how successful are we? *Expert Opin Investig Drugs* 18(1):45-56.
30. Borentain P*, et al.* (2017) Hepatocellular carcinoma complicating hepatitis E virus-related cirrhosis. *Hepatology*.

Supporting Information

SI Materials and Methods

Cell culture models and plasmids

Human hepatoma cells Huh7.5 were kindly provided by Professor Bart Haagmans from Department of Viroscience, Erasmus Medical Center. Human embryonic kidney 293 cells (HEK293) were originally obtained from ATCC (www.atcc.org). Huh7.5 and HEK293 cells were grown in Dulbecco's modified Eagle medium (DMEM) (Lonza Biowhittaker, Verviers, Belgium) supplemented with 10% (v/v) fetal calf serum (FCS) (Hyclone, Lonan, Utah) and antibiotics.). The HEV subgenomic model was based on Huh7.5 cells containing the subgenomic HEV sequence (Kernow-C1, P6-luc) coupled to a Gaussia luciferase reporter gene. HEV-infected cell models (named Huh7.5-P6, PLC/PRF/5-P6, HepaRG-P6, MRC5-P6 and HEK293-P6), electroporated with full-length HEV genome RNA were generated as described (1, 2). MEF cells (WT, STAT3-/- and STAT3-C) were kindly provided by Annalisa Camporeale (University of Turin) (3, 4). Plasmid STAT3-Luc was kindly provided by Michael R. Beard (University of Adelaide). Plasmid pLVX-ORF2-IRES-zsGrenn1 was kindly provided by Alexander Ploss (Princeton University) (5). Plasmid pEGFP-C1-ORF3 was constructed in our lab.

Immunohistochemistry (IHC) staining

Immunohistochemistry staining of HEV ORF2 viral protein or P-STAT3 (Y705) was performed to validate HEV infection and visualize phosphorylated-STAT3. In detail, the liver biopsies were fixed in 10% formalin for 1.5 h at room temperature, processed for paraffin embedding, and sectioned at a thickness of 4 μm. The sections were deparaffinized in xylene and rehydrated through graded ethanol treatment, followed by high pressure in citrate buffer (pH 6.0) for 3 min for antigen retrieval. Then they were blocked with 3% H_2O_2 in TBS for 15 min and further blocked with goat serum for 1 hour. The sections were then incubated with anti-HEV ORF2 viral protein (Millipore,1:600) or anti-P-STAT3 (Cell signaling,1:800) monoclonal antibody overnight at 4 °C, and incubated with goat anti-mouse/rabbit secondary antibody (ZSGB-BIO,KIT-5030) for 15 min at 37°C. Subsequently, the sections were developed in diaminobenzidine (DAB) (ZSGB-BIO, ZLI-9018), followed by counterstaining hematoxylin. Immunostained sections were scanned using Leica DFC400 digital camera and Leica Application Suite software (Leica Microsystems).

Gene knockdown by lentiviral vectors

Lentiviral pLKO knockdown vectors (Sigma–Aldrich) targeting IL6R, IFNAR1, IFNGR1, IFNLR1 or control were obtained from the Erasmus Biomics Center and produced in HEK293T cells as previously described (6). After a pilot study, the shRNA vectors exerting optimal gene knockdown were selected. These shRNA sequences are listed in Table S2. Stable gene knockdown cells were generated after lentiviral vector transduction and puromycin (4 µg/ml; Sigma) selection.

Measurement of luciferase activity

For HEV (ORF1)-related *Gaussia* luciferase analysis, the activity of secreted luciferase in the cell culture medium was measured by BioLux® *Gaussia* Luciferase Flex Assay Kit (New England Biolabs) according to the manufacturer's instructions. STAT3 promoter elements related luciferase activity (STAT3-luc) was measured using the Luciferase Assay System (Promega, Madison, WI). Data were normalized for the transfection efficiency by using the Dual Luciferase Reporter Assay system (Promega) according to the manufacturer's instructions. The luciferase activity was quantified with a LumiStar Optima luminescence counter (BMG Lab Tech, Offenburg, Germany).

Quantitative real-time polymerase chain reaction

RNA was isolated using a Machery-NucleoSpin RNA II kit (Bioke, Leiden, The Netherlands) and quantified using a Nanodrop ND-1000 (Wilmington, DE, USA). All RNA samples were adjusted to the concentration of 62.5ng/µl. 500 ng of RNA was used as template for cDNA preparation with the reverse transcription system(TAKARA BIO INC). The cDNA (10ng/well) of all detected genes was amplified for 50 cycles and quantified with a SYBRGreen-based real-time PCR (Applied Biosystems) according to the manufacturer's instructions. GAPDH was used as a reference gene for normalizing gene expression. Relative gene expressions were normalized to GAPDH using the formula $2^{-\Delta\Delta CT}$ ($\Delta\Delta CT = \Delta CT_{sample} - \Delta CT_{control}$). All the primer sequences are included in Table S3.

Transfection assay

FuGENE® HD Transfection Reagent was used for transfection assays. Cells were seeded in 96-well plates at a density of 1×10^4 cells per well. After 24h, the medium was removed and cell layer was washed by Opti-MEM. Plasmid constructs were transfected with FuGENE® HD Transfection Reagent in a total volume of 100 µL Opti-MEM according to the protocols. After 6 h, the medium was changed back to routine medium.

Confocal laser electroscope assay

Cells were seeded on glass coverslips. After 12 hours, cells were washed with PBS, fixed in 4% PBS-buffered formalin for 10 mins and blocked with tween-milk-glycine medium (PBS, 0.05% tween, 5g/L skim milk and 1.5g/L glycine). Samples were incubated with primary antibodies overnight at 4 °C. Subsequently, samples were incubated with 1:1000 dilutions of the anti-mouse IgG (H+L), F(ab')2 Fragment (Alexa Fluor® 488 Conjugate) or anti-rabbit IgG(H+L), F(ab') 2 Fragment (Alexa Fluor 488 conjugate) secondary antibodies. Nuclei were stained with DAPI (4,6-diamidino-2-phenylindole; Invitrogen). Images were detected using confocal electroscope.

HEV infection assay

HEV inoculation and infection assay was performed according to previously described protocols (7). Infectious HEV particles were collected from Huh7-P6 HEV model and purified by ultracentrifugation. The supernatant was first filtered through 0.45 mm filter followed by centrifugation at 10,000 rpm for 30 min to remove cell debris and then 22,000 rpm for 2 h to pellet HEV virus (SW 28 rotor). The pellet was suspended with DMEM and diluted to 1×10^7 HEV viral RNA copies/ml. The diluted HEV virus stock was stored at −80 °C. For HEV infection, cells were seeded into 12-well plates at a density of 7×10^4 cells per well and incubated for 24 h. Next, cells were incubated with 400 µl of the HEV stock (1×10^7 viral RNA copies/ml) per well at 37 °C for 3 days. Then, the inoculum was removed, and cell layers were washed three times with PBS.

Western blot assay

Cultured cells were lysed in Laemmli sample buffer containing 0.1 M DTT and heated for 5 min at 95 °C, followed by loading onto a 10% sodium dodecyl sulfate polyacrylamide gel and separation by electrophoresis. After 90 min running at 120 V, proteins were transferred onto a polyvinylidene difluoride membrane (Invitrogen) for 1.5 h with an electric current of 250mA. Subsequently, the membrane was blocked with a mixture of 2.5 ml blocking buffer (Odyssey) and 2.5 ml phosphate-buffered saline containing 0.05% Tween 20. This was followed by overnight incubation with primary antibodies (1:1000) at 4 °C. The membrane was washed 3 times followed by incubation with IRDye-conjugated secondary antibody (1:5000). After washing 3 times, protein bands were detected with the Odyssey 3.0 Infrared Imaging System.

Statistical analysis

All results were presented as mean ± SEM. Data analysis were performed with Mann-Whitney test. Differences were considered significant at a p-value less than 0.05 (single asterisks in figures), P values less than 0.01 (double asterisks) and 0.001 (triple asterisks) were considered highly significant.

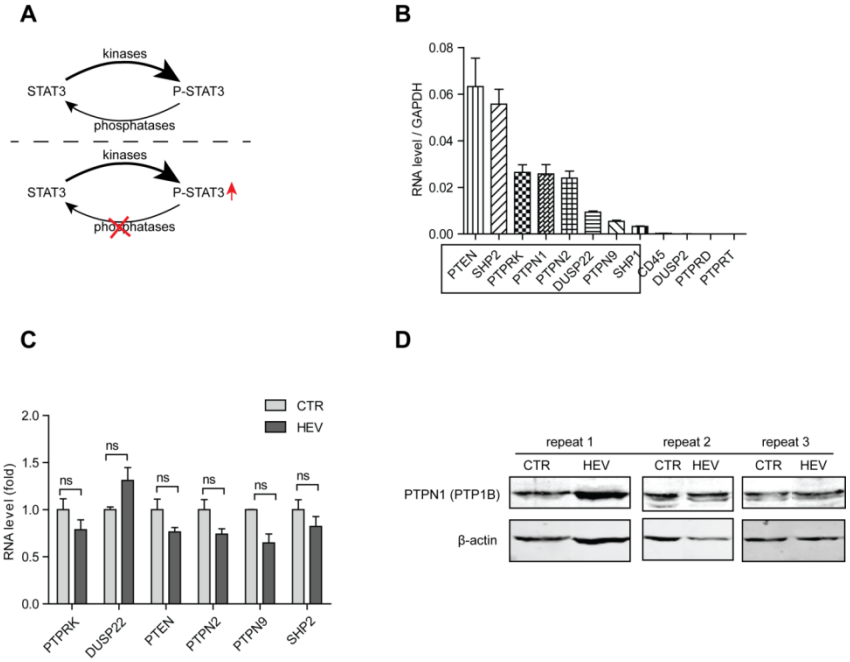

sFig. 1. HEV infection results in no significant effects on the levels of phosphatase. (A) The regulation of phosphorylation process of STAT3 was illustrated. Upon signaling transduction, STAT3 gets phosphorylated by specific kinases. Meanwhile, phosphorylated STAT3 undergoes dephosphorylation process by specific phosphatase. Thus, the phosphorylation and dephosphorylation process coordinate to maintain the phosphorylation level at a balanced state. Consequently, the inhibition of phosphatases will alter the balanced state, leading to higher levels of phosphorylated STAT3. (B) The expression levels of indicated phosphatases in Huh7.5 cells were analyzed by qRT-PCR. (C) qRT-PCR analysis of indicated phosphatases in Huh7.5 cells infected with HEV or controls. HEV infection exerted no significant effect on the expression levels of phosphatases. (D) Western blotting analysis of mock or HEV infected Huh7.5 cells with PTP1B antibody (H-135, sc-14021, Santa Cruz Biotechnology). HEV infection exerted no significant effect on the levels of PTP1B.

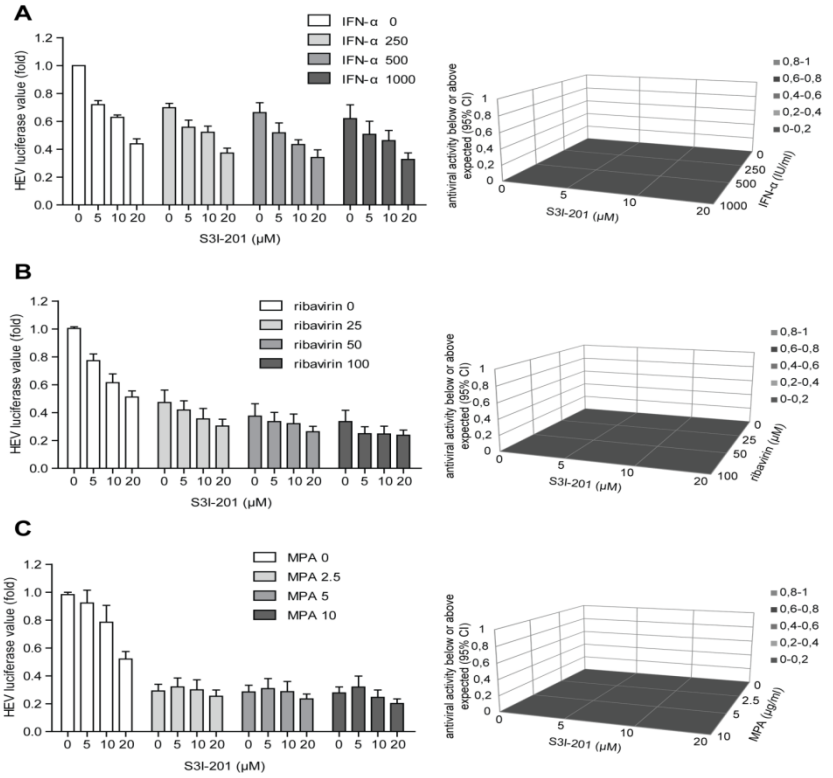

sFig. 2. The combination of STAT3 inhibitor S3I-201 with IFN-α, ribavirin or MPA results in no antagonistic or synergistic effect against HEV. The combinatory anti-HEV effects of two drugs were analyzed using the mathematical model MacSynergyII. The three-dimensional surface plot represents the differences (within 95% confidence interval) between actual experimental effects and theoretical additive effects of the combination at various concentrations (n = 5). The antiviral effects of S3I-201 in combination with IFN-α (A), ribavirin (B) or MPA (C) was analyzed by the MacSynergyII model.

Table S1. Patient information

	patient No.	Gender	Age	diagnosis	HEV-IgG	HEV-IgM	HEV staining	P-STAT3 staining
HEV patients	1	Female	38	acute non-icteric HEV	-	+	1-5%	1-5%
	2	Female	58	acute icteric HEV	weak +	-	5-10%	1-5%
	3	Male	42	acute icteric HEV	-	+	5-10%	1-5%
	4	Male	24	acute icteric HEV	+	+	5-10%	1-5%
	5	Male	20	acute icteric HEV	+	-	10-15%	10-15%
	6	Male	5	acute non-icteric HEV	-	+	1-5%	1-5%
	7	Male	38	acute icteric HEV	weak +	+	10-15%	0%
	8	Female	58	acute icteric HEV	+	+	0%	0%
	9	Male	58	acute icteric HEV	-	weak +	1-5%	1-5%
	10	Male	1,5	acute HEV	-	+	1-5%	1-5%
	11	Female	67	acute HEV	+	-	5-10%	1-5%
	12	Male	3	acute HEV	-	+	0%	1-5%
	13	Female	61	acute icteric HEV	+	+	1-5%	1-5%
	14	Male	40	acute icteric HEV	-	+	5-10%	1-5%
	15	Male	55	acute HEV	+	weak +	10-15%	1-5%
	16	Male	35	HEV	+	-	5-10%	10-15%
	17	Male	19	HEV	+	-	1-5%	1-5%
	18	Female	66	acute HEV	+	-	1-5%	1-5%
	19	Male	52	HEV	+	-	10-15%	5-10%
	20	Male	11	acute non-icteric HEV	+	+	5-10%	0%
	21	Male	36	chronic HEV	+	+	10-15%	5-10%
Negative controls	22	Female	40	hepatic hemangioma	-	-	0%	0%
	23	Female	44	hepatic hemangioma	-	-	0%	0%
	24	Male	49	hepatic hemangioma	-	-	0%	0%
	25	Female	48	hepatic hemangioma	-	-	0%	0%
	26	Female	43	hepatic hemangioma	-	-	0%	0%

+, postive. -, negative.

Table S2. qRT-PCR primer sequences (human)

Gene	F-Sequences (5' - 3')	R-Sequences (5' - 3')
IFNAR1	CGCCTGTGATCCAGGATTATCC	TGGTGTGTGCTCTGGCTTTCAC
IFNLR1	CAGCAAGTTCTCTAAGCCCACC	GTCATTCACGGACTCTGGTCTG
IFNGR1	AGTGCTTAGCCTGGTATTCATCTG	GGCTGGTATGACGTGATGAGTG
IL6R	GACTGTGCACTTGCTGGTGGAT	ACTTCCTCACCAAGAGCACAGC
IL10R	GCCGAAAGAAGCTACCCAGTGT	GGTCCAAGTTCTTCAGCTCTGG
HEV(P6)	ATCGGCCAGAAGTTGGTTTTTAC	CCGTGGCTATAACTGTGGTCT
GAPDH	TGTCCCCACCCCCAATGTATC	CTCCGATGCCTGCTTCACTACCTT

Table S3. qRT-PCR primer sequences (mouse)

Gene	F-Sequences (5' - 3')	R-Sequences (5' - 3')
IFNα-F	GGATGTGACCTTCCTCAGACTC	ACCTTCTCCTGCGGGAATCCAA
IFNβ-F	AAGAGTTACACTGCCTTTGCCATC	CACTGTCTGCTGGTGGAGTTCATC
IFIT1-F	TACAGGCTGGAGTGTGCTGAGA	CTCCACTTTCAGAGCCTTCGCA
MX1-F	TGGACATTGCTACCACAGAGGC	TTGCCTTCAGCACCTCTGTCCA
DDX58-F	AGCCAAGGATGTCTCCGAGGAA	ACACTGAGCACGCTTTGTGGAC
IFIH1-F	TGCGGAAGTTGGAGTCAAAGCG	CACCGTCGTAGCGATAAGCAGA
IRF9-F	CAACATAGGCGGTGGTGGCAAT	GTTGATGCTCCAGGAACACTGG
GAPDH-F	CATCACTGCCACCCAGAAGACTG	ATGCCAGTGAGCTTCCCGTTCAG

Table S4. Lentiviral shRNA sequences

Name	Oligo Sequences (5' - 3')
IL6R kd No.01	CCGGCTCTGGAAACTATTCATGCTACTCGAGTAGCATGAATAGTTTCCAGAGTTTTTG
IL6R kd No.02	CCGGAGCCCTTATGACATCAGCAATCTCGAGATTGCTGATGTCATAAGGGCTTTTTTG
IFNAR1 kd No.01	CCGGGCCAAGATTCAGGAAATTATTCTCGAGAATAATTTCCTGAATCTTGGCTTTTTG
IFNAR1 kd No.02	CCGGCCTTAGTGATTCATTCCATATCTCGAGATATGGAATGAATCACTAAGGTTTTTG
IFNLR1 kd No.01	CCGGCCAACAGACAAGATGGAAGAACTCGAGTTCTTCCATCTTGTCTGTTGGTTTTTG
IFNLR1 kd No.02	CCGGACACGTTCAGTGTCCCGAAATCTCGAGATTTCGGGACACTGAACGTGTTTTTTG
IFNGR1 kd No.01	CCGGGCCTATGCAAAGTCAGAAGAACTCGAGTTCTTCTGACTTTGCATAGGCTTTTTG
IFNGR1 kd No.02	CCGGCGGAAGTGAGATCCAGTATAACTCGAGTTATACTGGATCTCACTTCCGTTTTTG
IFNGR1 kd No.03	CCGGCCACCTCCTTTGGTTATGATACTCGAGTATCATAACCAAAGGAGGTGGTTTTTG

References

1. Xu L*, et al.* (2017) RIG-I is a key antiviral interferon-stimulated gene against hepatitis E virus regardless of interferon production. *Hepatology* 65(6):1823-1839.
2. Qu C*, et al.* (2017) Nucleoside analogue 2'-C-methylcytidine inhibits hepatitis E virus replication but antagonizes ribavirin. *Arch Virol*.
3. Camporeale A*, et al.* (2014) STAT3 Activities and Energy Metabolism: Dangerous Liaisons. *Cancers (Basel)* 6(3):1579-1596.
4. Costa-Pereira AP*, et al.* (2002) Mutational switch of an IL-6 response to an interferon-gamma-like response. *Proc Natl Acad Sci U S A* 99(12):8043-8047.
5. Ding Q*, et al.* (2017) Hepatitis E virus ORF3 is a functional ion channel required for release of infectious particles. *Proc Natl Acad Sci U S A* 114(5):1147-1152.
6. Wang W*, et al.* (2017) Unphosphorylated ISGF3 drives constitutive expression of interferon-stimulated genes to protect against viral infections. *Sci Signal* 10(476).
7. Wang W*, et al.* (2017) Biological or pharmacological activation of protein kinase C alpha constrains hepatitis E virus replication. *Antiviral Res* 140:1-12.

Chapter 16

Summary and Discussion

Hepatitis E virus (HEV) infection is the most common cause of acute hepatitis worldwide. Epidemics of hepatitis E occur periodically throughout the developing world. High mortality rate occurs in specific populations, in particular in pregnant women (1). **In Chapter 2**, I comprehensively reviewed the global burden of HEV outbreak. HEV outbreaks were mainly reported from Asian and African countries, and only a few from European and American countries. India represents the country with the highest number of reported HEV outbreaks. HEV genotypes 1 and 2 were responsible for most of the large outbreaks in developing countries. During the outbreaks in developing countries, a significantly higher case fatality rate was observed in pregnant women. The control measures mainly depend upon improvement of sanitation and hygiene. This study highlights that HEV is a continuous global health problem. Unfortunately, there is no effective prevention or treatment available in this setting, besides supportive care. Remarkably, chronic hepatitis E is emerging in developed countries, specifically in immunocompromised patients. Of note, chronic HEV infection could result in rapid progression to liver fibrosis and cirrhosis in organ transplant recipients, which is an important cause of graft loss and patient death. Although hepatitis E was discovered in early 1980s, not enough attention was paid to its clinical burden. Besides supportive care and off-label treatment for some cases, there is still no proven anti-HEV medication available. Fundamental and translational research has fallen far behind, when compared to the research on other hepatitis viruses. Therefore, there is an urgent need for the development of novel antivirals, which ideally should act on distinct mechanisms to maximize the antiviral effect, a strategy that has proven essential for successful control of other viruses, like HIV.

The role of interferon-stimulated genes in combating HEV infection

The interferon (IFN)-mediated cellular response is thought to be the first line of antiviral defense. IFN exerts its antiviral function by inducing the expression of the so-called IFN-stimulated genes (ISGs) (2, 3). There is accumulating data to indicate that host cells have evolved complex but elaborate systems to defend against virus infection, and that the pathways involved are not limited to the well-described action of IFNs. Recently, the existence of an antiviral pathway that acts before the production of IFNs was reported (4). Upon infection, a subset of NF-kB-inducible genes (*e.g.* CXCL9 and CXCL10) were induced apparently before IFNs were produced in the viral infection process, and these genes may thus be part of an auxiliary system combating viral disease. CXCL9 and CXCL10 were found to recruit neutrophils to exert their antiviral activity. Since some specific ISGs possess direct antiviral activity, ISGs expressed at a basal level can exert cell-autonomous antiviral activity, independent of virus-induced IFN production (4).

In Part I Chapter 3, I comprehensively reviewed the canonical and non-canonical regulation mechanisms of ISG transcription. I highlighted the non-canonical regulation of ISG expression that involved some unique pathways or complex, such as non-canonical ISGF3 complex, STAT5-CrkL complex and nucleotide synthesis pathway. This finding apparently expands our understanding of the regulation of ISG at transcriptional leve and shows that these mechanisms are more complex as thought but may also provide clues for the development of antiviral strategies. In **Chapter 4,** I discussed the IFN-independent antiviral mechanisms of some ISGs. Many important antiviral ISGs have the ability to activate or amplify ISG transcription apparently independent of IFN production. Some ISGs which are believed to exert antiviral function via induction of IFN production also have direct antiviral abilities. This is still a largely unexplored area in need of further investigation. Besides

IFN-α, TNF-α (Tumor Necrosis Factor-alpha) is also an important antiviral cytokine and its downstream NF-κB pathway plays essential roles in regulating the expression of inflammatory cytokines. In **Chapter 5**, I investigated the antiviral ability of TNF-α and its role in regulating ISG transcription (5). I first demonstrated that TNF-α exerts potent antiviral ability against HEV and HCV. I ruled out the possibility that TNF-α induces ISG expression through the production of IFN or JAK-STAT signaling. I found the TNF-α activates ISG transcription via its canonical downstream pathway, NF-κB. NF-κB protein complex, serving as an important transcription factor, directly binds to the promoter region of many ISGs. I further found that TNF-α cooperated with IFN-α in ISG induction and antiviral action against HCV and HEV.

Even without the presence of IFNs, many ISGs are constitutive expressed, which enable host cell to mount a rapid and direct response to viral infection. However, how host cells maintains ISGs expression at basal level is still not clear. In **Chapter 6,** I reported that the unphosphorylated ISGF3 (U-ISGF3) complex, which is constituted out of IRF9 together with unphosphorylated STAT1 and STAT2, drives the constitutive expression of ISGs under homeostatic conditions (6). Deletion of any element of this U-ISGF3 complex leads to the decreased expression of ISGs and increased viral replication. Conversely, the overexpression of these three proteins, not any one of them alone, increased ISG expression and inhibited viral replication. These results expand our knowledge on the regulation of ISG transcription. In **Chapter 7,** using a lentivirus-based experimental strategy, I profiled a cohort of human ISGs for their anti-HEV ability. RIG-I, MDA5 and IRF1 were identified as potent anti-HEV ISGs.I focused on RIG-I for further mechanistic study. RIG-I is a pattern recognition receptor (PRR) that mainly recognizes viral RNAs (7-9). Interestingly, I found that RIG-I is involved in IFN induced ISG transcription. The absence of RIG-I will attenuate IFN-initiated ISG expression while its overexpression appears to enhance ISG expression. It is generally believed that RIG-I exerts its antiviral action by the induction of IFN production. However, I found that RIG-I exerts its anti-HEV activity independent of IFN production. The overexpression of RIG-I activated the phosphorylation of STAT1 and the induction of ISGs without triggering IFN production.

Collectively, all these canonical and non-canonical mechanisms coordinately regulate the vast host antiviral web that is centered around the ISGs. With regards to the adverse effects of IFNs, ISG-based antiviral strategies could be the next promising frontier in drug development for controlling hepatitis E. Several ISGs have been identified to exert potent anti-HEV effect in our study. Based on the fact that ISGs encompass hundreds members, a comprehensive study to characterize individual ISGs with respect to their anti-HEV specificity is highly demanded. These data are invaluable for the development of ISG-based specific antivirals against HEV.

Direct-acting antiviral (DAA) agents against hepatitis E

A variety of nucleoside analogues have been widely used to treat viral infections due to their potent antiviral effects and high barrier to drug resistance development. Ribavirin, an guanosine analogue, is the drug of choice for treating most chronic HEV patients. Ribavirin monotherapy is effective for treating chronic HEV with sustained virological responses (SVRs) of 85–90% (10-12). However, for a few patients, ribavirin treatment fails (13, 14). Effective antiviral therapy is therefore needed for HEV-infected patients with ribavirin treatment failure. One study indicated that sofosbuvir, a direct-acting antiviral (DAA) agent against hepatitis C virus (HCV), can inhibit HEV replication and exert an additive effect when combined with ribavirin (15). Sofosbuvir is a specific and potent inhibitor that

targets the HCV NS5B RNA-dependent RNA polymerase. **In Part II Chapter 8**, I found that the in-vitro efficacy of sofosbuvir against HEV is modest even at high concentrations (16). **In Chapter 9**, I showed that sofosbuvir was effective at inhibiting HCV replication, but was much less efficacious against HEV in cell culture models of both monoinfection and HCV–HEV co-infection (16). **In Chapter 10**, I reviewed in-vitro and in-vivo data and concluded that sofosbuvir is unlikely to be the drug of choice for patients who do not clear HEV under ribavirin therapy (17). To develop effective DAAs for HEV, it is essential to gain more insight into the crystallographic structures of the viral proteins, particularly the HEV polymerase.

For HEV infection, antiviral is needed only for a subpopulation or limited number of patients, and pharmaceutical companies have no interest in therapeutic development, despite the necessity and urgency. Therefore, the discovery of potential anti-HEV candidates from pre-clinical or clinical used antiviral drugs represent an cost-effective but unconventional paths. The nucleoside analogue 2'-C-methylcytidine (2CMC), a viral polymerase inhibitor, has been shown to inhibit the infection of a variety of viruses (18, 19). **In Chapter 11**, I found that 2CMC significantly inhibits the replication of HEV. This result indicated that 2CMC constitutes a potential antiviral drug for the treatment of HEV infection(20). Favipiravir (T-705; 6-fluoro-3-hydroxy-2-pyrazinecarboxamide) is another antiviral drug, which selectively inhibits the RNA-dependent RNA polymerase of influenza virus (21). In addition to its anti-influenza activity, favipiravir also blocks the replication of many other RNA viruses. Therefore, it is also worthwhile to investigate the effect of favipiravir on HEV. With its direct mechanism of action and broad spectrum of antiviral activity, favipiravir may represent another promising drug candidate for HEV.

HEV-host interactions: the path to novel antiviral strategies

Viruses heavily rely on the host to complete their life-cycle. In turn, the human body possesses a powerful immune system to sense and defend against viral infections. Gaining insight how HEV triggers host antiviral defense and how the virus interferes with these mechanisms is essential for the development of new therapeutic approaches. Protein kinases are principal components of the machineries that orchestrate immune response against diverse pathogens. To comprehensively profile kinase-mediated cascades in cell–autonomous antiviral immunity, in **Part III Chapter 12**, I screened a library of pharmacological kinase inhibitors in Huh7.5 based HEV replication cell model. I identified protein kinase C alpha (PKCα) as an important cell host factor restricting HEV replication (22). In fact, except PKCα, several other kinases have also been identified either promoting or inhibiting HEV replication, (*e.g*. CDK, AKT). These kinases also represent good candidates to study the interaction between host kinome and HEV.

Since *de novo* nucleotide biosynthesis is essentially required for both host cell metabolism and viral replication, specific catalytic enzymes of these pathways have been explored as potential antiviral targets. **In Chapter 13**, I investigated the role of different enzymatic cascades of nucleotides biosynthesis in hepatitis E virus (HEV) replication. I found that targeting the early steps of the purine biosynthesis pathway led to enhancement of HEV replication; whereas targeting the later step resulted in potent antiviral activity. Interestingly, all these inhibitors with anti-HEV activity concurrently triggered the induction of ISGs. This study highlighted a crosstalk between nucleotide biosynthesis pathways and cellular antiviral immunity in constraining HEV infection (23). However,

the mechanism as to the inhibition of nucleotide biosynthesis can induce ISGs are still unknown. This also represents a non-canonical regulation of ISGs needing further investigation.

The outcomes of hepatitis E virus (HEV) infection are closely associated with the immunological status of the host. To understand the innate cellular response to HEV infection, in **Chapter 14**, I studied the phosphorylation of STAT1 (Y701), a hallmark of IFN-related antiviral response, in the liver of HEV infected patients. Maybe not surprisingly, I found that HEV RNA potently induces IFN production and antiviral response in both cell lines and 3D cultured primary liver organoids. Single-stranded HEV RNA (ssRNA) was sufficient to trigger this host response. This occurs in a RIG-I-, MDA5-, MAVS- and β-catenin-independent, but IRF3 and IRF7-dependent manner. Our result indicates that HEV RNA is likely recognized by an undefined or unknown cytosolic RNA-sensing systems. Until now, only limited numbers of intracellular RNA sensors are described, a comprehensive study to further explore undiscovered sensors will definitely facilitate the studies in this field.

Viruses heavily rely on the host to supply biochemical materials, and use essential cellular machineries of the host to complete their life-cycle. However, the knowledge related to host factors that impact the HEV life cycle are quite limited. In **Chapter 15**, the phosphorylation of STAT3 (Y705) was assessed in a cohort of HEV infected patients using paraffin embedded liver tissue. Consistent with the results obtained (which suggested that STAT3 activation is linked to HEV infection), the inoculation of model systems with HEV resulted in STAT3 phosphorylation in different *in vitro* cell lines. STAT3 activation occurs in a HEV replication dependent manner via the kinase activity of Janus kinases (JAKs) and Src kinase. Functional studies indicated that HEV-dependent STAT3 phosphorylation in turn created a favorable environment to facilitate HEV replication. Interestingly, constitutive STAT3 activation has been associated with malignant transformation. A large number of studies have been undertaken for the investigation of STAT3 as a cancer drug target, and several pharmacological inhibitors are at various stages of preclinical or clinical development (24). Interestingly, chronic HEV infection has been recently reported to be associated with the development of liver cancer (25). Therefore, the future clinical use of STAT3 inhibitors as anti-cancer drug will provide as an off-label therapy against HEV infection.

Final Remarks

- The ISGs network represents a complex butrobust and effective system defining the state of host anti-pathogen defense, which are not restricted to the well-described action of IFNs. Profiling individual ISGs with respect to their antiviral effects against HEV is highly called for. This knowledge is highly relevant for guiding the development of novel therapies that promote the clearance of HEV infection, but avoiding autoimmune diseases and toxic effects to the host.
- For HEV infection, antiviral therapy is needed only for a limited number of patients. Therefore, the discovery of potential anti-HEV candidates from pre-clinical or clinical used antiviral drugs represent a cost-effective but likely only to improve care for a restricted number of cases and thus such therapies shall remain unconventional in nature.
- Viruses heavily rely on the host to complete their life-cycle. In turn, the human body has evolved a powerful immune system to defend against viral infections. Gaining insight how HEV triggers host antiviral defence and how the virus interferes with these mechanisms will not resolve the clinical burden immediately. However, such fundamental knowledges will prove essential for exploiting the full potential of current anti-HEV therapy, as well as the development of new therapeutic approaches.

References

1. Hakim MS, Wang W, Bramer WM, Geng J, Huang F, de Man RA, Peppelenbosch MP, et al. The Global Burden of Hepatitis E Outbreaks: A Systematic Review. Liver Int 2016.
2. Xu L, Wang W, Peppelenbosch MP, Pan Q. Noncanonical Antiviral Mechanisms of ISGs: Dispensability of Inducible Interferons. Trends Immunol 2017;38:1-2.
3. Wang W, Xu L, Su J, Peppelenbosch MP, Pan Q. Transcriptional Regulation of Antiviral Interferon-Stimulated Genes. Trends Microbiol 2017.
4. Iversen MB, Reinert LS, Thomsen MK, Bagdonaite I, Nandakumar R, Cheshenko N, Prabakaran T, et al. An innate antiviral pathway acting before interferons at epithelial surfaces. Nat Immunol 2016;17:150-158.
5. Wang W, Xu L, Brandsma JH, Wang Y, Hakim MS, Zhou X, Yin Y, et al. Convergent Transcription of Interferon-stimulated Genes by TNF-alpha and IFN-alpha Augments Antiviral Activity against HCV and HEV. Sci Rep 2016;6:25482.
6. Wang W, Yin Y, Xu L, Su J, Huang F, Wang Y, Boor PPC, et al. Unphosphorylated ISGF3 drives constitutive expression of interferon-stimulated genes to protect against viral infections. Sci Signal 2017;10.
7. Xu L, Wang W, Li Y, Zhou X, Yin Y, Wang Y, de Man RA, et al. RIG-I Is A Key Antiviral Interferon-Stimulated Gene Against Hepatitis E Virus Dispensable Of Interferon Production. Hepatology 2017.
8. Wu J, Chen ZJ. Innate immune sensing and signaling of cytosolic nucleic acids. Annu Rev Immunol 2014;32:461-488.
9. Goubau D, Deddouche S, Reis e Sousa C. Cytosolic sensing of viruses. Immunity 2013;38:855-869.
10. Dalton HR, Kamar N, Izopet J. Hepatitis E in developed countries: current status and future perspectives. Future Microbiol 2014;9:1361-1372.
11. Kamar N, Rostaing L, Izopet J. Hepatitis E virus infection in immunosuppressed patients: natural history and therapy. Semin Liver Dis 2013;33:62-70.
12. Kamar N, Lhomme S, Abravanel F, Marion O, Peron JM, Alric L, Izopet J. Treatment of HEV Infection in Patients with a Solid-Organ Transplant and Chronic Hepatitis. Viruses 2016;8.
13. Debing Y, Gisa A, Dallmeier K, Pischke S, Bremer B, Manns M, Wedemeyer H, et al. A mutation in the hepatitis E virus RNA polymerase promotes its replication and associates with ribavirin treatment failure in organ transplant recipients. Gastroenterology 2014;147:1008-1011 e1007; quiz e1015-1006.
14. Debing Y, Ramiere C, Dallmeier K, Piorkowski G, Trabaud MA, Lebosse F, Scholtes C, et al. Hepatitis E virus mutations associated with ribavirin treatment failure result in altered viral fitness and ribavirin sensitivity. J Hepatol 2016;65:499-508.
15. Dao Thi VL, Debing Y, Wu X, Rice CM, Neyts J, Moradpour D, Gouttenoire J. Sofosbuvir Inhibits Hepatitis E Virus Replication In Vitro and Results in an Additive Effect When Combined With Ribavirin. Gastroenterology 2016;150:82-85 e84.
16. Wang W, Hakim MS, Nair VP, de Ruiter PE, Huang F, Sprengers D, Van Der Laan LJ, et al. Distinct Antiviral Potency of Sofosbuvir Against Hepatitis C and E Viruses. Gastroenterology 2016;151:1251-1253.
17. Nassim Kamar WW, Harry R Dalton, Qiuwei Pan. Direct-acting antiviral therapy for hepatitis E virus? The Lancet Gastroenterology & Hepatology 2017;2:154-155.
18. Lee JC, Tseng CK, Wu YH, Kaushik-Basu N, Lin CK, Chen WC, Wu HN. Characterization of the activity of 2'-C-methylcytidine against dengue virus replication. Antiviral Res 2015;116:1-9.
19. Rocha-Pereira J, Jochmans D, Dallmeier K, Leyssen P, Cunha R, Costa I, Nascimento MS, et al. Inhibition of norovirus replication by the nucleoside analogue 2'-C-methylcytidine. Biochem Biophys Res Commun 2012;427:796-800.
20. Qu C, Xu L, Yin Y, Peppelenbosch MP, Pan Q, Wang W. Nucleoside analogue 2'-C-methylcytidine inhibits hepatitis E virus replication but antagonizes ribavirin. Arch Virol 2017.
21. Furuta Y, Gowen BB, Takahashi K, Shiraki K, Smee DF, Barnard DL. Favipiravir (T-705), a novel viral RNA polymerase inhibitor. Antiviral Res 2013;100:446-454.
22. Wang W, Wang Y, Debing Y, Zhou X, Yin Y, Xu L, Herrera Carrillo E, et al. Biological or pharmacological activation of protein kinase C alpha constrains hepatitis E virus replication. Antiviral Res 2017;140:1-12.
23. Wang Y, Wang W, Xu L, Zhou X, Shokrollahi E, Felczak K, van der Laan LJ, et al. Cross Talk between Nucleotide Synthesis Pathways with Cellular Immunity in Constraining Hepatitis E Virus Replication. Antimicrob Agents Chemother 2016;60:2834-2848.
24. Yue P, Turkson J. Targeting STAT3 in cancer: how successful are we? Expert Opin Investig Drugs 2009;18:45-56.
25. Borentain P, Colson P, Bolon E, Gauchez P, Coso D, Gerolami R. Hepatocellular carcinoma complicating hepatitis E virus-related cirrhosis. Hepatology 2017.

Dutch Summary

Nederlandse samenvatting voor niet ingewijden

Het HEV (hepatitis E virus) is één van de voornaamste oorzaken van het ontstaan van virale hepatitis. Normalitair btreedt het HEV de bloedbaan via het maag-darm kanaal en infecteert het de lever waar het zich uitstekend vermenigvuldigen in de lever. Het beloop van een typische HEV-infectie wordt gekenmerkt door een aantal fases: van subklinisch, naar acuut en uiteindelijk naar fulminant. Hepatitis E wordt in steeds grotere mate gezien als een "public health concern" en in dit proefschrift voer ik ook een analyse uit in welke mate deze visie terecht is. Deze wordt beschreven in **hoofdstuk 2** en is ook gepubliceerd (Hakim MS, Wang W, Bramer WM, Geng J, Huang F, de Man RA, Peppelenbosch MP, Pan Q. The global burden of hepatitis E outbreaks: a systematic review. Liver Int. 2017 Jan;37(1):19-31). Ik concludeer in dit hoofdstuk dat alhoewel een mortaliteit van 0.2 tot 1.0 % in verhouding tot andere ziekten klein lijkt, deze bij zwangeren in het laatste trimester van de zwangerschap kan oplopen tot zo'n 20-25%. Ook zijn er substantiële zorgen met betrekking tor het risico van juist dit virus voor immuun-gecompromitteerde individuen en dan specifiek orgaantransplantatie-patiënten. HEV is dus inderdaad een groot probleem en ik richt me in mijn proefschrift dan ook verder met name op het verder begrijpen van de biologie die de interactie tussen men en virus onderligt alsmede op het exploreren van nieuwe therapeutische opties. Het proefschrift is daartoe verdeeld in drie delen, waarbij het eerste deel de moleculaire biologie van de afweer tegen HEV exploreert, het tweede deel de interactie van de moleculaire virale machinerie met potentiële geneesmiddelen onderzoekt en in het derde deel zich concentreert op de interactie van virussen met de gastheer en de mogelijkheden die daar liggen om tot nieuwe therapie te komen.

Helaas is er dan wel heel wat literatuur over de mechanismen waarmee het lichaam zichzelf verdedigt tegen HEV infectie, maar is deze is goed samengevat noch afdoende geanalyseerd. Om deze deficiëntie te repareren voer ik in **hoofdstuk 3** en **hoofdstuk 4** een systematisch literatuuronderzoek uit, waar ik mij met name concentreer op de interferonen (inflammatoire hormonen belangrijk bij de virale afweer) alsook de zogenaamde ISGs (genproducten die van het DNA worden afgeschreven volgend op stimulatie van cellen door interferonen en die de uiteindelijke antivirale werking uitvoeren). Deze analyse vormt de basis van experimentele studies in de daarop volgende hoofdstukken en werd gepubliceerd in twee artikelen (Wang W, Xu L, Su J, Peppelenbosch MP, Pan Q. Transcriptional Regulation of Antiviral Interferon-Stimulated Genes. Trends Microbiol. 2017 Jul;25(7):573-584 & Xu L, Wang W, Peppelenbosch MP, Pan Q. Noncanonical Antiviral Mechanisms of ISGs: Dispensability of Inducible Interferons. Trends Immunol. 2017 Jan;38(1):1-2). Met name op de mechanismen die leiden tot productie van antivirale genproducten heb ik vervolgens onderzocht. Het is welbekend dat het antivirale hormoon interferon de productie van dergelijke genproducten stimuleert en wel door het activeren van een zogenaamde STAT transcriptiefactor die direct aan de receptor voor interferon bindt, vervolgens gefosforileerd en geactiveerd wordt en dan in de kern aan promotor van de betrokken genproducten bindt en door het rekruteren van de transcriptionele machinerie naar deze promotoren de transcriptie van deze genen in gang zet. In praktijk zal echter bij virale infectie interferonen hun werking doen in de aanwezigheid van andere genproducten. Met name het inflammatoire hormoon TNF-alpha zal ook aanwezig zijn. In het **vierde hoofdstuk** ontrafel in de details van de resulterende interactie en laat

zien dat met name het activeren van zogenaamde NF-kappaB transcriptiefactoren door TNF een belangrijk synergistisch signaal dat samen met de interferon-afhankelijke signalen de transcriptie van de betrokken genen aanjaagt. Ook deze data zijn reeds gepubliceerd (Wang W, Xu L, Brandsma JH, Wang Y, Hakim MS, Zhou X, Yin Y, Fuhler GM, van der Laan LJ, van der Woude CJ, Sprengers D, Metselaar HJ, Smits R, Poot RA, Peppelenbosch MP, Pan Q. Convergent Transcription of Interferon-stimulated Genes by TNF-α and IFN-α Augments Antiviral Activity against HCV and HEV. Sci Rep. 2016 May 6;6:25482).

Dergelijke interacties laten onverlet dat zelfs in de afwezigheid van inflammatoire hormonen cellen al substantiële antivirale mechanismen kunnen activeren. In het **vijfde hoofdstuk** kijk ik hoe deze t eerste beschermingslinie tegen virale infectie in elkaar steekt. In stel vast dat ook zonder stimulatie en dus ook zonder fosforilatie de betrokken transcriptiefactoren al aan het DNA kunnen binden en transcriptionele machinerie kunnen rekruteren. Dit is in aanzienlijke tegenspraak met het dogma in de gedachten over de organisatie van deze verdediging en deze data werden dan ook gepubliceerd in een wetenschappelijk tijdschrift dat een duidelijke zichtbaarheid in het veld heeft (Wang W, Yin Y, Xu L, Su J, Huang F, Wang Y, Boor PPC, Chen K, Wang W, Cao W, Zhou X, LiuP, van der Laan LJW, Kwekkeboom J, Peppelenbosch MP, Pan Q. Unphosphorylated ISGF3 drives constitutive expression of interferon-stimulated genes to protect against viral infections. Sci Signal. 2017 Apr 25;10(476). Het betrokken mechanisme, dat dus ook belangrijk is in de afwezigheid van het anti-virale interferonhormoon werd verder uitgediept in **hoofdstuk 7**. Hier bleek dat met name het antivirale genproduct RIG-I een belangrijke effector vervult. Ook deze data kon ik een tijdschrift dat een grote zichtbaarheid geniet publiceren (Xu L, Wang W, Li Y, Zhou X, Yin Y, Wang Y, de Man RA, van der Laan LJW, Huang F, Kamar N, Peppelenbosch MP, Pan Q. RIG-I is a key antiviral interferon-stimulated gene against hepatitis E virus regardless of interferon production. Hepatology. 2017 Jun;65(6):1823-1839). Nu ik meer inzicht had gekregen in moleculaire mechanismen die het lichaam gebruikt om zich te verdedigen tegen HEV infectie, besloot ik uit te zoeken hoe afweer tegen HEV ondersteunt kan worden antivirale therapie. Dit vormt het tweede deel van dit proefschrift.

In eerste instantie onderzoek ik hierbij in welke het virale polymerase (een eiwit gecodeerd door het virale genoom dat essentieel is voor de vermenigvuldiging van het genetisch materiaal van het virus) een bruikbaar doelwit vorm voor dergelijke farmacologische therapie, een analyse die ik opgenomen heb in dit proefschrift in **hoofdstuk 8** maar die ik ook wereldkundig heb gemaakt middels een publicatie in wederom een vooraanstaand tijdschrift in mijn vakgebied (Wang W, Peppelenbosch MP, Pan Q. Targeting Viral Polymerase for Treating Hepatitis E Infection: How Far Are We? Gastroenterology. 2016 Jun;150(7):1690). In **hoofdstuk 9** ga ik dan in op het vermogen van Sofosbuvir om hepatitis E te bestrijden. Deze medicatie heeft een sterk effect op het hepatitis C virus en zou daarom ook een goede optie kunnen zijn bij de behandeling van hepatitis E. Ik laat echter zien dat de gevoeligheid van hepatitis C virus en HEV voor dit middel sterk verschillend is. Dit teleurstellend en daarom ook klinisch belangrijk effect werd wederom gepubliceerd in een gezichtsbepalend tijdschrift in mijn vakgebied (Wang W, Hakim MS, Nair VP, de Ruiter PE, Huang F, Sprengers D, Van Der Laan LJ, Peppelenbosch MP, Surjit M, Pan Q. Distinct Antiviral Potency of Sofosbuvir Against Hepatitis C and E Viruses. Gastroenterology. 2016 Dec;151(6):1251-1253). Op zoek naar een oplossing testte ik een andere medicatie, *in casu* het nucleoside-analoog (een namaak

DNA-base die de polymerase van het virus kan foppen en dus zo mogelijk de vermenigvuldiging van genetisch materiaal van het virus stoppen). Dit middel bleek inderdaad het virus te remmen. Echter, tegelijkertijd bleek het ook de werking van de enige medicatie met in ieder geval enige bewezen effectiviteit tegen HEV (ribavarine) te verstoren, waardoor de netto opbrengst van behandeling van hepatitis E met nucleoside analogen tegen valt en dus andere mogelijkheden onderzocht moesten worden. De betreffende experimenten en hun overkoepelende analyse staan beschreven in **hoofdstuk 10** en **hoofdstuk 11.** Ook deze data werden gepubliceerd in de wetenschappelijke literatuur (Qu C, Xu L, Yin Y, Peppelenbosch MP, Pan Q, Wang W. Nucleoside analogue 2'-C-methylcytidine inhibits hepatitis E virus replication but antagonizes ribavirin. Arch Virol. 2017 Jun 16 & Kamar N, Wang W, Dalton HR, Pan Q. Direct-acting antiviral therapy for hepatitis E virus? Lancet Gastroenterol Hepatol. 2017 Mar;2(3):154-155).

Nieuwe strategieën met betrekking tot de behandeling van hepatitis E kunnen heel wel ontwikkeld worden uit vergrootte kennis van de gastheercel met het HEV. Ik analyseer daarom in **hoofdstuk 12** de rol van zogenaamde kinasen (een verzamelnaam voor een groep enzymen die een fosfaatgroep kan aanbrengen op een ander eiwit of een ander molecuul (fosforylering), terwijl een fosfatase een dergelijke groep kan verwijderen (defosforylering). Vaak wordt door zo'n fosforylering of defosforylering het doeleiwit geactiveerd of gedeactiveerd. Deze schakelfunctie kan zo chemische reacties in de cel aansturen en vormt een belangrijke factor in de cel-interne signaaltransductie) en stel vast dat het zogenaamde proteïne kinase C een sleutelfunctie vervuld bij het opwekken van cellulaire reacties in de gastheercel. Ook deze data werden gepresenteerd aan de wetenschappelijke gemeenschap middels een publicatie (Wang W, Wang Y, Debing Y, Zhou X, Yin Y, Xu L, Herrera Carrillo E, Brandsma JH, Poot RA, Berkhout B, Neyts J, Peppelenbosch MP, Pan Q. Biological or pharmacological activation of protein kinase C alpha constrains hepatitis E virus replication. Antiviral Res. 2017 Apr;140:1-12). Hoe cellulaire biochemie en cel-autonome immuniteit dan samen het natuurlijk beloop van een HEV infectie kunnen verklaren wordt dan verder uitgezocht in **hoofdstuk 13** en is ook gepubliceerd in een wetenschappelijk tijdschrift (Wang Y, Wang W, Xu L, Zhou X, Shokrollahi E, Felczak K, van der Laan LJ, Pankiewicz KW, Sprengers D, Raat NJ, Metselaar HJ, Peppelenbosch MP, Pan Q. Cross Talk between Nucleotide Synthesis Pathways with Cellular Immunity in Constraining Hepatitis E Virus Replication. Antimicrob Agents Chemother. 2016 Apr 22;60(5):2834-48).1. Een volgend **hoofdstuk 14** exploreert dan welke elementen uit het genoom van HEV precies de cel-autonome antivirale immuniteit oproepen. Dit hoofdstuk is momenteel onder review bij het tijdschrift “Hepatology”. Het laatste experimenteel hoofdstuk karakteriseert de rol van STAT3 in de HEV replicatie. Heel spectaculair toont de kandidaat aan dat STAT3 een onmisbare co-factor is voor virale vermenigvuldiging. Een manuscript gebaseerd op deze data wordt nu klaar gemaakt om voor publicatie te worden aangeboden. Een overkoepelende samenvattende discussie is ook opgenomen in dit proefschrift.

Samen hoop ik met dit werk een wezenlijke bijdrage te hebben geleverd aan het begrijpen van de biologie van de interactie tussen levercel en het HEV en ook aanzetten te hebben gegeven voor nieuwe rationele behandeling van hepatitis E.

Appendix

Acknowledgements

Publications

PhD Portfolio

Curriculum Vitae

Acknowledgements

I would like to give my greatest gratitude to all of you, my families, my promoter, co-promoter, colleagues and friends. The work presented in this thesis would never be possible without your invaluable support and help.

Dr. Qiuwei (Abdullah) Pan, thank you for the enormous support and encouragement during my entire PhD study. You are such a brilliant , hard-working but also humble scientist, a model that I look up to! Your enthusiasm in science really motivates me a lot. I fully appreciate the way how you train us to do research and how to foster the scientific thinking. Just like the ancient Chinese proverb “Give a man a fish and you feed him for a day; teach a man to fish and you feed him for a lifetime.”(授人以鱼不如授人以渔). I really enjoy the time we working together. Thank you so much for guiding me through all the difficulties. It’s really my great honor to be your student.

Prof. Maikel P. Peppelenbosch, thank you for the suggestion and supervision for my research. You are a legendary scientist full of innovative and creative ideas. I enjoy every group discussion, weekly meeting and seminars that you attended. I am so impressed by the inspiring and mind-blowing questions or suggestions you raised. Thank you for all the support for my PhD study.

Dr. Dave Sprengers, I really enjoy the discussion during our weekly meeting. Your suggestions from the clinical perspective are really helpful for research. Dr. Ron Smits, you are a wonderful scientist full of knowledge and kindness. You always like to offer your helpful hand when we meet problems. I enjoy every discussion with you. Dr. Gwenny Fuhler, you are a knowledgeable scientist. Your valuable suggestions and input help me a lot. Thank you for all the collaboration and support.

Prof. Stephan Urban, thank you for inviting me to visit your lab. You are the leading scientist in the research field of HBV and HDV. I really enjoyed the scientific discussion with you and all you lab members.

Prof. Frank van Kuppeveld, I am so glad to meet you in the 2016 ECV conference. Thanks for your suggestions about how to do research. You encouraged me a lot.

Dr. Omry Koren, thank you for hosting me during my visit to your lab. I learnt a lot in the field of microbiome. Looking forward to visit you next time!

Dr. Lei Xu and Dr. Yuebang Yin, I am so glad to meet you in the Netherlands. We worked together for the past four years, and both of you gave me so much help and support for my projects. I learned a lot from you. We keep our friendship forever! Dr. Yijin Wang and Dr. Xinying Zhou, both of you helped me a lot when I first came to the lab. I really appreciate your invaluable support. Hoping both of you achieve great success.

Dr. Kan Chen, I really enjoyed the time together with you in the lab. Thank you for your encourage and support. Wenhui, my dear ‘sister’, so glad to meet you in Rotterdam. What a coincidence (we have the same family name and similar first name) ! Thank you for the support in the last four years. Wanlu, you are an excellent researcher full of idea and

persistence. Your hard-working will be paid off. Wen, thank you for organizing so many wonderful activities; Shan, you are the excellent combination of scientist, doctor and big chef; Pengyu, you are a knowledgeable researcher. Changbo, you are a very talented and humble person; Buyun, you are kind and smart, full of energy; Meng, you are the 'mitochondrial-expert' full of creative and scientific ideas . Menggang, you look more like an elder brother full of kindness. Thanks for the experiences and knowledge you shared with us. Guoying, you are an excellent researcher full of justice. Yingying, you are an prominent researcher full of kindness. Sunrui and Jiaye, you are the most creative members in our group. Hakim, you are kind and hard-working. I enjoyed the time we work together. Wish all of you success in your research projects.

To my former 'senior office members', Elmer, Rik, Wesley, Xiaolei, Michelle, Emmeloes, Renee, et al. To my 'junior office members', Aafke, Gulce, Monigue, Janine, Ishaki, et al. Thanks for the great time we had together.

To all MDL members, Andre, Hugo, Andrea, Auke, Jaap, Luc, Raymond, Leonie, Marcel, Monique, Thomas, Henk, Pauline, Adriaan, Jan, Paula, Patrick, Sonja, Anthonie, Martijn, Juan, Lauke, Gertine, Kim, Shanta, Petra et al., everyone in our lab are so great! I want to thank all of you for any help and support during my study here.

To my Chinese friends, Zhanmin, Xiaolei, Ruoyu, Changbin, Wu Bin, Huang Ling & Tongwei, Gao Wen & Ya, Ping Zhen, Lu Tao, Liu Fan & Wen Bei, Kuikui, Guannan, Shihao, Shaoshi, Liqin & Haobo, Danli, Yu Xue, et al. Wish you all the best!

To Dr. Jiakun Gong and Dr. Xiaoyan Zhao, Hongbo and I feel so lucky to meet you in Netherlands. You two are such nice, kind and thoughtful person. Thank you both for your invaluable help and encouragement.

To 中国农业科学院一级岗位杰出人才专家吴东来研究员，感谢在硕士研究期间对学生的指导和关心，感谢您对我出国求学的支持和鼓励。感谢孙恩成研究员 （亲师兄！）一直以来对我的鼓励和支持。感谢首席科学家步志高研究员以及重要人兽共患病与烈性外来病研究创新团队所有老师和同学的帮助。感谢山东农业大学刘思当教授，肖一红教授对学生的关心和支持。

感谢我的父母，岳父母，姐姐，姐夫和小外甥王赫，谢谢你们自始至终对我的支持和关心。家永远是幸福的港湾。

Last but not least, to Hongbo, my beloved wife, thank you for your enomous love and support. You are the one who always support and encourage me when I meet hardship. Thank you for taking really good care of me. All the best wishes to our bright future!

Publications list

1. **W.Wang**, Y. Wang, C. Qu, S. Wang, J. Zhou, W. Cao, L. Xu, B. Ma, M. S. Hakim, Y. Yin, T. Li, M. P. Peppelenbosch, J. Zhao, Q. Pan. The RNA genome of hepatitis E virus robustly triggers antiviral interferon response. **Hepatology**.
2. Yin, Y., W. Dang, X. Zhou, L. Xu, **W. Wang**, W. Cao, S. Chen, J. Su, X. Cai, S. Xiao, M. P. Peppelenbosch, and Q. Pan. 2017. PI3K-Akt-mTOR axis sustains rotavirus infection via the 4E-BP1 mediated autophagy pathway and represents an antiviral target. *Virulence*.
3. Xu, L., **W. Wang**, M. P. Peppelenbosch, and Q. Pan. 2017. Noncanonical Antiviral Mechanisms of ISGs: Dispensability of Inducible Interferons. *Trends Immunol* 38: 1-2.
4. Xu, L., **W. Wang**, Y. Li, X. Zhou, Y. Yin, Y. Wang, R. A. de Man, L. J. van der Laan, F. Huang, N. Kamar, M. P. Peppelenbosch, and Q. Pan. 2017. RIG-I Is A Key Antiviral Interferon-Stimulated Gene Against Hepatitis E Virus Dispensable Of Interferon Production. *Hepatology*.
5. **Wang, W**., Y. Yin, L. Xu, J. Su, F. Huang, Y. Wang, P. P. C. Boor, K. Chen, W. Wang, W. Cao, X. Zhou, P. Liu, L. J. W. van der Laan, J. Kwekkeboom, M. P. Peppelenbosch, and Q. Pan. 2017. Unphosphorylated ISGF3 drives constitutive expression of interferon-stimulated genes to protect against viral infections. *Sci Signal* 10.
6. **Wang, W**., L. Xu, J. Su, M. P. Peppelenbosch, and Q. Pan. 2017. Transcriptional Regulation of Antiviral Interferon-Stimulated Genes. *Trends Microbiol*.
7. **Wang, W**., Y. Wang, Y. Debing, X. Zhou, Y. Yin, L. Xu, E. Herrera Carrillo, J. H. Brandsma, R. A. Poot, B. Berkhout, J. Neyts, M. P. Peppelenbosch, and Q. Pan. 2017. Biological or pharmacological activation of protein kinase C alpha constrains hepatitis E virus replication. *Antiviral Res* 140: 1-12.
8. Qu, C., L. Xu, Y. Yin, M. P. Peppelenbosch, Q. Pan, and **W. Wang**. 2017. Nucleoside analogue 2'-C-methylcytidine inhibits hepatitis E virus replication but antagonizes ribavirin. *Arch Virol*.
9. Nassim Kamar, **W. Wang**., Harry R Dalton, Qiuwei Pan. 2017. Direct-acting antiviral therapy for hepatitis E virus? *The Lancet Gastroenterology & Hepatology* 2: 154-155.
10. Nano, J., M. Ghanbari, **W. Wang**, P. S. de Vries, K. Dhana, T. Muka, A. G. Uitterlinden, J. B. J. van Meurs, A. Hofman, B. consortium, O. H. Franco, Q. Pan, S. D. Murad, and A. Dehghan. 2017. Epigenome-Wide Association Study Identifies Methylation Sites Associated With Liver Enzymes and Hepatic Steatosis. *Gastroenterology* 153: 1096-1106 e1092.
11. Ikram, A., M. S. Hakim, J. H. Zhou, **W. Wan**g, M. P. Peppelenbosch, and Q. Pan. 2017. Genotype-specific acquisition, evolution and adaptation of characteristic mutations in hepatitis E virus. *Virulence*: 1-12.
12. Dang, W., Y. Yin, Y. Wang, **W. Wang**, J. Su, D. Sprengers, L. J. W. van der Laan, K. Felczak, K. W. Pankiewicz, K. O. Chang, M. P. G. Koopmans, H. J. Metselaar, M. P. Peppelenbosch, and Q. Pan. 2017. Inhibition of calcineurin or IMPDH exerts moderate to potent antiviral activity against norovirus replication. *Antimicrob Agents Chemother*.
13. Cao, W., K. Chen, M. Bolkestein, Y. Yin, M. M. A. Verstegen, M. J. C. Bijvelds, **W. Wang**, N. Tuysuz, D. Ten Berge, D. Sprengers, H. J. Metselaar, L. J. W. van der Laan, J. Kwekkeboom, R. Smits, M. P. Peppelenbosch, and Q. Pan. 2017. Dynamics of Proliferative and Quiescent Stem Cells in Liver Homeostasis and Injury. *Gastroenterology* 153: 1133-1147.
14. Zhou, X., L. Xu, **W. Wang**, K. Watashi, Y. Wang, D. Sprengers, P. E. de Ruiter, L. J. van der Laan, H. J. Metselaar, N. Kamar, M. P. Peppelenbosch, and Q. Pan. 2016. Disparity of basal and therapeutically activated interferon signalling in constraining hepatitis E virus infection. *J Viral Hepat* 23: 294-304.
15. Yin, Y. B., Y. J. Wang, W. Dang, L. Xu, J. H. Su, X. Y. Zhou, **W. Wang**, K. Felczak, L. J. W. van der Laan, K. W. Pankiewicz, A. A. van der Eijk, M. Bijvelds, D. Sprengers, H. de Jonge, M. P. G. Koopmans, H. J. Metselaar, M. P. Peppelenbosch, and Q. W. Pan. 2016. Mycophenolic acid potently inhibits rotavirus infection with a high barrier to resistance development. *Antivir Res* 133: 41-49.

16. Xu, L., X. Zhou, **W. Wang**, Y. Wang, Y. Yin, L. J. van der Laan, D. Sprengers, H. J. Metselaar, M. P. Peppelenbosch, and Q. Pan. 2016. IFN regulatory factor 1 restricts hepatitis E virus replication by activating STAT1 to induce antiviral IFN-stimulated genes. *FASEB J*.

17. Wang, Y., **W. Wang**, L. Xu, X. Zhou, E. Shokrollahi, K. Felczak, L. J. van der Laan, K. W. Pankiewicz, D. Sprengers, N. J. Raat, H. J. Metselaar, M. P. Peppelenbosch, and Q. Pan. 2016. Cross Talk between Nucleotide Synthesis Pathways with Cellular Immunity in Constraining Hepatitis E Virus Replication. *Antimicrob Agents Chemother* 60: 2834-2848.

18. **Wang, W**., L. Xu, J. H. Brandsma, Y. Wang, M. S. Hakim, X. Zhou, Y. Yin, G. M. Fuhler, L. J. van der Laan, C. J. van der Woude, D. Sprengers, H. J. Metselaar, R. Smits, R. A. Poot, M. P. Peppelenbosch, and Q. Pan. 2016. Convergent Transcription of Interferon-stimulated Genes by TNF-alpha and IFN-alpha Augments Antiviral Activity against HCV and HEV. *Sci Rep* 6: 25482.

19. **Wang, W**., M. P. Peppelenbosch, and Q. Pan. 2016. Targeting Viral Polymerase for Treating Hepatitis E Infection: How Far Are We? *Gastroenterology*.

20. **Wang, W**., M. S. Hakim, V. P. Nair, P. E. de Ruiter, F. Huang, D. Sprengers, L. J. Van Der Laan, M. P. Peppelenbosch, M. Surjit, and Q. Pan. 2016. Distinct Antiviral Potency of Sofosbuvir Against Hepatitis C and E Viruses. *Gastroenterology* 151: 1251-1253.

21. Hakim, M. S., **W. Wang**, W. M. Bramer, J. Geng, F. Huang, R. A. de Man, M. P. Peppelenbosch, and Q. Pan. 2016. The Global Burden of Hepatitis E Outbreaks: A Systematic Review. *Liver Int*.

22. Zhou, X., L. Xu, Y. Wang, **W. Wang**, D. Sprengers, H. J. Metselaar, M. P. Peppelenbosch, and Q. Pan. 2015. Requirement of the eukaryotic translation initiation factor 4F complex in hepatitis E virus replication. *Antiviral Res* 124: 11-19.

23. Hernanda, P. Y., K. Chen, A. M. Das, K. Sideras, **W. Wang**, J. Li, W. Cao, S. J. Bots, L. L. Kodach, R. A. de Man, J. N. Ijzermans, H. L. Janssen, A. P. Stubbs, D. Sprengers, M. J. Bruno, H. J. Metselaar, T. L. ten Hagen, J. Kwekkeboom, M. P. Peppelenbosch, and Q. Pan. 2015. SMAD4 exerts a tumor-promoting role in hepatocellular carcinoma. *Oncogene* 34: 5055-5068.

24. **Wang, W.**, E. C. Sun, Q. Y. Xu, T. Yang, Y. L. Qin, J. Zhao, Y. F. Feng, J. P. Li, P. Wei, C. Y. Zhang, and D. L. Wu. 2013. Identification of two novel BTV16-specific B cell epitopes using monoclonal antibodies against the VP2 protein. *Appl Microbiol Biotechnol* 97: 5933-5942.

25. **Wang, W.**, E. C. Sun, N. H. Liu, T. Yang, Q. Y. Xu, Y. L. Qin, J. Zhao, Y. F. Feng, J. P. Li, P. Wei, C. Y. Zhang, and D. L. Wu. 2013. Identification of three novel linear B-cell epitopes on the VP5 protein of BTV16. *Vet Microbiol* 162: 631-642.

26. Sun, E. C., J. Zhao, L. Sun, Q. Y. Xu, T. Yang, Y. L. Qin, **W. Wang**, P. Wei, J. Sun, and D. L. Wu. 2013. Comprehensive Mapping of Common Immunodominant Epitopes in the Eastern Equine Encephalitis Virus E2 Protein Recognized by Avian Antibody Responses. *Plos One* 8.

27. Sun, E., J. Zhao, TaoYang, Q. Xu, Y. Qin, **W. Wang**, P. Wei, and D. Wu. 2013. Antibodies generated by immunization with the NS1 protein of West Nile virus confer partial protection against lethal Japanese encephalitis virus challenge. *Vet Microbiol* 166: 145-153.

28. Qin, Y. L., E. C. Sun, N. H. Liu, T. Yang, Q. Y. Xu, J. Zhao, **W. Wang**, P. Wei, Y. F. Feng, J. P. Li, and D. L. Wu. 2013. Identification of a linear B-cell epitope within the Bluetongue virus serotype 8 NS2 protein using a phage-displayed random peptide library. *Vet Immunol Immunopathol* 154: 93-101.

29. EnCheng, S., Z. Jing, Y. Tao, X. QingYuan, Q. Yongli, **Wang. W**, W. Peng, S. Liang, S. Jing, and W. DongLai. 2013. Analysis of murine B-cell epitopes on Eastern equine encephalitis virus glycoprotein E2. *Appl Microbiol Biotechnol* 97: 6359-6372.

30. **Wang, W**., E. C. Sun, N. H. Liu, T. Yang, Q. Y. Xu, Y. L. Qin, J. Zhao, Y. F. Feng, J. P. Li, P. Wei, C. Y. Zhang, and D. L. Wu. 2012. Monoclonal antibodies against VP7 of bluetongue virus. *Hybridoma (Larchmt)* 31: 469-472.

PhD Portfolio

Name PhD Student Wenshi Wang

Erasmus MC Department Gastroenterology and Hepatology

Ph.D Period October 2013 - September 2017

Promotor Prof. Dr. Maikel P. Peppelenbosch

Copromotor Dr. Qiuwei Pan

General Courses

- 2014, the workshop on Photoshop and Illustrator CS5
- 2014, the Virology Course and Symposium
- 2014, Microscope Image Analysis: From Theory to Practice
- 2015, the Course Biomedical Research Techniques XIII
- 2017, the Course on Microbiomics I
- 2017, the Course Scientific Integrity

Academic Presentation (National and International)

- 2015, April. International Liver Congress™. Vienna, Austria.(one poster presentation)
- 2016, March. Dutch Experimental Gastroenterology and Hepatology Meeting. Eindhoven, Netherlands. (two oral presentation and one poster presentation)
- 2016，March. 20th Molecular Medicine Day, Erasmus Postgraduate School Molecular Medicine. Rotterdam, Netherlands (one poster presentation)
- 2016, April. International Liver Congress™ Barcelona, Spain.(one oral presentation and two poster presentation)
- 2016, October. 6th European Congress of Virology. Hamburg, Germany.(one poster presentation)
- 2017, March. Dutch Experimental Gastroenterology and Hepatology Meeting. Eindhoven, Netherlands.(one oral presentation)
- 2017，March. 21th Molecular Medicine Day, Erasmus Postgraduate School Molecular Medicine. Rotterdam, Netherlands (one poster presentation)
- 2017, April. Royal Dutch Society for Microbiology Spring Meeting. Arnhem, Netherlands.(one oral presentation)

- 2017, June. EMBO Conference on Hijacking host signaling and epigenetic mimicry during infections. Paris, France. (one poster presentation)

- 2017, July. Department of Infectious Diseases, Molecular Virology at Heidelberg University. Heidelberg, Germany. (Invited oral presentation)

Academic Awards

- FEMS Research and Training Grants, Federation of European Microbiology Societies. 2017

- Kiem Award for the best first publications written by young microbiologists (€500), Royal Dutch Society for Microbiology. 2017.

- ILC Full Bursary (€650), International Liver Congress™, Barcelona, Spain. 2016.

- ILC Full Bursary (€650), International Liver Congress™, Vienna, Austria. 2015.

- China Scholarship Council (CSC) Scholarship (201303250056), 2013.

- Highest-level Master Graduate Award, HVRI, Chinese Academy of Agricultural Science, China. 2013 (¥10,000).

- Excellent Master Graduate (*honor*), Graduate School of Chinese Academy of Agricultural Science, China. 2013.

- Excellent Master Graduate (*honor*), the Municipality of Beijing, People's Republic of China. 2013.

- Distinguished Master's Thesis Award, Chinese Academy of Agricultural Science, China. 2013. (¥5,000)
- National Scholarship for Graduate Students, People's Republic of China. 2013 (¥20,000)

Curriculum Vitae

Wenshi Wang was born on November 08, 1987, in Qingdao, Shandong Province, China. He grew up and attended primary, middle and high school in his hometown. In 2006, he moved to Tai'an in western Shandong Province to start his Bachelor study in veterinary medicine at Shandong Agriculturial University. He finished his study with a thesis, entitled "Identification of B-cell Epitopes on NS1 protein of West Nile Virus". In 2010, he started his master study at Graduate School of Chinese Academy of Agricultural Science (CAAS), Beijing, China. One year later, he formally started his master research training at the Department of Zoonosis, Harbin Veterinary Research Institute, CAAS. Under the supervision of Prof. Donglai Wu, he finished his thesis book, entitled "Preparation of Monoclonal Antibodies Against VP2 and VP5 Proteins of Bluetongue Virus 16 and Identification of B-cell Epitopes". In 2013, with the support of China Scholarship Council, he got an opportunity to start his Ph.D study at the department of Gastroenterology and Hepatology, Erasmus Medical Center Rotterdam, the Netherlands. Under the supervision of Prof. Maikel P. Peppelenbosch and Dr. Qiuwei Pan, he focused on the development of novel antiviral strategies for hepatitis E, including (I) Interferon-stimulated genes –based strategies; (II) Drug-based strategies; (III) Virus-host interaction-based strategies.